



**HAL**  
open science

# Huntingtin functions in the regulation of axonal transport : consequences on neuronal network homeostasis and behavior, in health and disease

Hélène Vitet

## ► To cite this version:

Hélène Vitet. Huntingtin functions in the regulation of axonal transport : consequences on neuronal network homeostasis and behavior, in health and disease. Neurobiology. Université Grenoble Alpes [2020-..], 2020. English. NNT : 2020GRALV038 . tel-03198814

**HAL Id: tel-03198814**

**<https://theses.hal.science/tel-03198814v1>**

Submitted on 15 Apr 2021

**HAL** is a multi-disciplinary open access archive for the deposit and dissemination of scientific research documents, whether they are published or not. The documents may come from teaching and research institutions in France or abroad, or from public or private research centers.

L'archive ouverte pluridisciplinaire **HAL**, est destinée au dépôt et à la diffusion de documents scientifiques de niveau recherche, publiés ou non, émanant des établissements d'enseignement et de recherche français ou étrangers, des laboratoires publics ou privés.



## THÈSE

Pour obtenir le grade de

## DOCTEUR DE L'UNIVERSITÉ GRENOBLE ALPES

Spécialité : Neurosciences - Neurobiologie

Arrêté ministériel : 25 mai 2016

Présentée par

**Hélène VITET**

Thèse dirigée par **Frederic SAUDOU**  
et co-encadrée par **Chiara SCARAMUZZINO**, Université  
Grenoble-Alpes

préparée au sein du **Laboratoire Grenoble Institut des  
Neurosciences**  
dans l'**École Doctorale Chimie et Sciences du Vivant**

**Conséquences de la régulation du transport  
axonal par la Huntingtine sur l'homéostasie  
de réseaux neuronaux et sur le  
comportement, en conditions saine et  
pathologique**

**Huntingtin functions in the regulation of  
axonal transport: consequences on neuronal  
network homeostasis and behavior, in health  
and disease**

Thèse soutenue publiquement le **11 décembre 2020**,  
devant le jury composé de :

**Monsieur FREDERIC SAUDOU**  
PROFESSEUR DES UNIVERSITES - PRATICIEN HOSPITALIER,  
UNIVERSITE GRENOBLE ALPES, Directeur de thèse

**Madame KARINE MERIENNE**  
DIRECTRICE DE RECHERCHE, CNRS DELEGATION ALSACE,  
Rapporteuse

**Madame CORALIE FASSIER**  
DIRECTRICE DE RECHERCHE, INSERM DELEGATION PARIS,  
Rapporteuse

**Monsieur ALAIN MARTY**  
DIRECTEUR DE RECHERCHE, CNRS DELEGATION ILE-DE-FRANCE  
VILLEJUIF, Examineur

**Monsieur ALAIN BUISSON**  
PROFESSEUR DES UNIVERSITES, UNIVERSITE GRENOBLE ALPES,  
Président



*À mon grand-père, dans l'espoir qu'il soit en paix avec  
l'usage que je fais du nom qu'il nous a transmis.*



## Preface

### L'état d'équilibre des déséquilibres

Avant de rentrer dans les profondeurs et méandres de la régulation du transport axonal, arrêtons-nous sur l'importance de l'homéostasie, l'état d'équilibre, de la cellule ou de tout autre système. La définition de l'homéostasie est fidèlement explicitée par son étymologie grecque ; « homéostasie » est composée de *hómoios*, « similaire », et de *stásis*, « stabilité ». Cette « stabilité similaire », du fait de sa capacité à s'autoentretenir, permet l'établissement d'un équilibre capable de répondre à des perturbations au sein d'un système. Ces perturbations peuvent être transitoires ou permanentes et impactantes menant soit à un rapide retour à un autre état d'équilibre soit à un emballement du système. Ces conséquences sont visibles au sein d'une cellule telle qu'un neurone régulant le transport d'une vésicule tout comme au sein d'une planète régulant sa température. Dans les deux cas, une perturbation importante, et donc une perte de l'homéostasie, amène à la neurodégénérescence ou au réchauffement climatique dont nous sommes aujourd'hui les témoins. Ainsi, sans profonde perturbations menant à l'emballement du système, l'essence même d'un état d'équilibre serait d'être perturbé, déséquilibré, modifié, mais jamais perdu ; l'équilibre sera toujours trouvé. Le chimiste trouve l'équilibre chimique d'une réaction en perturbant l'équilibre de plusieurs espèces par leur mélange. Le dramaturge se joue de l'élément perturbateur initial pour mettre en scène le chemin menant au prochain équilibre. Le musicien produit des mélodies en contrôlant les perturbations et le retour à l'équilibre de l'air en le faisant vibrer avec une corde.

L'équilibre, la physiologie, voilà ce que le chercheur étudie pour comprendre le déséquilibre, la pathologie. En pratique, c'est généralement l'observation de la pathologie qui arrive en premier. Claude Bernard a par exemple étudié l'effet du curare qui paralysait les animaux les proies des indiens d'Amazonie pour une meilleure compréhension du fonctionnement de la jonction neuromusculaire. De même pour la maladie d'Huntington, de nombreuses études se sont en premier lieu penchées sur les conséquences de l'induction d'effets toxiques provoqués par la maladie plutôt que la perte de fonctions physiologiques. Ainsi, c'est en investissant dans la recherche fondamentale centrée sur les phénomènes physiologiques que la science fondamentale permet l'application à la pathologie. En effet, en comprenant l'équilibre d'un système, il est possible de le rétablir lorsqu'il est perturbé ; la médecine aujourd'hui, réussit à perturber l'équilibre du système malade pour soigner, s'il ne s'est pas encore emballé.

Les déséquilibres apparaissent comme problématiques mais ne nous sont-ils pas également nécessaires ? L'équilibre apparaîtrait donc comme nécessaire aux déséquilibres et à leurs effets. En effet, les déséquilibres ne font-ils pas de nous des Hommes et non pas des machines, pour le pire et le

meilleur ? Sans déséquilibres, et sans sa capacité d'adaptation due à l'homéostasie, l'Homme n'aurait sûrement pas évolué de la façon dont il l'a fait. De plus, nos avancées scientifiques auraient été limitées car le chercheur a besoin de perturber l'équilibre pour le comprendre. Ainsi, ne faudrait-il donc pas atteindre un état d'équilibre des déséquilibres ? En effet, trop peu de perturbations de l'équilibre nous aurait peut-être empêché d'évoluer en tant qu'Hommes et scientifiques et *a contrario*, trop de perturbations peuvent mettre à mal l'homéostasie et créer de nouvelles conditions (climatiques par exemple) non compatibles avec la vie humaine. Enfin, la fin d'un sous-système par perte homéostasique peut également être considéré comme un mécanisme de préservation de l'homéostasie d'un système supérieur atteignant alors un nouvel état d'équilibre. Ceci ajoute finalement un caractère relatif à la notion d'équilibre.

A nous de trouver notre prochain équilibre ou les prochains déséquilibres y menant...

## Title

**Huntingtin functions in the regulation of axonal transport: consequences on neuronal network homeostasis and behavior in health and disease**

## Abstract

Neuronal circuits are at the basis of behaviors such as motor coordination or learning and memory. As being part of a network, neurons communicate at synapses through finely tuned molecular and cellular processes. One key mechanism regulating synapse homeostasis involves the transport of vesicles within axons and dendrites, which is dysregulated in many neurological disorders such as Rett syndrome, Alzheimer's (AD) and Huntington's diseases (HD). Thus, deciphering the regulation of vesicular transport within neurites in physiological context is crucial to understand, and potentially restore, the consequences of these dysregulations in pathological contexts.

Huntingtin (HTT) protein, known for its devastating role in HD when mutated, is a key actor of axonal transport. It promotes and regulates vesicular transport in neurites by scaffolding adaptors and molecular motors. Particularly, HTT phosphorylation status at S421 regulates the directionality of BDNF, APP and VAMP-7 vesicles within neurites in cultured and transfected neurons. However, several questions remain to be elucidated regarding the mechanisms and the consequences of this HTT-dependent regulation of vesicular transport such as the neuritic specificity (axons or dendrites) and the behavioral consequences of such modification. Finally, we do not know whether transport regulation can be influenced in pathological conditions to restore disease-associated phenotypes *in vivo*.

**This thesis aims at characterizing *in vivo* the mechanisms and the consequences of axonal transport regulation of three different types of vesicles through the phosphorylation of Huntingtin at S421 and to investigate its propensity to restore disease-associated phenotypes in mouse models of human neurological disorders.**

In order to reproduce *in vitro* the *in vivo* networks associated with neurological disorders we used microfluidic devices that allow the reconstitution of neuronal networks *in vitro*. We investigated the transport of Amyloid Precursor Protein (APP) vesicles, precursors of synaptic vesicles (SVPs) or dense-core vesicles (DCVs) in neurons in which the HTT phosphorylation status was modified. These neurons came from mice in which Serine 421 has been replaced by an aspartic acid to mimic the



phosphorylated form of HTT (HTT<sub>S421D</sub>) or by an alanine to mimic the unphosphorylatable form of HTT (HTT<sub>S421A</sub>).

APP homeostasis is impaired in AD. We investigated APP transport and accumulation at corticocortical synapses. We found that Akt-mediated HTT phosphorylation at S421 regulates the directionality of APP containing vesicles in axons but not in dendrites: the unphosphorylatable form of HTT decreases axonal anterograde flux of APP and reduces its levels at presynaptic zones both *in vitro* and *in vivo*. Reducing anterograde flux of APP in familial AD mouse model restored synapse homeostasis *in vivo* and memory deficits (Publication 1; Bruyere\*, Abada\*, Vitet\* *et al.*, eLife, 2020).

BDNF transport within DCVs is dysregulated in the corticostriatal network of Rett syndrome's patients. We found that endogenous HTT phosphorylation at S421 or a chemical inhibitor of calcineurin (FK506) rescue BDNF transport in the corticostriatal network, neuronal communication, and behaviors of Rett syndrome model mice (Publication 2; Ehinger *et al.*, Embo Mol Med, 2020).

Finally, it has been shown that SVP axonal transport regulates the number of SVs at the synapse, which, within a corticostriatal synapse, is essential for motor skill learning. We found that HTT phosphorylation increases the recruitment of the molecular motor KIF1A on SVPs, thus promoting anterograde transport and the probability of release. Silencing KIF1A in the corticostriatal network of HTT<sub>S421D</sub> mice, we found that pHTTS421 increases the number of SVs at the synapse and impairs procedural memory through a specific HTT-KIF1A dependent mechanism. This study defines a pathway by which axonal transport of SVP impact the behavioral phenotype (Publication 3; Vitet *et al.*, *in prep*).

## Keywords

Huntingtin, phosphorylation, serine 421, axonal transport, Brain-Derived-Neurotrophic-Factor, Amyloid Precursor Protein, Synaptic Vesicle Precursor, Alzheimer's disease, Rett syndrome, memory, microfluidics, cortical networks

## Titre

**Conséquences de la régulation du transport axonal par la Huntingtine sur l'homéostasie de réseaux neuronaux et sur le comportement, en conditions saine et pathologique**

## Résumé

Les circuits neuronaux régissent les comportements tels que la coordination motrice ou la mémoire et l'apprentissage. Au sein d'un réseau, les neurones communiquent par des processus moléculaires et cellulaires finement réglés à la synapse. Un des mécanismes régulant l'homéostasie synaptique, le transport de vésicules dans les neurones, est dérégulé dans les maladies neurologiques telles que le syndrome de Rett, la maladie d'Alzheimer et la maladie d'Huntington. Ainsi, investiguer la régulation du transport de vésicules dans les neurites dans un contexte physiologique est important pour comprendre, et potentiellement rétablir, les conséquences de ces dérégulations pathologiques.

La protéine Huntingtine (HTT), connue pour son implication dans la maladie d'Huntington, est un acteur clé du transport axonal. Elle promeut et influence le transport des vésicules en favorisant le recrutement des adaptateurs et des moteurs moléculaires. Sa phosphorylation à la sérine 421 (pHTTS421) régule la directionnalité des vésicules de BDNF, d'APP et de VAMP-7 dans des neurones transfectés *in vitro*. Cependant, les mécanismes et les conséquences de la régulation du transport par HTT, comme la spécificité neuritique et les conséquences comportementales, restent peu connues. Enfin, nous ignorons si la régulation du transport peut être influencée dans des conditions pathologiques afin de restaurer les phénotypes *in vivo*.

**Ce projet de thèse vise à caractériser les mécanismes et les conséquences de la régulation du transport axonal de trois types de vésicules par pHTTS421 et d'investiguer sa propension à restaurer les phénotypes associés à des maladies neurologiques dans des modèles murins.**

Dans le but de reproduire *in vitro* les réseaux associés à des maladies neurologiques, nous avons utilisé des chambres microfluidiques. Nous avons étudié le transport des vésicules d'APP, des précurseurs des vésicules synaptiques (PVSs) ou des vésicules à cœur dense (VCDs) contenant BDNF au sein d'un réseau neuronal dans lequel pHTTS421 a été modifiée. Ces neurones sont issus de souris pour lesquelles la sérine 421 a été remplacée par un acide aspartique ou par une alanine pour mimer respectivement l'état phosphorylé (HTT<sub>S421D</sub>) ou non phosphorylable (HTT<sub>S421A</sub>) de la HTT.

Dans la maladie d'Alzheimer, l'homéostasie d'APP est dérégulée. Nous avons donc étudié son transport et son accumulation synaptique dans un circuit corticocortical. Nous avons trouvé que la phosphorylation de la sérine S421 par Akt régule la directionnalité des vésicules d'APP uniquement dans les axones : HTT<sub>S421A</sub> diminue le flux antérograde axonal d'APP ainsi que ses niveaux à la synapse *in vitro et in vivo*. Réduire le flux antérograde d'APP dans un modèle murin d'Alzheimer restaure l'homéostasie synaptique *in vivo* et les déficits de mémoire associés (publication 1 ; Bruyère\*, Abada\*, Vitet\* *et al.*, eLife, 2020).

Le transport de BDNF est dérégulé dans le réseau corticostriatal des jeunes filles atteintes du syndrome de Rett. Nous avons observé que l'expression endogène de pHTTS421 ou l'injection d'un composé inhibant la calcineurine (FK506) restaure le transport de BDNF dans un réseau corticostriatal, la communication neuronale et les symptômes associés chez les souris modèles du syndrome de Rett (Publication 2 ; Ehinger *et al.*, Embo Mol Med, 2020).

Enfin, Le transport axonal des PVSs régule le nombre de vésicules synaptiques (VSs), ce qui, dans un réseau corticostriatal, est essentiel à l'apprentissage de compétences motrices. Nous avons montré que pHTTS421 augmente le recrutement de la kinésine KIF1A sur les PVSs, augmentant le transport antérograde et la probabilité d'exocytose. En réduisant les niveaux de KIF1A dans le réseau corticostriatal des souris HTT<sub>S421D</sub>, nous avons trouvé que pHTTS421 augmente le nombre de VSs et altère la mémoire procédurale. Cette étude décrit comment le transport axonal des PVSs impacte les phénotypes comportementaux (publication 3 ; Vitet *et al.*, *in prep*).

## Mots clés

Huntingtine, phosphorylation, sérine 421, transport axonal, BDNF, APP, Précurseur des Vésicules Synaptiques, maladie d'Alzheimer, syndrome de Rett, mémoire, microfluidique, réseaux corticaux

## Laboratory

Grenoble Institut des Neurosciences, INSERM U1216, Bâtiment Edmond J. Safra, Chemin Fortuné Ferrini, 38700 La Tronche

## Remerciements

L'ensemble de ce travail n'aurait pas été possible sans la volonté de certaines personnes de repousser les frontières de notre savoir, de créer une bonne atmosphère de travail ou de veiller à mon équilibre. Par ces quelques lignes, je voudrais leur rendre hommage et les remercier.

Mes premiers remerciements vont aux membres du jury, Alain Buisson, Alain Marty, et tout particulièrement à Karine Merienne et Coralie Fassier qui ont pris le temps de lire ce long manuscrit, pour avoir accepté de rejoindre mon jury de thèse. Par votre présence et votre appréciation, vous me permettez de repousser mes limites et celles de la science. Je tenais également à souligner le rôle important d'Alain Marty, Alain Buisson, Sébastien Carnicella, Laurent Venance et Sandrine Humbert pour leur participation à nos réflexions concernant mes projets lors de mes Comité de suivi de thèse.

Fred, je te remercie de m'avoir fait confiance tout au long de cette thèse et particulièrement dès le début où tu as pris le risque de commencer une thèse avec moi sans me connaître. Tu as été le seul directeur de recherche à le faire et j'en suis très reconnaissante. Grâce à toi j'ai beaucoup appris, notamment concernant l'écriture et le monde de la recherche en général. Merci de m'avoir fait confiance pour la rédaction de la revue, de la révision du papier APP mais aussi pour t'avoir secondé pendant le congrès de Montpellier. Merci également de m'avoir donné cette chance de pouvoir travailler sans me soucier de problèmes matériels ; c'est une chose rare que j'ai su apprécier.

Sandrine, je te remercie d'avoir considéré ma candidature spontanée que tu as reçu il y a maintenant plus de quatre ans. Ton accompagnement et tes conseils tout au long de mes projets ont également été très appréciés.

Je voulais également remercier ces gens de l'ombre, qu'on ne voit pas et qui ont pourtant été essentiels. Ces personnes m'ont permis, par le biais de leurs dons à la fondation pour la recherche médicale ou l'association Huntington France, de réaliser cette thèse et d'accroître nos connaissances pour trouver des solutions aux défis de santé actuels.

Jérôme, merci de m'avoir accueillie dans ton laboratoire alors que je ne savais ni pipeter ni parler anglais décemment. Mon séjour au Texas m'a profondément marquée et changée, tant personnellement que professionnellement. Tant et si bien que j'irai jusqu'à dire qu'il m'a été essentiel pour la réalisation de ma thèse.

Mes chers collègues qui, soyons honnêtes, sont également mes amis, je vous remercie d'avoir contribué à mon équilibre pendant ces quatre années.

Chiara, non so come ringraziarti per esserci stata quando ne avevo più bisogno. Non hai esitato un attimo a prendere il posto di Julie su un argomento che conoscevi solo superficialmente. Mi hai sostenuta quando ne avevo bisogno, sei stata la mia protezione, sei sempre stata lì per me. Mi ricorderò delle pause caffè che prendevamo sulla terrazza per parlare entrambe. Grazie Chiara.

Julie, bien plus qu'une encadrante, tu es devenue une vraie amie. Tu m'as tout appris, tes protocoles, tes petites manies, ta passion, j'ai tout pris. Si bien qu'on a fini par se comprendre sans même se parler, aujourd'hui encore. Ton enthousiasme était le mien. Tu m'as manquée mais on se voit bientôt à Tahiti !

Anne-Sophie, tu le sais, j'ai été très heureuse de travailler avec toi. Les bases de statistiques que nous avons établies ensemble au tout début m'ont suivi toute ma thèse. J'apprécie ta rigueur et je te souhaite sincèrement le meilleur dans tes nouveaux projets. Merci également d'avoir été présente tout au long de ma thèse pour répondre à chacune de mes questions.

Elo je te remercie pour ta disponibilité et l'intérêt désintéressé que tu portes aux gens. Merci de m'avoir aidé à démêler les profondeurs du striatum et adoucir les aspérités de l'électrophy.

Bobinette, que serais-je devenue sans ton soutien permanent et tes soirées crêpes mémorables ? Dès mes premiers pas au labo tu as su me mettre à l'aise. Puis se sont succédés les sorties au ski, en rando, le bloc, la bastille à 21h sur un coup de tête, les confidences dans ta voiture, les concerts d'électro plus ou moins appréciés, la soirée mémorable à Montpellier, la sortie roller à Aix les bains, ect.... Bref, merci d'avoir été toi pendant ces quatre années, tu as rendu cette thèse plus douce et plus facile.

Caro, nous avons peu travaillé ensemble mais j'ai apprécié ces moments. Tu m'as transmis tout ce que je sais de l'étude du comportement, merci. Je me souviendrai également de ce petit cocktail que nous avons partagé toutes les deux entre deux confidences, à refaire quand tu veux !

Les co-bureau, merci pour ces bonnes doses de rire que vous m'avez procurées. Max, merci de poser des questions naïves et improbables auxquelles personne ne pense. Mais merci aussi pour ta sensibilité et ta générosité dans ta manière d'être. Nagham, merci pour ces moments tard au bureau, ces moments ont été précieux parce que très simples et sincères. Peut-être que maintenant on arrivera à trouver du temps pour faire un time story ;) . Eve, tu savais animer ce bureau à coups d'affaires sensibles et de sujets de discussion improbables, merci d'avoir été présente quand j'en avais besoin. Amandine et Julie-Anne, vous m'avez guidée lors de mes premiers pas dans la thèse et j'ai apprécié travailler à vos côtés.

Les « nouveaux », Emeline, Anca, Johanna, j'aurais aimé prendre le temps de mieux vous connaître mais j'ai déjà apprécié les moments que nous avons partagés ensemble.

Nathalie, merci de nous avoir sauvés plus d'une fois dans ce labyrinthe que représente l'administration pour nous. Tu as plus d'une fois réparé nos bêtises avec toute ta bienveillance. Nous avons de la chance de t'avoir.

Cléopâtre et Maria, des stagiaires surprenantes par leur maturité et leur motivation. Je vous remercie toutes les deux de m'avoir soutenue dans mes projets par votre implication, nous formions de belles équipes. Je vous souhaite le meilleur pour la suite, vous le méritez.

Ensuite, un institut ne se limite pas à un laboratoire. Le GIN a cela de précieux qu'il réunit des personnes avec une grande intelligence à la fois scientifique et humaine. Je parle de Jacques, pour ses cours de statistiques très utiles et sa disponibilité, Karin, pour sa curiosité scientifique mais également pour son humanisme et les discussions que nous avons pu avoir au labo de ME ensemble. Nora, nous nous sommes peu parlé mais le peu de fois où nous l'avons fait, tu as su dire ce qu'il fallait. Merci. Toff, j'ai vraiment apprécié travailler à tes côtés, pour tes qualités d'encadrement et ton esprit scientifique. Béa, la dose de bonne humeur et d'air de la montagne du GIN. Merci pour les moments que nous avons partagés ensemble. Leticia, merci pour cette session de poster à parler d'APP à Héraklion, une piña colada à la main. Je referai l'un ou l'autre avec grand plaisir. Cécile, merci d'être l'oreille attentive dont les doctorants ont besoin.

Un grand merci également aux zootechs, Sylvain, Laure, Fabien et Flore qui font, comme l'ont démontré ces derniers mois, un travail indispensable à nos études. Mais plus encore, leur bienveillance nous permet de travailler dans de bonnes conditions. Merci d'avoir été à mes côtés pendant ces longues journées d'injections à savoir si j'avais besoin de quoique ce soit. Ça a beaucoup compté pour moi.

Les doctorants, continuez à former cette entité, ce groupe qui permettra d'amortir les coups et surtout, de les boire.

Enfin, je tiens à remercier ma famille. Papa, maman, merci pour tous ces sacrifices que vous avez fait depuis mes tous premiers pas pour me permettre d'accomplir mes plus grandes ambitions. Ma thèse était l'une d'entre elles, sans votre soutien tout au long de ses 27 années, rien n'aurait été possible. Vous avez fait de mes échecs des forces, de votre pugnacité au travail et humilité mes valeurs et je suis fière d'être votre fille. Choupie, tu constitues ce socle inébranlable qu'on appelle la famille, j'aurais aimé être plus présente pour tes premiers pas dans la vraie vie mais je sais que Fredo veille à ce que ma petite sœur soit heureuse. Papy et mamie vous m'avez transmis vos valeurs, votre douceur et votre ingéniosité, je suis si heureuse d'être à vos côtés. Je chérie chaque moment passé avec vous.

Pascal et Yvette, merci de m'avoir permis de me ressourcer dans votre petit paradis paisible. Vous m'avez permis de trouver l'équilibre dont j'avais besoin pour affronter les difficultés de la thèse. Merci pour votre accueil et votre bienveillance.

Enfin, mon homme, tu as su être l'oreille attentive et l'épaule dont j'avais besoin pendant ce marathon. Tu as été présent dans les bons comme dans les mauvais moments, tu me connais mieux que quiconque et tu sais ce dont j'ai besoin en toute circonstance. Mais tu as aussi su me pousser hors de ma zone de confort pour m'améliorer. Tu m'as aidé à tenir mon cap tout en étant mon ancre, tu m'as permis d'aller loin tout en me rappelant ce qui était important. Maintenant que ce cap est franchi, allons trouver le prochain. Qu'il soit au Chili ou à Taïwan, c'est lors de notre prochaine aventure que nous le franchirons. Te quiero.

## Table of contents

Preface.....	5
Abstract .....	7
Résumé.....	9
List of figures .....	17
List of abbreviations .....	21
Introduction.....	23
Chapter 1 - Behaviors are the result of the communication between central nervous system structures through neuronal network establishment.....	24
1. The brain as a combination of structures.....	24
2. Structures communication results in a behavior .....	28
3. The neuron: the structural and functional unit of the brain.....	33
4. The neuronal mechanisms underlying learning and memory.....	41
Chapter 2- Axonal transport of vesicles as a regulator of neuronal functions and survival through multi-protein interactions .....	45
1. Vesicles and cargoes.....	45
2. Vesicular transport .....	57
Chapter 3 - Example of a synaptic vesicle journey: how axonal transport ensures its neurotransmission function. ....	84
1. SV: a unique type of vesicle.....	84
2. SVs origin from SVP transport and maturation.....	101
Chapter 4 - Huntingtin as a crucial hub for protein interactions through its intrinsic molecular properties .....	114
1. HTT: a large, dynamic and ubiquitous protein .....	114
2. HTT & HD .....	119
Chapter 5 – Traffic signaling: new functions of Huntingtin and axonal transport in neurological disease.....	124
Results .....	135
Results – part 1: Presynaptic APP levels and synaptic homeostasis are regulated by Akt phosphorylation of Huntingtin.....	136



Summary & context of the study .....	136
Discussion .....	173
Results – part 2: Huntingtin phosphorylation governs BDNF homeostasis and improves the phenotype of Mecp2 knockout mice .....	178
Summary & context of the study .....	178
Discussion .....	193
Results – part 3: HTT acts as a scaffold for KIF1A-mediated-transport and regulates SVP axonal transport.....	196
Summary & context of the study .....	196
Discussion .....	242
Discussion .....	247
1. Experimental set up: looking for more integrative and relevant studies .....	247
2. S421 phosphorylation of HTT as a physiological regulator of vesicle transport. ....	258
3. Restoring vesicular transport in NDs, an efficient therapeutic strategy? .....	260
Conclusion .....	262
Perspectives.....	263
1. Technical challenges and future plans for research.....	263
2. Challenges in therapeutic strategies for pharmaceutical industry .....	264
Bibliography.....	266
Annex.....	322

## List of figures

Figure 1: Human brain is more complex and developed than mouse brain.....	24
Figure 2: brain is the sum of structures. ....	25
Figure 3: 3D reconstitution of the cortex.....	25
Figure 4: cortex is organized in layers of neurons.....	25
Figure 5: layer V.....	26
Figure 6: 3D reconstitution of the striatum .....	27
Figure 7: 3D representation of basal ganglia organization in a mouse brain. ....	27
Figure 8: 3D reconstitution of the hippocampus .....	27
Figure 9: cortex and hippocampus form a network.....	28
Figure 10: movements are controlled by two loops involving cortex and basal ganglia. ....	29
Figure 11: Different forms of memory involve specific networks and are evaluated by different behavioral protocols.....	31
Figure 12: cortical projections target different striatal zones.....	32
Figure 13: cellular homeostasis as a closed feedback loop regulating cellular functions.....	33
Figure 14: IGF-1 pathway regulates cell survival through Akt activation.....	34
Figure 15: neuronal shapes define neuronal functions.....	35
Figure 16: pyramidal cells display a specific organization.....	35
Figure 17: morphologic properties differentiate cortical pyramidal cells from MSN.. ....	36
Figure 18: neuronal networks morphology and function. ....	36
Figure 19: synapse morphology and function.....	37
Figure 20: MTs are a polarized structure. ....	38
Figure 21: MT dynamic is stable.....	39
Figure 22: actin filament structure.....	39
Figure 23: actin forms rings within the axon.....	40
Figure 24: synaptic homeostasis as a two compartments system.....	41
Figure 25: a vesicle journey .....	45
Figure 26: PTMs modify the chemical composition of amino acids.....	46
Figure 27: <i>De novo</i> production of vesicles is made in TGN.. ....	46
Figure 28: ER network is present in neurites. ....	47
Figure 29: different endocytic modes exist. ....	48
Figure 30: TGN vesicles are secreted through two pathways, CSP or RSP.....	49
Figure 31: DCVs are dense and bigger than SVs.....	50
Figure 32: endosome can undergo different pathways.....	52

Figure 34: secretory vesicles carry specific cargoes.....	53
Figure 35: excitatory and inhibitory synapses exhibit different structural characteristics.....	55
Figure 36: endosomal vesicles carry specific cargoes..	56
Figure 37: MTs constitute tracks for neuronal transport of vesicle.....	59
Figure 38: Tau homeostasis is crucial for MT stabilization which directly affects neuron survival. ....	59
Figure 39: Tau is mostly axonal whereas MAP-2 is dendritic.....	60
Figure 40: MT acetylation regulates molecular motor binding to MTS. ....	62
Figure 41: kinesin-1 and -3 exhibit different behavior according to MT PTM..	63
Figure 42: 3D representation of kinesin-1 and -3 structure.....	65
Figure 43: kinesin progression on MTs is ATP dependent..	66
Figure 44: kinesins within a family exhibit different structures.....	67
Figure 45: kinesins display specific velocity distributions. ....	68
Figure 46: kinesin number on a vesicle influences its velocity and run length.....	71
Figure 47: involvement of different kinesins on one vesicle display specific velocity distribution.. ....	71
Figure 48: dynein-1 structure .....	72
Figure 49: dynein regulators specify dynein mediated transport of cargoes. ....	73
Figure 50: dynactin structure serves dynein functions. ....	75
Figure 51: Hook and BicD acts as dynein regulators .....	75
Figure 52: kinesin and dynein are present on the same vesicle. ....	76
Figure 53: HTT interacts with both kinesin and dynein acting as a scaffold protein. ....	77
Figure 54: microfluidics device allows the study of axonal transport in connected neurons.....	79
Figure 55: kymographs are the 2D representation of a vesicle transport .....	79
Figure 56: the selective recruitment model.....	80
Figure 57: the tug-of-war model explains the bidirectional and non-processive transport.....	81
Figure 58: the coordination model explains the fast and processive transport of vesicles.....	82
Figure 59: the steric disinhibition model relies on a cooperation between the two motors. ....	82
Figure 60: Molecular model of an average SV. ....	87
Figure 61: SP interact with each other to regulate exocytosis.....	88
Figure 62: APP might be present on SVs. ....	91
Figure 63: SV diameter is around 40 nm. ....	91
Figure 64: SV size is dependent on SP steric hindrance. ....	91
Figure 65: SV are organized in three pools: RRP, recycling pool and the reserve pool. ....	92
Figure 66: RRP vesicles are docked to the PM..	93
Figure 67: CME forms clathrin coat around the endocytosed vesicle..	95
Figure 68: the reserve pool is further from the active zone and contains many SVs. ....	96

Figure 69: synapsin regulates the reserve pool size by sticking the SV all together.....	97
Figure 70: glutamate loading in SVs requires electric and chemical components.....	100
Figure 71: SVPs formed from the Golgi are the result of a specific and SNARE-dependent SP segregation. ....	101
Figure 72: KIF1A dimer structure. ....	103
Figure 73: KIF1A also transports BDNF vesicles and BACE1 vesicles.....	104
Figure 74: KIF1A activation follows KIF1A dimerization on the vesicle.....	106
Figure 75: KIF1A affinity for MT is increased thanks to the K-loop.....	106
Figure 76: DENN/MADD complex acts as an adaptor for KIF1A recruitment on SVP. ....	108
Figure 77: liprin- $\alpha$ acts as aKIF1A captor at dendritic spines. ....	108
Figure 78: KIF1A KO mice exhibit a decrease in the number of SV at the synapse.....	109
Figure 79: KIF1A mutation in human causes cerebellar atrophy. ....	110
Figure 80:KIF1A mutation decreases KIF1A velocity <i>in vitro</i> .....	110
Figure 81: KIF1A mutations in human diseases.....	111
Figure 82: SV cycle life lasts for more than 92h, from SVP biosynthesis to degradation. ....	112
Figure 83: 3D representation of HTT structure. ....	114
Figure 84: HT interacts with many proteins involved in large cellular functions.....	115
Figure 85: HTT regulates dynamin-1 activation. ....	116
Figure 86: HTT regulates transcription.....	117
Figure 87: HTT adopt multiple conformations according to the environment. ....	118
Figure 88: weak interaction between C- and N-term.....	118
Figure 89: HD provokes neurodegeneration leading to a reduction of brain weight. ....	119
Figure 90: HTT structures are affected by polyQ stretch. ....	121
Figure 91: APP cleavage by secretases produces many fragments.....	137
Figure 92: APP processing is dependent on APP transport and trafficking .....	139
Figure 93: AD provokes neurodegeneration of the cortex and the hippocampus .....	141
Figure 94: unphosphorylatable form of HTT rescues AD mouse model phenotypes. ....	173
Figure 95: Akt is overactivated in AD. ....	174
Figure 96: IGF-1 pathway regulates cell survival through Akt activation.....	175
Figure 97: balance of APP level at the synapse is important for neuronal homeostasis .....	177
Figure 98: BDNF level is crucial for neuronal homeostasis and subsequent behavior. ....	195
Figure 99: exocytosis is regulated by SNAREs. ....	197
Figure 100: facilitation results in a higher release of NT at the second stimulation.....	198
Figure 101: facilitation might be due to SVs forming a reserve for docked SVs. ....	199
Figure 102: time to fall of the accelerating rotarod over eight consecutive days of training.....	200

Figure 103: DLS and DMS are both involved in the procedural memory formation. ....	201
Figure 104: HTT acts as a scaffold for SVP transport.....	242
Figure 105: SV number is crucial for neuronal homeostasis and subsequent behavior. ....	245
Figure 106: HTT acts as a scaffold for glycolytic enzymes on the vesicle.....	251
Figure 107: DENN/MADD cellular functions. Scheme from Miyoshi & Takai, 2004 .....	253
Figure 108: APP transport and post signaling are impaired in HdhCAG140+/- corticostriatal network. .....	254
Figure 109: A $\beta$ peptides regulates SV cycle.....	256
Figure 110: S421 phosphorylation role in the homeostatic regulation of neurotransmission.....	261
Figure 111: axonal transport of a vesicle. ....	262

## List of abbreviations

Ach	Acetylcholine	ER	Endoplasmic Reticulum
AD	Alzheimer's Disease	FAD	Familial form of Alzheimer's Disease
ADP	Adenosin DiPhosphate	FAT	Fast Axonal Transport
AIS	Axon Initial Segment	GABA	Gamma-AminoButyric Acid
ALS	Amyotrophic Lateral Sclerosis	GDP	Guanosine DiPhosphate
AP	Action Potential	GPe	Globus Pallidus externus
APP	Amyloid Precursor Protein	GPi	Globus Pallidus internus
ATP	Adenosin TriPhosphate	GTP	Guanosine TriPhosphate
ASO	AntiSens Oligonucleotide	HD	Huntington's Disease
A $\beta$	Amyloid beta	HSANII	Hereditary Sensory and Autonomic Neuropathy type II
BDNF	Brain Derived Neurotrophic Factor	HSP	Hereditary Spastic Paraplegia
CA	Cornu Ammonis	HTT	Huntingtin
CME	Clathrin-Mediated Endocytosis	IGF-1	Insulin-like Growth Factor-1
CMT	Charcot-Marie-Tooth disease	IPSC	Inhibitory PostSynaptic Current
CNS	Central Nervous System	JIP1	JNK-interacting Protein-1
CSP	Constitutively Secretory Pathway	JNK	c-Jun N-terminal Kinase
DCV	Dense Core Vesicle	LDP	Long-Term Depression
DCX	Doublecortin	LTP	Long-Term Potentiation
DLS	DorsoLateral Striatum	MAP	Microtubule Associated Protein
DMS	DorsoMedial Striatum	MSN	Medium Spiny Neuron
EC	Entorhinal Cortex	MTs	MicroTubules
EPSC	Excitatory PostSynaptic Current		

MVB	Multi Vesicular Body	RRP	Readily Releasable Pool
NDs	Neurological Disorders	RSP	Regulatory Secretory Pathway
NMDAr	N-Methyl-D-Aspartate receptor	SNARE	Soluble NSF (N-ethylmaleimide Sensitive Fusion) Attachment Protein REceptor
NT	NeuroTransmitter	SP	Synaptic Protein
PD	Parkinson's Disease	STED	STimulated Emission Depletion
PEHO	Progressive encephalopathy with Edema, Hypsarrhythmia and Optic atrophy	STORM	Stochastic Optical Reconstruction Microscopy
PM	Plasma Membrane	SV	Synaptic Vesicle
PNS	Peripheral Nervous System	SVP	Synaptic Vesicle Precursor
PSC	PostSynaptic Current	TGN	Trans-Golgi Network
PSD	PostSynaptic Density		
PTM	Post-Translational Modification		

## Introduction

This work focuses on the consequences of Huntingtin (HTT) phosphorylation at S421 on cellular processes and mouse behavior in both physiological and pathological contexts. In order to appreciate and highlight the relevance of this study, we propose a top-bottom presentation of this work, from the macroscopic behavior to the nanometer structures responsible for its establishment.

The mouse brain will be first described as an assembly of structures communicating between themselves through neurons to regulate behavior.

Then, the neuronal communication and survival are described as relying on transport of different vesicles through the interaction with molecular motors. Later, the attention is brought to the role of adaptors on vesicular complexes modulating neuronal transport. The third chapter describes axonal transport of a specific type of vesicles, the synaptic vesicle precursors.

Finally, the fourth chapter focuses on HTT, described as a specific adaptor by its structure and functions, allowing the scaffolding of many proteins responsible for transport modulation. Then, we will understand the consequences of HTT phosphorylation at S421 on axonal transport.



## Chapter 1 - Behaviors are the result of the communication between central nervous system structures through neuronal network establishment

Behavior can be defined as the result of an information processed by the brain through neuronal connections able to select and modulate the nervous message. This chapter focuses on understanding how interconnected structures regulate behaviors based on the structural and functional properties of neural cells. Finally, attention will be brought to learning and memory mechanisms based on neuronal connection changes.

### 1. The brain as a combination of structures

#### a. Definition

Nervous system in human and in mammals in general is composed by the **central nervous system (CNS)** and the peripheral nervous system (PNS). The CNS is composed by the **brain** and the spinal cord.

Human brain differs from mouse brain from its organization in 4 lobes and its convoluted shape defined by grooves and gyri (Snyder et al., 2018) (figure 1). This structural property is thought to be an evolutionary adaptation to pack an increasing number of neurons into a limited space represented by the skull.

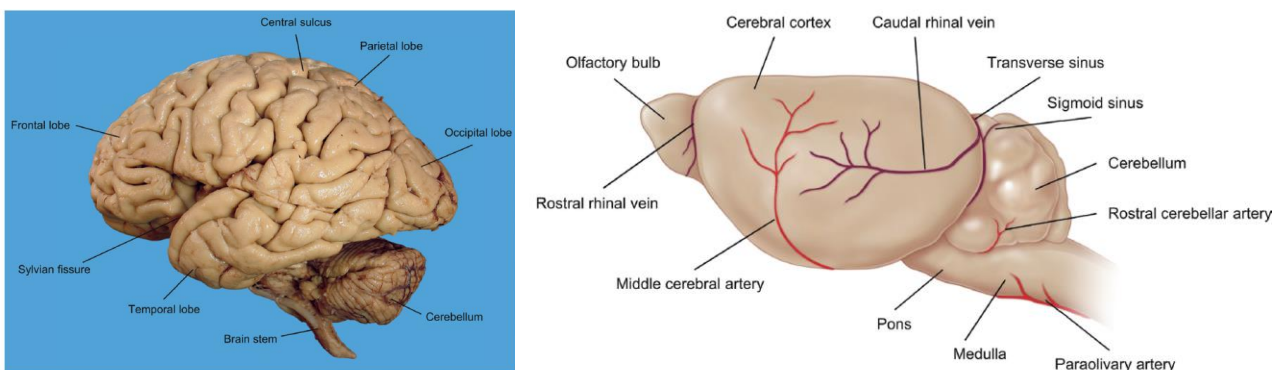


**Figure 1: Human brain is more complex and developed than mouse brain.** Comparison of the organization and the structure between a human brain (left) and a mouse brain (right) from (Snyder et al., 2018).

**Brain** is composed of six regions: the medulla, the pons, the midbrain, the cerebellum, the diencephalon, and the **telencephalon**. The medulla, pons and midbrain can be gathered in the brain stem controlling automatic functions. The cerebellum controls the body balance and the diencephalon regroups the thalamus and the hypothalamus. Hypothalamus regulates body temperature, hunger, sleep, emotion whereas thalamus is involved in movement and cognition through connection with other structures.

The **telencephalon** is composed of two hemispheres containing among others the **cortex** at the periphery, basal ganglia, and **hippocampus** (figure 2). In mice, basal ganglia are mostly formed by the **striatum** (figure 2). These structures are divided into areas exhibiting specific functions. The cortex regulates perceptual, motor and cognitive functions whereas basal ganglia play an important role in controlling movement. Hippocampus is associated with short-term and explicit memory. Neurodegeneration of specific regions in diseases such as PD, AD and HD is responsible for specific symptoms affecting memory, psychiatry and motor skills in each of these diseases.

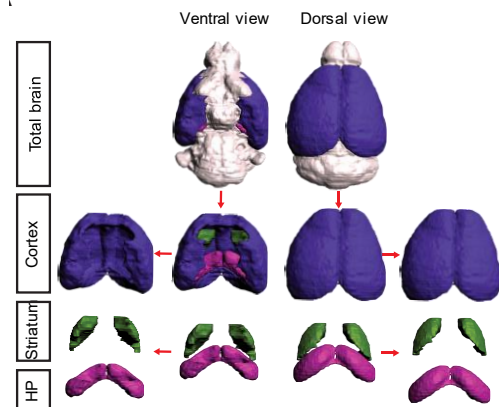


**Figure 2: brain is the sum of structures.** MRI reconstitution of a mouse brain. Blue: cortex, pink: hippocampus, green: striatum (Bruyère et al., 2020)

### b. Examples of brain structures in mouse brain: cortex, striatum and hippocampus

This work focuses on the understanding of the basis of communication between two types of neurons within the cortex or between cortex and striatum or cortex and hippocampus. Thus, the following part is dedicated to the structural and functional presentation of these structures in a mouse brain.

#### i. Cortex

The cortex at the periphery of the brain (neocortex)(figure 3) is organized into 6 layers and several columns of neurons, organized according to their role (Bayer & Altman, 1991). Each layer has intrinsic properties like width, density, type and morphology of neurons and connections to other structures (figure 4). Indeed, each layer receives specific inputs and send out outputs to specific structures.



**Figure 3:** 3D reconstitution of the cortex (left) opposed to a coronal slice in which the cortex is colored in blue (right).

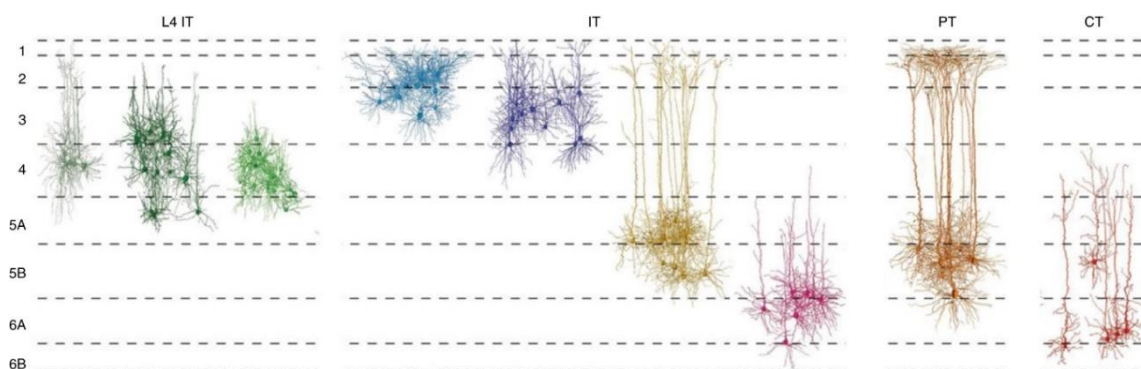


**Figure 4: cortex is organized in layers of neurons.** Cortical organization into layers in S1 barrel cortex. From Harris & Shepherd, 2015

The first layer from the pia mater, layer I, is called *molecular layer* and contains mostly dendrites and axons from deeper cortical layers. Layer II (*external granular cell layer*) and III (*external pyramidal cell layer*) contain respectively small and large pyramidal cells projecting to the same or other cortical areas, promoting intracortical communication. Layer IV, also called *internal granular cell layer*, contains small spherical neurons crucial for their roles in sensory function since this layer is the main recipient for sensory inputs from the thalamus. Layer V, the *internal pyramidal cell layer*, contains large pyramidal cells exhibiting a thick primary apical dendrite (Genc et al., 2019) (figure 5) and projecting axons communicating with the cortex and subcortical structures as the striatum. Finally, layer VI, the *polymorphic layer*, sends its projections to other cortical areas.

The layer V is of interest in this study because it is the main layer projecting to the striatum (McGeorge & Faull, 1989).

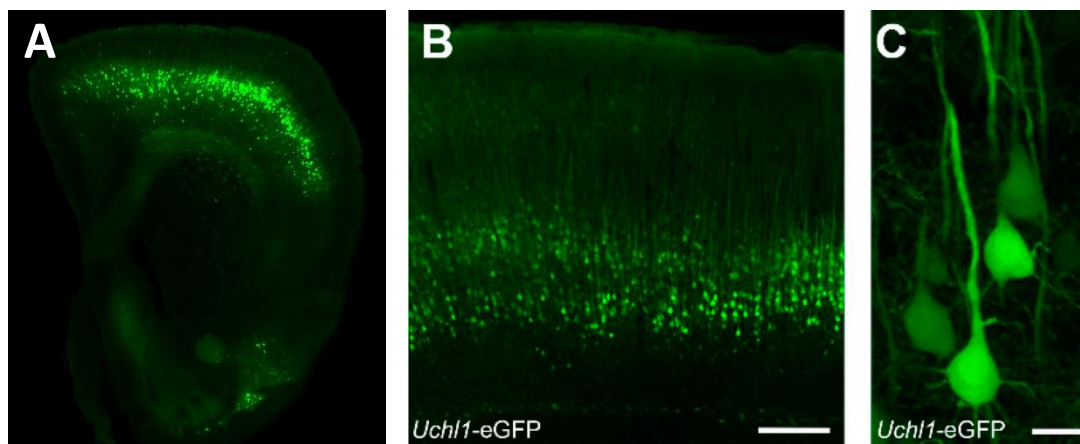


**Figure 5: layer V.** Layer V localization within a brain slice (A), within the cortex (B) and cortical pyramidal neurons (C). (B) and (C) from Genc et al., 2019.

According to the column division of the cortex, layer V neurons project to different part of the striatum: neurons residing in the associative and cingulate cortex project to the dorsomedial striatum (DMS) whereas sensorimotor neurons project to the dorsolateral striatum (DLS) (Costa et al., 2004; Mannella et al., 2013) (figure 12).

Although many cell types are encountered in the cortex, 80% or more of cortical neurons are excitatory (Georgiev & Glazebrook, 2018; K. D. Harris & Shepherd, 2015). Thus, the signal sent from the cortex is mainly exciting the targeted areas.

Cortical neurons also communicate with the hippocampus via a specific area, named as the entorhinal cortex (EC), that acts as an interface between the neocortex and the hippocampus. Interestingly in AD, the entorhinal cortex is one of the first structures to degenerate, underlying its relevance in the memory formation (Heiko Braak et al., 2006; Schmitz & Nathan Spreng, 2016).

## ii. Striatum & basal ganglia

In human, striatum is composed of caudate nucleus and putamen. In mouse, the two structures are not anatomically distinct and referred as striatum. Striatum is the major input structure of the basal ganglia which englobes the striatum, the globus pallidus (internal and external nuclei), the substantia nigra (pars compacta and pars reticula) and the subthalamic nucleus (A. Y. Kim et al., 2020) (figure 7). The striatum receives projections from the cortex (layer V), the thalamus, the limbic system and the brain stem (figure 10).

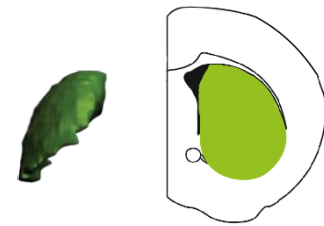


**Figure 7:** 3D reconstitution of the striatum (left) opposed to a coronal slice in which the striatum is colored in green (right).

Striatum is made of three compartments anatomically, biochemically and functionally different: an extrastriosomal matrix, reticular patches called striosomes and the recently added annular compartment (Perrin & Venance, 2019). The matrix contains the neurons mostly found in the striatum, the GABAergic medium spiny neurons (MSNs), named by the abundance of spines on their dendrites (Gritton et al., 2019). As an example, dorsal striatum is composed of 95% of MSNs (Jiang & North, 1991).

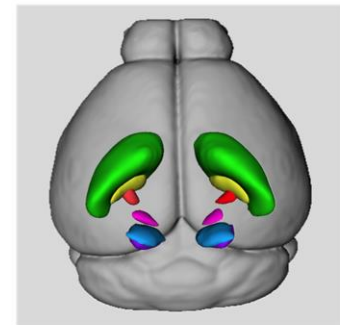


**Figure 6:** 3D representation of basal ganglia organization in a mouse brain. Green: striatum, yellow: globus pallidus external, red: globus pallidus internal, pink: subthalamic nucleus, blue: substantia nigra pars compacta and purple: substantia nigra pars reticula. From Kim *et al.*, 2020

MSN activity is driven by cortical inputs (Wilson, 1995) forming synapses with MSN spines only. MSN activity can be modulated by dopamine projections from the substantia nigra pars compacta or by the action of GABAergic interneurons (Parvalbumin, Neuropeptide Y, somatostatin) or cholinergic interneurons (CHI). Despite the interneuron low representation (<5% of each interneurons types), they play an essential role (Gritton et al., 2019). PV interneurons would best predict movement, whereas CHI interneurons have a selective role in recruiting and synchronizing MSN activity through the occurrence of a movement, irrespectively to a reward (Gritton et al., 2019).

## iii. Hippocampus

Hippocampus was named after its unusual and very organized sea-horse shape (figure 8). The hippocampus receives projections from the layer II or III of the entorhinal cortex (EC), and projects to subiculum or deep layers of the EC (figure 9). These bidirectional connections confer to the hippocampus a fundamental role in learning and memory.

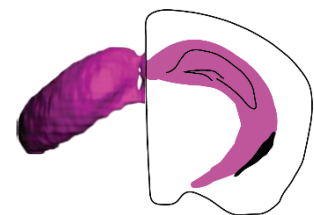


**Figure 8:** 3D reconstitution of the hippocampus (left) opposed to a coronal slice in which the hippocampus is colored in pink (right).

Cell bodies are densely concentrated in *Cornu Ammonis* (CA) areas and are discriminated according to their localization and functions: CA1, CA2 or CA3 (figure 9). Although hippocampus cells are in majority excitatory pyramidal cells, similar to the pyramidal cell in the cortex, astrocytes are known to form tripartite synapses regulating neuronal processes (Bosson et al., 2017).

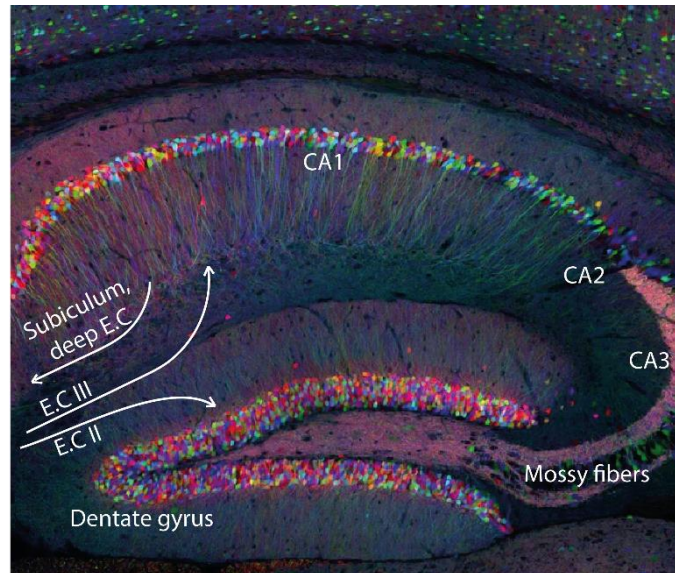


**Figure 9: cortex and hippocampus form a network.** Hippocampus organization and connections with the entorhinal cortex (E.C).

## 2. Structures communication results in a behavior

In the past, several experiments of ligation and lesion were realized in mammals proving that brain structures alone, disconnected of other structures, cannot play their role (Drewe, 1974; N. G. Müller & Knight, 2006; Nordborg & Johansson, 1995). Indeed, brain structures need to be interconnected and need to act cooperatively to produce a behavior adapted to the external stimuli. Each behavior is the product of a signal between and/or within brain structures. Neuronal networks resulting into a behavior can differ from an organism to the other, even between mammals. For example, 25% of human striatum possess different connectivity fingerprints compared to mice (Balsters et al., 2020). Despite these discrepancies, it is important to understand biological mechanisms in both physio- and pathological contexts in a simpler organism like the mouse at a first instance, in order to further apply the knowledge to human physiology and disease mechanisms (Collins et al., 2019).

This paragraph focuses on neuronal networks responsible for mouse behaviors studied during this work in physiological condition (procedural memory) and pathological condition in mouse model of human neurological disorders like AD (explicit memory) and Rett syndrome (motor coordination).

### a. Corticostriatal network & motor coordination

Thanks to its connections with the cortex, basal ganglia, limbic system and the thalamus, the striatum is critical for the control of voluntary movements, motor learning but is also able to link emotions, rewards, executive functions, and mood. In this paragraph, we focus on the striatal control of the voluntary movements.

The crucial role of the corticostriatal network in controlling the movements is illustrated by symptoms observed in neurological disorders in which the striatum is specifically affected. In HD, the degeneration of the cortex and the striatum leads to the apparition of hyperkinesia often referred as chorea. Rett syndrome provoking motor infirmity is another example illustrating the central role of the corticostriatal network.

Within the corticostriatal network, two cellular pathways are regulating the control of voluntary movements: the permissive and monosynaptic direct pathway and the inhibitory and polysynaptic indirect pathway (figure 10). Both pathways implicate MSNs (Brimblecombe & Cragg, 2015; Crittenden & Graybiel, 2011; Perrin & Venance, 2019) receiving excitatory afferences from neurons of cortical layer V within the motor or associative areas (respectively projecting to the dorsolateral or dorsomedial striatum). The direct pathway is then described as MSNs projecting to and inhibiting the GPi/SNr, nuclei known to inhibit the thalamus. Finally, the stimulated thalamus projects back to the cortex, completing the loop essential for smoothly executed movement.

On the other hand, the indirect pathway results in an inhibition of the thalamus through a GPe-mediated inhibition of the SNr or the STN (in the latter case, we term this network the hyperdirect pathway).

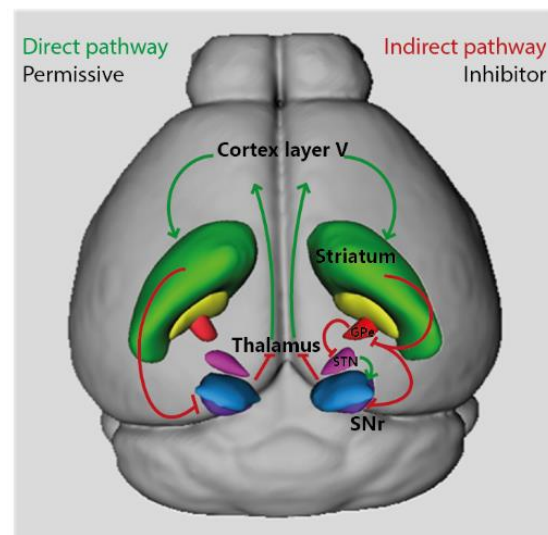


**Figure 10: movements are controlled by two loops involving cortex and basal ganglia.** Direct and indirect pathways of the corticostriatal loop. Green: striatum, yellow: globus pallidus external, red: globus pallidus internal, pink: subthalamic nucleus, blue: substantia nigra pars compacta and purple: substantia nigra pars reticula. Adapted from Kim et al., 2020

Chorea in HD is thought to be due to a loss of MSNs projecting to the GPe leading to an excessive inhibition of the subthalamic nucleus and a subsequent reduction in the basal ganglia output from the thalamus. This network dysfunction could explain the involuntary movements. However, rigidity and akinesia observed in the later stages of HD would impact the MSNs projecting to the GPi/SNr. Removing inhibition from those neurons could convert hyperkinetic movements into hypokinetic problems (rigidity and akinesia).

Cortical inputs from associative areas to MSNs can target DMS and control what we describe as goal directed behavior (Gangarossa et al., 2020; Hawes et al., 2015; Koralek et al., 2012; Ma et al., 2018; Shan et al., 2014), which is the decision of an action regarding the outcome in a specific situation and is directly dependent on the control of voluntary movements.

## b. Learning & Memories

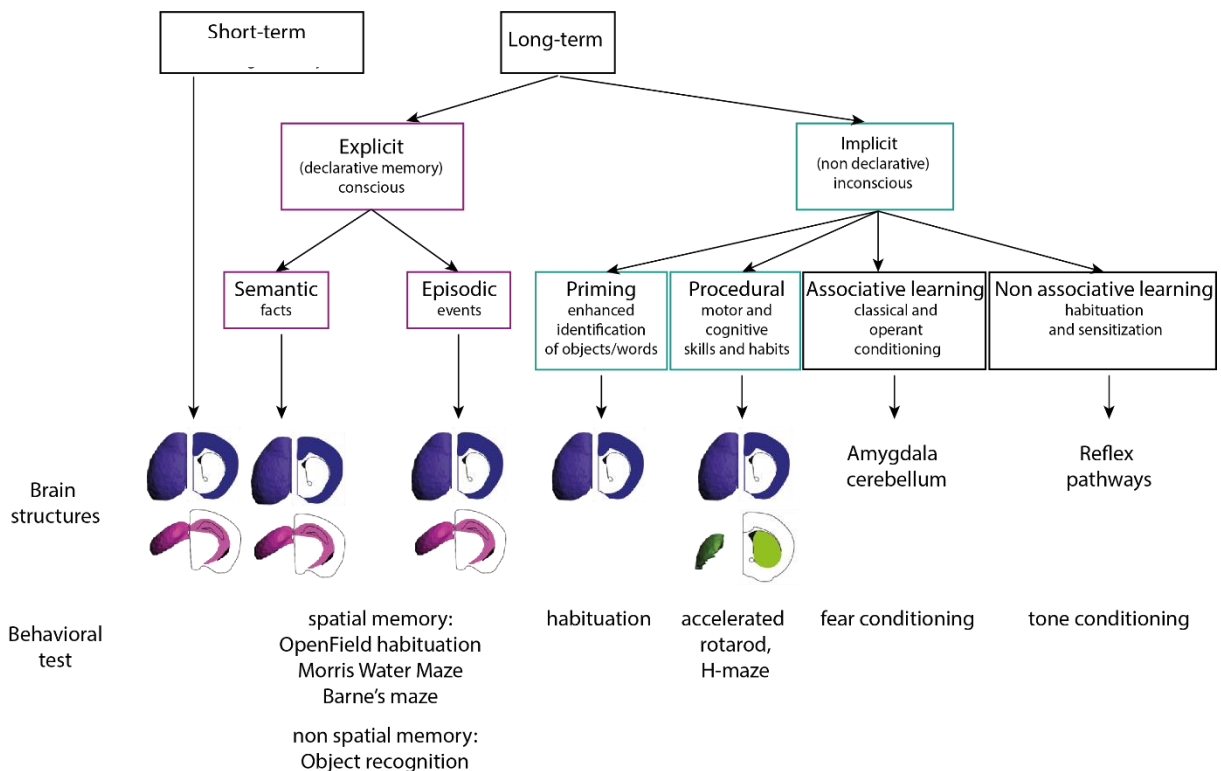
Learning and memory are behaviors often attributed to superior mammals like humans or primates but mice, flies or even worms also exhibit a certain form of learning and memory (L. B. Li et al., 2016; Phan et al., 2019). They are characterized by the sequence of three steps: the encoding of a new information into the neurons, the consolidation of this information for long-term memory and the retrieval.

Several forms of learning and memories exist and they rely on different brain structures (Camina & Güell, 2017; Quillfeldt, 2010) (figure 11) (to know more about memories: <http://memorya.org>). **Long-term** memory is opposed to the **short-term memory** which can be verbal or visual, lasting up to 1 minute and recruited to be used immediately (remembering a phone number for instance). Mice take advantage of the short-term working memory when trying to escape from a maze for few minutes. Differently, long-term memory can last minutes, days, months, up to lifespan. The shift, after few seconds, of encoding between forgetfulness (characterizing the short-term memory) and the maintenance of the memory characterizes the long-term memory and is based on the consolidation of the memory at both synaptic and system levels. The process of consolidation, that can occur during sleep, allows a reinforcement of the memory traces recently encoded that are thus, labile and fragile (Kitamura et al., 2017; Tonegawa et al., 2018). At the cellular level, consolidation reinforces the connections of specific cells: the engram cells. By modulating the activation of the engram cell, it is possible to activate or inhibit the retrieval (Tonegawa et al., 2018). Changes in the physical or chemical properties of the neurons (synaptic consolidation) with time create a new organization in time and in space of the stimulated neuronal network (systems consolidation). For instance, long term explicit memory is known to appear in the hippocampus during the encoding phase and is then transferred to the cortex thanks to consolidation processes. Engrams cells are known and found within corticohippocampal network (Kitamura et al., 2017) but might also be present in corticostriatal networks as revealed by their specific increase in activity within the striatum upon cortical stimulation and after training (Badreddine *et al.*, under revisions).

Long-term memory can refer to the **explicit memory**, highly flexible or to the **implicit memory** which stores knowledge acquired without conscious effort. Explicit memory is the memory intentionally recovered of facts, concepts (semantic) or personal experiences (episodic). This memory is stored in

the cortex and in the hippocampus. A mouse uses its explicit memory when remembering the localization of the platform in the Morris Water Maze. **Implicit memory**, tightly dependent on the conditions of learning, is involved in several processes like *priming*, *procedural memory* and *(non)associative memory*. Priming improves the perception of a word or an object by prior exposure. Associative learning associates an event with another; it is the case for fear conditioning experiments where an event (sound) is associated with electric foot shock. Non-associative learning is implicated through a change in the response of a stimuli due to repeated exposure.

Finally, **procedural memory**, is the memory of habits and is mobilized in human when we learn how to ride a bike or play an instrument. Habits can be defined by a stimulus-response association created only by the repetition of the stimuli rather than the desire or the fear of the outcome (associative learning). This memory is acquired through trials and errors, practice, and experience. To give a clear example, a mouse forms its procedural memory when falling off the accelerating rod repeatedly. At the end of the training, adapting its movements to the rod speed has become a habit. This type of



memory is known to be dependent on the corticostriatal network (Bosson et al., 2017; Costa et al., 2004; Perrin & Venance, 2019; Yin et al., 2009).

**Figure 11: Different forms of memory involve specific networks and are evaluated by different behavioral protocols.**



### i. Corticohippocampal and corticocortical networks & explicit memory

Thanks to its connection with the cortex, the hippocampus receives sensory and spatial information and is able to store this information for days to a lifetime period. The ultimate and long-term storage takes place, after consolidation, in the cortex through hippocampal output towards the deep layers of the entorhinal cortex or the subiculum.

Corticohippocampal network is defined by two pathways called **perforant pathways**: a *monosynaptic and direct pathway* and a *trisynaptic and indirect pathway*. In the direct pathway, projections from layer III of the entorhinal cortex form synapses with CA1 neurons which project back to the cortex. The indirect pathway is defined by the layer II of the entorhinal cortex projecting to the granule cells of the dentate gyrus through the mossy fibers which then project to the CA1 neurons through the Schaffer collateral. The existence of these two pathways is thought to be necessary for learning and memory because they allow the comparison of the outputs received through both pathways.

Spatial memory evaluated by the Morris-Water Maze test in mouse is dependent on cortical and hippocampal plasticity. In fact, a spatial map of the testing environment is formed in the hippocampus of the tested mouse through firing pattern of specific neurons in CA1 and CA3 regions: the place cells. Although spatial memory is hippocampus-dependent, it seems that is not the case for object recognition which is thought to depend more on the cortex (Oliveira et al., 2010).

### ii. Corticostriatal network & procedural memory

As detailed earlier, movement control is dictated through the loop involving mainly the cortex, the basal ganglia, and the thalamus. However, movement control is not only useful for goal directed behavior but also for learning and acquisition of new motor skills and habits, what we identify as the procedural memory (Costa et al., 2004; Graybiel & Grafton, 2015; Hawes et al., 2015; Hyungju Park et al., 2014; Yin et al., 2009). Interestingly, procedural memory, mainly dictated by the corticostriatal network, is known to be impaired in HD where this network is the first to degenerate (Heindel et al., 1989; Van Asselen et al., 2012). Cortical inputs reside in either the associative cortex projecting to DMS, either the sensorimotor cortex projecting to the DLS (Mannella et al., 2013; Miyachi et al., 1997, 2002) (figure 12). Regarding striatal outputs during procedural learning, both direct and indirect

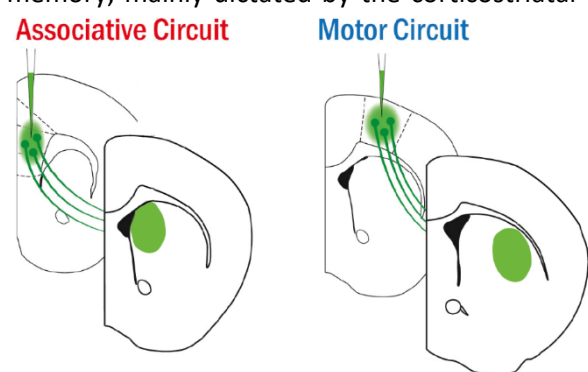


**Figure 12: cortical projections target different striatal zones.** associative cortex projects towards the DMS (left) whereas sensorimotor cortex projects towards DLS, from Corbit et al., 2017.

pathways seem to be used since both DLS outputs are strengthened (O’Hare et al., 2016).

Two phases are involved in the learning of a new motor skill: a fast acquisition phase relying on the goal-directed behavior, and a slow mastery phase where the movement becomes unconscious (or implicit) and the habit is formed (Corbit et al., 2017; Costa et al., 2004; Yin et al., 2009). Neuronal mechanisms responsible for the establishment of procedural memory are still being investigated and two models co-exist in the literature to explain the roles of each network. The first model relies on a control shift from associative cortex-DMS network, responsible for the early learning of a task, to the sensorimotor-DLS network later during the training (Costa et al., 2004; Yin et al., 2009). The other model relies on a co-engagement of the two networks during learning and competing for control (Kupferschmidt et al., 2017; Perrin & Venance, 2019).

Thus, communication between two neurons is crucial for the emergence of a behavior such as learning and memory. Consequently, it is important to understand how two neurons communicate. In the following paragraph, we will focus on how neuronal morphology serves neuronal functions and communication.

### 3. The neuron: the structural and functional unit of the brain

Brain structures’ communication is based on the functional transmission of information between two neurons. Before detailing neuron specificities, it is relevant to recapitulate the main hallmarks of the physiology of cells.

#### a. Cellular physiology

Cellular physiology represents the elements regulating the functions of a cell, among which the cellular homeostasis, regulated by cellular signaling pathways, is crucial for the establishment of the cell state equilibrium.

##### i. Cellular homeostasis

First conceptualized by Claude Bernard in the 19<sup>th</sup> century who investigated the stability of the “milieu interieur”, the cellular homeostasis has then been pointed out by Cannon for its crucial role in survival (Cannon & Rosenberg, 1932). Cellular homeostasis can be defined as a dynamic equilibrium of a cellular steady state (variable, set point) established by the response of the cell (feedback) from the reception of intra and extra-cellular events (information from a sensor) (Styr & Slutsky,

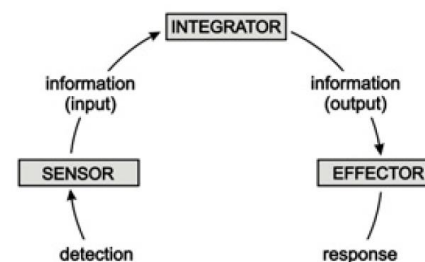


Figure 13: cellular homeostasis can be defined as a closed feedback loop regulating cellular functions. From Macleod & Zinsmaier, 2006

2018) (figure 13). When it is impaired in neurons, it is thought to be the source of neurological disorders like AD, PD and HD (D. Fernandes & Carvalho, 2016; Soukup et al., 2018). Cellular homeostasis depends partly on protein homeostasis since both protein quantity and quality are crucial for the good functioning of the cell. Thus, physiological protein levels and clearance of the damaged protein are important for the cell to keep its homeostasis. For instance, A $\beta$  peptides have been shown to be toxic for neuronal functions if they are either at high or low concentration (Abramov et al., 2009; Puzzo et al., 2008).

## ii. Cellular signaling pathways

Cellular homeostasis is regulated by an entire set up of cellular pathways. A dozen of signaling pathways are described in the literature and one particularly interesting is the IGF-1/Akt pathway.

IGF-1 (Insulin-like growth factor-1) is a growth factor able to activate many signaling pathways, thus responsible for several functions in cells like survival and differentiation (Bondy et al., 2006). When bound to its tyrosine kinase receptor at the surface of the cell, it causes the activation of intrinsic tyrosine kinases. Targeted protein like IRS-1 and Shc will then be phosphorylated leading to the activation of

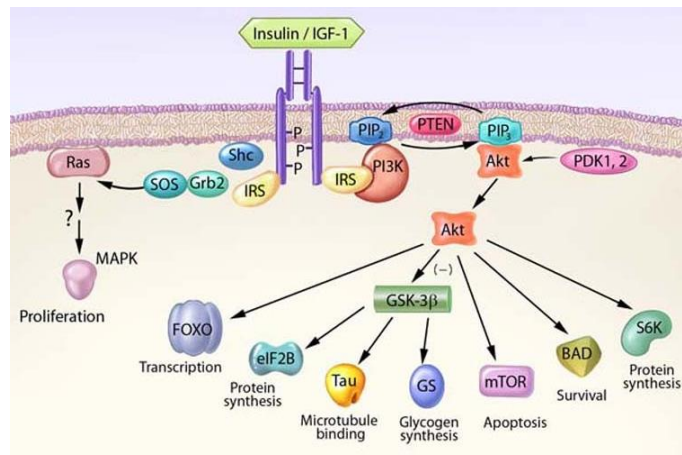


**Figure 14: IGF-1 pathway regulates cell survival through Akt activation.** From Bondy et al., 2006

several pathways including the one relying of the PI3K/Akt and the MAP kinase (ERK). PI3K activation leads to an Akt recruitment to the plasma membrane where it is phosphorylated by PDK-1 and -2 on Thr308 and Ser473. Akt, a serine/threonine kinase, is known for its roles in cell development, growth and survival when activated. This diversity of functions is the results of the many Akt targets like GSK-3 $\beta$ , Bad, caspases, mTOR and FOXO, promoting cell survival and inhibiting apoptosis (W. H. Zheng & Quirion, 2006) (figure 14). For instance, by inhibiting GSK-3 $\beta$ , Akt is able to prevent Tau accumulation observed in AD (Y. S. Hu et al., 2013; Kitagishi et al., 2014).

Thus, as any other cell, a neuron needs this equilibrium state to survive and perform its roles. However, a neuron is a specific cell in which cellular homeostasis can differ according to its type, its compartments, and its roles.

## b. The neuron: a highly specialized cell

A neuron is a specific cell whose shape is crucial for its function and vice versa.

### i. Different types of neurons

Throughout the brain, dozens of neuron types exist and are characterized by a morphology matching their functions (Weissman et al., 2007) (figure 15).

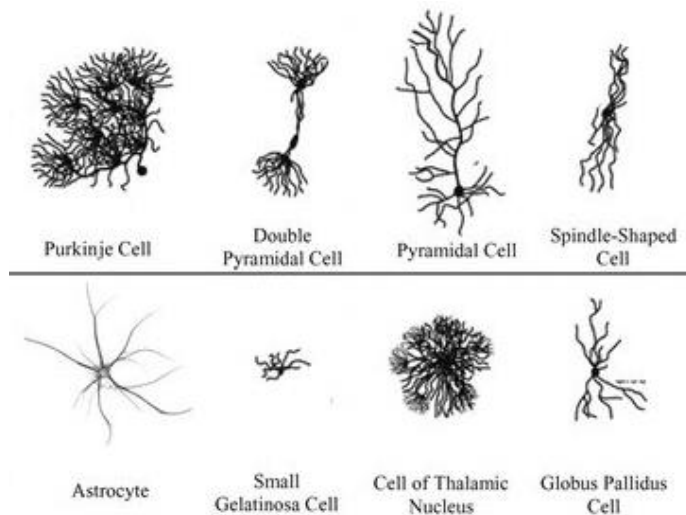


**Figure 15: neuronal shapes define neuronal functions.** From Weissman et al., 2007, adapted from Ramon y cajal drawings.

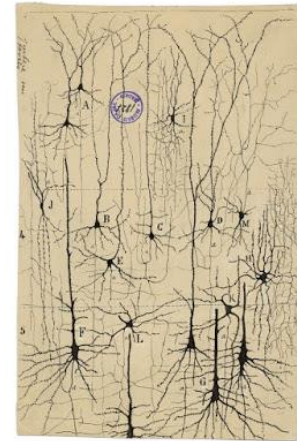


**Figure 16: pyramidal cells display a specific organization.** Santiago Ramón y Cajal, Golgi stained pyramidal cells of the cerebral cortex (detail) ink and pencil on paper. From Cajal Institute, Spanish National Research Council

For instance, pyramidal neurons in the cortex have been described at the end of the 19<sup>th</sup> century by Ramón y Cajal, famous for its functional and morphological drawings of neurons based on Golgi staining's (Llinás, 2003) (figures 15 and 16). Pyramidal cells present a primary and apical dendrite connected to the soma in a specific layer projecting its axons in specific output structures. Although this type of neurons is predominantly present within the cortex, one of Ramón y Cajal students, Rafael Lorente de Nó later identified more than 40 types of cortical neurons based on the distribution of the dendrites and axons.

Brain structures are often characterized by their types of neurons: Purkinje cells, presenting a huge dendritic arborization with many spines, are only found in the cerebellum whereas MSNs characterized by a high dendritic spine number are striatum-specific (Klapstein et al., 2001) (figure 15 and 17). These characteristics can be explained by the fact that the neuronal shape and neuronal function influence each other. For instance, MSNs are thought to compensate their smaller number within the striatum, compared to the number of cortical projecting neurons, by the high density of dendritic spines, emphasizing their central role in receiving and selecting the information from the different cortical areas (figure 17).

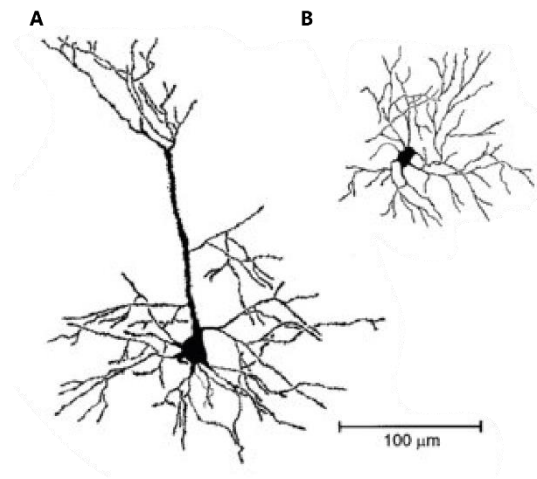


**Figure 17: morphologic properties differentiate cortical pyramidal cells from MSN.** 3D reconstitution of a pyramidal neuron (A) and a MSN (B), adapted from Klapstein et al., 2001.

## ii. A polarized structure

Both cell shape and neuronal function imply a polarity within the cell. All neurons are compartmentalized with neurites receiving or sending the signal in order to communicate. Polar morphology and function directly depend on the organization of the cytoskeleton (Kelliher et al., 2019).

### 1. Neuronal compartments

Neuronal communication is supported by a specific spatial compartmentalization of the neuron separating the neurite receiving the signal, the dendrite (input) and the one sending the signal, the axon (output) (figure 18). Between those two neurites stand the soma and its nucleus.

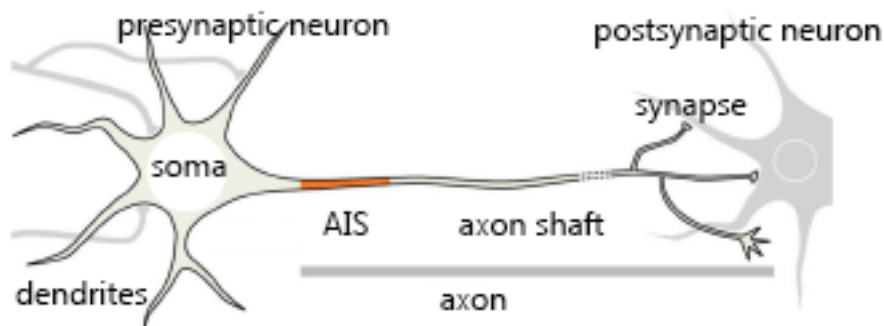


**Figure 18: neuronal networks are formed with a presynaptic neuron and a postsynaptic neuron communicating through a synapse.** Schematic representation of neuronal organization adapted from Leterrier, 2018.

## Dendrites

Dendrites are the neurites receiving the signal through their spines. Dendritic spines are small protrusions from the shaft whose morphology reflects maturation. Spine turnover is accelerated during learning and memory formation (Min Fu & Zuo, 2011; Montagna et al., 2017).

## Soma

The soma contains the genetic information within the nucleus connected to the endoplasmic reticulum. Even though some RNA translation and protein production are carried out within neurites, they essentially take place within the soma. Soma volume represents less than 1% of the entire neuron volume (Soukup et al., 2018).

## Axon

Connected to the soma, the axon is an extension that can measure up to one meter, in the case of the motor neuron. Axons can be divided in three parts: the axon initial segment (AIS), the axon shaft and the presynaptic terminal (Kelliher et al., 2019). **AIS** is the segment present on the first 20-60  $\mu\text{m}$  of the axon where an action potential, the electrical signal, is generated and shaped from the summation of synaptic inputs received by the post synaptic dendritic spines (Letierrier, 2018). AIS is thought to act as a filter, sorting molecules and regulating molecular motors recruitment to direct vesicles to their specific destination (Letierrier, 2018). It is able to select axonal vesicles and exclude dendritic cargoes. Once generated, the action potential is propagated along the **axon shaft** where it finally reaches the **presynaptic terminal**.

## Synapse

Axons connect to another neuron's dendrites through synapses, from the axon terminal or from the axon shaft (en passant boutons). According to its nature, a neuron can make up to 10 000 synapses with other cells in the mammalian brain, as it is the case for Purkinje cells. A chemical synapse is thus composed of a presynaptic element, the axon terminal, and a postsynaptic element, usually a dendritic spine, separated by a 30 nm synaptic cleft (figure 19). Active zones joined to the plasma membrane in the presynaptic element are characterized by their enrichment in vesicles ready to be released and

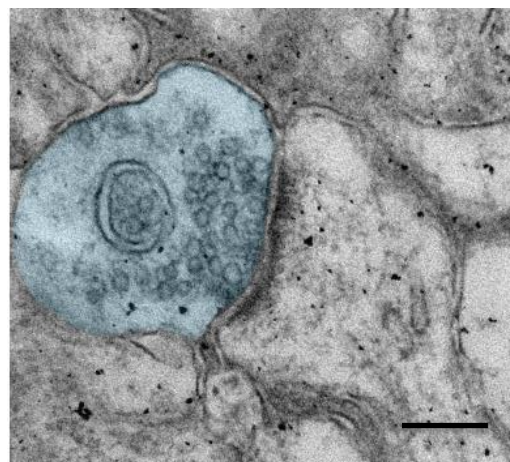


**Figure 19: a synapse is formed by a presynaptic compartment releasing NT into the synaptic cleft received by the postsynaptic compartment.** Picture of a corticostriatal synapse from an electron microscope. Blue: presynaptic compartment, scale = 200nm

in proteins; they are the release sites. Opposed to active zones in the postsynaptic element, stand a postsynaptic density (PSD), dense to electrons because of the high protein concentration (figure 19). Even though it is scarcer, a release site can be unpaired with a PSD on the postsynaptic neuron: the release is then termed extrasynaptic (Fuxe & Agnati, 1991; Sámano et al., 2012).

The electric signal (action potential) received from the dendrites is filtered in the AIS, transported along the axon and translated into a chemical signal (calcium influx) at the synapse. The signal is then encoded by the following release of signaling molecules (neurotransmitters) into the synaptic cleft (exocytosis) and their caption from receptors in the postsynaptic neuron. Then, thanks to several cellular signaling, the postsynaptic dendrites are able to translate the chemical signal into an electric one generating post synaptic currents (PSC), either excitatory (EPSC) or inhibitory (IPSC).

To conclude, neuronal shape is crucial for its function in transmitting the information. However, what are the cell components responsible for this architecture?

## 2. Cytoskeleton governs the cell architecture and its functions

Cytoskeleton has several important functions within the cell as it regulates the neuronal structure and functions. In fact, by modeling the cell, the cytoskeleton regulates neuronal migration, polarity, and differentiation (Kapitein & Hoogenraad, 2015). Moreover, it supports neuronal transport, thus functionalizing the neuronal segments (Kelliher et al., 2019). Different components of the cytoskeleton can be found based on the neuronal compartment and their roles, such as microtubules, actin and neurofilaments.

### a. Microtubules

Microtubules (MTs) are made up of heterodimers of  $\alpha$ - and  $\beta$ -tubulin bound altogether to form protofilaments that associate laterally and form a hollow tube, 25-nm wide (figure 20). Tubulin dimers are polarized structures and their head-to-tail assembly confers polarization to the MTs, revealed by the presence of a plus and a minus end (Kapitein & Hoogenraad, 2015; Kelliher et al., 2019). The polarity of MTs is crucial for neuronal functioning especially in axons where their organization is one of the cellular sensors for signal directionality.

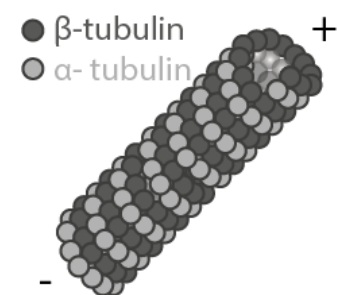


**Figure 20: MTs are a polarized structure.** Schematic representation of MT organization

Although they are components of the cell “skeleton”, it is important to consider MTs as dynamic structure: they are in constant polymerization and depolymerization processes, through GTP hydrolysis (figure 21) (Harvey et al., 2008). The plus-end is characterized by the assembly of GTP-bound

tubulin dimers which allows a rapid growth of MTs. On the other hand, GTP-tubulin can be hydrolyzed into GDP leading to its detachment from the depolymerizing MTs. When a neuron is mature and no longer needs to migrate or grow, MTs become relatively stable, but not static. Indeed, the coordination of this dynamics is well regulated in order to keep the length constant, while incorporating new tubulin monomers (Feinstein & Wilson, 2005; Ricard, 2006). These phenomena are quite relevant since they give the right structure to neurites. The roles of MTs as tracks for neuronal transport are detailed in the next chapter.

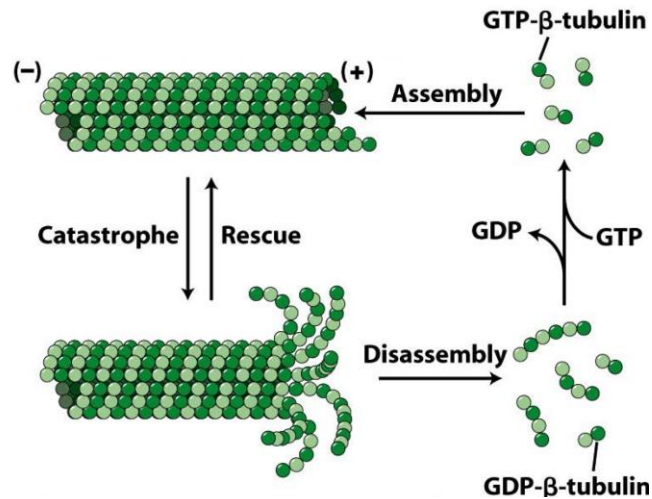


**Figure 21: MT dynamic is stable.** Schematic representation of incorporation or release of GTP- $\beta$ -tubulin responsible for MT dynamic stability, from Harvey et al., 2008.

#### b. Actin filaments

Another component of the cytoskeleton are actin filaments, which are 7-9 nm thick polymers made up of actin monomers organized in two strands. The actin filaments are also polarized and dynamic. Their formation depends on the assembly of the actin monomers at the barbed end and disassembly at the pointed end of the filament (figure 22). Actin filaments are known to be involved in many cellular processes involving force generation such as morphogenesis, elongation,



**Figure 22: actin filament structure.** Adapted from Wioland et al., 2017.

branching and specification (Papandréou & Leterrier, 2018).

Structurally, actin filaments were originally found under the plasma membrane, where MTs were absent, in synaptic regions like presynaptic terminals and dendritic spines but also in the growth cone of developing neurons (Hirokawa et al., 2010). Nowadays, thanks to the development of super-resolution microscopy techniques like STED or STORM or cryo-electron microscopy, actin has been detected along the neuron, from the tip of the dendrite to the AIS and within the axon shaft in which



actin forms rings (figure 23), hotspots or trails (Leterrier et al., 2017; Papandréou & Leterrier, 2018; Vassilopoulos et al., 2019; K. Xu et al., 2013).

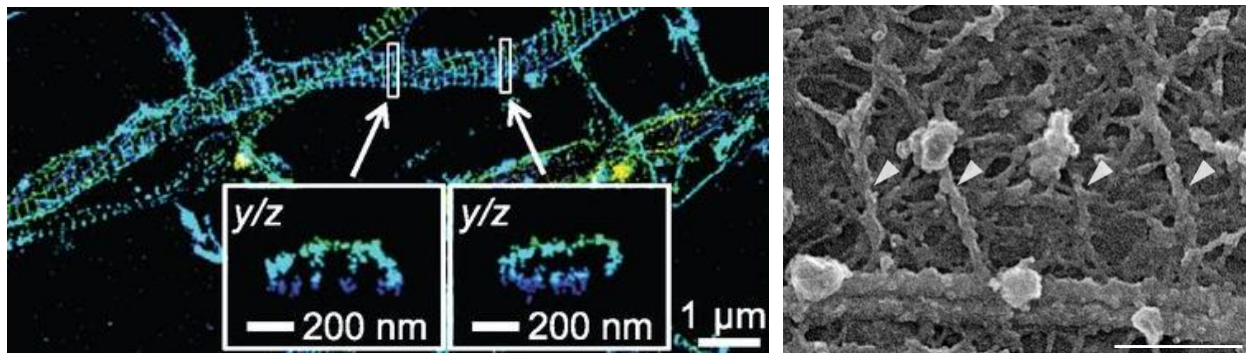


**Figure 23: actin forms rings within the axon.** Actin rings in the axon shaft observed with STORM (left from Xu et al., 2013) or with cryo electron microscopy (right, from Vassilopoulos et al., 2019)

Functionally, in addition to being crucial for the shape and integrity of neurons, actin filaments also play an important role in neuronal transport as they act as tracks for the molecular motor myosin (Hirokawa et al., 2010). Unlike the MTs, actin-based transport would allow a short and local trafficking of organelles, carried into synaptic areas by MT-based transport (Q. Cai & Sheng, 2009). This shift from MTs to actin is thought to modulate endosome motility or the SV trafficking within pools at the presynapse (between the reserve pool and the RRP after a stimulation, e.g.) (Miki et al., 2016; Owe et al., 2009; Papandréou & Leterrier, 2018; Rust & Maritzen, 2015).

It is interesting to note that MTs and actin filaments in axons, thanks to their dynamic state, are designed to ensure the structural plasticity necessary to modulate synaptic connections and therefore cellular mechanisms of learning and memory.

### c. Neurofilaments

Neurofilaments are a type of intermediate filaments found only in neurons (Gibbs et al., 2015; Yuan et al., 2017). They are the most abundant fibrillar components in axons (three to 10 times more than MTs) and are considered as the bones of the cytoskeleton. The peculiarity of this structure of 10 nm of diameter is that, unlike MTs and actin filaments, it is stable and almost completely polymerized in the cell.

Neurofilaments, are believed to support axonal structure and to regulate axon diameter (Gibbs et al., 2015). When neurofilament proteins are mutated in Charcot–Marie –Tooth disease, the diameter of the axons is reduced and nerve conduction is impaired (Yuan et al., 2017).

Neurofilaments are thought to play a role in neuronal transport by interconnecting with MTs or actin filaments to create a specific network that could serve as a docking platform for proteins and organelles (Yuan et al., 2017).

Therefore, the cytoskeleton is crucial for the shape and functions of a neuron as it creates a polarized cell that functionalizes the neuronal compartments allowing neuronal communication. But how are neurons responsible for macroscopic events such as memory and learning through neuronal communication? In which cellular mechanisms do memory and learning reside?

#### 4. The neuronal mechanisms underlying learning and memory

One of the key processes for memory mechanisms is based on synaptic homeostasis which constantly adapts and perceives environmental cues or changes. From there, the second key process is the brain's ability to remember and learn the coupling between homeostatic changes and output in terms of chemistry. This process is called plasticity.

##### a. Synapse homeostasis

Synaptic homeostasis is a specific cellular homeostasis because this dynamic equilibrium relies on the communication between two compartments to maintain a feedback loop: the pre- and the postsynaptic compartments (figure 24). This two-sided loop allows the integration of a change in the equilibrium from one compartment to another through diffusible molecules, which makes it able to drive signaling pathways that induce a compensatory mechanism and prevent degeneration of the nervous system (D. Fernandes & Carvalho, 2016; Yee et al., 2017). Synapse homeostasis regulates the synaptic performance according to the environment through constant remodeling (functional and morphological) in order to maintain the fidelity of communication within neuronal networks. This adaptability is called homeostatic plasticity. Functional remodeling may rely on regulation of **synaptic strength** through postsynaptic excitability, network modeling, or alteration of presynaptic functions (Styr & Slutsky, 2018; G. Turrigiano, 2012; G. G. Turrigiano, 2017; H. Wang et al., 2012). Morphological remodeling is characterized by the regulation of the size and the shape of dendritic spines, synapses, PSD areas or number of synapses (Marrone & Petit, 2002).

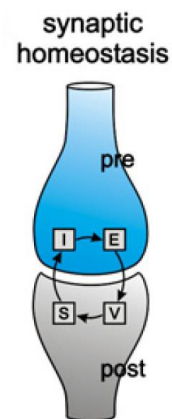


**Figure 24: synaptic homeostasis as a two compartments system.** schematic representation of synaptic homeostasis, from Macleod & Zinsmaier, 2006.

If the two compartments do not influence each other, adaptation to the environment is a **cell-autonomous** response and is considered as a cellular homeostasis rather than a synaptic homeostasis.

However, these two modes are not exclusive. In fact, synaptic homeostasis can be seen as the junction of two cellular homeostatic systems that interact through trans-synaptic signaling pathways. These trans-synaptic pathways can be supported by molecules responsible for the cell-cell interaction or cell adhesion by creating trans-synaptic connections such as integrins or **APP homodimers** (Fogel, et al., 2014; Frere & Slutsky, 2017; Huber, 2018; Macleod & Zinsmaier, 2006; Styr & Slutsky, 2018).

The fact that neurons are post mitotic cells implies their great dependence on efficient mechanisms that control protein and synapse homeostasis (Soukup et al., 2018), which are the basis for the establishment of the molecular pathway that regulates memory. Indeed, when synapse homeostasis is lost, like in PD, AD or HD (Styr & Slutsky, 2018; H. Vitet et al., 2020), the system is no longer able to adapt (*i.e.* is no longer able to change the balance). Therefore, memory mechanisms are not possible and the equilibrium is no longer dynamic.

### b. Synaptic strength

As previously mentioned, synapse homeostasis can regulate and adjust synaptic strength, which is known to be critical to the physiological function of the brain (D. Fernandes & Carvalho, 2016; Styr & Slutsky, 2018; G. G. Turrigiano, 1999). Synaptic strength is a parameter that can give access to synaptic function (Murthy, 1998). It is defined as the “amount of current produced in the postsynaptic neuron by an AP in the presynaptic” (Murthy, 1998). According to Katz’s theory, two parameters can influence synaptic strength: the **probability of release** (the ability for an AP to activate the release of at least one vesicle from the presynaptic neuron (Alabi & Tsien, 2012) and the quantal size (the current created in postsynaptic neuron from the NT release) (Allen & Stevens, 1994; P. S. Kaeser & Regehr, 2017). The probability of release depends both on the activation mechanism (*i.e.* the calcium influx) and on the activated process (the amount of release of NT). **The amount of NT release** depends on the number of release sites (usually 1 in the mammalian CNS) and the **number of SVs ready to be released (N)** (Dobrunz & Stevens, 1997; Matz et al., 2010; Murthy et al., 2001). The greater the number of SVs in the active zone, the greater is the probability of release. In hippocampal neurons, the probability of release was found to be low, less than 0.3 (Murthy et al., 1997).

### c. Plasticity

Synaptic strength can be modulated dramatically and rapidly by signals from intrinsic (high activity) or extrinsic (input from other neurons) factors. This change in synaptic strength can last for seconds to days and is called short-term or long-term plasticity, respectively. In other words, plasticity is the ability of a cell to change synaptic strength, based on the signal it received. The increase in synaptic strength is called potentiation, while a decrease is called depression. Short-term memory, like working memory, is believed to rely on short-term regulation of synaptic strength (neuronal firing).

During plasticity, pre- and postsynaptic elements communicate in a coordinated way, causing the perturbation of synaptic homeostasis, leading to an infinite strengthening of the connections (Hebb, 1949; H. Wang et al., 2012); this phenomenon is called long-term potentiation (LTP) and was first described by Hebb (Hebb, 1949). LTP is opposed to long-term depression (LTD), which characterizes the weakening of synaptic connections. LTP (or LTD) forms are varied and can use many molecular mechanisms that regulate synapse homeostasis such as sustained increase in the amplitude of ESPSPs, modulation of the number of glutamate receptors in postsynaptic element, or cellular pathways that regulate the gene expression (CREB)(Edelman & Gally, 2001). LTP also causes morphological changes as a change in synaptic curvature or in synapse perforation and an enlargement of dendritic spines and synapses (Bourne & Harris, 2011; Marrone & Petit, 2002). Since the synapse area is constant (Bourne & Harris, 2011), during LTP, synaptic density decreases and synapses get bigger with a larger PSD area, correlated to the mean EPSP amplitude (Holler-Rickauer et al., 2019). All of these changes in morphology serve to increase the probability of release by either regulating the calcium influx concentration or by decreasing the distance between the pre- and the postsynaptic neurons. This morphological plasticity is responsible for long-term changes in behavior such as learning or memory (Fields & Ellisman, 1985).

LTP and LTD have been shown to be implicated during various learning protocols in mice, emphasizing the fact that they may be the cellular substrates for memory formation (Wang et al., 2012). For instance, hippocampal long storage of information mobilized for spatial memory is thought to be directly linked to LTP. Implicit memory is thought to be driven by the strength of corticostriatal connections where LTP modulates MSNs activity by regulating glutamate receptor (NMDAR) (Perrin & Venance, 2019).

Interestingly, Hebbian plasticity illustrates well the need for homeostasis regulation (through homeostatic plasticity) since, without this regulation, LTP leads to a degradation of the neuronal network caused by a vicious cycle of excitation (Styr & Slutsky, 2018). For example, homeostatic-dependent regulation of the synaptic strength during activity through the regulation of the number of

glutamate receptors in the postsynaptic compartment is important to control the Hebbian-like LTP mechanisms responsible for memory (Styr & Slutsky, 2018; G. G. Turrigiano, 2017). Hence, homeostatic plasticity seems to counteract LTP-dependent perturbations by triggering homeostatic negative feedback mechanisms (D. Fernandes & Carvalho, 2016; G. Turrigiano, 2012; G. G. Turrigiano, 2017; H. Wang et al., 2012; Yee et al., 2017). The regulation of LTP-dependent perturbation by homeostatic plasticity is called metaplasticity (Cooper & Bear, 2012; Yee et al., 2017).

In conclusion, behaviors such as learning and memory, implicit or explicit, are the result of the communication between neurons from different brain structures that form networks. Therefore, neuronal communication and homeostasis appear to be crucial for the proper functioning of neuronal networks. This communication between two neurons is based on a specific neuronal morphology linked to its function with dendrites receiving the signal and axons sending it to another neuron through the synapse. The strength of this neuronal communication depends on the release of molecules at the synapse and can be modulated over a short or a long period by the plasticity properties of neurons. Long-term changes in synaptic strength are associated with LTP or LDP, which are thought to be the cellular substrates of long-term memory.

The communication between two neurons depends on the communication between the compartments within a given neuron. Therefore, understanding the mechanisms and consequences of the transport of molecules within neurites is important to characterize the physiological functioning of the system. But what is neuronal transport and how is it regulated?

## Chapter 2- Axonal transport of vesicles as a regulator of neuronal functions and survival through multi-protein interactions

This part focuses on a specific neuritic transport: axonal transport. Indeed, the aim of this study concerns the understanding of the transport within the axons of different vesicles containing a variety of molecules. We will first define what a vesicle is from its synthesis to its fusion with the plasma membrane and then the differences between the types of vesicles in terms of cargo and dynamics. Tracks for these vesicles will also be described alongside their role in the regulation of molecular motor driven axonal transport. However, tracks and molecular motors are not the only players regulating axonal transport: adaptors and scaffold proteins also play an important role. It is therefore important to identify those regulators to better understand the dynamics of axonal transport and its modalities and then try to restore it in a pathological context.

### 1. Vesicles and cargoes

#### a. Definition

A vesicle is a mobile organelle actively transported in neurons or astrocytes (Bohmbach et al., 2018; Verkhratsky et al., 2016), bounded by a lipid bilayer and containing cytoplasm that can be enriched with cargoes: molecules, peptides, proteins, or other vesicles (figure 25). Vesicles have specific biogenesis, morphology and dynamics depending on the cargo they carry which determines their roles.

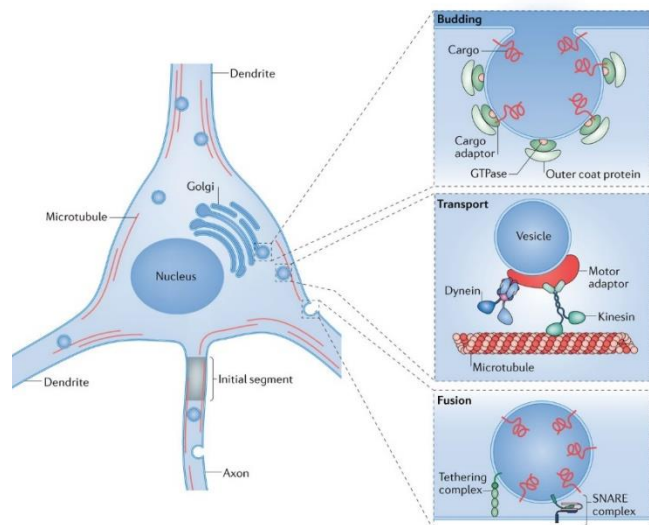


Figure 25: a vesicle journey from its biosynthesis in the Golgi apparatus to its exocytosis at the plasma membrane. From Bentley and Banker, 2016.

#### b. Vesicle biosynthesis

A simple description of a vesicle would consist of a sphere made of lipids and containing proteins. The lipids that form the vesicles are usually buddings from the membranes of organelles within the cell body or from the plasma membrane at axon terminals. These two cellular sub-compartments are also those in which proteins are inserted into the vesicles: by being produced *de novo in-situ*, by being sequestered in the invaginated membrane.

i. *De novo* vesicular production from the endoplasmic reticulum (ER)

Like any other protein in a secretory cell, proteins within a neuron are synthesized by ribosomal processing of mRNA. Located mainly on the cytosolic surface of the endoplasmic reticulum (ER) in the cell body, ribosomes can fully transfer polypeptides within the ER lumen to produce secretory proteins (such as neurotrophic factors) or not. In the latter case, if the transfer is incomplete, the newly synthesized protein will be anchored within the ER membrane and will become a transmembrane protein like APP or SNARE proteins. Once synthesized within the ER, proteins undergo many modifications to acquire three-dimensional conformation and post-translational modifications (PTMs) such as phosphorylation (figure 26) or glycosylation. They then leave the ER within transport vesicles and reach the Golgi apparatus. This transport is initially controlled by proteins that form layers around the vesicle: COPI and COPII. They control the evagination of the ER membrane into a bud-shaped vesicle and select the protein that will travel within these vesicles: the protein cargo.

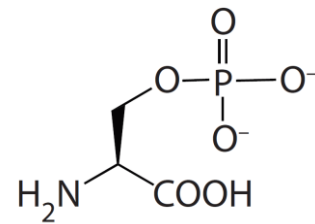


Figure 26: PTMs modify the chemical composition of amino acids. chemical representation of a phosphorylated serine

After 20 minutes of transit from the ER, transport vesicles reach the cis- side of the Golgi apparatus as a free vesicle (Gondré-Lewis et al., 2012) and use the SNARE system to fuse with the Golgi membrane (for more details, see chapter 3 1-a-iii). Once the protein cargo is within the Golgi, it travels through its different enzyme-enriched stacks to the trans-Golgi where it undergoes many PTMs. Finally, it emerges from the trans-Golgi network (TGN) as a free vesicle with a specific molecular composition and destination (figure 27).

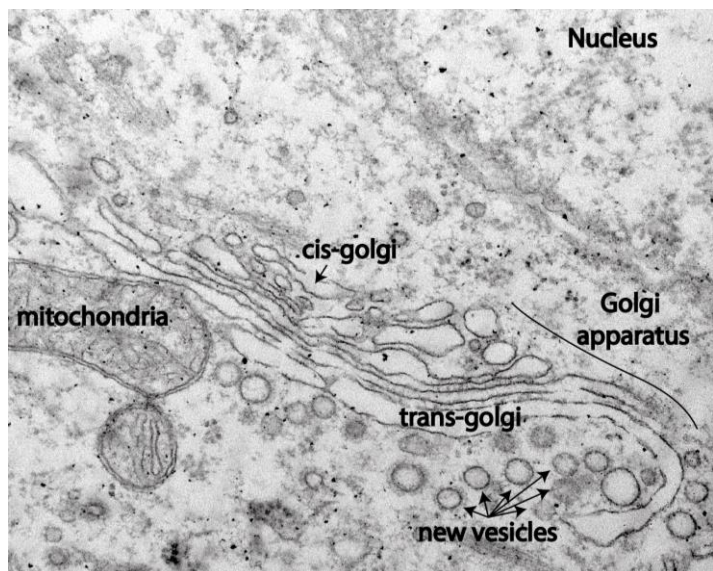
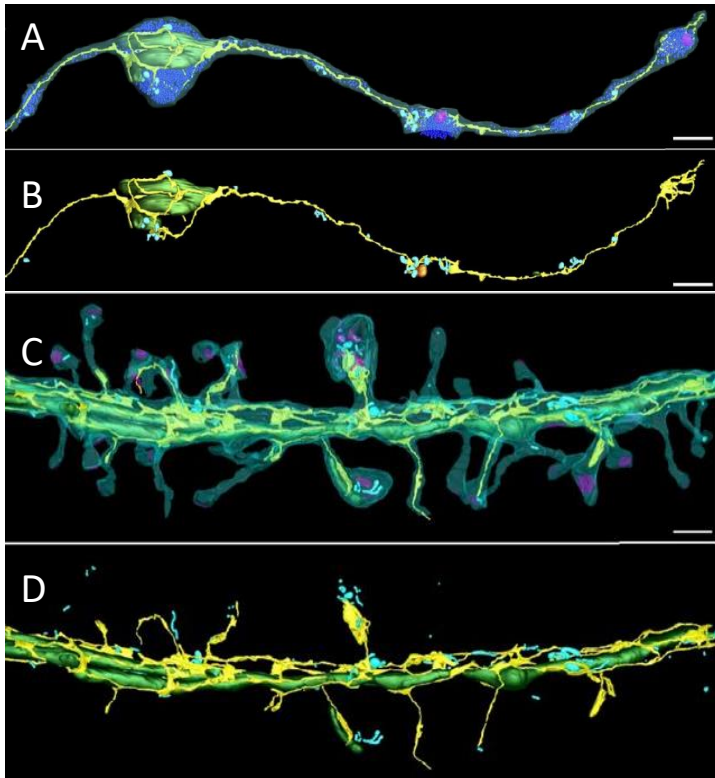


Figure 27: *De novo* production of vesicles is made in TGN. Picture of a Golgi apparatus and its biosynthesis of vesicle obtained from an electron microscope.



**Figure 28: ER network is present in neurites.** 3D representation of the ER network in axon (A) and (B) and in dendrite (C) and (D). yellow: ER, blue: PM, light blue: endosomes, dark blue: SVs, green: mitochondria, from Wu et al., 2017

However, neurons are very specific cells due to their polarized structure. Unlike non-polarized cells, neurons exhibit a continuous distribution of the ER and, although limited, discontinuous discrete Golgi structures (Golgi outposts, GOPs) within dendrites and axons (figure 28) (Valenzuela et al., 2014; Y. Wu et al., 2017). In the 1960s, some studies hypothesized the presence of mRNA and ribosomes in axons supporting the idea of intra-axonal protein synthesis (Bunge, 1973; Koenig, 1965). Nowadays, though controversial for many years (Sahoo et al., 2018; Steward, 1997), this hypothesis has been further investigated and validated *in vivo* in

mature mammalian axons (Perry & Fainzilber Mike, 2013; Sahoo et al., 2018). The mRNA can be transported via kinesin-mediated transport to the axon terminal where it is translated into proteins or docked to receptors (Sahoo et al., 2018). This mechanism allows the subcellular regulation of the proteome, essential for neurons and critical for their regeneration and repair (Gumy et al., 2011; Sahoo et al., 2018). But it also allows the communication between the axon terminal and the cell body through the retrograde transport of proteins synthesized in axons. This communication is known to be increased and dramatic in AD (Baleriola et al., 2014).

Furthermore, the biogenesis of vesicle can be regulated by many processes such as gene expression, post-transcriptional or post-translational modifications (Gondré-Lewis et al., 2012). This is the case, for example of the REST/NRSF transcriptional repressor, which, when not sequestered in the cytoplasm, is known to down-regulate the expression of genes required for vesicle secretion and vesicular protein production (Bruce et al., 2004; C. Zuccato et al., 2001).



ii. Vesicular production from endocytosis at the level of the plasma membrane

Another way of producing new vesicles within neurites is through the invagination of the plasma membrane (PM) which can carry extracellular material into the cell. Thus, instead of being a TGN expansion, vesicles are made up of lipids and proteins from the PM. Endocytosis can be observed in both dendrites and axons, and over a 40 year period, four main modes of endocytosis have been described: the clathrin mediated endocytosis (CME) (Figure 29B), the kiss-and-run (Figure 29C), the ultrafast endocytosis (Figure 29A) and the activity-dependent bulk endocytosis (ADBE) (Figure 29D) (Chanaday et al., 2019; Kononenko & Haucke, 2015; Y. Wu et al., 2014).

The CME mode, which predominates in mammalian synapse, is slow (10-30s) because it requires a significant and specific set of proteins to produce recycled vesicles with high quality and fidelity (Chanaday et al., 2019; Y. Wu et al., 2014). Briefly, adaptor proteins recruit clathrin proteins around the forming vesicle to build a clathrin coating. This coating is then stripped away by other proteins assembled into a ring structure around the neck of the forming vesicle which eventually frees itself from both the PM and the clathrin molecules (for more details, see chapter 3 1-a-v-2).

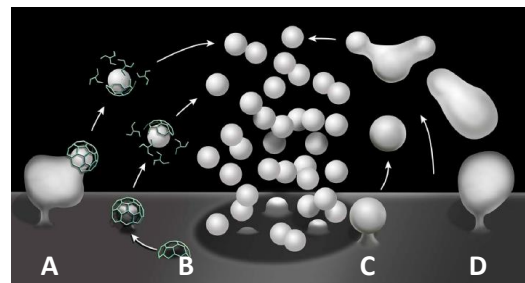


**Figure 29: different endocytic modes exist.** Schematic representation of different endocytic modes. (A) ultrafast endocytosis, (B) clathrin-mediated-endocytosis, (C) kiss-and-run, (D) activity-dependent bulk endocytosis, from Wu et al., 2014.

Conversely, the kiss-and-run endocytosis mode is faster (less than 1 or 2 seconds), because not only the opening of the fusion pore is reversed but also because it requires no adaptor or clathrin proteins. This endocytic modality would also be the most effective in terms of recycling (Chanaday et al., 2019; Schikorski, 2014; Y. Wu et al., 2014) and could explain the small proportion of lipid mixing between the PM and the synaptic vesicles found in Lewis' study (Lewis et al., 2017).

Furthermore, ultrafast endocytosis can be performed in 50 ms after exocytosis via endocytosis of a large amount of clathrin-free PM. Due to its ability to recover a big amount of PM in a short time, this recently discovered mechanism is thought to compensate for the excessive amount of lipids carried to the PM during exocytosis to maintain membrane tension (Chanaday et al., 2019). The bulk forming large endocytic vesicles (80 nm) can then lead to clathrin-mediated budding to produce smaller and mobile vesicles.

Finally, ADBE mode is a clathrin-independent mechanism, similar to ultrafast endocytosis, but differs in activation modality: long bursts of intense activity are required. It is also slower (1-2 sec) and the formed endosomes are larger (150 nm) (Chanaday et al., 2019).

The two modalities of vesicle production described above in the paragraph give specific morphology and dynamics to the new vesicles.

### c. Vesicle morphologies and dynamics

The electron microscopy technique provides direct access to the morphology and localization of vesicles. Observations and measurements led to the conclusion that a vesicle can be described based on its function, morphology, composition and dynamics, which are all interdependent. For example, we can distinguish secretory vesicles and endosomes from exosomes and each of them can be declined in different types of vesicles.

#### i. Secretory vesicles

In neurons, many of the newly formed vesicles in the Golgi apparatus are secreted at the plasma membrane to ensure neuronal communication by releasing molecules, survival cues, or cell-adhesion proteins. Despite their heterogeneity, they all contain the exocytotic machinery for merging with PM. Two main secretory pathways are described in the literature: the constitutive secretory pathway (CSP) and the regulated secretory pathway (RSP) (figure 30) (Gondré-Lewis et al., 2012).

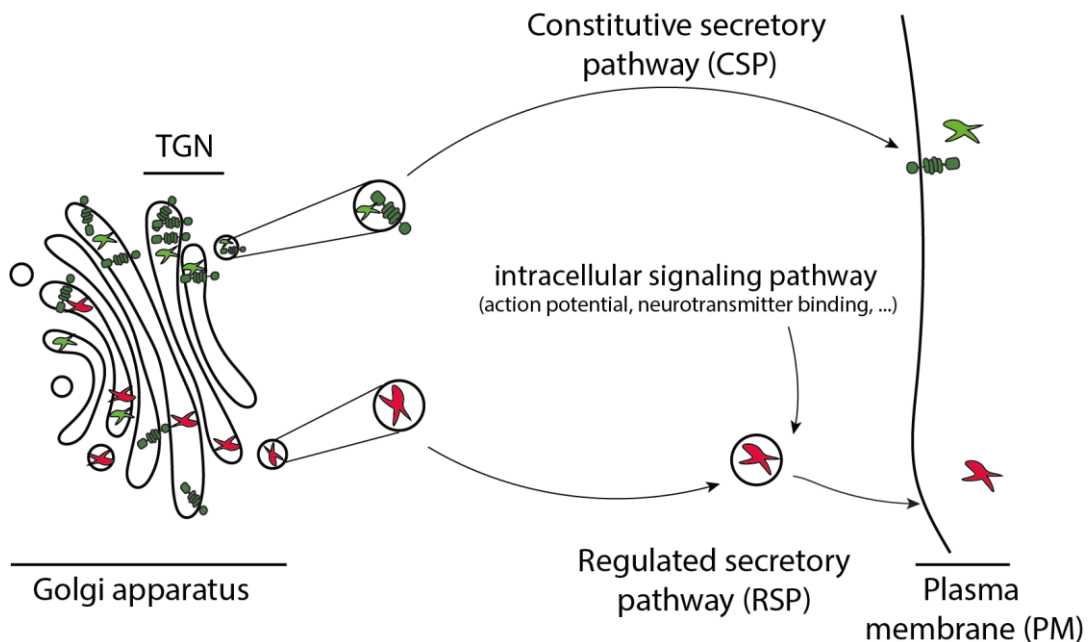


Figure 30: TGN vesicles are secreted through two pathways, CSP or RSP.

### 1. CSP vesicles

The vesicles formed by the Golgi apparatus are CSP vesicles by default because their production does not require processes of maturation, protein concentration or coating. These vesicles, also called transport vesicles or TGN-derived vesicles, emerge from the Golgi apparatus as clear and small vesicles (80-100 nm of diameter) and can contain both secretory (like growth factor) and/or membrane proteins (such as APP) (figure 30). Once produced, they are transported to the axon terminal where they fuse with the plasma membrane regardless of any external or calcium-related signal. Consequently, the CSP depends on the rate of *de novo* vesicle production and does not form any vesicle pool within the neurite (Gondré-Lewis et al., 2012).

### 2. CSP vesicles-like: synaptic vesicle precursors

Some CSP vesicles are specific because they differ in their composition. These CSP vesicles-like, also called Synaptic Vesicle Precursors (SVPs), possess a specific set of membrane proteins allowing exocytosis (described in chapter 3 2-a) that requires a preliminary protein concentration and sorting within the Golgi apparatus. Usually empty after their formation, SVPs are transported and secreted constitutively to the plasma membrane of the axon terminal, where they fuse and mature to become a neurotransmitter-filled synaptic vesicle (SV). At this stage, this CSP vesicle becomes a RSP vesicle because it needs a calcium influx to be fused with the PM and ensure the neuronal communication. Further details are described in chapter 3 1-a-iii.

### 3. RSP vesicles: dense core vesicles

Inside neurons, we can also find another type of secretory vesicle. Dense-core vesicles (DCVs) are RSP vesicles and their secretion depends on external signal translated into a  $\text{Ca}^{2+}$  entry. Contrary to the CSP vesicles, they need to be filled and enriched with a certain set of proteins, right from the exit of the Golgi apparatus in order to mature and be delivered to the PM. This process begins when DCV proteins reach the TGN and are sorted and aggregated at an acidic pH to finally bud and form immature clathrin-coated DCV (Sahu et al., 2017).

Maturation processes such as acidification, sorting, and cleavage (Gondré-Lewis et al., 2012; T. Kim et al., 2006; Mowla et al., 1999) allow the DCVs to be fully functional and pure. For example, lysosomal enzymes are separated from the immature DCV to be delivered to the endosomes during this process. The highly concentrated and condensed content of DCVs make this type of vesicle opaque, dense with electrons and larger than CSP vesicles (100-300 nm of diameter) (figure 31) (Dominguez et al., 2018).

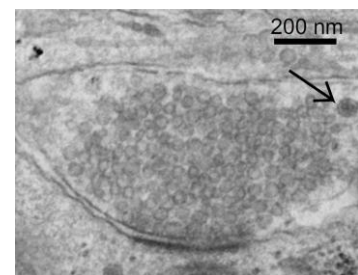


**Figure 31: DCVs are dense and bigger than SVs.** Picture of DCV and SV within an axon terminal, from an electron microscope, in Dominguez et al., 2018

DCVs are located throughout the neuron (Persoon et al., 2018), transported bidirectionally into both dendrites and axons (Stucchi et al., 2018), stored in actin-rich domains under the plasma membrane in dendrites (Washburn et al., 2002) and fuse mainly in the axon terminals where on average 2 or 3 DCVs can be found (Persoon et al., 2018). DCV exocytosis requires external signal and intracellular calcium.

## ii. Endocytic vesicles: Endosomes

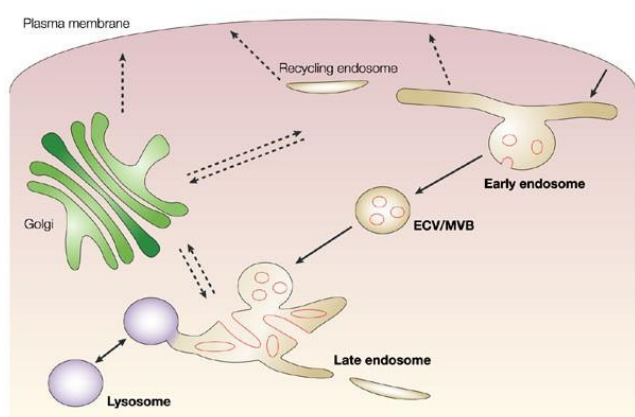
Newly formed vesicles from endocytosis are called endosomal vesicles. Depending on the mode of endocytosis or the nature of the endocytosed proteins, the morphology of endosomal vesicles is different as they undergo different pathways to reach a specific target. Three main paths related to cellular functions can be identified: recycling, degradation, or signaling.

### 1. Recycling endosomes

Once the endosomal vesicle has been created in a clathrin-dependent mode, it is likely that its lipid and protein components are about to be recycled to the PM (Yamashita & Kuruville, 2016). Cell cycle recycling is direct and rapid or indirect and slow through endosome recycling (Gruenberg & Stenmark, 2004). Recycling is a crucial process because it regulates the concentration of a protein at the PM. For example, it can limit the number of receptors at the PM thus decreasing the communication between two neurons (Yamashita & Kuruville, 2016). This recycling route also promotes SV maturation.

### 2. Degradation endosomes

Clathrin-independent endocytosis may be a signal of degradation (Yamashita & Kuruville, 2016) that begins with the entry of the vesicle into an early endosome thus forming intraluminal vesicles. Then, the early endosome becomes an intermediate endosome (also called Multi Vesicular Body) and becomes latter, a late endosome that eventually fuses with a lysosome responsible for degradation (figure 32) (Gruenberg & Stenmark, 2004). Each of these



Nature Reviews | Molecular Cell Biology

**Figure 32: endosome can undergo different pathways.** Scheme from Gruenberg & Stenmark, 2004

endosomes possesses a specific morphology and protein composition: late endosomes are larger and more pleiomorphic than MVBs which are spherical and around 400-500 nm wide. Degradation in

neurons is crucial because clearance of proteins avoids their accumulation and, by extensions, preserves these postmitotic cells which cannot divide.

### 3. Signaling endosomes

Finally, a small proportion of endosomes (Yamashita & Kuruvilla, 2016) contains signaling molecules bound to their PM receptor. They are retrogradely transported to the cell body, mainly through the interaction of dynein, where signaling molecules are able to regulate gene expression and promote the strengthening of the synapse. These signaling endosomes and their transport are important because they support neurotrophic communication between neurons (Scaramuzzino et al., *in prep*).

#### iii. Endocytic & secretory vesicles: exosomes

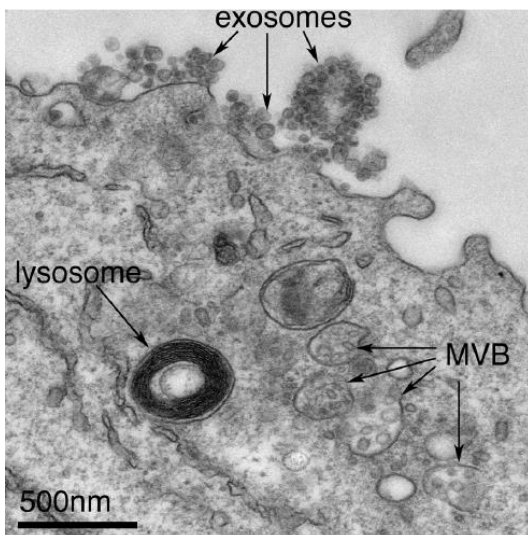


**Figure 33: exosomes are specific vesicles.** Picture of exosomes and MVB within a neuron from an electron microscope, in Edgar, 2016

Depending on their lipidic composition, some endocytosed vesicles within the late endosomes can be directed to the PM for exocytosis of its intraluminal vesicles (exosomes) (Edgar, 2016; Raposo & Stoorvogel, 2013). These vesicles are large (40-1000 nm) (figure 33) and have a specific molecular signature as they contain endosomal proteins (Rab, SNARE, Alix) and cytosolic proteins or molecules such as RNA (Raposo & Stoorvogel, 2013). However, this form of release was found to account for only 1% of the total peptide secretion (Rajendran et al., 2006).

#### d. To each vesicle its cargo

As previously described, vesicles within neurites show different morphologies and dynamics depending in their roles, which are mainly dictated by their cargo. Here, we will discuss about the main cargo properties of the three types of secretory vesicles described above: Amyloid Precursor Protein (APP) transported within CSP vesicles, neurotransmitters trafficked within synaptic vesicles and Brain-Derived Neurotrophic Factor (BDNF) transported within DCVs (figure 34). Endosome cargoes will be described briefly and not exhaustively. The fact that these three cargoes are carried by different type of vesicles reflects the need of compartmentalization: a cargo must be transported to a specific target zone through a precise route within a specific type of vesicle in order to fulfil its role.

## secretory vesicles

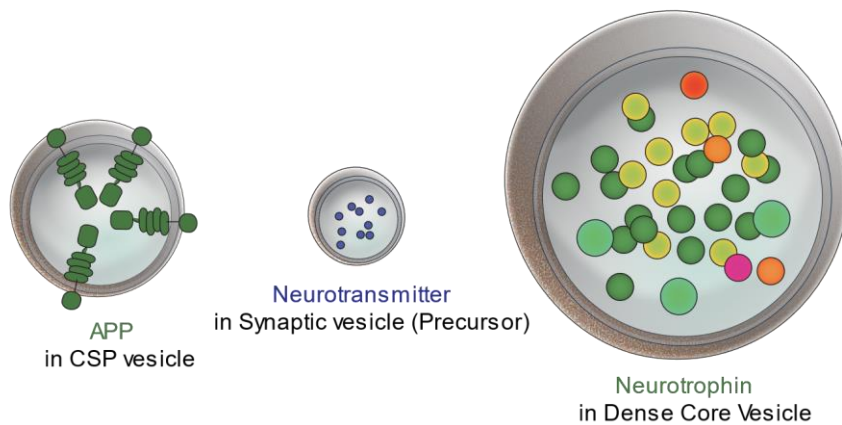
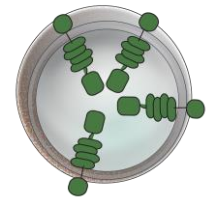


**Figure 34: secretory vesicles carry specific cargoes.** Representative scheme of APP transported in CSP vesicles, NT in SV(P) and neurotrophins like BDNF in DCVs.

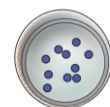
### i. CSP vesicles contain PM proteins and/or secretory molecules

CSP vesicles contain transmembrane proteins and/or secretory molecules such as growth factor. To name just a few of the many transmembrane proteins, we can list receptors, active zone proteins, t-SNARE proteins, channels or APP. The role of APP on synaptic homeostasis, which is impaired in Alzheimer's disease, is crucial and was the subject of the first study included in this work (Bruyère et al., 2020). Since secretion rate of CSP vesicles is known to be independent of neuronal activity, it is interesting to understand that if the system is challenged by a APP overexpression or an addition of transgene, the level of constitutively secreted APP will increase. As for growth factors, one of them (Nerve Growth factor - NGF) is known to be constitutively secreted, unlike BDNF (Mowla et al., 1999).



### ii. Synaptic Vesicles contain neurotransmitter (NT)

The synaptic vesicles found at the axon terminal fuse with the PM as a result of neuronal activity. These vesicles are peculiar because they contain the molecules responsible for delivering the message: neurotransmitters (NTs). A neurotransmitter could be simply defined as a molecule released by the presynapse, received by a receptor in the postsynaptic neuron which then converts the chemical signal into an electric signal from a cascade of events. A NT is the unity of the nervous message.



All NTs satisfy four criteria:

- ✓ It is synthesized within the presynaptic bouton
- ✓ It is localized within the presynaptic terminal and released in sufficient quantities to induce a postsynaptic response
- ✓ It has an identity of action; exogenous NT mimics the action of endogenous NT
- ✓ It undergoes specific and rapid processing to be removed from the synaptic cleft.

Many molecules fit this definition and are classified despite their diversity into two categories based on their size and their role: the classic and the neuromodulator (or co-transmitters). The classics, the smallest, are amino acids or transmitters (acetylcholine, dopamine, serotonin, glycine, glutamate, GABA, etc.) transported within dense core vesicles (DCVs) or SVs (Sámano et al., 2012). The other category is composed of neuropeptides (neuropeptide Y, oxytocin, melatonin, etc.), bigger molecules and are carried only by DCVs.

A NT is usually excitatory or inhibitory: glutamate or norepinephrine are mainly associated with excitatory mechanisms, while GABA or serotonin are mostly associated with inhibitory mechanisms. However, it is important to point out that for some NTs, the nature of the message does not depend on their property, but rather on the type of receptor that receives the NT and translates the message. The receptors determine the action of NT. For example, the action of acetylcholine (ACh) and dopamine depend on their receptor. Indeed, ACh can bind to nAChR or mAChR and dopamine to D1 or D2, to transduce both and respectively an excitatory or inhibitory message.

Until the late 1970s, it was thought that a neuron could send only one neurotransmitter (Eccles, 1957; Sámano et al., 2012). However, some evidence showed a few years later that it is not always the case and proved the existence of co-transmission. It was discovered for the first time that some classical NTs are co-expressed in the same neuron. This is the case for glutamate and GABA which send opposite signals to the postsynaptic: they are known to be released simultaneously in the auditory synapse of the brainstem, in the olfactory bulb or in the cerebellum (Seal & Edwards, 2006). This is also the case for glutamate and dopamine co-released by neurons that project into the ventral striatum (modulation of motivated behavior) (Hnasko et al., 2010; Stuber et al., 2010). The segregation of the two NTs into different vesicles would allow a good management of the co-release and an adaptation of the response (Marder, 1999). Although some scientists claim that co-transmission is the rule rather than the exception (Trudeau & Gutiérrez, 2007), it is commonly accepted that under physiological conditions and in most cases, a neuron mainly releases one type of NT which plays a role of activation or inhibition.

Knowing this, can we characterize a neuron by the type of action of both its NT and postsynaptic receptors? A vast field of research focuses on the study of the neuronal network based on this property: synapses are either excitatory or inhibitory. By activating a specific neuron or structure, we get a specific response from the neuronal network. For example, striatal neurons are known to be mainly inhibitory (Persoon et al., 2018). The type of connection can be distinguished by their function using electrophysiology recordings for example or by its morphology using electron microscopy. According to Gray's description, glutamatergic synapses (asymmetric synapse) have round SVs, a dark active zone, a wide synaptic cleft and a thick, large PSD. In contrast, GABAergic synapses (symmetric synapses) have pleomorphic SVs, a narrow synaptic cleft and a thin PSD (Gray, 1969; Gray & Guillery, 1966; Merchán-Pérez, Rodríguez, Alonso-Nanclares, et al., 2009; Merchán-Pérez, Rodríguez, Ribak, et al., 2009) (figure 35).

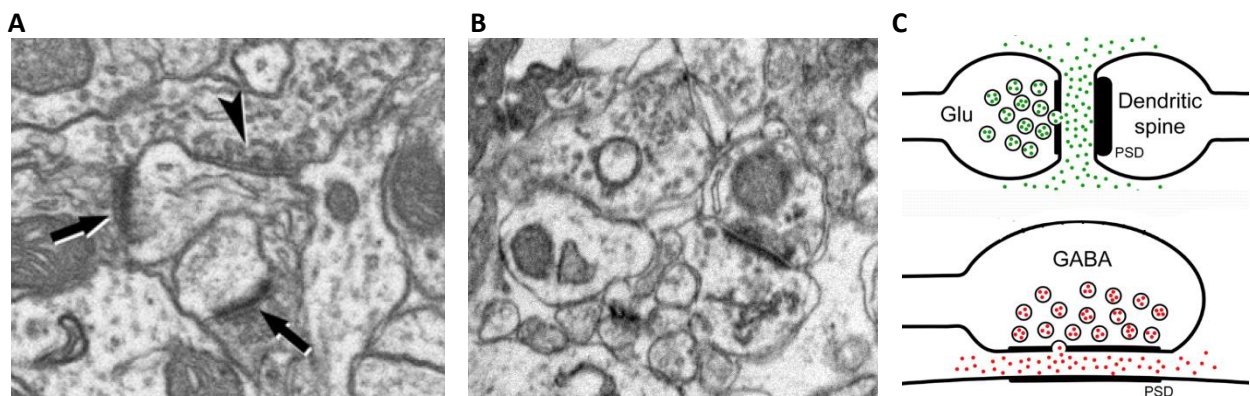


**Figure 35: excitatory and inhibitory synapses exhibit different structural characteristics.** (A) asymmetric (arrow) and symmetric (arrowhead) synapses, from Merchán-Pérez et al., 2009 or from mouse striatum (B). (C) representative scheme of the structural differences of excitatory and inhibitory synapses, adapted from Merchán-Pérez et al., 2009.

### iii. Dense-Core vesicles contain BDNF

DCVs are mainly filled with neuropeptides and neurotrophins which can function as neuromodulator or neurohormones (Gondré-Lewis et al., 2012), but it is also possible to find other proteins such as endorphins, proteases, membrane protein (vmat2, transporter of monoamines) or matrix protein (chromogranin) (Gabrych et al., 2019; Gondré-Lewis et al., 2012). Neurotrophins are a type of growth factors necessary for neuronal survival, development, and plasticity. For their action, they are essential for many neuronal functions (neurogenesis, plasticity, development...) and act as modulators of synaptic transmission that influence synaptic efficacy (Gondré-Lewis et al., 2012; Hyungju Park & Poo, 2013; Russo, 2017). Two main neurotrophins are found in DCVs: brain-derived neurotrophic factor (BDNF) and the neuropeptide Y (Gabrych et al., 2019; Lou et al., 2005). Here, we will focus on BDNF as a representative





cargo of DCVs, which is the main neuronal growth factor and essential for neuronal survival. Knock out BDNF mice die shortly after birth (Ernfors et al., 1994) and the lack of cortical BDNF transmission to striatum is responsible for the striatal neurodegeneration observed in HD (Altar et al., 1997). Besides being a cue of survival, BDNF is also critical for learning and long-term synaptic plasticity in the cortex, striatum and hippocampus (Gangarossa et al., 2020; Matsumoto et al., 2008) because it can for example modulate SV docking and enhance quantal NT release (William J. Tyler et al., 2006).

#### iv. Endosomes contain PM proteins

PM proteins can be found in all endosomes. In fact, over the course of its lifetime, a PM protein can be recycled, carried into the cell body, and degraded. This is for example the case of a growth factor receptor: to control its availability, the cell can modulate its presence at the PM by regulating its endocytosis either by recycling or by degrading it. A growth factor receptor can also be transported to the cell body as a signaling molecule.

However, based on their role, endosomes contain a specific set of proteins, known as Rab family of proteins. They are members of the Ras superfamily of small G proteins and are involved in membrane trafficking, such as membrane fusion and vesicle formation. Rab proteins are commonly used as markers to identify the nature of an endosome such as, for example, Rab 4 and 5 positive endosomes are usually defined as “early”, whereas “late” endosome are usually Rab 7 positives and “recycling” endosome are Rab 11 positive (Stenmark, 2009). Signaling endosomes can be differentiated by the presence of bound ligand and receptor in its core (Ayloo et al., 2017; Cosker et al., 2008; Liot et al., 2013).

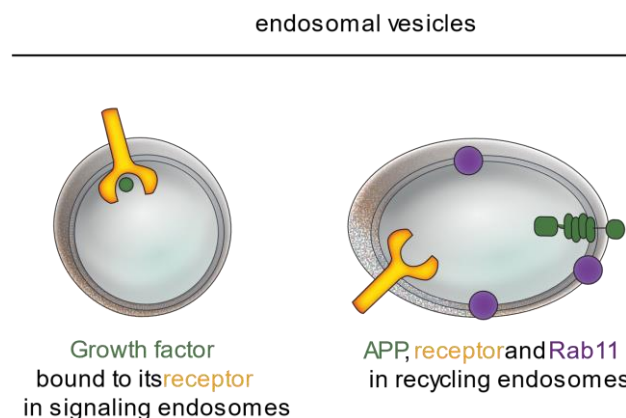
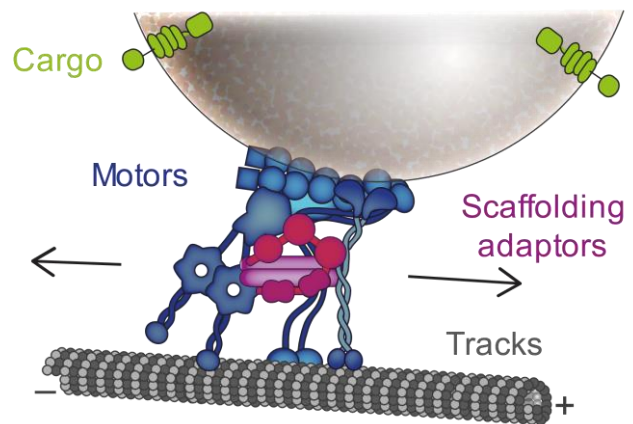


**Figure 36: endosomal vesicles carry specific cargoes.** Representative scheme of BDNF transported in signaling endosomes and APP in recycling endosomes.

In conclusion, vesicles are essential organelles for a neuronal life and play a vital role starting during the development and throughout the life of neuronal cells. Their role mainly depends on their ability to be transported inside the neuron, since their location affects their functions. But how are they transported? What are the mechanisms and actors responsible for axonal transport of vesicles?

## 2. Vesicular transport

The transport of cargoes within neurites is crucial for neuronal functions and homeostasis because, despite the elongated and polarized shape, the neuron needs to communicate in both directions with other cells that may be far from the biosynthesis site of the cargo. Consequently, two types of transport can be distinguished within a neuron, which are axonal and dendritic transports.



Depending on the compartment from which they origin and the one they are intended, the transport of the cargo takes place either from the soma to the synapse (**anterograde**) or from the synapse to the cell body (**retrograde**). In fact, bidirectional transport is the key process for neuronal communication to and from a neuron.

**Anterograde** axonal and dendritic transports from cell body to the axon terminal allow the supply of proteins, lipids, mitochondria, mRNA and neurotrophin at the synapse, necessary for neuronal metabolism and maintenance (Hirokawa et al., 2010; Millecamps & Julien, 2013; Sahoo et al., 2018; Schlager & Hoogenraad, 2009). Anterograde axonal transport also allows for neuronal transmission through SVPs transport. **Retrograde axonal** and dendritic transports to the cell body are also crucial. They not only convey information from the synapse to the cell body via signaling endosomes (Scaramuzzino *et al.*, *in prep*, Cosker et al., 2008; Ginty & Segal, 2002; Olenick & Holzbaur, 2019; Salinas et al., 2008) but they also clear recycled, misfolded, or old proteins through degradation endosomes in order to avoid their accumulation and the formation of toxic aggregates which lead to neurodegeneration (Bentley & Banker, 2016; Millecamps & Julien, 2013).

Since defective axonal or dendritic transport have been shown to be involved in several neurodegenerative disorders, many studies have described and characterized neuronal transport (Gauthier et al., 2004; Guedes-Dias & Holzbaur, 2019; Gunawardena et al., 2013; Holzbaur & Scherer, 2011; Hung & Coleman, 2016). Two terms have been dedicated to describe the movement of a cargo: transport and traffic. Transport is considered as a general term that characterizes the neurite or the

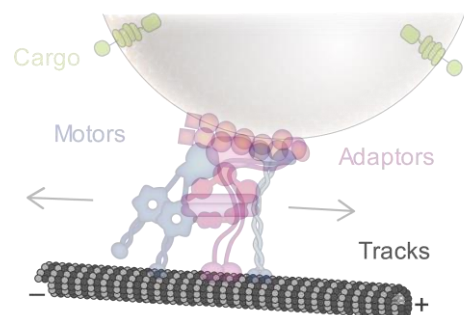
directionality of a moving cargo. However, trafficking is more related to a movement of cargoes between a sub-cellular compartment. For example, it is possible to describe a transport of CSP vesicle to the axon terminal which can be followed by its trafficking between different pools or endosomes.

Although distinct, transport and trafficking within neurons share the need of four actors to be efficient: cargoes (free or within a vesicle), motors (molecular motors), tracks (cytoskeleton) and adaptors regulating the movement. If neuronal transport or trafficking is compromised by mutation, dysregulation or dysfunction of one of these actors, the resulting “transportopathy” leads to neurodegeneration that causes neurological disorders such as AD, HD, PD, Rett syndrome, spastic paraplegia, ALS and Charcot–Marie–Tooth peripheral neuropathy (Gabrych et al., 2019; M.-V. Hinckelmann et al., 2016; Millecamps & Julien, 2013). It is therefore of the utmost importance to understand the mechanisms and regulation of neuronal transport in order to consider them as potential therapeutics target (De Vos & Hafezparast, 2017).

In the following pages the tracks, motors and adaptors involved in axonal transport of the vesicles will be described and it will be clear that these actors interact and adapt themselves with each other through different combinations to regulate axonal transport.

#### a. Microtubules: the main tracks of axonal and dendritic transport

Neurons are highly polarized and compartmentalized cells that rely on the neuronal ability to receive or send information through neuronal transport. Each compartment plays a pivotal role in neurotransmission, and MTs, within a compartment, display different organizations and functions that can be regulated by PTM and/or association with MAPs (Kelliher et al., 2019). Therefore, it is understandable that MTs, based on their properties and structure (length, density, stability), “set the upper rate limit of efficient transport” (William J. Tyler et al., 2006).



#### i. MT properties essential for neuronal transport

MTs constitute the tracks for neuronal transport thanks to the ability of tubulin heterodimers to bind to the catalytic core of molecular motors (figure 37) (Lacey et al., 2019; Mizuno et al., 2004; Song & Mandelkow, 1993; Vale & Milligan, 2000). They are the necessary structure for neuronal transport. Polarization confers the functionality on the MTs, so molecular motors and other proteins are able to perceive this polarity and consequently modulate the directionality of the transport, essential for regulating the direction of the message (Kelliher et al., 2019). In axons, the MTs are all

oriented in the same direction, as the plus end points towards the synapse. However, in dendrites, MTs display a mixed-orientation (Baas et al., 1988; Conde & Cáceres, 2009; Kapitein & Hoogenraad, 2015) but are still organized. Indeed, it was recently discovered that MTs with the same polarity are bundled together in dendrites (Kelliher et al., 2019; Tas et al., 2017).

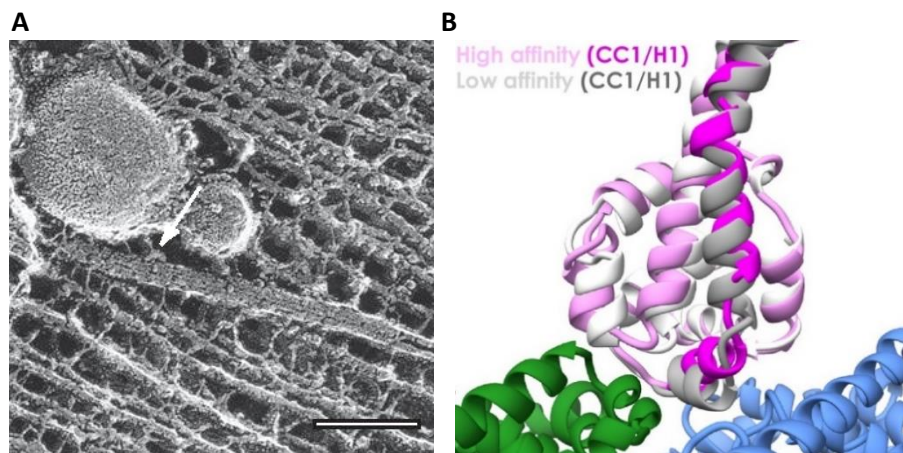


**Figure 37: MTs constitute tracks for neuronal transport of vesicle.** (A) picture from electron microscope showing a vesicle transported by a molecular motor (arrow) on MTs, from Hirokawa *et al.*, 2010. (B) 3D representation of interaction between tubulin dimer (green and blue) and dynein motor binding domain (pink), from cryo-electron microscopy in Lacey *et al.*, 2019.

## ii. Microtubules associated proteins (MAPs) acting as points

The dynamic stability of MTs, essential for neuronal functions (Feinstein & Wilson, 2005) and vesicular transport, is regulated by microtubule-associated proteins (MAPs). These proteins interact with MTs to locally regulate cytoskeletal assembly and/or stability due to their compartmental specificity.

For example, **Tau** is known to regulate MT dynamics. It binds directly to MTs and stabilizes their axonal dynamics by promoting polymerization and assembly of tubulin and inhibiting its depolymerization (Buée et al., 2000; Feinstein & Wilson, 2005; Venkatramani & Panda, 2019). But tau is also known as a direct modulator of anterograde transport due to its ability to inhibit the binding of kinesins (-1 and -3) to MTs (Guedes-Dias & Holzbaaur, 2019). Homeostasis of Tau is crucial because its excessive binding to MTs

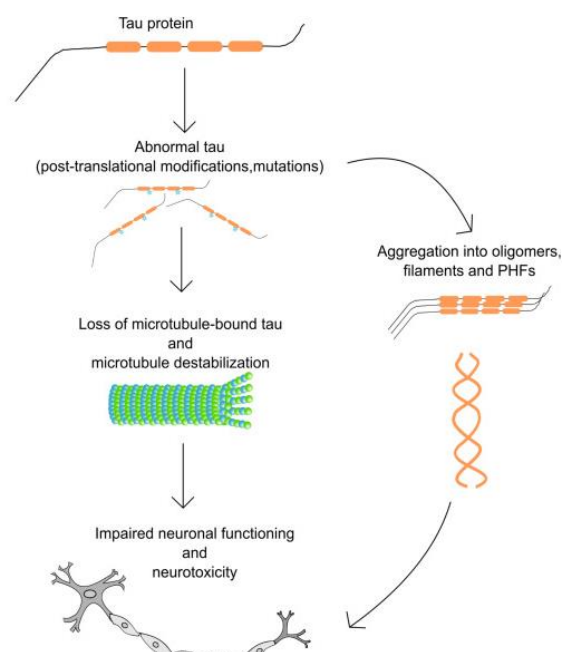


**Figure 38: Tau homeostasis is crucial for MT stabilization which directly affects neuron survival.** From Venkatramani *et al.*, 2019

suppresses the dynamics of MTs, leading to cell death (Feinstein & Wilson, 2005). Conversely, the lack of Tau binding on MTs, caused by gene mutations or hyper-phosphorylation in AD (Kopke et al., 1993), destabilizes the MT network, leading to cell death (Feinstein & Wilson, 2005; Venkatramani & Panda, 2019) (figure 38). In AD, Tau phosphorylation is thought not only to reduce Tau affinity for MTs but also to promote Tau aggregation which finally lead to neurofibrillary tangles production, an AD hallmark.

Tau is part of the MAP2/Tau family of MAPs. Tau and MAP2 are both found in neurons, but show compartment-specific localization as MAP2 is found mainly in somatodendritic regions while tau is found in axons (Deshpande et al., 2008; Dotti et al., 1988; Gumy et al., 2017; Lipka et al., 2016) (figure 39). Although MAPs share the ability to stabilize MTs (Dehmelt & Halpain, 2004), they have their own peculiarities. For example, it has been recently shown that **MAP2** acts as a filter in the proximal axon to select DCVs transported by both kinesin-3 and kinesin-1, therefore regulating axonal transport (Gumy et al., 2017; Kelliher et al., 2019).

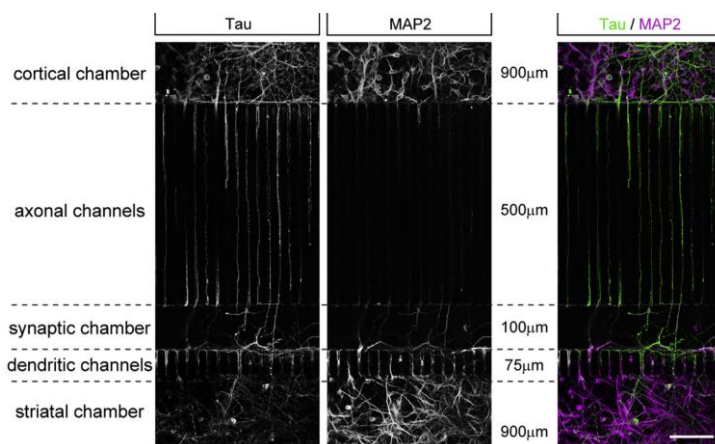


**Figure 39: Tau is mostly axonal whereas MAP-2 is dendritic.** Tau and MAP2 stainings within a microfluidics device, from Virlogeux et al., 2018

**MAP9, Doublecortin (DCX)** and its homolog **DCLK1** also deserve mention as MAPs because they have been found to control polarized cargo transport in dendrites. These three MAPs bind to both the dendritic MTs, based on their phosphorylation, and the motor domain of kinesin-3. They act as a local signal to enhance the motor activity of kinesin-3 and inhibit the transport of kinesin-1 into dendrites thus regulating dendritic outgrowth and branching (Monroy et al., 2020). DCX promotes transport by increasing KIF1A affinity for MTs by a factor two, thus avoiding its detachment from MTs (Lipka et al., 2016). The depletion or mutation of DCX or DCLK1 impairs the transport of DCVs and SVPs by disrupting the DCX/KIF1 interaction thus reducing the run length of KIF1. In humans, DCX mutations

have been found in X-linked lissencephaly and double brain cortex syndrome (Gleeson et al., 1999) causing intellectual disabilities and epilepsy.

**Spastin** is known for its role of regulating the stability and integrity of MTs by severing them. When spastin is mutated or deleted, MT cutting off is reduced and axonal transport is impaired, leading to axonal swelling in cortical neurons and appearance of Hereditary Spastic Paraplegia (HSP) in humans (Fassier et al., 2013; Millecamps & Julien, 2013; Tarrade et al., 2006).

To sum up, MAPs are important indicators and regulators of local, compartment specific MTs dynamics. However, their MTs binding properties can be influenced by tubulin PTMs (Fukushima et al., 2009), which then appear as additional regulators of MT dynamics.

### iii. Tubulin PTMs

Neuronal transport in a compartment can also be spatially and temporally regulated by specific PTMs on tubulin, such as acetylation, (de)tyrosination, poly-glutamylation, phosphorylation, polyglycylation and palmitoylation, through the regulation of MT dynamics and motor affinity (Fukushima et al., 2009). Here, we will focus on two of them for their new insights and relevance for neurological disorders (NDs): acetylation and tyrosination.

**Acetylation** (addition of a  $-CO-CH_3$  group) by  $\alpha$ TAT1 on K40 of  $\alpha$ -tubulin, in the MT lumen, is believed to promote the persistence of MTs in the cell. It strengthens the stability of old MTs making them resilient to mechanical stress thus preserving stable connections (Kelliher et al., 2019; Magiera et al., 2018; Sadoul et al., 2018). Consequently, acetylated MTs are more stable and highly prone to bind with molecular motors (Dompierre et al., 2007), thus promoting an efficient neuronal transport (Sadoul et al., 2018). Indeed, physiological acetylation levels are crucial for neuronal transport as it has been shown to be defective in a  $\alpha$ TAT1 knockout mouse model (Even et al., 2019). Furthermore, several diseases are linked to a reduced acetylation of tubulin: Charcot-Marie-Tooth, AD, HD, PD, Amyotrophic Lateral Sclerosis (ALS) and more generally, ciliopathies, bleeding disorders or cancer (Dompierre et al., 2007; Fukushima et al., 2009; Magiera et al., 2018; Sadoul et al., 2018). Interestingly, the increase in acetylation by inhibiting deacetylation enzymes (HDAC6, SIRT2) has been shown to stimulate kinesin-1 mediated transport by increasing its binding to MTs and to rescue some phenotypes in mouse model of NDs (Dompierre et al., 2007; Fukushima et al., 2009; Magiera et al., 2018) (figure 40).

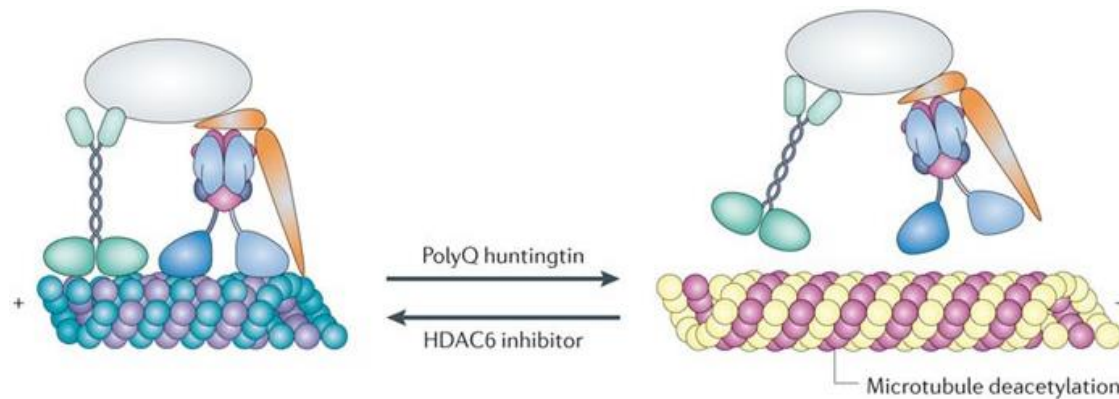


**Figure 40: MT acetylation regulates molecular motor binding to MTS.** Scheme from Millecamps & Julien, 2013. Light green: kinesin, blue: dynein, orange: dynactin.

**(De)tyrosination** of  $\alpha$ -tubulin consists in the removal of a tyrosine residue on its C-terminal by a tubulin carboxypeptidase (TCP) or its replacement by the tubulin tyrosine ligase (TTL). Despite that identity of TTL has been discovered for many years, TCP identity has just been identified (Aillaud et al., 2017). The tyrosination of MTs is directly related to their dynamics and is a marker of a MTs population, as it is present in the newly formed MT localized in distal regions of neurites such as growth cones and absent in stable and long-lasting MTs (Fukushima et al., 2009; Sadoul et al., 2018). Although no ND has so far been described as direct result of a dysregulation of this detyr-tyr cycle (Sadoul et al., 2018), this specific tubulin PTM is important because it can modulate neuronal transport by selecting molecular motors (Konishi & Setou, 2009). For example, detyrosination inhibits the disassembly of MTs by preventing the binding of molecular motors responsible for MT depolymerization (kinesin-13) (Peris et al., 2009; Sadoul et al., 2018).

**Poly- or de-glutamylaton** of tubulin monomers constitute another type of tubulin PTMs where the glutamate amino acid is incorporated, forming a side chain branching from the main peptidic chain of the tubulin (Janke & Magiera, 2020). This PTM is of interest because the dysregulation of its equilibrium state, caused by changes in the genes coding the enzymes responsible for deglutamylation (CCP1) or polyglutamylaton (TLL1), impacts MT biological functions. Indeed, an increase in polyglutamylaton, caused by a decrease in CCP1 expression, increases neurodegeneration, supposedly by impairing axonal transport and MT dynamics, thus impairing synaptic transmission. This is the case for several mouse models generating respiratory disorders, photoreceptor degeneration in the retina, cerebellar atrophy and motor neuron degeneration (Magiera et al., 2018; Shashi et al., 2018). In Humans, mutation in the CCP1 gene causes a developmental delay as well as a cerebellar atrophy and motor neuropathy (Shashi et al., 2018).

Therefore, tubulin PTMs are able to regulate axonal transport in neurons by changing MT properties but they may not be sufficient on their own (Walter et al., 2012). Indeed, tubulin PTMs combined with MAPs and molecular motors, form a “code” to regulate neuronal transport (Fukushima et al., 2009).

#### iv. Cracking the tubulin code

Compartment specificity, MT polarity, tubulin PTMs and MAPs combine to create or translate a plethora of cellular situations to precisely regulate neuronal transport. All these combinations are referred to as the “tubulin code” (Kelliher et al., 2019; Verhey & Gaertig, 2007). Many studies worked to crack this code to understand the coordination between MT polarity, tubulin PTMs and MAPs. For example, we now know one of the correlations between MT polarity, tubulin PTM and recruited molecular motors. In dendrites, acetylated (and detyrosinated) MTs plus-end point towards the cell body and favor the transport mediated by the molecular motor kinesin-1 (KIF5C- see next paragraph for insights on molecular motors). Inversely tyrosinated MTs point their plus-end towards the distal part of the dendrite and favor kinesin-3 mediated transport (Tas et al., 2017) through its recruitment mediated by DCLK1, DCX or MAP9 (Fukushima et al., 2009; Kelliher et al., 2019; Konishi & Setou, 2009; Lipka et al., 2016; Monroy et al., 2020; Sadoul et al., 2018) (figure 41). In this scenario, detyrosination, acetylation and/or absence of DCX/DCLK1/MAP9 on MTs would act as directional signals for kinesin-1-mediated transport to the axon by increasing its binding to MTs (Konishi & Setou, 2009; Monroy et al., 2020). This molecular motor recruitment depending on the combination of tubulin PTMs and MAPs appears important, especially for directing kinesins carrying vesicles in both axons and dendrites such as KIF1A and KIF21B (Lipka et al., 2016).

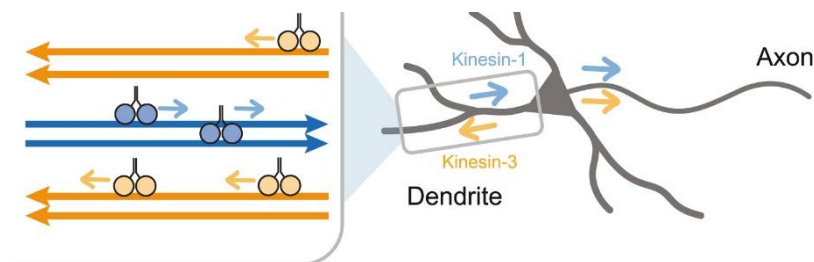
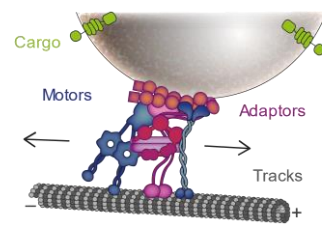


**Figure 41: kinesin-1 and -3 exhibit different behavior according to MT PTM.** Orange MT: tyrosinated MT, blue MT: acetylated MT, orange kinesin: kinesin-3 and blue kinesin: kinesin-1, from Tas et al., 2017.



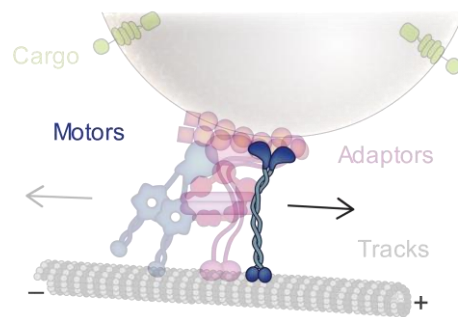
## b. Molecular motors

In order to be transported or trafficked from one compartment to another, cargoes cannot rely on mere diffusion because this mode of transport would be too slow for them to reach their destination. Therefore, active transport is necessary and is ensured by molecular motors. These proteins use the energy of ATP hydrolysis to move along MTs. Depending on the directionality of a cargo, specific motors ensure transport through MTs: kinesins and dynein (Hirokawa et al., 2010). Although initially thought to function separately, new modes of operation have been discovered based on a cooperation between motors and the regulation of their properties by adaptors. Finally, we will focus on how neuronal transport has been examined in this work and why it is important to study neuronal transport.



### i. Kinesins are responsible for axonal anterograde transport

Kinesins (KIFs) are molecular motors mainly responsible for anterograde transport of vesicles in axons. They are crucial proteins because they are involved in brain functions such as learning and memory, neuronal morphology and function, development and plasticity (Hirokawa & Tanaka, 2015; Muhia et al., 2016; Y. V. Zhang et al., 2017). Understanding their structures, functions, specificities, and regulations is of the utmost importance for characterizing therapeutic strategies based on neuronal transport. Indeed, dysregulated or dysfunctional KIFs are involved in some NDs such as KIF17 in Schizophrenia, KIF3 in ALS, KIF1A in SGP-30, KIF5 in SPG-10 and KIF21B in intellectual disability (Asselin et al., 2020; M. V. Hinckelmann et al., 2013; Hirokawa & Tanaka, 2015). This work focuses mainly on KIF5C and KIF1A (described later) as they are the kinesins dedicated to axonal and anterograde transport of the cargoes studied.



#### 1. Kinesin structure serves kinesin functions

Forty-five kinesin proteins belong to the kinesin superfamily, which contains three subgroups based on the location of the motor domain where ATP hydrolysis occurs: at the N-terminal (N-KIFs, 39 in mammals), at the center of the KIF (M-KIFs, 3 in mammals) or at the C-terminal (C-KIFs, 3 in mammals) (Hirokawa et al., 2010; Maday et al., 2014). Since N-KIFs are predominant and of interest in this work, we will focus on these kinesins, which are known to move towards MT plus end, as opposed to C-KIFs.

This N-KIF group was then subdivided into 15 subfamilies accordingly to their structure, functions, or cargo (Hirokawa et al., 2010). The kinesin structures, although dependent on its sub family, are similar in that they all have a motor domain (in blue in figure 42) linked to the rest of the kinesin by a neck linker (Vale, 2003). This 15-amino acid segment is mobile and flexible in the presence of ADP. Follow the neck linker, a coiled-coil domain (in grey in figure 42) with a variable length depending on the kinesin, is important for protein-protein interactions. This stalk domain is followed by the tail domain, the C-terminal part of the kinesin, which can display specific domains such as a Pleckstrin homology (PH). This is the case of KIF1A which exhibits a PH domain (in purple in figure 42), considered to be crucial for the binding of the cargo (for more details see chapter 3 2-b-i). Thus, the kinesin structure allows for its binding to MTs, cargo and several other adaptors capable of controlling kinesin activity and cargo binding (Verhey & Hammond, 2009).

Most kinesins form dimers. KIF5C as a dimer is composed by two kinesin heavy chains (KHC) (containing the motor domain, coiled-coil stalk) and two kinesin light chains (KLCs, green in figure 42).

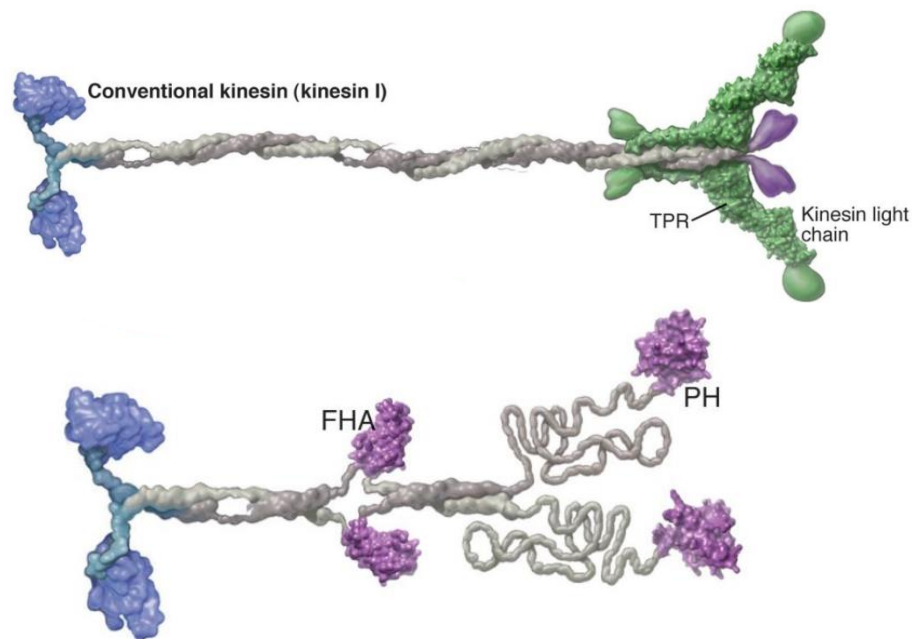


**Figure 42: 3D representation of kinesin-1 and -3 structure.** Blue: microtubule binding domain, gray: coiled-coil and stalk domains, purple: PH domain in kinesin-3, green: kinesin heavy chains, from Vale, 2003.

## 2. Self-inhibition of kinesin regulates neuronal transport

The number of active kinesins within a cell is crucial for many cellular processes such as axon outgrowth (kinesin-3), cargo localization in dendrites and synapse formation (kinesin-4), size and density (Kelliher et al., 2018, 2019; Niwa et al., 2016). In fact, kinesins control axonal anterograde transport and, consequently, the number of vesicles reaching their target area. In order to regulate this vesicle flow to save time and resources, to prevent unnecessary degradation of ATP or saturation

of MT tracks, molecular motors can be activated or inhibited through autoinhibition (Tomishige et al., 2002; Verhey & Hammond, 2009).

In the absence of cargo, kinesin dimers are found free in the cytoplasm under their self-inhibited conformation (Verhey & Hammond, 2009), although this is not yet clear for KIF1A (for more details, see chapter 3 2-b-ii). Autoinhibition function is allowed by the structure of kinesin: self-inhibited kinesins are folded which joins the non-motor regions to the motor domain, inhibiting the ATPase activity (Verhey & Hammond, 2009). More precisely for kinesin-1, the tail binds to the motor and the coiled-coil domain preventing the undocking of the neck linker responsible for the release of ADP (Kaan et al., 2011; Verhey & Hammond, 2009). Upon activation signals, such as binding to regulatory proteins (JIP1 for kinesin-1) or cargo, kinesin becomes activated and binds to MTs.

### 3. Kinesin active movement

Once on the MT tracks, each motor domain of the dimerized kinesin is bound to a tubulin heterodimer of the same protofilament by electrostatic interactions between the positive charges of the motor domain and the negative charges of the tubulin (Guedes-Dias & Holzbaaur, 2019). After ATP binding to the leading head (right blue structure figure 43), the neck linker is docked to the motor domain with its COOH terminus pointed towards the plus-end of the MTs. The hydrolysis of ATP then provides the energy necessary for the conformational change of the neck linker (red in 1 figure 43) which results in its forward motion, displacing any (macro)molecule attached to it, including the other motor domain. Due to its ability to modify conformational changes on the ATP binding, the neck linker is considered as the power stroke. Indeed, one study underlines the importance of the length of this neck linker for its processive motor function (Shastry & Hancock, 2010). Then, the new main motor domain binds tightly to the new tubulin site and produces a force that pushes the cargo forward by 8 nm, which corresponds to the length of a tubulin heterodimer (Guedes-Dias & Holzbaaur, 2019; Vale & Milligan, 2000). Finally, ADP is released by the catalytic core of the first motor domain and another ATP molecule binds to the new leading motor domain. This mechanism is described as 'hand-over-hand' manner.

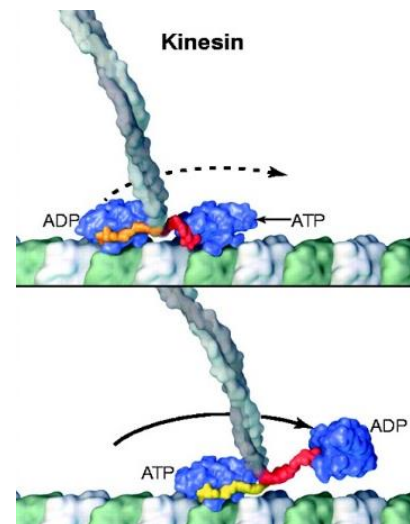


**Figure 43: kinesin progression on MTs is ATP dependent.** Blue: microtubule binding domain, red: neck linker. Scheme from Vale & Milligan, 2000.

#### 4. Kinesin specificities

Although the N-kinesins share a homology of 30-60% of their motor domain (Hirokawa et al., 2010) and may be redundant in their functions, some specificities can be noted, even between two motors within a same sub-family. The peculiarities in their structure create specificity of cargo, speed and processivity for each kinesin.

##### a. Cargo specificity?

This is for example the case of the kinesin-3 family containing KIF1A, KIF1B $\beta$  both carrying SVPs (Niwa et al., 2008; Okada et al., 1995; C. Zhao et al., 2001), KIF1B $\alpha$  transporting mitochondria and KIF13B transporting PiP<sub>3</sub> (Hirokawa et al., 2010). Interestingly, KIF1B $\alpha$  and - $\beta$  originate from the same gene and differ only

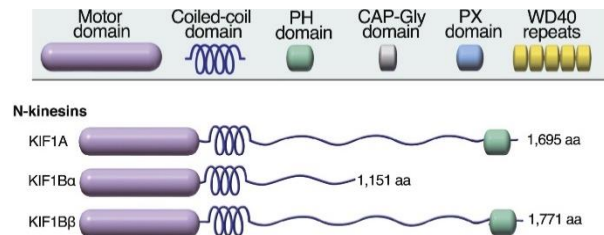


**Figure 44: kinesins within a family exhibit different structures.** Purple: motor domain, blue: coiled-oil domain, green: PH domain, from Hirokawa et al., 2010.

by an alternative splicing of mRNA (figure 44). These differences in the structure functionalize these two kinesins very differently: the first drives mitochondrial transport whereas the second one is important for SVP transport in neurons and for the one of mRNA-protein complex in glia (Hirokawa et al., 2010). Thus, each kinesin seems to have its cargo.

However, this cargo specificity may not be as specific: a kinesin can transport different types of cargo (KIF1B $\beta$ : SVPs and mRNA-protein complex, KIF5C: mRNA-protein complex, mitochondria, DCVs, APP vesicles, endosomal vesicles), but one cargo can also be transported by different kinesins (redundancy of the motors). For example, mitochondria are known to be transported by KIF1B $\alpha$  and/or KIF5C, DCVs by KIF1A and/or KIF5C (Arpağ et al., 2019; Gumy et al., 2017), TrkB-vesicles by KIF21B or KIF5 and mRNA-protein complex by KIF1B $\beta$  and/or KIF5 (Hirokawa et al., 2010) (table 1).

## b. Kinesin motility characteristics

In neurons, and mainly axons, two types of kinesin transport are described: slow transport of cytosolic or cytoskeleton proteins (less than 0.1  $\mu\text{m/s}$ ) and fast transport of membranous organelles (between 0.5 and 4  $\mu\text{m/s}$ ) (Hirokawa et al., 2010; Hirokawa & Tanaka, 2015). Although the role of fast axonal transport (FAT) within long range connection is easily understood, slow axonal transport (SAT) is also important because its impairment is believed to contribute to severe NDs like Charcot-Marie-Tooth, Amyotrophic Lateral Sclerosis, and PD (Gabrych et al., 2019; Yuan et al., 2017). SAT is mainly processed by kinesin-1 members (Hirokawa & Tanaka, 2015).

The rate of FAT depends on many parameters (like tubulin PTMs, MAPs, adaptors) including the type of kinesin. In fact, based on their affinity for MTs and their ability to release ADP, kinesins have intrinsically different speed and processivity (Hirokawa et al., 2010). For example, the transport of Kinesin-1 family has been shown to be slower than the one of kinesin-3 family (respectively and on average, 1-2 and 2-3  $\mu\text{m/s}$ ) which is also more processive (for more details see chapter 3 2-b-iv)(Arpağ et al., 2019) (table 1 and figure 45).

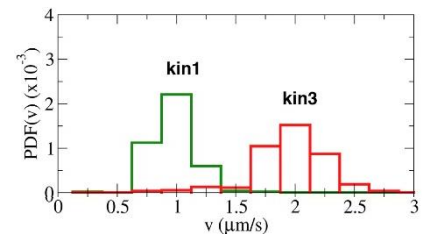


**Figure 45: kinesins display specific velocity distributions.** Velocity distribution for kinesin-1 (green) and kinesin-3 (red). PDF ( $v$ ): probability distribution function, from Arpağ et al., 2019.

The following table (table 1) recapitulates the kinesin specificities for KIF5C, KIF1A and KIF21B, the three kinesins studied in this project (publications 1,2,3 and annex 1) in term of cargoes, speed, adaptors and their impact in NDs.

## c. Compartment specificity

For a long time, it has been thought that kinesins were specific to axon or dendrite. Recently, it was discovered *in vitro* that most kinesins operate only in axons, while some of them (KIF1A, -B, -C, KIF21A, -B) functioned in both compartments (Asselin et al., 2020; Lipka et al., 2016). The compartmentalization of kinesins relies on tubulin PTMs and the ability of MAPs to concentrate kinesins (Lipka et al., 2016) by controlling the entry of a motor into a compartment (Kelliher et al., 2019). For example, MAP2 acts as a filter within the proximal axon by selecting only DCVs transported by both kinesin-3 and kinesin-1 (Gumy et al., 2017), while septin 9 prevents vesicles transported by kinesin-1 to reach the dendrites (Karasmanis et al., 2018; Kelliher et al., 2019).

<b>Kinesin family</b>	<b>KIF</b>	<b>cargoes</b>	<b>Speed/run length</b>	<b>Adaptor/regulators</b>	<b>Related NDs</b>	<b>references</b>
<b>Kinesin-1</b>	KIF5C KIF5A	Secretory vesicles DCVs APP vesicles Endosomal vesicles TrkB vesicles GABA <sub>A</sub> r Organelles mitochondria mRNA-protein complex	Run length: 1 $\mu$ m (100 steps per run) Speed: between 1 and 2 $\mu$ m/s	JIP-1 Milton-Miro HAP1 HTT	SPG-10 (KIF5A) Lissencephaly (pachygyria) and microcephaly (KIF5C)	(Cavallin et al., 2016; Colin et al., 2008; Guedes-Dias & Holzbaur, 2019; Muresan & Muresan, 2005; Reid et al., 2002; Twelvetrees et al., 2010)
<b>Kinesin-3</b>	KIF1A (KIF1B $\beta$ )	Secretory vesicles SVPs DCVs BACE-1 vesicles	Run length: 8 $\mu$ m (500 steps per run) Speed: between 2 and 3 $\mu$ m/s	DENN/MADD Doublecortin KBP Arl8	SPG-30, Goldberg-Shprintzen syndrome	(Guedes-Dias & Holzbaur, 2019; Kevenaar et al., 2016; Lipka et al., 2016; Niwa et al., 2008; Okada et al., 1995)
<b>Kinesin-4</b>	KIF21B	Endosomal vesicles NMDAr TrkB vesicles	Run length: between 6 and 12 $\mu$ m Speed: around 0.4 $\mu$ m/s	TRIM3	Intellectual disability, brain malformations, microcephaly. Multiple sclerosis	(Asselin et al., 2020; Ghiretti et al., 2016; Gromova et al., 2018; Muhia et al., 2016)

**Table 1: KIF5C, KIF1A and KIF21B specificities and related NDs**

## 5. *Modulators of kinesin activity*

Once kinesins are activated, several processes in addition to MAP functions can regulate their activity, thus affecting neuronal transport. This is, for example, the case of modulator proteins capable of binding kinesins, or of PTMs able of influencing the activity of kinesin or the number of kinesins on a vesicle.

### a. Kinesin modulator: example of KBP

The kinesin inhibitor protein (KBP) is required for axonal growth and maintenance through its regulation of organelle axonal transport and MT dynamics (Kevenaar et al., 2016; Lyons et al., 2008). It interacts directly with different types of kinesins such as KIF1A (SVP transport) and KIF18A (MT depolymerization) to block their activity by binding to their motor domain, thus preventing their attachment to MTs (Kevenaar et al., 2016; N. Siddiqui & A. Straube, 2017). Interestingly, when KBP levels are reduced by nonsense mutations, it causes the Goldberg-Shprintzen syndrome leading to intellectual disability, microcephaly and axonal neuropathy (Kevenaar et al., 2016; Lyons et al., 2008). These defects may be caused by an accumulation and mislocalization of mitochondria (Lyons et al., 2008) but also by the increase in anterograde axonal transport which causes an accumulation of SVPs at the axon terminal, as seen in animal model where KBP was knocked down (Kevenaar et al., 2016; Lyons et al., 2008).

### b. Kinesin PTM: example of phosphorylation

Another way to modulate kinesin activity is based on kinesin PTMs. One of these is the phosphorylation of the motor domain of KIF5C on S176 by JNK3 (Morfini et al., 2009; Padzik et al., 2016). It has been shown that JNK3 phosphorylation of KIF5 promotes the dissociation of KIF5 from MTs when not bound to the cargo but facilitates its transport when it is bound to a cargo (Morfini et al., 2009; Padzik et al., 2016). The non-physiological level of kinesin phosphorylation is believed to participate in NDs such as AD or HD (Morfini et al., 2009).

### c. Kinesin number on a vesicle

The motility of kinesins can also depend on the number and types of kinesin present on a vesicle. In fact, it is possible to find up to four kinesins on the same SVP (Hayashi et al., 2018). The number of motors on a vesicle has been shown to modulate transport parameters such as vesicle run length, kinesin force, vesicular binding rate to MTs (Gutiérrez-Medina et al., 2018) or dwell times at MT intersections (Osunbayo et al., 2015). A recent single molecule study showed that this is specifically the case for SVPs, as the number of kinesins on an SVP can regulate its transport by changing the run length and the speed of the SVP through changes in the MT binding rate (Furuta et al., 2013; Guedes-Dias & Holzbaaur, 2019; Hayashi et al., 2018) (figure 46). The change of vesicular speed based on the number of kinesin on a vesicle could be explained by the load distribution on the motors; the more kinesins are present on a vesicle the less heavy is the load for each kinesin (Hayashi et al., 2018). Interestingly, the number of kinesins on a vesicle can be regulated by adaptors/regulators. ARL8, for example, has been shown to decrease the number of kinesins on a SVP resulting in a striking decrease in their run length (Hayashi et al., 2018).

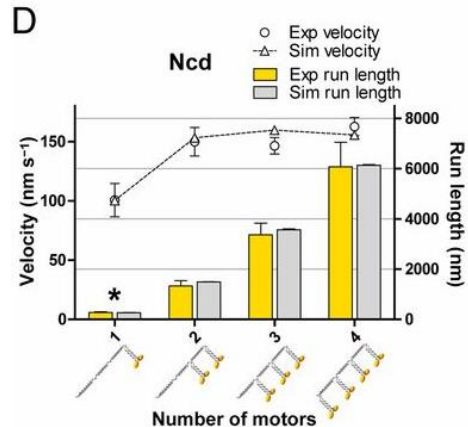


**Figure 46: kinesin number on a vesicle influences its velocity and run length.** Velocity and run length evaluation according to the number of kinesin-14 on a vesicle, from Furuta et al., 2013

Although increasing the number of a type of kinesin on a vesicle has a summative effect on their properties, this may not be the case with heterogenous kinesins on one vesicle. For example, *in vitro* data show that a cargo co-transported by kinesin-1 and kinesin-3 will show the speed of a kinesin-1-transported vesicle due to a dominant prevalence of kinesin-1 (Arpağ et al., 2019) and as a result of stochastic effects (Furuta et al., 2013; Kunwar et al., 2008) (figure 47). Collaborative transport between kinesin-3 and kinesin-1 has been demonstrated for 20% of DCVs in *Drosophila* neurons (Lim et al., 2017) and is thought to control the entry of cargoes into a neuron. Without KIF1A, KIF5 alone is not able to drive long-distance transport of DCVs in DRG axons through MAP2 regulation (Gumy et al., 2017).

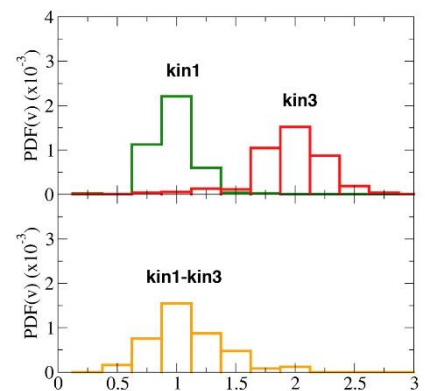
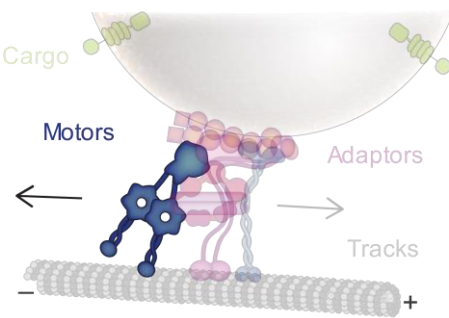


**Figure 47: involvement of different kinesins on one vesicle display specific velocity distribution.** Velocity distribution for kinesin-1 (green), kinesin-3 (red) and kinesin-1 and 3 (yellow). PDF (v): probability distribution function, from Arpağ et al., 2019.



## ii. Retrograde transport: dynein

Dynein-mediated transport is crucial for neuronal functions because it prevents accumulation of old, toxic or misfolded protein and supports synapse-cell communication in the body by carrying signaling endosomes through retrograde transport of cargo (M. V. Hinckelmann et al., 2013; Millecamps & Julien, 2013; Olenick & Holzbaaur, 2019). In mice, deletion of the dynein heavy chain gene is embryonic lethal (Harada et al., 1998) and in humans point mutations on any dynein subunit or dynein regulator gene lead to severe NDs like CMT, malformations of cortical development, intellectual disability, spinal muscular atrophy, perry syndrome or HSP (Lipka et al., 2013).



### 1. The structure of dynein serves the function of dynein

Contrary to kinesins, only one dynein isoform is responsible for neuronal transport: dynein-1 (Cianfrocco et al., 2015; Reck-Peterson et al., 2018). Therefore, since several retrograde cargoes are essential for neuronal functions, dynein-1 is capable of carrying a plethora of cargoes such as endosomes, autophagosomes, lipid droplets, mitochondria, mRNAs and secretory vesicles (Cianfrocco et al., 2015; Guedes-Dias & Holzbaaur, 2019; Reck-Peterson et al., 2018).

Dynein is formed as a dimer in which each monomer contains (Cianfrocco et al., 2015) ( figure 48):

- a microtubule binding domain, which binds to a similar MT kinesin binding site, in the cleft between  $\alpha$ - and  $\beta$ -tubulin
- a motor domain, carried by heavy chains, forming a ring composed by 6 sub-domains involved in ATP hydrolysis and in conformational changes. The motor domain is also known to interact with Lis1, one of the dynein regulators.
- a linker that act as a power stroke.

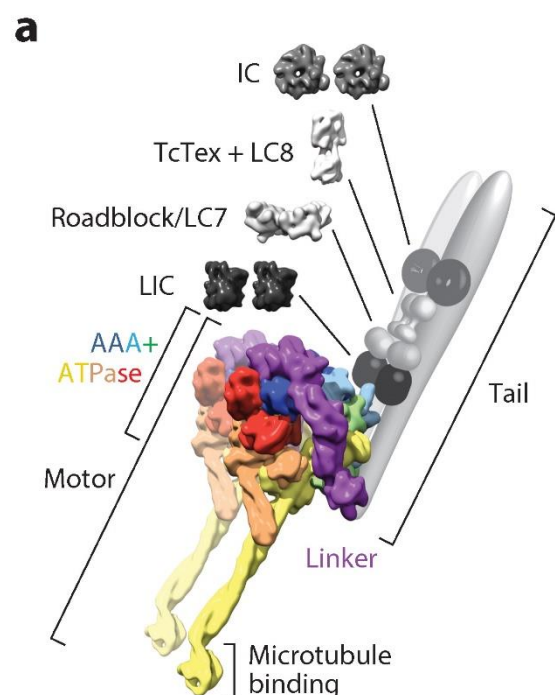


Figure 48: dynein-1 structure, from Cianfrocco et al., 2015

- a tail as a scaffold for dimerization, other chain attachments (intermediate, light and light intermediate) and cargo binding. Intermediate chains (ICs) are important because they can bind to other major dynein regulators: dynactin and Nudel/NudE.

Dynein in the cytoplasm is also known to first form an inhibited dimer. Once activated by its regulator or cargo association, the dynein binds to the plus-end of MTs and begins to move. Since the mechanism of ATP hydrolysis and subsequent movement on MTs share a similar mechanism with that of kinesin, with the linker as a power stroke, it will not be explained here but it is fully and well described in Cianfrocco et al., 2015. However, unlike kinesin, the step size of dynein can range from 8 to 32 nm (Guedes-Dias & Holzbaaur, 2019).

## 2. Dynein activators and regulators

The retrograde motor is modulated by many regulators which compensate for the lack of specificity in the transport of cargoes (Cianfrocco et al., 2015; Reck-Peterson et al., 2018) (figure 49). These modulators can be cargo specific and can modify the dynein run lengths (from 5 to 10 mm) and the dynein speed (from 0.8 to 1.3  $\mu\text{m/s}$ ) (Guedes-Dias & Holzbaaur, 2019). The following list of such regulators and activators is non exhaustive and focuses primarily on their roles.

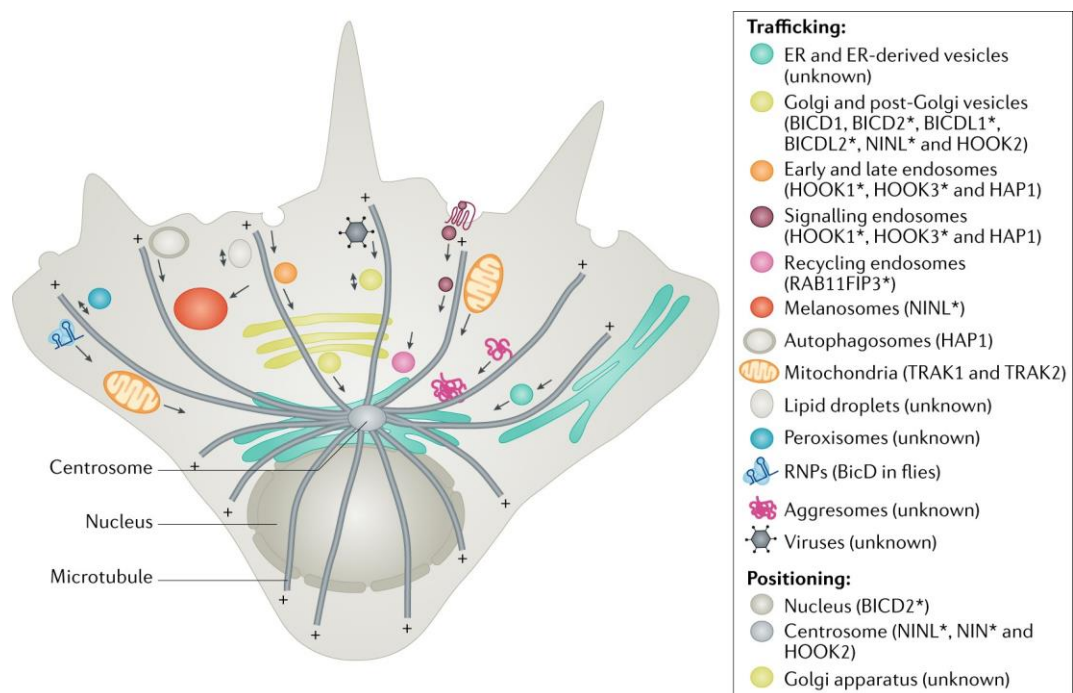


Figure 49: dynein regulators specify dynein mediated transport of cargoes. From Reck-Peterson *et al.*, 2018

a. Lis1 as a dynein activator that release autoinhibition

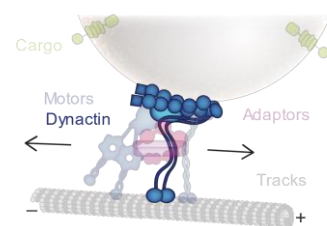
The role of **Lis1** has been extensively studied in this past year (Elshenawy et al., 2020; Htet et al., 2020; Marzo et al., 2020). Thanks to recently developed techniques such as cryo-EM and single molecule experiments, we now better understand the role of this protein that, when mutated in humans, leads to lissencephaly accompanied by a smooth brain surface, cognitive defects and seizures (Cianfrocco et al., 2015; McKenney, 2020). Lis1 is now considered as a dynein activator because it allows the release of dynein autoinhibition thanks to its direct link with the dynein motor domain which causes important conformational changes (Cianfrocco et al., 2015; Htet et al., 2020). But more than activating dynein, Lis1 seems also to promote other adaptor or even other dynein dimers recruitment on dynein. This recruitment regulates dynein motility (Elshenawy et al., 2020; Htet et al., 2020; McKenney, 2020) and the consequent transport of cargoes such as mitochondria, endosomes and lysosomes (M. J. Egan et al., 2012). Once the dynein is mobile, Lis1 detaches from the complex.

b. NudE as a compartment regulator

**Nudel/NudE**, two mammalian homologues (also called Ndel1) interact *in vivo* with both Lis1 and the dynein intermediate chain (DIC). They are thought to increase Lis1 effect on dynein motility by helping its binding to dynein (Cianfrocco et al., 2015). The Knock out mice of one of them is sufficient to reduce the brain volume or to cause non-viability (Cianfrocco et al., 2015). More specifically, Ndel1 is important for regulating dendritic transport and for maintaining axonal identity. Indeed, its enrichment within the AIS redirects the dendritic cargo to the dendrites by transferring the cargo to the dynein present in the AIS (Guedes-Dias & Holzbaaur, 2019; Kelliher et al., 2019).

c. Dynactin as transport initiator and activator

**Dynactin** is known as a dynein activator because it initiates transport when the dynein is in an open conformation and improves its processivity (K. Zhang et al., 2017). This large structure is composed of a cargo-binding domain called the shoulder complex that can be related to an actin filament (Cianfrocco et al., 2015; Maday et al., 2014), a long



and thin motor binding domain (p510<sup>Glued</sup>) and ends with a MT binding domain, which allows dynactin to bind to both dynein and MTs (figure 50). Therefore, due to its structure, dynactin can promote the MT binding of dynein (Guedes-Dias & Holzbaaur, 2019). When the structure of dynactin is compromised by a mutation on p150<sup>Glued</sup>, for example, its retrograde function is impaired and leads to severe NDs

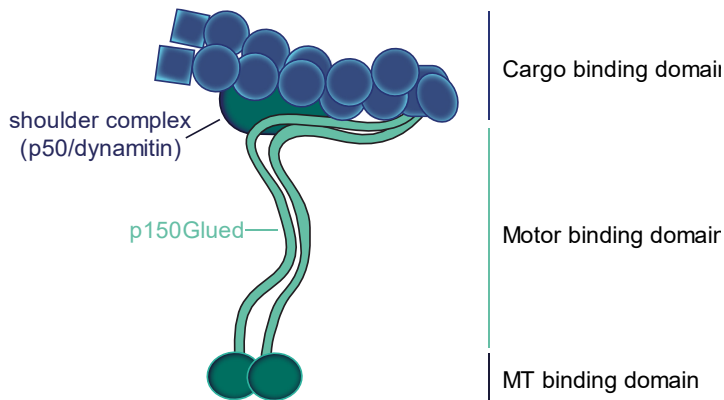


**Figure 50: dynactin structure serves dynein functions.**

such as Perry Syndrome (an aggressive form of Parkinsonism) or other motor neuron diseases (Cianfrocco et al., 2015; Guedes-Dias & Holzbaur, 2019; Lipka et al., 2013; Millecamps & Julien, 2013). On the other hand, and as an example of the importance of protein homeostasis, overexpression of p50/dynamitin in mice leads also to motor neuron degeneration (LaMonte

et al., 2002) through the non-functional dissociation of dynactin (Echeverri et al., 1996; Eckley et al., 1999), thus inhibiting retrograde transport (LaMonte et al., 2002). Interestingly, the affinity of dynactin for MTs depends on the tyrosination level of tubulin (Guedes-Dias & Holzbaur, 2019) and on the MAPs present on MTs as MAP9 is known to inhibit the binding of p150 to MTs (Monroy et al., 2020).

#### d. Hook and BicD as cargo regulators and activating adaptors

Hook and BicD proteins act similarly: each of them can bind to the dynein-dynactin complex to form a tripartite complex, improving its stability (Allan, 2014; Guedes-Dias & Holzbaur, 2019; Olenick & Holzbaur, 2019; Reck-Peterson et al., 2018) (figure 51). As a result, dynein motility is activated, showing longer run lengths (dynein is then highly processive) and higher velocity (Cianfrocco et al., 2015; Guedes-Dias & Holzbaur, 2019; Olenick & Holzbaur, 2019). Hook and a BicD-related protein are also able to increase the number of dynein recruited on a vesicle (which can reach the value of five (Guedes-Dias & Holzbaur, 2019)), further improving the velocity of the vesicle and the force produced (Guedes-Dias & Holzbaur, 2019; Olenick & Holzbaur, 2019; Reck-Peterson et al., 2018). However, they differ from the cargo of which they support the transport. Hook1 has been shown to activate retrograde transport of signaling endosomes only through its association with membranes derived from clathrin-independent endocytosis (Cianfrocco et al., 2015; Reck-Peterson et al., 2018) while BicD is more associated with Golgi vesicles through its interaction with Rab6 (Guedes-Dias & Holzbaur, 2019; Olenick & Holzbaur, 2019; Reck-Peterson et al., 2018).

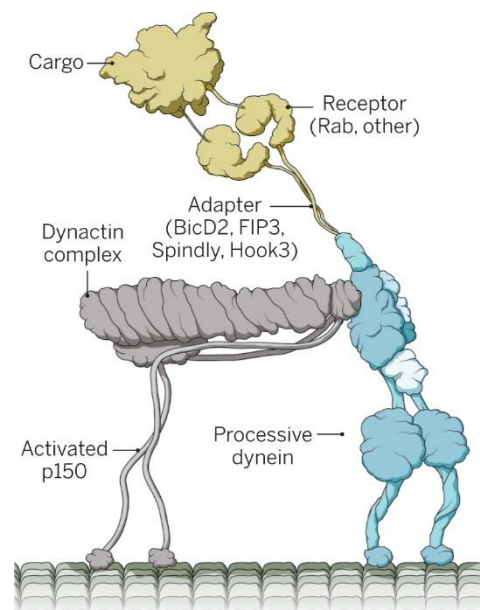


**Figure 51: Hook and BicD acts as dynein regulators and activating adaptors forming a tripartite complex with dynein and dynactin.** From Allan, 2014

To summarize, neuronal transport is performed by molecular motors, dynein and kinesins, which govern the directionality and the speed of the vesicles. However, some regulators or adaptors can modify molecular motor properties such as their autoinhibition, dimerization and localization within the neuron. Interestingly, many of these actors were found on the same vesicle. For example, despite their opposite directions, kinesin and dynein have been found to colocalize on a vesicle (figure 52) (Encalada et al., 2011; Hendricks et al., 2012; Soppina et al., 2009; Szpankowski et al., 2012).

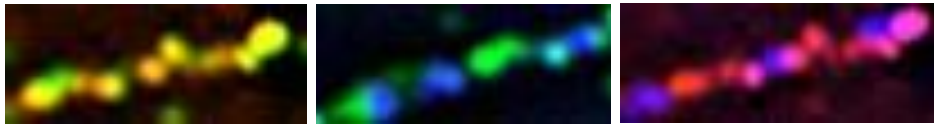
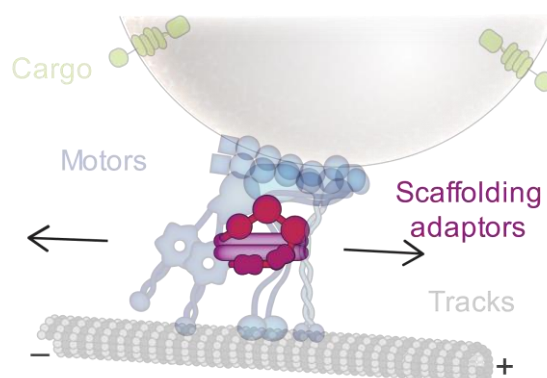


**Figure 52: kinesin and dynein are present on the same vesicle.** Immunostainings of kinesin (green), APP (red) and dynein (blue), from Szpankowski et al., 2012.

Although the reasons why kinesin and dynein can be found on the same vesicle will be explained later, we can first ask how both molecular motors along with their own adaptors can be recruited to the same vesicle. The next part focuses on the proteins that allow this protein scaffold on a vesicle.

### c. Scaffolding adaptors

As we just discussed, many proteins are on board the vesicles: opposite molecular motors, regulators, activators, and adaptors. Therefore, the structural and functional regulations of these actors seem important. These are the roles of scaffolding proteins that enable the formation of an integrated regulatory vesicular unit (Meng-meng Fu & Holzbaur, 2014). These large proteins or complexes have the property of making many interactions with molecular motors, cargoes but also with cytosolic proteins such as kinases. They act structurally as a binding platform to increase the stability of the machinery supporting the transport, functionally as a hub by integrating cellular signals and locally regulating the transport (Meng-meng Fu & Holzbaur, 2014; Gibbs et al., 2015).



### i. Scaffolding of machinery to recruit molecular motors

As one of their properties, most of the scaffolding proteins have the ability to bind to many proteins, including both molecular motors (kinesin and dynein). This is for example the case of huntingtin (HTT) which binds directly to dynein (DIC) and indirectly, through HAP1 interaction, to kinesin (KLC) and dynactin (p150<sup>Glued</sup>) (Meng-meng Fu & Holzbaaur, 2014; Saudou & Humbert, 2016) (figure 53). When HTT is mutated in HD with a polyQ expansion in the N-ter of HTT, HTT interaction with molecular machinery is altered and, specifically, increased between HAP1 and HTT leading to a reduction in motors association with MTs. This impairment of HTT-scaffolding role is responsible for the reduced BDNF transport that causes HD (Gauthier et al., 2004). HTT is also known to scaffold enzymes responsible for the glycolytic pathway on vesicles to provide energy locally (M.-V. Hinckelmann et al., 2016; H. Vitet et al., 2020; Zala, Hinckelmann, Yu, et al., 2013).

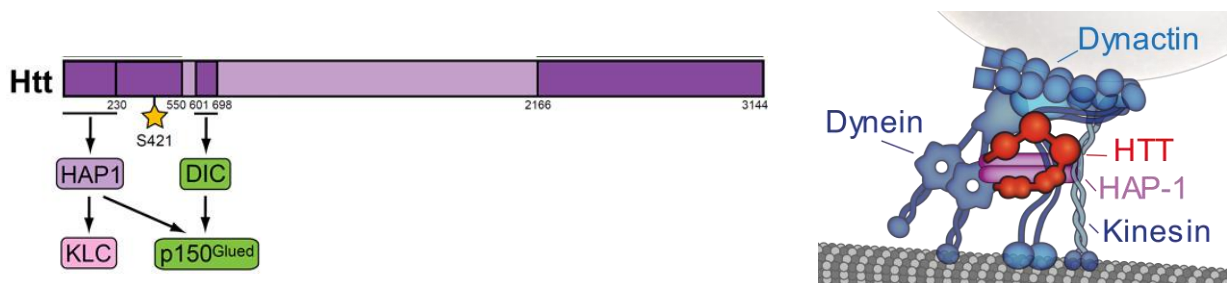


**Figure 53: HTT interacts with both kinesin and dynein acting as a scaffold protein.** Representative schemes of HTT interacting with molecular motors (left: Fu & Holzbaaur, 2014).

Interestingly, the past decade has shown that some regulators that were originally thought to be motor specific are now considered to be scaffolding proteins that bind both motors. This is the case for Hook3 which binds to dynein and KIF1C (Kendrick et al., 2019), JIP-1 which binds to dynein and KIF5 to regulate APP transport (Meng-meng Fu & Holzbaaur, 2013) and BicD related protein (BicDR-1) which coordinates bidirectional transport of DCVs by binding to dynein and KIF1 at early stages of development (Lipka et al., 2016; Olenick & Holzbaaur, 2019).

### ii. Scaffolding of machinery to integrate cellular cues

The second consequence of this binding platform is that it favors the binding of partners or PTMs that act as regulatory signals (Olenick & Holzbaaur, 2019).

#### 1. PTMs on scaffolding proteins: example of phosphorylation

Many kinases are described as adaptive targets of axonal transport such as Akt, GSK3 $\beta$ , ERK1/2, Cdk5, JNK or p38 MAPK, and their dysregulation impact axonal transport in NDs (as in the case of ALS, AD, CMT-2F, HD or PD) (Olenick & Holzbaaur, 2019). JIP-1 and HTT, two major scaffolding proteins, are known to act as molecular switches since when they are phosphorylated – both on S421-, they favor

anterograde transport of their cargo (Bruyère et al., 2020; Colin et al., 2008; Meng-meng Fu & Holzbaur, 2013). JIP-1 is known to be phosphorylated by JNK and appears to be specific for APP-containing-vesicle (Meng-meng Fu & Holzbaur, 2013). Instead, HTT has been shown to be phosphorylated by Akt and/or SGK and to regulate not only the directionality of APP-containing-vesicle, but also BDNF and vamp-7 vesicles (Bruyère et al., 2020; Colin et al., 2008; Humbert et al., 2002; Rangone et al., 2005). It has been found that S421 phosphorylation of HTT increases both the number of kinesin-1 recruited on BDNF vesicles and the affinity of kinesin-1 for MTs (Colin et al., 2008).

## 2. Partner binding

Scaffold proteins are able to integrate a cellular signal thanks to their multiple bindings. For example, calcineurin, the phosphatase that targets HTT dephosphorylation at S421, has been shown to be at the edge of the vesicle (Scaramuzzino *et al.*, *in prep*). The presence of Rab proteins is also an example of the importance of scaffolding proteins as they can sense the environment and translate it into a transport regulation signal by binding to the GTPases protein (White et al., 2015; White et al., 2020). Rab5, for example, can bind to HTT through HAP40 interaction and regulate endosomal trafficking (Pal et al., 2006).

If all of these transport regulators are present on board of a vesicle, how does the vesicle move and in which modality? Is it unidirectional or bidirectional? But before studying the modes of transport, it is important to set up conditions under which neuronal connections are controlled. Indeed, if a neuron is able to make thousands of connections with another neuron, how can we study vesicular transport within a specific neuronal compartment?

### d. Microfluidics: a way to study neuronal transport in specific networks and compartments

In order to study the neuronal transport in a specific compartment, neurites must be isolated. To do this, we used microfluidics devices which allow us to discriminate the axons from the dendrites, thanks to the specific dimension of the channels and the creation of a laminin gradient. The microchamber pattern used in this study is composed of three chambers: the presynaptic chamber containing cortical neurons that project their axons in 500 nm long channels to finally reach the synaptic chamber where they form synapses with cortical or striatal dendrites coming from the post synaptic chamber through 75-nm long channels (figure 54). A higher concentration of laminin within the postsynaptic chamber attracts the axons, thus the majority of post synaptic axons lie in the post synaptic compartment. Moreover, the length of the presynaptic microchannels avoids that presynaptic

dendrites reach the synaptic compartment. This device has been characterized in term of kinetics and cellular signaling and has been shown to reproduce *in vitro* an *in vivo* network (Agasse et al., 2020; Bruyère et al., 2020; Yann Ehinger et al., 2020; Moutaux, Charlot, et al., 2018; Moutaux, Christaller, et al., 2018). To specifically study axonal transport, presynaptic neurons are transduced with a fluorescent labeled cargo or adaptor which is then followed by video microscopy acquisition (thanks to a confocal microscope coupled with spinning disk unit). The analysis of transport dynamics using ImageJ with KymoToolBox plugin allows to generate kymographs, representing the space localization of a single vesicle according to the time. Kymographs drawing and analysis generate different parameters such as velocity, number of vesicles moving in a given direction or pausing and the directionality of the transport (figure 55).

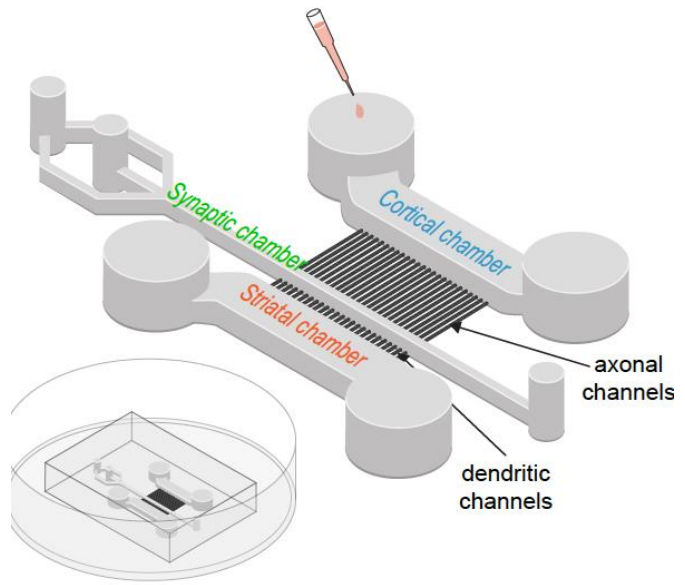


**Figure 54: microfluidics device allows the study of axonal transport in connected neurons.**

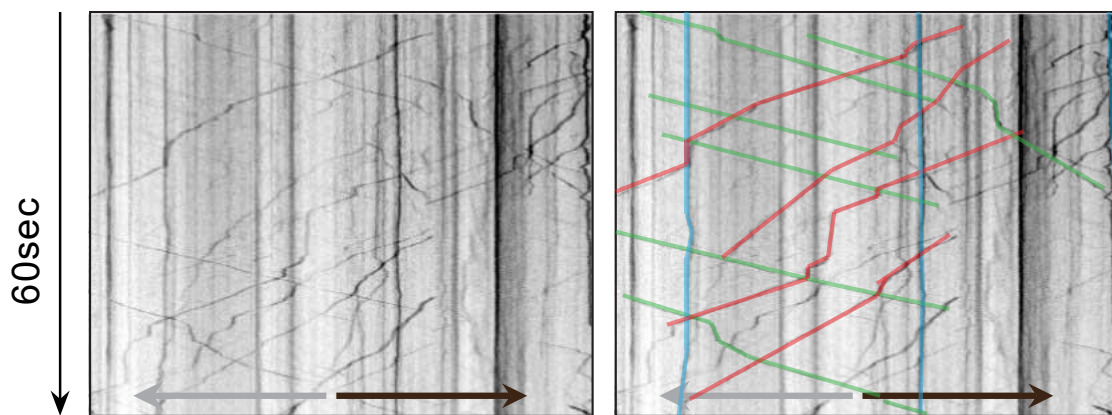


**Figure 55: kymographs are the 2D representation of a vesicle transport displaying the distance over time. Green: anterograde vesicle, red: retrograde vesicle and blue: static vesicles. Total axon length: 100µm.**

### e. Transport modes

Over the years, different modes of transport have been described and modeled in the literature to better understand how a vesicle is transported within a neurite. Some of them are discussed below and it is interesting to remember that these models are not exclusive and they can, indeed, complement each other.



### i. Selective recruitment model

The simplest model to describe neuronal transport would be to say that it is the result of the selective recruitment of kinesin or dynein to a vesicle. Although it may be more of a model than a reality, this model could explain the unidirectional and highly processive vesicle transport (Meng-meng Fu & Holzbaaur, 2014). However, the lack of adaptors that facilitate the transport would make them move slower (figure 56).

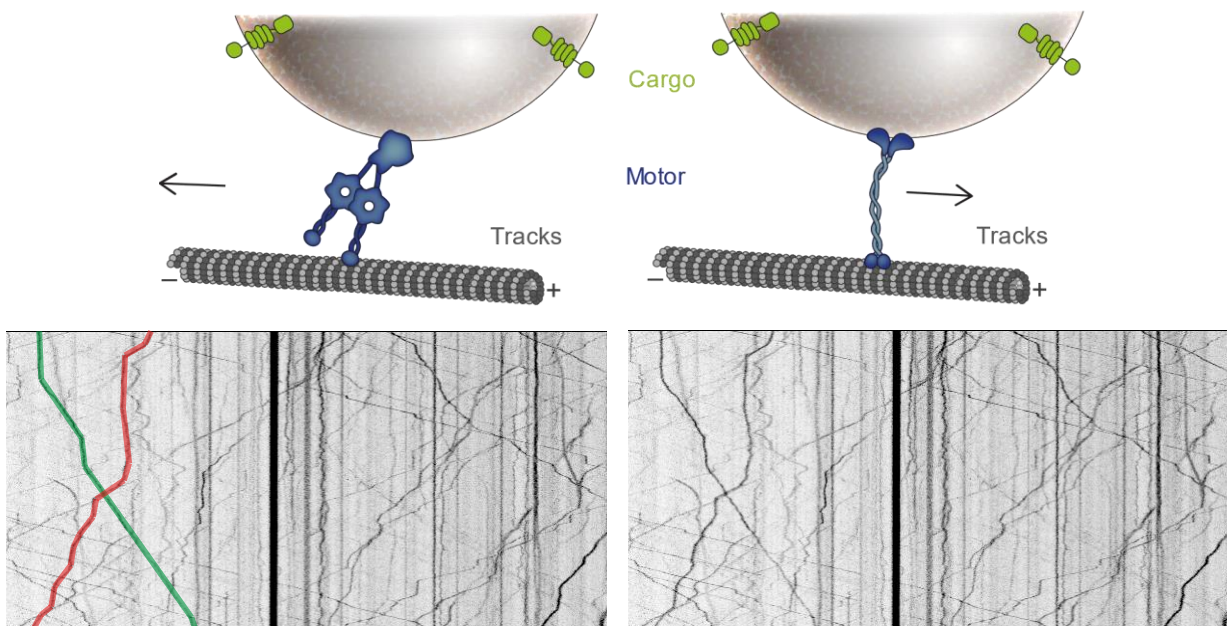


**Figure 56: the selective recruitment model explains the unidirectional and processive transport of vesicles.** Representative schemes and possible kymographs for selective recruitment model. Green: anterograde vesicle and red: retrograde vesicle.

### ii. Tug-of-war model

However, both kinesin and dynein have been found to colocalize on the same moving vesicle (Encalada et al., 2011; Hendricks et al., 2012; Soppina et al., 2009; Szpankowski et al., 2012). Several models have been proposed over the past decade to understand how opposing motors can work together (Meng-meng Fu & Holzbaaur, 2014; Hancock, 2014). The tug-of-war mechanism is based on the fact that the two opposed motors are present on the vesicle and that the one producing the greatest force (i.e., strongest pull), the dominant motor, “wins” the fight and drives the vesicle towards its preferred MT end. In this model, the number of recruited motors is important because it changes the force produced (Meng-meng Fu & Holzbaaur, 2014; Gutiérrez-Medina et al., 2018; Leidel et al., 2012). Since the force produced by kinesins is most often greater than that of dynein (respectively 5-7 pN and 1 pN), with a 1:1 ratio of the two motors, and accordingly to the type of kinesin, this transport would results in short movements marked by many directional switches but overall anterograde (Meng-meng Fu & Holzbaaur, 2014). So, once the kinesin detaches from the vesicle, tug-of-war vesicles will not be pausing but will be rather retrograde. This model fits the idea that decreasing KHC levels

increases the frequency of directional changes (Kaether et al., 2000). These vesicles are therefore bidirectional, non-processive and dedicated to a short-range transport, as it is expected and effectively modeled for the transport of late endosomes/lysosomes or the vesicular transport at MT intersection (Hendricks et al., 2012; Maday et al., 2014; M. J. I. Müller et al., 2008; Osunbayo et al., 2015) (figure 57).

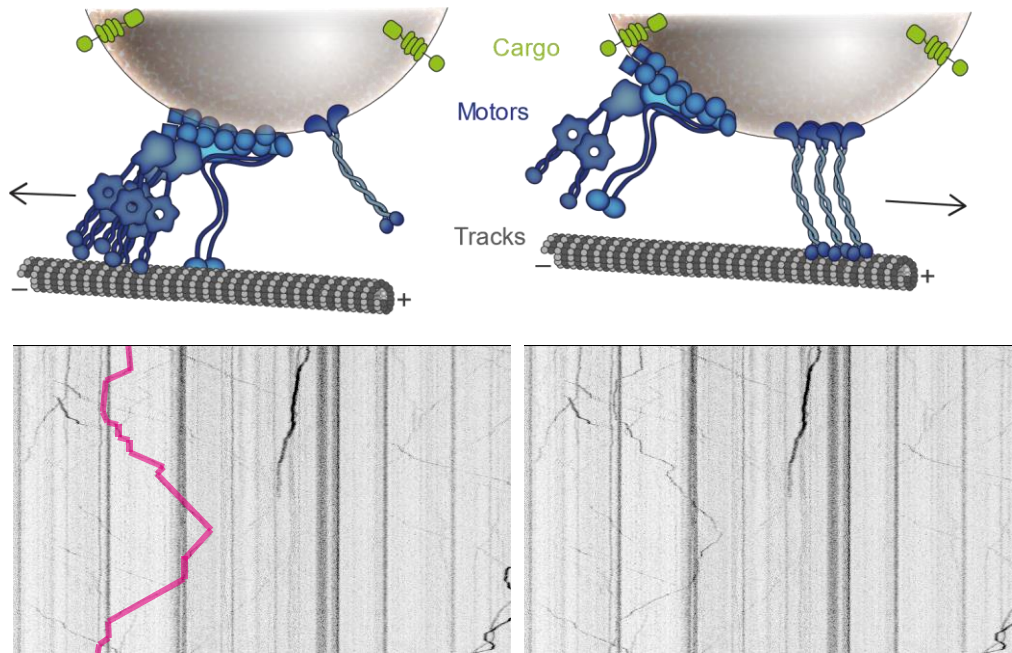


**Figure 57: the tug-of-war model explains the bidirectional and non-processive transport of vesicles.** Representative schemes and possible kymographs for the tug-of-war model.

### iii. Coordination model

However, several studies have shown that only one type of motor can be active on a vesicle (Leidel et al., 2012). The subsequent coordinated model postulates that although both opposed motors are bound to the vesicle, their activity level is different and regulated by PTMs or scaffolding proteins as discussed earlier (for more details see chapter 2 2-b-i-5-b and 2-c-i). This is the case with most of the organelles examined to date (Guedes-Dias & Holzbaur, 2019). For instance, an adaptor or a scaffolding protein could coordinate the activation of the dynein-dynactin complex and the autoinhibition of kinesin. This model explains the fast and processive transport of vesicle with few changes of direction and is more dedicated to the long-range transport (figure 58) of autophagosome for example (Meng-meng Fu & Holzbaur, 2014; Maday et al., 2012). It would provide quick responses in terms of directional changes due to modification of local environment or to avoid traffic jams, for instance (Meng-meng Fu & Holzbaur, 2014).

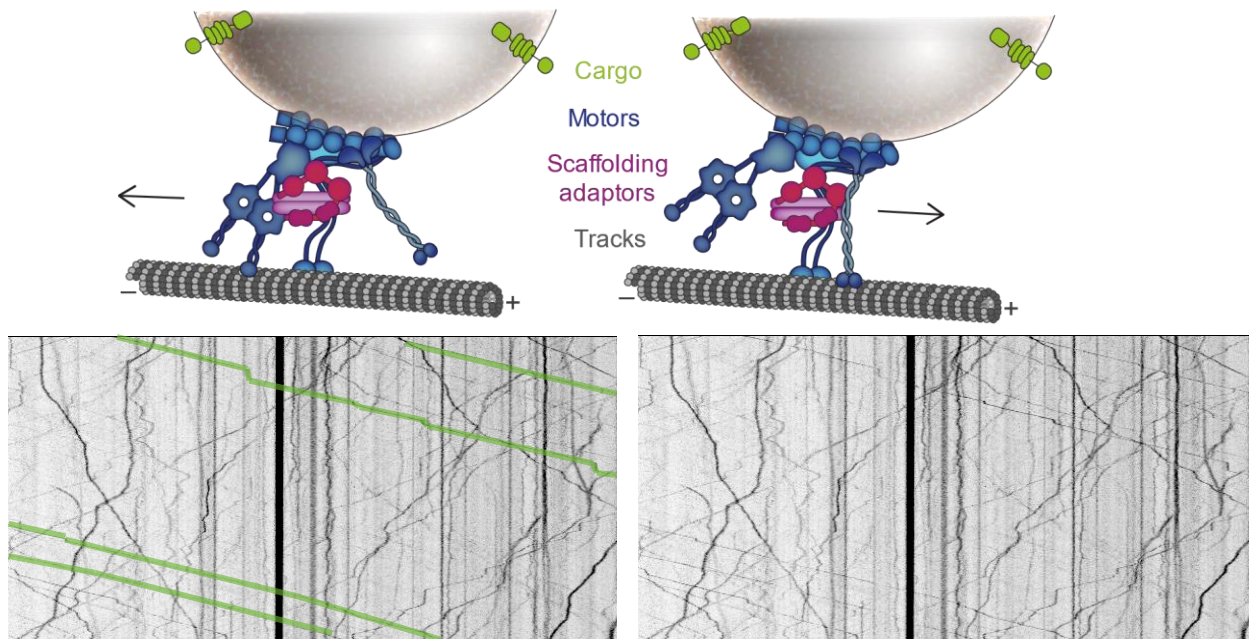


**Figure 58: the coordination model explains the fast and processive transport of vesicles.** Representative schemes and possible kymographs for coordinating model.

#### iv. Steric disinhibition

Another model has emerged in the last decade: the steric disinhibition model. This model is based on the fact that the motor interacts directly with its opposed motor to reduce its autoinhibition, which in turns become active (C. W. Chen et al., 2019; Encalada et al., 2011; Hancock, 2014; Koushika et al., 2004) (figure 59). In this model, anterograde and retrograde machineries support and activate each other (Ally et al., 2009). Indeed, when one motor is dysregulated, the velocities and run length of both motors are affected (Encalada et al., 2011). For example, it has been shown that knocking down in *C. elegans* dynein or dynactin reduces the velocity and run length of UNC104 (KIF1A homolog). Dynein is therefore believed to trigger UNC104 activity (C. W. Chen et al., 2019).

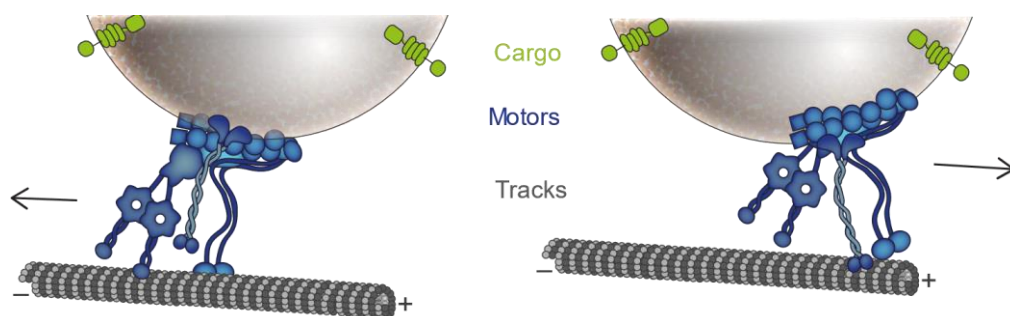


**Figure 59: the steric disinhibition model relies on a cooperation between the two motors.**

To conclude, in order to fulfill its diverse roles, a given neuron needs its different cargoes to be located in a specific neuronal subcompartment. To reach their destination, the cargoes can be transported inside vesicles formed from the TGN or the PM. According to its physiological role, a cargo can be found within a specific vesicle. Moreover, transport within neurites requires tracks, formed by microtubules and molecular motors, known as kinesin and dynein. These two players can be modified to affect axonal transport by MAPs for microtubules, and by adaptors or regulators for molecular motors. Finally, scaffolding proteins as HTT allow the assembling of all these proteins responsible for regulating axonal transport to finely adapt it in time and space. Axonal transport studies based on kymographs have reported several modes of FAT that integrate the functions of some of the aforementioned players.

## Chapter 3 - Example of a synaptic vesicle journey: how axonal transport ensures its neurotransmission function.

Now that all the actors for axonal transport have been identified in detail, we focus on the axonal transport of a previously described type of vesicles, the SVPs. We will understand why those vesicles are specific, for their constitution in lipids and proteins, morphology and behavior. After maturation, SVPs become SVs which are organized in pools at the synapse. SVs contain the molecules responsible for delivering the signal to the postsynaptic neuron (the neurotransmitters), which is why SVP transport to the synapse is crucial.

### 1. SV: a unique type of vesicle

#### a. SV from the outside: when interactions between lipids and proteins regulate neurotransmission

##### i. Definition of a SV

As previously described, a vesicle is an organelle bounded by a lipid bilayer and containing cytoplasm. Synaptic vesicles (SVs) are the most abundant vesicles in the axons of the CNS. In a single human CNS neuron, a presynapse can contain between 40 and 850 synaptic vesicles (Guedes-Dias & Holzbaaur, 2019). Structure, location within the neurite, and function confer unique characteristics to SVs. They were named and first described by De Robertis and Bennett in 1955 thanks to a technique emerging at that time, known as electron microscopy (De Robertis & Bennett, 1955). They described SV in the presynaptic element like “*numerous scattered granules or vesicles (SV), about 100 to 300 Å in diameter*”. However, their function was discovered earlier than their structure when Katz and colleagues (Del Castillo & Katz, 1954; Fatt & Katz, 1952) proposed a quantal theory of transmitter release. Both findings suggested that these vesicles are filled with neurotransmitters (NT) released from the presynaptic terminals in discrete ‘quanta’. More than 60 years later, this definition still stands out, but it has been deeply extended. Today, it is commonly accepted that SVs in CNS are dynamic lipid organelles of 40 nm of diameter, enriched with synaptic proteins and concentrated at the axon terminal. They must be transported from the Golgi apparatus to the axonal tip, described as synaptic vesicle precursors (SVPs). SVs are full of molecules carrying messages (NT, quanta) and are prone to exocytosis at the presynaptic plasma membrane after calcium influx. This event leads to the release of neurotransmitters and the spread of messages to the postsynaptic neuron.

For their work on SV trafficking and the discovery of the major proteins responsible for exo- or endocytosis, Südhof, Rothman and Schekman won the Nobel Prize in Physiology or Medicine in 2013.

## ii. Lipidic composition of a SV

Although lipids are widely considered as structural molecules that “simply” compartmentalize the cell, it is interesting to study their role as modulators during neurotransmission. Indeed, the specific lipidic composition of SVs gives them the ability to undergo exocytosis and endocytosis and to interact with synaptic proteins (Mochel et al., 2018; Puchkov & Haucke, 2013). For many years it was thought that lipid composition of SVs was mainly made of phospholipids (Baker et al., 1975; Benfenati et al., 1989; Michaelson et al., 1983; Westhead, 1987). However, some researches have shown that the percentage of cholesterol was underestimated in previous studies (Shigeo Takamori et al., 2006; Westhead, 1987). Despite the rapid progress of lipidomic analysis, membrane lipid composition of SVs is still not very well characterized (Postila & Róg, 2019). Nowadays, it is believed that some classes of lipids (like cholesterol, sphingolipids, triacylglycerides and phospholipids) are present on SVs and regulate neurotransmission by modulating lipid dynamics and/or interacting with proteins (Camoletto et al., 2009; Lewis et al., 2017; Puchkov & Haucke, 2013).

**Cholesterol**, which represents more than 40% of SV lipids (Shigeo Takamori et al., 2006) can be considered as a membrane organizer (Puchkov & Haucke, 2013). Thanks to its ability to form lipid rafts slowing down the dynamics of lipids, cholesterol stabilizes the highly curved membrane making it more rigid (Bruckner et al., 2009). This property allows the sequestration of synaptic proteins (SPs), leading to their enrichment in the microdomains (Jia et al., 2006). Furthermore, it has been proposed that the organization and concentration of SPs within the lipidic bilayer may be crucial for presynaptic function (Jia et al., 2006; Rohrbough & Broadie, 2005). For example, during endocytosis, cholesterol could prevent the rapid dispersion of SPs away from the fusion site (Lingwood & Simons, 2010; Puchkov & Haucke, 2013). Cholesterol also regulates presynaptic functions by interacting with proteins such as **synaptophysin** to modulate its interaction with **synaptobrevin/VAMP-2** (Mitter et al., 2003; Puchkov & Haucke, 2013; Thiele et al., 2000).

Another type of lipids, **sphingolipids**, which are one of the main constituents of SVs (Lewis et al., 2017), can be considered as regulators of exocytosis and endocytosis (Puchkov & Haucke, 2013). They self-aggregate in the membrane domain with cholesterol (Lingwood & Simons, 2010) and regulate protein interactions. For example, sphingosine regulates the interaction of Munc18-1 with **syntaxin-1** (Camoletto et al., 2009).

Finally, **phospholipids**, although more abundant on the plasma membrane than on SVs (Lewis et al., 2017), are present on SVs and can be considered protein-recruitment hubs (Lauwers et al., 2016; Puchkov & Haucke, 2013). These lipids bind to many SPs, such as **synaptotagmin-1**, **synaptobrevin/VAMP-2**, Mint, **syntaxin-1**, Munc-13, and Huntingtin-interacting-protein 1 (HIP1), giving them the role of major players in exo/endocytosis coupling (Martens et al., 2007; Nyenhuis et al., 2019; Paddock et al., 2011).

The importance of a correct lipid composition in the CNS is reported in several papers showing, for example, that an alteration of the metabolism of sphingolipids is involved in a plethora of diseases such as early onset PD, epilepsy or sphingolipidoses (Krebs et al., 2013; Mochel et al., 2018). Sphingolipidoses in humans displays neurological phenotypes (seizures, dystonia, abnormalities in gait, decreased attentiveness and more) that are consistent with the relevant role for sphingolipids in the nervous system (Kolter & Sandhoff, 2006; Puchkov & Haucke, 2013). In mice, removal of the enzyme responsible for the metabolism of Phosphatidylinositol-4,5-bisphosphate (PIP<sub>2</sub>) causes postnatal lethality due to the severe defects in NT release and SV membrane retrieval (Di Paolo et al., 2004). Furthermore, the alteration of lipid composition in hippocampal neurons is mediated by an increase in sphingolipids at the presynaptic terminal thus increasing glutamate release (Riganti et al., 2016). Taken together, these pieces of evidence underscore the importance of lipids for neuronal functions.

However, lipids alone are unable to efficiently fuse with the plasma membrane to ensure the physiological needs of neurons because the energy required for fusion is very high (between 15 and 50 k<sub>B</sub>T (Grafmüller et al., 2009)). Without any facilitation process, the fusion would be very slow. Therefore, this mechanism is facilitated by the presence of SPs within the SVs and the energy is provided by a protein machinery (SNARE complex), which reduces the activation energy (Fang & Lindau, 2014).

### iii. Protein composition of a SV

Although the amount of protein is low within a SV, the protein/lipid ratio is extremely high and proteins represent more than 60% of the total mass (Shigeo Takamori et al., 2006). Only a small variety of SV anchored SPs can be found, leading to speculation that SPs fulfill only a small and specific set of functions. Among them, we can mention proteins for exocytosis or endocytosis (**synaptobrevin/VAMPs**, **Syntaxins**), GTPases (Rab3), other trafficking proteins (**synaptophysin**, **synaptotagmins**, synapsin, Munc-18) and channel transporter (**VGLUT-1**) (Shigeo Takamori et al., 2006). This paragraph will focus on SP properties necessary for exocytosis.

Exocytosis requires many protein interactions between the SV membrane and the plasma membrane triggering membrane fusion (figure 61). The interplay between trafficking proteins and SNARE proteins allows for the fine regulation of this crucial process over time and space. SNARE family (Soluble NSF Attachment Proteins receptor) includes v-SNARE (protein anchored within the vesicle) and t-SNARE proteins (protein anchored within the target, the plasma membrane). SNARE proteins are characterized by sequences called SNARE motifs with a high probability forming coiled coils. This unique feature allows *syntaxin-1*, *SNAP25* and *synaptobrevin/vAMP-2* to form a highly stable “SNARE complex” constituted by a parallel four-helix bundle (trans-SNARE complex) (Rizo & Rosenmund, 2008) which is essential for exocytosis (figure 61). The crucial role of these SNARE proteins in stimulus-driven NT release has been demonstrated using a neurotoxin that cleaves SNARE proteins at a specific site (Schiavo et al., 2000).

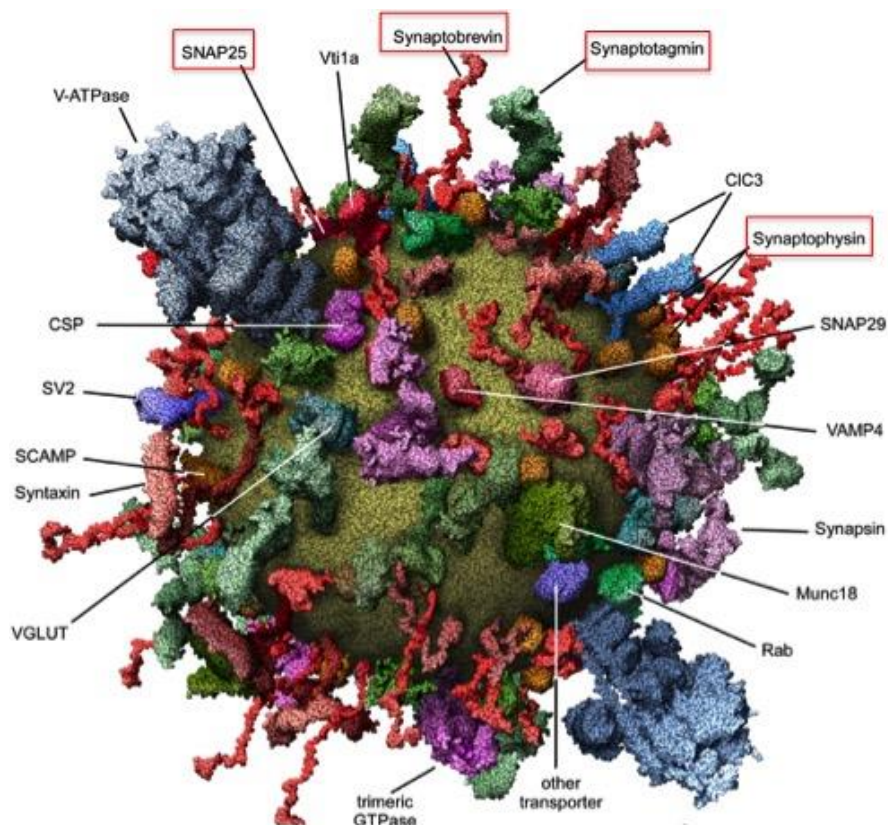


**Figure 60: Molecular model of an average SV. Outside view.** Adapted from Takamori et al., 2006

This section will be devoted to the presentation of four main actors of exocytosis: *synaptobrevin/VAMP*, *synaptophysin* (p38), *synaptotagmin* (Syt) and *SNAP25* (figure 60 and 61) (Quentin et al., 2018).



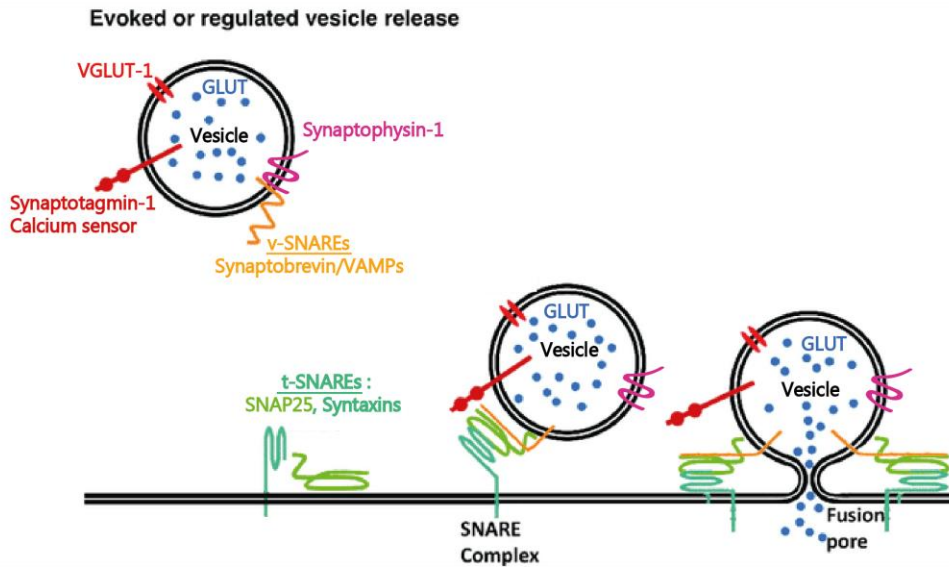
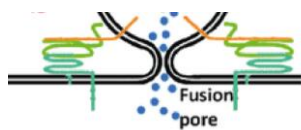
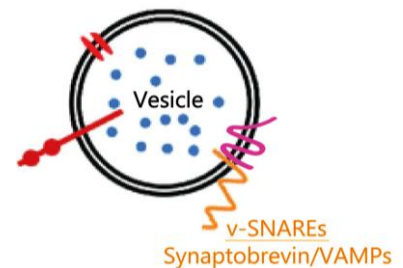


Figure 61: SP interact with each other to regulate exocytosis. Scheme modified from Quentin et al., 2018

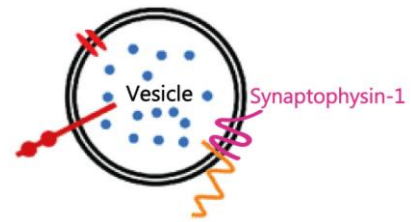
**Synaptobrevin/VAMP** (vesicle associated membrane protein) is a **v-SNARE** family containing less than 10 members, all involved differently in vesicle fusion. As an example of their diversity, Vamp-1 plays an essential role in exocytosis in the murine neuro-muscular junction (Y. Liu et al., 2011) while Vamp-7/Ti-VAMP is a specific v-SNARE localized in late endosomes which mediates neurite outgrowth and neuronal morphogenesis (Y. Wang & Tang, 2006). Exocytosis in the CNS is largely mediated by VAMP-2 (Quetglas et al., 2002)



which appears to be crucial for the establishment of the SNARE complex, leading to **membrane fusion**. Indeed, in mice, the knock-out of VAMP-2 is lethal after birth and exhibits 100-fold fewer synaptic fusion events in mutant hippocampal slices compared to wild type ones (Schoch et al., 1999). *De novo* mutations in patients along the SNARE motif of VAMP-2 cause neurodevelopmental disorders such as intellectual disability, autistic features, hyperkinetic movement disorder or epilepsy. One of these mutations (S75P) induces the loss of hydrogen bonds, reducing interaction with **syntaxin-1** thus affecting the vesicular fusion rate (Salpietro et al., 2019) .

**Synaptophysin-1** (Syp-1, also called p-38) is known as one of the most present proteins on board on SVs. Although it is commonly accepted that Syp-1 positive vesicle are SVs, its role has puzzled neuroscientist for many years. Indeed, this protein discovered in 1985 is thought to play an important role in exocytosis since it was abundant in nerve terminal, having the ability to modulate

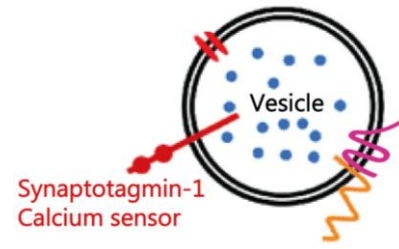
neurotransmission (J. Alder et al., 1995; Janet Alder et al., 1992; Thomas et al., 1988). However, mice lacking *syp-1* showed no deterioration of synaptic properties (synaptic transmission, synaptic plasticity and probability of release) (Janz et al., 1999; McMahon et al., 1996). The authors concluded therefore that Syp-



1 was not essential for synaptic transmission. The only significant feature that they observed in Syp-1 knock-out mice was a 20% decrease in expression of *synaptobrevin/VAMP-2* protein, known to interact with Syp-1 (Calakos & Scheller, 1994; Edelmann et al., 1995; McMahon et al., 1996; P Washbourne et al., 1995). This specific change in *VAMP-2* expression, can potentially be explained by the role of Syp-1 in protein sorting (Pennuto et al., 2003). Nowadays, the complexity of Syp-1's role has been deciphered and it is commonly accepted that Syp-1 participates in SV **exocytosis, endocytosis and biogenesis**. The binding of Syp-1 to *VAMP-2* is mutually exclusive to the SNARE complex and can finely regulate the delivery of *VAMP-2* to the other SNARES for fusion pore formation. Consequently, Syp-1 can be considered as a key actor that ensures **excitation-secretion coupling** (Valtorta et al., 2004). However, the main role of Syp-1 may lie in the efficient **retrieval or clearance of Vamp-2 from the active zone, upstream of the endocytosis** that supports NT release (Harper et al., 2017; Kokotos et al., 2019; Rajappa et al., 2016; Valtorta et al., 2004). During this process, the need for a subtle balance was highlighted by the description of a specific stoichiometry of Syp-1/*VAMP-2* (1:2), which has been proved to be crucial for Syp-1 to modulate the retention of *Vamp-2* at the nerve terminal (Gordon et al., 2016).

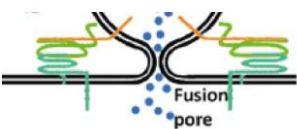
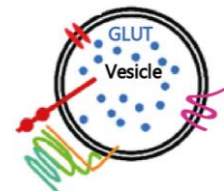
The absence of defect in synaptic transmission in Syp-1 KO mice was better understood when a study proposed that the large amount of *VAMP-2* present on SV (around 70 copies (Shigeo Takamori et al., 2006)) renders *VAMP-2* in excess comparing of the low number needed for SV fusion (between 1 and 3) (Kokotos et al., 2019; Mohrmann et al., 2010; Sinha et al., 2011; Van Den Bogaart et al., 2010). This may explain why presynaptic defects only appear when frequent SV turnover is induced (Kokotos et al., 2019). Another explanation could lie in the redundancy of the isoforms. Indeed, Syp-1 KO mice show defects in the organization of the cell membrane and also a reduced number of SVs in photoreceptors of retinal rod, characterized by a high concentration of Syp-1 and an absence of Syp-2 (Spiwox-Becker et al., 2001). Furthermore, knocking down the four Syp-1 isoforms, or related proteins, increases the probability of SV release (Davis et al., 2019), which is consistent with Syps blocking exocytosis.

The **Synaptotagmin (Syt)** family of proteins contains more than 15 members capable to bind calcium (Pang & Südhof, 2010). Isoforms appear to play different roles. For example, Syt-2 has been found to modulate synchronous release, while syt-7 modulates the asynchronous component of release in Zebrafish



(Wen et al., 2010). Syt-1, similar to Syt-2, is a key player in exocytosis due to its two calcium binding sites (C2A and C2B), acting as **calcium sensor for SV release** (Südhof, 2013). The importance of Syt-1 in the coordinated release of NT with calcium has been demonstrated by many experiments. The knock-down of Syt-1 abolishes the fast synchronous NT release (Geppert et al., 1994; Littleton et al., 1993) and increases the neuronal frequency of spontaneous release (Chicka et al., 2008). A proposed mechanism is that Syt-1 inhibits fusion in absence of action potential inducing a  $Ca^{2+}$  entry (Chicka et al., 2008; Tucker et al., 2004).

The **SNAP-25 (synaptosomal associated protein)** sub-family is unique due to its two SNARE motifs within each of its 4 members: SNAP-25 (the founder of this family), SNAP-23, SNAP-29 and SNAP-47 (Kádková et al., 2019). Briefly, SNAP-29 and SNAP-47 are thought to bind to some VAMPs to form cis-complexes necessary for non-exocytic fusion reactions, especially during post-Golgi secretion and endosomal/lysosomal/autophagy pathway (Itakura et al., 2012; Kádková et al., 2019; Kuster et al., 2015).



SNAP-25 is a t-SNARE partner of the SNARE complex, where it engages two of the four helices needed to form the bundle that allows the fusion between SV and plasma membrane. SNAP-25 is devoted entirely to evoked synaptic transmission ( $Ca^{2+}$  triggering) as SNAP-25 knock-out mice show mEPSCs but do not exhibit depolarization-driven exocytosis (Philip Washbourne et al., 2002). Moreover, this team

demonstrated that the ablation of this gene is lethal at embryonic stages. G protein and SNAP25 prevents the binding of synaptotagmin to SNAP-25 and inhibits the exocytosis triggered by  $Ca^{2+}$  raise (Zurawski et al., 2017). These interactions among others appear to be physiologically very sensitive since when compromised because of SNAP-25 polymorphisms, SNARE complexes are either too weak or too strong. In both cases, its functions are impaired and lead to bipolar disorder, autistic disorder syndrome, schizophrenia or attention-deficit hyperactivity disorder in child (Karmakar et al., 2019; Y. S. Liu et al., 2017; Ramos-Miguel et al., 2019).

Thanks to more resolutive techniques, we can now detect another type of protein present in 10% of the SVs and in small quantities (Ikin et al., 1996), known as APP (Groemer et al., 2011) (figure 62). Indeed, APP can be considered a “bona fide” SP since once at the PM, it is trafficked (but not transported) by SVs (Del Prete et al., 2014; Groemer et al., 2011; Kohli et al., 2012; Nigam et al., 2016). However, the presence of APP within SVs is still controversial (Laßek et al., 2013; Weingarten et al., 2017). The  $\alpha$ - and  $\beta$ -secretases, two enzymes responsible for the production of APP-CTF resulting from APP cleavage, were also observed within SVs and along with their cleavage products (Del Prete et al., 2014; Lundgren et al., 2015). However, A $\beta$  peptides are not produced within SVs because  $\gamma$ -secretase subunits are not present (or in low levels) inside SVs, which may explain SV enrichment in APP-CTFs (Lundgren et al., 2015).

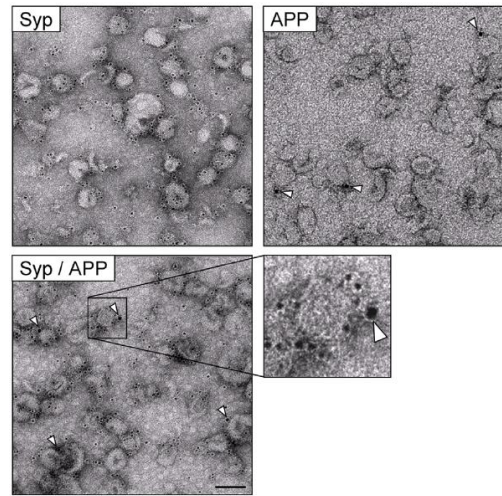


**Figure 62: APP might be present on SVs.** Immunolabelling of Syp (small dots) and APP (big dot) from Groemer et al., 2011

#### iv. Size of SVs

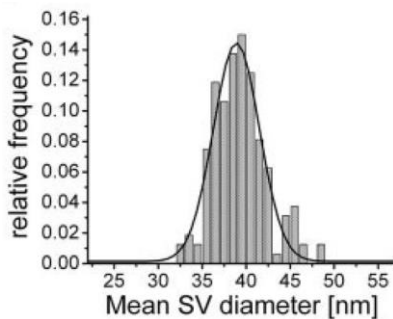


**Figure 63: SV diameter is around 40 nm.** Relative frequency of SV diameter, from Hu et al., 2008.

The size of SV has been well characterized, since it is a specific feature of these organelles, and in excitatory neurons of the CNS its diameter is around 40 nm (figure 63) (Dittman & Ryan, 2009; K. M. Harris & Sultan, 1995; Y. Hu et al., 2008; Jahn et al., 1994). Although SV diameter may differ from one species to another, it is very similar from one synapse to another of the same species. Indeed, the SV diameter is not correlated with the PSD area size nor with the number of SVs within the bouton or with neuronal activity (Qu et al., 2009).

The size of SV would depend on the curvature driven by lipid properties and the steric hindrance of SP (Jahn & Südhof, 1993). SPs such as **synaptobrevin** or **synaptotagmin**, with a large cytoplasmic domain and a small luminal domain (in red and green respectively in figure 64), can form oligomeric structures (Bowen et al., 2002) and appear to form clusters, which promotes a high membrane curvature (Poudel & Bai, 2014).

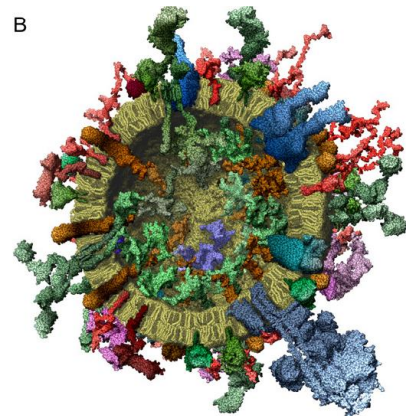


**Figure 64: SV size is dependent on SP steric hindrance.** Representative cross section of a SV from Takamori et al., 2006

Once the SVs are formed, they retain their acquired size thanks to some soluble proteins such as synapsin or Rab5 which prevent the SV from fusing together (H. Shimizu et al., 2003).

Finally, endocytosis protein like dynamin-1, AP-2 or clathrin modulate SV size by controlling the amount of PM retrieved or the interactions with other proteins (Mahapatra et al., 2016; Nakatsu et al., 2004; Nonet et al., 1999; B. Zhang et al., 1998).

#### v. SV pools

Historically, using electron microscopy, different SV pools have been observed and described based on their localization to the release site in the plasma membrane (the active zone). Following morphological observations, functional properties were assigned to each pool. As shown in figure 58, after non-physiologic stimulation of goldfish bipolar cells (Denker & Rizzoli, 2010), three kinetics components of release on depolarization can be observed, which are linked with the presence of three pools (Neves & Lagnado, 1999). The first phase is a rapid increase in the fluorescence change (related to the membrane surface), then a linear phase appears and finally comes the third phase, slower and continuous (figure 65). These three phases led to the conclusion that three distinct SV pools co-exist: the readily releasable pool (RRP, exhausted within 20 ms of depolarization, figure 65), the recycling pool (exhausted within 1s of depolarization, figure 58) and the reserve pool (not depleted over a 5s period of depolarization, figure 58) (Neves & Lagnado, 1999; Rizzoli & Betz, 2005; Santos et al., 2009).

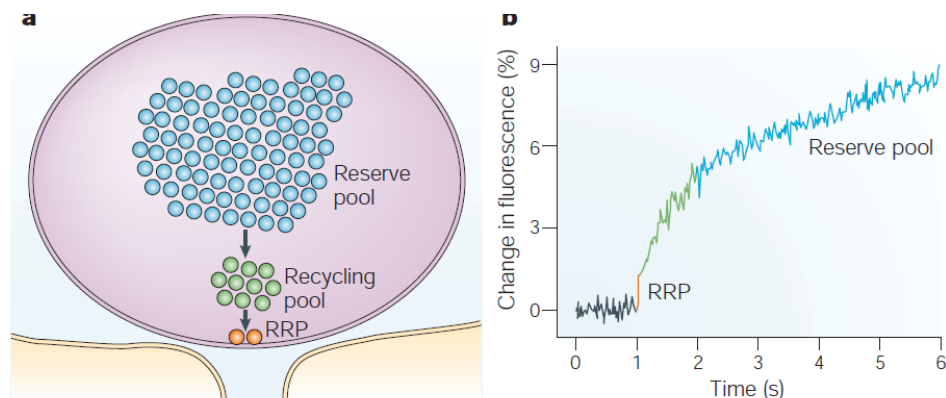


**Figure 65: SV are organized in three pools: RRP, recycling pool and the reserve pool.** Representative scheme and graph from Rizzoli & Betz, 2005

Over the years, thanks to extensive research, new subpopulations of pools have emerged as well as different nomenclatures and definitions. A universal list of these pools is missing today. In this manuscript, we will use the most accepted classification cited above.

## 1. RRP

The RRP, first hypothesized in the 60s (Bircks & MacIntosh, 1961; Elmqvist & Quastel, 1965), is the pool located at the active zone, ready to be released (less than 1 second is needed for their release, as seen in the first phase of the graph figure 58) (Rizzoli & Betz, 2005). It represents 1-2 % of the vesicles present at the presynapse and for example, in mouse hippocampal neurons, it is composed of between 5 and 13 vesicles (Alabi & Tsien, 2012; Rizzoli & Betz, 2005; Schikorski & Stevens, 1997).

### a. RRP composition

RRP consists of docked SVs that are attached to the plasma membrane at the active zone through SNARE interactions (figure 66) (Imig et al., 2014). These interactions play an important role in anchoring because when the amount of SNARE-interacting protein is decreased, the number of docked vesicles is increased (Nonet et al., 1999), the probability of release is lower, thus affecting the learning and memory processes (De Rossi et al., 2020). Docked vesicles become competent for fusion thanks to a maturation process called priming (Imig et al., 2014; Südhof, 2013) where Rab-3 and Munc13 plays a crucial role (Schlüter et al., 2006; Varoqueaux et al., 2002). The knock-out mouse of Munc-13 showed altered priming mechanisms and a decrease in the number of docked vesicles (Imig et al., 2014; P. Kaeser, 2011). Thanks to these properties, docked SVs have the highest probability of fusion, so they are the first SVs to be released after the calcium influx.

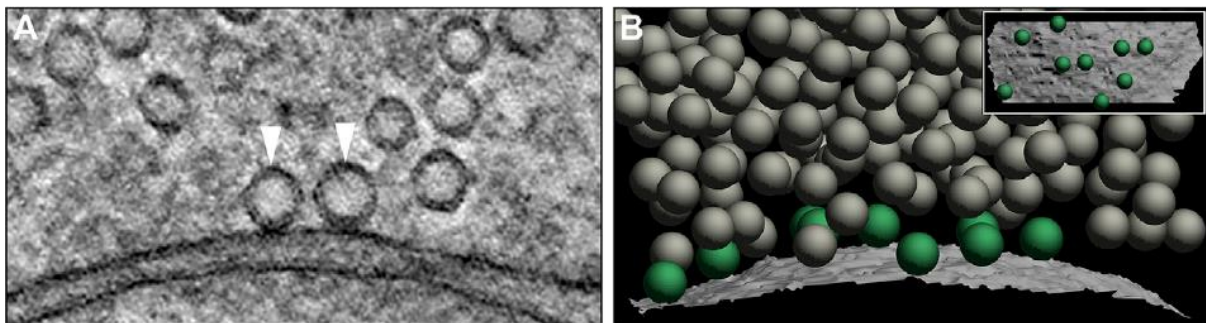


**Figure 66: RRP vesicles are docked to the PM.** RRP vesicles observed with an electron microscope and localization within the SV pools, from Imig et al., 2014.

Interestingly, not all docked vesicles are released upon activation and the opposite is also true: RRP is not composed only of anchored vesicles (Rizzoli, 2014). Some undocked vesicles that are close to the PM can be released by RRP-depleting stimuli, suggesting that localization within the bouton alone could regulate the release (P. S. Kaeser & Regehr, 2017) (figure 66). SVs closer to  $\text{Ca}^{2+}$  channel may, for example, have higher probability to fuse (Crawford & Kavalali, 2015; Fowler & Staras, 2015). This localization may be dictated by their distinct molecular composition which can modify their ability to fuse and modify the standard view of the pool classification (Crawford & Kavalali, 2015; Fowler &

Staras, 2015). This is for example the case of vesicles enriched with vamp4 or vamp7 (Matz et al., 2010; Schikorski & Stevens, 1997; Thanawala & Regehr, 2016).

b. RRP function is partly governed by its size

The size of RRP (i.e the number of SVs within the RRP) is crucial because it regulates its function: it is proportional to the probability of a vesicle release and consequently to the synaptic strength (Goda & Stevens, 1998; Matz et al., 2010; Schikorski & Stevens, 1997; Thanawala & Regehr, 2013). RRP is replenished from the reserve pool, which is vital for sustaining response (P. S. Kaeser & Regehr, 2017) and is rapidly depleted after 5-15 high frequency electrical stimulations (Rizzoli & Betz, 2005) or between 10 and 50 action potential at 10-20 Htz (Hyocheon Park et al., 2012). Once exhausted, it is filled with SVs coming mainly from the recycling pool (Alabi & Tsien, 2012; Schikorski, 2014). Many studies have focused on understanding the mechanisms that regulate RRP size and the consequences on NT release and synaptic strength (Bacaj et al., 2015; Baldelli et al., 2007; S. Chang et al., 2018; Imig et al., 2014). Reducing the size of RRP has been shown to reduce EPSC amplitude in the calyx of the Held synapse (by reducing calcium influx) (Thanawala & Regehr, 2013) and in the avian nucleus magnocellularis (Taruno et al., 2012), to increase synaptic depression in GABAergic neurons (Baldelli et al., 2007) and to alter homeostatic plasticity in the neuromuscular junction of *Drosophila* (by RIM KO) (M. Müller et al., 2012). Likewise, delaying the reloading of the RRP increases synaptic depression (Mochida et al., 2016). The increase in the size of the RRP however, allows for a transient augment of synaptic efficacy in the Calyx of Held (Habets & Borst, 2007; Mahapatra et al., 2016), and an increase in EPSC size along with reinforced synaptic strength in the glutamatergic hippocampal synapses (Stevens & Sullivan, 1998).

Thanks to its functional role, RRP is the easiest pool of SVs to quantify. After triggering the RRP depletion by different means (prolonged presynaptic voltage steps, evoked currents, photolytic presynaptic calcium release, or applications of hypertonic sucrose), three main techniques are used today to quantify the RRP size (P. S. Kaeser & Regehr, 2017; Thanawala & Regehr, 2016). They measure the post synaptic currents (EPSC), the capacity changes in the presynapse due to the addition of membrane during fusion or the rate of exocytosis with optical methods.

## 2. Recycling pool

The second phase observed in the graph figure 65 is due to the presence of the recycling pool which is released more slowly than the RRP. Its release occurs once the RRP is exhausted and precedes the mobilization of the reserve pool (Rizzoli & Betz, 2005).

The SVs function of the recycling pool is the biological response to the too high energy consumption necessary for SV synthesis. Instead of producing *de novo* SVs, which is a costly mechanism in term of energy and time, the neuron has the ability to recycle the SVs that have just been exocytosed. Once incorporated into the PM, lipids and proteins of SVs are recovered by endocytosis. This mechanism has more than one consequence: it also prevents the accumulation of new lipids to limit the expansion of the PM, and preserving membrane integrity and synapse homeostasis (Puchkov & Haucke, 2013).

Several endocytosis mechanisms are described in the literature (see chapter 2 1-b-ii) (figure 29) (Gan & Watanabe, 2018) but we will focus on the most common: the clathrin-mediated mechanism (Chanaday et al., 2019). When the SVs are inside the PM, they are recognized by cofactors/adaptors, some of them are activated by PiP2 of the PM (AP2 for example, (Höning et al., 2005)). The activation will trigger a cascade of events that will lead to the formation of a clathrin-coated vesicles (Kononenko & Haucke, 2015). Thus, in order to be free from the PM, the coated vesicle must be severed/pinched off. This process is ensured by dynamin, recruited by the cofactors, which will assemble to form a ring structure around the neck of the endocytosed vesicles. The free SV will then lose its clathrin coating (figure 67) with the help of non-coating factors and fuse with early or sorting endosomes through a reaction involving Rab5 (Rizzoli, 2014).

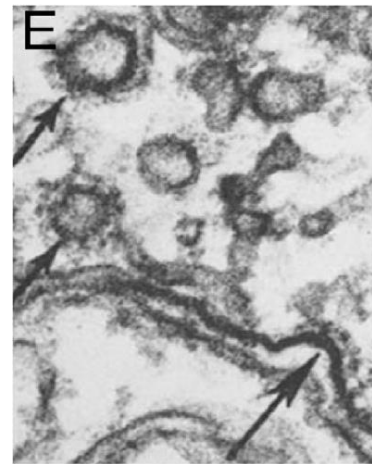


**Figure 67: CME forms clathrin coat around the endocytosed vesicle.** Picture of endocytosed vesicle surrounding by clathrin coat from electron microscopy in Kononenko & Haucke, 2015.

The SVs formed by endocytosis are specific in terms of lipid and protein composition and it depends on which part of the PM has been endocytosed. In fact, at the end of exocytosis, the lipids from the exocytosed SVs such as cholesterol and sphingolipids formed SPs containing microdomains. Some other PM proteins can be found in these microdomains, such as APP (Groemer et al., 2011; Guardia-Laguarta et al., 2009). Thus, thanks to its physical properties and protein interactions, these entire lipidic microdomains will be endocytosed along with their proteins. The same mechanism can be observed for release from endosomes. This is why we can find some PM or endosomal proteins, like Rab-5, integrated into newly synthesized SVs (Groemer et al., 2011; Guardia-Laguarta et al., 2009).



Understanding the mechanisms of SVs endocytosis is interesting because it allows the scientists to manipulate pathways and uncover consequences on SV release. For instance, by slowing down the recycling pathway, it is possible to delay the filling of the RRP, which causes synaptic depression and alters synaptic plasticity (Ivanova et al., 2020; Mochida et al., 2016). Conversely, increasing the recycling rate increases the number of SVs within a bouton in the hippocampus, thus leading to short-term facilitation and aberrant behavior such as increased exploration-related behavior in mice (Kononenko et al., 2013). Interestingly, it has been shown recently that the size of the recycling pool naturally increases after LTP induction (Rey et al., 2020).

### 3. Reserve pool

The third phase observed in graph figure 65 represents the release of the reserve pool, which is even slower than the release of the recycling pool and continuous. The SVs of the reserve pool represent between 80 and 90% of SVs within the synaptic bouton and are believed to be the oldest (Alabi & Tsien, 2012; Fernandez-Alfonso & Ryan, 2008; Rizzoli & Betz, 2005; Truckenbrodt et al., 2018). They are located farther from the active zone and are only released upon intense or prolonged stimulation after depletion of both RRP and recycling pool (figure 68).

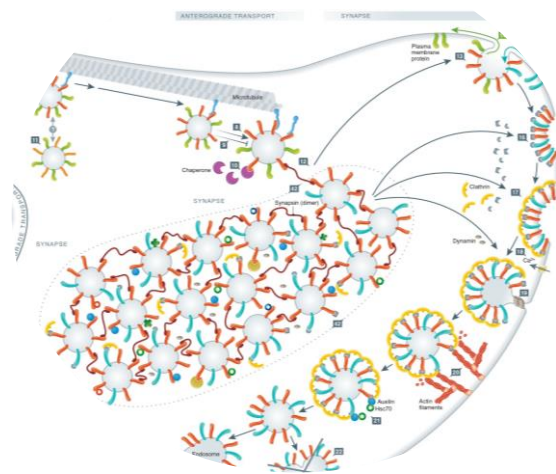


**Figure 68: the reserve pool is further from the active zone and contains many SVs.** Scheme from Rizzoli, 2014 showing the reserve pool of SVs coated with blue and red SPs.

To date, the roles of the reserve pool are not very well understood but its reduction in size causes an increase in synaptic depression, memory deficits and epilepsy (Skorobogatko et al., 2014). Several hypotheses may explain the role of the reserve pool in supporting neurotransmission. This SV pool could act as a buffer for recycling of SVs and soluble proteins to be provided on demand during synaptic activity (Denker et al., 2011). With this mechanism, the size of the reserve pool controls the recycling rate and the recycling pool and, consequently, the SV release. As mentioned before, this pool could also be heterogeneous due to the different composition of its SVs; some are thought to be interchanged between boutons (Fernandez-Alfonso & Ryan, 2008) and some may be responsible for the spontaneous fusion of the vesicles (Fredj & Burrone, 2009).

Controlling the size of the reserve pool could rely on protein modification linked to calcium influx. This is particularly the case with Syt-7, a member of the synaptotagmin family which is a calcium sensor that monitors both the reserve pool and the recycling pool sizes making the vesicles unavailable for

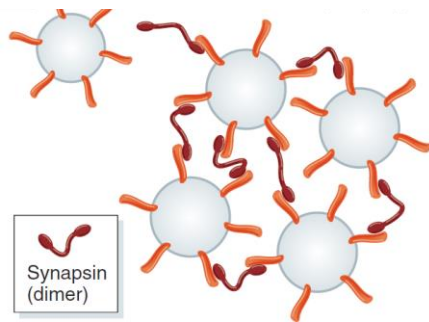


**Figure 69: synapsin regulates the reserve pool size by sticking the SV all together.**  
Scheme from Rizzoli, 2014

release (Durán et al., 2018). Synapsin could be the main regulator of reserve pool size. Indeed, knock-out mice of this protein exhibit incompletely functional synapses because the reserve pool is greatly reduced. These mice show defects in synaptic plasticity (synaptic depression), cognitive decline and seizure (Corradi et al., 2008; Gitler et al., 2008). In humans, synapsin I has been found to be mutated in patients affected by epilepsy and autism spectrum disorder (Fassio et al., 2011; Garcia et al., 2004). This phosphoprotein acts as a scaffold for SVs: the unphosphorylated form is present on the SV and its “sticky” propriety provokes the crosslinking of all the neighbor SVs to form a block that cannot fuse together. Synapsin forms a cage around the SV which prevents its fusion with other SV from the reserve pool (figure 69). When phosphorylated by calcium-activated kinases following intense and non-physiologic stimulation, synapsin is released from the vesicle which becomes free from the pool and can move. Mutation of its phosphorylation site to alanine increased the size of the reserve pool (Skorobogatko et al., 2014) and in a HD mouse model, synapsin phosphorylation has been found to predict neuronal transmission impairment (Liévens et al., 2002).

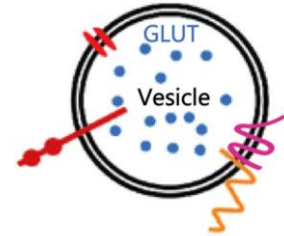
To conclude, due to their dynamics and localization within the axon terminal, vesicle pools are able to regulate synaptic strength and plasticity taking into account many presynaptic processes. Therefore, synaptic pools are crucial for behaviors such as learning and memory (Alabi & Tsien, 2012).

To conclude, from the outside view, a SV is a 40 nm transparent vesicle at the axon terminal with a very specific lipid and protein composition that allows the vesicle to fuse with the plasma membrane. Both its distance from the active zone and its molecular composition confer a functional role on SV. But what is the role of SVs? What does they carry inside?

**b. SV from the inside: the vesicle containing the message unit. Example of SV containing glutamate**

**i. SVs are filled with NT**

The discovery, thanks to electron microscopy, of the external view of an SV coincided with the theory emitted by Katz and colleagues about the inside view and the functional role of a SV.



Although the chemical nature of the messenger that sends information from the nerve to an organ was highlighted in the early 1900s (Curtis & Watkins, 1961), , Katz was a pioneer in the discovery of NT-mediated mechanisms of nervous message diffusion. In 1954 with Del Castillo, they proposed a quantal theory of transmitter release from their studies on the nerve-muscle synapse of the frog (Del Castillo & Katz, 1954). Transmitters are molecules that are released in “packets” from the presynaptic to generate a postsynaptic potential. Each packet (later called the synaptic vesicle) contains a fixed amount of NT (up to several thousand NT molecules): a quantum.

The small and clear vesicles in the presynaptic terminal observed with electron microscopy was the structural answer of the discovery of NT released in fixed quanta.

However, thanks to extensive research, this definition evolved over the years; nowadays, it is very well described that SVs are filled with neurotransmitters, molecules that make up the essence of the message sent by a neuron. NTs have already been described (see chapter 2 1-d-ii), but to briefly remind, a neurotransmitter could be simply defined as a molecule released by the presynapse, received by a receptor which then converts the chemical signal into an electric signal from a cascade of events. In this part, we will focus on glutamate as it is the main neurotransmitter found in cortical neurons that project towards the striatum (Fonnum, 1984).

**ii. Glutamate definition**

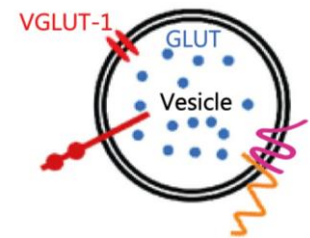
Many studies have focused on glutamate intake because it is the NT that is most frequently found in excitatory synapses and one of the first to be identified by electrophysiological studies (Fonnum, 1984).

Glutamate is the main amino acid found in the brain (Shigeo Takamori et al., 2006) and was first suggested by Krebs in 1935 to play an important role in brain metabolism. Its production from  $\alpha$ -ketoglutarate occurs in the mitochondria during the “Krebs cycle”. The fact that glutamate is an amino acid and therefore present in all neurons, including inhibitory neurons, implies the need to discriminate between the two types of glutamate.

### iii. Loading of glutamate into SVs

Once glutamate is present in the neuron, it must be concentrated within a SV, up to 100.000 times more than in cytoplasm. This process requires energy to overcome the concentration gradient and active transport is required. The transport of glutamate in SV is carried by a specific vesicular transporter, which is VGLut. The needs of energy for this transport explain the presence one to two vacuolar-type H<sup>+</sup>-ATPases (V-ATPase) within each SV along with transporters (Shigeo Takamori et al., 2006). V-ATPases are responsible for the ATP hydrolysis which produces H<sup>+</sup> and is slowed down when the SV membrane potential is positive.

VGLut proteins appear under 3 isoforms: vGlut-1, vGlut-2 and vGlut-3. The two firsts isoforms are expressed in the adult brain with a complementary pattern of expression throughout the brain. vGlut-1 is the main glutamate transporter in the cortex, hippocampus and cerebellar cortex while vGlut-2 is preferentially present in the thalamus and brainstem (Bellocchio et al., 2000; S. Takamori et al., 2001; F. X. Zhang et al., 2018).



vGlut-1 is a voltage-H<sup>+</sup> antiporter that can be activated by a positive membrane potential ( $\Psi$ ) or a H<sup>+</sup> gradient, thus transporting glutamate in exchange for a proton (Martineau et al., 2017). Very recently, vGlut has been found to allow glutamate to enter an SV along with a P<sub>i</sub> and a proton (H<sup>+</sup>) through ATP hydrolysis (Preobraschenski et al., 2018).

SV loading with glutamate can be described by 3 steps (figure 70) (Chaudhry et al., 2008; R. H. Edwards, 2007; Martineau et al., 2017):

#### 1/ Electric component drives the beginning of the loading

When SVs are empty of NT, they are enriched with Cl<sup>-</sup>. This accumulation of negative charges increases the membrane potential ( $\Psi$ ), activating vGlut1 which loads the glutamate in the SV in exchange for an H<sup>+</sup> produced by V-ATPase. The activity of vGlut-1 is high and there is a massive glutamate import. In this first phase, there is no accumulation of H<sup>+</sup> because the high concentration of Cl<sup>-</sup> prevents the activity of V-ATPase.

2/ The chemical component takes over: SV becomes acidic

When the concentration of  $\text{Cl}^-$  decreases within the SV, the electrical component vanishes and the activity of vGlut-1 is interrupted. However, it also causes the disinhibition of V-ATPase. Therefore,  $\text{H}^+$  accumulates in the SV which becomes acidic and activates vGlut-1. Glutamate is still imported but at a slower rate than  $\text{H}^+$ , which is imported from the V-ATPase.

3/ End of the loading

SV loading ends when its pH reaches 5.5 and there is a 100-fold  $\text{H}^+$  gradient that blocks the V-ATPase. This process allows 1800 molecules of glutamate to enter a vesicle (Shigeo Takamori et al., 2006)

#### iv. Supply and recycling of SVs transporting glutamate

Once glutamate is released into the synaptic cleft, it is then taken up by transporters within the membrane of astrocyte (Balcar & Johnston, 1972). This transport allows both the clearance of glutamate inside the synaptic cleft (which is one of the properties of NT) and the recycling of glutamate. Once glutamate is transported through EAAT2 in astrocytes, it is then converted into glutamine by glutamine synthase, which is mainly present in astrocytes (W. Chen et al., 2004; McKenna, 2007). Glutamine then diffuses back into neurons where it is hydrolyzed by the phosphate-activated-glutaminase (PAG) into glutamate within mitochondria located near a synapse (Schousboe et al., 2014).

This glutamate/glutamin cycle was first validated in the late 1900s by biochemistry and only recently by electrophysiology (Tani et al., 2014). Interestingly, the contribution of other mechanisms of neuronal glutamate via neuronal EAAT2 (Furness et al., 2008) or *de novo* production are to a lesser extent and are still debated (Danbolt et al., 2016).

To sum up, from the inside, a SV is filled with neurotransmitters, which are molecules responsible for neurotransmission after being released from the synapse. But how does a SV reach the synapse?

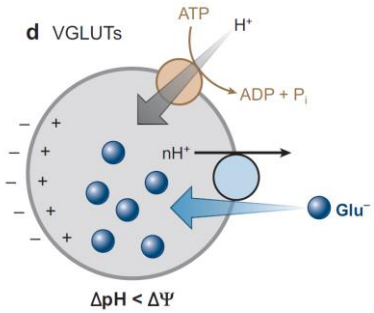


**Figure 70: glutamate loading in SVs requires electric and chemical components.** Scheme from Chaudhry et al., 2008

## 2. SVs origin from SVP transport and maturation

Before becoming an SV containing all SPs, its precursor must first be synthesized, then transported into the synapse to be exocytosed and then endocytosed to finally become an SV in itself. The precursor of SV (called SVP) is interesting because it travels inside the axon and if its transport is compromised, the size of pools will change and, consequently, also post synaptic responses. The mechanism of SVP axonal transport as the same features described earlier (vesicles attached to motors following microtubules direction). However, some specificities can be noted and are well described in the literature, and new regulatory mechanisms still remain to be elucidated.

### a. *De novo* production of SVPs

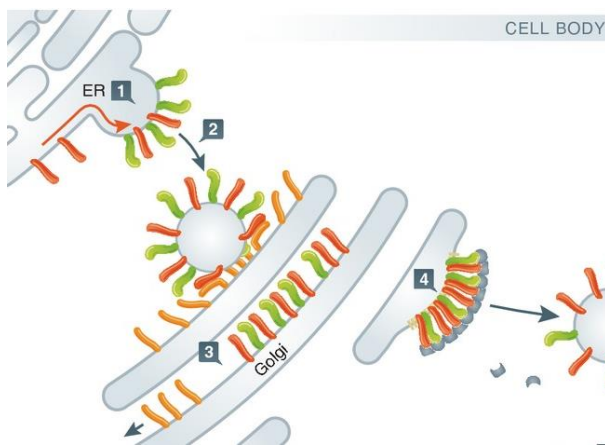


**Figure 71: SVPs formed from the Golgi are the result of a specific and SNARE-dependent SP segregation.** Scheme from Rizzoli, 2014

The *de novo* production of secretory vesicles has already been described in the chapter 2 1-c-i-2. To deepen the characterization of SVP production, we can emphasize the importance of protein and lipid segregation during this process. In fact, it is known that synaptophysin and cholesterol bind to each other inside the ER, thus forming domains and causing a slower diffusion of lipids (Régnier-Vigouroux et al., 1991; Thiele et al., 2000). These domains will be enriched in SPs such as syntaxin and synaptobrevin/vamp thanks to their

interactions (Rizzoli, 2014) and will therefore form a new vesicle when leaving the ER (figure 71). The newly formed vesicles then reach the *cis*- side of the Golgi apparatus as free vesicles and use the synaptic proteins anchored in their membrane (*i.e.*, the SNARE system) to fuse with the Golgi membrane (see chapter 3 1-a-iii). These proteolipid patches will diffuse inside the Golgi membrane to finally bud from the trans Golgi network (TGN) and to be released in the cytoplasm (figure 71). This *de novo* production machinery is responsible for the generating 17 to 35 SVPs per second in the cell body (Guedes-Dias & Holzbaaur, 2019). However, the Golgi is unable to form perfect SVs containing all the SPs they need to play their role in neurotransmission. For this reason, the precursor leaving the TGN requires maturation which consists of another fusion with the plasma membrane (PM), also containing synaptic proteins. Thus, SVPs are transported from the Golgi anterogradely to the axon terminal thanks to motors and adapter proteins. However, some studies pointed out that the transport to the PM can also be carried out throughout the dendrite (Sampo et al., 2003; Wisco et al., 2003), even if SVPs are mainly transported in the axon (Guedes-Dias & Holzbaaur, 2019; Staras et al., 2010).

## b. Anterograde molecular motor of SVPs: KIF1A

In the case of SVP axonal transport, KIF1A or KIF1B $\beta$  are recruited based on the subset of SVPs they carry (Okada et al., 1995; Santos et al., 2009). For example, synaptophysin is transported by KIF1A (Okada et al., 1995). Although KIF5B has been shown to transport SVPs (Q. Cai et al., 2007), the main anterograde molecular motor for the precursors is KIF1A (C. W. Chen et al., 2019; Maeder et al., 2014; N. Siddiqui & A. Straube, 2017; Okada et al., 1995).

### i. Structure and functions of KIF1A

The kinesin-3 family sequence is highly conserved (Gabrych et al., 2019) and KIF1A homologs can be found in *C. elegans* (UNC-104), *Drosophila* (Imac), mouse and human. Its conservation between species highlights its importance, particularly in terms of vesicular transport, neuroplasticity, spontaneous release and synaptic organization (Okada et al., 1995; Yonekawa et al., 1998; Y. V. Zhang et al., 2017). This subfamily is composed by KIF1A and KIF1B $\beta$ , but while KIF1A is expressed only in neurons, KIF1B $\beta$  is also present in glial cells (Hirokawa et al., 2010).

A few years after the discovery of the functional role of KIF1A, Okada demonstrated in 1999 that unlike other molecular motors, KIF1A has the ability to move along MT in its monomeric form (Okada & Hirokawa, 1999). However, kinesins were thought to move according to the hand-over-hand model due to their dimerized structure. So how can a monomeric motor move? Although it is now known that KIF1A also forms dimers to move anterograde, thanks to many structural studies, we now better know the monomeric KIF1A motility mechanism.

Like any other kinesin, KIF1A is composed of a motor domain on its N-terminal end where ATP is hydrolyzed and a cargo-binding domain on its C-terminal end. Specific domains within the stalk domain are described and lie between these two ends: the motor domain is connected to a neck coil domain (NC) by a flexible neck linker (NL). NC is followed by a first coiled-coil domain (CC-1), a forked head associated domain (FHA), two other coiled-coil domains (CC2 and CC3) which are linked to the Pleckstrin homology domain (PH) (figure 72).

*Motor domain:* in its N-terminal part, it is characterized by its catalytic core in which the P-loop (phosphate binding loop) acts as a nucleotide binding pocket (Hirokawa et al., 2009). This is where ATP binds and is hydrolyzed. On its C-terminal part, the motor domain shows a positively charged (lysine-enriched) K-loop interacting with the negatively charged MT hook (E-hook) (Soppina & Verhey,

2014). This weak interaction ( $\sim 0.15$  pN) allows KIF1A to move to the next binding site using diffusion without detaching from the MTs (Hirokawa et al., 2009). However, this diffusion is very slow ( $0.15 \mu\text{m} / \text{s}$ ) and cannot alone explain the high KIF1A processivity (N. Siddiqui & A. Straube, 2017).

*Neck Linker:* Completely detached from the catalytic core in the ADP state, but during the exchange of nucleotides (ADP to ATP) the neck linker attaches to the catalytic nucleus. This docking is responsible for the hand-over-hand mechanism as it transforms the chemical reaction into mechanical energy. It is considered as the power stroke: it generates force (Hirokawa et al., 2009).

*Stalk domain:* thanks to its structure mediates protein-protein interactions. An example of interacting proteins is the DENN / MADD adapter (see paragraph...). Moreover, the coiled-coil domains mediate motor dimerization (Y. Shimizu et al., 2005) and CC1-FHA is known as a central hub for the control of motor activation (Huo et al., 2012). Finally, the FHA-CC2 region is autoinhibitory and blocks access to microtubules (Hammond et al., 2009) and FHA is known to play a crucial role in cargo binding for other kinesins.

*PH domain:* due to its high affinity for PIP2, it is believed to be important for binding of cargo vesicle (Klopfenstein & Vale, 2004). However, this domain has been found not to be sufficient (Hirokawa et al., 2010), possibly due to the preferred localization of PM PIP2.

## ii. KIF1A cargoes

KIF1A was first discovered for its role in **SVP** transport because it allows the one of synaptophysin (Okada et al., 1995). Since then, the KIF1A-mediated transport of SVP has been confirmed as other SPs are essentially transported by KIF1A: vamp-2 and syt-1 (J. S. Liu et al., 2012; Sgro et al., 2013; Yonekawa et al., 1998).

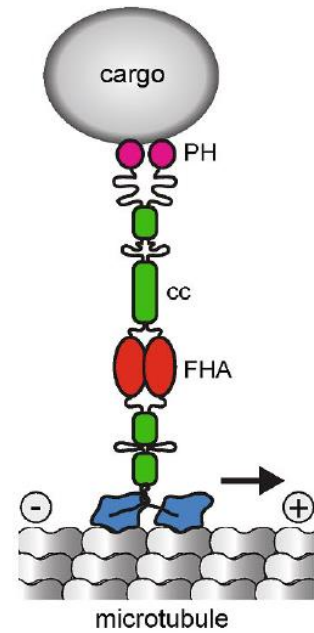


**Figure 72: KIF1A dimer structure.** Scheme from N.Siddiqui & A.Straube, 2017



Although KIF1A is known for carrying SVPs, it can also transport other types of vesicles:

- Dense Core Vesicles

During the last decade, DCVs have been found to be transported by KIF1A or UNC104 by the colocalization of several DCV proteins or peptides with KIF1A during transport: BDNF (Barkus et al., 2008; Hung & Coleman, 2016; Kondo et al., 2012; Lo et al., 2011), neuropeptide-Y (Lo et al., 2011), syt-4 (Arthur et al., 2010; Bharat et al., 2017), endosomes containing TrKA (Tanaka et al., 2016) and autophagosome containing ATG-9 (Stavoe et al., 2016) (Gabrych et al., 2019; N. Siddiqui & A. Straube, 2017). Indeed, KIF1A vesicles

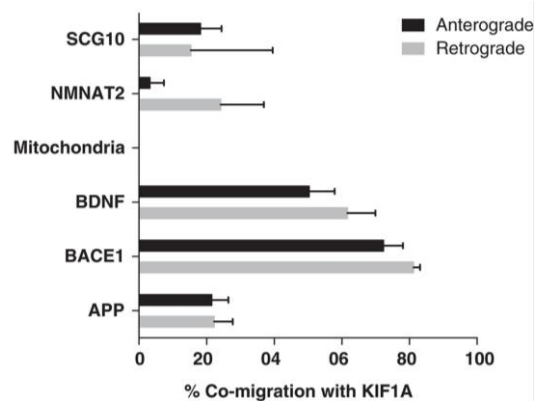


**Figure 73: KIF1A also transports BDNF vesicles and BACE1 vesicles.** Percentage of co-migration of KIF1A and several cargoes, from Hung & Coleman, 2016

colocalize with 15% of BDNF vesicles in the axons of cultured neurons in the hippocampus (R. Yang et al., 2019). Other studies have found that BDNF primarily uses KIF1A to be transported (Hung & Coleman, 2016; Lo et al., 2011) (figure 73). These results were inconsistent with kinesin-1 believed to be responsible for DCV transport (Butowt & Von Bartheld, 2007; Dompierre et al., 2007; Gauthier et al., 2004; Lim et al., 2017). Redundancy was the first hypothesis to explain how these two motors can regulate the transport of the same cargo (Gabrych et al., 2019; R. Yang et al., 2019) but it turned out not to be true in *Drosophila*; Overexpression of KHC does not save UNC104 RNAi phenotypes in the larva (Lim et al., 2017). Rather than conflicting, these two kinesins both appear to be necessary for DCV transport: they both associate with DCV (Lim et al., 2017). UNC104 first associates with DCV to promote transport from the cell body to the axon where it co-assembles with Kinesin-1, which is required for anterograde transport and responsible for the correct distribution of DCV within the axon. The mechanism is still unknown, but they appear to act in a complementary way: kinesin-1 could help kinesin-3 to maintain its dimerized form to enable processive and fast axonal transport of DCV. By binding to the same DCV, the two motors combine their properties to regulate the speed and stroke length of the vesicle (Lim et al., 2017).

- APP containing vesicles

APP is known to be transported primarily and anterograde in TGN-derived vesicles, other than SVP, with the kinesin-1 family (KIF5C) (DeBoer et al., 2008; Kaether et al., 2000; Szodorai et al., 2009). APP vesicles contain Rab-3a, SNARE proteins (SNAP25, syntaxin-1, VAMP-2), synapsin and active zone proteins but most of them are specific and differ from SVP since they do not contain Syp (Kaether et al., 2000; Szodorai et al., 2009). Furthermore, although it has been shown that 20% of APP positive

vesicles are carried with KIF1A or Vamp-2 (Gabrych et al., 2019; Hung & Coleman, 2016; Kohli et al., 2012) (figure 73), KIF1A mutation or silencing does not affect axonal transport of APP (Hung & Coleman, 2016; Kaether et al., 2000). Indeed, in these experiments, APP vesicles moved at the same speed as before treatment (on average 4.5  $\mu\text{m}/\text{s}$ ) and over longer distances than syp-containing vesicles which moved four times slower (0.9  $\mu\text{m}/\text{s}$ ).

- BACE1 containing vesicles

It has been shown that BACE1, the  $\beta$ -secretase that cleaves APP, is mainly transported by KIF1A, in distinct vesicles from APP vesicles, avoiding APP cleavage. Furthermore, the transport mechanism of BACE1 and APP appears to be different as a KIF1A mutation alters the transport of BACE1 without affecting the transport of APP (Hung & Coleman, 2016).

iii. KIF1A inhibition / activation by dimerization

Today, the regulation of KIF1A activity is not fully understood due to its complexity (Gabrych et al., 2019). Despite Okada's findings in 1999, we now believe that when KIF1A is monomeric, free within the cytosol or bound to a vesicle, it is autoinhibited (Al-Bassam & Nithianantham, 2018). However, it is still not clear whether KIF1A needs to be dimerized on the cargo membrane to be activated (Soppina et al., 2014; Tomishige et al., 2002) or whether the dimerized KIF1A is autoinhibited and needs an additional signal to become active (Hammond et al., 2009).

In the latest and most approved model (Al-Bassam & Nithianantham, 2018), KIF1A activation follows dimerization on the cargo membrane (figure 74). This dimerization not only abrogates monomeric autoinhibition, but also activates the motor functions of KIF1A. As a monomer, KIF1A is self-inhibited by the interaction of the neck coil domain and CC1, which is relieved by the interaction with the neck coil domain of another kinesin (Gabrych et al., 2019; Huo et al., 2012; Soppina et al., 2014) (figure 74). The dissociation of this dimer alters KIF1A-mediated transport in *C. elegans* and influences its behavior (Yue et al., 2013). In the case of SVP, ARL8 would be involved in the relief of autoinhibition by allowing dimerization, also regulated by liprin- $\alpha$  (Hirokawa et al., 2010; O. I. Wagner et al., 2009). These interactions are possible due to the high probability of protein interaction of the stalk domain.

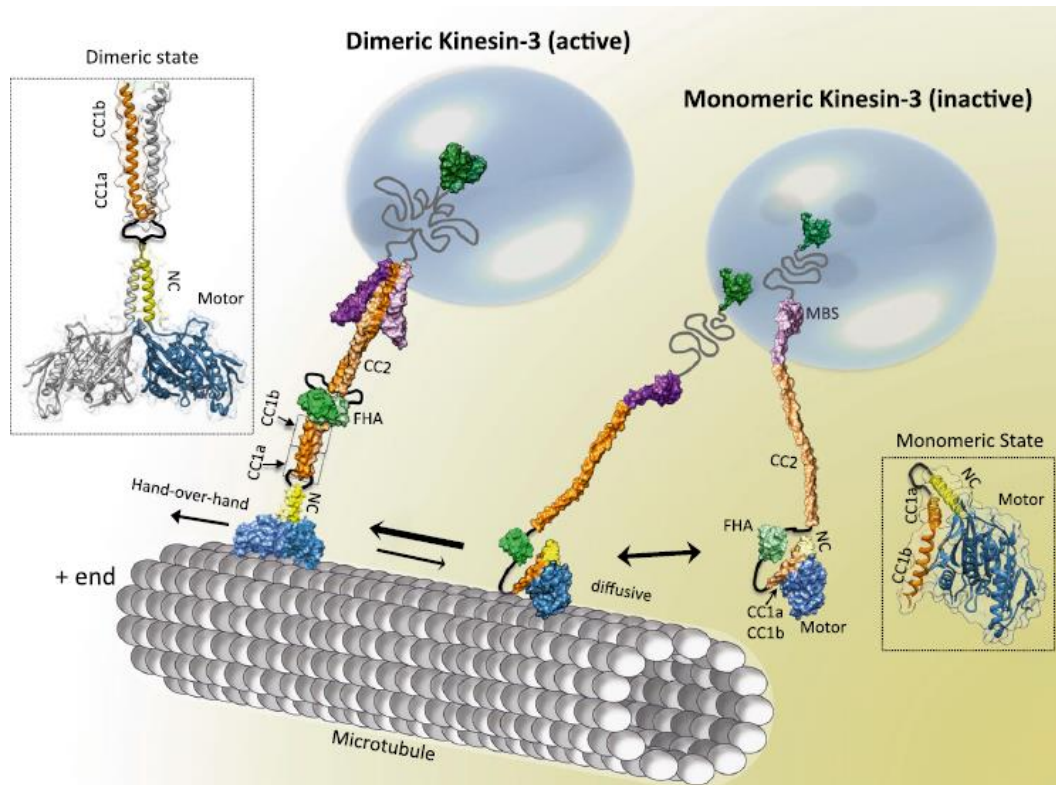


Figure 74: KIF1A activation follows KIF1A dimerization on the vesicle. Scheme from Al-bassam et al., 2018

#### iv. KIF1A processivity

KIF1A, like other members of the Kinesin-3 family, is unique for its particularly efficient super-processive motion for long-range axonal transport (Soppina & Verhey, 2014). Its processivity is defined both by the low number of pauses that occur in a run and by its speed.

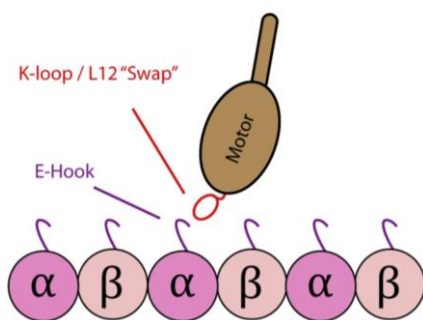


Figure 75: KIF1A affinity for MT is increased thanks to the K-loop. Scheme from Arpağ et al., 2019

The low number of pauses is partly due to the high affinity between the motor domain (k-loop) and the MTs ( $\epsilon$ -loops), which is approximately 250 times higher than kinesin-1 and MTs (Atherton et al., 2014; Guedes-Dias & Holzbaaur, 2019; N. Siddiqui & A. Straube, 2017) (figure 75). The high affinity between the two loops increases the attachment rate of KIF1A without changing its velocity, making it highly processive (Arpağ et al., 2019), (Soppina & Verhey, 2014). Furthermore, when KIF1A pauses occur, KIF1A specifically stops at the MT terminal (Yogev et al., 2016), which can connect multiple MT segments together and thereby increase the processivity of other running KIF1As (Lessard et al., 2019).

A vesicle carried by KIF1A can easily reach speeds of 3  $\mu\text{m} / \text{s}$  or more thus covering between 3 and 8  $\mu\text{m}$  of MT in a single run (Guedes-Dias & Holzbaur, 2019; Lessard et al., 2019). These maximum speeds could be allowed by the multimerization of KIF1A (N. Siddiqui & A. Straube, 2017) on a vesicle (see chapter 2 b-i-5-c). For example, an SVP can be transported from 1 to 4 kinesin-3 in *C.elegans* (Hayashi et al., 2018).

When this high affinity between KIF1A and MT is reduced, in a double curtain depletion model, for example, the lengths of the KIF1A series are reduced (Lipka et al., 2016; J. S. Liu et al., 2012).

#### v. Adaptors

Due to its stalk domain, KIF1A can easily form protein-protein interactions. Their diversity allows for precise regulation at different stages of cargo transport. The activation, processivity, delivery of the cargo and specificity of KIF1A are regulated by adaptors. Interestingly, two of these rely on the interaction between a GTP-ase within the SVP, providing insights for the regulation of KIF1A and a scaffold protein that binds to KIF1A. This is not surprising because Rab proteins, once activated, are known to bind to the vesicles and become a target marker; the activated Rab-3-containing vesicle has a specific compartment of destination with which it should fuse (H. Cai et al., 2007; N. Siddiqui & A. Straube, 2017; Stenmark, 2009).

- **Arl8/ALR8B & BORC complex:** this small arf-like guanosine triphosphatase (GTPase) found on SV (Shigeo Takamori et al., 2006) also binds to the stalk domain of inactive KIF1A (Y. E. Wu et al., 2013). When acquiring its GTP from, the Arl8 / ALR8B interaction with **activates UNC104/KIF1A** unlocking KIF1A self-inhibition in *C.elegans* (Niwa et al., 2016). The crucial role of Arl8 is illustrated by its need for SVP transport in *C.elegans* (Klassen et al., 2010; L. B. Li et al., 2016). . This mechanism ensures that UNC104 / KIF1A is activated specifically on the cargo vesicles which will then bind together. Arl8 is thought to be activated and recruited into SVPs by the BLOC-1 related complex (BORC), known for its regulation of lysosomal transport. More specifically, one of its six subunits, SAM-4 / Myrlysin, promotes the PIL-to-GTP exchange of Arl8 in vitro and recruits Arl8 to SVP in vivo in *C.elegans* (Niwa et al., 2017). Interestingly, this complex proved unnecessary and absent on SVPs within rat neurons, suggesting that the SVP transport mechanism may differ by species (here, *C.elegans* and mouse) (Pace et al., 2020).

- **Rab3 & DENN/MADD:** the DENN / MADD death domain binds to the KIF1A stem and the MADD domain binds to the small guanosine triphosphatase (GTPase) Rab3 present within the SVP membrane (Shigeo Takamori et al., 2006) (figure 76). These interactions regulate the

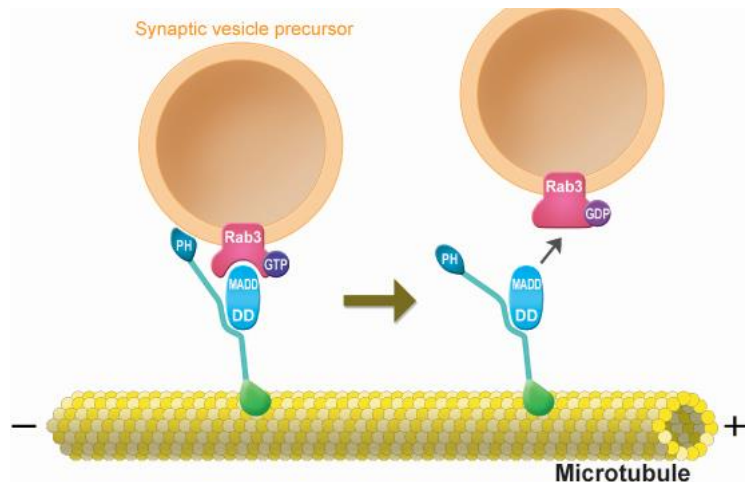
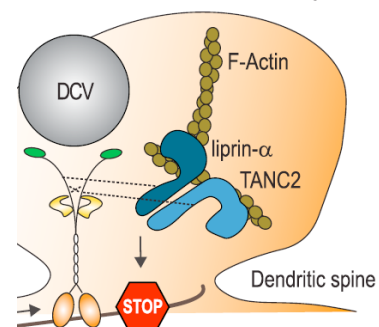


**Figure 76: DENN/MADD complex acts as an adaptor for KIF1A recruitment on SVP.** Scheme from Niwa et al., 2008

binding of SVP to MTs based on the nucleotide state of Rab3; in its GTP-Rab3 form, SVP binding is more effective (Hirokawa et al., 2010; Niwa et al., 2008; O. I. Wagner et al., 2009). These adapters are believed to be important for load binding specificity (Hirokawa et al., 2010) but also for preventing SVPs from escaping the presynapse (Guedes-Dias & Holzbaaur, 2019). However, in *C. elegans* lacking the DENN/MADD homolog, the transport of synaptotagmin is not impaired (Mahoney et al., 2006). This suggests that other proteins are involved in the regulation of SVP transport (Hirokawa et al., 2010).

- **Liprin- $\alpha$ :** Known for its role in PSD scaffolding, this protein may be a potential KIF1A adapter, although its mechanism of action in SVP transport is still unknown. First described as a KIF1A receptor due to its ability to bind to the tail region of KIF1A (Shin et al., 2003), it was later thought to be a scaffolding protein for regulating KIF1A motility and transport efficiency (O. I. Wagner et al., 2009). For example, liprin could increase LIN2 / CASK recruitment into the KIF1A stalk domain, forming a complex that has been shown to increase KIF1A series

**KIF1A recruitment in spines**



liprin- $\alpha$ /TANC2 capture KIF1A-driven DCVs

**Figure 77: liprin- $\alpha$  acts as a KIF1A captor at dendritic spines.** Scheme from Stucchi et al., 2018

lengths (G. H. Wu et al., 2016). Liprin and the mutant *Drosophila* LIN2 and *C. elegans* show a decrease in the anterograde processivity of SVP and an increase in the initiation of retrograde transport (Miller et al., 2005; O. I. Wagner et al., 2009; G. H. Wu et al., 2016). However, nowadays, this hypothesis is being re-evaluated due to the ability of liprin to form KIF1A clusters at the axon terminal (Hsu et al., 2011; O. I. Wagner et al., 2009), and

also due to its synaptic localization and unaltered distribution in mutants (Sieburth et al., 2005; Stucchi et al., 2018). In a recent study, it was found that liprin acts as a KIF1A collector by transporting DCV within the dendritic spines rather than a cargo adaptor (Stucchi et al., 2018) (figure 77).

Of note, until now, no studies have investigated whether and how all these adapters are linked together with KIF1A. One hypothesis could be that a large scaffold adapter could pick up all of these proteins to allow for fine regulation of KIF1A transport.

vi. SVP targeted to the synapse resulting from the release of SVP from KIF1A

Once KIF1A is activated, it carries the SVPs following the plus end of the MTs. But how does KIF1A unload cargo at the axon terminal? It all lies in the high density of GTP-rich microtubule lattices in the presynapse, the discharge zone. First, KIF1A and its cargo are detached from MTs at presynapse due to the low affinity KIF1A has for GTP-rich microtubule lattices (Guedes-dias et al., 2019).

The high density of GTP will also increase GTP hydrolysis by both Arl8 which will lead to inactivation of KIF1A (Niwa et al., 2016) and Rab3 which will decrease the KIF1A affinity for MT through the DENN / interaction MADD, releasing SVPs at the synapse (Niwa et al., 2008).

vii. KIF1A mutations: loss and gain of functions

In many – if not all- organisms, KIF1A is a sensitive protein due to its crucial role in long-distance transport of cargoes. Its downregulation or the presence of mutations cause changes in cellular dynamics, morphology and behavior in fungi, nematodes, flies, zebrafish, mice and humans (Esmaeeli Nieh et al., 2015; Kern et al., 2013; Lyons et al., 2008; Ohba et al., 2015; Otsuka et al., 1991; Pack-chung et al., 2007; Phan et al., 2019; Yonekawa et al., 1998; Zekert & Fischer, 2009), generating a “transportopathy” (Gabrych et al., 2019).

In mice, knocking out KIF1A results in a decrease in the transport of SVP in axons and in the accumulation of SP and SV at the synapses leading to neuronal degeneration and perinatal death (Yonekawa et al., 1998) (figure 78). In *C. elegans* and *Drosophila*, UNC1014 KO causes deficits in axonal transport and in the learning and memory of these animals (L. B. Li et al., 2016; Phan et al., 2019). In humans, KIF1A mutations are often dominant negative (Cheon et al., 2017; Esmaeeli Nieh et al., 2015) and are

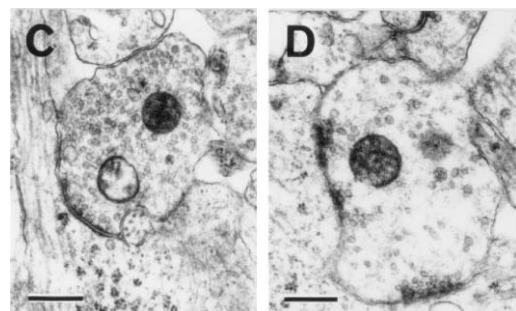


**Figure 78: KIF1A KO mice exhibit a decrease in the number of SV at the synapse.** Pictures from electron microscopy from WT (C) and KIF1A KO (D) brains from Yonekawa et al., 1998

responsible for SPG-30, an hereditary spastic paraplegia (HSP), causing neurodegeneration in which stiffness of the legs, shaking, ataxia and intellectual disability (cortical visual impairment, epilepsy) are the main symptoms (Esmaeeli Nieh et al., 2015; Hedera, 2000). These neurological symptoms could be explained by the progressive cerebral and cerebellar atrophy revealed by MRI (figure 79). Related rare diseases have been reported to be due to KIF1A mutations such as HSANII (hereditary sensory and autonomic neuropathy type II) and PEHO (Gabrych et al., 2019; Rivière et al., 2011).

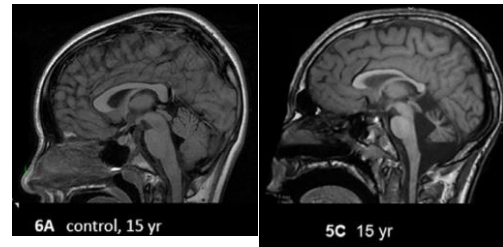


**Figure 79: KIF1A mutation in human causes cerebellar atrophy.** MRI images from a control 15-year-old child (left) or from a 15-year old child with a R216H mutation on KIF1A, from Esmaeeli Nieh et al., 2015

KIF1A mutations have been shown to be the source of loss of physiological functions but also of gains of functions. Although their mechanisms are different, they both lead to aberrant subcellular localizations of neuronal cargoes. In human, most of KIF1A mutations are found within the motor domain and lead to its loss of function by altering protein dynamics (Cheon et al., 2017) or ATP binding / hydrolysis (Esmaeeli Nieh et al., 2015). This is for example the case of the T99M mutation which decreases ATP binding by reducing KIF1A nucleotide affinity. This mutation dramatically decreases KIF1A velocity on MTs (figure 80) and is believed to be responsible for the cerebellar atrophy (Esmaeeli Nieh et al., 2015). Of all the other mutations found in humans, one has shed some light on the importance of motor release from SVPs. Indeed, the T258M reduces SVP retention at presynapses by modifying the affinity of KIF1A for microtubules (Cheon et al., 2017; Guedes-dias et al., 2019), thus causing a decrease in presynaptic strength in hippocampal neurons (Guedes-dias et al., 2019).

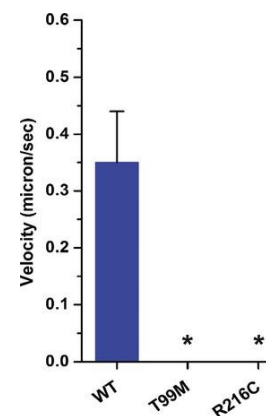


**Figure 80: KIF1A mutation decreases KIF1A velocity *in vitro*.** Velocity of KIF1A in WT condition or with mutation (T99M or R216C), from Esmaeeli Nieh et al., 2015

Some human SPG mutations can strengthen KIF1A which becomes hypermotile or acquires a greater affinity for MTs, conferring a gain of a new function to the motor (Gabrych et al., 2019; Niwa et al., 2016). For instance, R350G and A255V mutations (figure 81) were found to increase KIF1A velocity and accumulate SVPs at the axon terminal on *C. elegans* neurons respectively (Chiba et al., 2019). Other mutations found in the stalk and motor domains of UNC104 increase MTs and cargo vesicle binding by

disrupting autoinhibition and causing an excessive activation that is responsible for a decreased in synaptic density and size (Niwa et al., 2016).

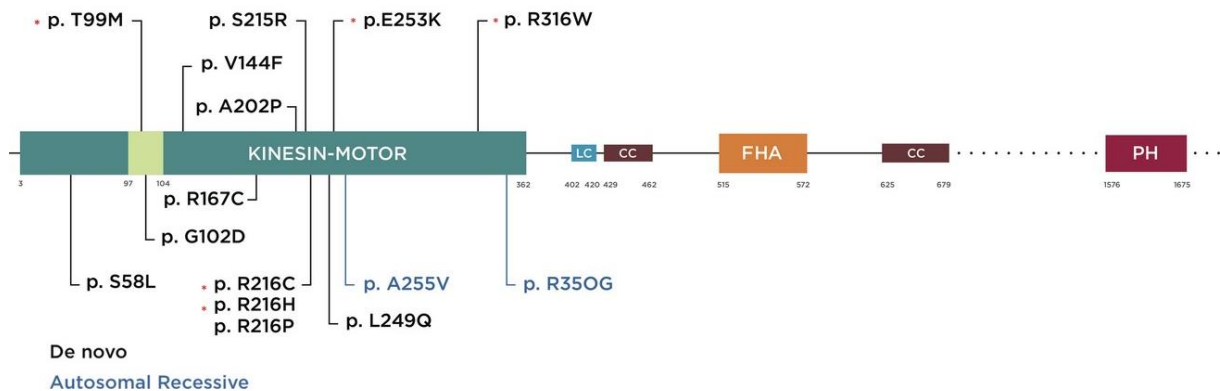


**Figure 81: KIF1A mutations in human diseases.** Scheme from Esmaeeli Nieh et al., 2015

Understanding of the consequences of these mutation on neuronal dynamics suggests that axonal transport is a key regulator for synapse homeostasis and that cargo accumulation or decrease at the synapse may be pathogenic (Gabrych et al., 2019).

To conclude, SVP are immature SV transported to the axon terminal anterogradely by KIF1A. Therefore, KIF1A is partly responsible for the number of SVs at the axon terminal. This molecular motor which carries various cargoes must be activated to be highly processive. Due to its structure, KIF1A can bind to many adaptors that regulate its activation, motility and cargo delivery. When KIF1A structure is modified by mutations, loss-of-function and gain-of-function appear along with SVP mislocalisation and cause “transportopathies”, dramatic neurodegenerative disorders like HSP. How does a KIF1A transported SVP becomes an SV?

### c. From immature SV to old SV

Thanks to kinesin-mediated anterograde transport, presynaptic sites are replenished with 20-40 new SVPs per day (Guedes-Dias & Holzbaur, 2019). Once the SVPs are delivered to the presynapse, they undergo a first fusion with the PM to mature (Matteoli et al., 2004; Régnier-Vigouroux et al., 1991). This first cycle of exo- and endocytosis will add PM proteins to immature SVPs. After endosomal fusion, the newly formed SVs go to the recycling pool, are filled with NT and are then exocytosed following the influx of calcium. These newly formed SVs are responsible for all NT release during physiological activity (Truckenbrodt et al., 2018). SVs will undergo a few hundred cycles of exo-endocytosis over about 24 hours and will eventually become old and reluctant to release. After 24-48h



of permanence inside the reserve pool, they will be transported retrogradely and then degraded (figure 82) (Guedes-Dias & Holzbaaur, 2019; Truckenbrodt et al., 2018).

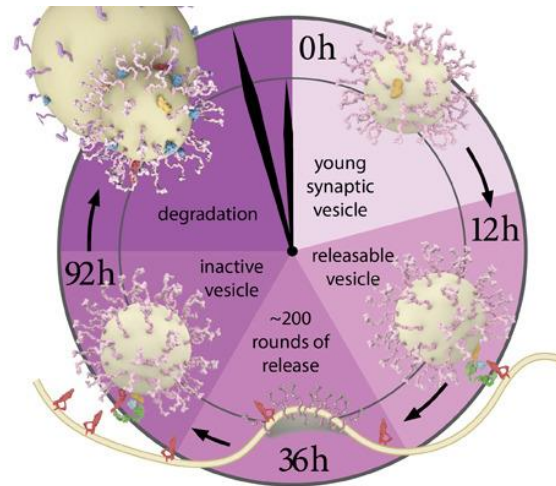


**Figure 82: SV cycle life lasts for more than 92h, from SVP biosynthesis to degradation. Scheme from Truckenbrodt et al., 2018**

#### d. Retrograde transport of SV: Dynein interacts with KIF1A

Altered or damaged proteins within a SV are likely to be targeted to degradation due to the importance of maintaining protein homeostasis in the neuron. Aggregates of damaged proteins alter protein homeostasis and, therefore, are a major cause of neurodegenerative disorders like AD, HD or PD (Cornejo et al., 2017; H. Vitet et al., 2020; Yap et al., 2018). The damaged SPs are believed to be inactivated with the help of SNAP25, ubiquitinated and targeted for degradation into lysosomes in the cell body through Rab7 recognition (Rizzoli, 2014; Truckenbrodt et al., 2018). This retrograde transport of SV to the soma is effected by dynein: when mutated in *C.elegans*, SV and UNC104 appear to accumulate at the nerve terminal due to impaired retrograde transport (C. W. Chen et al., 2019; Koushika et al., 2004).

Dynactin and its p150<sup>Glued</sup> subunit bind to dynein for cargo specificity and other adaptors can be found on this dynactin-dynein complex to regulate its motility towards the MT minus end: LIS1, BICD1, NDEL and Hook3 (C. W. Chen et al., 2019; Guedes-Dias & Holzbaaur, 2019; N. Siddiqui & A. Straube, 2017). Interestingly, KIF1A can act as a component of this complex (Barkus et al., 2008; C. W. Chen et al., 2019; Koushika et al., 2004) as it is able to bind to both dynein and dynactin through CC2, CC3 and FHA domains (C. W. Chen et al., 2019). The interactions between motors and adaptors could be explained by the “motor coordination model” described in chapter 2 2-e-iii. But more than regulating the directionality of SVs, the dynein/dynactin complex appears to be required for SV transport mediated by UNC104 or KIF1A (Barkus et al., 2008; C. W. Chen et al., 2019; Koushika et al., 2004). It would act as

an UNC104 activator since when this complex is mutated, both the anterograde and retrograde velocities of UNC104 are drastically affected (C. W. Chen et al., 2019).

Knowing that HTT can impale both dynactin and dynein and that KIF1A is part of the HTT interactome (Shirasaki et al., 2012), it would not be surprising if HTT acted as a scaffold that supports SVP transport. This scaffolding would allow the presence of the two opposing motors and other adaptors localized on a vesicle and could regulate the transport via post translational modification occurring on HTT.

As we have seen, KIF1A-driven SVP axonal transport determines the fate of SVs and thus neuronal communication. However, the regulators of this KIF1A-driven axonal transport are still under discussion (de pace 2020) and the consequences of their actions in vivo remain unknown.

## Chapter 4 - Huntingtin as a crucial hub for protein interactions through its intrinsic molecular properties

The main objective of my PhD has been to understand the role of HTT as a scaffolding protein facilitating and regulating axonal transport. But before detailing the roles of HTT in FAT, it is important to describe the current knowledge on the biology of HTT and the relation between its structure and its functions. Studying HTT physiological functions is likely to lead to a better understanding of the consequences of its loss of functions partly responsible for HD.

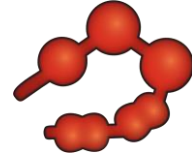


**Figure 83: 3D representation of HTT structure.**  
From Saudou & Humbert, 2016

### 1. HTT: a large, dynamic and ubiquitous protein

Both embryonic lethality at day 7.5 of HTT KO mice (Zeitlin et al., 1995) and symptom severity of HD patients emphasize the fact that HTT plays major role in the development and in physiological context in adult.

Huntingtin is a large protein (348 KDa) detected in most tissues (Marques Sousa & Humbert, 2013), with higher levels in the brain. HTT is expressed from development to adulthood and in many different cell types, from epithelial cells, to neurons or muscle. In neuronal cells, HTT is found in neurons, interneurons but also in astrocytes and oligodendrocytes (Creus-Muncunill & Ehrlich, 2019; Saudou & Humbert, 2016).

HTT being a very large protein, made the study of its biology difficult. Indeed, most of the investigations have been using overexpression of N-terminal parts of HTT to overcome these difficulties. However, such approaches had caveats since they potentially lead to overexpression artefacts and also because it neglected important parts of the protein such as the C-terminal part of HTT (El-Daher et al., 2015).

#### a. HTT structure creates a hub which is critical for multiple cellular functions

Bioinformatics study revealed that HTT is composed of 16 to 36 heat repeats which are solenoid like structure composed of anti-parallel alpha-helices essential for protein-protein interactions with other proteins or with HTT itself (Palidwor et al., 2009; Saudou & Humbert, 2016). These heat repeats are packed into larger domains (3 to 7) (figure 83 and 84) separated by disordered regions, known to contain post-translational modifications. Since the mutation on HTT leading to HD is located on the very N-terminal part of HTT, this portion is well described. It is composed of 17 amino acids involved in nuclear export signal, followed by a polyQ stretch, which has been found flexible,

unlike the following amino acids forming the Proline Rich Domain (PRD) that is critical for protein-protein interactions.

The complete structure of HTT at a 4 Å resolution has been recently resolved using Cryo-EM; It is composed by a large N-terminal part linked to the C-terminal part by a flexible bridge (Guo et al., 2018). This structure allows HTT to interact and scaffold various protein. In particular, the first structure shows that both N- and C-part of HTT scaffold the protein HAP40.

Although the complete list of HTT interactors is still not know for now, more than 300 HTT interactors have been found (Culver et al., 2012; Saudou & Humbert, 2016), indicating that HTT could participate to cellular dynamics, metabolism, protein turnover, gene expression or signal transduction (J. P. Liu & Zeitlin, 2017; Saudou & Humbert, 2016). Thus, by its structure, size, number of partners and the specific cellular processes it controls, HTT acts as a scaffold for proteins thus acting as a hub to finely control cellular processes (Guo et al., 2018; Saudou & Humbert, 2016).

Following is a non-exhaustive list of some HTT interactors and the role they play in different cellular processes (figure 84).

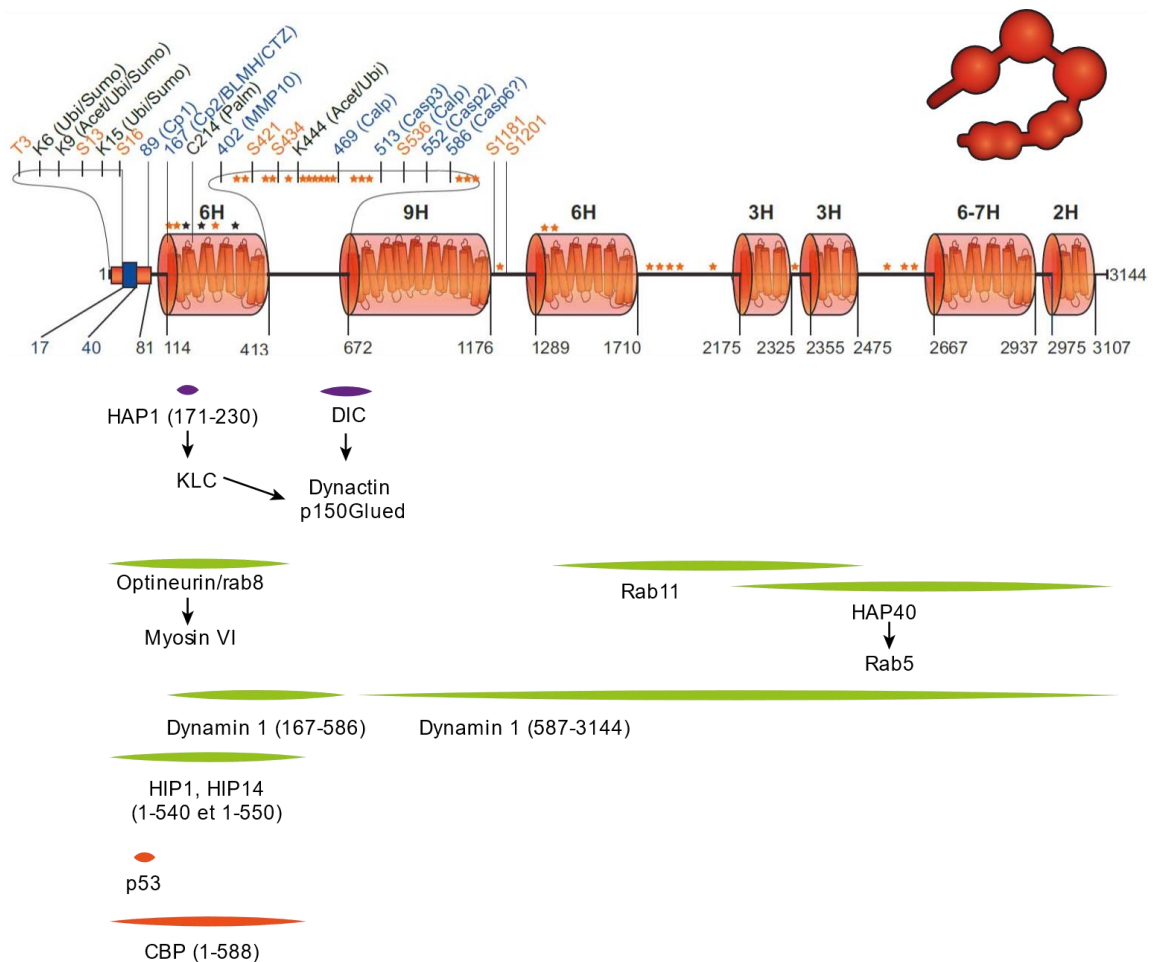
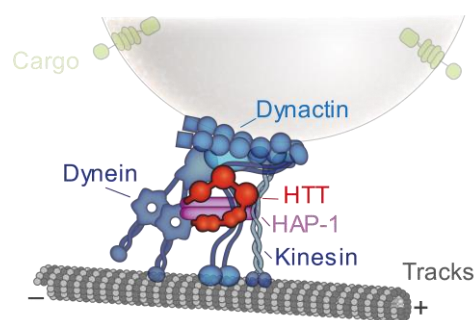


**Figure 84: HT interacts with many proteins involved in large cellular functions.** Purple: transport, green: endocytosis, orange : transcription, adapted from Saudou & Humbert, 2016

### i. Interaction with molecular motors

HTT acts as a scaffold by interacting directly or indirectly (through HAP1) with both dynein and kinesin respectively to control cellular dynamics like neuronal transport, cell division or ciliogenesis (Caviston et al., 2007; Colin et al., 2008; Gauthier et al., 2004; Gunawardena et al., 2003; J. P. Liu & Zeitlin, 2017; Saudou & Humbert, 2016; Twelvetrees et al., 2010).



Roles of HTT interactions on **neuronal transport** are detailed in the next chapter.

During **cell division**, HTT is targeted on the spindle poles through its dynein interaction to accumulate proteins that are essential for mitosis. Then, this complex is targeted to the cell cortex through kinesin-1 transport to bring the material able to generate pulling forces on astral MTs allowing a good positioning of the mitotic spindle (Elias et al., 2014; Godin et al., 2010; Saudou & Humbert, 2016).

HTT also controls the time and space location of essential proteins for **ciliogenesis**. Indeed, by regulating the transport of PCM1 to the base of the cilium, HTT regulates proper ciliogenesis (Keryer et al., 2011; Saudou & Humbert, 2016).

### ii. Interaction with endocytic machinery

HTT not only regulates transport but also trafficking between endosomes and thus participates to cellular events like clathrin mediated endocytosis and recycling.

By its interaction with HIP1/HIP12, HTT supports the plasma membrane invagination and the assembly of clathrin coating during **endocytosis**. In parallel, HTT also regulates dynamin-1 activation which is essential for the endocytosed vesicle to be separated from the membrane (El-Daher et al., 2015) (figure 85).

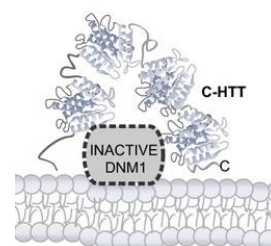


**Figure 85: HTT regulates dynamin-1 activation.** Scheme from El-Daher et al., 2015

HTT also interacts with Rab proteins such as Rab11 for **vesicle recycling** (but also for migration during development (Barnat et al., 2017) and polarity in epithelial cells (Elias et al., 2015)) and Rab5 through HAP40 interaction to reduce endosome motility (Pal et al., 2006). Transition of endosomes between MTs and actin is also controlled by HTT through its binding to Rab8/optineurin complex and myosin VI (Sahlender et al., 2005).

### iii. Interaction with gene expression modulators

More than being a scaffold to control cellular dynamics, HTT also acts as a scaffold to control **gene transcription and epigenetic regulation** (Francelle et al., 2017). By mediating the binding between transcription factors (like CBP, p53, REST/NRSF) and transcriptional regulators, HTT acts itself like a transcription factor since it can potentiate or inhibit a repressor or an activator. By this mechanism, HTT positively regulates NRSF expression, which is a transcription factor for several genes like BDNF (Saudou & Humbert, 2016; Chiara Zuccato et al., 2003) (figure 86).

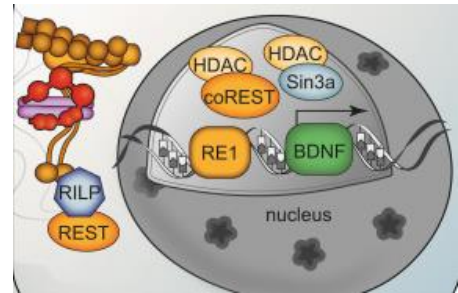


**Figure 86: HTT regulates transcription.** Scheme from Saudou & Humbert, 2016

### iv. Interactions with autophagy-related proteins

Thanks to its unique structure and the presence of LC3-interacting repeats, HTT shares similar properties with proteins responsible for scaffolding autophagy-related proteins like Atg11 (Ochaba et al., 2014). Loss of HTT protein reduces cargo recognition and loading to the autophagosome. HTT is thus thought to act here also as a scaffold for autophagy processes, regulating both cargo recognition and autophagy induction.

As a conclusion, HTT act as a scaffold tethering multiple partners into complexes according to cellular cues and processes. Some of these partners, like dynein, are effectors and some of them can be considered as regulators of the assembly and disassembly of complexes in time and space on the HTT hub (Saudou & Humbert, 2016). These proteins are thought to be involved in signaling like JIP3, Akt or Rab proteins and their action depend on their activation or location, reflecting the needs of activating specific signals at specific location within the cell. Interestingly, many Rab proteins have been found to interact in a direct or indirect way with HTT: Rab3 (SVPs), Rab19 (recycling vesicles), Rab7 (late endosomes) (J. A. White et al., 2015), Rab5 (endosome), Rab11 (recycling vesicles), Rab8 (endosomes) (Hattula & Peränen, 2000)(J. A. White et al., 2020) underlying the central role for HTT and Rab proteins interaction in regulating cellular trafficking.

### b. HTT PTMs regulate its functions

Due to its large size and specific structure, HTT exhibits many PTM sites. For instance, more than 70 phosphorylation sites have been reported from human cells (Hornbeck et al., 2012). These PTMs are located in disordered regions (fig 85) (Ehrnhoefer et al., 2011; Saudou & Humbert, 2016). In addition to phosphorylation, HTT undergoes other types of PTMs like ubiquitination, sumoylation, acetylation and palmitoylation (figure 85, (Saudou & Humbert, 2016)). Although the role of all these

PTMs in physiological condition are not known, some studies begin to put some light on them. For instance, acetylation, at low levels, has been shown to mediate HTT clearance (Jeong et al., 2009) whereas phosphorylation is neuroprotective (Humbert et al., 2002). Other PTMs like palmitoylation might be a good strategy to reduce some HD phenotypes (Virlogeux et al., *under revision*). PTM roles on axonal transport are detailed in the next chapter.

An approach to study the role of PTMs in HTT *in vivo* involves the generation of knock-in mice. It is the case for HTT<sup>S421D</sup> and HTT<sup>S421A</sup> mice in which the serine 421 has been replaced by either and respectively an aspartic acid to mimic constitutive phosphorylation or by an alanine to mimic the unphosphorylatable form of HTT.

### c. HTT: a flexible protein

3D HTT structure has been investigated for many years but the structure has only been recently reported given the difficulty to express high levels of HTT (Guo et al., 2018). HTT can acquire multiple conformations according to the context (Seong et al., 2009) (figure 87).

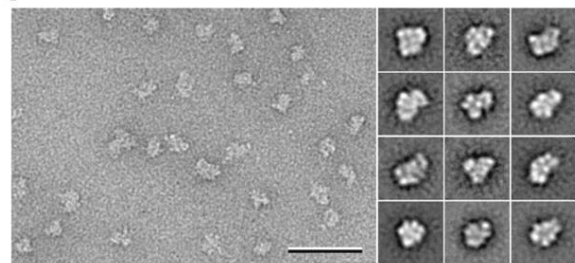


**Figure 87: HTT adopt multiple conformations according to the environment.** Picture of HTT conformations by electron microscopy from Seong et al., 2009

Recently, cryo-EM on HTT-HAP40 complex described HTT as a structure composed by three parts: the N-terminal part which has the ability to bind proteins on its two sides (internal and external), a flexible bridge (1685 – 2091) and a C-terminal part. Besides the highly flexible bridge, some N-ter and C-ter domains were found to also be flexible like the exon 1 and the 2062-2092 domain. Interestingly, N-ter and C-ter interactions are weak, which explains the high dynamics of HTT when it is not bound to any partner (Guo et al., 2018) (figure 88).

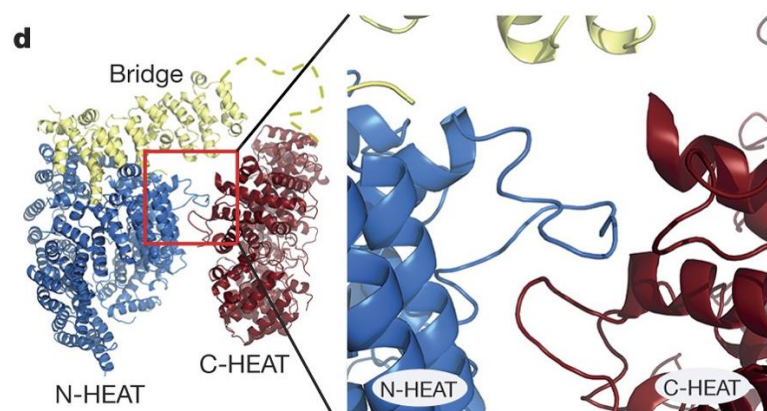


**Figure 88: weak interaction between C- and N-term.** 3D representation of N-ter and C-ter interaction from Guo et al., 2018

HTT high flexibility due to of intrinsically disordered regions (IDRs) leads to a lack of a stable secondary and tertiary structure. Thus, HTT, like any other protein containing IDRs does not follow the classical protein “structure-function” paradigm (Birol & Melo, 2020) relying on a unique 3D structure established by a specific amino acid sequence corresponding to a specific function. The last two decades proved that these proteins containing IDRs exhibit specific properties supporting their diversity in term of cellular functions (Birol & Melo, 2020). In fact, they are able to respond quickly to cellular cues, they have multiple partners and they are tightly regulated by PTMs (Birol & Melo, 2020). Years of studying the physiological roles of HTT and the consequences of its PTMs proved that HTT corresponds to all these criteria (Saudou & Humbert, 2016).

Roles of IDRs containing proteins are crucial because they are implicated in several NDs when they are mutated or misfolded, provoking their aggregation like it is seen in AD ( $A\beta$ ), PD ( $\alpha$ -synuclein) and HD (mHTT) (Birol & Melo, 2020). It is therefore not surprising that any HTT mutation like the polyQ extension or a point mutation on an amino acid carrying PTM leads to cellular dysfunctions.

## 2. HTT & HD

### a. Huntington’s disease (HD)

Huntington’s disease is a genetically inherited dominant neurological disease with a late onset which affects 5 to 10 individuals per 100.000 in the Caucasian population (orphanet, (Saudou & Humbert, 2016)); in France, it represents around 18.000 individuals (“dossier inserm”). One allele is sufficient to cause the disease and most of the patients are heterozygotes for the mutation. HD is characterized by the degeneration of neurons within the striatum and the cortex leading to a 30% reduction of brain weight (Rosas et al., 2008) (figure 89). HD patients carry a mutation that is located within the first exon of HTT gene (IT15) (MacDonald et al., 1993). It consists in an abnormal expansion of a CAG repeat coding for a polymorphic glutamine stretch (polyQ) on the N-terminal of HTT (MacDonald et al., 1993). If this stretch reaches 37 repeats or more, the protein is mutated and induces pathology. Number of repeats higher than 37 correlates with the age at onset (Saudou & Humbert, 2016). Juvenile forms of HD (5% of the cases) are generally caused by more than 55 CAGs in the polyQ stretch and are accompanied with epilepsy (Saudou & Humbert, 2016).



Figure 89: HD provokes neurodegeneration leading to a reduction of brain weight.

Symptoms are crippling by their diversity, their nature and their severity and start to appear around 30-40 years even though neuronal abnormalities can be observed as early as developmental stages



(Barnat et al., 2020). They are known to form a triad with motor dysfunctions (choreiform movements, bradykinesia, rigidity), cognitive decline (cognitive slowing, decrease in attention and mental flexibility) and psychiatric abnormalities (depression, irritability, impulsions, apathy, social disinhibition) (Saudou & Humbert, 2016). Other non-CNS-related symptoms can also be noted like metabolic and immune disturbances, cardiac failure, osteoporosis, ... (Saudou & Humbert, 2016). HD patients usually die around 20 years later, mostly from pneumonia caused by bradykinesia (orphanet).

Dozens of clinical trials have been launched in the last decade, but none of them brought a curative treatment against this disease (Tabrizi, Ghosh, et al., 2019, clinicaltrials.gov website). Nowadays, hopes are turned towards gene therapy through the use of antisense oligonucleotide (ASOs) (Barker et al., 2020; Tabrizi, Ghosh, et al., 2019; Tabrizi, Leavitt, et al., 2019) to reduce the gain of toxic functions and restore the HTT physiological functions.

#### **b. HD & HTT gain of toxic functions**

By its polyglutamine expansion at the N-terminal of HTT, the mutation responsible for HD leads to a gain of toxic functions. In HD patient brains, mHTT has been found to produce oxidative stress, excitotoxic processes and energy metabolism dysfunctions (M. Borrell-Pagès et al., 2006; Saudou & Humbert, 2016), affecting cell homeostasis and leading to cell death. Indeed, mHTT causes, for instance and non-exhaustively, a disruption of calcium homeostasis, a reduced trophic support, an inhibition of the proteasome and autophagy, mitochondrial abnormalities, an alteration in endocytosis and in vesicle transport and an increase of glutamate release (excitotoxicity). Besides the direct and negative consequences on cell homeostasis, some of these processes lead, more or less directly, to an activation of caspases which then cleave mHTT. Multiple cleavages of mHTT excessively produce N-ter fragments with the polyQ expansion and C-ter fragments of HTT, the two of them being known to be toxic for the cells (M. Borrell-Pagès et al., 2006; El-Daher et al., 2015; Gauthier et al., 2004; Saudou & Humbert, 2016). The polyQ Nter fragments are prone to aggregate and form neuritic, cytoplasmic and nuclear inclusions. The translocation into the nucleus of the polyQ-Nter fragments is a key step in HD because they affect transcription of classes of genes, like the BDNF gene or other gene important for neuronal development and function. Indeed, these fragments are able to sequester or interact with transcription factor (CBP, REST/NRSF), leading to a dysregulation of the transcription (M. Borrell-Pagès et al., 2006; Saudou & Humbert, 2016).

However, intranuclear aggregates are not directly correlated with neuronal death and their role in HD is still being discussed (M. Borrell-Pagès et al., 2006; Saudou & Humbert, 2016).

### c. HD & HTT loss of functions

The fact that HD pathology affects mostly adults and is very different to what is observed in the genetic invalidation of HTT in mice (embryonic lethality) led to the suggestion that HD could induce neurodegeneration through the gain of new toxic functions that are not related to HTT. However, the observation that loss or alteration of HTT function induce and/or modulate neurodegeneration indicates that HTT function plays an important role in pathogenesis. Indeed, although several toxic effects elicited by mHTT have been reported, these approaches were usually based on the expression at high levels of short fragments containing a high number of glutamines. Conversely, studies addressing HTT functions revealed that most, if not all, of these described functions are affected in HD (neurogenesis, axonal transport ciliogenesis, autophagy, etc.) suggesting that alterations of HTT functions have to be considered for understanding HD pathogenesis.

#### i. Potential mechanisms for HTT loss of function

How mHTT could induce alteration of HTT functions? One possibility is that elongation of the polyQ stretch on HTT could change HTT structure by affecting intramolecular interactions between the HEAT repeats (Vijayvargia et al., 2016) (figure 90). These structural changes could also modify also the inter-protein interactions (Ratovitski et al., 2012; Saudou & Humbert, 2016) since six phosphorylation sites have been found to be negatively affected by mHTT: pS421, pS434, pS1181, pS1201, pS1876 and pS2116 (Jung et al., 2019). Consequently, such modifications could affect HTT functions in the regulation of neuronal survival (e.g.: phosphorylation of S421).

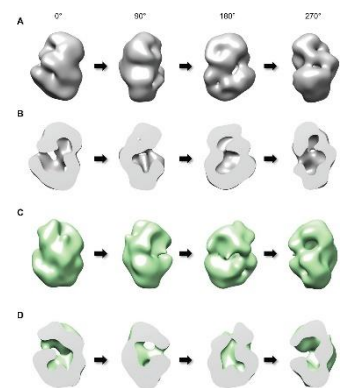


**Figure 90: HTT structures are affected by polyQ stretch.** 3D representation from Vijayvargia et al., 2016

In addition, in HD, heterozygotes patients for the mutation, possess one mutated and one wt allele (Saudou & Humbert, 2016). The fact that heterozygous and homozygous HD patients show no difference in their age at onset (Cubo et al., 2019) suggests that HD is a pure dominant disorder or that mHTT could exert a dominant negative effect on the wt HTT allele in heterozygous HD patients. In support of the last hypothesis, the specific silencing of mHTT in neurons derived from human embryonic stem cells showed a restoration of BDNF transport to what is observed in WT cells (Drouet et al., 2014). Overexpressing wt HTT but not mHTT can restore BDNF transport in heterozygous cells showed that HTT expression can overcome mHTT defects while mHTT cannot (Gauthier et al., 2004; Leavitt et al., 2006). In HD patients, this ratio of mhtt and HTT can be naturally changed by non-coding SNPs able to delay or anticipate the age of onset (Becanovic et al., 2015). In conclusion, the observation that the level of mutant HTT relative to the level of its wt form can have profound consequences on

HTT-mediated function and disease progression suggests that at least for BDNF transport, mHTT could act as a dominant negative protein over the wt HTT form.

## ii. Consequences of HTT loss of function

Loss of HTT function provoked by silencing, inactivating or KO of HTT has been studied both *in vitro* and *in vivo*. Among other read outs, HTT silencing leads to a reduced neuronal transport of BDNF, APP vesicles and autophagosomes in cells and flies (Caviston et al., 2007; Gauthier et al., 2004; Gunawardena et al., 2003; L. Her & Goldstein, 2008; Zala et al., 2008; Zala, Hinckelmann, & Saudou, 2013). *In vivo*, when HTT is inactivated during embryonic development, it affects neuronal morphology at adulthood (Barnat et al., 2017, 2020). Loss of HTT functions participate to neurodegeneration, motor phenotype and a reduced lifespan, in a similar way than in HD context, arguing for a loss of function role in HD (Burrus et al., 2020; Dragatsis et al., 2000; Gunawardena et al., 2003). Loss of HTT in striatal projecting neurons for example causes motor dysfunctions and hyperactivity, by dysregulating electrophysiological properties of these neurons (Burrus et al., 2020). Recently, loss of wt HTT consequences in a HD context has been revealed and described as the only cause for endocytosis defect (McAdam et al., 2020). Together, these studies show that alterations of wt HTT levels and function have profound consequences on brain functions, not only during development but also in adults.

## d. Clinical trials & loss of (m)HTT

Current clinical trials have focused their strategy mostly on DNA targeting using antisense oligonucleotides (Barker et al., 2020; Tabrizi, Ghosh, et al., 2019; Tabrizi, Leavitt, et al., 2019), mHTT clearance (Tabrizi, Ghosh, et al., 2019) or calcium homeostasis using pridopidine, an antagonist to sigma1 receptor (Eddings et al., 2019).

Antisense oligonucleotide (ASO) administration is the most promising strategy nowadays since it has been proven recently not to have any “serious adverse events” (Tabrizi, Ghosh, et al., 2019). ASO administration aims at decreasing the expression of both mHTT and wt HTT in HD patients by 60-75% of total HTT levels (J. P. Liu & Zeitlin, 2017) to limit toxic functions of mHTT. However, to our understanding and according to loss of functions studies on HTT, reducing wt HTT levels could potentially be detrimental. This is for example the case of some patients affected by Rett-syndrome like phenotypes associated with HTT mutations predicted to reduce HTT function (Rodan et al., 2016). More studies have yet to be performed to determine the minimal amount of wt HTT required for it to be fully functional (Barker et al., 2020; J. P. Liu & Zeitlin, 2017). However, decreasing specifically mHTT

expression by targeting HD-SNPs or CAG expansion in HD patients appears more promising (Southwell et al., 2018; Zeitler et al., 2019).

In conclusion, HTT by its structure, is able to interact with many proteins and form a large array of protein complexes, which could then regulate several aspects of neuronal homeostasis. Its multiple PTM sites and its flexibility are important for the regulation of HTT functions. In HD, mutation of HTT leads to the gain of toxic functions but also to the loss of some functions leading to a loss of homeostasis, participating to the neurodegeneration. Loss of HTT functions in HD are crucial to be determined because one current therapeutic strategy is based on the reduction of both mutated and wild type allele of HTT in HD patients. This is why we investigated here the physiological roles of HTT in axonal transport and more specifically the consequences of its phosphorylation at serine 421.

## Chapter 5 – Traffic signaling: new functions of Huntingtin and axonal transport in neurological disease

In this last chapter, we focus on the roles on axonal transport regulation of different HTT PTMs, namely, methylation and phosphorylation at different sites. We first emphasize the crucial HTT role on maintaining synapse homeostasis through its role in transport regulation. Then, HTT importance is highlighted by the multiplicity of both PTMs and mechanisms responsible for transport regulation; each PTM regulates axonal transport in a specific way. Finally, our interest is brought towards S421 phosphorylation impacts on axonal transport in pathological context like AD and Rett syndrome, which are the two first studies of this project.



## Traffic signaling: new functions of huntingtin and axonal transport in neurological disease

Hélène Vitet, Vicky Brandt and Frédéric Saudou



Over the past twenty years there have been numerous advances in our understanding of Huntington's disease (HD) and other neurodegenerative proteopathies such as Alzheimer's disease and Parkinson's disease. In each case, disease-specific proteins are expressed and accumulate; what has been less clear is precisely what problems are caused by the accumulation. Recently we have begun to appreciate that increased protein levels or changes in the ratios of different isoforms affect the movement of molecules along the axon, thereby disrupting neuronal function. Huntingtin, the protein involved in HD, plays a special role in axonal transport, and very recent studies have found that its activity — and the movement of its cargoes — is altered not only in HD but in other neurological diseases. Here, we contextualize these studies and consider how modulating huntingtin activity could provide new avenues to therapy.

### Address

Univ. Grenoble Alpes, Inserm, U1216, CHU Grenoble Alpes, Grenoble Institut Neurosciences, GIN, 38000 Grenoble, France

Corresponding author: Saudou, Frédéric ([frederic.saudou@inserm.fr](mailto:frederic.saudou@inserm.fr))

Current Opinion in Neurobiology 2020, 63:122–130

This review comes from a themed issue on Cellular neuroscience

Edited by Hollis Cline

For a complete overview see the [Issue](#) and the [Editorial](#)

Available online 12th May 2020

<https://doi.org/10.1016/j.conb.2020.04.001>

0959-4388/© 2020 Elsevier Ltd. All rights reserved.

### Introduction: the importance of intracellular transport in neurons

The intracellular environment has been justly compared to a bustling city, with a complex network of highways and railways along which membrane-bound vesicles, organelles, proteins, and other molecules travel to and fro. These 'transportation routes' are formed by different elements of the cytoskeleton — actin, intermediate filaments, and microtubules — that each plays distinct roles in enabling various cargoes to reach their proper destinations. In neurons, the microtubule network conducts traffic along the axons. Microtubules are polar molecules, with a stable minus end that points toward the cell body and a dynamic plus end that grows toward the axon

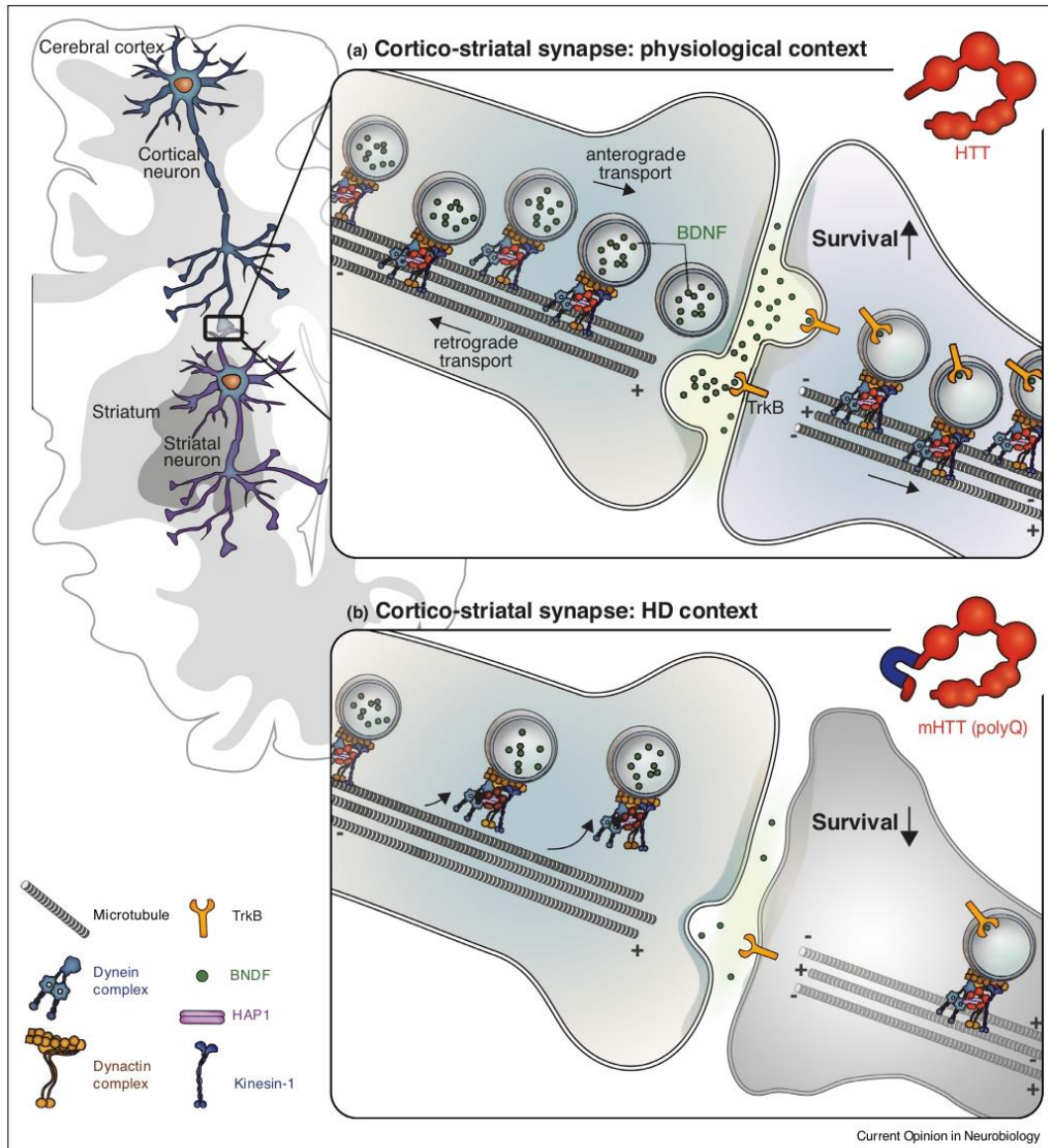
terminal. This polarity helps determine the direction of axonal transport. Kinesin motor proteins move in an anterograde direction, carrying newly synthesized molecules from the cell body toward the growth cones and synapses, while dynein proteins proceed in a retrograde direction, carrying signals for growth factors to the soma and returning aging proteins and organelles for recycling. Damage to the microtubule network is extremely detrimental: hyperphosphorylation of tau proteins, which help maintain microtubules in axons, leads to the formation of inclusions or neurofibrillary tangles that are seen in Alzheimer's disease, frontotemporal dementia, chronic traumatic encephalopathy, and other 'tauopathies.' Long before these accumulations become evident, however, hyperphosphorylated tau disturbs axonal transport; even changes in the ratio of different tau isoforms alters the direction and speed of vesicular traffic [1\*,2\*].

Axonal transport can be influenced by many factors other than the microtubule network itself. A build-up of cellular detritus, as occurs when a certain protein is either overexpressed or fails to be properly cleared (recycled), could impede trafficking, and this may be what happens in the larger family of proteopathies that includes Alzheimer's, Parkinson's and Huntington's disease. In this review, however, we will be focusing on the protein Huntingtin (HTT), whose mutation (a polyglutamine expansion) underlies Huntington's disease (HD). HTT is a large scaffolding protein that interacts with both kinesin-1 and dynein motors, as well as over four hundred other proteins, many of which are active in microtubule-based or actin-based transport [3]. In HD neurons, flies, and mice, mutant HTT (mHTT) impedes fast axonal transport and interferes directly with the trafficking of brain-derived neurotrophic factor (BDNF) and autophagosomes [4–6]. This ability to move BDNF and autophagosomes, two cargoes that are extremely important for neuronal health, suggests that modulating HTT activity might prove beneficial for a variety of neurological diseases.

### HD as a disease of defective transport

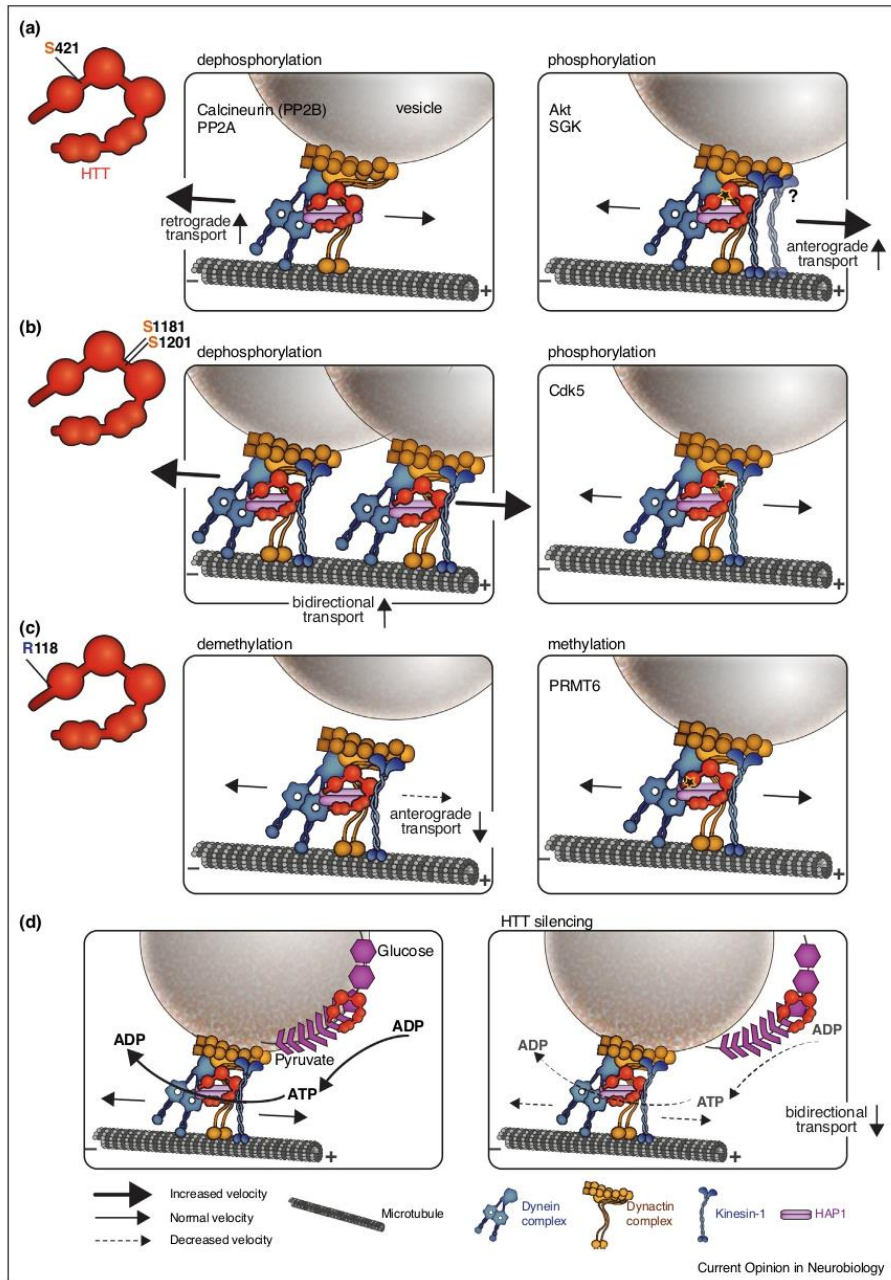
Like the tauopathies mentioned above, Huntington disease (HD) causes cognitive deterioration and personality changes long before motor symptoms appear. The disease is typically diagnosed in the fifth decade of life, by which time there is already considerable dysfunction and death of neurons within the corticostriatal circuit [7]. The HD mutation is an abnormal expansion of a CAG repeat in *HTT* that is translated into an

Figure 1



Huntingtin transports vesicles along microtubules toward the synapse. **(a)** Huntingtin facilitates anterograde transport of various vesicles, such as those containing the Brain-Derived Neurotrophic Factor (BDNF). When released at the synapse, BDNF will bind its receptor TrkB, which will be internalized and transported back to the soma of the striatal neurons where it will elicit a survival signal. **(b)** In HD, BDNF-containing vesicles are transported less efficiently because they tend to detach from microtubules. As a result, BDNF release at the synapse, TrkB receptor activation, and survival signaling are all reduced, leading to dysfunction and death of striatal neurons.

Figure 2



Post-translational modifications of Huntingtin modify its interactions with other proteins to govern the speed and directionality of transport. **(a)** The Serine/Threonine kinase Akt and the serum- and glucocorticoid-induced kinase SGK are able to phosphorylate HTT at S421; this residue is dephosphorylated by calcineurin and PP2A. HTT phosphorylation at S421 recruits kinesin-1 to the dynein/dynactin complex, which promotes anterograde transport of specific vesicles. In contrast, dephosphorylation of HTT S421 detaches kinesin-1 to promote retrograde vesicular



abnormally long polyglutamine (polyQ) tract in the N-terminal part of the mutant HTT (mHTT) protein. HTT is ubiquitously expressed, and is found not only in neurons but also astrocytes and oligodendrocytes [8,3,9].

Most HD patients carry one normal and one mutant allele; because of the dominant inheritance pattern, HD was first thought to be due solely to a toxic gain of HTT function. Loss of wild-type HTT function, however, also contributes to the disease, and mHTT exerts dominant-negative effects on the wild-type HTT and its normal functions in intracellular trafficking, cell division, ciliogenesis, migration, autophagy, and transcription [3]. HTT's ability to interact with such a large number of proteins is facilitated by its structure, which consists of large N-terminal and C-terminal domains linked by a flexible bridge [10\*\*], with the two sides of the N terminal (internal and external) being accessible for protein binding.

One of the first HTT interactors to be identified, Huntingtin-associated protein 1, HAP1, linked HTT to axonal transport through the dynein/dynein complex [11,12] and then later on through the kinesin-1 complex [13]. HTT also binds directly with the dynein intermediate chain [14]. Through these interactions, HTT facilitates the transport of vesicles by decreasing their pausing time along microtubules and determining their direction of movement. HTT transports vesicles that contain brain-derived neurotrophic factor (BDNF) [5], the amyloid precursor protein, APP [15,16], VAMP7 [15], Rab proteins [17], GABA receptors [18], autophagosomes [6], endosomes and lysosomes [19,20], precursors of synaptic vesicles [21], and protein complexes and RNA [22]. Overexpression of full-length HTT or N-terminal fragments in cells or *in vivo* in fly larvae increases transport efficiency, while silencing HTT reduces transport [4,5,21]. In the context of HD, mutant HTT (mHTT) binds with a higher affinity to HAP1 and the molecular motors, which induces vesicles to detach prematurely from the microtubules, thereby diminishing the efficacy of transport overall. Selective silencing of the mutant allele in human embryonic neural stem cells restores axonal transport [23].

Of all the specific cargos associated with HTT, BDNF appears to be the most essential for maintaining the health of the corticostriatal circuit, which is the primary site of degeneration in HD. Striatal neurons depend heavily on trophic support from corticostriatal afferents [24\*\*,25\*,26] — so much so that loss of BDNF from these corticostriatal projecting neurons is sufficient to induce

neurodegeneration [27–29]. Conversely, restoring secretion of BDNF has a neuroprotective effect on the striatum and corticostriatal synapses [30]. Thus, both the loss of function of wild-type HTT and the interference in transport caused by mHTT reduce BDNF trophic support to the striatum, making BDNF insufficiency an important part of HD pathogenesis (Figure 1).

### Post-translational modifications of HTT regulate speed and direction of transport

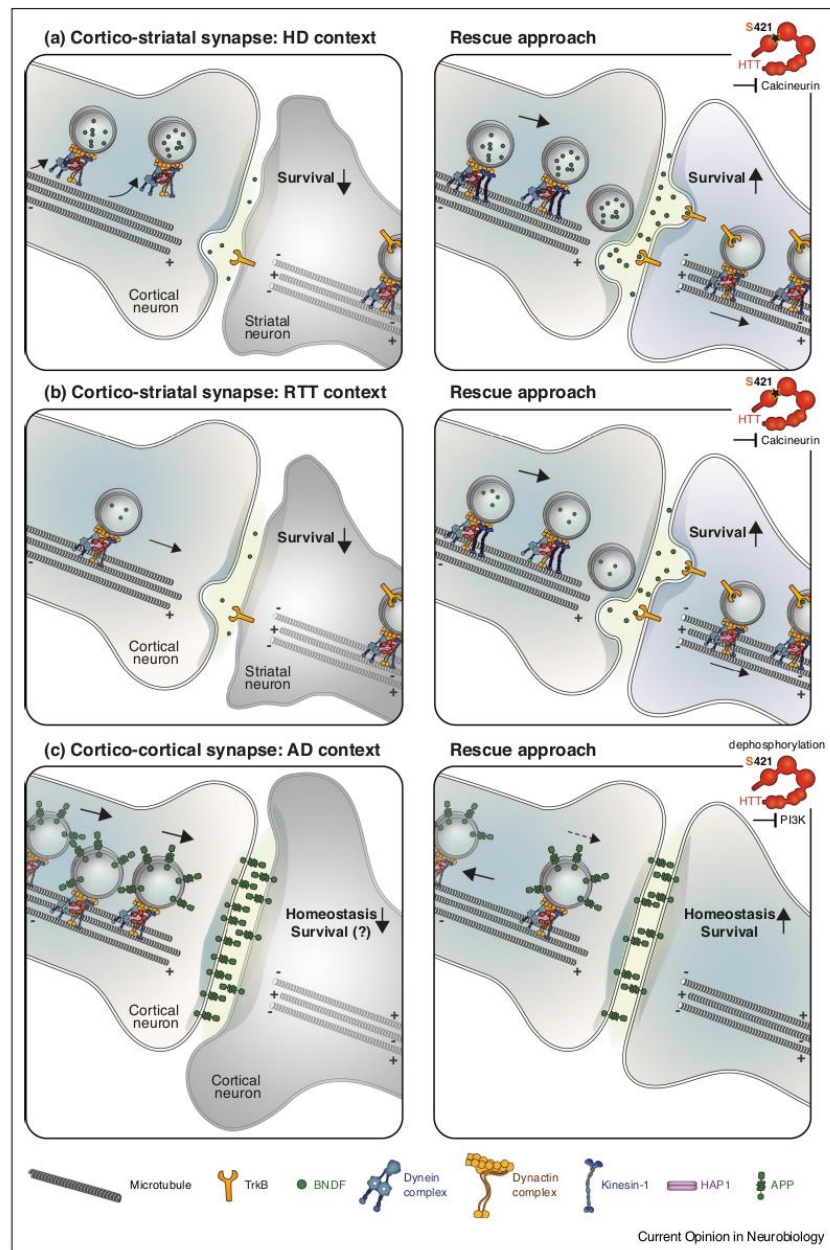
It is likely that the expanded polyglutamine tract alters the conformation of mHTT in such a way as to alter the protein's amenability to post-translational modifications. Phosphorylation, for example, is a major mechanism for regulating HTT-mediated transport, yet it is decreased overall in HD [31] (Figure 2). Phosphorylation of serine 421 determines the direction of transport by recruiting kinesin-1, thereby favoring anterograde transport of vesicles — including those carrying BDNF and APP — and synaptic vesicle precursors (SVPs) [3,15,32\*]. In the absence of S421 phosphorylation, HTT co-migrates with dynein and the dynactin complex rather than kinesin, and so travels in a retrograde direction instead. S421 can be phosphorylated by Serine/Threonine Akt (also known as Protein kinase B), phosphatidylinositol 3-kinase, and Serum- and glucocorticoid-induced kinase (SGK) [33]; it is dephosphorylated by Calcineurin (PP2B) [34] and PP2A [35]. Restoring phosphorylation, either by generating mHTT containing a mutation that mimics phosphorylation at S421 or by inhibiting calcineurin, restores BDNF transport to the corticostriatal circuit and improves survival in neuronal culture and in rodents [34,36–39] (Figure 3).

HTT phosphorylation by the serine-threonine cyclin-dependent kinase 5 (Cdk5) regulates transport efficiency [40]. Cdk5 phosphorylates HTT at several positions [3,41], but S1181 and S1201 are particularly important for controlling the speed of BDNF. Lack of HTT phosphorylation at these sites increases the velocity of BDNF-containing vesicles in both anterograde and retrograde directions and reduces their pausing time by enhancing recruitment of the dynein/dynactin complex and BDNF to microtubules [42] (Figure 2).

Arginine methylation by protein arginine methyltransferase (PRMT6) enhances HTT's association with vesicles and increases their speed [43]. PRMT6 was shown to methylate several residues on HTT several years ago [41], but the effect on transport was unknown. More recent work found that absence of methylation at R118

**(Figure 2 Legend Continued)** transport. **(b)** Cdk5 phosphorylates HTT at S1181 and S1201 to detach vesicles and motor complexes from microtubules, thereby reducing their transport in both anterograde and retrograde directions. **(c)** The protein Arginine Methyltransferase 6 (PRMT6) methylates HTT at R118, promoting the attachment of vesicles to HTT and the dynein/dynactin/kinesin complex. Absence of methylation specifically reduces anterograde transport. **(d)** HTT scaffolds the glycolytic enzyme GAPDH on vesicles to provide energy for the molecular motors. Absence of HTT detaches GAPDH from the vesicles and reduces transport efficiency in both directions.

Figure 3



Huntingtin post-translational modifications could provide a strategy to restore proper axonal transport in Rett Syndrome and Alzheimer's disease. (a) Phosphorylating HTT at S421 restores axonal transport in HD and (b) also in Rett syndrome, which is characterized by reduced expression of BDNF, HTT and molecular motors. (c) Alzheimer's disease is characterized by an abnormal accumulation of APP at the presynaptic terminals, which leads to larger spines and fewer synapses (not shown). Reducing the anterograde transport of APP-containing vesicles by promoting

reduces HTT association with vesicles, thereby diminishing anterograde transport. Conversely, increasing PRMT6 levels rescues transport in a R118-HTT-dependent manner. This suggests that HTT's stoichiometry on the vesicle influences its scaffolding function [43].

HTT ensures transport efficiency by another method that does not involve post-translational modifications. Rather, it involves HTT binding to the glyceraldehyde 3-phosphate dehydrogenase, GAPDH, an essential enzyme of the glycolytic machinery, on vesicles. This appears to guarantee the energy supply for molecular motors and accelerates transport in both directions [44,45\*\*] (Figure 2). Whether this function is altered in any disease state remains to be established.

### Restoring HTT-mediated BDNF transport improves the phenotype of the mouse model of Rett syndrome

Given the centrality of BDNF to neuronal health, alterations in its availability are implicated in a number of neurological conditions. For example, BDNF expression is profoundly reduced in Rett syndrome (RTT), a severe neurodevelopmental disorder caused by mutations in *MECP2* that alter the expression of thousands of genes [46]. Other proteins whose levels are reduced in RTT include HTT, HAP1, dynactin-1, and dynein cytoplasmic 1 heavy chain, which suggests that not only is BDNF downregulated but that defects in its transport could account for the specific dysfunction of the corticostriatal circuit in RTT [47]. Indeed, Ehinger *et al.* recently showed that restoring BDNF transport by promoting phosphorylation either genetically (via a phospho-mimetic mutation) or pharmacologically (via calcineurin inhibition) rescues synapse homeostasis and improves certain aspects of the *Mecp2* KO mouse phenotype [32\*] (Figure 3). Thus, drugs promoting BDNF transport through HTT-specific pathways may be of interest not only for HD but for other neurological disorders such as RTT and Parkinson's disease, which also involve disrupted axonal trafficking and impaired BDNF signaling [48].

### HTT dephosphorylation counteracts APP accumulation in a mouse model of AD

Amyloid precursor protein (APP) is a type-1 transmembrane glycoprotein that accumulates in Alzheimer's disease, Lewy body dementia, and cerebral amyloid angiopathy [49]. It is believed to play a crucial role in synapse formation, activity and maintenance [50]. APP is transported in both axons and dendrites and localizes in both the pre-synaptic and post-synaptic compartments, where it could associate with synaptic release machinery to

regulate neuronal transmission [51–55] and synaptic maintenance [49,56]. In the context of Alzheimer's disease (AD), axonal transport is impaired [57] and APP accumulates at synapses. A $\beta$  production is also increased, leading to lower synaptic density and 'stubrier' spines [58]. A $\beta$  oligomers also impede the transport of BDNF, mitochondria, and recycling endosomes, all of which are crucial for synaptic maintenance [59].

Early studies focusing on HTT noticed that reducing HTT phosphorylation also happens to reduce APP transport in axons and prevent the accumulation of APP at the synapse [15]. More recently, Martinez-Marmol *et al.* [60\*\*] found that inhibiting the phosphoinositide 3 kinase (PI3K) reduces APP anterograde transport, decreases APP and A $\beta$  accumulation, and prevents cognitive decline in the APP/PS1 mouse model of familial AD. Now another study has now shown that reducing APP transport via HTT dephosphorylation counteracts the overexpression of wild-type APP in neurons, reducing APP accumulation at synapses in the APP/PS1 mice [61]. Like HTT, JIP1 has the capacity to switch the direction of APP transport, and thus may represent an alternative or complementary approach to regulate APP trafficking to synapses [62]. Another recent study showed that curcumin exerts protective effects in AD both by promoting autophagic flux and by enhancing retrograde axonal transport of APP by increasing HTT protein levels [63]. Modulation of specific transport pathways may thus prove beneficial by enhancing functions that have been compromised by a variety of neurological diseases.

### Concluding remarks

It is likely that neurons are more sensitive to slight increases or decreases in protein levels than other cell types because of their unique dependence on axonal transport for synaptic homeostasis; in fact, some of the studies considered here indicate that small changes in the levels of a particular protein, even just at the synapse, can cause neuronal dysfunction and death.

The identification of HTT's roles in health and disease has revealed unexpected insights into intracellular trafficking, such as the use of phosphorylation sites to determine the direction of transport or the capacity of vesicles to produce their own energy. Although these discoveries raise the possibility of therapeutically stimulating HTT-mediated transport, both the direction of trafficking that is stimulated and the effects on other cargoes must be considered. For example, boosting HTT activity could augment BDNF transport but at the same time cause APP to accumulate. We therefore need to understand the

(Figure 3 Legend Continued) dephosphorylation of HTT or by inhibiting PI3K, an upstream Akt-activating kinase, slows the anterograde transport of APP vesicles, reduces its accumulation at the presynapse, and restores synaptic homeostasis. (Since blocking a pathway pharmacologically is easier than stimulating it, this approach may be easier than trying to induce more tau-mediated retrograde transport of APP.)

exact circuits involved and the mechanisms controlling synapse specificity.

Besides HTT, several other adaptors such as JIP1 appear to fine-tune axonal transport. Future studies are warranted to better understand the specificity of these adaptors, how they route cargos to specific neuronal compartments, and how this regulation may open new avenues to therapy.

### Conflict of interest statement

F.S. is on the scientific advisory board of Servier (Neurosciences Department) and a consultant for TEVA and Wave Life Sciences. The other authors declare that they have no competing interests.

### CRedit authorship contribution statement

**Hélène Vitet:** Conceptualization, Writing - original draft.  
**Vicky Brandt:** Conceptualization, Writing - review & editing.  
**Frédéric Saudou:** Conceptualization, Writing - review & editing.

### Acknowledgments

We thank Agnieszka Kawka for the illustrations and Sandrine Humbert for helpful discussions and comments on the manuscript. Research in the Saudou lab is supported by grants from Agence Nationale de la Recherche (ANR-15-IDEX-02 NeuroCoG in the framework of the "Investissements d'avenir" program; ANR-18-CE16-0009-01 AXION; ANR-18-CE16-0022-03 HDEV; ANR-18-CE13-0029-04 TELOPOST); the AGEMED program from INSERM; and funding from the European Research Council (ERC) under the European Union's Horizon 2020 research and innovation programme (AdG grant agreement No 834317). The Saudou lab is part of the Grenoble Center of Excellence in Neurodegeneration (GREEN). H.V. was supported by a PhD fellowship from Association Huntington France and FRM (FDT201904008035).

### References and recommended reading

Papers of particular interest, published within the period of review, have been highlighted as:

- of special interest
- of outstanding interest

1. Butler VJ, Salazar DA, Soriano-Castell D, Alves-Ferreira M, Dennissen FJA, Vohra M, Oses-Prieto JA, Li KH, Wang AL, Jing B *et al.*: **Tau/MAPT disease-associated variant A152T alters tau function and toxicity via impaired retrograde axonal transport.** *Hum Mol Genet* 2019, **28**:1498-1514
2. Lacovich V, Espindola SL, Alloati M, Pozo Devoto V, Cromberg LE, Cama ME, Forte G, Gallo JM, Bruno L, Stokin GB *et al.*: **Tau isoforms imbalance impairs the axonal transport of the amyloid precursor protein in human neurons.** *J Neurosci* 2017, **37**:58-69
- In healthy human brains, tau isoforms containing 3 or 4 microtubule-binding repeats are expressed in a one-to-one ratio; deviations from this ratio are observed in several tauopathies, but the effect of this change was unknown. This study perturbed the ratio in human-derived neurons and, using live-cell imaging, found that higher levels of isoform 3R increase the velocity and number of APP-carrying vesicles in the anterograde direction, whereas higher levels of 4R bias transport in the retrograde direction.
3. Saudou F, Humbert S: **The biology of huntingtin.** *Neuron* 2016, **89**:910-926.
4. Gunawardena S, Her LS, Brusch RG, Laymon RA, Niesman IR, Gordeky-Gold B, Sintasath L, Bonini NM, Goldstein LS: **Disruption of axonal transport by loss of huntingtin or expression of pathogenic polyQ proteins in Drosophila.** *Neuron* 2003, **40**:25-40.
5. Gauthier LR, Charrin BC, Borrell-Pages M, Dompierre JP, Rangone H, Cordelieres FP, De Mey J, MacDonald ME, Lessmann V, Humbert S *et al.*: **Huntingtin controls neurotrophic support and survival of neurons by enhancing BDNF vesicular transport along microtubules.** *Cell* 2004, **118**:127-138.
6. Wong YC, Holzbaur EL: **The regulation of autophagosome dynamics by huntingtin and HAP1 is disrupted by expression of mutant huntingtin, leading to defective cargo degradation.** *J Neurosci* 2014, **34**:1293-1305.
7. Sapp E, Penney J, Young A, Aronin N, Vonsattel JP, DiFiglia M: **Axonal transport of N-terminal huntingtin suggests early pathology of corticostriatal projections in Huntington disease.** *J Neuropathol Exp Neurol* 1999, **58**:165-173.
8. Ghosh R, Tabrizi SJ: **Huntington disease.** *Handb Clin Neurol* 2018, **147**:255-278.
9. Creus-Muncunill J, Ehrlich ME: **Cell-Autonomous and non-cell-autonomous pathogenic mechanisms in huntingtin's disease: insights from in vitro and in vivo models.** *Neurotherapeutics* 2019, **16**:957-978.
10. Guo Q, Bin H, Cheng J, Seefeldler M, Engler T, Pfeifer G, Oeckl P, Otto M, Moser F, Maurer M *et al.*: **The cryo-electron microscopy structure of huntingtin.** *Nature* 2018, **555**:117-120
- This study reports the first high-resolution structure of HTT, illuminating the basis of its scaffolding capacity.
11. Engelender S, Sharp AH, Colomer V, Tokito MK, Lanahan A, Worley P, Holzbaur EL, Ross CA: **Huntingtin-associated protein 1 (HAP1) interacts with the p150Glued subunit of dynein.** *Hum Mol Genet* 1997, **6**:2205-2212.
12. Li SH, Gutekunst CA, Hersch SM, Li XJ: **Interaction of huntingtin-associated protein with dynein P150Glued.** *J Neurosci* 1998, **18**:1261-1269.
13. McGuire JR, Rong J, Li SH, Li XJ: **Interaction of Huntingtin-associated protein-1 with kinesin light chain: implications in intracellular trafficking in neurons.** *J Biol Chem* 2006, **281**:3552-3559.
14. Caviston JP, Ross JL, Antony SM, Tokito M, Holzbaur EL: **Huntingtin facilitates dynein/dynein-mediated vesicle transport.** *Proc Natl Acad Sci U S A* 2007, **104**:10045-10050.
15. Colin E, Zala D, Liot G, Rangone H, Borrell-Pages M, Li XJ, Saudou F, Humbert S: **Huntingtin phosphorylation acts as a molecular switch for anterograde/retrograde transport in neurons.** *EMBO J* 2008, **27**:2124-2134.
16. Her LS, Goldstein LS: **Enhanced sensitivity of striatal neurons to axonal transport defects induced by mutant huntingtin.** *J Neurosci* 2008, **28**:13662-13672.
17. White JA 2nd, Anderson E, Zimmerman K, Zheng KH, Rouhani R, Gunawardena S: **Huntingtin differentially regulates the axonal transport of a sub-set of Rab-containing vesicles in vivo.** *Hum Mol Genet* 2015, **24**:7182-7195.
18. Twelvetrees AE, Yuen EY, Arancibia-Carcamo IL, MacAskill AF, Rostaing P, Lumb MJ, Humbert S, Triller A, Saudou F, Yan Z *et al.*: **Delivery of GABAARs to synapses is mediated by HAP1-KIF5 and disrupted by mutant huntingtin.** *Neuron* 2010, **65**:53-65.
19. Caviston JP, Zajac AL, Tokito M, Holzbaur EL: **Huntingtin coordinates the dynein-mediated dynamic positioning of endosomes and lysosomes.** *Mol Biol Cell* 2011, **22**:478-492.
20. Liot G, Zala D, Pla P, Mottet G, Piel M, Saudou F: **Mutant Huntingtin alters retrograde transport of TrkB receptors in striatal dendrites.** *J Neurosci* 2013, **33**:6298-6309.
21. Zala D, Hinkelmann MV, Saudou F: **Huntingtin's function in axonal transport is conserved in Drosophila melanogaster.** *PLoS One* 2013, **8**:e60162.
22. Savas JN, Ma B, Deinhardt K, Culver BP, Restituito S, Wu L, Belasco JG, Chao MV, Tanese N: **A role for huntingtin disease**

- protein in dendritic RNA granules. *J Biol Chem* 2010, **285**:13142-13153.**
23. Drouet V, Ruiz M, Zala D, Feyeux M, Auregan G, Cambon K, Troquier L, Carpentier J, Aubert S, Merienne N *et al.*: **Allele-specific silencing of mutant huntingtin in rodent brain and human stem cells.** *PLoS One* 2014, **9**:e99341.
24. Virlogeux A, Moutaux E, Christaller W, Genoux A, Bruyere J, •• Fino E, Charlot B, Cazorla M, Saudou F: **Reconstituting corticostriatal network on-a-chip reveals the contribution of the presynaptic compartment to Huntington's disease.** *Cell Rep* 2018, **22**:110-122
- This study reports the development and use of microfluidic devices to reconstitute corticostriatal networks-on-a-chip that enable examination of subcellular compartments. It showed that altering the status of the presynaptic compartment (cortical neurons) is sufficient to damage or restore the whole corticostriatal circuit.
25. Zhao X, Chen XQ, Han E, Hu Y, Paik P, Ding Z, Overman J, Lau AL, Shahmoradian SH, Chiu W *et al.*: **TRiC subunits enhance BDNF axonal transport and rescue striatal atrophy in Huntington's disease.** *Proc Natl Acad Sci U S A* 2016, **113**:E5655-5664
- This study used microfluidic devices to reconstitute corticostriatal networks from the BACHD model of HD and showed that the synthesis and transport of BDNF from WT neurons rescues the HD striatal neurons. They also show that the chaperonin T-complex 1 (TCP-1) ring complex (TRiC) reduces levels of mHTT in BACHD cortical neurons, enhances release of BDNF, and rescues striatal neurons.
26. Wang N, Gray M, Lu XH, Cantle JP, Holley SM, Greiner E, Gu X, Shirasaki D, Cepeda C, Li Y *et al.*: **Neuronal targets for reducing mutant huntingtin expression to ameliorate disease in a mouse model of Huntington's disease.** *Nat Med* 2014, **20**:536-541.
27. Baquet ZC, Gorski JA, Jones KR: **Early striatal dendrite deficits followed by neuron loss with advanced age in the absence of anterograde cortical brain-derived neurotrophic factor.** *J Neurosci* 2004, **24**:4250-4258.
28. Altar CA, Cai N, Bliven T, Juhasz M, Conner JM, Acheson AL, Lindsay RM, Wiegand SJ: **Anterograde transport of brain-derived neurotrophic factor and its role in the brain.** *Nature* 1997, **389**:856-860.
29. Park H: **Cortical axonal secretion of BDNF in the striatum is disrupted in the mutant-huntingtin knock-in mouse model of Huntington's disease.** *Exp Neurol* 2018, **27**:217-225.
30. Borrell-Pages M, Canals JM, Cordelieres FP, Parker JA, Pineda JR, Grange G, Bryson EA, Guillemier M, Hirsch E, Hantraye P *et al.*: **Cystamine and cysteamine increase brain levels of BDNF in Huntington disease via HsJ1b and transglutaminase.** *J Clin Invest* 2006, **116**:1410-1424.
31. Warby SC, Chan EY, Metzler M, Gan L, Singaraja RR, Crocker SF, Robertson HA, Hayden MR: **Huntingtin phosphorylation on serine 421 is significantly reduced in the striatum and by polyglutamine expansion in vivo.** *Hum Mol Genet* 2005, **14**:1569-1577.
32. Ehinger Y, Bruyere J, Panayotis N, Abada YS, Borloz E, Matagne V, • Scaramuzzino C, Vitet H, Delatour B, Saidi L *et al.*: **Huntingtin phosphorylation governs BDNF homeostasis and improves the phenotype of Mecp2 knockout mice.** *EMBO Mol Med* 2020, **12**:e10889
- This study demonstrates that chronic phosphorylation of HTT S421 increases BDNF availability, enhances synaptic connectivity *in vivo*, and improves the phenotype of Mecp2 knockout mice, a model of Rett syndrome, even though treatment began after the mice had developed symptoms.
33. Rangone H, Poizat G, Troncoso J, Ross CA, MacDonald ME, Saudou F, Humbert S: **The serum- and glucocorticoid-induced kinase SGK inhibits mutant huntingtin-induced toxicity by phosphorylating serine 421 of huntingtin.** *Eur J Neurosci* 2004, **19**:273-279.
34. Pardo R, Colin E, Regulier E, Aebischer P, Deglon N, Humbert S, Saudou F: **Inhibition of calcineurin by FK506 protects against polyglutamine-huntingtin toxicity through an increase of huntingtin phosphorylation at S421.** *J Neurosci* 2006, **26**:1635-1645.
35. Metzler M, Gan L, Mazarei G, Graham RK, Liu L, Bissada N, Lu G, Leavitt BR, Hayden MR: **Phosphorylation of huntingtin at Ser421 in YAC128 neurons is associated with protection of YAC128 neurons from NMDA-mediated excitotoxicity and is modulated by PP1 and PP2A.** *J Neurosci* 2010, **30**:14318-14329.
36. Humbert S, Bryson EA, Cordelieres FP, Connors NC, Datta SR, Finkbeiner S, Greenberg ME, Saudou F: **The IGF-1/Akt pathway is neuroprotective in Huntington's disease and involves Huntingtin phosphorylation by Akt.** *Dev Cell* 2002, **2**:831-837.
37. Zala D, Colin E, Rangone H, Liot G, Humbert S, Saudou F: **Phosphorylation of mutant huntingtin at S421 restores anterograde and retrograde transport in neurons.** *Hum Mol Genet* 2008, **17**:3837-3846.
38. Pineda JR, Pardo R, Zala D, Yu H, Humbert S, Saudou F: **Genetic and pharmacological inhibition of calcineurin corrects the BDNF transport defect in Huntington's disease.** *Mol Brain* 2009, **2**:33.
39. Kratter IH, Zahed H, Lau A, Tsvetkov AS, Daub AC, Weiberth KF, Gu X, Saudou F, Humbert S, Yang XW *et al.*: **Serine 421 regulates mutant huntingtin toxicity and clearance in mice.** *J Clin Invest* 2016, **126**:3585-3597.
40. Cruz JC, Tsai LH: **A Jekyll and Hyde kinase: roles for Cdk5 in brain development and disease.** *Curr Opin Neurobiol* 2004, **14**:390-394.
41. Ratovitski T, O'Meally RN, Jiang M, Chaerkady R, Chighladze E, Stewart JC, Wang X, Arbez N, Roby E, Alexandris A *et al.*: **Post-translational modifications (PTMs), identified on endogenous huntingtin, cluster within proteolytic domains between HEAT repeats.** *J Proteome Res* 2017, **16**:2692-2708.
42. Ben M'Barek K, Pla P, Orvoen S, Benstaali C, Godin JD, Gardier AM, Saudou F, David DJ, Humbert S: **Huntingtin mediates anxiety/depression-related behaviors and hippocampal neurogenesis.** *J Neurosci* 2013, **33**:8608-8620.
43. Migazzi A, Scaramuzzino C, Anderson E, Tripathy D, Hernandez I, Virlogeux A, Zuccato C, Caricasole A, Ratovitski T, Ross CA *et al.*: **Huntingtin-mediated axonal transport requires arginine methylation by PRMT6.** 2020 <http://dx.doi.org/10.2139/ssrn.3520100>.
44. Zala D, Hinckelmann MV, Yu H, Lyra da Cunha MM, Liot G, Cordelieres FP, Marco S, Saudou F: **Vesicular glycolysis provides on-board energy for fast axonal transport.** *Cell* 2013, **152**:479-491.
45. Hinckelmann MV, Virlogeux A, Niehage C, Pujol C, Choquet D, •• Hoflack B, Zala D, Saudou F: **Self-propelling vesicles define glycolysis as the minimal energy machinery at transport.** *Nat Commun* 2016, **7**:13233
- It had been known that the glycolytic enzyme GAPDH facilitates fast axonal transport, but it was unclear whether glycolysis alone is sufficient for the reaction. In this study, proteomic analysis revealed that most glycolytic enzymes are associated with vesicles and provide energy 'autonomously' for axonal transport.
46. Chang Q, Khare G, Dani V, Nelson S, Jaenisch R: **The disease progression of Mecp2 mutant mice is affected by the level of BDNF expression.** *Neuron* 2006, **49**:341-348.
47. Roux JC, Zala D, Panayotis N, Borges-Correia A, Saudou F, Villard L: **Modification of Mecp2 dosage alters axonal transport through the Huntingtin/Hap1 pathway.** *Neurobiol Dis* 2012, **45**:786-795.
48. Fang F, Yang W, Florio JB, Rockenstein E, Spencer B, Orain XM, Dong SX, Li H, Chen X, Sung K *et al.*: **Synuclein impairs trafficking and signaling of BDNF in a mouse model of Parkinson's disease.** *Sci Rep* 2017, **7**:3868.
49. Muller UC, Deller T, Korte M: **Not just amyloid: physiological functions of the amyloid precursor protein family.** *Nat Rev Neurosci* 2017, **18**:281-298.
50. Deyts C, Thinakaran G, Parent AT: **APP receptor? To be or not to be.** *Trends Pharmacol Sci* 2016, **37**:390-411.
51. Das U, Wang L, Ganguly A, Saikia JM, Wagner SL, Koo EH, Roy S: **Visualizing APP and BACE-1 approximation in neurons yields**

- insight into the amyloidogenic pathway. *Nat Neurosci* 2016, **19**:55-64.
52. Buggia-Prevot V, Fernandez CG, Riordan S, Vetrivel KS, Roseman J, Waters J, Bindokas VP, Vassar R, Thinakaran G: **Axonal BACE1 dynamics and targeting in hippocampal neurons: a role for Rab11 GTPase.** *Mol Neurodegener* 2014, **9**:1.
  53. Groemer TW, Thiel CS, Holt M, Riedel D, Hua Y, Huve J, Wilhelm BG, Klingauf J: **Amyloid precursor protein is trafficked and secreted via synaptic vesicles.** *PLoS One* 2011, **6**:e18754.
  54. Fanutza T, Del Prete D, Ford MJ, Castillo PE, D'Adamio L: **APP and APLP2 interact with the synaptic release machinery and facilitate transmitter release at hippocampal synapses.** *eLife* 2015, **4**:e09743.
  55. Klevanski M, Herrmann U, Weyer SW, Fol R, Cartier N, Wolfer DP, Caldwell JH, Korte M, Müller UC: **The APP intracellular domain is required for normal synaptic morphology, synaptic plasticity, and hippocampus-dependent behavior.** *J Neurosci* 2015, **35**:16018-16033.
  56. Soba P, Eggert S, Wagner K, Zentgraf H, Siehl K, Kreger S, Lower A, Langer A, Merdes G, Paro R *et al.*: **Homo- and heterodimerization of APP family members promotes intercellular adhesion.** *EMBO J* 2005, **24**:3624-3634.
  57. Adalbert R, Milde S, Durrant C, Ando K, Stygelbout V, Yilmaz Z, Gould S, Brion JP, Coleman MP: **Interaction between a MAPT variant causing frontotemporal dementia and mutant APP affects axonal transport.** *Neurobiol Aging* 2018, **68**:68-75.
  58. Androuin A, Potier B, Nagerl UV, Cattaert D, Danglot L, Thierry M, Youssef I, Triller A, Duyckaerts C, El Hachimi KH *et al.*: **Evidence for altered dendritic spine compartmentalization in Alzheimer's disease and functional effects in a mouse model.** *Acta Neuropathol* 2018, **135**:839-854.
  59. Umeda T, Ramser EM, Yamashita M, Nakajima K, Mori H, Silverman MA, Tomiyama T: **Intracellular amyloid beta oligomers impair organelle transport and induce dendritic spine loss in primary neurons.** *Acta Neuropathol Commun* 2015, **3**:51.
  60. Martínez-Mármol R, Mohannak N, Qian L, Wang T, Gormal RS, Ruitenber MJ, Vanhaesebroeck B, Coulson EJ, Meunier F: **PI3-kinase inhibition perturbs APP and TNF $\alpha$  trafficking, reduces plaque burden, dampens neuroinflammation, and prevents cognitive decline in an Alzheimer's disease mouse model.** *J Neurosci* 2019, **39**:7976-7991
- This study demonstrates that inhibition of the PI3K reduces anterograde transport of APP and improves cognitive function in the APP/PS1 mouse model of AD, providing a link between APP anterograde transport and APP/A $\beta$  accumulation.
61. Bruyere J, Abada Y-S, Vitet H, Fontaine G, Deloulme JC, Cès A, Denarier E, Pernet-Gallay K, Andrieux A, Humbert S, Potier MC *et al.*: **Presynaptic APP levels and synaptic homeostasis are regulated by Akt phosphorylation of Huntingtin.** *bioRxiv* 2020 <http://dx.doi.org/10.1101/2020.04.21.052506>. (In press).
  62. Fu MM, Holzbaur EL: **JIP1 regulates the directionality of APP axonal transport by coordinating kinesin and dynein motors.** *J Cell Biol* 2013, **202**:495-508.
  63. Liang J, Zhou F, Xiong X, Zhang X, Li S, Li X, Gao M, Li Y: **Enhancing the retrograde axonal transport by curcumin promotes autophagic flux in N2a/APP695swe cells.** *Aging (Albany NY)* 2019, **11**:7036-7050.

This introduction is a trial for a state-of-the-art sum up of what is known so far on the consequences of FAT in cellular processes and behavior. However, some questions remain about the importance of this dynamic mechanism on neurological disorders and its ability to be reversed or modulated as a therapeutic strategy. In the three following studies, we aimed at restoring FAT of APP in an AD mouse model, of BDNF in Rett syndrome mouse model and of SVP in HTTS421D mice and FAT.

# Results



## Results – part 1: Presynaptic APP levels and synaptic homeostasis are regulated by Akt phosphorylation of Huntingtin

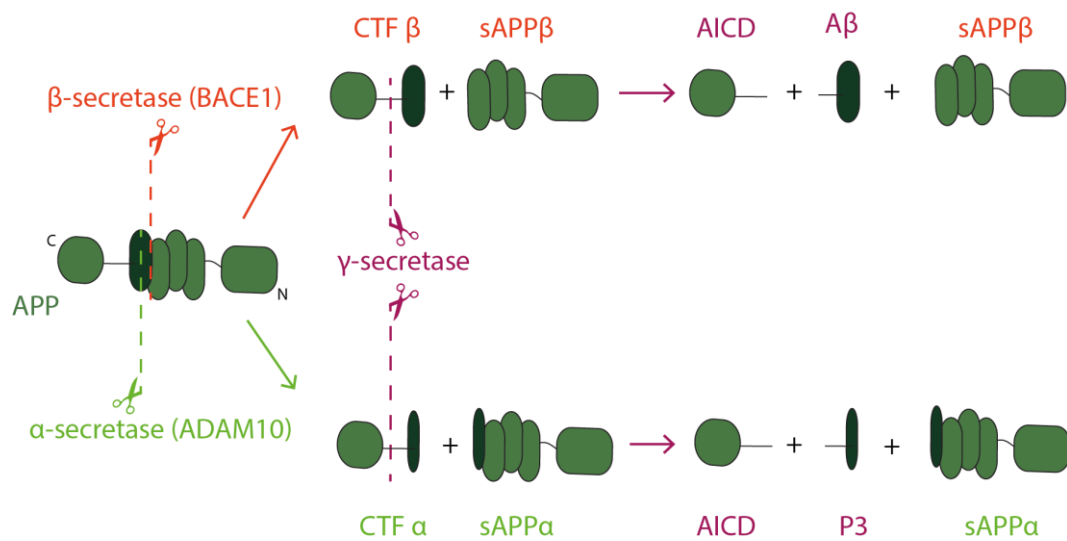
### Summary & context of the study

This study focused on the role of HTT in regulating APP levels at the plasma membrane. The lab has previously shown that APP levels could be regulated by HTT phosphorylation at S421. However, few studies have investigated the consequences of modulating APP levels at synapses on synapse homeostasis and behavior. The generation in the lab of mice knock-in for the S421 site led us to investigate whether modulation of endogenous HTT phosphorylation impacts APP axonal dynamics and synapse homeostasis both *in vitro* and *in vivo*. We also investigated the consequences of modulating APP transport on a mouse model of FAD *in vivo*. Before describing the results of the study, a brief review of the literature on mechanisms regulating APP transport and functions and on Alzheimer's disease is given below.

#### *APP homeostasis*

APP is a type-1 transmembrane glycoprotein well known because of its implication in Alzheimer's Disease (AD). Physiologically, APP and its fragments can be cleaved by three secretases:  $\alpha$ - (ADAM10),  $\beta$ - (BACE1) and  $\gamma$ - (containing presenilin-1). When APP is cleaved by  $\alpha$ -secretase at the plasma membrane, it can no longer be cleaved by  $\beta$ -secretase and the non-amyloidogenic pathway is triggered producing CTF  $\alpha$ . On the other hand, the  $\beta$ -secretase is responsible for the triggering of the amyloidogenic pathway, leading to the production of CTF  $\beta$  fragments. Both CTF fragments can be cleaved by the  $\gamma$ -secretase producing AICD and P3 or A $\beta$  peptides (figure 91). Each fragment resulting from APP cleavage has specific roles. For instance, sAPP $\alpha$  is known to have a protective effect (Y. W. Zhang et al., 2011) and A $\beta$  peptides, according to the levels, can be either protective and responsible for memory formation and neuroprotection (Abramov et al., 2009; Puzzo et al., 2008) or toxic because it leads to an increased apoptosis (Toshiyuki et al., 2000), increased ROS or decreased synaptic release (Shankar & Walsh, 2009). A $\beta$  oligomers also impede the transport of BDNF, mitochondria, and recycling endosomes, all of which are crucial for synaptic maintenance (Umeda et al., 2015). However, an increasing number of studies point out that APP is not only the precursor for A $\beta$  peptides but is also a cell adhesion molecule and/or a receptor acting as a hub for proteins interaction that activate signaling pathways and provoke physiological responses (Deyts et al., 2016; Matrone et al., 2019).

### Amyloidogenic pathway



### Non-amyloidogenic pathway

Figure 91: APP cleavage by secretases produces many fragments

Thanks to its processing, its PTM through phosphorylation at the  $_{682}\text{YENPTY}_{687}$  domain and its ability to interact with many proteins, APP can be seen as a multirole player controlling synaptic homeostasis:

- APP as a receptor transducing a signal

APP possesses receptor properties that allows it to act as a signal transducer, comparable to a G protein-coupled receptor. It can receive the signal from the extracellular medium through soluble proteins or growth factor like Grb2 (growth factor receptor bound, IGF-1-pathway-downstream molecule) and convert this signal into intracellular signaling affecting spine plasticity for example (Deyts et al., 2016; Montagna et al., 2017). This signal transduction is possible given the plethora of proteins able to bind to APP or to its cleavage products. For instance, AICD can interact with the  $G_{\alpha s}$  subunit of the G protein, activating PKA and inhibiting GSK3 $\beta$  signaling cascades thus, enhancing axonodendritic arborization (Deyts et al., 2016). Interestingly, other signaling pathways can also be induced since CTF interacts with the  $G_{\alpha 0}$  subunit of the G protein (Deyts et al., 2016). Grb2 APP binding, regulated by APP phosphorylation, induces the activation of MAP kinase pathway, regulating cell survival and apoptosis (Deyts et al., 2016). APP phosphorylation around the YENPTY site can be considered as a “biochemical switch” since it drastically changes APP interactome (Matrone, 2013), APP sorting and trafficking, notably through JIP-1 modulation interaction (Scheinfeld et al., 2003).

As a receptor, APP could also have the ability to downregulate its own production or to cause its own desensitization through its internalization mediated by its interaction with clathrin/AP2 complex (la Rosa et al., 2015) and caused by the binding of ligand (Deyts et al., 2016).

- APP as a dimer that regulates synapse formation, plasticity and stability

One of APP interactors is APP itself or one of its isoforms. Since APP is both present in the pre- and in the post-synaptic neuron, APP can dimerize. By forming a physical bridge between the two neurons, APP dimer facilitates the interaction between the two neurons (Brunholz et al., 2012), which participates to synapse formation and stabilization (Deyts et al., 2016; Montagna et al., 2017). This dimerization is reinforced in the presence of APP ligand molecules within the ECM like collagen, heparin and laminin, further modulating the dendritic spines stability or plasticity (Montagna et al., 2017).

- APP as gene expression regulator

AICD produced by the  $\gamma$ -secretase, can be sent to the nucleus and activate several transcription factors which are known to be involved in the regulation of dendritic spine plasticity. Some target genes have been observed like GSK3 $\beta$ , p53 or  $\alpha$ 2-actin to organize the actin cytoskeleton (Montagna et al., 2017).

- APP as trophic / paracrine molecule

When APP is cleaved by  $\alpha$ -secretase in the plasma membrane, the N-terminal part of APP (sAPP $\alpha$ ) is released into the extracellular medium as a soluble form of APP. Acting as a paracrine molecule (Brunholz et al., 2012), sAPP $\alpha$  can modulate several signaling pathways involved in neuroprotection, plasticity and axonal outgrowth (Deyts et al., 2016).

- APP as a modulator of postsynaptic response & learning

Finally, APP can regulate the post synaptic response thus plasticity by regulating NMDARs trafficking to the plasma membrane. This is another way, of how APP FL can regulate learning and memory (Hoe et al., 2012).

To sum up, APP regulates spine structure, density and functions which contributes to learning and memory through plasticity driven connection strengthening (Octave et al., 2013; H. Wang et al., 2012). Although APP role on synapse homeostasis is acknowledged and even though some mechanisms have been proposed, APP homeostasis remains unclear. For instance, Weyer et al., (Weyer et al., 2014) and Lee (K. J. Lee et al., 2010) showed that dendritic spine density decreases in

APP-KO CA1 whereas Bittner and colleagues showed earlier an increase of dendritic spine number in neurons from the somatosensory cortex of these APP KO mice (Bittner et al., 2009). Although APP FL physiologic roles have to be better understood, it is acknowledged that its processing, along with other processes, participates to AD.

### *APP transport & trafficking*

Several studies have demonstrated that APP processing is transport-dependent (Anderson & Ii, 2014; Stokin et al., 2005; Tan & Gleeson, 2019; Vagnoni et al., 2012). Even if the majority of APP is localized within the Golgi (X. Zhang & Song, 2013), it needs to be transported to the plasma membrane of the synapse to play its role of cell adhesion molecule or to regulate synapse formation and/or maturation (Deyts et al., 2016); 10% of APP proteins are found at the synapse (Thinakaran & Koo, 2008). For this purpose, APP FL is anterogradely transported from the Golgi apparatus to the synapse in transport vesicles carried out by Kinesin-1 (Kaether et al., 2000; Stokin et al., 2005) (figure 92). APP can also be directly directed to the endosomes. Once at the plasma membrane, APP is either cleaved by  $\alpha$ -secretase, quickly endocytosed and directed to early endosomes enriched in Rab5 or transported to lysosomes (Brunholz et al., 2012). Most of vesicular APP has been found to be associated with Rab-5 compartment and is thought to spend most time in the endocytic rather than exocytic pathways and barely recycled (Ikin et al., 1996). There, APP vesicles can fuse with vesicles containing  $\beta$ - and  $\gamma$ -secretases and be cleaved into A $\beta$  peptides or P3 if it has already been cleaved by  $\alpha$ -secretase.

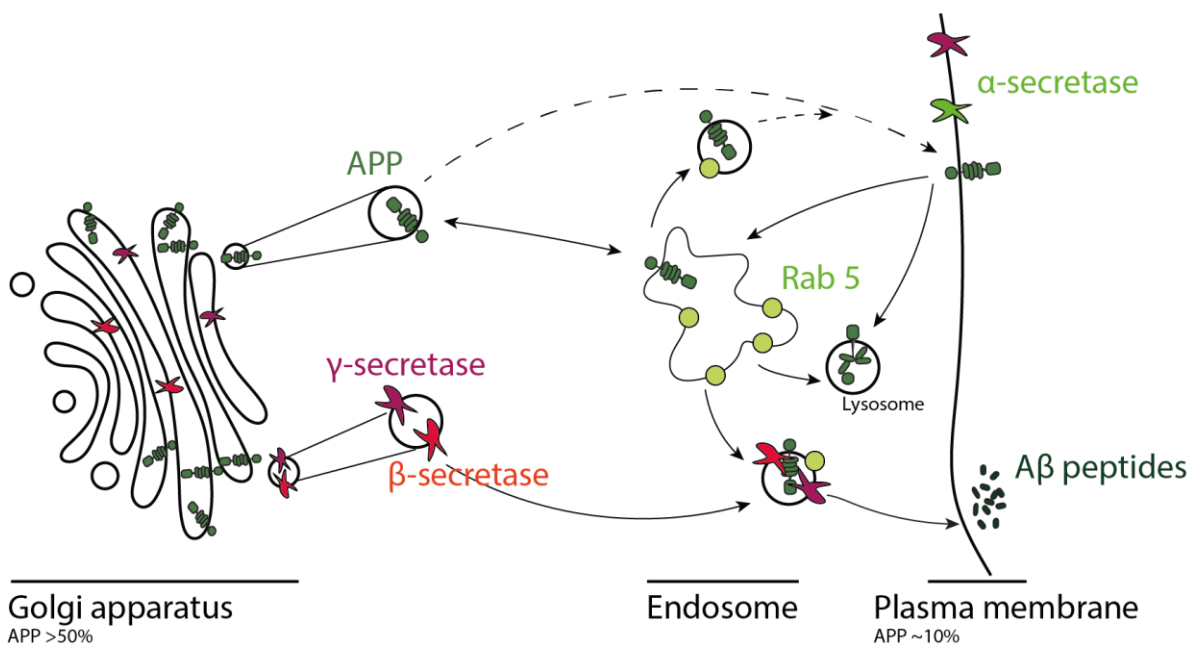


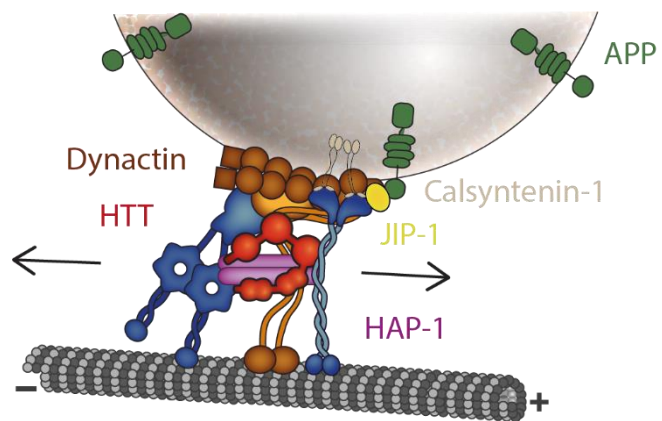
**Figure 92: APP processing is dependent on APP transport and trafficking**

Thus, APP processing is directly correlated to retrograde transport (Tan & Gleeson, 2019) which is able to enhance APP accessibility to its secretases (Kamenetz et al., 2003).

Because of subcellular localization of secretases, in different moving vesicles or at the plasma membrane, APP is not cleaved during its anterograde transport (Kamenetz et al., 2003). Since APP transport is crucial for its homeostasis, it is understandable that impaired APP transport leads to disruption of motor neuron function in *Drosophila* (Araki et al., 2007).

#### *APP transport adaptors and regulation*

Because APP and its fragments play a crucial role and are partly responsible of the main neurodegenerative disorder man is experiencing nowadays, APP transport has been well studied (Tan & Gleeson, 2019). Adaptors to its transport for example, have been described: we can list HAP-1 (Mcguire et al., 2006; G. Z. Yang et al., 2012), JIP<sub>1</sub> (Chiba et al., 2019; Meng-meng Fu & Holzbaaur, 2013; Muresan & Muresan, 2005), Huntingtin (Colin



et al., 2008; L. Her & Goldstein, 2008), calsyntenin-1 (Araki et al., 2007; Vagnoni et al., 2012) or AHI<sub>1</sub> (Ting et al., 2019). Some of them could directly bind to APP thanks to phosphotyrosine-binding domains able to dock on the APP YENPTY domain; this is the case for JIP1 (Deyts et al., 2016). These adaptors facilitate APP transport; if one of them is removed, APP transport is negatively impacted (Meng-meng Fu & Holzbaaur, 2013; Mcguire et al., 2006) and can lead to loss of function of APP. For example, siRNA loss of calsyntenin-1 or JIP<sub>1</sub> KO decreases APP containing vesicle velocities (Meng-meng Fu & Holzbaaur, 2013; Vagnoni et al., 2012). They also regulate APP transport because by their presence or by PTMs, they can change APP vesicle directionality. It is the case for JIP<sub>1</sub> which, when phosphorylated, stabilizes JIP1-kinesin-1 interaction and by this way, increases APP anterograde transport. On the opposite, when JIP<sub>1</sub> is not phosphorylated, retrograde APP transport is increased (Meng-meng Fu & Holzbaaur, 2013). Work from the lab also proposed that HTT phosphorylation at S421 could regulate APP transport with phosphorylation promoting anterograde transport while the non phosphorylatable form would promote the retrograde transport (Colin et al., 2008). However, such experiments were performed in neurons in which axons and dendrites could not be distinguished and used overexpression of HTT fragments. This study is at the basis of the work described below.

### *APP homeostasis is dysregulated in AD*

Alzheimer's disease is one of the main challenges our modern society has to face in term of healthcare. To illustrate this affirmation, in 2019, one American in 10 age 65 and older has Alzheimer's disease (Alzheimer's association). AD patients exhibit memory loss, challenges in planning, confusion with time and place and changes in mood and can struggle with words. This neurodegenerative disease is mostly sporadic and linked with the environment but can be inherited (familial form <10%) (Y. W. Zhang et al., 2011) and caused by gene mutations, notably with the PSEN1 gene provoking its hyperactivation. A plethora of studies were performed in the last decade to better understand the mechanisms leading to the death of the

cortical and hippocampal neurons (figure 93). Two main hypotheses were followed: the tau hyperphosphorylation leading to the production of neurofibrillary tangles (Buée et al., 2000; Y. W. Zhang et al., 2011) and the amyloid plaques accumulation which leads to toxic processes. These two AD's hallmarks were described by Braak as being

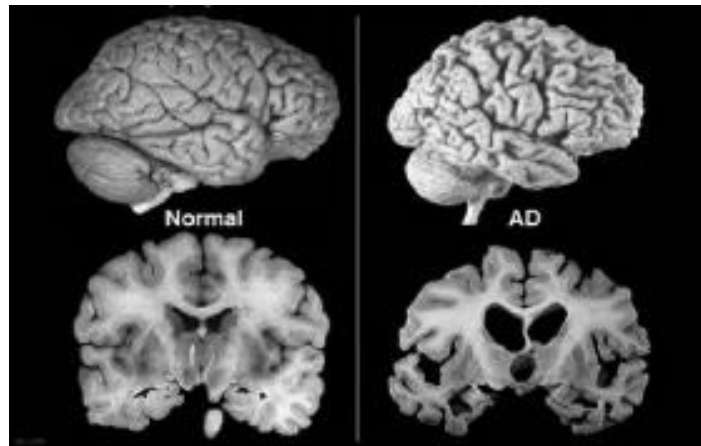


**Figure 93: AD provokes neurodegeneration of the cortex and the hippocampus**

dependent on the stage of the disease (H Braak & Braak, 1997). Recently, another cause for AD has been investigated, which is the dysregulation of synaptic homeostasis (Styr & Slutsky, 2018). In fact, during the development of this neurodegeneration, homeostasis is perturbed, and cellular and molecular changes can be observed. It is for example the case of APP FL physiology: APP transport from and to the synapse is thought to be impaired (Adalbert et al., 2018; Cash et al., 2003; Poulsen et al., 2017; Stokin et al., 2005; Woodruff et al., 2016), its phosphorylation at T668 is increased (M. S. Lee et al., 2003; Triaca et al., 2016), as well as its cleavage (Y. W. Zhang et al., 2011). Intracellular signaling pathways are also dysregulated: IGF-1 pathway, known for its crucial role in neuronal growth, synaptic maintenance, neuroprotection (Van Dam & Aleman, 2004), neuronal survival (B. Kim & Feldman, 2012) and learning and memory (B. Kim & Feldman, 2015) through Akt and ERK regulation, is altered (Bedse et al., 2015; George et al., 2017). This insulin resistance is believed to cause an Akt hyperactivation (figure 94), a subsequent desensitization of PI-3K/Akt pathway, enhancing APP phosphorylation (B. Kim et al., 2019) at the neurite endings (Iijima et al., 2000). APP phosphorylation in physiological conditions is low thanks to NGF downregulation of JNK(p54) which phosphorylates APP and thus, promote APP trafficking to Golgi by increasing APP binding to TrkA (Triaca et al., 2016). When APP is phosphorylated at T668, it is thought to decrease APP-TrkA affinity, promoting APP transport to BACE1

vesicles (B. Kim et al., 2019; Triaca et al., 2016). This change in APP dynamics is partly responsible for A $\beta$  accumulation and phosphorylated tau aggregation (B. Kim et al., 2019).

Pointing out APP FL homeostasis importance can be a key to understand why some clinical trials did not work. For instance, many of them tried to avoid A $\beta$  production but failed to cure AD patients (Coimbra et al., 2018; Congdon & Sigurdsson, 2018; M. F. Egan et al., 2019; Kametani & Hasegawa, 2018; Karran & De Strooper, 2016). By modulating APP processing, APP homeostasis would be changed, and this could trigger a combination of signaling pathways that could be detrimental for the cells. Clinical trials tried also to modulate IGF-1 pathway to rescue AD phenotypes but show mixed effects, even though a recent one proved that regular insulin treatment improve memory of AD patients (Craft et al., 2017).

#### *Mouse model for AD*

In order to model the pathology, mouse models were created using AD linked mutation found in human familial forms of the pathology. In the APP-PS1 model, human APP<sub>swe</sub> is overexpressed, and PSEN-1 is mutated, which both increase APP cleavage (Radde et al., 2006). In this model, APP transport is impaired (Götz et al., 2006; Gunawardena & Goldstein, 2001; Lazarov et al., 2007; Rusu et al., 2007; X. L. Zhao et al., 2010), amyloid plaque deposition in the cortex and in the hippocampus appears from 7 months of age and APPPS1 mice exhibit memory loss and cognitive deficits around the same age (S. R. Edwards et al., 2014; Puzzo et al., 2014). They also display higher APP levels in the brains and in hippocampal axons, consequently to its transgenic nature (Bitsikas et al., 2014). Morphologically, synaptic density is lower than WT mice, which could explain the memory impairment (Octave et al., 2013) and spine are bigger and stubbier (Androuin et al., 2018; Neuman et al., 2015).

As a conclusion, an important role for APP is to participate to synapse homeostasis and loss of APP homeostatic regulation could cause pathological outcomes (Deyts et al., 2016). For instance, whether APP is overexpressed or knocked out, synaptic activity is increased (Busche et al., 2012; Palop et al., 2007; Poll et al., 2020; Priller et al., 2006; Verret et al., 2012; Vossel et al., 2013). As stated previously, this role could be of importance since loss of synapse homeostasis rather than A $\beta$  or Tau accumulation is believed to trigger AD symptoms (Frere & Slutsky, 2017; Karran & De Strooper, 2016). This homeostasis collapse could be the trigger to switch synaptic and cognitive impairments into neurodegeneration. Our work on the link on HTT role in APP transport and that is described thereafter support this hypothesis.

# Presynaptic APP levels and synaptic homeostasis are regulated by Akt phosphorylation of huntingtin

Julie Bruyère<sup>1†</sup>, Yah-Se Abada<sup>2†</sup>, H  l  ne Vitet<sup>1†</sup>, Ga  lle Fontaine<sup>2</sup>, Jean-Christophe Deloulme<sup>1</sup>, Aur  lia C  s<sup>2</sup>, Eric Denarier<sup>1</sup>, Karin Permet-Gallay<sup>1</sup>, Annie Andrieux<sup>1</sup>, Sandrine Humbert<sup>1</sup>, Marie-Claude Potier<sup>2</sup>, Beno  t Delatour<sup>2</sup>, Fr  d  ric Saudou<sup>1\*</sup>

<sup>1</sup>Univ. Grenoble Alpes, Inserm, U1216, CHU Grenoble Alpes, CEA, Grenoble Institut Neurosciences, Grenoble, France; <sup>2</sup>Institut du Cerveau et de la Moelle   pini  re, ICM, Inserm U1127, CNRS UMR 7225, Sorbonne Universit  , Paris, France

**Abstract** Studies have suggested that amyloid precursor protein (APP) regulates synaptic homeostasis, but the evidence has not been consistent. In particular, signaling pathways controlling APP transport to the synapse in axons and dendrites remain to be identified. Having previously shown that Huntingtin (HTT), the scaffolding protein involved in Huntington’s disease, regulates neuritic transport of APP, we used a microfluidic corticocortical neuronal network-on-a-chip to examine APP transport and localization to the pre- and post-synaptic compartments. We found that HTT, upon phosphorylation by the Ser/Thr kinase Akt, regulates APP transport in axons but not dendrites. Expression of an unphosphorylatable HTT decreased axonal anterograde transport of APP, reduced presynaptic APP levels, and increased synaptic density. Ablating in vivo HTT phosphorylation in APPPS1 mice, which overexpress APP, reduced presynaptic APP levels, restored synapse number and improved learning and memory. The Akt-HTT pathway and axonal transport of APP thus regulate APP presynaptic levels and synapse homeostasis.

\*For correspondence:  
frederic.saudou@inserm.fr

<sup>†</sup>These authors contributed equally to this work

**Competing interests:** The authors declare that no competing interests exist.

**Funding:** See page 22

**Received:** 25 February 2020

**Accepted:** 11 May 2020

**Published:** 26 May 2020

**Reviewing editor:** Harry T Orr, University of Minnesota, United States

   Copyright Bruy  re et al. This article is distributed under the terms of the [Creative Commons Attribution License](https://creativecommons.org/licenses/by/4.0/), which permits unrestricted use and redistribution provided that the original author and source are credited.

## Introduction

Synaptic homeostasis stabilizes neural circuits and ensures faithful communication within networks that are being continuously remodeled. It involves a complex interplay between presynaptic and postsynaptic proteins that modulates synaptic morphology and strength (S  dhof, 2018). Several studies suggest that amyloid precursor protein (APP) contributes to synapse homeostasis (for reviews see Hoe et al., 2012; M  ller et al., 2017), and although the evidence is not entirely consistent, this possibility has intuitive appeal because of APP’s involvement in diseases of cognition (e.g., Alzheimer’s disease, Lewy body dementia, and cerebral amyloid angiopathy)(M  ller et al., 2017). Some studies suggest that loss of APP reduces synapse density (Weyer et al., 2014), while others show that it increases the number of synapses (Bittner et al., 2009). More firmly established is the fact that APP is transported both in axons and dendrites and localizes in both the pre- and post-synaptic compartments, where it could associate with synaptic release machinery to regulate neuronal transmission (Buggia-Pr  vot et al., 2014; Das et al., 2016; Fanutza et al., 2015; Groemer et al., 2011; Klevanski et al., 2015). In addition, APP may function as an adhesion molecule at the synapse (M  ller et al., 2017; Soba et al., 2005). Any modification in the transport of APP in either axons or dendrites thus has the potential to disrupt synaptic function or homeostasis. Therefore, there is a need to identify mechanisms and/or pathways that specifically regulate APP transport both in axons and/or dendrites and to determine whether manipulating these pathways control APP accumulation and synapse homeostasis.



APP is transported from the Golgi apparatus to the synapse in either dendrites or axons, and in both anterograde and retrograde directions by kinesin-1 and dynein, respectively (Brunholz *et al.*, 2012; Gibbs *et al.*, 2015; Toh and Gleeson, 2016). We and others have shown that wild-type huntingtin (HTT), but not the polyglutamine-expanded HTT that causes Huntington's disease (HD), facilitates APP transport by increasing the velocity of APP-containing vesicles (Colin *et al.*, 2008; Her and Goldstein, 2008). HTT is a large scaffold protein that interacts with various protein complexes including molecular motor proteins and, regulates consequently the transport of several cargos (Saudou and Humbert, 2016). APP transport into neurites is altered upon reduction of HTT levels or by the presence of polyQ expansion on HTT (Colin *et al.*, 2008; Her and Goldstein, 2008). However, these studies did not distinguished axons from dendrites and did not investigate the consequences on APP levels at the synapse both in vitro and in vivo. Consequently, several questions remain to be addressed regarding the interplay between HTT and APP and its physiological consequences.

To answer these questions, we studied APP and HTT in a microfluidic device that reconstitutes a corticocortical neuronal network with separate presynaptic, synaptic, and postsynaptic compartments, and further tested our findings in APPPS1 mice, which display AD-like pathology. We find that subtle modifications of axonal transport of APP change synaptic levels of APP and have dramatic consequences on synapse function.

## Results

### Developing an in vitro corticocortical network using microfluidic chambers

One of the major impediments to assessing APP transport in axons and dendrites under physiological conditions is the difficulty of recreating a mature neuronal network in a dish. Primary cultures are usually randomly distributed, with multidirectional, random connections. The use of Campenot chambers or microfluidic devices made it possible to separate axons from dendrites and soma, but neurons in these chambers are still not integrated into networks as they would be in vivo (Taylor *et al.*, 2005). We therefore turned to later-generation devices (Taylor *et al.*, 2010) and modified them to reconstitute an oriented network with optimized connections (Moutaux *et al.*, 2018; Virlogeux *et al.*, 2018). These devices contain three compartments (presynaptic, synaptic, and postsynaptic) that are fluidically isolated and separated by microchannels that are 5  $\mu\text{m}$  high and 5  $\mu\text{m}$  wide, but of two different lengths: 500  $\mu\text{m}$  and 75  $\mu\text{m}$  (Figure 1A). The 500  $\mu\text{m}$  channels allow only axons from the presynaptic compartment to reach the synaptic compartment (Taylor *et al.*, 2005). The 75  $\mu\text{m}$  long microchannels allow dendrites to cross from the postsynaptic to the synaptic compartment, where MAP2 staining shows they connect with axons coming from the presynaptic compartment (Figure 1B). We reconstructed a corticocortical network-on-a-chip since APP protein is expressed in the cortex, and AD largely targets iso- and archicortical brain regions. In these microfluidic devices, we observed full maturation of the corticocortical neuronal network between days in vitro (DIV) 10 and 15, as revealed by uptake of FM4-64, an indicator of endocytosis/exocytosis of functional synapses (Figure 1C). This device is thus optimized for studying the sub-cellular dynamics of APP.

### APP is transported to synapses from both pre- and post-synaptic neurons

We transduced mouse cortical neurons at DIV eight with lentiviruses expressing APP tagged with mCherry at the C terminus (APP-mCherry), which retains APP characteristics (Kaether *et al.*, 2000; Marquer *et al.*, 2014). We recorded the movements of APP-mCherry vesicles at high frequency frame rate using spinning disk confocal microscopy and found that velocities reach a maximum at DIV13, when the network is fully mature, with established synapses (Figure 1B and C, Figure 1—figure supplement 1). To assess axonal transport, we first focused on the distal part of the 500  $\mu\text{m}$  long microchannels (Figure 1B) to follow APP-mCherry vesicles within neurons transduced in the presynaptic compartment (Figure 2A, Video 1), which can be reached only by presynaptic axons (Moutaux *et al.*, 2018; Taylor *et al.*, 2005; Virlogeux *et al.*, 2018). To assess dendritic transport of APP-mCherry vesicles, we transfected the postsynaptic neurons with a MAP2-GFP plasmid and

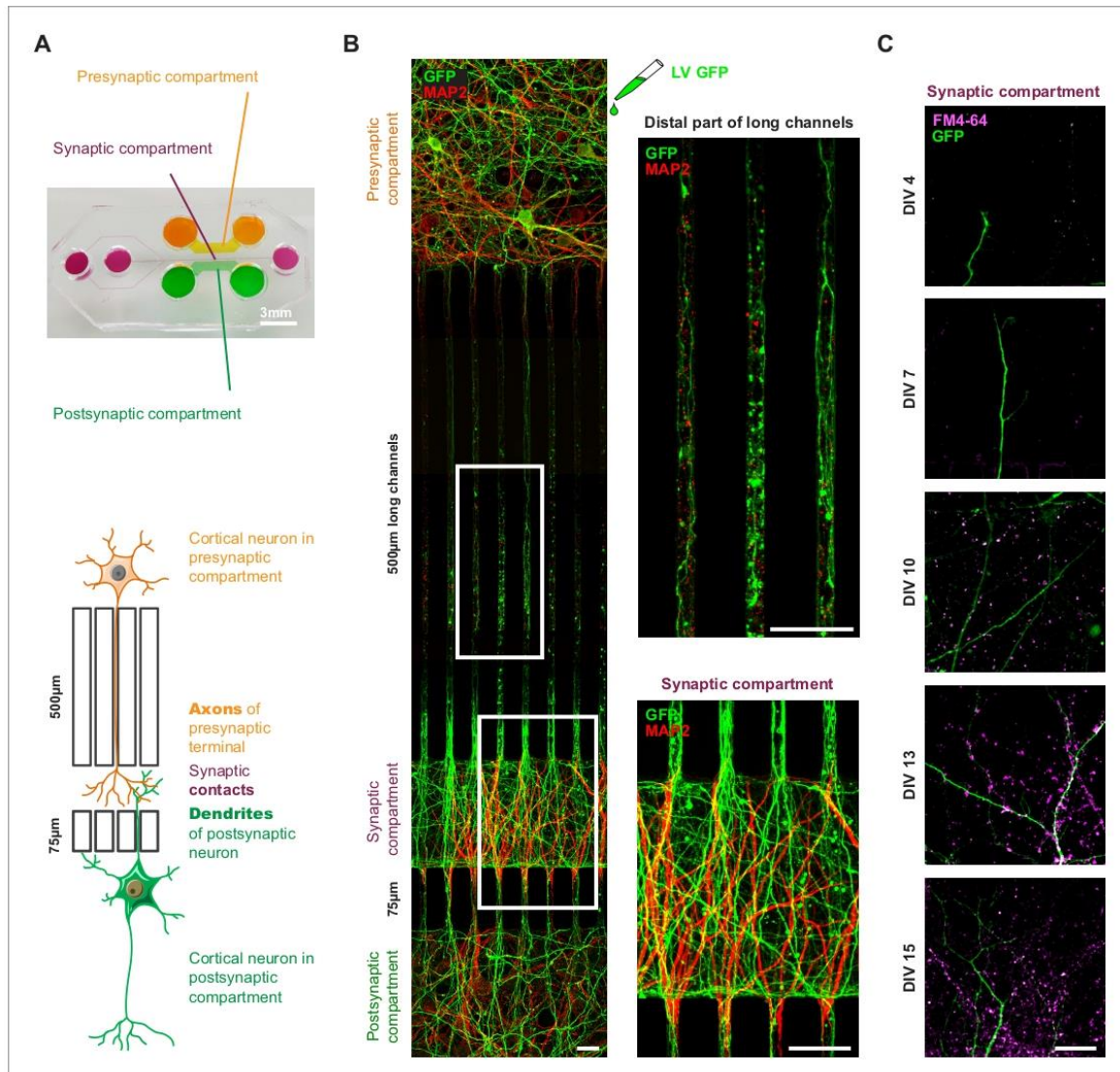


**Figure 1.** Reconstituted corticocortical mature neuronal circuit. (A) Image and schematic representation of the 3-compartment microfluidic chamber that allows the reconstitution of a corticocortical mature network compatible with live-cell imaging of axons and dendrites. (B) Presynaptic neurons were transduced with GFP (green) to visualize axons into microgrooves and MAP2 (red) immunostaining was applied on the entire microchambre at DIV13. Magnification shows axons into distal part of long microchannel but not MAP2-positive dendrites (C) Functional synapses were detected using FM4-64 dye (purple) that labels active presynaptic boutons on GFP dendrites (green) upon 50 mM KCl stimulation. Images represent a projection of 5 µm Z stacks. The highest number of functional corticocortical synapses is visualized between DIV10 and DIV15 in this microfluidic device. Scale bar = 20 µm. The online version of this article includes the following figure supplement(s) for figure 1:

**Figure supplement 1.** Time course of kinetics of anterograde and retrograde APP-mCherry axonal velocity after plating neurons into microchambers.

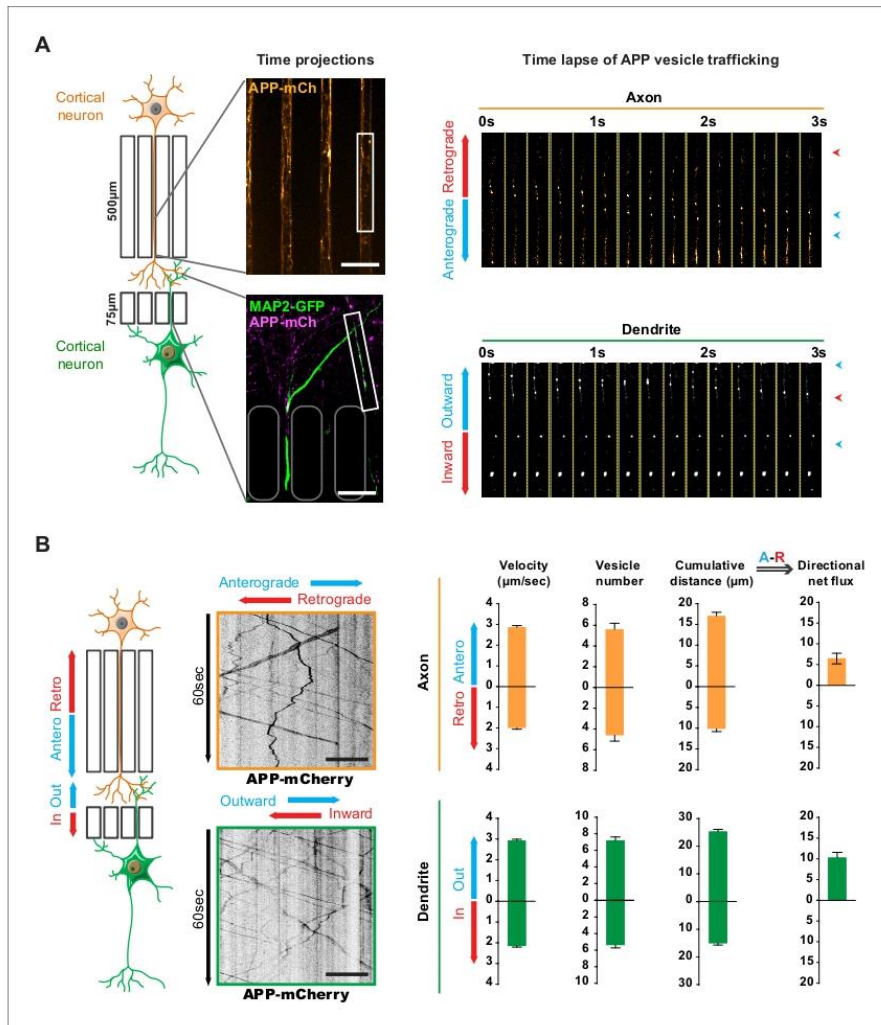
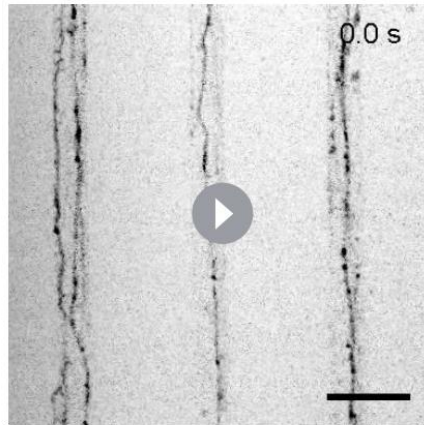


**Figure 2.** Transport of APP in axons and dendrites in reconstituted corticocortical mature neuronal circuit. (A) APP-mCherry was transduced into the presynaptic compartment for axonal transport analysis or into the postsynaptic compartment for dendritic trafficking. Postsynaptic neurons were transfected with MAP2-GFP (green) to visualize dendrites that cross the short microchannels. APP-mCherry transport along the axons or the dendrites are represented in time projections of maximum signal intensities for 60 s (middle panels) and real time-lapse analysis of anterograde/retrograde or inward/outward vesicles in axons and dendrites respectively (right panel). Scale bars = 20 μm. (B) Kymograph analyses of APP-mCherry axonal or dendritic transport at DIV13 from time-lapse images acquired every 200 ms during 60 s. Transport characteristics such as the anterograde/retrograde or outward/inward vesicle velocities, moving vesicle number per 100 μm of neurite length, the cumulative distances travelled by vesicles and thus the directional net flux of APP-mCherry trafficking into axons (upper panel) or dendrites (lower panel) are represented by means ± SEM of 3 independent experiments, 40 axonal and 120 dendritic axons and 674 axonal and 1160 dendritic vesicles. Scale bars = 20 μm. (see also *Videos 1* and *2*).

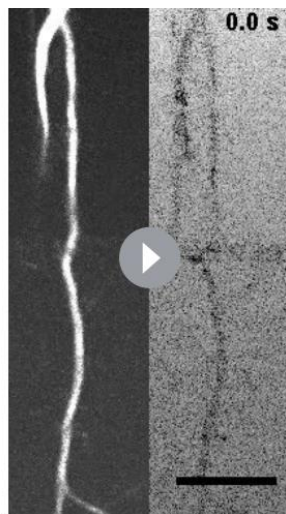
selected only the APP-mCherry vesicles that crossed the 75-μm-long microchannels (*Figure 2A*, *Video 2*). MAP2-GFP transfection did not modify the transport of APP by itself (data not shown).

We generated kymographs from the axonal and dendritic recordings (*Figure 2B*) and measured several transport parameters (see Materials and methods): the velocity of APP-mCherry vesicles, their number, and the cumulative distance they travelled in anterograde and retrograde directions



**Video 1.** Axonal Transport of APP-mCherry in presynaptic cortical neurons at DIV13. Vesicles were recorded for 60 s at 5 Hz. Axons are oriented from soma (top of the channel) to neurite terminals (bottom) with anterograde vesicles going down. Scale bar, 20  $\mu$ m.

<https://elifesciences.org/articles/56371#video1>



**Video 2.** Transport of APP-mCherry (right panel) in MAP2-GFP positive postsynaptic cortical dendrites (left panel) at DIV13. Vesicles were recorded for 60 s at 5 Hz. Dendrites are oriented from soma (top of the channel) to neurite terminals (bottom) with outward vesicles going down. Scale bar, 20  $\mu$ m.

<https://elifesciences.org/articles/56371#video2>

within axons. We defined the overall direction of APP-mCherry vesicle transport in axons by adding the anterograde cumulative distance to the negative retrograde cumulative distance, so that positive values indicate a net anterograde flux from the soma towards the synapse (**Figure 2B**). We also measured dendritic transport, expressed as inward (from postsynaptic compartment to soma) or outward (from soma to postsynaptic site), since microtubules in dendrites (unlike in axons) are not fully oriented with the plus ends towards the dendrite's extremities (**Kapitein and Hoogenraad, 2015; van Beuningen and Hoogenraad, 2016; Figure 2B**). Our analysis showed a net anterograde axonal and outward dendritic flux for APP-mCherry-containing vesicles, indicating that there is a significant transport of APP to the synapse from both pre- and postsynaptic neurons (**Figure 2B**). These findings in a mature network are in accordance with the reported velocities of APP vesicles (**Fu and Holzbaaur, 2013; Her and Goldstein, 2008; Marquer et al., 2014; Rodrigues et al., 2012; Vagnoni et al., 2013**).

### Huntingtin phosphorylation regulates axonal but not dendritic transport of APP

We had previously shown that phosphorylation of HTT at Serine 421 determines the direction in which various cargoes are transported in neurites (**Colin et al., 2008**). These experiments over-expressed short HTT fragments containing mutations at Serine 421 in neurons that were randomly cultured (i.e., not integrated into a mature network) and in which axons and dendrites could not be discriminated. To study the role of HTT phosphorylation at S421 in APP transport in axons versus dendrites, we took advantage of our microfluidic system and two lines of homozygous knock-in mice: one in which Serine 421 is replaced by an alanine ( $Htt^{S421A/S421A}$  or  $HTT_{SA}$ ), mimicking the absence of phosphorylation, and another in which Serine 421 is replaced by aspartic acid ( $Htt^{S421D/S421D}$  or  $HTT_{SD}$ ), mimicking constitutive phosphorylation (**Thion et al., 2015**). It is important to note that neither mutation affects the level of HTT expression (**Ehinger et al., 2020**).

We isolated  $HTT_{SA}$  and  $HTT_{SD}$  cortical neurons from the mice and plated them in both pre- and postsynaptic compartments of our microfluidic device as in **Figure 1A**. Abolishing HTT phosphorylation at Serine 421 increased the velocity of retrograde vesicles, increased their cumulative distance travelled, and reduced the net

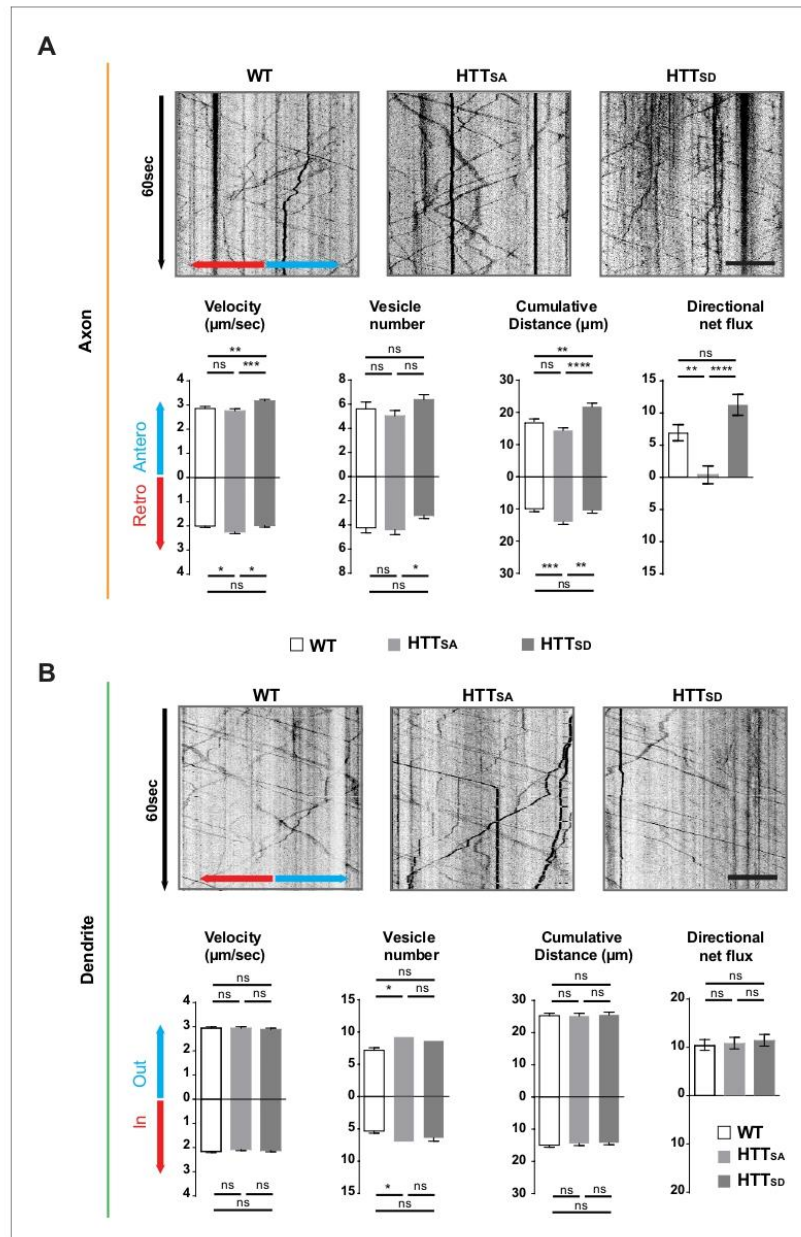


**Figure 3.** Axonal but not dendritic transport of APP depends on HTT phosphorylation. (A) Kymographs and quantifications of APP-mCherry into WT, HTT<sub>SA</sub> and HTT<sub>SD</sub> axons. Velocity, vesicle number per 100 μm of neurite length, cumulative distance and directional net flux were measured. Histograms represent means +/- SEM of 3 independent experiments, 41 WT, 52 HTT<sub>SA</sub> and 63 HTT<sub>SD</sub> axons and 674 WT, 602 HTT<sub>SA</sub> and 493 HTT<sub>SD</sub> vesicles. Significance was determined using an unpaired t-test; \*p<0.05, \*\*p<0.01, \*\*\*p<0.001, \*\*\*\*p<0.0001, ns = not significant. Scale bar = 20 μm. (B) Kymographs and quantifications of APP-mCherry into WT, HTT<sub>SA</sub> and HTT<sub>SD</sub> dendrites. Significance was determined using an unpaired t-test; \*p<0.05, \*\*p<0.01, \*\*\*p<0.001, \*\*\*\*p<0.0001, ns = not significant. Scale bar = 20 μm.

Figure 3 continued on next page

## Figure 3 continued

dendrites. Dendritic inward and outward velocity, vesicle number per 100  $\mu\text{m}$  of neurite length, cumulative distance and directional net flux were measured. Histograms represent means  $\pm$  SEM of 4 independent experiments, 122 WT, 99 HTT<sub>SA</sub> and 109 HTT<sub>SD</sub> dendrites, 1171 WT, 1119 HTT<sub>SA</sub> and 1074 HTT<sub>SD</sub> vesicles. Significance was determined using an unpaired t-test; \* $p < 0.05$ ; ns = not significant. Scale bar = 20  $\mu\text{m}$ . (see also **Video 3**).

The online version of this article includes the following source data and figure supplement(s) for figure 3:

**Source data 1.** Statistical analysis of APP axonal transport.

**Source data 2.** Statistical analysis of APP dendritic transport.

**Figure supplement 1.** Cellular distribution of kinesin and dynactin in WT and HTT<sub>SA</sub> mouse brains.

**Figure supplement 1—source data 1.** Statistical analysis of total KHC levels.

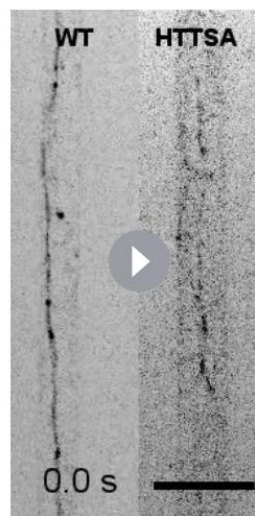
**Figure supplement 1—source data 2.** Statistical analysis of vesicular and cytosolic KHC levels.

anterograde flux of APP vesicles in axons (**Figure 3A**, **Video 3**), whereas HTT<sub>SD</sub> neurons showed an increase in anterograde velocity and greater cumulative distance travelled by APP compared to HTT<sub>SA</sub> or wild type (WT) neurons. Nevertheless, the net flux, which reflects the flow of vesicles from the soma to axon terminals, was not significantly different from that observed in WT neurons. This indicates that in our experimental conditions, most of the WT HTT is in its phosphorylated form. Phosphorylation status did not, however, modify APP transport in dendrites (**Figure 3B**). We conclude that HTT phosphorylation regulates axonal but not dendritic transport of APP to the synapse.

Given that microtubule polarity influences selective cargo trafficking in axons and dendrites (*van Beuningen and Hoogenraad, 2016*), it is interesting to note that the axon-specific effect of HTT phosphorylation correlates with axons' preferential plus-end microtubule orientation (dendrites have mixed microtubule polarity). To further understand the selective effect in axons versus dendrites, we investigated the interaction of non-phospho HTT with kinesin-1, the molecular motor responsible for the transport of APP (*Matsuda et al., 2001; Verhey et al., 2001*). Because most WT HTT is already in its phosphorylated form in our experimental conditions, we compared HTT<sub>SA</sub> with WT (rather than HTT<sub>SD</sub>) neurons. We found no difference between WT and HTT<sub>SA</sub> neurons in their total kinesin heavy chain (KHC) levels (**Figure 3—figure supplement 1A**), but HTT<sub>SA</sub> neurons had less KHC in the vesicular fraction than in the cytosolic fraction (**Figure 3—figure supplement 1B**). These results are in agreement with our previous study suggesting HTT dephosphorylation decreases the association of kinesin-1 with vesicles (*Colin et al., 2008*).

### HTT regulation of APP anterograde axonal transport is mediated by akt phosphorylation

HTT phosphorylation at S421 depends on the Akt kinase (*Humbert et al., 2002*). We therefore investigated whether Akt could modify anterograde transport of APP and whether this required HTT phosphorylation. We transduced cortical neurons with APP-mCherry and a construct encoding constitutively active Akt (Akt-CA) or a form of Akt (Akt-N) that has no kinase activity with and IRES-GFP or the corresponding empty GFP vector (GFP) as a control. As expected, Akt induced endogenous HTT phosphorylation in WT neurons but was unable to do so in HTT<sub>SA</sub> neurons (**Figure 4A**). In addition,



**Video 3.** APP-mCherry transport in WT (left panel) or HTT<sub>SA</sub> (right panel) axons at DIV13. Vesicles were recorded for 60 s at 5 Hz. Axons are oriented from soma (top of the channel) to neurite terminals (bottom) with anterograde vesicles going down. Scale bar, 20  $\mu\text{m}$ .

<https://elifesciences.org/articles/56371#video3>

HTT phosphorylation was reduced upon Akt-N expression.

To ensure Akt was not affecting neuronal growth and maturation, we transduced neurons at DIV8 and analyzed APP trafficking at DIV13. Expressing Akt-CA and APP-mCherry in WT cortical neurons had no effect on vesicle number but markedly increased anterograde velocity of APP and the cumulative distances travelled by anterograde APP-mCherry-containing vesicles, which in turn led to an increase of their net anterograde flux (*Figure 4B and C, Video 4*). In contrast, in HTT<sub>SA</sub> neurons, Akt-CA was unable to modify the different transport parameters. Thus, Akt activation increases APP anterograde transport in axons by phosphorylating HTT at Serine 421. These results identify Akt-HTT signaling as a new mechanism that regulates axonal trafficking of APP.

### Huntingtin-mediated axonal transport determines presynaptic APP levels

To determine whether reduced anterograde axonal transport of APP affects the targeting of APP at the plasma membrane, we used TIRF (total internal reflection fluorescence) microscopy and a super-ecliptic version of pHluorin (SEP) fused to the N-terminal part of APP to monitor insertion of APP into the plasma membrane. As we could not reliably detect APP-SEP at the membrane in primary cultures of neurons, we transfected the APP-SEP construct with versions of full-length wild type HTT (pARIS HTT) (*Pardo et al., 2010*) or full-length HTT containing the S421A mutation (pARIS HTT<sub>SA</sub>) into COS cells that are known to have their plus-end microtubules oriented toward the plasma membrane (*Takemura et al., 1995*). We detected far fewer APP-SEP dots per minute in cells expressing pARIS HTT<sub>SA</sub> than in cells expressing pARIS HTT (*Figure 5A, Video 5*). This result suggests that reducing transport of APP to the plasma membrane by dephosphorylating HTT decreases APP targeting at the plasma membrane.

The fluidic isolation of the synaptic compartment enabled us to collect proteins and investigate the targeting of APP at synapses by measuring APP levels by western blot. We first verified that the synaptic chamber is enriched with synaptic marker synaptophysin and empty of nuclear marker lamin B1 (*Figure 5B*). Lack of HTT phosphorylation led to a reduction of APP protein levels at synapses but no real change in the soma-containing chamber (*Figure 5B*).

We then investigated APP targeting in vivo. We first prepared synaptosomal fractions from WT mouse brains and purified post-synaptic density fractions (PSD, enriched in postsynaptic proteins) and non-PSD fractions that are enriched with presynaptic proteins. As expected, we detected synaptophysin, a presynaptic marker, and PSD95, a postsynaptic marker, in the non-PSD and PSD enriched fractions, respectively (*Figure 5C*). We detected APP in both fractions. We found that most of the synaptosomal APP was enriched in the non-PSD fraction, which suggests that a significant fraction of APP found at synapses originates from the presynaptic compartment. Since anterograde axonal transport of APP is controlled by HTT phosphorylation, we measured APP within fractions prepared from HTT<sub>SA</sub> homozygous mouse brains (*Figure 5D*). APP levels were lower in the non-PSD fraction of HTT<sub>SA</sub> mouse brains (enriched with presynaptic proteins), but APP levels did not differ significantly between WT and HTT<sub>SA</sub> mouse brains in the PSD fraction (*Figure 5D*). Together, our results indicate that the absence of HTT phosphorylation reduces anterograde transport of APP in axons, but not in dendrites, and subsequently regulates the levels of APP in the presynaptic compartment both in vitro and in vivo.

### HTT chronic dephosphorylation alters brain morphology and synapse size and number

The previously generated HTT<sub>SA</sub> mice have no obvious phenotype but were not fully characterized for brain-related behavior and morphology (*Thion et al., 2015*). Subsequent analyses of the mice at 6 months of age did not reveal any behavioral abnormalities (*Ehinger et al., 2020*). Given our observation that anterograde transport and presynaptic accumulation of APP are both reduced in HTT<sub>SA</sub> mice and that APP is associated with late-onset defects, we subjected the mice to complete behavioral analysis (SHIRPA *Rogers et al., 1997*, open field, grip test and elevated plus Maze) when they were 12 months old, and again found no significant differences in behavior (*Figure 6—figure supplement 1 and Supplementary file 1*).

We then performed anatomical ex vivo MRI of young adult WT and HTT<sub>SA</sub> mice (*Figure 6A and B*). HTT<sub>SA</sub> mice between 8 and 11 weeks of age showed greater whole brain volume (4.8%) affecting

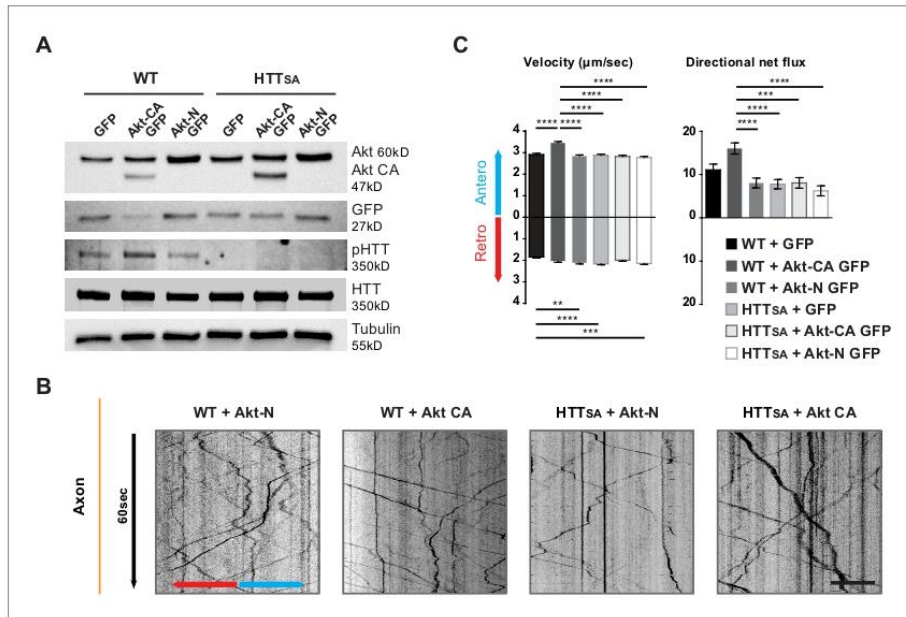


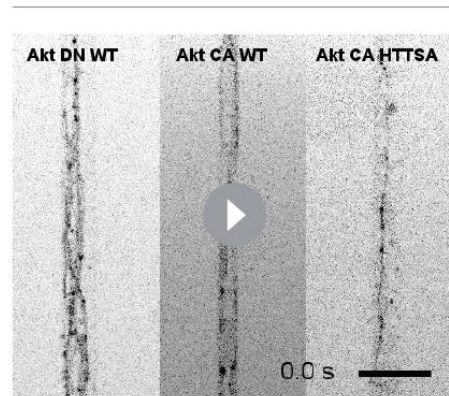
**Figure 4.** Akt regulates APP transport in a HTT phospho-dependent manner. (A) WT and HTT<sub>SA</sub> neurons transduced with constitutively active Akt (Akt-CA GFP) or an inactive form of Akt (Akt-N GFP) in IRES GFP constructs or with empty GFP vector (GFP) were analyzed by western blotting with Akt, GFP, phosphorylated HTT, total HTT and tubulin antibodies. (B) Kymographs of APP-mCherry from WT and HTT<sub>SA</sub> neurons seeded in microchambers and transduced with APP-mCherry and GFP, Akt-CA GFP or Akt-N GFP. Scale bar 20 μm. (see also [Video 4](#)). (C) Velocity and directional net flux of APP-mCherry vesicles were quantified. Histograms represent means +/- SEM of 3 independent experiments, 936 WT GFP, 988 WT AKT CA, 1261 WT AKT N, 1357 HTT<sub>SA</sub> GFP, 1048 HTT<sub>SA</sub> AKT CA and 1177 HTT<sub>SA</sub> AKT N vesicles. Significance was determined using one-way ANOVA followed by Tukey's post-hoc analysis for multiple comparisons; \*p<0.05, \*\*p<0.01, \*\*\*p<0.001, \*\*\*\*p<0.0001. The online version of this article includes the following source data for figure 4:

**Source data 1.** Statistical analysis of APP axonal transport according to Akt activity.

the hippocampus (8.5%) and the cortex (3.7%) but not the striatum. To determine whether HTT<sub>SA</sub> produced more subtle changes in synapse number and morphology, we quantified synaptic density and spine size in WT and HTT<sub>SA</sub> mice by electron microscopy. HTT<sub>SA</sub> mice had more synapses than WT mice but no difference in spine size ([Figure 6C](#)).

To further investigate the contribution of transport and APP levels on synapse number, we took advantage of the microfluidic devices and, using pre- and post-synaptic markers (synaptophysin and PSD95, respectively), measured the number of synaptic contacts in the synaptic compartment within WT and HTT<sub>SA</sub> mature neuronal circuits at DIV12. In agreement with our in vivo experiments ([Figure 6C](#)), we found an increase in the number of synaptic contacts in the HTT<sub>SA</sub> circuit ([Figure 7A](#)).

To determine whether APP overexpression would increase the quantity of APP within the



**Video 4.** Effect of Akt on the axonal transport of APP-mCherry in presynaptic cortical neurons from WT or HTT<sub>SA</sub> mice at DIV13. Vesicles were recorded for 60 s at 5 Hz. Axons are oriented from soma (top of the channel) to neurite terminals (bottom) with anterograde vesicles going down. Scale bar, 20 μm.

<https://elifesciences.org/articles/56371#video4>



presynaptic cortical compartment of a WT or HTT<sub>SA</sub> network (**Figure 7B**), we transduced WT or HTT<sub>SA</sub> neurons with a lentivirus expressing APP-mCherry at DIV7 and measured synapse number at DIV12. Overexpressing APP-mCherry in WT presynaptic cortical neurons decreased synaptic contacts, but overexpressing APP-mCherry in HTT<sub>SA</sub> presynaptic cortical neurons restored synaptic contacts back to the levels seen in WT neurons (**Figure 7B**). The presynaptic level of APP thus appears to determine synapse number and can be modulated by HTT phosphorylation; this further supports a role for the Akt-HTT-APP pathway in synapse homeostasis. To ensure that the HTT<sub>SA</sub> mutation was not affecting neurodevelopment, we transduced a WT circuit at DIV8, when axon growth has ended (**Moutaux et al., 2018**), with lentiviruses expressing APP-mCherry and either an N-terminal HTT construct containing the first 480 amino acids (HTT-480-WT) or a construct in which the S421 has been mutated into alanine (HTT-480-SA). We found that expressing the HTT-480-SA construct in mature neurons led to an increase in synaptic contacts similar to what is observed in HTT<sub>SA</sub> neurons differentiated in microchambers (**Figure 7A and C**). This suggests that the HTT S421A mutation has no major role in axon growth and/or that the increase of synaptic contacts seen in HTT<sub>SA</sub> neurons is not due to changes in neurodevelopment but rather results from reduced transport and accumulation of APP at the presynapses. We then investigated the effect of APP overexpression in WT neurons. As in **Figure 7B**, APP-mCherry overexpression in WT neurons transduced with HTT-480-WT led to a decrease in the number of synaptic contacts. However, it had no effect in neurons expressing HTT-480-SA, indicating that HTT dephosphorylation attenuates the effect of APP overexpression on synapse number (**Figure 7D**). We conclude that reducing anterograde axonal transport of APP either during axonal growth or in mature networks is sufficient to modulate synaptic contact number.

### Unphosphorylatable HTT reduces APP presynaptic levels in APPPS1 mouse model

HTT-mediated transport clearly modulates presynaptic levels of APP in a corticocortical circuit, but we wanted to investigate the consequences of chronic HTT dephosphorylation *in vivo*, in a mouse line that overexpresses APP. We chose APPPS1 mice—double transgenics that bear a human APP transgene with the Swedish mutation (APP<sup>Swe</sup>) and a mutant human presenilin 1 (PS1<sup>L166P</sup>) transgene (**Radde et al., 2006**)—which express human APP at three times the level of murine APP and mimic familial Alzheimer's. These mice show reduced synapse density (**Alonso-Nanclares et al., 2013; Bittner et al., 2012; Hoe et al., 2012; Müller et al., 2017; Priller et al., 2009; Radde et al., 2006; Zou et al., 2015**). We crossed HTT<sub>SA</sub> phospho-mutant mice with APPPS1 mice to generate APP<sup>Swe</sup>; PS1<sup>L166P</sup>;Htt<sup>S421A/S421A</sup> mice, heretofore referred to as APPPS1/HTT<sub>SA</sub> mice.

The levels of APP in the non-post-synaptic density fraction of APPPS1/HTT<sub>SA</sub> mice were significantly lower than in APPPS1 mice at 10 months (**Figure 8A and B**). Since the PS1<sup>L166P</sup> mutation promotes APP cleavage, thereby increasing A $\beta$ 42 production (**Radde et al., 2006**), we biochemically quantified A $\beta$  levels (**Figure 8—figure supplement 1A**) and performed histological measurements of plaque loads using the 4G8 antibody that recognizes both human and murine A $\beta$  (**Figure 8—figure supplement 1B**). We also measured amyloid burden using Congo red to stain amyloid plaques, and OC and A11 antibodies to recognize amyloid fibrils, fibrillary oligomers, and prefibrillar oligomers (**Kayed et al., 2007**) in 19-month-old APPPS1 and APPPS1/HTT<sub>SA</sub> mouse brains, a time that corresponds to the final behavioral evaluation of the mice before histopathological analyses (**Figure 8—figure supplement 1C**). We found no significant differences between genotypes, indicating that loss of HTT phosphorylation has no effect on A $\beta$  level, amyloid load, A $\beta$  oligomer load or plaque aggregation. These results indicate that HTT dephosphorylation regulates presynaptic levels of APP<sup>Swe</sup> without affecting downstream A $\beta$  production and/or accumulation.

We next quantified the number and the size of the spines in the CA1 region of 19-month-old mice by electron microscopy. As previously described for APP<sup>Swe</sup>-PS1<sup>ΔE9</sup> mice, 5xFAD Tg mice, and APPxPS1-KI mice (**Androuin et al., 2018; Koffie et al., 2009; Neuman et al., 2015**), APPPS1 mice showed lower synaptic density and larger spines than WT mice (**Figure 8C**). Strikingly, unphosphorylatable HTT (HTT<sub>SA</sub>) significantly increased spine density and completely rescued APPPS1-induced increase of spine size (**Figure 8C**).

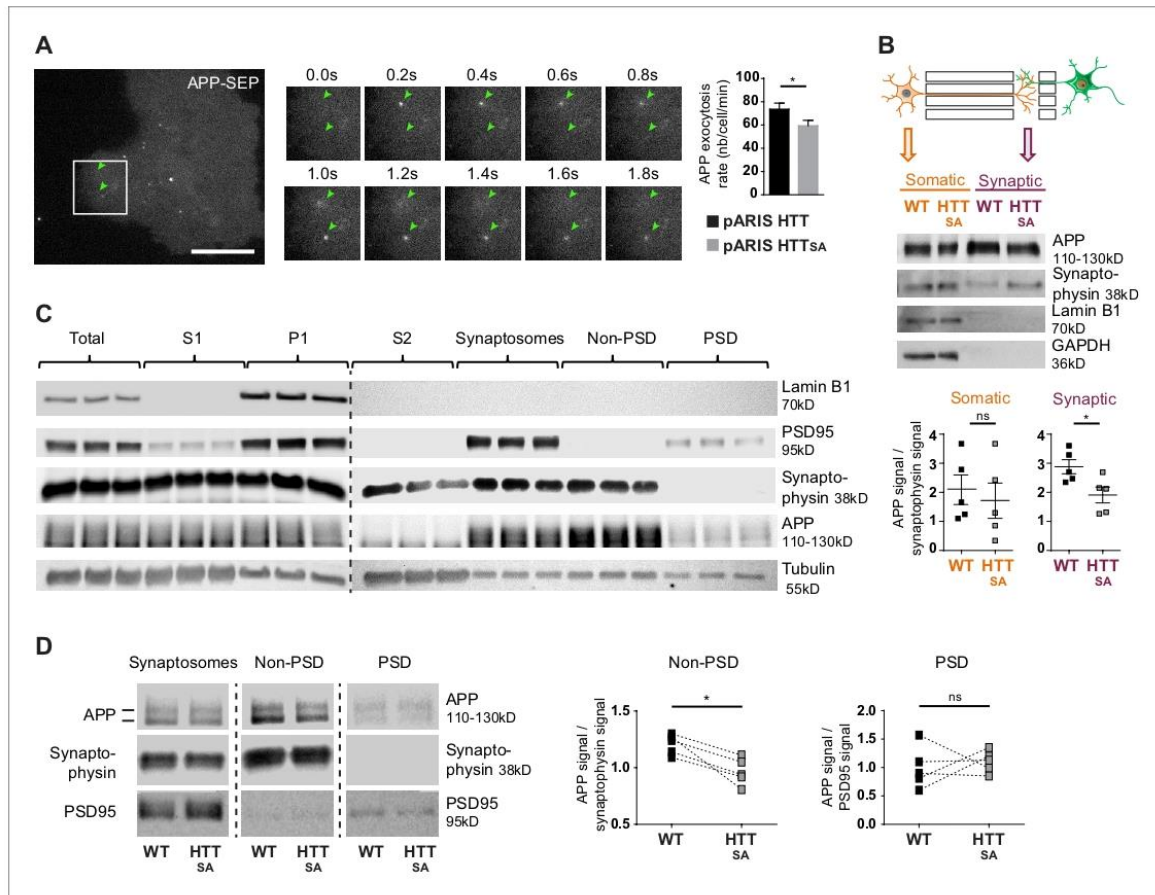


**Figure 5.** HTT S421 phosphorylation affects presynaptic APP targeting. (A) Effect of HTT S421 phosphorylation on exocytosis rate of APP was analyzed in COS cells co-transfected with APP-SEP (Super Ecliptic pHluorin) and with pARIS HTT or pARIS HTT<sub>SA</sub> visualized by TIRF microscopy. Magnification represents a time lapse of events showing 2 events of APP vesicle exocytosis (green arrows). Histograms represent means  $\pm$  SEM of exocytosis event number per minute in 39 HTT and 40 HTT<sub>SA</sub> cells from four independent experiments. Significance was determined using an unpaired t-test; \* $p < 0.05$ . Scale bar = 20  $\mu$ m. (see also *Video 5*). (B) Effect of HTT S421 phosphorylation on APP targeting at the synapse was assessed by anti-APP western blotting (22C11) analysis of extracts from synaptic chambers of a WT or HTT<sub>SA</sub> corticocortical network. SNAP25 was used as a control for protein content in the synaptic compartment and nuclear marker Lamin B1 for the somatic compartment. Histograms represent means  $\pm$  SEM of APP signal per synaptophysin signal on five independent experiments. Significance was determined using a Mann-Whitney test; \* $p < 0.05$ , ns = not significant. (C) Western blotting analysis of pre- and postsynaptic fractions obtained from synaptosome preparations. Fractionation gives the first pellet, P1, the first supernatant, S1, and the second supernatant, S2. Lamin B1, a nuclear marker is enriched in P1 fraction. The pre- (non-PSD) and the post-synaptic (PSD) fractions are respectively enriched in synaptophysin and PSD95. (D) APP from WT or HTT<sub>SA</sub> cortices fractions was quantified by western blotting analyses. APP signal was quantified as the ratio of synaptophysin signal for non-PSD fraction and as the ratio of PSD95 signal for PSD fraction. One line represents one experiment. Significance was determined using Mann-Whitney test; \* $p < 0.05$ , ns = not significant. The online version of this article includes the following source data for figure 5:

**Source data 1.** Statistical analysis of APP exocytosis rate.

**Source data 2.** Statistical analysis of APP levels in microfluidics device.

**Source data 3.** Statistical analysis of APP levels in synaptosome from brains.

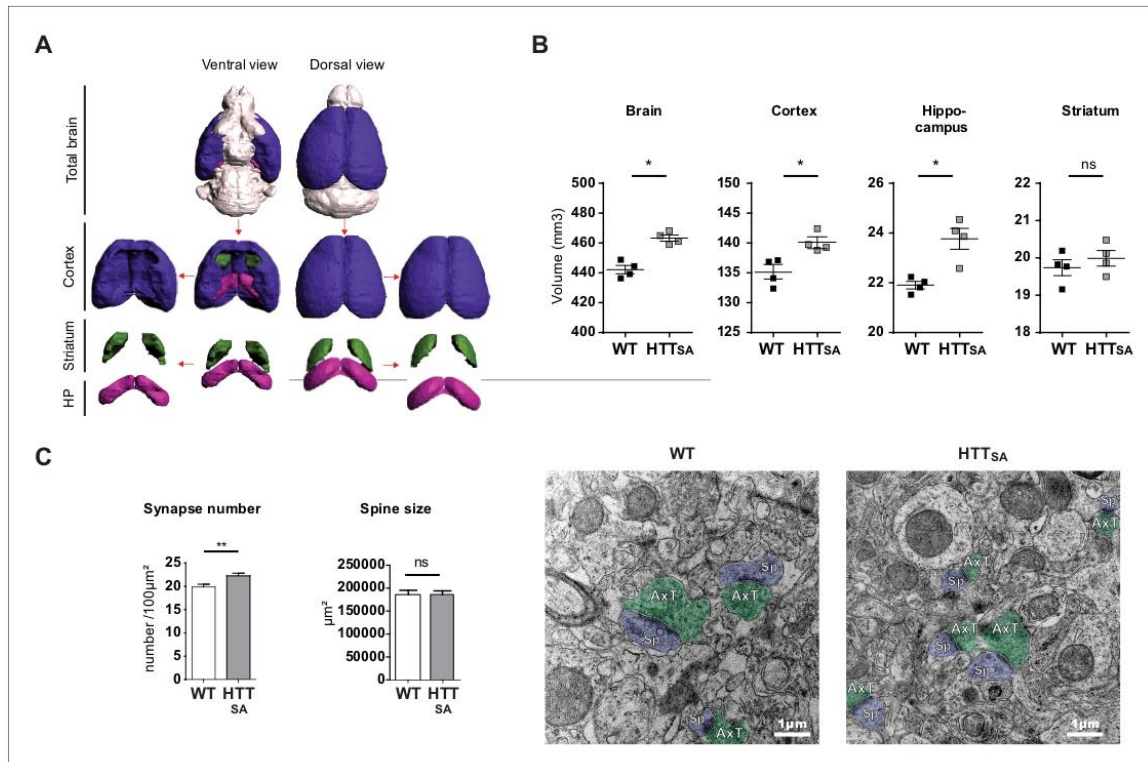


**Figure 6.** HTT dephosphorylation induces changes in brain morphology and synapse number. (A) Representative 3D reconstructions of WT brain areas built from high spatial resolution ex vivo MRI-T<sub>1w</sub> data. Each brain structure is represented with a specific color: cortex (purple), hippocampal formation (pink), striatum (green), and other structures (light grey). (B) Quantification of the volumes of the different cerebral regions represented in (A). The graphics show volumes for these regions (in mm<sup>3</sup>) of 2 and 3-month-old WT and HTT<sub>SA</sub> mice. Black bars represent the mean of 4 WT and 4 HTT<sub>SA</sub> mice, Mann and Whitney two tails, \**P* < 0.05; \*\**P* < 0.01; \*\*\**P* < 0.001). (C) Synapse number and size in CA1 region of 19-month-old WT or HTT<sub>SA</sub> mice were quantified by electron microscopy. Axon terminals (AxT) and spines (Sp) are colored with green and purple respectively. Histograms represent means ± SEM of 3 brains with 134 (WT) and 203 (HTT<sub>SA</sub>) fields analyzed and 225 (WT) and 218 (HTT<sub>SA</sub>) synapses. Significance was determined using an unpaired t-test; \*\**p* < 0.01, ns = not significant. Scale bar = 1 μm.

The online version of this article includes the following source data and figure supplement(s) for figure 6:

**Source data 1.** Statistical analysis of brain structure volumes of HTT<sub>SA</sub> mice.

**Source data 2.** Statistical analysis of synapse number and spine size in HTT<sub>SA</sub> brains.

**Figure supplement 1.** Behavioral analyses of the locomotion, force and anxiety in WT and HTT<sub>SA</sub> mice.

**Figure supplement 1—source data 1.** Statistical analysis of the distance moved in an open field by HTT<sub>SA</sub> mice.

**Figure supplement 1—source data 2.** Statistical analysis of the time spent in the periphery of an open field by HTT<sub>SA</sub> mice.

**Figure supplement 1—source data 3.** Statistical analysis of grip force test by HTT<sub>SA</sub> mice.

**Figure supplement 1—source data 4.** Statistical analysis of EPM test by HTT<sub>SA</sub> mice.

## Unphosphorylatable HTT improves learning and memory in APPPS1 mice

We next investigated the behavior of WT, APPPS1, and APPPS1/HTT<sub>SA</sub> mice. Extensive phenotypic analysis of the HTT<sub>SA</sub> mice using a modified SHIRPA primary screen and various behavioral tests (**Figure 6—figure supplement 1** and **Supplementary file 1**) revealed no significant changes in the behavioral-neurological status of 12 to 15 month-old HTT<sub>SA</sub> mice compared to WT mice. When we

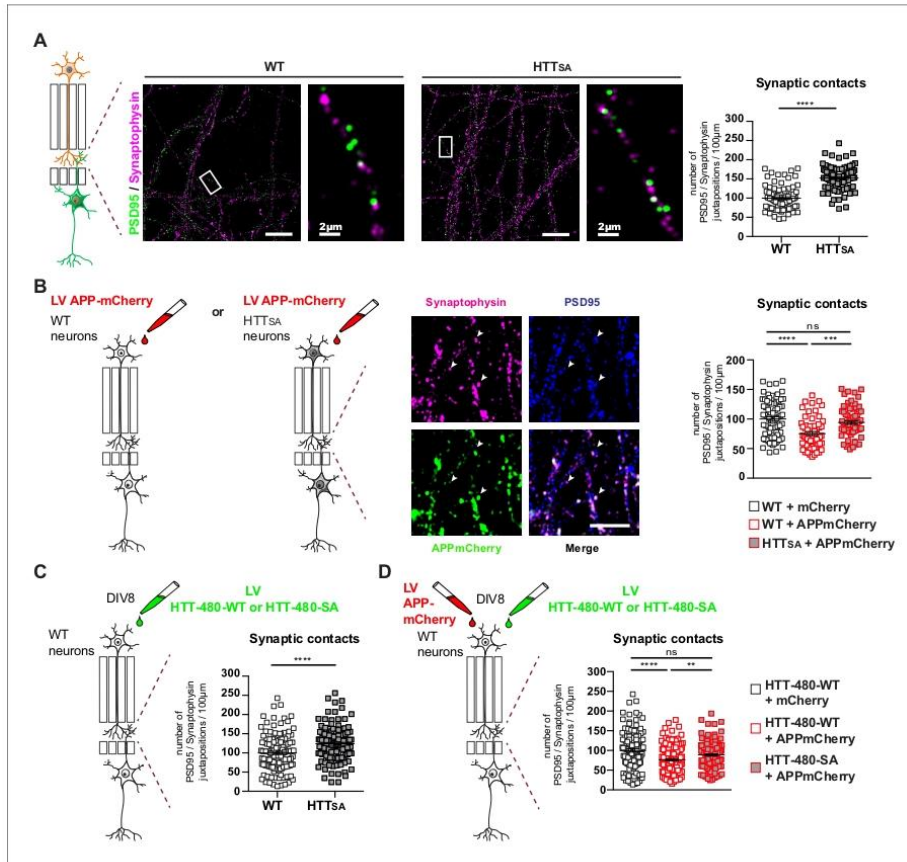


**Figure 7.** HTT phosphorylation regulates synaptic contacts by reducing presynaptic APP levels. (A) Number of PSD95/Synaptophysin contacts in the synaptic chamber of WT and HTT<sub>SA</sub> network. Right microphotographs for each genotype show magnification of representative neurites. Scale bars = 20  $\mu$ m (low magnification) or 2  $\mu$ m (high magnification). Histograms represent means  $\pm$  SEM of 3 independent experiments and 85 WT and 91 HTT<sub>SA</sub> neurites. Significance was determined using an unpaired t-test; \*\*\*\* $p$ <0.0001. (B) Representative image of APP-mCherry transduced presynaptic neurons. APP-mCherry is present in axon terminals positive for synaptophysin (white arrows). Scale bar = 2  $\mu$ m. Number of PSD95/Synaptophysin contacts in the synaptic chamber of WT and HTT<sub>SA</sub> network transduced at presynaptic site with APP-mCherry or mCherry as a control. Histograms represent means  $\pm$  SEM of 3 independent experiments and 75 WT + mCherry, 59 WT + APP-mCherry and 71 HTT<sub>SA</sub> APP-mCherry neurites. (C) Number of PSD95/Synaptophysin contacts in the synaptic chamber of WT mature network transduced at presynaptic site with a lentivirus encoding an HTT construct containing the first 480 amino acids without (HTT-480-WT) or with the S421A mutation (HTT-480-SA). Histograms represent means  $\pm$  SEM of at least three independent experiments and 132 HTT-480-WT and 130 HTT-480-SA neurites. Significance was determined using Mann and Whitney test; \*\*\*\* $p$ <0.0001. (D) Number of PSD95/Synaptophysin contacts in the synaptic chamber of WT mature network transduced at presynaptic site with APP-mCherry or mCherry as a control and with a lentivirus encoding a HTT-480-WT or HTT-480-SA. Histograms represent means  $\pm$  SEM of 3 independent experiments and 132 HTT-480-WT + mCherry, 134 HTT-480-WT + APP mCherry and 136 HTT-480-SA + APP mCherry neurites. Significance was determined using one-way Kruskal-Wallis test followed by Dunn's post-hoc analysis for multiple comparisons; \*\* $p$ <0.01, \*\*\* $p$ <0.001, \*\*\*\* $p$ <0.0001, ns = not significant.

The online version of this article includes the following source data for figure 7:

- Source data 1.** Statistical analysis of the number of synaptic contacts in HTT<sub>SA</sub> neurons.
- Source data 2.** Statistical analysis of the number of synaptic contacts in APP transduced neurons.
- Source data 3.** Statistical analysis of the number of synaptic contacts in HTT transduced neurons.
- Source data 4.** Statistical analysis of the number of synaptic contacts in APP and HTT transduced neurons.

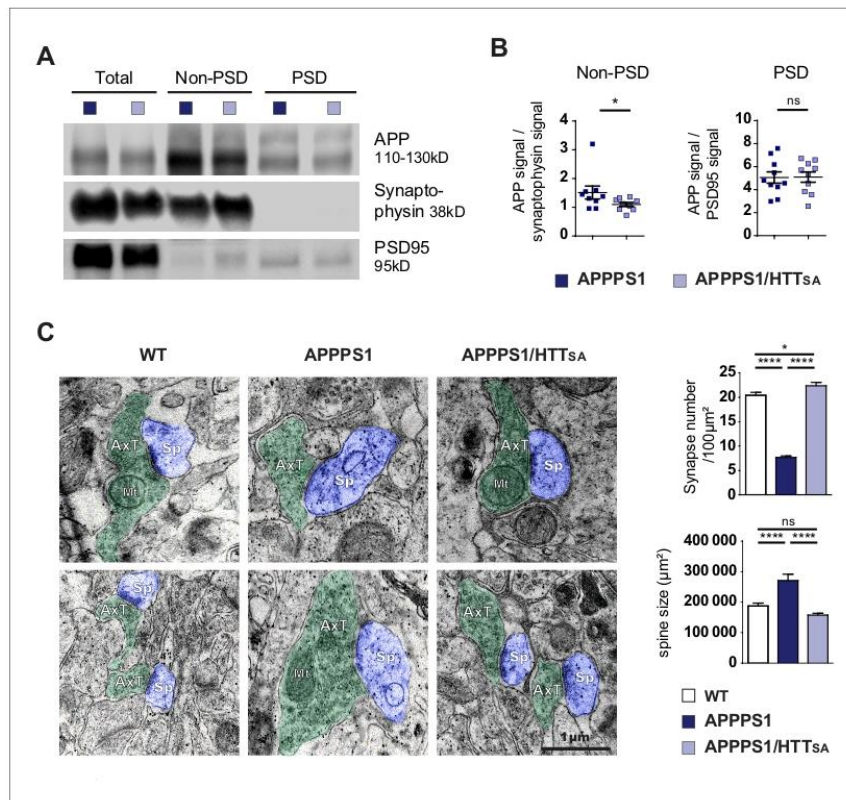


**Figure 8.** HTT S421 dephosphorylation rescues synapse number in APPPS1 mice. (A) APP levels from APPPS1 and APPPS1/HTT<sub>SA</sub> cortical fractions were quantified by western blotting analyses after synaptosomes fractionation. (B) APP signal was quantified as the ratio of synaptophysin signal for non-PSD fraction and as the ratio of PSD95 signal for PSD fraction. Histograms represent means  $\pm$  SEM of 9 experiments. Significance was determined using Wilcoxon test; \* $p < 0.05$ , ns = not significant. (C) Synaptic number and postsynaptic density (PSD) length of CA1 region of hippocampi from 19-month-old APPPS1 and APPPS1/HTT<sub>SA</sub> mice were quantified by electron microscopy. Axon terminals (AxT) and spines (Sp) are colored with green and purple, respectively. Scale bar = 1  $\mu$ m. (D) Histograms represent means  $\pm$  SEM of 3 brains; 153 APPPS1 and 152 APPPS1/HTT<sub>SA</sub> fields and 182 APPPS1 and 350 APPPS1/HTT<sub>SA</sub> synapses were analyzed. Significance was determined using one-way ANOVA followed by Tukey's multiple comparisons test; \* $p < 0.05$ , \*\*\*\* $p < 0.0001$ ; ns = not significant.

The online version of this article includes the following source data and figure supplement(s) for figure 8:

**Source data 1.** Statistical analysis of APP levels in synaptosomes from APPPS1/HTT<sub>SA</sub> brains.

**Source data 2.** Statistical analysis of synapse number and spine size of APPPS1/HTT<sub>SA</sub> brains.

**Figure supplement 1.** Analysis of soluble A $\beta$ 42 levels, amyloid plaques and amyloid load in APPPS1 and APPPS1/HTT<sub>SA</sub> mice.

**Figure supplement 1—source data 1.** Statistical analysis of soluble of A $\beta$ 42 levels in APPPS1/HTT<sub>SA</sub> brains.

**Figure supplement 1—source data 2.** Statistical analysis of amyloid load in APPPS1/HTT<sub>SA</sub> brains.

compared WT, APPPS1, and APPPS1/HTT<sub>SA</sub> mice, we found no significant differences in locomotor activity or anxiety-related behavior in the open field test (**Figure 9—figure supplement 1**).

We then evaluated spatial learning of 12- to 15-month-old APPPS1 and APPPS1/HTT<sub>SA</sub> mice in the Morris water maze paradigm. As expected, APPPS1 mice took longer paths to reach the platform of the water maze (**Figure 9A**). APPPS1/HTT<sub>SA</sub> mice performed better than APPPS1 mice, although not to the level of WT mice. Comparing the early and late stages of learning in the APPPS1/HTT<sub>SA</sub> mice, we found that APPPS1/HTT<sub>SA</sub> mice performed about as poorly as the APPPS1 mice in the early stages of learning (first training sessions). In the late training sessions, however, they performed much better than APPPS1 mice and showed a substantial recovery of performance

(Figure 9B). Finally, we evaluated their memory of the platform location by subjecting the mice to a probe trial. APPPS1 mice explored all quadrants of the pool equally, whereas both WT and APPPS1/HTT<sub>SA</sub> mice showed a preference for the target quadrant, indicating that their memory of the platform was intact (Figure 9C).

We also subjected the mice to the novel object recognition test (Figure 9D). APPPS1 mice spent similar time investigating familiar and novel objects, indicating a memory deficit (indicated by a memory index close to 50%). In contrast, APPPS1/HTT<sub>SA</sub> mice behaved as WT mice and showed a marked preference for the novel object (significantly different from the theoretical 50% random score), suggesting that unphosphorylatable HTT can mitigate the memory deficit observed in APPPS1 mice.

We conclude that blocking Akt phosphorylation at HTT S421 reduces APP presynaptic levels, improving learning and memory in APPPS1 mice.

## Discussion

We used high-resolution live-cell imaging of isolated axonal and dendritic compartments in a mature corticocortical network-on-a-chip to investigate the influence of HTT phosphorylation on APP

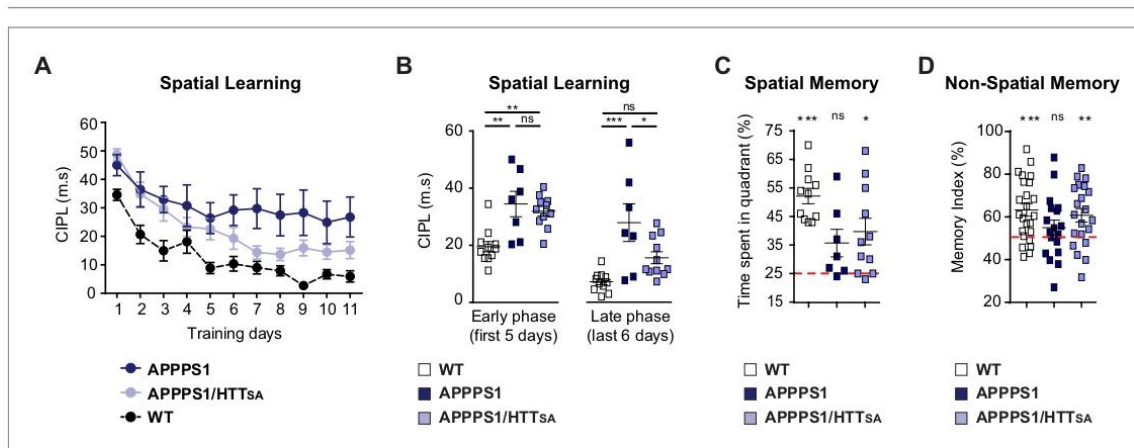


**Figure 9.** HTT S421 dephosphorylation enhances learning and memory in APPPS1 mice. (A) Spatial learning of 7 APPPS1 mice (dark blue), 11 APPPS1/HTT<sub>SA</sub> mice (light blue), and 11 WT mice (black dotted line) was assessed by measuring CIPL (Corrected Integrated Path Length), an unbiased measure of learning in the Morris water maze test over 11 days of training. Data are represented as mean  $\pm$  SEM. (B) Cumulative CIPL during the early phase (first 5 days) and the late phase (last 6 days) of training is depicted for WT, APPPS1 and APPPS1/HTT<sub>SA</sub> mice. All values are means  $\pm$  SEM. Significance was determined using one-way ANOVA test followed by Tukey's post-hoc analysis for multiple comparisons; \* $p < 0.05$ , \*\* $p < 0.01$ , \*\*\* $p < 0.001$ ; ns = not significant. (C) Spatial memory of 11 WT, 7 APPPS1 and 11 APPPS1/HTT<sub>SA</sub> mice was assessed on a probe trial performed 72 hr after the last training day and during which the percentage of time spent in the target quadrant was quantified. All values are means  $\pm$  SEM. Significance above the 25% chance level was determined using a one-sample t-test for each group. \* $p < 0.05$ , \*\*\* $p < 0.001$ ; ns = not significant. (D) Non-spatial memory of 24 WT, 18 APPPS1 and 21 APPPS1/HTT<sub>SA</sub> mice was assessed by the novel object recognition memory test. Memory index is calculated as the percentage of time spent exploring a novel object versus the time spent exploring both familiar and novel objects after a retention interval of 3 hr. All values are means  $\pm$  SEM. A score of 50% indicates no preference (i.e., no memory). Performance significantly above the 50% chance level was determined using a one-sample t-test for each group. \*\* $p < 0.01$ , \*\*\* $p < 0.001$ ; ns = not significant.

The online version of this article includes the following source data and figure supplement(s) for figure 9:

**Source data 1.** Statistical analysis of spatial learning of APPPS1/HTT<sub>SA</sub> mice.

**Source data 2.** Statistical analysis of cumulative CIPL.

**Source data 3.** Statistical analysis of spatial memory of APPPS1/HTT<sub>SA</sub> mice.

**Source data 4.** Statistical analysis of non spatial memory of APPPS1/HTT<sub>SA</sub> mice.

**Figure supplement 1.** Behavioral analyses of the locomotion and anxiety-related behavior in WT, APPPS1 and APPPS1/HTT<sub>SA</sub> mice.

**Figure supplement 1—source data 1.** Statistical analysis of the distance moved in an open field by APPPS1/HTT<sub>SA</sub> mice.

**Figure supplement 1—source data 2.** Statistical analysis of the time spent in the periphery of an open field by APPPS1/HTT<sub>SA</sub> mice.

trafficking. We then evaluated the consequences of HTT phosphorylation on brain morphology and function in both wild-type mice and in transgenic mice with AD-like neuropathology. We propose a model in which axonal transport of APP, APP presynaptic levels, and synapse homeostasis require an intact Akt-HTT pathway.

### HTT links APP axonal transport to presynaptic levels of APP

We find that axonal, but not dendritic, transport of APP is regulated by Akt-phosphorylated HTT. We previously showed that HTT phosphorylation at Serine 421 recruits kinesin-1 to the molecular motor complex and promotes anterograde transport of vesicles to the plus end of microtubules in axons (Colin *et al.*, 2008). Given the mixed polarity of microtubules in dendrites (Kapitein and Hoogenraad, 2015; Yau *et al.*, 2016), modifying HTT phosphorylation affects APP transport only in axons, where all the microtubules are oriented with the plus end towards the axon terminal. Our finding that the modulation of axonal transport of APP regulates synaptic APP homeostasis is in agreement with nerve ligation studies, which showed early on that blocking traffic from the entorhinal cortex to the dentate gyrus greatly reduced APP levels at the synapse (Koo *et al.*, 1990). Results obtained by pulse-chase labeling experiments and unilateral lesions of the perforant path, a circuit by which axons from the entorhinal cortex connect to the dentate gyrus, also accord with these results (Buxbaum *et al.*, 1998; Lazarov *et al.*, 2002). Moreover, studies investigating the composition of APP vesicles report that most proteins co-transported with APP are presynaptic (Kohli *et al.*, 2012; Szodorai *et al.*, 2009) and that APP colocalizes with presynaptic proteins at the presynaptic bouton (Groemer *et al.*, 2011). Notwithstanding the contribution of dendritic APP to synapse homeostasis (Niederst *et al.*, 2015), our results demonstrate that APP levels at presynaptic membranes rely on HTT-dependent axonal transport.

### HTT phosphorylation, APP presynaptic levels and synapse homeostasis

The absence of HTT phosphorylation reduced presynaptic levels of APP, restored synapse number and PSD length, and attenuated memory deficits in APPS1 mice. In contrast, there was no effect of the HTT S421A mutation on amyloid plaques, on different pools of A $\beta$  oligomers, or on extracellular and intracellular A $\beta$ 42 levels in brain, although the existence of a pool of vesicular presynaptic A $\beta$  has been recently reported (Yu *et al.*, 2018). These results suggest that HTT dephosphorylation regulates synapse homeostasis by modulating presynaptic APP levels rather than modulating APP-derived A $\beta$  production. Notwithstanding the synaptic toxicity of A $\beta$  peptides (Klementieva *et al.*, 2017; Mucke and Selkoe, 2012; Palop and Mucke, 2010; Selkoe and Hardy, 2016; Wei *et al.*, 2010), our findings dovetail nicely with previous results showing presynaptic APP contributes to synapse formation, function, and maintenance (Hoe *et al.*, 2012; Müller *et al.*, 2017; Nicolas and Hassan, 2014).

Our results are also in accord with reports that *App* knockout increases the number of functional synapses in vitro (Priller *et al.*, 2006) and augments synaptic density in vivo, as visualized by two-photon in vivo microscopy through a cranial window (Bittner *et al.*, 2009). Indeed, we found that reducing APP presynaptic levels by blocking HTT phosphorylation increases synapse density, and that this effect can be reversed by over-expressing APP in presynaptic neurons. Conversely, and again in agreement with previous studies (Alonso-Nanclares *et al.*, 2013; Bittner *et al.*, 2012; Priller *et al.*, 2009), we found that overexpressing APP and PS1 mutations in vivo reduced synaptic density, an effect that can be restored by HTT-mediated reduction of APP presynaptic levels, without having significant effects on A $\beta$  levels. Although the precise physiological function of APP at the synapse remains to be elucidated, changes in synapse homeostasis could be linked to the potential function of APP as an adhesion molecule that forms homo and/or heteromeric complexes with APP family members (Müller *et al.*, 2017; Soba *et al.*, 2005).

### Relevance to disease pathogenesis

Our identification of an Akt-HTT pathway that regulates APP and synapse homeostasis might be of relevance for AD pathophysiology. Post-mortem analyses of AD patient brains report increased levels of activated Akt in mid-temporal and mid-frontal cortex soluble fractions (Rickle *et al.*, 2004) as well as increased phosphorylation of Akt and of Akt substrates in membrane-bound fractions (Griffin *et al.*, 2005). Our finding that inhibiting Akt-mediated HTT phosphorylation reduces APP

presynaptic levels in APPS1 mice suggests that increased Akt activity might contribute to higher presynaptic APP levels in AD brains, leading to synapse loss and cognitive decline. Our findings may also relate to studies that show rescue of synaptic and behavioral deficits in AD mouse models by knocking down the IGF-1 receptor and inhibiting the phosphoinositide three kinase (PI3K), which are upstream of Akt-htt (Cohen et al., 2009; Humbert et al., 2002; Martínez-Mármol et al., 2019). Prior to this study, the JNK-interacting protein 1 (JIP1) was identified as a scaffold for APP (Muresan and Muresan, 2005). JIP1 determines the directionality of APP trafficking through its phosphorylation at a JNK-dependent phosphorylation site (Fu and Holzbaur, 2013) and could regulate amyloid-independent mechanisms of AD pathogenesis (Margevicius et al., 2015). This study and ours highlight the complexity of the regulation of APP trafficking in neurons, with different kinases (JNK and Akt) responding to specific signaling pathways.

Defects in APP trafficking could also contribute to synaptic defects observed in HD, as we found that the Akt-htt pathway is down-regulated in HD patient brain samples and lymphoblasts as well as in HD rodent models (Colin et al., 2005; Humbert et al., 2002). Several studies have reported a notable reduction in the number of synapses particularly within the corticostriatal circuit, which is the most profoundly affected in HD (Virlogeux et al., 2018). A better understanding of htt-APP relationship could help unravel mechanisms of interest for both Huntington's disease and Alzheimer's disease.

### Contact for reagent and resource sharing

Further information and requests for resources and reagents should be directed to and will be fulfilled by the Lead Contact, Frédéric Saudou (Frederic.saudou@inserm.fr).

## Materials and methods

### Mice

The APP<sup>swe</sup>;PS1L166P (Tg Thy1-APP<sup>KM670/671 NL</sup>;Thy1-PS1L166P referred as APPS1) mouse strain (#21; C57Bl6/J background) was obtained from Dr. M. Jucker's laboratory (Radde et al., 2006). Heterozygous *Htt*<sup>S421A/+</sup> Knock-In mice (C57Bl6/J background) were generated at the Mouse Clinical Institute (Strasbourg, France) by introduction of a point mutation into Exon 9 (AGC >GCC, Ser >Ala) or (AGC >GAC, Ser >Asp) concomitant with introduction of repeated regions LoxP<sub>Neo</sub>-LoxP in intron nine for genotyping and a FseI restriction site in intron eight for cloning purpose. Homozygous *Htt*<sup>S421A/S421A</sup> Knock-In mice (HTT<sub>SA</sub>) were generated and did not show obvious phenotype as shown previously (Thion et al., 2015) and in this study. Transgenic APPS1 mice in a *Htt*<sup>S421A/S421A</sup> (HTT<sub>SA</sub>) genetic background mice were obtained by crossing homozygous *Htt*<sup>S421A/S421A</sup> mice with transgenic APPS1 mice thus generating APPS1;*Htt*<sup>S421A/+</sup> mice that were crossed with heterozygous *Htt*<sup>S421A/+</sup> mice to obtain APPS1;*Htt*<sup>S421A/S421A</sup> mice, heretofore referred to as APPS1/HTT<sub>SA</sub> mice. WT mice used for backcrossing and mouse amplification are C57Bl6/J mice from Charles River Laboratories (L'Arbresle, France). WT mice used for behavioral and biochemical experiments are littermates of APPS1/HTT<sub>SA</sub> and, of HTT<sub>SA</sub> and APPS1 mice respectively.

The general health of the mice was regularly checked and body weights were assessed weekly throughout the experimental period. Animals were held in accordance with the French Animal Welfare Act and the EU legislation (Council Directive 86/609/EEC) and the ARRIVE (Animal Research: Reporting of In Vivo Experiments) guidelines. The French Ministry of Agriculture and the local ethics committee gave specific authorization (authorization no. 04594.02) to BD to conduct the experiments described in the present study.

To evaluate the effects of HTT<sub>SA</sub> mutation on a WT background, a total of 23 mice were used. To evaluate the effects of HTT<sub>SA</sub> mutation on an APPS1 transgenic background, a total of 84 mice were used. Only male mice were studied, to avoid any potential effects of the estrus cycle on behavioral responses. Behavioral phenotypes were analyzed between 12 and 15 months of age, a time at which behavioral defects are observed in APPS1 mice (Radde et al., 2006).

### Behavioral and cognitive evaluation

The behavioral testing battery consisted of: primary modified SHIRPA screen (Rogers et al., 1997), open field, elevated plus maze, novel object recognition, Morris water maze, and grip strength tests.



All tests were performed during light phases of the diurnal cycle. Mice were group housed (4–6/ cage) and had free access to food and water except during experiments. They were transported to the behavioral testing room and allowed to acclimate for at least 1 hr prior to initiating experiments.

### Novel object recognition test (NOR)

The object recognition test is based on the natural tendency of rodents to spend more time investigating a novel object than a familiar one (*Ennaceur and Delacour, 1988*). The choice to explore the novel object reflects the use of recognition memory. Our protocol is similar to that previously described (*Scholtzova et al., 2009*). The object recognition test was carried out in an illuminated (30 lux) square gray PVC open field box (50 cm x 50 cm x 30 cm). The test consists of a familiarization session of 15 min in which mice explored the open field arena containing two identical, symmetrically placed objects (A1 and A2). The following day, a training session of 15 min was run with two novel identical objects (B1 and B2). Retention was tested 3 hr after the training session to evaluate object memory. During the retention trial, mice were exposed to a third exemplar of the familiar object (B3) and to a novel object (C1) for 10 min. Behavioral monitoring was done with ANY-maze (Stoelting, USA). The results were expressed as a recognition index, defined as percentage of the time spent exploring the new object over the total time exploring the two objects. Experiments with animals whose exploration was not considered sufficient to allow recognition (less than 6 s of exploration time during training and retention sessions) were discarded from analysis.

### Morris water maze test (MWM)

Spatial learning capacity was tested in the standard hidden-platform Morris water maze (MWM). The maze consisted of a large circular pool (diameter 150 cm) filled with water to a depth of 35 cm. The MWM protocol was adapted from a previous description (*Lo et al., 2013*). Briefly, mice were trained for 11 days to find a hidden platform (10 cm diameter) set at 1 cm beneath the surface of the water at a fixed position in a selected, constant quadrant. The water was opacified with non-toxic white paint (ACUSOL, Brenntag, Belgium) to prevent animals from seeing the platform. The water temperature was maintained at 25–26°C with four thermostatically controlled heaters (Askoll Therm XL 200W, Truffaut, France). The pool was situated at the center of a brightly lit room (~320 lux) with various fixed posters and visual cues placed on the walls to act as distal landmarks. There were four trials per training day with an inter-trial interval of 30 min. The mice were released into water at semi-randomly chosen cardinal compass points (N, E, S, and W). Mice failing to reach the platform within 90 s were gently guided to the platform and were left on it for 15 s, before being dried and returned to their home cages. Two days of rest were given after the 5th and 10th day of training. On the 11th day of training (i.e.: 72 hr after last training session), a probe trial was performed to evaluate robustness of spatial memory. During the probe trial, the platform was removed and mice were released into the pool from the side diagonally opposite to where the platform was located and allowed to swim freely for 90 s.

During all testing phases, a video camera was positioned above the pool for trial recording and the ANY-maze videotracking software was used. Rather than measuring latency or distance traveled, which could be biased by variations in swim speeds and path tortuosity, we analyzed the Corrected Integrated Path Length (CIPL) (*Gallagher et al., 1993*) to assess learning during the 11 training days. During the probe test the percent of time spent in each quadrant was assessed.

### Antibodies, plasmids and lentiviruses

Antibodies used are anti-: HTT (clone D7F7, Cell Signaling; 5656), pHTT-S421 pAb 3517 (*Colin et al., 2008*), GFP (for western blotting, Institut Curie, A-P-R#06), SNAP25 (AbCam, sb24737), Synaptophysin (Cell Signaling; s5768), PSD95 (Millipore; mab1598), p38 (AbCam, ab14692), APP (clone 22C11, Millipore; mab348), Lamin B1 (AbCam; ab133741), KHC (clone SUK4, Covance; MMS-188P), p-150 (BD Transduction Laboratories, 610474), MAP-2 (Millipore; AB5622), GFP (for immunofluorescence experiments, AbCam; Ab13970), HA (clone 6E2, Cell Signaling, mAb#2367), Tubulin (Sigma; t9026) and GAPDH (Sigma; G9545).

APP-mCherry (*Marquer et al., 2014*) plasmid was cloned into pSIN lentiviral vector (*Drouet et al., 2009*) by Gateway system (Life Technology) using sense primer 5'-GGGGACAAGTTGTACAAAAAAGCAGGCTTCAATTCTGCAGTCGACGG-3' and anti-sense primer 5'-

GGGGACCACTTTGTACAAGAAAGCTGGGTGCGGCCGCCCTACTTGTACA-3' and recombination. We verified whether APP-mCherry is cleaved in neuronal culture by endogenous secretases but did not find aberrant cleavage of APP in our experimental conditions indicating that most of the APP-containing vesicles correspond to full length APP (data not shown). Plasmids coding for pHRIG-Akt1 (Akt-CA) and pHRIG-AktDN (Akt-N) were gifts from Heng Zhao (Addgene plasmids # 53583 and 53597 respectively). MAP2-GFP was previously described (Liot *et al.*, 2013). Lentiviruses encoding the first 480 amino acids of HTT with 17Q and with the S421A mutation have been previously described (Pardo *et al.*, 2006). Plasmid coding for GFP lentivector was a gift from Dr J. M. Heard. Lentivectors were produced by the ENS Lyon Vectorology Facility with titer higher than  $10^8$  UI/ml.

### Vesicular transport imaging into microchambers

Cortical neurons were isolated from mouse embryos (E15.5) according to Liot *et al.*, 2013. Neurons were seeded on 12-well plate coated with poly-L-lysine (1 mg/ml) or into microchambers coated with poly-D-lysine (0.1 mg/ml; presynaptic and synaptic compartments) or poly-D-lysine and laminin 10  $\mu$ g/ml (Sigma; postsynaptic compartment) and cultured at 37°C in a 5% CO<sub>2</sub> incubator for 13 days. For dendritic trafficking, mouse neurons were transfected before plating with 5  $\mu$ g of MAP2-GFP plasmid using a Nucleofector (Lonza) according to the manufacturer's specifications. After 8 days in vitro (DIV8), neurons were transduced as previously described (Bruyère *et al.*, 2015) into presynaptic neuron chamber for axonal transport analysis or into the postsynaptic neuron chamber for the dendritic transport analysis. Acquisitions were done at DIV13 on microgrooves, at the limit of the synaptic compartment, at 5 Hz for 1 min on inverted microscope (Axio Observer, Zeiss) coupled to a spinning-disk confocal system (CSU-W1-T3; Yokogawa) connected to an electron-multiplying CCD (charge-coupled device) camera (ProEM+1024, Princeton Instrument) at 37°C and 5% CO<sub>2</sub>. Vesicle velocity, directional net flux and vesicle number were measured on 100  $\mu$ m of neurite using KymoTool Box ImageJ plugin as previously described (Virlogeux *et al.*, 2018). Vesicle velocity corresponds to segmental anterograde or retrograde velocity. Directional net flux is the anterograde cumulative distance minus the retrograde cumulative distance. Regarding vesicle number, a vesicle is considered anterograde when the distance travelled by one vesicle is more anterograde than retrograde.

### Detection of active synapses

Neurons were seeded into microfluidic devices and transduced at DIV1 with GFP lentivirus. The synaptic chamber was incubated at indicated time with 10  $\mu$ M of FM4-64 styryl dye (ThermoFischer Scientific) into high KCl Tyrode solution (2 mM NaCl; 50 mM KCl; 2 mM CaCl<sub>2</sub>; 1 mM MgCl<sub>2</sub>; 10 mM Glucose and 1 mM Hepes buffer pH7.4) during 1 min at 37°C. After three washes with Tyrode solution (150 mM NaCl; 4 mM KCl; 2 mM CaCl<sub>2</sub>; 1 mM MgCl<sub>2</sub>; 10 mM Glucose and 1 mM Hepes buffer pH7.4) containing inhibitors of additional firing (1 mM kynurenic acid and 10 mM MgCl<sub>2</sub>), acquisitions were made on inverted microscope (Axio Observer, Zeiss) coupled to a spinning-disk confocal system (CSU-W1-T3; Yokogawa) connected to an electron-multiplying CCD (charge-coupled device) camera (ProEM+1024, Princeton Instrument) at 37°C and 5% CO<sub>2</sub> with z stacks of 5  $\mu$ m.

### Quantification of exocytosis rate

COS-1 cells were plated at low density on glass coverslips and transfected with APP-SEP (super ecliptic pHluorin) and with pARIS HTT or pARIS HTT<sub>SA</sub> (Pardo *et al.*, 2010) using calcium phosphate. Acquisitions were made the day after transfection at 5 Hz during 1 min using an inverted microscope (Eclipse Ti, Nikon) with a X60 1.42 NA APO TIRF oil-immersion objective (Nikon) coupled to a CCD camera (CoolSnap, Photometrics) and maintained at 37°C and 5% CO<sub>2</sub>. Analysis was done on area delimited by cell edges and exocytosis rate was quantified using ExocytosisAnalyser macro on ImageJ developed by Marine Scoazec.

### Quantification of APP in the synaptic chamber

Thirteen days after plating, media from synaptic or presynaptic compartments of 9 microchambres per condition were removed. Lysis buffer containing 4 mM Hepes, pH 7.4, 320 mM sucrose and protease inhibitor cocktail (Roche) mixed with 1X Laemmli buffer was added on synaptic and

presynaptic compartments during 30 min. Harvested media containing lysed neurites and synapses were analyzed on western blot.

### Fractionation of Synaptosomes, PSD and non-PSD fractions

Synaptosome purification was performed as previously described (Frändemiché *et al.*, 2014). Cortex was homogenized in cold buffer containing 4 mM HEPES, pH 7.4, 320 mM sucrose and protease inhibitor cocktail (Roche). Homogenates were cleared at 1000 g for 10 min to remove nuclei and large debris. The resulting supernatants were concentrated at 12,000 g for 20 min to obtain a crude membrane fraction, which was then resuspended twice (4 mM HEPES, 1 mM EDTA, pH 7.4, 20 min at 12,000 g). Then, the pellet was incubated (20 mM HEPES, 100 mM NaCl, 0.5% Triton X-100, pH 7.2) for 1 hr at 4°C with mild agitation and centrifuged at 12,000 g for 20 min to pellet the synaptosomal membrane fraction. The supernatant was collected as the non-postsynaptic density membrane fraction (non-PSD) or Triton-soluble fraction. The pellet was then solubilized (20 mM HEPES, 0.15 mM NaCl, 1% Triton X-100, 1% deoxycholic acid, 1% SDS, pH 7.5) for 1 hr at 4°C and centrifuged 15 min at 10,000 g. The supernatant contained the PSD or Triton-insoluble fraction. The non-PSD integrity was checked by synaptophysin immunoblotting and the PSD fraction was confirmed by the PSD-95 immunoblotting enriched in this compartment.

### Synapse analysis by electron microscopy

Mice were anesthetized at 19 months of age with pentobarbital (120 mg/kg) and then transcardially perfused with phosphate-buffered saline solution. Hippocampi were dissected and fixed with 2% glutaraldehyde and 2% paraformaldehyde in 0.1 M phosphate buffer pH 7.2 during 48 hr at 4°C; the CA1 area was dissected under the binocular and further fixed during 72 hr in the same solution. Samples were then washed with buffer and post-fixed with 1% Osmium tetroxide and 0.1 M phosphate buffer pH 7.2 during 1 hr at 4°C. After extensive washing with water, cells were further stained with 1% uranyl acetate pH four in water during 1 hr at 4°C before being dehydrated through graded ethanol (30%–60%–90%–100%–100%–100%) and infiltrate with a mix of 1/1 epon/alcohol 100% during 1 hr and several bath of fresh epon (Flukka) during 3 hr. Finally, samples were included in a capsule full of resin that was let to polymerize during 72 hr at 60°C. Ultrathin sections of the samples were cut with an ultramicrotome (Leica), sections were post-stained with 5% uranyl acetate and 0.4% lead citrate before being observed with a transmission electron microscope at 80 kV (JEOL 1200EX). Images were acquired with a digital camera (Veleta, SIS, Olympus) and morphometric analysis was performed with iTEM software (Olympus). Quantification of synaptic density was done on axon-free neuropil regions (Zhang *et al.*, 2015).

### Immunostaining into microchambers

Neurons within microchambers were fixed with a PFA/Sucrose solution (4%/4% in PBS) for 20 min at room temperature (RT). The fixation buffer was rinsed three times with PBS and neurons were incubated for 1 hr at RT with a blocking solution (BSA 1%, normal goat serum 2%, Triton X-100 0.1%). For PSD95 and synaptophysin immunofluorescence, the synaptic compartment was then incubated overnight at 4°C with primary antibodies PSD95 (Millipore, #MAB1598, 1:1,000) and Synaptophysin (Abcam, #AB14692, 1:200). For GFP and MAP-2 immunofluorescence, all compartments were incubated with primary antibodies against MAP-2 (Millipore; AB5622) and GFP (AbCam; Ab13970). After washing with PBS, appropriate fluorescent secondary antibodies were incubated for 1 hr at RT. The immunofluorescence was maintained in PBS for a maximum of one week in the dark at 4°C. Immunostainings were acquired with a X63 oil-immersion objective (1.4 NA) using an inverted confocal microscope (LSM 710, Zeiss) coupled to an Airyscan detector to improve signal-to-noise ratio and to increase resolution. Juxtaposition analyses were performed using ImageJ. Airyscan images were thresholded to remove non-specific signal and an area of interest of at least 100  $\mu\text{m}$  in length was defined around neurites. The number of synaptophysin spots overlapping, juxtaposed or separated by no more than two pixels (130 nm) to PSD95 spots were counted manually. Results were expressed as a function of neurite length and were normalized to 100  $\mu\text{m}$  and WT condition. Each condition was tested using at least two chambers per culture from at least two independent cultures. In each chamber, three fields were analyzed in which at least 3 regions of interest were selected ( $n$  = number of fields).

## MRI analyses

### Brain preparation for ex vivo MRI acquisitions

Skulls were processed as described in *Pagnamenta et al., 2019*. Briefly, four male mice of each genotype aged between 8 and 11 weeks were transcardially perfused with 4% paraformaldehyde solution in phosphate buffered saline containing 6.25 mM of Gd-DOTA (Guerbet Laboratories, Roissy, France). This contrast agent is added to reduce the MRI acquisition time. Skin and head muscles were removed to expose the skull, which was then immersed in the fixing solution for 4 days. The skull was then transferred to a Fomblin (FenS chemicals, Goes, Netherlands) bath for at least 7 days for the distribution of Gd-DOTA to be homogeneous throughout the whole brain.

### MRI acquisitions

Ex vivo 3D MRI acquisitions were performed as described in *Pagnamenta et al., 2019*. Briefly, skulls were put in a 9.4 T MRI (Bruker Biospec Avance III; IRMaGe facility) and a volume coil for transmission and a head surface cryocoil for reception were used.

To quantify brain volume, the brain was segmented with a 3D T<sub>1W</sub> gradient-echo MRI sequence (repetition time: 35.2 ms, echo time: 8.5 ms, flip angle: 20 degrees, field of view: 12 × 9 × 18.1 mm<sup>3</sup>, isotropic spatial resolution: 50 μm, four signal accumulations, total acquisition time per brain: 2 hr 32 min).

### Quantitative analysis of brain volumes

Quantitative analysis of brain volume was performed as described in *Pagnamenta et al., 2019*. Briefly, from 3D T<sub>1W</sub> gradient-echo MRI images, brain structures were delimited manually with the help of Allen mouse brain atlas (<http://atlas.brain-map.org/atlas>) every five slices by defining regions of interest (ROIs) on the coronal orientation using Fiji software. Then, interpolation was applied using the segmentation editor plug-in ([http://fiji.sc/Segmentation\\_Editor](http://fiji.sc/Segmentation_Editor)) for the brain structures (total brain, cortex, hippocampus and striatum) to be reconstructed. A color was attributed to each structure and its 3D reconstruction and volume were determined using the Voxel counter plug-in in the Fiji software ([https://imagej.net/3D\\_Viewer](https://imagej.net/3D_Viewer)). Volume was calculated as following: number of voxels × voxel volume. All segmentations were done blind to the genotype. Mann and Whitney test was used for comparison.

## Statistical analyses

All cellular biology experiments were repeated in at least in three different batches of cultures. Normality of data distribution was verified by graphical analysis of the data distribution and residues. For data with assumed normal distribution, groups were compared by parametric tests followed by post hoc analyses for multiple comparisons. Non-parametric tests were used for western blot analyses and Aβ dosages. \*p<0.05; \*\*p<0.01; \*\*\*p<0.001; \*\*\*\*p<0.0001; ns, not significant. Statistical calculations were performed using GraphPad Prism 6.0.

## Acknowledgements

We thank Luc Buée, Alain Buisson, Bassem Hassan, Subhojit Roy, Rémy Sadoul, and members of the Saudou, Humbert and Potier labs for comments; Vicky Brandt for critical reading; Caroline Benstaali, Anne Bertrand, Camille Brochier, Aurélie Genoux, Félicie Lorenc, Jessica Roland, Chiara Scaramuzino, Marine Scoazec and Gisela Zalcmann for technical help and/or initial experiments; Daniel Choquet for the gift of Super-Ecliptic-pHluorin-APP plasmid, Y Saoudi and the GIN imaging facility (PICGIN) for help with image acquisitions; G Froment, D Nègre, and C Costa from SFR Biosciences (UMS3444/CNRS, US8/Inserm, ENS de Lyon, UCBL) for lentivirus production; Emmanuel Barbier and Olivier Montigon (UMS 3552/US17 IRMaGe) for MRI acquisitions; the technical staff of the PHENO-PARC platform and the HISTOMICS platform of the ICM for behavioral and histological studies. This work was supported by grants from Agence Nationale de la Recherche: ANR-12-MALZ-0004 HuntA-beta, FS and MCP; ANR-14-CE35-0027-01 PASSAGE, FS; ANR-15-IDEX-02 NeuroCoG (FS) and ANR-10-IAIHU-06 (MCP) in the framework of the 'Investissements d'avenir' program), Fondation pour la Recherche Médicale (FRM, DEI20151234418, FS; DEQ20170336752, SH), Fondation pour la Recherche sur le Cerveau (FRC)(FS), Fondation Bettencourt Schueller (FS) and AGEMED program

from INSERM (FS and SH). IRMaGe is partly funded by 'Investissements d'Avenir' run by the French National Research Agency, grant 'Infrastructure d'avenir en Biologie Santé' (ANR-11-INBS-0006). FS laboratory is member of the Grenoble Center of Excellence in Neurodegeneration (GREEN). HV was supported by a PhD fellowship from Association Huntington France and by a FRM fellowship (FDT201904008035)

## Additional information

### Funding

Funder	Grant reference number	Author
Agence Nationale de la Recherche	ANR-12-MALZ-0004 HuntAbeta	Marie-Claude Potier Frédéric Saudou
Fondation pour la Recherche Médicale	DEI20151234418	Frédéric Saudou
Fondation pour la Recherche sur le Cerveau		Frédéric Saudou
Inserm	AGEMED	Sandrine Humbert Frédéric Saudou
Fondation Bettencourt Schueller		Frédéric Saudou
Association Huntington France		Hélène Vitet
Agence Nationale de la Recherche	ANR-14-CE35-0027-01 PASSAGE	Frédéric Saudou
Agence Nationale de la Recherche	ANR-15-IDEX-02 NeuroCoG	Frédéric Saudou
Agence Nationale de la Recherche	ANR-10-IAIHU-06	Marie-Claude Potier
Fondation pour la Recherche Médicale	DEQ20170336752	Sandrine Humbert
Fondation pour la Recherche Médicale	FDT201904008035	Hélène Vitet

The funders had no role in study design, data collection and interpretation, or the decision to submit the work for publication.

### Author contributions

Julie Bruyère, Conceptualization, Formal analysis, Investigation, Visualization, Methodology, Writing - original draft, Writing - review and editing; Yah-Se Abada, Formal analysis, Investigation, Visualization, Methodology, Writing - original draft, Writing - review and editing; Hélène Vitet, Formal analysis, Investigation, Visualization, Methodology, Writing - review and editing; Gaëlle Fontaine, Aurélia Cès, Investigation, Acquisition of data, or analysis and interpretation of data, Final approval of the version to be published; Jean-Christophe Deloulme, Formal analysis, Investigation, Visualization, Methodology; Eric Denarier, Formal analysis, Methodology; Karin Pernet-Gallay, Formal analysis, Investigation, Visualization; Annie Andrieux, Supervision, Writing - review and editing; Sandrine Humbert, Conceptualization, Supervision, Methodology, Writing - review and editing; Marie-Claude Potier, Conceptualization, Supervision, Funding acquisition, Methodology, Writing - original draft, Writing - review and editing; Benoît Delatour, Conceptualization, Supervision, Visualization, Methodology, Writing - original draft, Writing - review and editing; Frédéric Saudou, Conceptualization, Supervision, Funding acquisition, Visualization, Methodology, Writing - original draft, Project administration, Writing - review and editing

### Author ORCIDs

Hélène Vitet  <https://orcid.org/0000-0003-2899-1064>

Jean-Christophe Deloulme  <http://orcid.org/0000-0002-2234-5865>

Eric Denarier  <http://orcid.org/0000-0002-4169-397X>  
 Annie Andrieux  <http://orcid.org/0000-0002-4022-6405>  
 Sandrine Humbert  <https://orcid.org/0000-0002-9501-2658>  
 Frédéric Saudou  <https://orcid.org/0000-0001-6107-1046>

### Ethics

Animal experimentation: Animals were held in accordance with the French Animal Welfare Act and the EU legislation (Council Directive 86/609/EEC) and the ARRIVE (Animal Research: Reporting of In Vivo Experiments) guidelines. The French Ministry of Agriculture and the local ethics committee gave specific authorization (authorization no. 04594.02) to BD to conduct the experiments described in the present study.

### Decision letter and Author response

Decision letter <https://doi.org/10.7554/eLife.56371.sa1>

Author response <https://doi.org/10.7554/eLife.56371.sa2>

## Additional files

### Supplementary files

- Supplementary file 1. The modified SHIRPA primary screen in WT and  $HTT_{S\Delta}$  mice. Results are presented in percentages unless otherwise indicated. No significant differences between genotypes were observed.
- Transparent reporting form

### Data availability

All data generated or analysed during this study are included in the manuscript and supporting files.

## References

- Alonso-Nanclares L, Merino-Serrais P, Gonzalez S, DeFelipe J. 2013. Synaptic changes in the dentate gyrus of APP/PS1 transgenic mice revealed by electron microscopy. *Journal of Neuropathology & Experimental Neurology* **72**:386–395. DOI: <https://doi.org/10.1097/NEN.0b013e31828d41ec>, PMID: 23584198
- Androuin A, Potier B, Nägerl UV, Cattaert D, Danglot L, Thierry M, Youssef I, Triller A, Duyckaerts C, El Hachimi KH, Dutar P, Delatour B, Marty S. 2018. Evidence for altered dendritic spine compartmentalization in Alzheimer's disease and functional effects in a mouse model. *Acta Neuropathologica* **135**:839–854. DOI: <https://doi.org/10.1007/s00401-018-1847-6>, PMID: 29696365
- Bittner T, Fuhrmann M, Burgold S, Jung CK, Volbracht C, Steiner H, Mitteregger G, Kretschmar HA, Haass C, Herms J. 2009. Gamma-secretase inhibition reduces spine density in vivo via an amyloid precursor protein-dependent pathway. *Journal of Neuroscience* **29**:10405–10409. DOI: <https://doi.org/10.1523/JNEUROSCI.2288-09.2009>, PMID: 19692615
- Bittner T, Burgold S, Dorostkar MM, Fuhrmann M, Wegenast-Braun BM, Schmidt B, Kretschmar H, Herms J. 2012. Amyloid plaque formation precedes dendritic spine loss. *Acta Neuropathologica* **124**:797–807. DOI: <https://doi.org/10.1007/s00401-012-1047-8>, PMID: 22993126
- Brunholz S, Sisodia S, Lorenzo A, Deyts C, Kins S, Morfini G. 2012. Axonal transport of APP and the spatial regulation of APP cleavage and function in neuronal cells. *Experimental Brain Research* **217**:353–364. DOI: <https://doi.org/10.1007/s00221-011-2870-1>, PMID: 21960299
- Bruyère J, Roy E, Ausseil J, Lemonnier T, Teyre G, Bohl D, Etienne-Manneville S, Lortat-Jacob H, Heard JM, Vitry S. 2015. Heparan sulfate saccharides modify focal adhesions: implication in mucopolysaccharidosis neuropathophysiology. *Journal of Molecular Biology* **427**:775–791. DOI: <https://doi.org/10.1016/j.jmb.2014.09.012>, PMID: 25268803
- Buggia-Prévot V, Fernandez CG, Riordan S, Vetrivel KS, Roseman J, Waters J, Bindokas VP, Vassar R, Thinakaran G. 2014. Axonal BACE1 dynamics and targeting in hippocampal neurons: a role for Rab11 GTPase. *Molecular Neurodegeneration* **9**:1. DOI: <https://doi.org/10.1186/1750-1326-9-1>, PMID: 24386896
- Buxbaum JD, Thinakaran G, Koliatsos V, O'Callahan J, Slunt HH, Price DL, Sisodia SS. 1998. Alzheimer amyloid protein precursor in the rat Hippocampus: transport and processing through the perforant path. *The Journal of Neuroscience* **18**:9629–9637. DOI: <https://doi.org/10.1523/JNEUROSCI.18-23-09629.1998>, PMID: 9822724

- Cohen E, Paulsson JF, Blinder P, Burstyn-Cohen T, Du D, Estepa G, Adame A, Pham HM, Holzenberger M, Kelly JW, Masliah E, Dillin A. 2009. Reduced IGF-1 signaling delays age-associated proteotoxicity in mice. *Cell* **139**: 1157–1169. DOI: <https://doi.org/10.1016/j.cell.2009.11.014>, PMID: 20005808
- Colin E, Régulier E, Perrin V, Dürr A, Brice A, Aebischer P, Déglon N, Humbert S, Saudou F. 2005. Akt is altered in an animal model of Huntington's disease and in patients. *European Journal of Neuroscience* **21**:1478–1488. DOI: <https://doi.org/10.1111/j.1460-9568.2005.03985.x>, PMID: 15845076
- Colin E, Zala D, Liot G, Rangone H, Borrell-Pagès M, Li XJ, Saudou F, Humbert S. 2008. Huntingtin phosphorylation acts as a molecular switch for anterograde/retrograde transport in neurons. *The EMBO Journal* **27**:2124–2134. DOI: <https://doi.org/10.1038/emboj.2008.133>, PMID: 18615096
- Das U, Wang L, Ganguly A, Saikia JM, Wagner SL, Koo EH, Roy S. 2016. Visualizing APP and BACE-1 approximation in neurons yields insight into the amyloidogenic pathway. *Nature Neuroscience* **19**:55–64. DOI: <https://doi.org/10.1038/nn.4188>, PMID: 26642089
- Drouet V, Perrin V, Hassig R, Dufour N, Auregan G, Alves S, Bonvento G, Brouillet E, Luthi-Carter R, Hantraye P, Déglon N. 2009. Sustained effects of nonallele-specific huntingtin silencing. *Annals of Neurology* **65**:276–285. DOI: <https://doi.org/10.1002/ana.21569>, PMID: 19334076
- Ehinger Y, Bruyère J, Panayotis N, Abada YS, Borloz E, Matagne V, Scaramuzzino C, Vitet H, Delatour B, Saidi L, Villard L, Saudou F, Roux JC. 2020. Huntingtin phosphorylation governs BDNF homeostasis and improves the phenotype of *Mecp2* knockout mice. *EMBO Molecular Medicine* **12**:e10889. DOI: <https://doi.org/10.15252/emmm.201910889>, PMID: 31913581
- Ennaceur A, Delacour J. 1988. A new one-trial test for neurobiological studies of memory in rats. 1: behavioral data. *Behavioural Brain Research* **31**:47–59. DOI: [https://doi.org/10.1016/0166-4328\(88\)90157-X](https://doi.org/10.1016/0166-4328(88)90157-X), PMID: 3228475
- Fanutza T, Del Prete D, Ford MJ, Castillo PE, D'Adamo L. 2015. APP and APLP2 interact with the synaptic release machinery and facilitate transmitter release at hippocampal synapses. *eLife* **4**:e09743. DOI: <https://doi.org/10.7554/eLife.09743>, PMID: 26551565
- Frändemichle ML, De Seranno S, Rush T, Borel E, Elie A, Arnal I, Lanté F, Buisson A. 2014. Activity-dependent tau protein translocation to excitatory synapse is disrupted by exposure to amyloid-beta oligomers. *Journal of Neuroscience* **34**:6084–6097. DOI: <https://doi.org/10.1523/JNEUROSCI.4261-13.2014>, PMID: 24760868
- Fu MM, Holzbaur EL. 2013. JIP1 regulates the directionality of APP axonal transport by coordinating kinesin and dynein motors. *The Journal of Cell Biology* **202**:495–508. DOI: <https://doi.org/10.1083/jcb.201302078>, PMID: 23897889
- Gallagher M, Burwell R, Burchinal M. 1993. Severity of spatial learning impairment in aging: development of a learning index for performance in the morris water maze. *Behavioral Neuroscience* **107**:618–626. DOI: <https://doi.org/10.1037/0735-7044.107.4.618>, PMID: 8397866
- Gibbs KL, Greensmith L, Schiavo G. 2015. Regulation of axonal transport by protein kinases. *Trends in Biochemical Sciences* **40**:597–610. DOI: <https://doi.org/10.1016/j.tibs.2015.08.003>, PMID: 26410600
- Griffin RJ, Moloney A, Kelliher M, Johnston JA, Ravid R, Dockery P, O'Connor R, O'Neill C. 2005. Activation of Akt/PKB, increased phosphorylation of Akt substrates and loss and altered distribution of Akt and PTEN are features of Alzheimer's disease pathology. *Journal of Neurochemistry* **93**:105–117. DOI: <https://doi.org/10.1111/j.1471-4159.2004.02949.x>, PMID: 15773910
- Groemer TW, Thiel CS, Holt M, Riedel D, Hua Y, Hüve J, Wilhelm BG, Klingauf J. 2011. Amyloid precursor protein is trafficked and secreted via synaptic vesicles. *PLOS ONE* **6**:e18754. DOI: <https://doi.org/10.1371/journal.pone.0018754>, PMID: 21556148
- Her LS, Goldstein LS. 2008. Enhanced sensitivity of striatal neurons to axonal transport defects induced by mutant huntingtin. *Journal of Neuroscience* **28**:13662–13672. DOI: <https://doi.org/10.1523/JNEUROSCI.4144-08.2008>, PMID: 19074039
- Hoe HS, Lee HK, Pak DT. 2012. The upside of APP at synapses. *CNS Neuroscience & Therapeutics* **18**:47–56. DOI: <https://doi.org/10.1111/j.1755-5949.2010.00221.x>, PMID: 21199446
- Humbert S, Bryson EA, Cordelières FP, Connors NC, Datta SR, Finkbeiner S, Greenberg ME, Saudou F. 2002. The IGF-1/Akt pathway is neuroprotective in Huntington's disease and involves Huntingtin phosphorylation by Akt. *Developmental Cell* **2**:831–837. DOI: [https://doi.org/10.1016/S1534-5807\(02\)00188-0](https://doi.org/10.1016/S1534-5807(02)00188-0), PMID: 12062094
- Kaether C, Skehel P, Dotti CG. 2000. Axonal membrane proteins are transported in distinct carriers: a two-color video microscopy study in cultured hippocampal neurons. *Molecular Biology of the Cell* **11**:1213–1224. DOI: <https://doi.org/10.1091/mbc.11.4.1213>, PMID: 10749925
- Kapitein LC, Hoogenraad CC. 2015. Building the neuronal microtubule cytoskeleton. *Neuron* **87**:492–506. DOI: <https://doi.org/10.1016/j.neuron.2015.05.046>, PMID: 26247859
- Kayed R, Head E, Sarsoza F, Saing T, Cotman CW, Neula M, Margol L, Wu J, Breydo L, Thompson JL, Rasool S, Gurlo T, Butler P, Glabe CG. 2007. Fibril specific, conformation dependent antibodies recognize a generic epitope common to amyloid fibrils and fibrillar oligomers that is absent in prefibrillar oligomers. *Molecular Neurodegeneration* **2**:18. DOI: <https://doi.org/10.1186/1750-1326-2-18>, PMID: 17897471
- Klementieva O, Willén K, Martinsson I, Israelsson B, Engdahl A, Cladera J, Uvdal P, Gouras GK. 2017. Pre-plaque conformational changes in Alzheimer's disease-linked A $\beta$  and APP. *Nature Communications* **8**:14726. DOI: <https://doi.org/10.1038/ncomms14726>, PMID: 28287086
- Klevanski M, Herrmann U, Weyer SW, Fol R, Cartier N, Wolfer DP, Caldwell JH, Korte M, Müller UC. 2015. The APP intracellular domain is required for normal synaptic morphology, synaptic plasticity, and Hippocampus-Dependent behavior. *Journal of Neuroscience* **35**:16018–16033. DOI: <https://doi.org/10.1523/JNEUROSCI.2009-15.2015>, PMID: 26658856

- Koffie RM, Meyer-Luehmann M, Hashimoto T, Adams KW, Mielke ML, Garcia-Alloza M, Micheva KD, Smith SJ, Kim ML, Lee VM, Hyman BT, Spires-Jones TL. 2009. Oligomeric amyloid beta associates with postsynaptic densities and correlates with excitatory synapse loss near senile plaques. *PNAS* **106**:4012–4017. DOI: <https://doi.org/10.1073/pnas.0811698106>, PMID: 19228947
- Kohli BM, Pflieger D, Mueller LN, Carbonetti G, Aebbersold R, Nitsch RM, Konietzko U. 2012. Interactome of the amyloid precursor protein APP in brain reveals a protein network involved in synaptic vesicle turnover and a close association with Synaptotagmin-1. *Journal of Proteome Research* **11**:4075–4090. DOI: <https://doi.org/10.1021/pr300123g>, PMID: 22731840
- Koo EH, Sisodia SS, Archer DR, Martin LJ, Weidemann A, Beyreuther K, Fischer P, Masters CL, Price DL. 1990. Precursor of amyloid protein in alzheimer disease undergoes fast anterograde axonal transport. *PNAS* **87**:1561–1565. DOI: <https://doi.org/10.1073/pnas.87.4.1561>, PMID: 1689489
- Lazarov O, Lee M, Peterson DA, Sisodia SS. 2002. Evidence that synaptically released beta-amyloid accumulates as extracellular deposits in the hippocampus of transgenic mice. *The Journal of Neuroscience* **22**:9785–9793. DOI: <https://doi.org/10.1523/JNEUROSCI.22-22-09785.2002>, PMID: 12427834
- Liot G, Zala D, Pla P, Mottet G, Piel M, Saudou F. 2013. Mutant huntingtin alters retrograde transport of TrkB receptors in striatal dendrites. *Journal of Neuroscience* **33**:6298–6309. DOI: <https://doi.org/10.1523/JNEUROSCI.2033-12.2013>, PMID: 23575829
- Lo AC, Tesseur I, Scopes DI, Nerou E, Callaerts-Vegh Z, Vermaercke B, Treherne JM, De Strooper B, D'Hooge R. 2013. Dose-dependent improvements in learning and memory deficits in APPS1-21 transgenic mice treated with the orally active  $\beta$  toxicity inhibitor SEN1500. *Neuropharmacology* **75**:458–466. DOI: <https://doi.org/10.1016/j.neuropharm.2013.08.030>, PMID: 24035915
- Margevicius DR, Bastian C, Fan Q, Davis RJ, Pimplikar SW. 2015. JNK-interacting protein 1 mediates alzheimer's-like pathological features in AICD-transgenic mice. *Neurobiology of Aging* **36**:2370–2379. DOI: <https://doi.org/10.1016/j.neurobiolaging.2015.04.013>, PMID: 26022769
- Marquer C, Laine J, Dauphinot L, Hanbouch L, Lemerrier-Neuillet C, Pierrot N, Bossers K, Le M, Corlier F, Benstaali C, Saudou F, Thinakaran G, Cartier N, Octave JN, Duyckaerts C, Potier MC. 2014. Increasing membrane cholesterol of neurons in culture recapitulates alzheimer's disease early phenotypes. *Molecular Neurodegeneration* **9**:60. DOI: <https://doi.org/10.1186/1750-1326-9-60>, PMID: 25524049
- Martínez-Mármol R, Mohannak N, Qian L, Wang T, Gormal RS, Ruitenber MJ, Vanhaesebroeck B, Coulson EJ, Meunier FA. 2019. p110 $\delta$  PI3-Kinase inhibition perturbs APP and tnf $\alpha$  trafficking, reduces plaque burden, dampens Neuroinflammation, and prevents cognitive decline in an Alzheimer's Disease Mouse Model. *The Journal of Neuroscience* **39**:7976–7991. DOI: <https://doi.org/10.1523/JNEUROSCI.0674-19.2019>, PMID: 31363064
- Matsuda S, Yasukawa T, Homma Y, Ito Y, Niikura T, Hiraki T, Hirai S, Ohno S, Kita Y, Kawasumi M, Kouyama K, Yamamoto T, Kyriakis JM, Nishimoto I. 2001. c-Jun N-terminal kinase (JNK)-interacting protein-1b/islet-brain-1 scaffolds alzheimer's amyloid precursor protein with JNK. *The Journal of Neuroscience* **21**:6597–6607. DOI: <https://doi.org/10.1523/JNEUROSCI.21-17-06597.2001>, PMID: 11517249
- Moutaux E, Christaller W, Scaramuzzino C, Genoux A, Charlot B, Cazorla M, Saudou F. 2018. Neuronal network maturation differently affects secretory vesicles and mitochondria transport in axons. *Scientific Reports* **8**:13429. DOI: <https://doi.org/10.1038/s41598-018-31759-x>, PMID: 30194421
- Mucke L, Selkoe DJ. 2012. Neurotoxicity of amyloid  $\beta$ -protein: synaptic and network dysfunction. *Cold Spring Harbor Perspectives in Medicine* **2**:a006338. DOI: <https://doi.org/10.1101/cshperspect.a006338>, PMID: 22762015
- Müller UC, Deller T, Korte M. 2017. Not just amyloid: physiological functions of the amyloid precursor protein family. *Nature Reviews Neuroscience* **18**:281–298. DOI: <https://doi.org/10.1038/nrn.2017.29>, PMID: 28360418
- Muresan Z, Muresan V. 2005. Coordinated transport of phosphorylated amyloid-beta precursor protein and c-Jun NH2-terminal kinase-interacting protein-1. *Journal of Cell Biology* **171**:615–625. DOI: <https://doi.org/10.1083/jcb.200502043>, PMID: 16301330
- Neuman KM, Molina-Campos E, Musial TF, Price AL, Oh KJ, Wolke ML, Buss EW, Scheff SW, Mufson EJ, Nicholson DA. 2015. Evidence for alzheimer's disease-linked synapse loss and compensation in mouse and human hippocampal CA1 pyramidal neurons. *Brain Structure and Function* **220**:3143–3165. DOI: <https://doi.org/10.1007/s00429-014-0848-z>, PMID: 25031178
- Nicolas M, Hassan BA. 2014. Amyloid precursor protein and neural development. *Development* **141**:2543–2548. DOI: <https://doi.org/10.1242/dev.108712>, PMID: 24961795
- Niederst ED, Reyna SM, Goldstein LS. 2015. Axonal amyloid precursor protein and its fragments undergo somatodendritic endocytosis and processing. *Molecular Biology of the Cell* **26**:205–217. DOI: <https://doi.org/10.1091/mbc.E14-06-1049>, PMID: 25392299
- Pagnamenta AT, Heemeryck P, Martin HC, Bosc C, Peris L, Uszynski I, Gory-Fauré S, Couly S, Deshpande C, Siddiqui A, Elmonairy AA, Jayawant S, Murthy S, Walker I, Loong L, Bauer P, Vossier F, Denarier E, Maurice T, Barbier EL, et al. 2019. Defective tubulin detyrosination causes structural brain abnormalities with cognitive deficiency in humans and mice. *Human Molecular Genetics* **28**:3391–3405. DOI: <https://doi.org/10.1093/hmg/ddz186>, PMID: 31363758
- Palop JJ, Mucke L. 2010. Amyloid-beta-induced neuronal dysfunction in Alzheimer's disease: from synapses toward neural networks. *Nature Neuroscience* **13**:812–818. DOI: <https://doi.org/10.1038/nn.2583>, PMID: 20581818
- Pardo R, Colin E, Régulier E, Aebischer P, Déglon N, Humbert S, Saudou F. 2006. Inhibition of calcineurin by FK506 protects against polyglutamine-huntingtin toxicity through an increase of huntingtin phosphorylation at



- S421. *Journal of Neuroscience* **26**:1635–1645. DOI: <https://doi.org/10.1523/JNEUROSCI.3706-05.2006>, PMID: 16452687
- Pardo R, Molina-Calavita M, Poizat G, Keryer G, Humbert S, Saudou F. 2010. pARIS-htt: an optimised expression platform to study huntingtin reveals functional domains required for vesicular trafficking. *Molecular Brain* **3**:17. DOI: <https://doi.org/10.1186/1756-6606-3-17>, PMID: 20515468
- Priller C, Bauer T, Mitteregger G, Krebs B, Kretschmar HA, Herms J. 2006. Synapse formation and function is modulated by the amyloid precursor protein. *Journal of Neuroscience* **26**:7212–7221. DOI: <https://doi.org/10.1523/JNEUROSCI.1450-06.2006>, PMID: 16822978
- Priller C, Mitteregger G, Paluch S, Vassallo N, Staufenbiel M, Kretschmar HA, Jucker M, Herms J. 2009. Excitatory synaptic transmission is depressed in cultured hippocampal neurons of APP/PS1 mice. *Neurobiology of Aging* **30**:1227–1237. DOI: <https://doi.org/10.1016/j.neurobiolaging.2007.10.016>, PMID: 18077058
- Radde R, Bolmont T, Kaeser SA, Coomaraswamy J, Lindau D, Stoltz L, Calhoun ME, Jäggi F, Wolburg H, Gengler S, Haass C, Ghetti B, Czech C, Hölscher C, Mathews PM, Jucker M. 2006. Abeta42-driven cerebral amyloidosis in transgenic mice reveals early and robust pathology. *EMBO Reports* **7**:940–946. DOI: <https://doi.org/10.1038/sj.embor.7400784>, PMID: 16906128
- Rickle A, Bogdanovic N, Volkman I, Winblad B, Ravid R, Cowburn RF. 2004. Akt activity in Alzheimer's disease and other neurodegenerative disorders. *NeuroReport* **15**:955–959. DOI: <https://doi.org/10.1097/00001756-200404290-00005>, PMID: 15076714
- Rodrigues EM, Weissmiller AM, Goldstein LSB. 2012. Enhanced  $\gamma$ -secretase processing alters APP axonal transport and leads to axonal defects. *Human Molecular Genetics* **21**:4587–4601. DOI: <https://doi.org/10.1093/hmg/dds297>
- Rogers DC, Fisher EM, Brown SD, Peters J, Hunter AJ, Martin JE. 1997. Behavioral and functional analysis of mouse phenotype: shirpa, a proposed protocol for comprehensive phenotype assessment. *Mammalian Genome* **8**:711–713. DOI: <https://doi.org/10.1007/s003359900551>, PMID: 9321461
- Saudou F, Humbert S. 2016. The biology of huntingtin. *Neuron* **89**:910–926. DOI: <https://doi.org/10.1016/j.neuron.2016.02.003>, PMID: 26938440
- Scholtzova H, Kascsak RJ, Bates KA, Boutajangout A, Kerr DJ, Meeker HC, Mehta PD, Spinner DS, Wisniewski T. 2009. Induction of toll-like receptor 9 signaling as a method for ameliorating alzheimer's disease-related pathology. *Journal of Neuroscience* **29**:1846–1854. DOI: <https://doi.org/10.1523/JNEUROSCI.5715-08.2009>, PMID: 19211891
- Selkoe DJ, Hardy J. 2016. The amyloid hypothesis of Alzheimer's disease at 25 years. *EMBO Molecular Medicine* **8**:595–608. DOI: <https://doi.org/10.15252/emmm.201606210>, PMID: 27025652
- Soba P, Eggert S, Wagner K, Zentgraf H, Siehl K, Kreger S, Löwer A, Langer A, Merdes G, Paro R, Masters CL, Müller U, Kins S, Beyreuther K. 2005. Homo- and heterodimerization of APP family members promotes intercellular adhesion. *The EMBO Journal* **24**:3624–3634. DOI: <https://doi.org/10.1038/sj.emboj.7600824>, PMID: 16193067
- Südhof TC. 2018. Towards an understanding of synapse formation. *Neuron* **100**:276–293. DOI: <https://doi.org/10.1016/j.neuron.2018.09.040>, PMID: 30359597
- Szodorai A, Kuan YH, Hunzelmann S, Engel U, Sakane A, Sasaki T, Takai Y, Kirsch J, Müller U, Beyreuther K, Brady S, Morfini G, Kins S. 2009. APP anterograde transport requires Rab3A GTPase activity for assembly of the transport vesicle. *Journal of Neuroscience* **29**:14534–14544. DOI: <https://doi.org/10.1523/JNEUROSCI.1546-09.2009>, PMID: 19923287
- Takemura R, Okabe S, Umeyama T, Hirokawa N. 1995. Polarity orientation and assembly process of microtubule bundles in nocodazole-treated, MAP2c-transfected COS cells. *Molecular Biology of the Cell* **6**:981–996. DOI: <https://doi.org/10.1091/mbc.6.8.981>, PMID: 7579713
- Taylor AM, Blurton-Jones M, Rhee SW, Cribbs DH, Cotman CW, Jeon NL. 2005. A microfluidic culture platform for CNS axonal injury, regeneration and transport. *Nature Methods* **2**:599–605. DOI: <https://doi.org/10.1038/nmeth777>, PMID: 16094385
- Taylor AM, Dieterich DC, Ito HT, Kim SA, Schuman EM. 2010. Microfluidic local perfusion chambers for the visualization and manipulation of synapses. *Neuron* **66**:57–68. DOI: <https://doi.org/10.1016/j.neuron.2010.03.022>, PMID: 20399729
- Thion MS, McGuire JR, Sousa CM, Fuhrmann L, Fitamant J, Leboucher S, Vacher S, du Montcel ST, Bièche I, Bernet A, Mehlen P, Vincent-Salomon A, Humbert S. 2015. Unraveling the role of huntingtin in breast Cancer metastasis. *Journal of the National Cancer Institute* **107**:djv208. DOI: <https://doi.org/10.1093/jnci/djv208>, PMID: 26293574
- Toh WH, Gleeson PA. 2016. Dysregulation of intracellular trafficking and endosomal sorting in Alzheimer's disease: controversies and unanswered questions. *Biochemical Journal* **473**:1977–1993. DOI: <https://doi.org/10.1042/BCJ20160147>, PMID: 27407168
- Vagnoni A, Glennon EB, Perkinton MS, Gray EH, Noble W, Miller CC. 2013. Loss of c-Jun N-terminal kinase-interacting protein-1 does not affect axonal transport of the amyloid precursor protein or  $\text{A}\beta$  production. *Human Molecular Genetics* **22**:4646–4652. DOI: <https://doi.org/10.1093/hmg/ddt313>, PMID: 23825109
- van Beuningen SF, Hoogenraad CC. 2016. Neuronal polarity: remodeling microtubule organization. *Current Opinion in Neurobiology* **39**:1–7. DOI: <https://doi.org/10.1016/j.conb.2016.02.003>, PMID: 26945466
- Verhey KJ, Meyer D, Deehan R, Blenis J, Schnapp BJ, Rapoport TA, Margolis B. 2001. Cargo of kinesin identified as JIP scaffolding proteins and associated signaling molecules. *Journal of Cell Biology* **152**:959–970. DOI: <https://doi.org/10.1083/jcb.152.5.959>, PMID: 11238452

- Virlogeux A, Moutaux E, Christaller W, Genoux A, Bruyère J, Fino E, Charlot B, Cazorla M, Saudou F. 2018. Reconstituting corticostriatal network on-a-Chip reveals the contribution of the presynaptic compartment to Huntington's Disease. *Cell Reports* **22**:110–122. DOI: <https://doi.org/10.1016/j.celrep.2017.12.013>, PMID: 29298414
- Wei W, Nguyen LN, Kessels HW, Hagiwara H, Sisodia S, Malinow R. 2010. Amyloid beta from axons and dendrites reduces local spine number and plasticity. *Nature Neuroscience* **13**:190–196. DOI: <https://doi.org/10.1038/nn.2476>, PMID: 20037574
- Weyer SW, Zagrebelsky M, Herrmann U, Hick M, Ganss L, Gobbert J, Gruber M, Altmann C, Korte M, Deller T, Müller UC. 2014. Comparative analysis of single and combined APP/APLP knockouts reveals reduced spine density in APP-KO mice that is prevented by app $\alpha$  expression. *Acta Neuropathologica Communications* **2**:36. DOI: <https://doi.org/10.1186/2051-5960-2-36>, PMID: 24684730
- Yau KW, Schätzle P, Tortosa E, Pagès S, Holtmaat A, Kapitein LC, Hoogenraad CC. 2016. In Dendrites in vitro and in vivo contain microtubules of opposite polarity and axon formation correlates with uniform Plus-End-Out microtubule orientation. *Journal of Neuroscience* **36**:1071–1085. DOI: <https://doi.org/10.1523/JNEUROSCI.2430-15.2016>, PMID: 26818498
- Yu Y, Jans DC, Winblad B, Tjernberg LO, Schedin-Weiss S. 2018. Neuronal  $\alpha$ 42 is enriched in small vesicles at the presynaptic side of synapses. *Life Science Alliance* **1**:e201800028. DOI: <https://doi.org/10.26508/lsa.201800028>, PMID: 30456353
- Zala D, Hinckelmann MV, Yu H, Lyra da Cunha MM, Liot G, Cordelières FP, Marco S, Saudou F. 2013. Vesicular glycolysis provides on-board energy for fast axonal transport. *Cell* **152**:479–491. DOI: <https://doi.org/10.1016/j.cell.2012.12.029>, PMID: 23374344
- Zhang Z, Song M, Liu X, Su Kang S, Duong DM, Seyfried NT, Cao X, Cheng L, Sun YE, Ping Yu S, Jia J, Levey AI, Ye K. 2015. Delta-secretase cleaves amyloid precursor protein and regulates the pathogenesis in Alzheimer's disease. *Nature Communications* **6**:8762. DOI: <https://doi.org/10.1038/ncomms9762>, PMID: 26549211
- Zou C, Montagna E, Shi Y, Peters F, Blazquez-Llorca L, Shi S, Filser S, Dorostkar MM, Herms J. 2015. Intraneuronal APP and extracellular  $\alpha$ 42 independently cause dendritic spine pathology in transgenic mouse models of Alzheimer's disease. *Acta Neuropathologica* **129**:909–920. DOI: <https://doi.org/10.1007/s00401-015-1421-4>, PMID: 25862638

## Appendix 1

### Supplemental Methods

#### Vesicular fractionation

Three 6/7-month-old mice were used per genotype. The protocol was adapted from *Zala et al., 2013*. Briefly, frozen brains were homogenized in 700  $\mu$ L of homogenization buffer (320 mM sucrose) by triturating with a Dounce homogenizer. Then, samples were centrifuged twice at 47,000 rcf for 10 min and the two supernatants were combined (S1). From S1, another ultracentrifugation was performed at 120,000 rcf for 40 min to obtain S2 and P2. The S2 fraction was put in another tube and 280  $\mu$ L of 700 mM sucrose buffer was added under the S2 fraction. After a 2 hr centrifugation at 260,000 rcf, S3 and P3 were obtained. P3 fraction was resuspended in 50  $\mu$ L of Re-suspension buffer (10 mM HEPES pH 7.3 and 320 mM sucrose). Antibodies used for western blot analysis are KHC (clone SUK4, Covance; MMS-188P,) and p150 (BD Transduction Laboratories, 610474).

#### Primary Screen (modified SHIRPA)

The testing was carried out using a modified version of the standard protocol (*Rogers et al., 1997*).  $HTT_{SA}$  and WT littermate control mice were examined at 12 months of age. The primary screen began by observing undisturbed behavior in a viewing jar (clear Perspex cylinder, 15 cm x 11 cm) for 30 s (section 1). Thereafter, the mouse was transferred in the arena (55 cm x 33 cm x 18 cm) for testing of transfer arousal and observation of normal behavior (section 2). The observer also looked for any manifestation of bizarre or stereotyped behavior, convulsions and indications of spatial disorientation. This was followed by a sequence of manipulations using tail suspension and the grid across the width of the arena (section 3). To complete the assessment, the animal was restrained in a supine position to record autonomic behaviors (section 4).

#### Open field activity (OF)

The open field test was used to assess locomotor activity (and anxiety-related behaviors). Mice were tested in a homogeneously illuminated (50 lux) circular open field arena made of white plastic (diameter: 54 cm) with 30 cm-high walls. Monitoring was done by an automated video tracking system (AnyMaze, Stoelting, Wood Dale, IL, USA). The main behavioral parameters analyzed during a single 10 min session in the OF were the total traveled distance and also the center-to-periphery exploration ratio.

#### Grip force test

Mice were scruffed by the lower back and lowered towards a mesh grip piece attached to a force gauge (Bioseb) until the animal grabbed it with both front paws. The animal was then lowered toward the platform and gently pulled straight back with consistent force until it released its grip. The forelimb grip force was recorded on the strain gauge.

#### Elevated plus maze (EPM)

The EPM was made of beige PVC and the center of the field illuminated at 70 lux. The apparatus was elevated 50 cm above floor level and consisted of four arms (35 cm x 5 cm). Two of the arms contained 15 cm-high walls (enclosed arms) and the other two had no walls (open arms). Each mouse was placed in the middle section facing an open arm and left to explore the maze for a single 5 min session with the experimenter out of view. Animals were video-recorded and their behavior automatically analyzed with the ANY-maze software.

Percent time spent in open arms which is supposed to be inversely correlated to anxiety levels was measured for each mouse.

### Neuropathology

Following completion of behavioral testing, at 19 months of age, mice were anesthetized with pentobarbital (120 mg/kg) and then transcardially perfused with phosphate-buffer saline solution. The brain was extracted and carefully weighed on a precision balance. One hemisphere was snap frozen in liquid nitrogen and then stored at  $-80^{\circ}\text{C}$  for subsequent biochemical analysis. The other half brain was fixed by immersion in freshly-made formaldehyde solution (3–4 days), then cryoprotected in a 2% - DMSO – 20% glycerol solution and finally cut on a freezing microtome (serial sections of  $40\ \mu\text{m}$  of the entire brain).

Amyloid deposits were labeled by standard Congo red staining (30 min in an 80% ethanol solution saturated with Congo red and sodium chloride). Microscopic scans of whole sections (pixel size  $0.25\ \mu\text{m}^2$ ) were acquired with a NanoZoomer 2.0-RS slide scanner (Hamamatsu Photonics, Hamamatsu, Japan). Amyloid loads were quantified using computer-based segmentation methods using the spot detector plugin of the ICY software (<http://icy.bioimageanalysis.org>) that automatically calculates the proportion of stained tissue ( $p = \text{stained area} / \text{total area}$ ), providing unbiased stereological measurements.

### Immunolabelling

For immunostaining, free-floating sections were washed in PBS 0.1M to remove cryoprotectant. The sections were treated with hydrogen peroxide for 10 min to quench endogenous peroxidase activity, permeabilized with 0.25% Triton X-100 in PBS 0.1M (PBSTx) for 20 min, pre-incubated in a 5% PBS-Tx normal goat serum (NGS) blocking solution and then incubated overnight at room temperature (RT) with the following primary antibodies : a biotinylated mouse anti-A $\beta$  (4G8) (1:3000, Covance Antibody Products), a rabbit polyclonal antibody recognizing amyloid fibrils and fibrillary A $\beta$  oligomers (OC) (1:3000, StressMarq Biosciences) and a rabbit polyclonal anti-prefibrillar A $\beta$  oligomers (A11) (1:1000, generous gift of Dr. Kaye Rakez). The sections were incubated with a secondary biotinylated goat anti-rabbit antibody at RT for 90 min (this step was omitted for 4G8 antibody that was already biotinylated). Tissues were then incubated in the Vector Elite avidin-biotin peroxidase kit (1:800) for 90 min at RT. Finally, after washes in PBS-Tx and Tris 0.1M solutions, immunoreactivity was revealed using diaminobenzidine (DAB) as chromogen to visualize the reaction product. The sections were then mounted on Superfrost slides, dehydrated in a series of alcohols (30%, 50%, 70%,  $2 \times 90\%$  and  $2 \times 100\%$ ), cleared in xylene, and coverslipped with EUKITT mounting medium.

### Analysis

Microscopic scans of immunostained brain sections were acquired with a NanoZoomer 2.0-RS slide scanner (Hamamatsu Photonics) at 40X magnification (pixel size  $0.25\ \mu\text{m}^2$ ). Selected regions of interest (ROIs) were delineated by using the Paxinos and Franklin Mouse Brain Atlas: sensori-motor (SM), Frontal (FR) and the hippocampus (HPC). ROIs were assessed across 2 to 6 consecutive serial sections (depending on structure) and were manually outlined on digitized sections. Computer-based segmentation methods were applied for 4G8 and OC immunostaining using the Best threshold plugins of the ICY software (<https://icy.bioimageanalysis.org>) that automatically calculate the proportion of stained tissue ( $p = \text{stained area} / \text{total area}$ ) in each ROIs. For A11 immunostained sections, A $\beta$  loads were calculated using the Ilastik interactive learning and segmentation toolkit software (<https://ilastik.org/index.html>). The frontal cortex, the sensori-motor cortex and the hippocampus brain regions were manually outlined on digitized sections. To evaluate the 4G8-detected A $\beta$  loads, reference background staining of the corpus callosum was used to binarize the digitized image to 8-bits black and white image. The mean number of thresholded pixels per ROI was automatically

calculated using an ICY image analysis software script. A minimum of 3 sections per brain ROIs per animal were analyzed and counting's were reported to the overall ROI surface to provide the 4G8 amyloid loads.

### A $\beta$ 42 dosages

Hemi-forebrains (~200 mg) were harvested in 500  $\mu$ l of solution containing 50 mM Tris-HCl (pH 7.6), 0.01% NP-40, 150 mM NaCl, 2 mM EDTA, 0.1% SDS, 1 mM phenylmethylsulfonyl fluoride (PMSF), and protease inhibitor cocktail (Sigma). Soluble, extracellular-enriched proteins were collected from mechanically homogenized lysates following centrifugation for 10 min at 3,000 g. Cytoplasmic proteins were extracted from cell pellets mechanically dissociated with a micropipettor in 500  $\mu$ l buffer containing 50 mM Tris-HCl (pH 7.6), 150 mM NaCl, 0.1% Triton X-100 following centrifugation 90 min at 11,000 g. Supernatant was collected for dosages. Supernatants from cortical neurons plated in microchambers were collected on ice in polypropylene tubes (Corning, Corning, NY, USA) containing a protease inhibitor cocktail (Roche) and were then stored at  $-80^{\circ}\text{C}$ . Concentration of A $\beta$  peptides were measured by Electro-Chemiluminescence Immuno-Assay (ECLIA) performed according to the manufacturer's instructions Meso Scale Discovery (MSD). Briefly, samples were analyzed using MSD SECTOR Imager 2400 (Meso Scale Discovery, Gaithersburg, MD, USA), with the Rodent A $\beta$  triplex kit (from MSD) on carbon 96-well plates. 100  $\mu$ l of blocking buffer solution were added to avoid non-specific binding. The plates were then sealed, wrapped in tin foil, and incubated at room temperature on a plate shaker (300 rpm) for 1 hr. Wells were then washed three times with washing buffer, and 25  $\mu$ l of the standards and samples were then added to the wells, followed by an A $\beta$ -detecting antibody at 1  $\mu\text{g}/\text{ml}$  (MSD) labelled with a Ruthenium (II) trisbipyridine N-hydroxysuccinimide ester; this detection antibody was 4G8. Plates were then aspirated and washed three times. MSD read buffer (containing TPA) was added to wells before reading on the Sector Imager. A small electric current passed through a microelectrode present in each well producing a redox reaction of the Ru $^{2+}$  cation, emitting 620 nm red light. The concentration of A $\beta$  was calculated for each sample, using dose-response curves, the blank being cell-less culture medium. All the conditions were tested in duplicate. A $\beta$  levels were normalized with total amount of proteins quantified by Bradford dosage.

## Discussion

Using HTT phosphorylation as a molecular tool to specifically increase APP anterograde axonal transport, we proved that APP transport regulation has consequences on APP accumulation at the synapse. Then, knowing that APP quantities at the synapse are important for its role on synapse homeostasis, we proved that APP axonal transport mediates APP role on synapse homeostasis. Finally, we demonstrated that the rescue of APPS1 memory observed in our study is due to a decreased level of phosphorylation of HTT, a Akt downstream target (figure 95), thus raising questions about the link between AD and the IGF-1/Akt pathway.

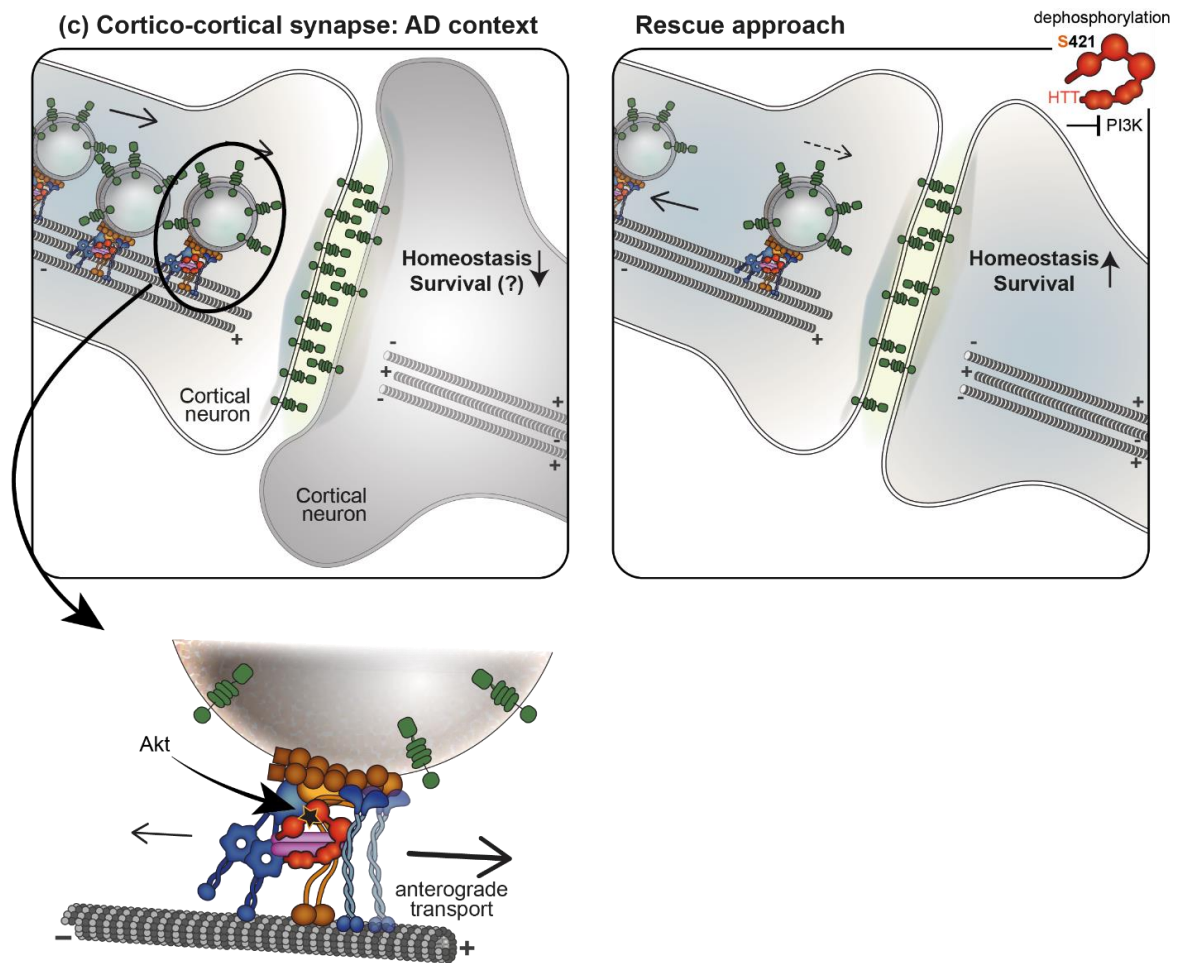
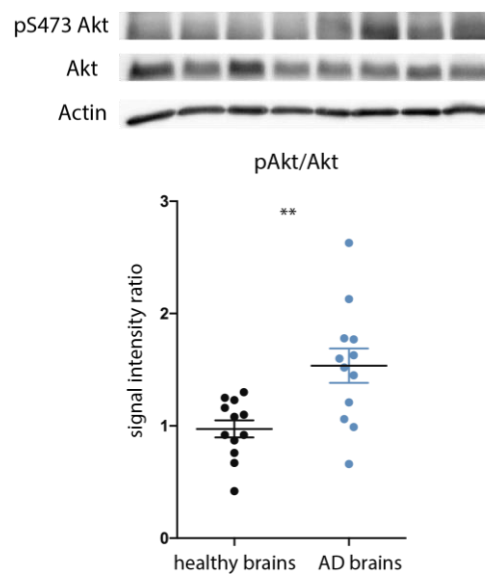


Figure 94: unphosphorylatable form of HTT rescues AD mouse model phenotypes through APP transport.

## AD and the IGF-1/Akt pathway

Our study points out the crucial role of APP transport mediated by HTT through Akt phosphorylation at S421 to the plasma membrane in APP PS1 mice. By crossing  $HTT_{SA}$  mice with APPPS1 mice, APP levels at the synapse were restored as well as the synapse number and size and the non-spatial memory of APPPS1 mice. These results are in agreement with the fact that Akt is hyperactivated in AD (figure 95) and is dependent on the AD stage. In AD, despite the fact that its transport has been reported to be negatively impaired, APP could accumulate at the synapse through Akt hyperactivation. The down regulation of this Akt-induced signal via  $HTT_{S421A}$  mutation represent therefore a strategy to attenuate Akt hyperactivation in AD.



**Figure 95: Akt is overactivated in AD.** Western blot analysis of at least four healthy or AD human brains and corresponding analysis.

Another way to regulate IGF-1 pathway could involve PI3K that is the upstream kinase of Akt (figure 96). Inhibiting PI3K action by a point mutation in its ATP binding site, or surprisingly activating Akt, decreased APP anterograde transport from Golgi (Martínez-Mármol et al., 2019; Shineman et al., 2009). Consequently, PI3K inhibition restores APP density within hippocampal axons, reduced  $A\beta$  burden and restored survival and learning acquisition in APP/PS1 mice (Martínez-Mármol et al., 2019).

Finally, a precursor study investigated the consequence of abolishing the entire IGF-1 pathway by knocking down the IGF-1 receptor. Heterozygous mice for IGF-1R KO, showing a reduced IGF-1 signaling, were crossed with an AD mouse model similar to APP/PS1 model. This IGF-1 regulation in AD mouse model caused a reduction of memory impairment and neuronal loss (Cohen et al., 2009).

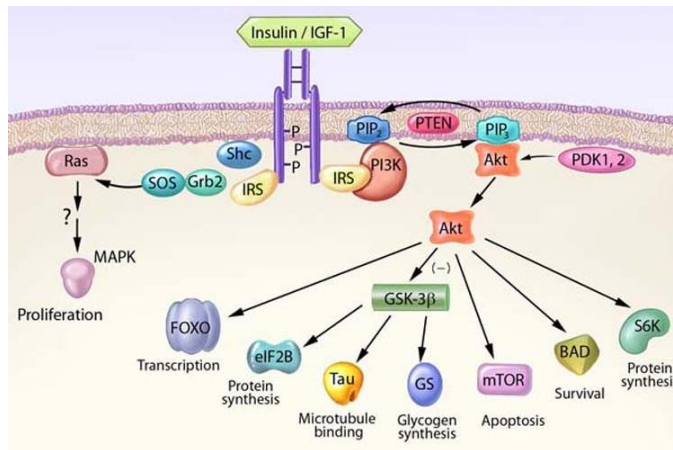


**Figure 96: IGF-1 pathway regulates cell survival through Akt activation.** Scheme from Bondy et al., 2006

Altogether, our study is in agreement with previous work aiming at decreasing Akt signaling that is hyperactivated in AD. Compared to other ways of down regulating IGF-1 pathway, our study has the advantage to be very specific and this way, can avoid off-target.

### **APP accumulation at the PM results in cognitive impairments**

Although it is believed that APP trafficking is impaired in AD and notably, its endocytic pathway (X. H. Liu et al., 2015; Poulsen et al., 2017), its accumulation at the synapse in AD patients remains unknown for the moment. However, in APP/PS1 model, we demonstrated that APP levels in the presynapse were higher. In this paragraph, we will explore the possibility to describe AD as a disease caused by APP accumulation at the PM

APP/PS1 mice exhibit an impaired synaptic homeostasis since their spine density is lower and spine size is larger than the physiological spine density (Androuin et al., 2018). Since APP, overexpressed in this model, regulates synapse homeostasis, one can wonder if APP accumulation at the PM could lead to these structural and functional impairments causing their loss of memory. Indeed, this increase in APP levels by itself could be responsible of this disrupted synapse homeostasis since overexpression of APP is sufficient to decrease the number of synapses (Bruyère et al., 2020; Kamenetz et al., 2003) and to affect short term synaptic plasticity (Rusu et al., 2007).

In humans, one disease exhibits an APP increased expression: Down syndrome (DS). Indeed, APP gene is located on the chromosome 21 which is duplicated in this disease: in DS, APP is present in triplicate. Interestingly, a mouse model of DS, trisomic for APP, exhibit a lower spine density and larger spines (Belichenko et al., 2004; A. J. Villar et al., 2005), just like the AD mouse model. Most of the DS patients



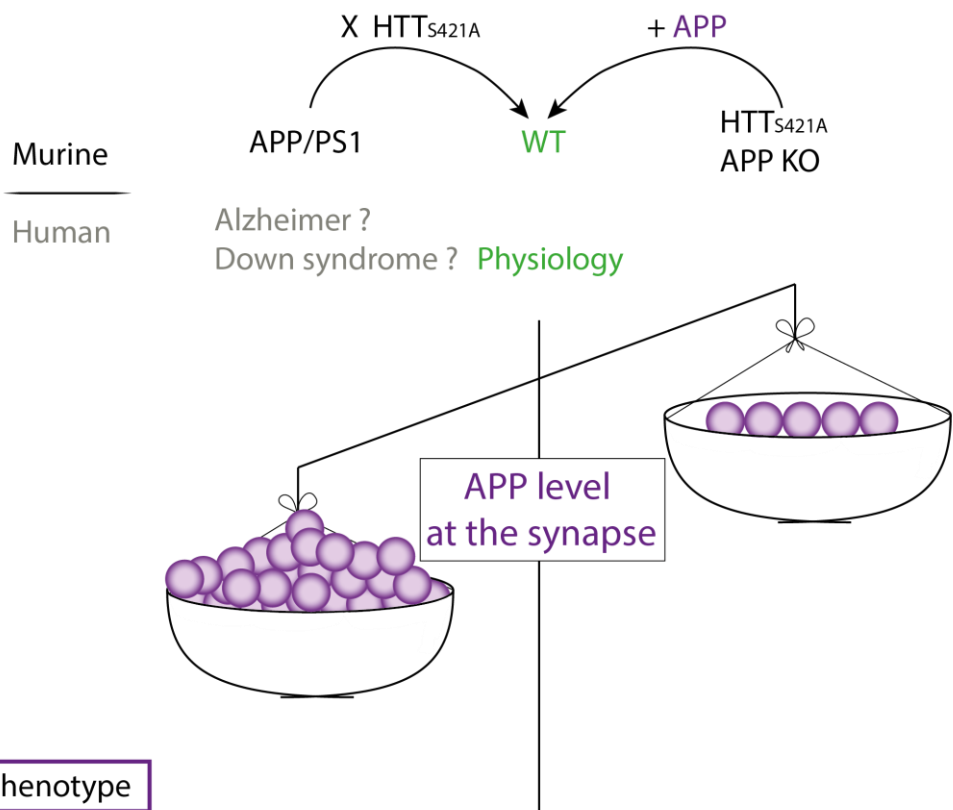
show AD characteristics at the age of 40 and it has been shown to be directly linked with APP triplicates. Indeed, very interestingly, a study reveals that one DS patient had a partial trisomy in which the chromosome 21 was partly replicated such as, the APP gene was not replicated. This patient did not show any dementia or main neuropsychological impairments (Doran et al., 2017). This opportunity confirms the fact that increased APP levels is toxic for the synapse homeostasis.

Finding the exact mechanisms responsible for the toxicity of APP accumulation at the PM would be challenging because of its multiple roles. However, one hint could be that APP accumulation would increase APP dimerization, known to activate the p38 cascade, and lead to tau phosphorylation along with neurofibrillary tangles (E. K. Kim & Choi, 2010).

Thus, instead of considering A $\beta$  production or tau phosphorylation as one of AD causes, maybe one good option would be to consider it as a consequence of APP homeostasis dysregulation (Kametani & Hasegawa, 2018) (figure 96).

To conclude this study, we can claim that APP level at the synapse is crucial for neuronal homeostasis. If it is increased like it is observed in APPPS1 AD mouse model or in human in down syndrome, it could potentially lead to the observed phenotypes in terms of synapse homeostasis and cognitive deficits. Crossing of APPPS1 mice with HTTS421A mice restored the APP-induced phenotypes. On the opposite, not enough APP at the synapse could be responsible for the dysregulation of synapse homeostasis observed in APP KO mice. Adding APP to APP KO neurons is sufficient to restore the observed phenotypes (Galanis *et al.*, 2020, under revision) (figure 97).

**Mutation or disease**



**Phenotype**

- |        |  |  |
|--------|--|--|
| Murine | <ul style="list-style-type: none"> <li>↘ synapse number</li> <li>↗ spine size</li> <li>↘ spatial memory</li> </ul>   | <ul style="list-style-type: none"> <li>↗ synapse number</li> <li>↘ spine size</li> </ul> |
| Human  | <ul style="list-style-type: none"> <li>memory loss</li> <li>challenges in planning</li> <li>confusion with time or space</li> <li>-</li> <li>mental retardation</li> <li>seizures</li> <li>young AD onset</li> </ul> |  |

**Figure 97: balance of APP level at the synapse is important for neuronal homeostasis**

## Results – part 2: Huntingtin phosphorylation governs BDNF homeostasis and improves the phenotype of *Mecp2* knockout mice

### Summary & context of the study

#### *Rett syndrome*

Rett syndrome (RTT) is a severe neurological disorder caused by mutations in the *MECP2* gene located on the X chromosome. This non-inherited disease affecting one out of 15 000 young girl from 1- to 2-year-old, is characterized by a dramatic and global disturbance of the CNS. Symptoms include intellectual disability, seizures, motor infirmity (affecting speech, walk and hand movements) and respiratory difficulties (apneas and hyperventilation) (orphanet website, (Yann Ehinger et al., 2020; Roux et al., 2012)). These symptoms are the results of a cerebral atrophy causing a reduction of the number of neuronal connections.

#### *MECP2 influences BDNF production and transport*



*MECP2* gene codes the MeCP2 protein (Methyl-CpG binding protein 2) which acts as a gene expression regulator. MeCP2 targets the expression of thousands of genes including *BDNF*, *HTT* and *HAP-1*, which are known to be implicated in axonal transport (Roux et al., 2012). Thus, *Mecp2* KO mice exhibit reduced levels of the corresponding proteins. Work of the Roux and Saudou labs showed a reduction of both BDNF levels in the striatum and BDNF transport in cortical neurons. This suggests that the decrease in the level of HTT could be responsible in part of the decreased BDNF levels observed in the striatum and the associated motor incoordination, apneas, and early onset of the death in these mice.

#### *BDNF, HTT and Rett Syndrome*

BDNF release in the corticostriatal network is crucial for striatal survival because this neurotrophic factor is not produced in the striatal cells (Altar et al., 1997; Baquet et al., 2004); it directly depends on the BDNF released from the cortex. BDNF acts as a survival cue through its release from the presynaptic neuron provoking the activation of TrkB receptors followed by their internalization in the postsynaptic neuron. Retrograde transport of these signaling endosomes then follows, mediated by the HTT-Dynein complex, to reach the cell bodies where cell survival pathways are activated (Liot et al., 2013). BDNF axonal transport in the cortical presynaptic neuron and its release are thus crucial for striatal signaling and survival (Baquet et al., 2004; Virlogeux et al., 2018; Vonsattel et al., 1985). BDNF is transported within DCVs through kinesin-1 and/or kinesin-3 binding (Arpağ et al., 2019; Dompierre et al., 2007; Lim et al., 2017; Lo et al., 2011; Yano & Chao, 2004), which can be modulated by HTT (Colin et al., 2008;

Gauthier et al., 2004). Such alteration of transport in HD is critical for pathogenesis but as discussed previously, impairment of BDNF transport within the corticostriatal network of Mecp2 KO mice could also be an important factor for the RTT phenotypes. The findings that HTT phosphorylation increases anterograde transport of BDNF vesicles, (Colin et al., 2008) led us to hypothesize that chronic HTT phosphorylation could rescue BDNF trafficking in Mecp2 deficient neurons and ameliorate symptoms in Mecp2 KO mice.

# Huntingtin phosphorylation governs BDNF homeostasis and improves the phenotype of *Mecp2* knockout mice

Yann Ehinger<sup>1,†,¶</sup>, Julie Bruyère<sup>2,¶</sup>, Nicolas Panayotis<sup>1,‡</sup>, Yah-Se Abada<sup>3</sup>, Emilie Borloz<sup>1</sup>, Valérie Matagne<sup>1</sup>, Chiara Scaramuzzino<sup>2</sup>, Hélène Vitet<sup>2</sup>, Benoit Delatour<sup>3</sup>, Lydia Saidi<sup>1,§</sup>, Laurent Villard<sup>1</sup>, Frédéric Saudou<sup>2,\*</sup>  & Jean-Christophe Roux<sup>1,\*\*</sup> 

## Abstract

Mutations in the X-linked *MECP2* gene are responsible for Rett syndrome (RTT), a severe neurological disorder for which there is no treatment. Several studies have linked the loss of MeCP2 function to alterations of brain-derived neurotrophic factor (BDNF) levels, but non-specific overexpression of BDNF only partially improves the phenotype of *Mecp2*-deficient mice. We and others have previously shown that huntingtin (HTT) scaffolds molecular complexes, transports BDNF-containing vesicles, and is under-expressed in *Mecp2* knockout brains. Here, we demonstrate that promoting HTT phosphorylation at Ser421, either by a phospho-mimetic mutation or inhibition of the phosphatase calcineurin, restores endogenous BDNF axonal transport *in vitro* in the corticostriatal pathway, increases striatal BDNF availability and synaptic connectivity *in vivo*, and improves the phenotype and the survival of *Mecp2* knockout mice—even though treatments were initiated only after the mice had already developed symptoms. Stimulation of endogenous cellular pathways may thus be a promising approach for the treatment of RTT patients.

**Keywords** Mecp2; Rett; BDNF; huntingtin; axonal transport

**Subject Categories** Genetics, Gene Therapy & Genetic Disease; Neuroscience; Pharmacology & Drug Discovery

**DOI** 10.15252/emmm.201910889 | Received 16 May 2019 | Revised 3 December 2019 | Accepted 5 December 2019 | Published online 8 January 2020

**EMBO Mol Med (2020) 12: e10889**

## Introduction

MeCP2 (Methyl-CpG-binding protein 2) is one of the most abundant proteins in the brain, yet the precise nature of its activities remains

controversial. It was originally discovered as a DNA methylation-dependent transcriptional repressor (Meehan *et al*, 1992), but has also been shown to play various roles in chromatin compaction, global gene expression, alternative splicing, and miRNA processing (Young *et al*, 2005; Chahrouh *et al*, 2008; Skene *et al*, 2010; Cheng *et al*, 2014). Interest in this protein rose sharply after it was discovered that mutations in *MECP2* cause Rett syndrome (RTT), a severe developmental disorder (Amir *et al*, 1999; Lyst & Bird, 2015). Females with RTT begin life apparently healthy, but between 6 and 18 months of age they undergo regression of early milestones, with deterioration of motor skills, eye contact, speech, and motor control; they then develop a range of neurological symptoms, including anxiety, respiratory dysrhythmias, and seizures (Lyst & Bird, 2015; Katz *et al*, 2016). Whereas loss of MeCP2 function leads to RTT, duplication or triplication of the locus leads to intellectual disability, autistic features, and motor dysfunction, as observed in males with *MECP2* duplication syndrome (Van Esch, 2012).

Disease-causing mutations in *MECP2* alter the expression of thousands of genes (Chahrouh *et al*, 2008). Among these, brain-derived neurotrophic factor (BDNF), a neuronal modulator that plays a key role in neuronal survival, development, and plasticity (Cheng *et al*, 2011), is one of the best studied (Chen *et al*, 2003, 2015; Chang *et al*, 2006; Sampathkumar *et al*, 2016). BDNF appears to be involved in the appearance and progression of the RTT phenotype in mice: *Mecp2* knockout mice (KO) present lower BDNF levels, and conditional BDNF deletion in *Mecp2* KO mice accelerates the onset of RTT-like symptoms (Chang *et al*, 2006). Conversely, conditional BDNF overexpression in the brain of *Mecp2* knockout mice leads to an improvement of certain locomotor and electrophysiological deficits (Chang *et al*, 2006). Although it is possible that the incomplete rescue reflects that MeCP2 has much broader regulatory effects than BDNF, it is possible that BDNF overexpression fails to restore

<sup>1</sup> Aix Marseille Univ, INSERM, MMG, UMR\_S 1251, Marseille, France

<sup>2</sup> Univ. Grenoble Alpes, Inserm, U1216, CHU Grenoble Alpes, Grenoble Institut Neurosciences, GIN, Grenoble, France

<sup>3</sup> Sorbonne Université, Institut du Cerveau et de la Moelle épinière, ICM, Inserm U1127, CNRS UMR 7225, Paris, France

\*Corresponding author. Tel: +33 4565 20514; E-mail: frederic.saudou@inserm.fr

\*\*Corresponding author. Tel: +33 4913 24904; E-mail: jean-christophe.roux@univ-amu.fr

†These authors contributed equally to this work

‡Present address: Department of Neurology, University of California, San Francisco, San Francisco, CA, USA

§Present address: Department of Biomolecular Sciences, Weizmann Institute of Science, Rehovot, Israel

¶Present address: Department of Psychiatry and Neuroscience, Faculty of medicine, Centre de recherche CERVO, Université Laval, Quebec City, QC, Canada

synaptic and neuronal function because it does not target the appropriate neurons. In support of this hypothesis, recent evidence suggests that MeCP2 deficiency leads to the disruption of cell-autonomous and autocrine BDNF signaling in excitatory glutamatergic neurons, and that increasing BDNF levels in diseased neurons restores their growth and ability to form synapses (Sampathkumar *et al*, 2016).

We have previously shown that BDNF homeostasis and transport involve huntingtin (HTT) and HTT-associated protein 1 (Hap1) (Roux *et al*, 2012; Saudou & Humbert, 2016). Levels of both these proteins are lower than normal in excitatory cortical neurons deficient for *Mecp2* (Roux *et al*, 2012). Here, we tested whether activating HTT, by a genetic or pharmacological approach, could improve BDNF homeostasis in *Mecp2*-deficient neuronal circuits and in *Mecp2* KO mice.

## Results

### BDNF transport is slowed in *Mecp2*-deficient axons

To examine BDNF transport in *Mecp2*-deficient neurons, we took advantage of the recent development and validation of microfluidic devices to reconstitute a neuronal network and monitor intracellular dynamics (Taylor *et al*, 2010; Virlogeux *et al*, 2018). We focused here on the corticostriatal network, which is altered in RTT and *Mecp2* KO mice (Roux *et al*, 2012; Xu *et al*, 2014). The device consists of a presynaptic compartment containing cortical neurons, a postsynaptic chamber containing striatal neurons, and a synaptic chamber containing corticostriatal contacts. Cortical neurons plated in the first compartment extend axons that connect to striatal dendrites within the synaptic compartment (Fig 1A), thus creating an oriented corticostriatal network on-a-chip (Virlogeux *et al*, 2018). This network reproduces the physiological network as we previously showed that cortical neurons from embryonic day (E) 15.5 are enriched in CTIP2/TBR1 neurons that correspond to the deepest layers of the cortex that send axons to the striatum. Also, most striatal neurons correspond to enkephalin-positive neurons that are the output-projecting neurons of the striatum (Virlogeux *et al*, 2018). Cortical neurons were transduced with mCherry-tagged BDNF lentivirus (BDNF-mCherry), and we used spinning disk confocal videomicroscopy to record the dynamics of BDNF-mCherry containing vesicles within microchannels in the axons (Fig 1A and Movie EV1). The dynamics of vesicles are in agreement with our recent studies using this technology (Moutaux *et al*, 2018; Virlogeux *et al*, 2018).

We transfected neurons with *Mecp2* siRNA, which reduced *Mecp2* protein levels by 63% compared to WT (Fig EV1A). This reduced the mean velocity and overall linear flow of BDNF vesicles reaching the corticostriatal contacts (Fig 1B). The number of moving vesicles was unchanged (Fig EV1B).

### HTT phosphorylation status influences anterograde and retrograde BDNF transport

Overexpression of phosphorylated HTT at S421 leads to increased outward transport in cells (Colin *et al*, 2008), but the role of endogenous HTT phosphorylation in axons remains unknown. We

isolated cortical neurons from homozygous knock-in mice in which S421 of HTT was replaced by an alanine ( $HTT^{S421A/S421A}$  or  $HTT_{SA}$ ), mimicking the absence of phosphorylation, or by an aspartic acid ( $HTT^{S421D/S421D}$  or  $HTT_{SD}$ ), mimicking constitutive phosphorylation (Thion *et al*, 2015). Mutating HTT at S421 abrogated the capacity of our phospho-HTT specific antibody to recognize endogenous phosphorylated protein (Fig EV1C). Importantly, the S into A or into D mutations had no effect on HTT protein levels, as quantification showed no difference in HTT protein expression between WT,  $HTT_{SD}$ , and  $HTT_{SA}$  mice (Fig EV1C). Also, we found that the mutations had no effect on cell viability, as shown by the MTT assay (Fig 1C). We then reproduced a corticostriatal network by plating the neurons within microfluidic devices. Phospho-mimetic HTT ( $HTT_{SD}$ ) significantly increased the speed of BDNF vesicles moving in the anterograde direction (Fig 1D, Movie EV1) without affecting the number of moving BDNF vesicles (Fig EV1D). In contrast, the absence of HTT phosphorylation ( $HTT_{SA}$ ) significantly increased the retrograde velocity of BDNF vesicles (Fig 1D). Thus, HTT phosphorylation status influences the velocity of BDNF vesicles in axons.

We next investigated whether HTT phosphorylation status influences the observed dysregulation of BDNF transport in *Mecp2* siRNA-transfected neurons (Figs 1E and EV1E and F). Phospho-mimetic HTT ( $HTT_{SD}$ ) rescued both anterograde and retrograde transport of BDNF, along with the mean velocity of BDNF vesicles and linear flow (Fig 1E). Preventing HTT phosphorylation ( $HTT_{SA}$ ) restored only the retrograde velocity of BDNF and linear flow rate to control levels (Fig 1E). The overall effect of HTT phosphorylation on BDNF transport under normal or low-*Mecp2* conditions was not due to a change in the number of moving BDNF vesicles (Fig EV1D and F) or in cell viability, since we observed no toxicity in *Mecp2* siRNA-transfected  $HTT_{SD}$  or  $HTT_{SA}$  neurons compared to *Mecp2* siRNA-transfected WT neurons (Fig 1F). These results demonstrate that genetically promoting HTT phosphorylation at S421 rescues the transport of BDNF vesicles in projecting corticostriatal siMecp2 neurons.

### Constitutive phosphorylation of HTT rescues corticostriatal BDNF transport and increases postsynaptic TrkB phosphorylation and markers of postsynaptic density *in vivo*

*Mecp2* KO mice show altered corticostriatal connections and reduced BDNF levels in the striatum (Roux *et al*, 2012). We therefore assessed the impact of huntingtin phosphorylation on BDNF transport *in vivo*. We crossed *Mecp2* KO mice with either  $HTT_{SA}$  or  $HTT_{SD}$  mice. The resulting double-mutant male mice, deficient for the *Mecp2* gene (KO) and homozygous for the S421A ( $HTT^{S421A/S421A}$ ) or S421D mutation ( $HTT^{S421D/S421D}$ ), will from hereon be referred to as KO/ $HTT_{SA}$  and KO/ $HTT_{SD}$ , respectively. Most of the BDNF protein located in the striatum comes from the cortex by anterograde transport within corticostriatal afferences (Altar *et al*, 1997). We therefore quantified the level of BDNF proteins using ELISA at the site of translation (the cortex) and the target site (the striatum) of 55-day-old WT mice, KO, KO/ $HTT_{SD}$ , and KO/ $HTT_{SA}$  mice (Fig 2A). The ratio of striatal and cortical BDNF is an indicator of the *in vivo* efficacy of BDNF axonal transport to the corticostriatal synapses. The ratio we observed in KO/ $HTT_{SD}$  mice ( $1.57 \pm 0.3$ ) was equivalent to what we observed in

WT mice ( $1.57 \pm 0.6$ ) and was significantly higher than that in *Mecp2* KO mice ( $1.14 \pm 0.1$ ) or KO/HTT<sub>SA</sub> mice ( $1.1 \pm 0.2$ ). These results suggest that HTT phosphorylation rescues corticostriatal BDNF transport *in vivo*.

We also found that improved corticostriatal BDNF transport in KO/HTT<sub>SD</sub> mice increased levels of TrkB phosphorylation at the postsynaptic level compared to KO WT (+36%,  $P < 0.05$ ) and

KO/HTT<sub>SA</sub> (+35%,  $P < 0.05$ ), showing that the BDNF release is stimulated *in vivo* (Figs 2A and EV1G). As a consequence, the post-synaptic marker PSD-95 is increased in KO/HTT<sub>SD</sub> striatum compared to KO/WT striatum (+37%,  $P < 0.01$ ) (Figs 2A and EV1G). We conclude that promoting HTT phosphorylation stimulates striatal BDNF pathways and helps maintain corticostriatal synapse homeostasis *in vivo*.

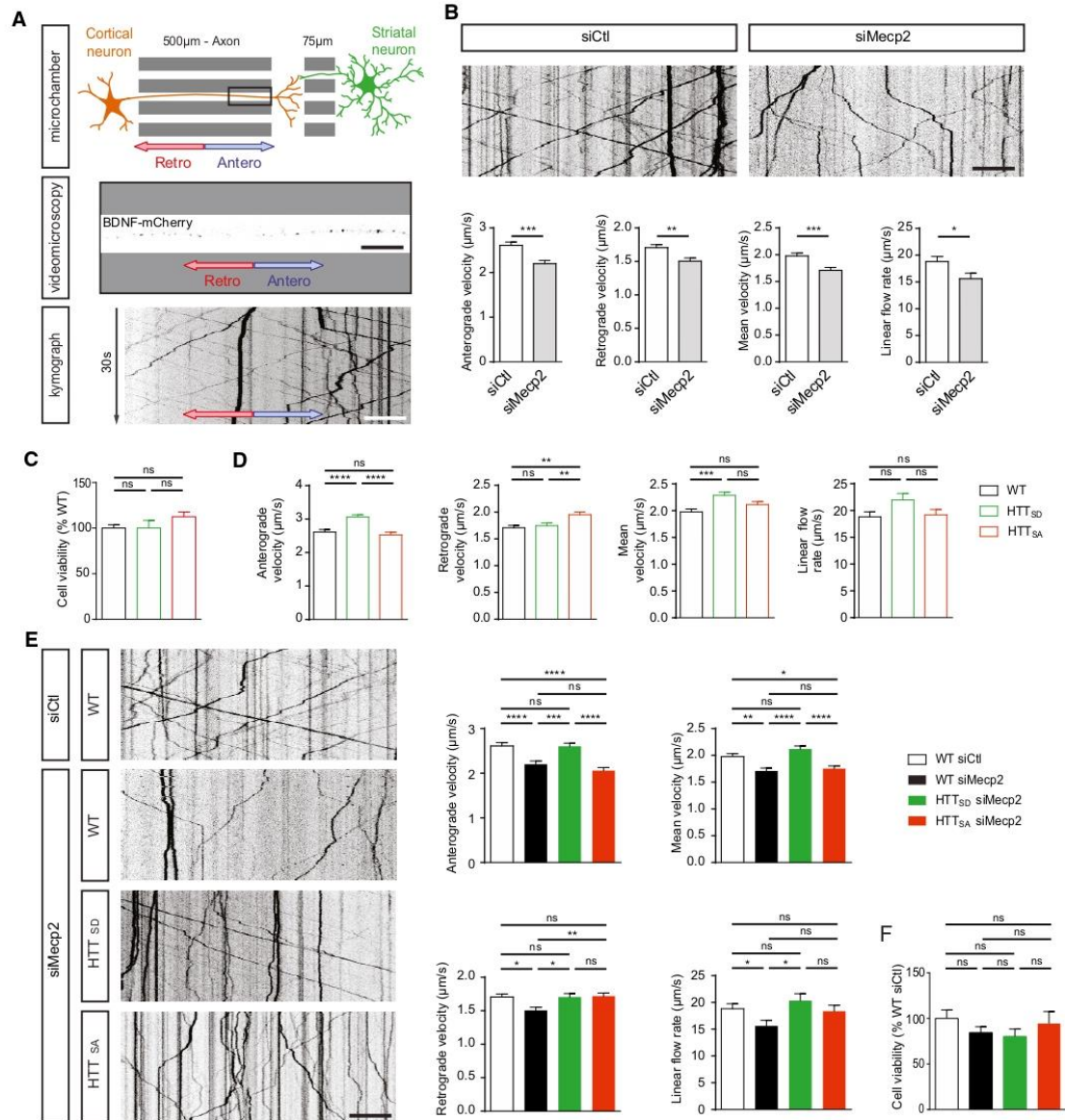


Figure 1.

**Figure 1. Huntingtin phosphorylation rescues BDNF transport in Mecp2-deficient axons.**

- A Microchamber that allows the isolation of axons within a corticostriatal network and live-cell imaging of axonal BDNF-mCherry transduced into mouse primary cortical neurons.
- B Representative kymographs and quantification of anterograde, retrograde, mean velocity, and linear flow rate of BDNF-mCherry-containing vesicles in cortical neurons transfected with siMecp2 ( $n = 753$  vesicles/81 axons) or siControl (siCtl) ( $n = 894$  vesicles/94 axons), inducing significant silencing of *Mecp2* (3 independent experiments; unpaired t-test).
- C Quantification of anterograde, retrograde, mean velocity, and linear flow rate of BDNF-mCherry trafficking into cortical neurons obtained from WT ( $n = 753$  vesicles/81 axons), HTT<sub>SA</sub> ( $n = 812$  vesicles/81 axons), or HTT<sub>SD</sub> ( $n = 787$  vesicles/82 axons) homozygous knock-in mice in which S421 of HTT was replaced by an alanine (HTT<sup>S421A/S421A</sup> or HTT<sub>SA</sub>), mimicking the absence of phosphorylation, or by an aspartic acid (HTT<sup>S421D/S421D</sup> or HTT<sub>SD</sub>), mimicking constitutive phosphorylation (3 independent experiments; one-way ANOVA test with Tukey's multiple comparisons).
- D Cell viability in WT ( $n = 3$ ), HTT<sub>SA</sub> ( $n = 1$ ), or HTT<sub>SD</sub> ( $n = 2$ ) neurons measured by MTT assay. No differences were observed between the different groups (three independent experiments; one-way ANOVA Kruskal–Wallis test,  $P = 0.5701$ ).
- E Kymographs and quantification of anterograde, retrograde, mean velocity, and linear flow rate of BDNF-mCherry axonal trafficking into WT ( $n = 894$  vesicles/94 axons), HTT<sub>SA</sub> ( $n = 812$  vesicles/82 axons), or HTT<sub>SD</sub> ( $n = 787$  vesicles/94 axons) cortical neurons transfected with siCtl or siMecp2, which significantly silenced *Mecp2* (three independent experiments; one-way ANOVA with Tukey's multiple comparisons).
- F Cell viability in WT, HTT<sub>SA</sub>, or HTT<sub>SD</sub> neurons transfected with siCtl or siMecp2 measured by MTT assay (WT siCtl:  $n = 3$ ; WT siMecp2:  $n = 3$ ; HTT<sub>SD</sub> siMecp2:  $n = 3$ ; HTT<sub>SA</sub> siMecp2:  $n = 2$ ). No differences were observed between the different groups (three independent experiments; one-way ANOVA Kruskal–Wallis test,  $P = 0.5701$ ).
- Data information: Scale bars = 20  $\mu$ m. \* $P < 0.05$ , \*\* $P < 0.01$ , \*\*\* $P < 0.001$ , \*\*\*\* $P < 0.0001$ , ns = not significant. Data are presented as the means  $\pm$  SEM.

#### Constitutive phosphorylation of HTT reduces the loss of body weight of *Mecp2* KO mice and extends their lifespan

We next investigated whether manipulating HTT phosphorylation *in vivo* could have an effect on *Mecp2* KO mouse symptoms. We first assessed the behavior of HTT<sub>SA</sub> and HTT<sub>SD</sub> homozygous mice using a modified SHIRPA primary screen (Appendix Table S1) and various behavioral assays (Fig EV2A–D) and found no significant differences between WT and HTT<sub>SA</sub> or HTT<sub>SD</sub> mice at 6 months in motor activity, strength, coordination, exploratory behavior, or body weight. *Mecp2* KO mice carrying the S421D mutation (KO/HTT<sub>SD</sub>) had a longer lifespan than *Mecp2* KO mice, though they still were subject to premature lethality, whereas KO/HTT<sub>SA</sub> mice showed no improvement over that of *Mecp2* KO mice (Fig 2B). KO/HTT<sub>SD</sub> mice also had greater body weight than the *Mecp2* KO mice, whereas the absence of phosphorylation in the KO/HTT<sub>SA</sub> mice had no effect on weight (Figs 2C and EV2E).

#### Constitutive phosphorylation of HTT reduces apneas in *Mecp2* KO mice

Breathing disturbances are prominent and deleterious in RTT patients (Kerr *et al*, 1997) and *Mecp2* KO mice (Viemari *et al*, 2005). We found that apnea frequency increased with age in *Mecp2* KO mice, from P35 to P55 (Fig 2D). The KO/HTT<sub>SD</sub> mice had significantly fewer apneas than *Mecp2* KO mice at both time points (Fig 2D). The absence of HTT phosphorylation slightly worsened this phenotype.

These data suggest that promoting HTT phosphorylation *in vivo* improves respiration in *Mecp2* KO mice.

#### Constitutive phosphorylation of HTT improves motor function of *Mecp2* KO mice

We next investigated motor coordination on the accelerating rotarod test (Pratte *et al*, 2011). In agreement with previous studies, *Mecp2* KO mice showed a progressive, significant decrease in the latency to fall relative to WT mice (Fig 2E). Promoting HTT phosphorylation delayed the appearance of motor incoordination until P55, but ablating HTT phosphorylation worsened motor coordination at both time

points (Fig 2E). HTT phosphorylation had no effect on the overall exploration pattern of *Mecp2* KO mice in the open-field (OF) test (Fig EV2F), but the time before initiation of the first movement was significantly longer for the *Mecp2* KO than WT mice (Fig 2F). The latency to explore the OF arena was further increased in KO/HTT<sub>SA</sub> mice, whereas it was reduced in the KO/HTT<sub>SD</sub> mice toward the values observed for WT mice (Fig 2F).

We next monitored circadian activity and found no deregulation in the circadian rhythm in the different genotypes during the day (Fig EV2G). There was, however, a striking suppression of spontaneous locomotion in the absence of *Mecp2* during the dark phase (7:00 PM–7:00 AM) (Fig EV2G). Promoting HTT phosphorylation enhanced spontaneous night activity, increasing the distance travelled by the KO/HTT<sub>SD</sub> mice, although it did not reach the value of the WT mice (Fig EV2H). Conversely, the distance travelled by the KO/HTT<sub>SA</sub> mice was significantly less than that covered by the KO/HTT<sub>SD</sub> mice. Overall, these results show that promoting HTT phosphorylation improves sensorimotor coordination and locomotor activity in *Mecp2* KO mice.

#### Inhibition of calcineurin by FK506 restores BDNF transport in *Mecp2*-silenced axons

Since chronic phosphorylation rescues BDNF trafficking *in vitro* and improves symptoms in mice, we investigated whether pharmacological induction of HTT phosphorylation could be of therapeutic value in RTT. We previously reported that HTT phosphorylation can be inhibited by the protein phosphatase calcineurin (Pardo *et al*, 2006; Pineda *et al*, 2009). We therefore evaluated whether FK506, a calcineurin inhibitor, can restore BDNF transport in *Mecp2*-silenced neurons by increasing HTT phosphorylation. Cortical neurons connected to striatal neurons within the microfluidic devices were transduced with the BDNF-mCherry lentiviral vector and a siRNA targeting either a control sequence or that of *Mecp2*. Five days after plating, we incubated the microfluidic chambers for 1 h with 1  $\mu$ M FK506 or vehicle and recorded BDNF axonal transport.

FK506 treatment increased HTT phosphorylation (Fig 3A) and rescued the reduced BDNF trafficking measured after *Mecp2* silencing (Fig 3B and C, Movie EV2). Both mean anterograde and



retrograde vesicle velocities were increased in *siMecp2*-transfected neurons, with a significant overall effect on mean velocity and linear flow (Fig 3C). The number of moving vesicles did not

change (Fig 3C). FK506-induced calcineurin inhibition thus mitigates deficits of BDNF transport observed in *Mecp2*-silenced neurons.

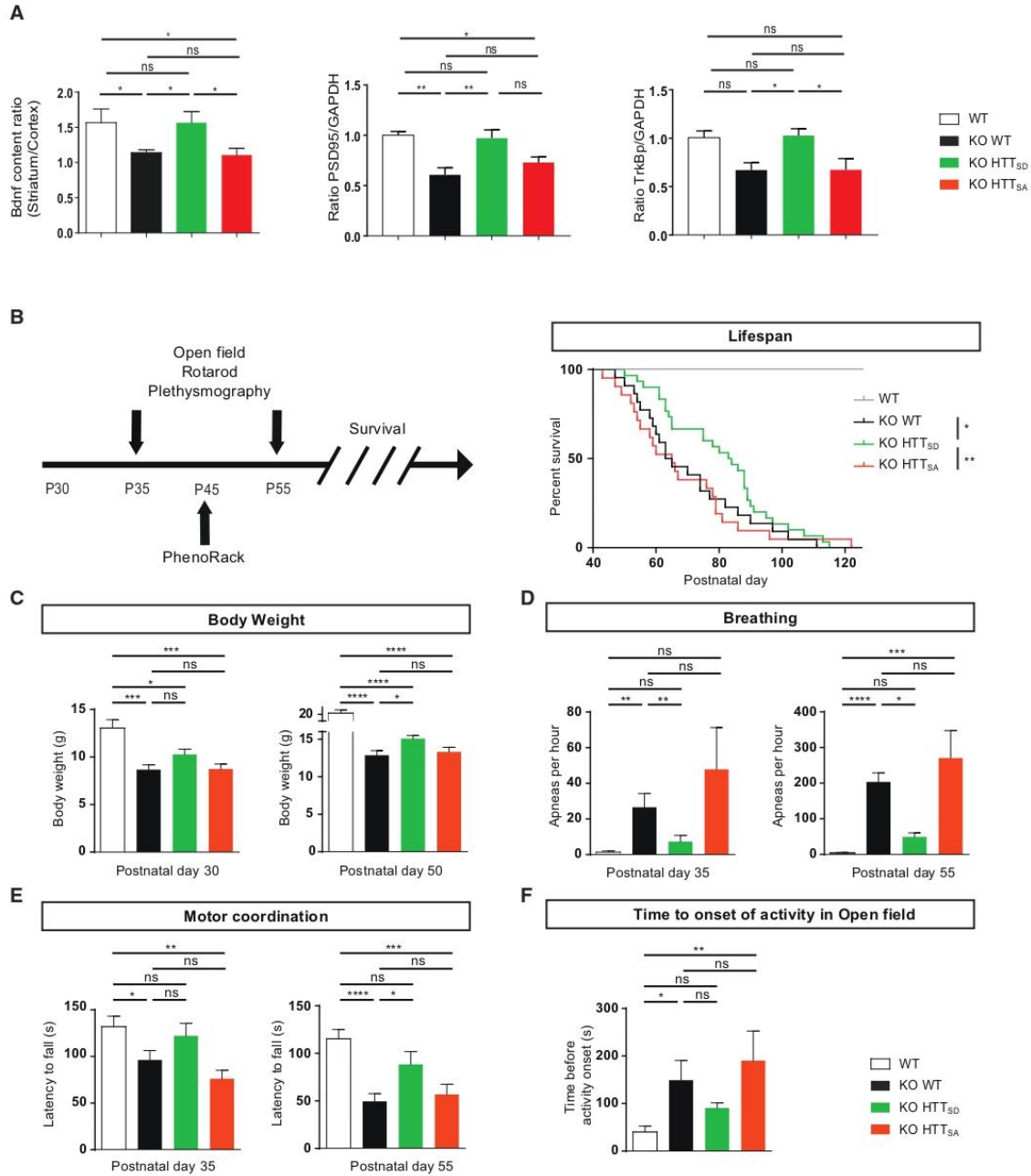


Figure 2.

**Figure 2. The S421D mutation improves BDNF corticostriatal transport *in vivo*, the motor and autonomic functions of *Mecp2*-deficient mice and increases their lifespan.**

A Left: The ratio between the striatal and the cortical BDNF determined by quantifying the level of BDNF proteins at the cortex and the striatum of 55-day-old WT ( $n = 8$ ), *Mecp2* KO ( $n = 6$ ), *Mecp2* KO/HTT<sub>SD</sub> (mimicking the absence of phosphorylation) ( $n = 4$ ), and *Mecp2* KO/HTT<sub>SA</sub> mice (mimicking constitutive phosphorylation) ( $n = 5$ ). Since striatal BDNF depends only on BDNF transport from the cortex, this ratio reflects BDNF transport through corticostriatal pathway (Mann–Whitney test). Right: Quantitative analysis of phospho-TrkB protein level in striatum of KO WT mice and KO HTT<sub>SD</sub> mice by immunoblotting. The relative expression levels of phospho-TrkB were normalized against GAPDH and are presented as the ratio ( $n = 6$  mice per group) (Mann–Whitney test). Middle: Quantitative analysis of PSD-95 protein level in striatum of *Mecp2* KO/HTT WT mice and KO/HTT<sub>SD</sub> mice by immunoblotting. The relative expression levels of PSD-95 were normalized against GAPDH and are presented as the ratio ( $n = 6$  mice per group) (Mann–Whitney test).

B Left: We investigated the behavior of *Mecp2* KO mice at 35, 45, and 55 days of age and assessed their survival. Right: KO/HTT<sub>SD</sub> mice ( $n = 30$ ) and WT mice ( $n = 17$ ) had a significantly longer lifespan than KO ( $n = 22$ ) or KO/HTT<sub>SA</sub> mice ( $n = 21$ ) (Kaplan–Meier survival test).

C Body weight of 10 WT, 24 KO, 32 KO/HTT<sub>SD</sub>, and 24 KO/HTT<sub>SA</sub> mice at P30 and P50 (one-way ANOVA with Tukey's comparison).

D Frequency of apnea of 9 WT, 10 KO, 14 KO/HTT<sub>SD</sub>, and 9 KO/HTT<sub>SA</sub> mice at P35 and P55 (Kruskal–Wallis test with Dunn's comparison).

E KO/HTT<sub>SD</sub> mice ( $n = 19$ ) performed as well as WT ( $n = 17$ ) at P35 on the accelerating rotarod test and continued to outperform *Mecp2* KO ( $n = 16$ ) and KO/HTT<sub>SA</sub> ( $n = 13$ ) at P55 (one-way ANOVA with Fisher's LSD test).

F Time before the onset of spontaneous locomotor activity of 17 WT, 20 KO, 19 KO/HTT<sub>SD</sub>, and 17 KO/HTT<sub>SA</sub> mice at P55. (Kruskal–Wallis test with Dunn's comparison).

Data information: Data are presented as the means  $\pm$  SEM. \* $P < 0.05$ , \*\* $P < 0.01$ , \*\*\* $P < 0.001$ , \*\*\*\* $P < 0.0001$ , ns = not significant.

### FK506 increases HTT phosphorylation in *Mecp2* KO mice

To determine whether calcineurin inhibition via FK506 treatment could improve *Mecp2* KO mouse symptoms, we treated *Mecp2* KO, WT and HTT<sub>SA</sub> mice with FK506 to induce HTT phosphorylation. Mice were first injected intraperitoneally with FK506 (5 mg/kg) and sacrificed 2 h after administration, as previously described (Pardo *et al*, 2006). We analyzed HTT phosphorylation at S421 by immunoblotting fresh whole-brain protein extract (Figs 4A and EV3A and B). As previously described, administration of FK506 in WT mice increased HTT phosphorylation, by about 1.3-fold (Pardo *et al*, 2006). In *Mecp2* KO mice, FK506 doubled HTT phosphorylation relative to vehicle. FK506 had no effect on HTT phosphorylation in HTT<sub>SA</sub> mice (Fig EV3A and B).

### FK506 treatment improves respiration and motor function of *Mecp2* KO mice and extends their lifespan via HTT phosphorylation

To determine whether FK506 could improve the *Mecp2*-deficient phenotype, we treated *Mecp2* KO mice by intraperitoneal FK506 injection (10 mg/kg), three times a week, starting at P30. We choose P30 as a starting point, since the onset of the *Mecp2*-knockout phenotype is already apparent at this stage as breathing abnormalities, locomotor deficits, and body weight loss (Guy *et al*, 2001; Viemari *et al*, 2005; Matagne *et al*, 2017). FK506 treatment significantly increased the lifespan of *Mecp2* KO mice (Fig 4B) and

induced a significant increase in body weight by P55 (Fig 4C). The number of apneas was significantly lower in the FK506-treated group than the vehicle group at P35 and remained lower at P55 (Fig 4D). FK506-treated *Mecp2* KO mice performed better on the accelerating rotarod at P50 (Fig 4E) and showed better forelimb muscle strength than the vehicle group (Fig 4F). We next investigated cell death in the striatum of these mice. In accord with previous reports (Reiss *et al*, 1993; Kishi & Macklis, 2004; Armstrong, 2005; Roux *et al*, 2007), we did not detect any cell death in *Mecp2* KO mice by cleaved caspase-3 immunodetection or by TUNEL assay (Fig EV4A and B). Importantly, we found that FK506 treatment did not induce any neuronal toxicity or cell death after 20 days of treatment (Fig EV4A and B).

We also verified the induction of HTT phosphorylation in *Mecp2*-deficient mice after 20 days of FK506 chronic treatment. Mouse brain samples were analyzed 2 hrs after the last treatment. We did not detect any difference in *Mecp2* protein levels or in HTT phosphorylation in wild-type mice treated with FK506 (Fig EV3B and C). However, at this time point we did not detect elevated HTT phosphorylation in the samples treated with FK506 relative to DMSO-treated animals, likely because repeated treatments desensitize the pathway. We observed a trend toward reduction in cFos staining in *Mecp2*-deficient mice that was increased back to control levels in FK506-treated *Mecp2* KO mice, suggesting a positive treatment effect (Fig EV4C and D).

To establish that the beneficial effect of FK506 is mediated by HTT phosphorylation at S421, we treated KO/HTT<sub>SA</sub> mice by intraperitoneal FK506 injection as previously done (Fig 4).

**Figure 3. FK506 restores BDNF axonal transport in *Mecp2*-silenced axons.**

A Western blot analysis of DIV 5 cortical neurons transfected with siMecp2 or siControl (siCtl) and treated with 1  $\mu$ M FK506 or vehicle for 1 h, and quantification of pS421 HTT ( $n = 9$  per group). Data are presented as means  $\pm$  SEM, \* $P < 0.05$ , \*\* $P < 0.01$ , \*\*\* $P < 0.001$ , Mann–Whitney test.

B Representative kymographs showing axonal trafficking of BDNF-mCherry-containing vesicles in cortical neurons transfected with siMecp2 or siControl (siCtl) and treated with 1  $\mu$ M FK506 or vehicle for 1 h. Scale bar = 20  $\mu$ m.

C Quantification of anterograde, retrograde, mean velocity, linear flow rate, and number of BDNF-mCherry-containing vesicles from the data in (A) (siMecp2+Vehicle:  $n = 801$  vesicles/95 axons; siMecp2+FK506:  $n = 1020$  vesicles/116 axons; siCtl+Vehicle:  $n = 780$  vesicles/83 axons; siCtl+FK506:  $n = 1,029$  vesicles/102 axons). Data are presented as the mean  $\pm$  SEM of at least three independent experiments (one-way ANOVA with Tukey's comparison). \* $P < 0.05$ , \*\* $P < 0.01$ , \*\*\* $P < 0.001$ , \*\*\*\* $P < 0.0001$ , ns = not significant.

Source data are available online for this figure.

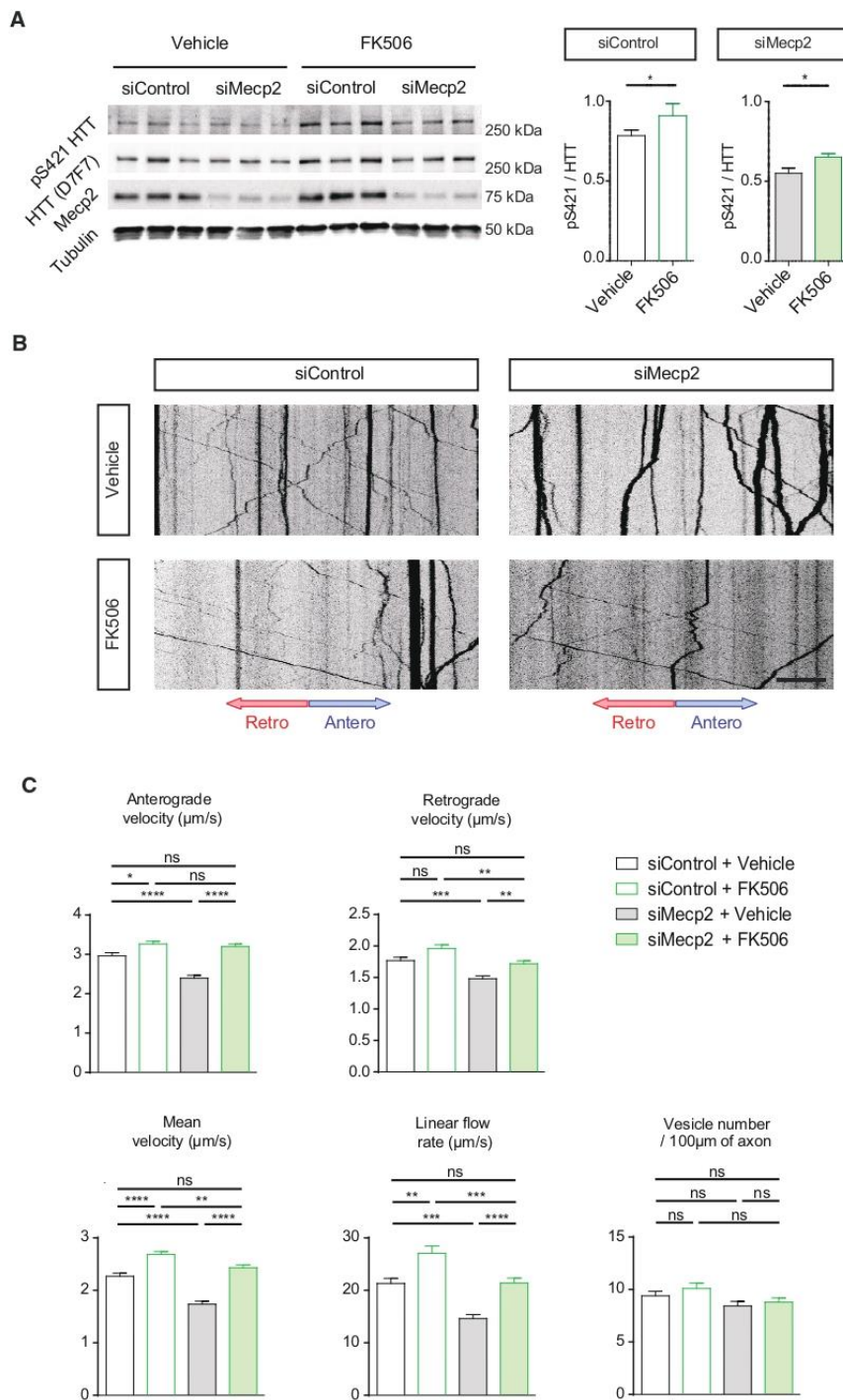
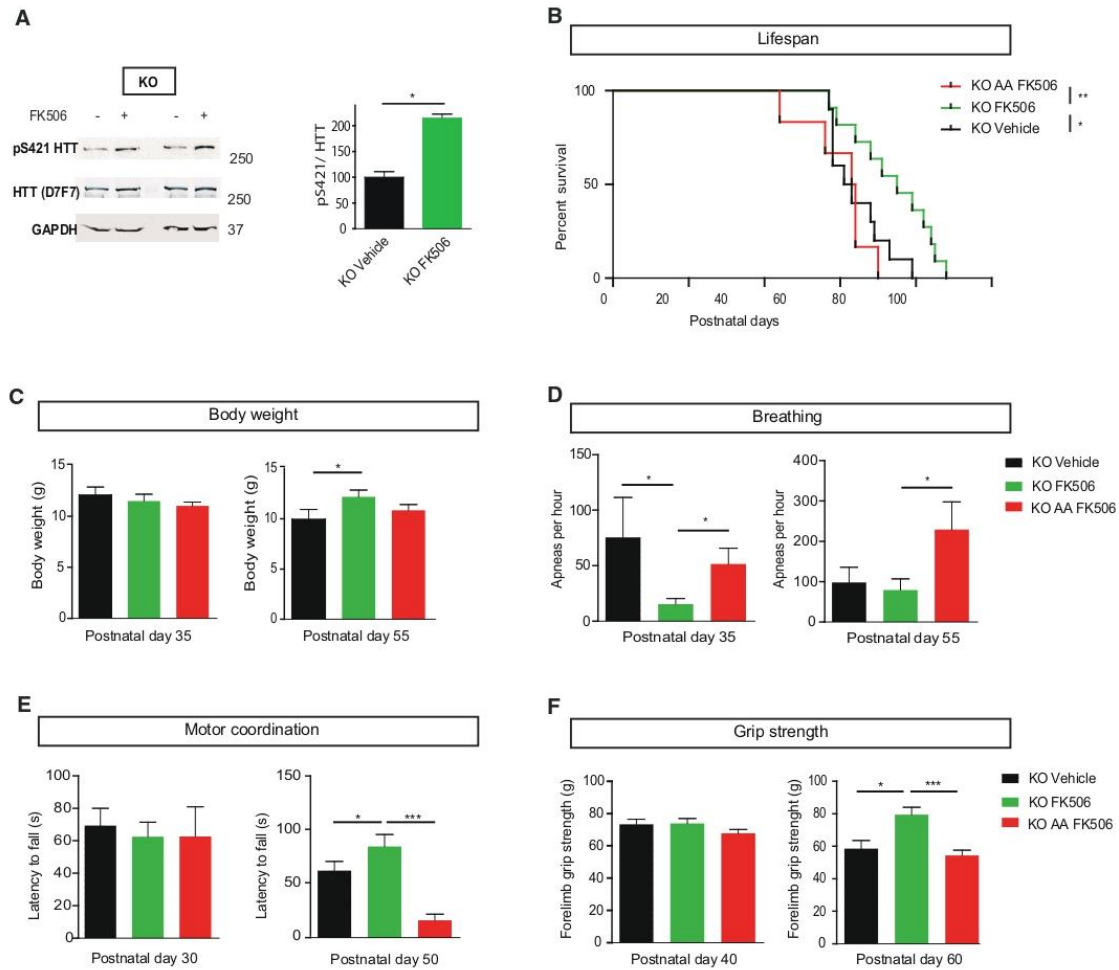


Figure 3.



**Figure 4. Calcineurin inhibition by FK506 in *Mecp2*-deficient mice improves motor and autonomic functions and extends lifespan through huntingtin-dependent phosphorylation.**

**A** Western blot of HTT S421 phosphorylation. We treated 30-day-old *Mecp2* KO mice intraperitoneally with FK506 (5 mg/kg) or vehicle and analyzed brain extracts for endogenous HTT phosphorylation by Western blotting, 2 h after administration, using an anti-phospho-HTT-S421 specific antibody. The D7F7 antibody recognizes total HTT. The relative protein level of phospho-HTT was normalized to total HTT protein level and is presented as the ratio (KO FK506  $n = 4$ , KO Vehicle  $n = 4$ ). Data are presented as means  $\pm$  SEM, \* $P < 0.05$ , Mann-Whitney test).

**B–F** We treated 30-day-old *Mecp2* KO mice ( $n = 10$ ) and KO/HTT<sub>SA</sub> mice ( $n = 10$ ) with 5 mg/kg FK506 three times a week by intraperitoneal injection and assessed them in various behavioral tests. (B) FK506-treated KO mice lived longer than vehicle-treated KO mice and FK506-treated KO HTT<sub>SA</sub> mice (Kaplan–Meier survival test). (C) Body weight of FK506-treated KO, FK506-treated KO HTT<sub>SA</sub>, and vehicle-treated KO mice at P35 and P55 (Mann–Whitney test). (D) Frequency of apnea of FK506-treated KO, FK506-treated KO HTT<sub>SA</sub>, and vehicle-treated KO mice at P35 and P55 (Mann–Whitney test). (E) Motor coordination of FK506-treated KO, FK506-treated KO HTT<sub>SA</sub>, and vehicle-treated KO mice on the accelerating rotarod test at P30 and P50 (Mann–Whitney test). (F) Forelimb strength of FK506-treated KO, FK506-treated KO HTT<sub>SA</sub>, and vehicle-treated KO mice assessed by the grip strength test at P40 and P60 (Mann–Whitney test).

Data information: \* $P < 0.05$ , \*\* $P < 0.01$ , \*\*\* $P < 0.001$ , ns = not significant. Data are means  $\pm$  SEM.

Source data are available online for this figure.

Interestingly, the lifespan of *Mecp2* KO/HTT<sub>SA</sub> mice was significantly shorter than that of *Mecp2* KO mice (Fig 4B). Moreover, FK506 treatment affected neither motor function nor apneas of

KO HTT<sub>SA</sub> mice (Fig 4D–F). These results demonstrate that HTT phosphorylation at S421 is essential for the therapeutic effect of FK506.

## Discussion

Here, we demonstrate that genetically or pharmacologically inducing HTT phosphorylation at S421 rescues BDNF vesicular transport in *Mecp2*-silenced projecting corticostriatal neurons and improves several pathophysiological features of *Mecp2* KO mice. The ability of FK506 as a proof-of-principle candidate to improve *Mecp2* symptoms highlights the feasibility of pharmacological stimulation of HTT S421-P in a mouse model of RTT. Importantly, our findings show that HTT phosphorylation can stimulate endogenous machinery to promote BDNF trafficking in the corticostriatal network.

There has been considerable interest in modulating BDNF expression and signaling as a treatment for RTT. Unfortunately, BDNF itself has very low blood-brain barrier (BBB) permeability, precluding its peripheral administration as a potential therapy. Several studies have used indirect stimulation of BDNF metabolism via fingolimod (Deogracias *et al*, 2012) or ampakine treatment (Ogier *et al*, 2007) to circumvent this limitation, but these pharmacological treatments only partially improved the phenotype of *Mecp2* KO mice. Daily injection of IGF-1, another neurotrophic factor that can cross the BBB and is known to induce Akt phosphorylation (Humbert *et al*, 2002), has been found to improve survival, locomotor activity, and respiratory rhythm in *Mecp2* KO mice (Tropea *et al*, 2009). Finally, potential agonists of the TrkB receptor, such as 7,8-dihydroxyflavone (Johnson *et al*, 2012) and LM22A-4 (Schmid *et al*, 2012; Kron *et al*, 2014; Li *et al*, 2017), improved breathing patterns in *Mecp2* KO mice. It is important to note, however, that the improvements observed in these different studies required that pharmacological treatments be initiated before the appearance of the first symptoms.

Given that RTT is not diagnosed until long after symptoms have begun, we searched for a more practical translational approach based on observed improvements in the RTT phenotype by constitutive phosphorylation of HTT. We selected FK506 because Pardo *et al* (2006) found that this drug increases phosphorylation of mutant HTT. Importantly, FK506 also induces HTT phosphorylation in *Mecp2* KO mice. Our results showed that FK506 treatment, starting at an already-symptomatic stage, improved the lifespan, motor strength and coordination, and exploratory behavior, and reduced the frequency of apneas in *Mecp2* KO mice in a manner that requires HTT phosphorylation at S421. Thus, part of the beneficial effect of FK506 treatment is due to the stimulation of the HTT-dependent transport of BDNF. It is possible that FK506 also modulates the trafficking of other cargo, such as mitochondria, which could contribute to the *in vivo* improvement we saw in the *Mecp2* KO mice. Future studies investigating such additional effects would be of interest, as they would increase the therapeutic relevance of FK506 treatment for *Mecp2* symptoms (Reddy *et al*, 2012).

We conclude that BDNF trafficking and supply are diminished in the absence of *Mecp2* and can be effectively stimulated by promoting HTT phosphorylation. Our results are in accord with a recent study that demonstrated that BDNF acts cell-autonomously in an autocrine loop, as wild-type neurons were unable to rescue growth deficits of neighboring *Mecp2*-deficient neurons (Sampathkumar *et al*, 2016). Thus, HTT phosphorylation may increase the bioavailability of BDNF at the synapse through autocrine and paracrine mechanisms in the brains of *Mecp2* KO mice and likely represents a

strategy of therapeutic interest versus a general, non-synapse-specific increase of BDNF levels in the brain.

## Materials and Methods

### Mouse breeding and genotyping

All mouse lines were on a C57BL/6J genetic background. The *Mecp2*<sup>tm1-1Bird</sup> *Mecp2*-deficient mice were obtained from the Jackson Laboratory and maintained on a C57BL/6 background by using C56BL/6J male breeders (also from the Jackson Laboratory). The HTT knock-in mice were previously generated by inserting a point mutation in exon 9 (AGC>GAC, Ser>Asp called S421D or AGC>GCC, Ser>Ala called S421A) (Thion *et al*, 2015). To obtain double-mutant mice (*Mecp2* KO and S421A or S421D), heterozygous females (*Mecp2*<sup>+/-</sup>) were crossed with homozygous S421D or S421A males.

Hemizygous mutant males (*Mecp2*<sup>-/-</sup> also called *Mecp2* KO) were generated by crossing heterozygous females (*Mecp2*<sup>+/-</sup>) with C57BL/6 males. Genotyping was performed by routine PCR technique following a previously described protocol (Roux *et al*, 2012). Animals were housed under standard conditions of temperature (21 ± 2°C) and humidity (55 ± 5%), with food and water *ad libitum* in a 12:12 h day/night cycle.

Only male mice were used for all genotypes and experiments.

Experimental protocols were approved by the ethical committee of the Aix Marseille University and the French M.E.N.E.S.R. minister (Permit Number: 02910.02).

The experimental procedures were carried out in keeping with the European guidelines for the care and use of laboratory animals (EU directive 2010/63/EU), the guide for the care and use of the laboratory animals of the French national institute for science and health (INSERM). All experiments were made to minimize animal suffering. In order to reduce animal suffering, endpoints were fixed as weight loss limit (below 80% of maximum weight), obvious breathing defects, or severe injury. In these cases, animals were euthanized with an overdose of pentobarbital (100 mg/kg BW i.p., Ceva Santé Animale, La Ballastiere, France).

### FK506 chronic *in vivo* treatment of *Mecp2*-deficient mice (KO and KO/HTT<sub>SA</sub>)

*Mecp2* KO mice were randomly assigned in groups. From P30, animals received an i.p. injection three times a week of either 10 mg/kg FK506 in 17% DMSO or vehicle alone (17% DMSO). The first group was used for behavioral testing and evaluating survival (see below). A second group was used to assess the chronic effects of FK506 treatment from P30 to P50 on cellular and molecular parameters.

### Behavioral testing

All mice were weighed every 5 days and assessed for survival. At P35, P45, and P55, each animal underwent a set of behavioral tests to assess motor function, activity, and breathing pattern (Fig 2). All testing occurred during the light phase of the light-dark cycle (except for the PhenoRack monitoring). All the behavioral experiments were performed blinded to HTT genotype and treatment.

**Open field**

An arena made of clear perspex (38 × 30 cm), under controlled light conditions (300 lx), was used for the FK506 study. For the genetic study, mice were placed in a 1-m-diameter arena under controlled light conditions (300 lx). Activity was recorded using the Videotrack software (Viewpoint, Lyon, France) for 20 min. Activity and average velocity (cm/s) were determined from the total distance moved and activity duration. Vertical activity (rearing, leaning, and grooming) was noted by an experimenter blind of the genotype.

**Rotarod**

Sensorimotor abilities were assessed by the accelerating Rotarod apparatus (Panlab LE-8200, Harvard Apparatus). Each trial started at 4 rpm and reached 40 rpm speed after 300 s. Mice underwent three trials, with 5-min rest time in between. The trial ended when the mouse fell off the rod or after 300 s. Latency to fall (in second) was measured, and only, the best trial was recorded. In the case of mice clinging to the rod, the trial was stopped and the passive rotation was considered a failure in performance like falling (Brown *et al*, 2005).

**Grip strength**

A Bioseb grip strength meter (Panlab) was used to measure forelimb strength. Five measures for each mouse were taken, and means were calculated from the three best trials.

**Whole-body plethysmography**

To assess apneas, mice were placed in a clear plexiglass chamber (200 ml) and allowed to breathe naturally under conscious and unrestrained conditions. After a ~30-min adaptation, breathing was recorded: The spirogram was obtained by recording the pressure difference between the two chambers, and then, the signal was amplified, filtered and fed to an analog-to-digital converter (sampling frequency, 1 kHz), and finally analyzed by the Spike2 interface and software (v.5.04, Cambridge Electronic Design Ltd., Cambridge, UK). Apneas were defined by more than 1s without breathing, as previously described (Roux *et al*, 2007). Breathing cycles were divided into four groups according to their duration: hyperventilation (including cycles in the range 0–0.3 s range); ventilation (0.3–0.7 s); hypoventilation (0.7–1 s); and apneas (1–∞ s). The breathing variability was calculated as the mean standard variability. Breathing parameters were obtained from the analysis of quiet period of at least 100 consecutive cycles (Fig EV5).

**Home cage activity**

To analyze spontaneous activity and circadian rhythm, mice were put in individual cages and monitored by the PhenoRack system (Viewpoint, Lyon, France). Mice locomotion was tracked by infrared light during 48 h, and after a 24-h adaptation phase, only the last 24-h activity was analyzed. The recorded data allowed us to analyze activity, distance (cm), and velocity (cm/sec).

**BDNF immunoassay**

P55 ( $n = 4$  Wt;  $n = 4$  *Mecp2* KO;  $n = 4$  KO/HTT<sub>SD</sub>;  $n = 5$  KO/HTT<sub>SA</sub>) male mice were euthanized by cervical dislocation, and their brains were dissected out within the first 2 min post-mortem. The cortex and the striatum were microdissected using a punching

needle (0.5 mm in diameter). Briefly, brain area dissection was performed on cryostat brain sections with the help of a 5× magnifying lens, following their stereotaxic coordinates (Paxinos and Franklin, 2001). We dissected cortical and striatal samples only coming from the same slice in the same rostro-caudal level. Tissue samples were freshly isolated and lysed in 200 μl of the extraction buffer (100 mM Tris-pH 7.5, 125 mM NaCl, 0.1 mM EGTA, 0.1% Triton X-100, Roche<sup>®</sup> protease inhibitors cocktail), sonicated, centrifugated. The supernatant was stored at –80°C until assay. Total protein concentration was determined by using the bicinchoninic acid (BCA) protein assay (Thermo Fisher scientific) and measured with a spectrophotometer (Glomax, Promega). The level of BDNF protein from tissue extracts was determined with the BDNF Emax<sup>®</sup> ImmunoAssay System (Promega) using the manufacturer's instruction. In the present study, we measured only free mature BDNF, and therefore, we proceeded directly to the ELISA protocol avoiding any acid treatment. In each assay, duplicate wells were assigned for each sample. A Victor 4 PerkinElmer microplate reader was used to measure signal intensity from the wells at 450 nm. A linear standard curve was generated with standard BDNF from 5.8 to 500 pg/ml. The total amount of BDNF per well was calculated based on the standard curve, and each sample value was within the linear range. The relative BDNF value was then calculated by normalizing the amount of BDNF against the total amount of protein input.

**Western blotting**

Adult (P55) male mice were euthanized by cervical dislocation, and their brains were dissected out within the first 2 min post-mortem. Brains were dissected on ice, and proteins were extracted by sonication and isolated in a lysis buffer containing 50 mM Tris-HCl (pH = 7.5), 150 mM NaCl, 2 mM EGTA, 2 mM EDTA, 1% Triton X-100, 10 mM betaglycerophosphate, 5 mM sodium pyrophosphate, 50 mM sodium fluoride, and Halt<sup>™</sup> proteases and phosphatases inhibitor cocktail (Pierce Thermo Fisher). Proteins were extracted from neuronal culture with lysis buffer containing 4 mM HEPES, pH 7.4, 320 mM sucrose, and protease inhibitor cocktail (Roche). Protein concentrations were determined by the bicinchoninic acid method. After a denaturation step at 96°C for 5 min, proteins (100 μg) were separated on 4–20% SDS-polyacrylamide gel (Life technology) and transferred onto a nitrocellulose membrane by electroblotting using the Trans-Blot turbo transfer system (Bio-Rad). The membrane was blocked with blocking buffer (Millipore, WBAVDFL01) for 1 h at room temperature. Primary antibodies for HTT [1:1,000, rabbit, clone D7F7, CST (Lunkes *et al*, 2002)], HTT-pS421 [1:500, rabbit homemade previously described (Humbert *et al*, 2002)], *Mecp2* [1:1,000, rabbit, CST], TRKB-p816 (Millipore ABN1381), PSD-95 [1:1,000, Neuromab], Tubulin [1:5,000, mouse, Sigma], GAPDH [1:5,000, rabbit, Sigma], Actin [1:10,000, mouse, Millipore], and Calnexin [1:1,000, rabbit, Sigma C4731] were diluted in the same solution and incubated overnight at 4°C. The membrane was incubated using appropriate HRP secondary antibodies (donkey anti-rabbit 711-035-152 and donkey anti-mouse 715-035-150; Jackson ImmunoResearch Laboratory and Bio-Rad ChemiDoc XRS System) or fluorescent secondary antibodies (IRDye 800 CW, IRDye 680 RD, LI-COR, and LI-COR Odyssey Imager). Quantitative analyses of signal intensity were performed using ImageJ software. For

quantification, total (phospho-independent) protein signals were used to normalize the phospho-protein signal.

### Immunohistochemistry

Mice were euthanized with pentobarbital and transcardially perfused with 0.01 M PBS followed by 4% paraformaldehyde (PFA) in phosphate buffer. Brains were removed, fixed in 4% PFA overnight at 4°C, and then cryopreserved in 20% sucrose for 3 days. Brains were then rapidly frozen and coronally sectioned into 50- $\mu$ m sections using a Leica VT1200s cryostat (Leica Biosystems). Sections were rehydrated in PBS three times for 10 min and blocked with 7% normal goat serum in PBS for 1 h and then incubated overnight at room temperature (RT) with anti-cFos (1/200, rabbit, Abcam ab209794) or anti-cleaved caspase-3 (1/400, rabbit, Cell signaling) antibodies. The sections were then washed three times for 10 min each in PBS followed by incubation for 2 h with the following secondary antibodies: Alexa Fluor 488-labeled goat anti-rabbit at 1/400. After staining, the sections were washed three times, for 10 min each in PBS, and then incubated 10 min in DAPI. After a last 10-min wash, sections were mounted in Immu-mount (Thermo Scientific). The immunolabeled slices were digitized and recorded using an Apotome Axioimager 2 (Carl Zeiss) or a Zeiss Lumar stereomicroscope coupled to AxioCam digital camera (Axiovision 4.4, Carl Zeiss).

### Videomicroscopy

Embryonic (E15.5) neuronal cultures were prepared as previously described (Liot *et al.*, 2013). Ganglionic eminences and cortex were dissected, and dissociated cortical neurons were nucleofected with ON-TARGET plus mouse Mecp2 siRNA or Non-targeting siRNA 1 (Dharmacon) according to the protocol of Amaxa Nucleofection (Lonza). Then, neurons were plated into microchambers coated with poly-D-lysine (0.1 mg/ml) in the cortical and synaptic compartment or poly-D-lysine and laminin (10  $\mu$ g/ml, Sigma) into the striatal compartment and cultured at 37°C in a 5% CO<sub>2</sub> incubator for 5 days. After 24 h in culture, cortical neurons were transduced with lentivector coding for BDNF-mCherry into presynaptic neuron chamber for axonal transport analysis as previously described (Virlogeux *et al.*, 2018). Acquisitions were done on microgrooves, at the limit of the synaptic compartment, at 5 Hz for 30 s on inverted microscope (Axio Observer, Zeiss) coupled to a spinning disk confocal system (CSU-W1-T3; Yokogawa) connected to an electron-multiplying CCD (charge-coupled device) camera (ProEM+1024, Princeton Instrument) at 37°C and 5% CO<sub>2</sub>. Quantifications of vesicle velocity, linear flow rate, and vesicle number were done on 100  $\mu$ m of axon using KymoTool Box ImageJ plug-in as previously described (Zala *et al.*, 2013; Virlogeux *et al.*, 2018). Vesicle velocity corresponds to segmental anterograde or retrograde velocity. Directional net flux is the anterograde cumulative distance minus the retrograde cumulative distance. Regarding vesicle number, a vesicle is considered anterograde when the distance travelled by one vesicle is more anterograde than retrograde.

### MTT assay

In a corticostriatal network, at DIV 11 or 12, presynaptic chamber was filled with MTT 1/10<sup>6</sup> from MTT solution at 5 mg/ml. After a

3.5-h incubation at 37°C, MTT solution was carefully removed from the presynaptic chamber and MTT solvent was added (10% SDS, 1.2 mM HCl) for 30 min under agitation. Then, MTT solvent was removed from the microfluidics device and put in a well within a 96-well plate. The absorbance was read at 490 nm on a microplate reader (PHERAstar FS, BMG labtech). Negative controls (dead cells) were treated with H<sub>2</sub>O<sub>2</sub> at 100 mM for 48 h before the experiment.

### Terminal deoxynucleotidyl transferase dUTP nick end labeling (TUNEL) of apoptotic cells

Cell apoptosis was measured *in vivo* using the Click-It™ Plus TUNEL Assay (Invitrogen) according to the manufacturer's protocol.

### Statistical analysis

All analyses were performed using GraphPad Prism for Windows/MacOS (GraphPad Software, La Jolla, California, USA, www.graphpad.com). The results are reported as mean  $\pm$  standard error of the mean (SEM). A  $P < 0.05$  was considered to be statistically significant. For group comparisons, normality distribution of the datasets was tested before performing any statistical test by Shapiro's test. In case of non-normal distribution, a non-parametric test was performed. When ANOVA was used, Brown Forsythe's test verifies that the variance is homogenous. One-way ANOVAs were performed as indicated with Dunnett's post-hoc analysis for pairwise comparisons when normal distribution. Kruskal–Wallis test with Dunn's multiple comparison was performed on datasets without normal distribution. When appropriate, two groups were compared with an unpaired two-way *t*-test or Mann–Whitney test on datasets without normal distribution. The Kaplan–Meier log-rank test was used for survival studies.

**Expanded View** for this article is available online.

### Acknowledgements

We thank S. Humbert for sharing the *HTT*<sup>5421A</sup> and *HTT*<sup>5421D</sup> mice and for advice; the GIN imaging facility (PIC-GIN) for help with image acquisitions; G. Froment, D. Nègre, and C. Costa from the lentivirus production facility of SFR Biosciences (UMS3444/CNRS, US8/Inserm, ENS de Lyon, UCBL); and V. Brandt for critical reading of the manuscript. This work was supported by grants from Agence Nationale pour la Recherche (ANR-2012-BSV1-0003-03 ANTARES, J.C.R. & F.S., ANR-14-CE35-0027-01 PASSAGE, F.S.; ANR-15-JPWG-0003-05 EU Joint Program-Neurodegenerative Disease (JPND) Research project CircProt (no. 643417), (F.S.), Fondation pour la Recherche Médicale (FRM, équipe labellisée, F.S.), Fondation Bettencourt Schueller (F.S.), Fédération pour la Recherche sur le Cerveau (F.S.), Inserm (J.C.R. & F.S.), Aix-Marseille Université (J.C.R.), AFSR (J.C.R.), Institut d'établissement d'AMU "Marseille Maladies Rares" (MarMaRa) (J.C.R.), Promex Stiftung Für Die Forschung (J.C.R.), Rettsyndrom.org (J.C.R.), and NeuroCoG in the framework of the "Investissements d'avenir" program (ANR-15-IDEX-02, F.S.). F.S. laboratory is member of the Grenoble Center of Excellence in Neurodegeneration (GREEN).

### Author contributions

YE, JB, NP, Y-SA, BD, LV, FS, and JCR designed experiments. YE, JB, NP, Y-SA, LS, VM, CS, EB, and HV performed experiments. YE, JB, NP, Y-SA, LS, VM, CS, HV, BD, LV, FS, EB, and J-CR analyzed the data, and YE, JB, FS, and J-CR wrote the manuscript.

**The paper explained****Problem**

Rett syndrome (RTT) is a severe neurodevelopmental disorder that becomes apparent in the second year of life, robbing girls of the motor, language, and social skills they acquired and replacing them with learning impairments, stereotypic behaviors, seizures, respiratory dysrhythmias, and a host of other symptoms. RTT is caused by mutations in the X-linked gene *MECP2* (Methyl-CpG-binding protein 2), which encodes the MeCP2 protein, an epigenetic factor that governs the expression of thousands of neuronal genes. Even if gene therapy becomes possible, the introduction of the *MECP2* gene into a cell already expressing a wild-type copy would cause a problem of MeCP2 dosage (MeCP2 duplication syndrome is an equally severe disorder). We therefore need viable approaches to therapy. Several studies have linked the loss of MeCP2 function to reductions in the levels of BDNF (brain-derived neurotrophic factor) in the brain of RTT patients as well as in mouse models. BDNF is crucial to learning and memory, but transport of BDNF-containing vesicles from the cortex to the striatum is abnormally reduced in *Mecp2* knockout (KO) mouse neurons. Intriguingly, BDNF is transported within neurons by the Huntingtin protein (HTT), so named because mutations in HTT underlie Huntington's disease. In the present study, we tested whether promoting HTT's transport function by stimulating its phosphorylation at serine 421 (S421) might restore BDNF transport.

**Results**

We used genetic and pharmacological approaches to promote HTT phosphorylation at S421 in both *Mecp2*-deficient neurons and *Mecp2* knockout mice. We also evaluated the consequences of HTT S421 phosphorylation on BDNF axonal trafficking in projecting corticostriatal neurons using microfluidic devices that mimic the excitatory network. We found that promoting huntingtin phosphorylation restores the intracellular trafficking of BDNF in *Mecp2*-silenced neurons, dramatically improves several key symptoms in *Mecp2* knockout mice, and extends their lifespan.

**Impact**

Our data demonstrate that promoting BDNF transport in the appropriate neuronal circuits is more effective at restoring normal function in *Mecp2*-deficient neurons than non-specific BDNF overexpression. Stimulation of endogenous cellular pathways, such as HTT phosphorylation at S421, may provide a promising new approach for the treatment of RTT patients.

**Conflict of interest**

The authors declare that they have no conflict of interest.

**References**

- Altar CA, Cai N, Bliven T, Juhasz M, Conner JM, Acheson AL, Lindsay RM, Wiegand SJ (1997) Anterograde transport of brain-derived neurotrophic factor and its role in the brain. *Nature* 389: 856–860
- Amir RE, Van den Veyver IB, Wan M, Tran CQ, Francke U, Zoghbi HY (1999) Rett syndrome is caused by mutations in X-linked *MECP2*, encoding methyl-CpG-binding protein 2. *Nat Genet* 23: 185–188
- Armstrong DD (2005) Neuropathology of Rett syndrome. *J Child Neurol* 20: 747–753
- Brown SDM, Chambon P, de Angelis MH, Eumorphia Consortium (2005) EMPRESS: standardized phenotype screens for functional annotation of the mouse genome. *Nat Genet* 37: 1155
- Chahrouh M, Jung SY, Shaw C, Zhou X, Wong STC, Qin J, Zoghbi HY (2008) MeCP2, a key contributor to neurological disease, activates and represses transcription. *Science* 320: 1224–1229
- Chang Q, Khare G, Dani V, Nelson S, Jaenisch R (2006) The disease progression of *Mecp2* mutant mice is affected by the level of BDNF expression. *Neuron* 49: 341–348
- Chen WG, Chang Q, Lin Y, Meissner A, West AE, Griffith EC, Jaenisch R, Greenberg ME (2003) Derepression of BDNF transcription involves calcium-dependent phosphorylation of MeCP2. *Science* 302: 885–889
- Chen L, Chen K, Lavery LA, Baker SA, Shaw CA, Li W, Zoghbi HY (2015) MeCP2 binds to non-CG methylated DNA as neurons mature, influencing transcription and the timing of onset for Rett syndrome. *Proc Natl Acad Sci USA* 112: 5509–5514
- Cheng P-L, Song A-H, Wong Y-H, Wang S, Zhang X, Poo M-M (2011) Self-amplifying autocrine actions of BDNF in axon development. *Proc Natl Acad Sci USA* 108: 18430–18435
- Cheng T-L, Wang Z, Liao Q, Zhu Y, Zhou W-H, Xu W, Qiu Z (2014) MeCP2 suppresses nuclear microRNA processing and dendritic growth by regulating the DGCR8/Drosha complex. *Dev Cell* 28: 547–560
- Colin E, Zala D, Liot G, Rangone H, Borrell-Pagès M, Li X-J, Saudou F, Humbert S (2008) Huntingtin phosphorylation acts as a molecular switch for anterograde/retrograde transport in neurons. *EMBO J* 27: 2124–2134
- Deogracias R, Yazdani M, Dekkers MPJ, Guy J, Ionescu MCS, Vogt KE, Barde Y-A (2012) Fingolimod, a sphingosine-1 phosphate receptor modulator, increases BDNF levels and improves symptoms of a mouse model of Rett syndrome. *Proc Natl Acad Sci USA* 109: 14230–14235
- Guy J, Hendrich B, Holmes M, Martin JE, Bird A (2001) A mouse *Mecp2*-null mutation causes neurological symptoms that mimic Rett syndrome. *Nat Genet* 27: 322–326
- Humbert S, Bryson EA, Cordelières FP, Connors NC, Datta SR, Finkbeiner S, Greenberg ME, Saudou F (2002) The IGF-1/Akt pathway is neuroprotective in Huntington's disease and involves Huntingtin phosphorylation by Akt. *Dev Cell* 2: 831–837
- Johnson RA, Lam M, Punzo AM, Li H, Lin BR, Ye K, Mitchell GS, Chang Q (2012) 7,8-dihydroxyflavone exhibits therapeutic efficacy in a mouse model of Rett syndrome. *J Appl Physiol* 112: 704–710
- Katz DM, Bird A, Coenraads M, Gray SJ, Menon DU, Philpot BD, Tarquinio DC (2016) Rett syndrome: crossing the threshold to clinical translation. *Trends Neurosci* 39: 100–113
- Kerr AM, Armstrong DD, Prescott RJ, Doyle D, Kearney DL (1997) Rett syndrome: analysis of deaths in the British survey. *Eur Child Adolesc Psychiatry* 6(Suppl 1): 71–74
- Kishi N, Macklis JD (2004) MeCP2 is progressively expressed in post-migratory neurons and is involved in neuronal maturation rather than cell fate decisions. *Mol Cell Neurosci* 27: 306–321
- Kron M, Lang M, Adams IT, Sceniak M, Longo F, Katz DM (2014) A BDNF loop-domain mimetic acutely reverses spontaneous apneas and respiratory abnormalities during behavioral arousal in a mouse model of Rett syndrome. *Dis Model Mech* 7: 1047–1055
- Li W, Bellot-Saez A, Phillips ML, Yang T, Longo FM, Pozzo-Miller L (2017) A small-molecule TrkB ligand restores hippocampal synaptic plasticity and object location memory in Rett syndrome mice. *Dis Model Mech* 10: 837–845
- Liot G, Zala D, Pla P, Mottet G, Piel M, Saudou F (2013) Mutant Huntingtin alters retrograde transport of TrkB receptors in striatal dendrites. *J Neurosci* 33: 6298–6309
- Lunke A, Lindenberg KS, Ben-Haiem L, Weber C, Devys D, Landwehrmeyer GB, Mandel J-L, Trotter Y (2002) Proteases acting on mutant huntingtin



- generate cleaved products that differentially build up cytoplasmic and nuclear inclusions. *Mol Cell* 10: 259–269
- Lyst MJ, Bird A (2015) Rett syndrome: a complex disorder with simple roots. *Nat Rev Genet* 16: 261–275
- Matagne V, Ehinger Y, Saidi L, Borges-Correia A, Barkats M, Bartoli M, Villard L, Roux J-C (2017) A codon-optimized Mecp2 transgene corrects breathing deficits and improves survival in a mouse model of Rett syndrome. *Neurobiol Dis* 99: 1–11
- Meehan RR, Lewis JD, Bird AP (1992) Characterization of MeCP2, a vertebrate DNA binding protein with affinity for methylated DNA. *Nucleic Acids Res* 20: 5085–5092
- Moutaux E, Christaller W, Scaramuzzino C, Genoux A, Charlot B, Cazorla M, Saudou F (2018) Neuronal network maturation differently affects secretory vesicles and mitochondria transport in axons. *Sci Rep* 8: 13429
- Ogier M, Wang H, Hong E, Wang Q, Greenberg ME, Katz DM (2007) Brain-derived neurotrophic factor expression and respiratory function improve after amphetamine treatment in a mouse model of Rett syndrome. *J Neurosci* 27: 10912–10917
- Pardo R, Colin E, Régulier E, Aebischer P, Déglon N, Humbert S, Saudou F (2006) Inhibition of calcineurin by FK506 protects against polyglutamine-huntingtin toxicity through an increase of huntingtin phosphorylation at S421. *J Neurosci* 26: 1635–1645
- Paxinos G, Franklin KBJ (2001) *The mouse brain in stereotaxic coordinates*, 2<sup>nd</sup> edn. San Diego: Academic Press
- Pineda JR, Pardo R, Zala D, Yu H, Humbert S, Saudou F (2009) Genetic and pharmacological inhibition of calcineurin corrects the BDNF transport defect in Huntington's disease. *Mol Brain* 2: 33
- Pratte M, Panayotis N, Ghata A, Villard L, Roux J-C (2011) Progressive motor and respiratory metabolism deficits in post-weaning Mecp2-null male mice. *Behav Brain Res* 216: 313–320
- Reddy PH, Tripathi R, Troung Q, Tirumala K, Reddy TP, Anekonda V, Shirendeb UP, Calkins MJ, Reddy AP, Mao P et al (2012) Abnormal mitochondrial dynamics and synaptic degeneration as early events in Alzheimer's disease: implications to mitochondria-targeted antioxidant therapeutics. *Biochim Biophys Acta* 1822: 639–649
- Reiss AL, Faruque F, Naidu S, Abrams M, Beaty T, Bryan RN, Moser H (1993) Neuroanatomy of Rett syndrome: a volumetric imaging study. *Ann Neurol* 34: 227–234
- Roux J-C, Dura E, Moncla A, Mancini J, Villard L (2007) Treatment with desipramine improves breathing and survival in a mouse model for Rett syndrome. *Eur J Neurosci* 25: 1915–1922
- Roux J-C, Zala D, Panayotis N, Borges-Correia A, Saudou F, Villard L (2012) Modification of Mecp2 dosage alters axonal transport through the Huntingtin/Hap1 pathway. *Neurobiol Dis* 45: 786–795
- Sampathkumar C, Wu Y-J, Vadhvani M, Trimbuch T, Eickholt B, Rosenmund C (2016) Loss of MeCP2 disrupts cell autonomous and autocrine BDNF signaling in mouse glutamatergic neurons. *Elife* 5: e19374
- Saudou F, Humbert S (2016) The biology of huntingtin. *Neuron* 89: 910–926
- Schmid DA, Yang T, Ogier M, Adams I, Mirakhor Y, Wang Q, Massa SM, Longo FM, Katz DM (2012) A TrkB small molecule partial agonist rescues TrkB phosphorylation deficits and improves respiratory function in a mouse model of Rett syndrome. *J Neurosci* 32: 1803–1810
- Skene PJ, Illingworth RS, Webb S, Kerr ARW, James KD, Turner DJ, Andrews R, Bird AP (2010) Neuronal MeCP2 is expressed at near histone-octamer levels and globally alters the chromatin state. *Mol Cell* 37: 457–468
- Taylor AM, Dieterich DC, Ito HT, Kim SA, Schuman EM (2010) Microfluidic local perfusion chambers for the visualization and manipulation of synapses. *Neuron* 66: 57–68
- Thion MS, McGuire JR, Sousa CM, Fuhrmann L, Fitamant J, Leboucher S, Vacher S, du Montcel ST, Bièche I, Bernet A et al (2015) Unraveling the role of huntingtin in breast cancer metastasis. *J Natl Cancer Inst* 107: djv208
- Tropea D, Giacometti E, Wilson NR, Beard C, McCurry C, Fu DD, Flannery R, Jaenisch R, Sur M (2009) Partial reversal of Rett Syndrome-like symptoms in Mecp2 mutant mice. *Proc Natl Acad Sci USA* 106: 2029–2034
- Van Esch H (2012) MECP2 duplication syndrome. *Mol Syndromol* 2: 128–136
- Viemari J-C, Roux J-C, Tryba AK, Saywell V, Burnet H, Peña F, Zanella S, Bévengut M, Barthelemy-Requin M, Herzing LBK et al (2005) Mecp2 deficiency disrupts norepinephrine and respiratory systems in mice. *J Neurosci* 25: 11521–11530
- Virlogeux A, Moutaux E, Christaller W, Genoux A, Bruyère J, Fino E, Charlot B, Cazorla M, Saudou F (2018) Reconstituting corticostriatal network on-a-chip reveals the contribution of the presynaptic compartment to Huntington's disease. *Cell Rep* 22: 110–122
- Xu X, Kozikowski AP, Pozzo-Miller L (2014) A selective histone deacetylase-6 inhibitor improves BDNF trafficking in hippocampal neurons from Mecp2 knockout mice: implications for Rett syndrome. *Front Cell Neurosci* 8: 68
- Young JI, Hong EP, Castle JC, Crespo-Barreto J, Bowman AB, Rose MF, Kang D, Richman R, Johnson JM, Berget S et al (2005) Regulation of RNA splicing by the methylation-dependent transcriptional repressor methyl-CpG binding protein 2. *Proc Natl Acad Sci USA* 102: 17551–17558
- Zala D, Hinckelmann M-V, Yu H, Lyra da Cunha MM, Liot G, Cordelières FP, Marco S, Saudou F (2013) Vesicular glycolysis provides on-board energy for fast axonal transport. *Cell* 152: 479–491



**License:** This is an open access article under the terms of the Creative Commons Attribution 4.0 License, which permits use, distribution and reproduction in any medium, provided the original work is properly cited.

## Discussion

This study found a new therapeutic strategy for Rett syndrome based on the HTT property of acting as a molecular switch upon S421 phosphorylation. Increasing S421 phosphorylation in Rett mice, either by a crossing with HTTS421D mice or with a calcineurin inhibitor (FK506), Rett mice symptoms are restored. These findings raise new questions about other strategies able to increase vesicular transport.

### **Calcineurin inhibitors or HTT phospho-activators as possible strategy for RTT?**

Currently, no treatment has been found for this rare disease and the drugs administrated to the young girls aimed only at relieving the symptoms (Sandweiss et al., 2020). Several approaches are being explored or tested to find a cure to RTT, relying mostly on modulating Mecp2 targets known to be downregulated in RTT or on editing genes (Sandweiss et al., 2020) but none of them has yet shown a full recovery.

Concerning **gene editing using gene therapy or antisense oligo nucleotides**, it is a challenging method because of the importance of MecP2 homeostasis. Indeed, MECP2 overexpression leads to another intellectual disability called the *MECP2* duplication syndrome (Van Esch, 2012). Thus, a fine control of the MECP2 levels is crucial. Actual hopes on the genetic approach lie on the CRISPR-Cas9 modification of MECP2 (Sandweiss et al., 2020).

In order to increase the expression of Mecp2 target in RTT, one potential strategy involved the restoration of BDNF. However, overexpressing BDNF in mice or stimulating BDNF production in young girls with a glatiramer acetate treatment came out to produce only partial rescue (Q. Chang et al., 2006; Tropea et al., 2009) in mice and drawbacks in girls (Nissenkorn et al., 2017; Sandweiss et al., 2020).

Since overexpressing BDNF failed to rescue RTT phenotypes in girls, another possibility is to increase its targeting to synapses by increasing the level of IGF-1 in RTT mouse model or RTT patients. A recent phase 2 clinical trial has proven that treating young RTT girls with a terminal tripeptide of IGF-1 improved some of RTT symptoms suggesting that activation of the IGF-1 pathway could be of therapeutic interest (Glaze et al., 2019; Sandweiss et al., 2020). Thus, according to our study, some of the beneficial effects observed could involve the phosphorylation or decreasing dephosphorylation of IGF-1/PI3K/Akt targets such as HTT, and possibly restoration of BDNF homeostasis.

However, it is important to note that increasing IGF-1 induces the activation of many proteins besides HTT. Furthermore, even if HTT was the sole target of this pathway, HTT phosphorylation regulates the

transport of many cargos as it is illustrated in this thesis. Indeed, as discussed here, HTT phosphorylation affect the anterograde transport of several types of vesicle including APP vesicles (Bruyère et al., 2020; Colin et al., 2008), vamp-7 vesicles (Colin et al., 2008) and Vamp-2 vesicles (vitet *et al.*, *in prep*). Thus, the rescue of BDNF transport might not be the only explanation to the improvement of MECP2 KO mice behavior.

In addition to neurons, improving transport in astrocytes could also be of interest. Enhancing MT-dependent transport to rescue RTT symptoms in mice has also been shown to be effective for lysosomes transport in astrocytes of a mouse model of RTT and derived from iPSC of RTT patient (Delépine et al., 2016). Indeed, by stabilizing MTs, it is possible to decrease and rescue the number of vesicles showing a low displacement length in higher in MECP2 mutant mouse astrocytes.

Thus, efforts are still needed to find an effective strategy relieving young girls from crippling symptoms. Moreover, since RTT is diagnosed long after the symptoms apparition because of the combination of similarities with autism spectrum disorder and normal development until 6 months, it is crucial to find a treatment which is effective even after the apparition of symptoms.

To conclude this study, we can claim that BDNF level at the synapse is crucial for neuronal homeostasis and subsequent behavior (figure 98). If it is increased like it could be the case for the glatiramer acetate treatment tested on Rett patients, it could lead to sever cognitive and motor impairments. On the opposite, a lower level of BDNF at the synapse is found in MeCP2 KO and BACHD mouse models of respectively Rett syndrome and HD and could be responsible for the decrease impaired motor coordination among other impairments. Some studies focused on the potential beneficial effect of S421 phosphorylation on those two mouse models and reported full restoration of the associated phenotypes (Yann Ehinger et al., 2020; Kratter et al., 2016).

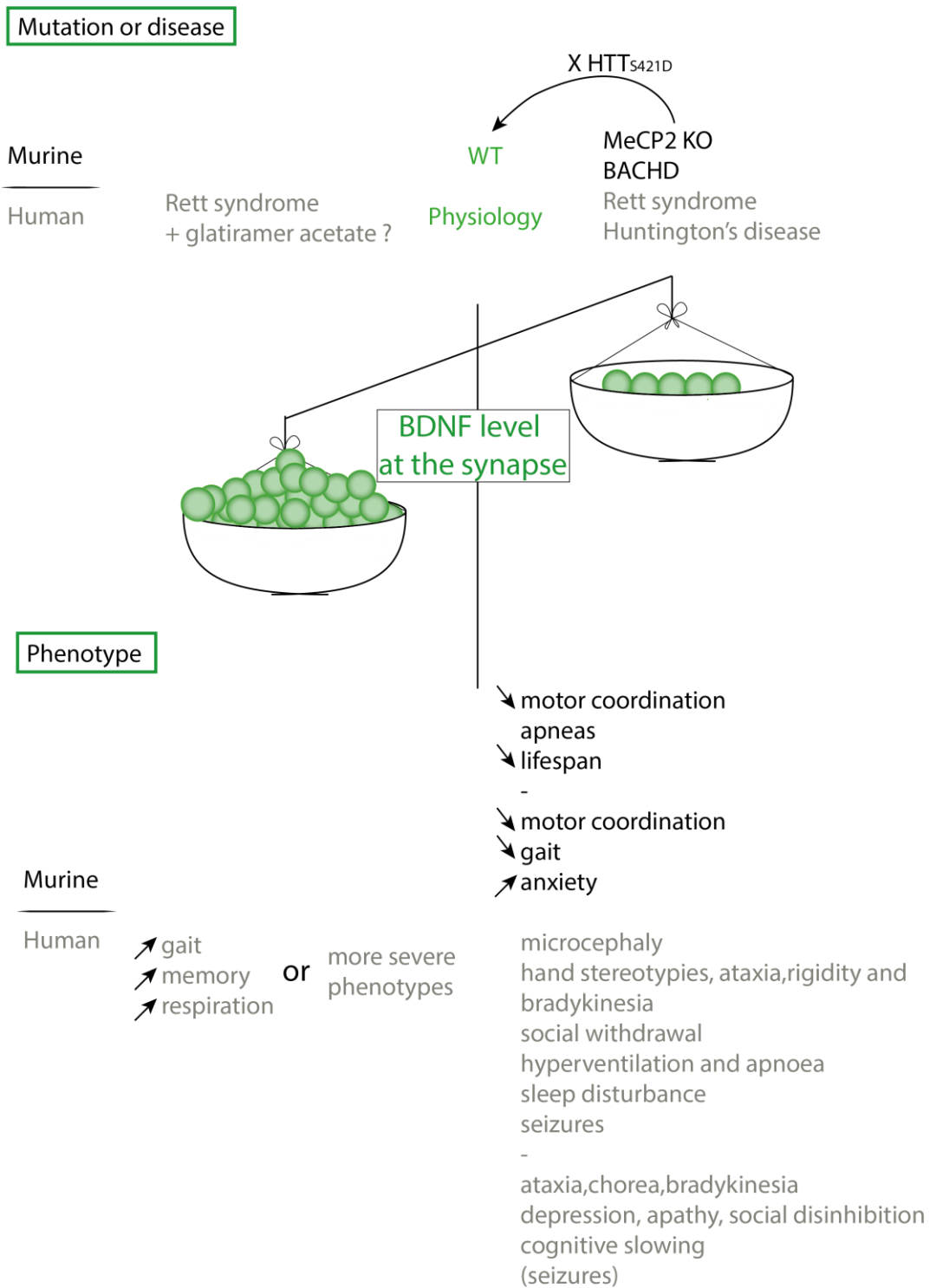


Figure 98: BDNF level at the synapse is crucial for neuronal homeostasis and subsequent behavior.

## Results – part 3: HTT acts as a scaffold for KIF1A-mediated-transport and regulates SVP axonal transport

### Summary & context of the study

Synaptic vesicles precursors (SVPs) are responsible for the localization and the production of synaptic vesicles (SVs), the vesicles that transmit signal to the post synaptic neuron. The transport of SVPs is mediated in part by the molecular motor KIF1A. KIF1A is known to interact with adaptors to regulate SVP activation or binding to MTs like DENN/MADD complex interacting with Rab3. Interestingly, neither the knockout of DENN/MADD in *C. elegans* nor RAB3 KO mice exhibit an impaired SVP transport, suggesting that other adaptors could regulate the transport of SVPs (Pace et al., 2020). In support for the existence of several KIF1A adaptor on a SVP is the report that dynein and dynactin interact and regulate KIF1A activity (C. W. Chen et al., 2019). However, no scaffolding proteins for KIF1A have been found yet (Niwa et al., 2008; Pace et al., 2020; O. I. Wagner et al., 2009). We made the hypothesis that HTT could act as a scaffolding protein for the KIF1A complex and as such could regulate the transport of SVPs. This hypothesis of HTT regulating SVP transport was supported by results showing that HTT reduction in *Drosophila* larval segmental nerves leads to a decrease in SVP transport and to an accumulation of SVP within the nerves (Gunawardena et al., 2003; Weiss & Littleton, 2016). The lab also previously showed that HTT phosphorylation at S421 regulates the directionality of late endosomes containing a specific v-SNARE, VAMP-7 (Colin et al., 2008). Finally, HTT interactome (Shirasaki et al., 2012) and HTT mass spectrometry from vesicles, indicated the possibility that HTT could scaffold KIF1A and consequently regulate KIF1A-mediated-transport of SVP containing v-SNAREs. In support with our working hypothesis, HTT has been later found in the KIF1A interactome (Stucchi et al., 2018).

Importantly, the number of SVs at the synapse is key as it regulates the NT release probability impacting synaptic strength and subsequent plasticity. Long term changes in synaptic strength of a specific network are known to be at the basis of learning and memory. In our study we focused on the activity of the corticostriatal network and its role in regulating the procedural memory, also called the memory of habit formation. In order to better understand the context of our study, an update of the literature on neurotransmission as well as on the link between the corticostriatal circuitry and habit formation is provided.

### *Number of SVs influences neurotransmission*

The number of SVs within the presynaptic bouton is important because it impacts the size of the different pools (RRP, recycling pool and the reserve pool) known to regulate synaptic strength and subsequent learning and memory behavior (Alabi & Tsien, 2012). From Katz theory on frog neuromuscular junction to recent studies on CNS mammalian synapse (Katz B, 1969; Malagon et al., 2020; Pulido & Marty, 2017), the number of RRP or docked vesicles has been directly linked to the amplitude of the induced postsynaptic current by the following equation:

$$I = Npq$$

Although the meaning of those terms can vary according to different paradigms, the amplitude of postsynaptic current (I) created in a “simple” CNS synapse follows this binomial distribution that is dependent on the probability of release of one vesicle (p), the number of released vesicles (q, the quantal size) and the number of vesicles able to be released (N). To be more specific, N can represent the “number of reactive units” (Katz B, 1969), the number of vesicles in the RRP or the number of docked vesicles and p relates to the release probability per “reactive unit” (Katz B, 1969), per RRP vesicle or per docking site (Pulido & Marty, 2017). For clarity, this specific probability of release will be termed  $p_{ves}$  (fusion probability) thereafter.

Studies demonstrated that impairing vesicle fusion with the plasma membrane ( $p_{ves}$ ), leads to defects in neurotransmission that could be responsible for neurological disorders (Alabi & Tsien, 2012; Cho & Askwith, 2008).

Indeed, once a vesicle is docked or primed, v-SNARE protein (synaptobrevin) partially form complexes with t-SNAREs (syntaxin-1, SNAP25) (Ryu et al., 2016). Then, upon calcium influx within the active zone and subsequent calcium binding to synaptotagmin, the two membranes fuse and the neurotransmitter is released into the synaptic cleft (figure 99).

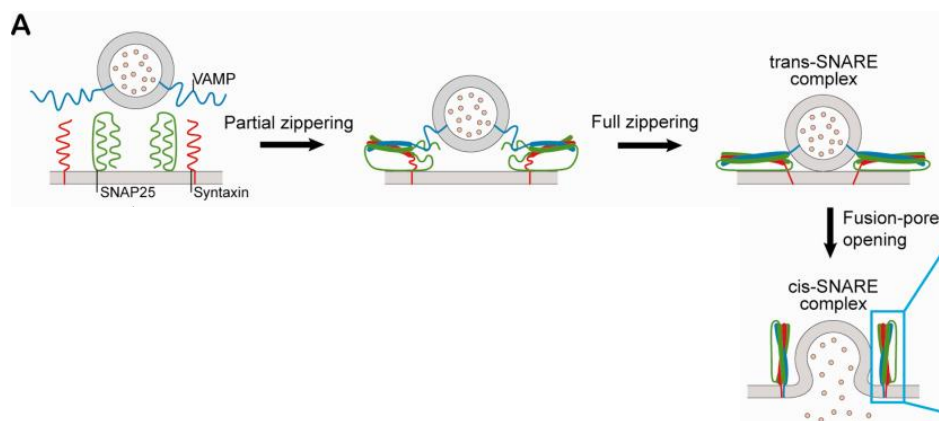


**Figure 99: exocytosis is regulated by SNAREs.** Scheme from Ryu et al.,2016

The neurotransmitter then activates its receptors located within the PSD, which are AMPA, NMDA or metabotropic receptors in the case of glutamate. AMPA and NMDA receptors convert the biochemical signal into a fast and brief electric signal by opening ion channels thus directly creating a postsynaptic current (EPSC). These ionoreceptors are thought to mediate behaviors from simple reflexes to complex cognitive processes. In addition, the metabotropic receptor act indirectly to create a postsynaptic current by changing the postsynaptic cell biochemistry state through second messengers and signaling pathways. This action is slow and long lasting (up to minutes), this is why it is thought to modulate behaviors, contributing to long lasting changes in neuronal networks underlying learning and memory.

The number of SVs at the axon terminal ( $N$ ) is crucial since NT concentration within the synaptic cleft ( $q$ ) is important for the triggering of a post synaptic response ( $I$ ) (and EPSC) (Pulido & Marty, 2017).

*Number of SVs influences the probability of release and consequent plasticity*

The number of SVs and especially of RRP vesicles also correlates with a presynaptic component of the neurotransmission, that is the probability of release ( $Pr$ ) (Dobrunz & Stevens, 1997). Indeed,  $Pr$  correlates positively with the number of SVs that are docked or primed. The changes in  $Pr$  that can occur physiologically in the presynaptic compartment are the triggered mechanisms for short-term plasticity (STP) (Biró et al., 2005; Thomson, 2000). This phenomenon is related to LTP in its roles of modulating synaptic efficacy, except that it is a short-term process. STP can be declined into STD or facilitation, both observed respectively by a decrease or an increase in postsynaptic response during repetitive presynaptic stimulation (Liley & North, 1953). STD is revealed by a paired-pulse ratio experiment. STD can be explained when the release of SVs is occurring faster than the replenishment of the reserve pool (Bircks & MacIntosh, 1961; Elmqvist & Quastel, 1965). This results in the depletion of the RRP and a decrease in NT release (Jackman & Regehr, 2017; Zucker & Regehr, 2002). Conversely, facilitation enhances synaptic transmission and has a role in working memory (Abbott & Regehr, 2004; Jackman & Regehr, 2017). Facilitation appears as a process to counteract synaptic depression caused by repeated stimulations (figure 100). Indeed, facilitation results in

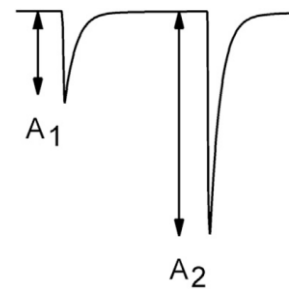


**Figure 100: facilitation results in a higher release of NT at the second stimulation.** Scheme from Jackman & Regehr, 2017

an increase of  $Pr$  (3-fold increase, (Malagon et al., 2020)) in a frequency-dependent manner by either increasing the number of SVs (Del Castillo & Katz, 1954) either the calcium influx (Jackman & Regehr, 2017). Thus, when  $Pr$  is low in a presynaptic compartment, facilitation is high (Abramov et al., 2009) and leads to an increase of NT release at the second stimulation (Jackman & Regehr, 2017; Thanawala & Regehr, 2013). However, when  $Pr$  is high, many vesicles fuse at the first stimulation, impeding

facilitation, the RRP becomes depleted and STD appears until RRP is replenished (Jackman & Regehr, 2017).

In term of mechanisms, the docking site concept might be one key to understand STP (Pulido & Marty, 2017). The concept lies on the fact that each active zone (AZ) host several docking sites (between 2 and 10, (Pulido & Marty, 2017)) for a SV to interact with AZ proteins and to be primed. Interestingly, the AZ size or the synaptic size vary with the number of docked vesicles and the probability of release of those vesicles. At rest, not all the docking sites are used (around 70%) (K. M. Harris & Sultan, 1995; Pulido & Marty, 2017) but each of them is associated with a replacement site (Pulido & Marty, 2017) containing a SV from the reserve pool (figure 101). During the first stimulus, the docked vesicles are exocytosed and free the docking sites. Then, many of the SVs within the replacement sites transit to the docking sites by an active myosin II transport (Miki et al., 2016; Pulido & Marty, 2017), resulting in a higher number of docked vesicles compared to the resting state (figure 101). This mechanism could

explain why the second stimulation induces higher release of NT. Thus, this mechanism relying on changes in docking site occupancy could determine facilitation and depression at synapses (Malagon et al., 2020; Miki et al., 2016, 2018; Pulido et al., 2015; Pulido & Marty, 2017).

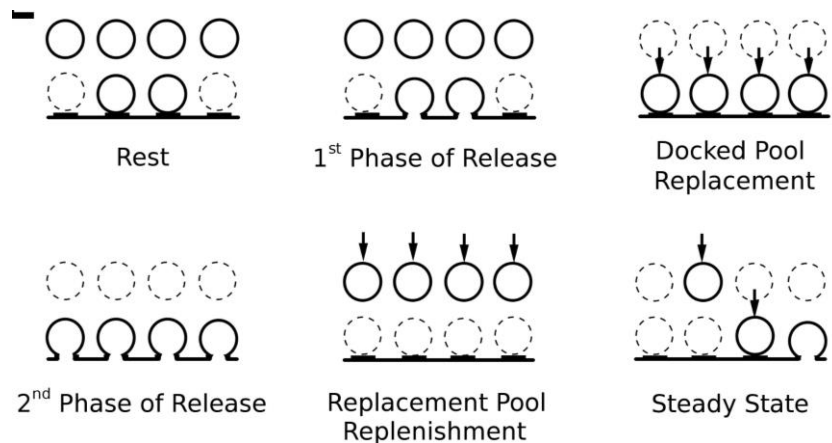


**Figure 101: facilitation might be due to SVs forming a reserve for docked SVs.** Scheme from Pulido & Marty, 2017

### *Corticostriatal plasticity influences procedural memory in mice*

We focused here on the plasticity occurring within the corticostriatal network, known to regulate procedural memory (Costa et al., 2004; Koralek et al., 2012; Yin et al., 2009). Corticostriatal plasticity appears to be necessary and responsible for learning new motor skills (Koralek et al., 2012; Perrin & Venance, 2019). During such learning, both cortical and striatal activities as well as connectivity, plasticity and strength of the circuit are modulated, resulting in long-lasting changes in glutamatergic transmission (Brasted & Wise, 2004; Costa et al., 2004; Kleim et al., 1998; Yin et al., 2009). These changes occur in more than 50% of the cells in the striatum and the motor cortex (Costa et al., 2004).

Skill motor learning can be assessed by different behavioral protocol like the T-maze, the double H-maze (Kirch et al., 2015) or the accelerating rotarod that is by far the most used approach. Accelerating rotarod is a protocol using a rotating rod whose speed increases over time. The mouse placed on the



rod has to learn this task by staying on the rod despite the accelerating speed. Ten trials per day over more than five consecutive days are needed for the task to become a habit (Kupferschmidt et al., 2017; Yin et al., 2009). The time spent on the rotarod by the mouse is recorded and display two phases according to the training: a fast improvement on the first day, the early training, and a slower one from day 2 to the end of the training, the late training (Kupferschmidt et al., 2017; Yin et al., 2009) (figure 102). One of the advantages of the accelerating rotarod protocol is that it only gives access to motor skill learning and not to associative and working memory components of other motor learning skills (Costa et al., 2004).

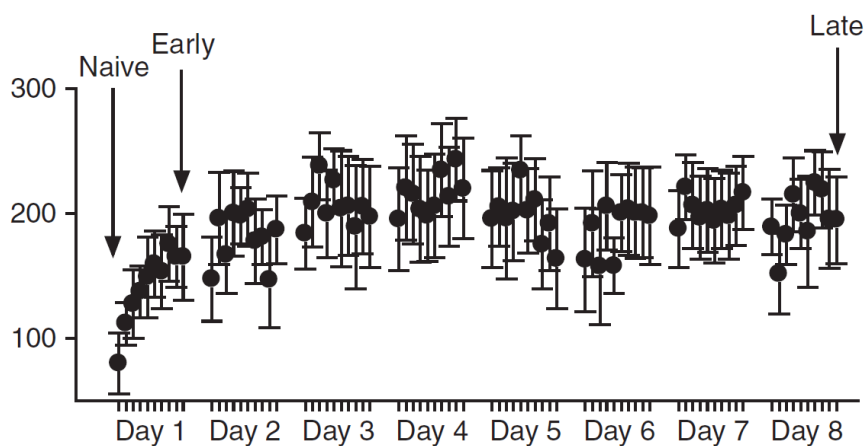


**Figure 102: time to fall of the accelerating rotarod over eight consecutive days of training.** Graph from Yin et al., 2009

As previously explained, two models are currently being developed to understand the striatal reorganization caused by the consolidation of the memory upon those two phases of learning. The first one relies on the DMS involvement during an early training and the DLS involvement during the late training (Costa et al., 2004; Koralek et al., 2012; Yin et al., 2009). The other model relies on a co-engagement of the two networks during learning and competing for control (Kupferschmidt et al., 2017; Perrin & Venance, 2019).

Recently, an elegant study proposed another model combining the two first models. By recording *in vivo*, the activity of MSNs from DMS or DLS in running mice performing an accelerating rotarod protocol over five days, authors showed that the two networks are co-engaged at the beginning of the learning, but disengaged in different patterns later during the training (Kupferschmidt et al., 2017) (figure 103). The associative cortex – DMS network would be engaged only strongly in the early training (first day) and starts its disengagement on day 2 to day 5 of the behavioral task. The sensorimotor cortex-DLS network would be strongly engaged from the beginning of the training (naïve mice) to an

early training and would then gradually be disengaged across training. However, during a late training, its engagement would still be higher than the associative cortex-DMS. This observation agrees with the idea that sensorimotor cortex-DLS network rather than the associative cortex-DMS circuit is more responsible for the execution of mastered skills (or habit) (Corbit et al., 2017; Yin et al., 2009). The lower global engagement of the sensorimotor-DLS network once the habit is formed could be explained by the need of fewer neurons to form smaller clusters that encode the activity, that could be called engram cells (Corbit et al., 2017; Badreddine *et al.*, *under revision*).

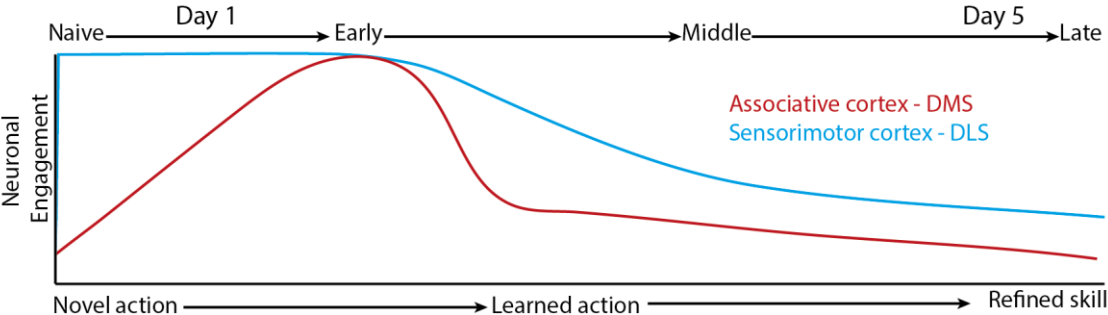


**Figure 103: DLS and DMS are both involved in the procedural memory formation during the first days of accelerating rotarod.** Scheme from Corbit *et al.*, 2017 and Kupferschmidt *et al.*, 2017.

## **Release probability is controlled by HTT dependent SVP transport in corticostriatal network impairing procedural memory in mice\***

Vitet H, Bruyère J, Xu H, Nassar M, Brocard J, Abada Y.S, Brodier C, Delatour B, Scaramuzzino C, Venance L, Humbert S, Saudou F\*\*

\* The version of this paper is still in preparation; some data and indications are being collected

\*\* author list and order presented here are not definitive.

### **Abstract**

Procedural memory, the memory of habits, mostly depends on the strength of neurotransmission within the corticostriatal circuit through glutamate release at the synapse. Synaptic strength depends on release probability and quantal size of glutamate synaptic vesicles (SVs) present at corticostriatal synapses thanks to the transport along axons of their precursor (SVPs). SV homeostasis is a highly regulated mechanism but whether modulation of SVP transport efficacy impacts synapse communication and subsequent behavior in mice remain to be investigated. Huntingtin (HTT), the protein that when mutated causes Huntington disease, facilitates the transport of many cargoes, including SVP by scaffolding molecular motors and adaptors. In particular, HTT phosphorylation at Serine 421 modulates the transport of vesicles containing trophic factors but it is not known whether HTT phosphorylation controls the directionality of SVPs in axons and whether this regulation can impact specific circuits and behaviors *in vivo*. Here we show that HTT phosphorylation, by recruiting the kinesin motor KIF1A, increases axonal transport of SVPs and glutamate release in a cortico-striatal circuit on-a-chip. *In vivo*, chronic HTT phosphorylation increases the number of SVs at synapses, the release probability and alters procedural memory that could be restored by the selective silencing of KIF1A in the corticostriatal circuit. Together, the HTT-KIF1A-dependent transport of SVPs in axons is a determinant of SV homeostasis and links the regulation of axonal transport of SVPs within specific circuits, here the corticostriatal network, to a specific behavior, procedural memory.

**running title:** HTT regulates release probability through SVP axonal transport

### **Key words:**

Synaptic Vesicle Precursors, Huntingtin phosphorylation, axonal transport, corticostriatal synapse, microfluidics, probability or release, procedural memory

## Introduction

Procedural memory is the memory responsible for the formation of habits after a long training (Costa et al., 2004; Yin et al., 2009). It relies mostly on the communication between the cortex and the striatum (Graybiel & Grafton, 2015; Hawes et al., 2015; Hyungju Park et al., 2014; Yin et al., 2009). Two corticostriatal connections have been found to finely regulate procedural memory and subsequent habit formation (Costa et al., 2004; Kupferschmidt et al., 2017; Hyungju Park et al., 2014; Perrin & Venance, 2019; Yin et al., 2009). Glutamatergic neurons from the layer V of the associative cortex project to the dorsomedial striatum (DMS) whereas neurons from the sensorimotor cortex project to the dorsolateral striatum (DLS) (Yin et al., 2009). DMS activation has for a long time been thought to be responsible for the goal directed behavior occurring in the early phase of the learning, contrary to DLS which was thought to intervene principally in the late phases of learning. Recently, these two corticostriatal connections have been found to be co-engaged during the beginning of the motor skill learning of the accelerating rotarod and then disengaged differently (Kupferschmidt et al., 2017). Thus, neuronal communication between the cortex and the striatum through glutamate release appears to be a key regulator of procedural memory. Memory is thought to rely on long-term changes of synaptic strength of a neuronal network, which depends on the release probability of synaptic vesicles (SVs) and the quantal size, according to Katz's theory (Katz B, 1969) and is proportional to the number of release sites and SVs at the synapse .

SVs localized at the axon terminal contain SNARE proteins such as VAMP-2 that allows exocytosis and vGLUT-1 responsible for the replenishment of glutamate (Shigeo Takamori et al., 2006). Thus, by transporting SVs to the nerve terminal, axonal transport of SV precursors (SVPs) is likely to impact the neurotransmission in specific circuits and consequently affect relevant behaviors (Klopfenstein & Vale, 2004; L. B. Li et al., 2016; Pack-chung et al., 2007; Yonekawa et al., 1998; Y. V. Zhang et al., 2017; Q. Zheng et al., 2014). Axonal transport of SVPs to the synapse is mediated mostly by two kinesin-3 family members: KIF1A and KIF1B $\beta$  (Kevenaar et al., 2016; J. S. Liu et al., 2012; Okada et al., 1995; Pack-chung et al., 2007; Sgro et al., 2013; Yonekawa et al., 1998). KIF1A is known to be very processive and its motility is regulated by modulators like KBP or MAPs (Kevenaar et al., 2016; Lipka et al., 2016; Lyons et al., 2008; Monroy et al., 2020). Other proteins referred as adaptors are known to regulate KIF1A functions by binding both to KIF1A and the SVP. It is the case of DENN/MADD or the BORC complex in *C. Elegans* that regulates KIF1A functions through Rab3 interaction (Niwa et al., 2008; Pace et al., 2020; O. I. Wagner et al., 2009). However, both of them have been shown to be non-essential for SVP transport, raising the question of the identity of a *bona fide* SVP transport adaptor (Mahoney et al., 2006; Pace et al., 2020). Furthermore, dynein is also present on SVPs with KIF1A (Barkus et al., 2008; C. W. Chen et al., 2019; Koushika et al., 2004) but we still do not know whether and how SVP

directionality is regulated and what are the consequences on SV stoichiometry at synapses, neurotransmission and behavior.

Huntingtin (HTT) when mutated, is responsible for Huntington disease (HD), an adult-onset neurological disorder. HTT is involved in several cellular functions including in particular the regulation of axonal transport of many cargoes in neurons (Gauthier et al., 2004; Her & Goldstein, 2008; Saudou & Humbert, 2016; H. Vitet et al., 2020; J. Ag. White et al., 2020; Wong & Holzbaur, 2014). Specifically, HTT acts as a scaffold for both molecular motors such as kinesin -1 and dynein and adaptors such as HAP1, and regulates the transport of vesicles containing BDNF, APP, as well as endosomes, autophagosomes and synaptic vesicles and SVPs (DiFiglia et al., 1995; Meng-meng Fu & Holzbaur, 2013; Gauthier et al., 2004; Gunawardena et al., 2003; L.-S. Her & Goldstein, 2008; H. Li et al., 2003; Weiss & Littleton, 2016; Wong & Holzbaur, 2014). Moreover, HTT can be phosphorylated at a particular Serine (S421), which in turn regulates the directionality of vesicles such as those containing BDNF and APP (Bruyère et al., 2020; Colin et al., 2008; Y. Ehinger et al., 2020). However, it remains to be elucidated whether HTT phosphorylation impacts on the anterograde transport of SVPs in axons and whether this can influence neurotransmission and behavior.

Here we investigated the consequences of constitutive phosphorylation of HTT on axonal transport of SVPs *in vitro* using reconstituted corticostriatal circuit on-a-chip and *in vivo* in mice. We reveal a functional link between efficiency of the anterograde transport of SVPs, mediated by HTT phosphorylation and KIF1A recruitment on SVPs, within corticostriatal projecting neurons, release probability of SVs and procedural memory.

## **Results:**

### **HTT phosphorylation at S421 impairs procedural memory**

To study the impact of HTT phosphorylation on behavior, we took advantage of mice in which the phosphorylation status is controlled by a point mutation (Thion et al., 2015). S421 phosphorylation is mimicked by the replacement of the serine by an aspartic acid (S421D, hereafter referred as HTT-SD mice) whereas the unphosphorylatable form of HTT is mimicked by the replacement of the serine by an alanine (S421A, hereafter referred as HTT-SA mice) (Thion et al., 2015). HTT-SD and HTT-SA mice have been characterized for their behavior and do not show any major impairment in weight, muscle force and motor coordination and in anxio-depressive behavior when compared with WT mice (Bruyère et al., 2020; Y. Ehinger et al., 2020) (Fig sup1A and B). However, when investigating specifically procedural memory using the 8-consecutive days accelerating rotarod protocol (Fig 1A), we found that HTT-SD mice show impaired procedural memory at 3 months and later (Fig 1B and C, Fig sup 1C). Briefly, this behavioral test consists in measuring the time for a mouse to fall of the accelerating rotarod over the 10 sessions per day and during 8 consecutive days (Figure 1A). HTT-SD mice spend less time in total on the rotarod during the 80 sessions than the wild type mice (Fig 1B). Since their motor ability could not explain this reduced performance, we next assessed their procedural memory. Whereas wild type (WT) mice performance reached a plateau from the third day, after the learning phase at day 3, the performance of HTT-SD decreased and reached a plateau that was significantly lower (Fig. 1C). In order to better understand the component responsible for this overall decrease in the performance in HTT-SD mice, we focused on the first and the last days. Although a trend appears from the very first day (Fig 1F, G) the decrease of performance was clearly stabilized during the last day of training (Fig 1J, K) suggesting that the impairment of procedural memory begins from the first day of training, before the formation of the habit. We performed the same experiments on the HTT-SA mice, but we did not observe difference between the wild type mice and the HTT-SA mice (Fig. 1D, E, H, I, L,M). Together, our results show that HTT-SD mice, unlike HTT-SA mice, exhibit an impaired procedural memory when tested on an accelerating rotarod protocol over 8 days. Thus, we focused thereafter our investigation on HTT-SD mice.

## **HTT phosphorylation at S421 regulates the number of SVs at the axon terminal and the release probability**

Procedural memory relies on the communication and on the long-term changes of synaptic strength of the corticostriatal network striatum (Graybiel & Grafton, 2015; Hawes et al., 2015; Hyungju Park et al., 2014; Yin et al., 2009). In order to assess the *in vivo* synaptic strength in HTT-SD mice, we first investigated the postsynaptic response provoked by an action potential in the presynaptic compartment by studying the electrophysiological properties and the sEPSCs in medium spiny neurons (MSNs) of the DLS. We found that the frequency but not the amplitude of sEPSCs was increased in HTT-SD MSNs (Fig 2A and B) suggesting that the properties of the corticostriatal network in HTT-SD mice depend on the presynaptic activity. We then investigated one of the presynaptic parameters able to influence the probability of release and focused on the number of SVs (Alabi & Tsien, 2012; Hanse & Gustafsson, 2001; Hyoukeun Park et al., 2012; Pulido & Marty, 2017) at the axon terminal within the somatosensory cortex-DLS network using electron microscopy. According to the morphology of both the spines and the synapses, we specifically counted the number of SVs in DLS glutamatergic afferences and found that HTT phosphorylation increases the number of SVs at the axon terminals (Fig 2C and D) while there was no difference in the number of synapses (Fig sup 2A). To test the possibility that the observed increase in the number of SVs at the presynapse could induce changes in the probability of release, we next studied neuronal facilitation with a 2-stimuli protocol and found that facilitation was completely abolished in HTT-SD slices (Fig 2 E and F). This lack of facilitation was particularly marked at repeated stimulations with short intervals and may result from the high level of SVs release during the first stimulation.

To further demonstrate that the number of SVs released at synapse is increased in HTT-SD neurons, we used microfluidic devices that allows to reconstitute mature corticostriatal networks on-a-chip, in which cortical neurons project to striatal target neurons through oriented axonodendritic connections. We recently validated such approaches to study the functioning of corticostriatal circuits in health and disease conditions (Moutaux, Christaller, et al., 2018; Virlogeux et al., 2018) These devices allow to study intracellular transport in isolated axons as well as neurotransmitter release at synapses. We plated cortical neurons from HTT-SD mice in the pre- and striatal neurons in the postsynaptic compartment and infected cortical neurons with a lentivirus expressing vGlut1-pHluorin. When the circuit was mature (DIV11), we treated the presynaptic compartment with 4AP/bicuculline and measured the number of exocytic events per active synapse by recording fluorescence within the synaptic compartment. While the amplitude of vGlut1 release was similar in WT compared with HTT-SD neurons, we observed a tendency towards an increase in the number of events at synapses when HTT is constitutively phosphorylated (Fig 2G). Together, these results indicate that in HTT-SD

corticostriatal network, the high number of SVs at the axon terminals could enhance the probability of release leading to higher exocytosis rate as revealed by a higher frequency of sEPSCs and the loss of facilitation. These changes in electrophysiologic properties could be at the basis of the impaired memory in HTT-SD mice.

### **HTT phosphorylation at S421 regulates SVP directionality in axons**

Since the number of SVs reaching the axon terminal depends on the axonal transport of SVs containing VAMP2 (Gunawardena et al., 2003; Pack-chung et al., 2007; Yonekawa et al., 1998; Q. Zheng et al., 2014), we investigated the regulation of SVP axonal transport in HTT-SD neurons. We expressed VAMP2-mCherry in cortical neurons connected to striatal neurons within microfluidic devices and recorded using spinning videomicroscopy Vamp-2-mCherry transport in the distal part of cortical axons when the circuit is mature (DIV12) (Fig 3A). Kymographs analysis showed that HTT phosphorylation increases specifically the anterograde velocity of VAMP-2 positive vesicles (Fig 3B and C). The S421D mutation increased specifically the number of anterograde vesicles while reducing the number of static vesicles (Fig 3D, E, F) and increased both the linear flux and the anterograde directionality (Fig 3G). Together, we conclude that HTT phosphorylation at S421 increases the anterograde flux of SVs towards the presynapse.

### **Phosphorylated HTT scaffolds KIF1A on VAMP2 vesicles**

SVP transport is known to be largely mediated by KIF1A and KIF1B $\beta$  (Kevenaar et al., 2016; J. S. Liu et al., 2012; Okada et al., 1995; Sgro et al., 2013; Yonekawa et al., 1998). Kinesin-3 family member KIF1A is responsible for the anterograde transport of SVs but participates also to the transport of dense core vesicles containing BDNF but not APP (Hung & Coleman, 2016; Kaether et al., 2000; Lim et al., 2017; Lo et al., 2011). Since the velocity of a vesicle depends on the number of recruited kinesins (Furuta et al., 2013; Guedes-Dias & Holzbaur, 2019; Hayashi et al., 2018) we investigated the stoichiometry of KIF1A molecules attached to vesicles isolated from HTT-SD brains. We enriched vesicles by successive centrifugation and investigated KIF1A protein levels. While KIF1A was found at the same level in the total fraction (Fig sup 3A), KIF1A was enriched specifically in the vesicular fraction of HTT-SD neurons (fig 4B). Thus, S421 phosphorylation leads to an increased level of KIF1A protein on vesicles. This KIF1A enrichment could be responsible for the increased anterograde transport of VAMP2 vesicles in axons (Fig 3C and 3F).

Although KIF1A is found in the HTT interactome and conversely (Shirasaki et al., 2012; Stucchi et al., 2018), no functional colocalization between the proteins has been reported. We recently reported the proteome of HTT-specific vesicles, i.e., the identity of proteins that are present on HTT-immunopositive vesicles (Migazzi, BioRx). Interestingly, we found KIF1A to be present on HTT positive



vesicles (Fig 4B). Moreover, dynein has been reported to interact with KIF1A (C. W. Chen et al., 2019), which suggested to us that HTT could, as shown for KIF5C (Gauthier et al., 2004), also scaffold KIF1A with dynein (Fig 4C). We therefore performed immunocytochemistry on isolated axons within microfluidic devices. As shown in figure 4D, we found KIF1A immunopositive vesicles to be stained for HTT and Vamp2-mCherry (3<sup>rd</sup> and 4<sup>th</sup> peak), which lead us to picture HTT acting as a scaffold for the molecular machinery dedicated to SVP transport (Fig 4E). Quantification using Mandel coefficient and calculating the number of colocalizing pixels confirmed this KIF1A presence on HTT positive vesicles (Fig 4F and 4G) and importantly, the colocalization increased when HTT contains the S421D mutation (Fig 4F and 4G). Together, we conclude that KIF1A and HTT colocalize on VAMP-2 positive vesicles and that S421 phosphorylation increases KIF1A stoichiometry on SVPs.

### **The kinesin KIF1A propels HTT-dependent SVPs in axons**

Our results indicate that HTT phosphorylation increases KIF1A recruitment on SVPs and increases their anterograde transport in axons. We therefore aimed to unequivocally demonstrate that the HTT-SD-mediated increase in axonal transport is linked to KIF1A using silencing approaches. To directly link the change in cellular dynamics and processes observed in HTT-SD corticostriatal network to a change in the flux of SVPs, we decreased the level of KIF1A using a shKIF1A (Kevenaar et al., 2016). We validated a lentiviral shRNA that decreases the expression of KIF1A by approximately 83% in cortical neurons (Fig sup 3B). We introduced the lentiviral construct into cortical neurons plated in microfluidic devices and measured axonal transport of VAMP2-mCherry vesicles at DIV12 (Fig 5A and 5B). Silencing KIF1A on cortical neurons within microfluidics device, slightly decreased, although not significantly, the VAMP-2 anterograde vesicle velocity in WT axons (fig 5B, C). This might be due to the potential redundant role of KIF1B $\beta$  on SVPs transport (Niwa et al., 2008; Nakamura et al., 2002; Okada et al., 1995). Reducing KIF1A, in contrast was effective to reduce the retrograde velocity of VAMP2-mCh vesicles. Such an effect on retrograde transport might be linked to the reported dynein activator role for KIF1A (Chen et al., 2019). We next silenced KIF1A in HTT-SD cortical axons and observed a significant reduction of both anterograde and retrograde transport of VAMP2-mCh vesicles back to values found in WT neurons for the anterograde speed (Fig 5C). Interestingly, when further analyzing the velocity distribution of VAMP2-mCh vesicles, silencing KIF1A was particularly efficient on vesicles moving at high speed (3 to 4  $\mu\text{m/s}$ ) (Fig 5D). In addition to velocities, shKIF1A abrogated the phospho-HTT-mediated increase in the number of anterograde vesicles (Fig 5E) as well as the linear flux (Fig 5G). Together, we conclude that HTT phosphorylation increases axonal transport of SVPs via KIF1A.

We have observed *in vitro* and *in vivo* an increase, upon HTT phosphorylation, of the number of SVs at synapses and of glutamate release. However, such phenotypes might be due in part to synergistic action of BDNF at synapses. Indeed, KIF1A also transports BDNF vesicles (Hung & Coleman, 2016; Lim et al., 2017; Lo et al., 2011) whose level at the synapse are known to change plasticity and SV release (De Pins et al., 2019; Gangarossa et al., 2020; Rauti et al., 2020; Shimojo et al., 2015; William J. Tyler et al., 2006). Lastly, we showed and that HTT phosphorylation also increases anterograde transport of BDNF (Colin et al., 2008; Y. Ehinger et al., 2020). We therefore silenced KIF1A in cortical axons and measured BDNF-mCherry axonal transport in the distal part of axons (Fig 5H). While chronic HTT phosphorylation increased anterograde transport as previously reported (Colin et al., 2008; Y. Ehinger et al., 2020), we found no effect of shKIF1A on anterograde transport, linear flow or the directionality (fig 5I,J and K). These experiments further support our hypothesis of a scaffolding role for HTT on SVPs through the recruitment of KIF1A. Together, we conclude that in corticostriatal projecting neurons, HTT phosphorylation enhances the anterograde transport of SVPs via KIF1A, while it promotes the anterograde transport of BDNF mostly via KIF5C (Colin et al., 2008; Dompierre et al., 2007).

#### **Huntingtin S421 phosphorylation regulates SV number at synapses via the KIF1A-dependent modulation of axonal transport**

We next investigated whether the impairment in procedural memory that is observed in HTT-SD mice is due to the abnormal accumulation of SVs at the presynapse subsequently to the phospho-HTT-KIF1A-mediated increase in the anterograde transport of SVPs. We therefore injected either lentiviral sh-scramble or sh-KIF1A in the layer V of the motor cortex from HTT-SD mice (Fig 6A,B) whose neurons project to the DLS part of the striatum (Fig 6D) (Mannella et al., 2013; Perrin & Venance, 2019)(Allen brain atlas experience #141602484). To control the efficiency of the injection, we assessed the levels of KIF1A by western blot analysis of brain punches performed at the injection sites and observed a reduction of KIF1A level (Fig 6C). We then quantified the number of SVs at corticostriatal synapses from EM sections prepared from WT and HTT-SD brains injected with lentiviral sh-Scr or sh-KIF1A. We observed a significant reduction in the number of SVs in WT sh-KIF1A presynapses when compared to WT sh-Scr presynapses (Fig 6E). As previously shown (Fig 2C), HTT S421 phosphorylation increased the number of SVs at presynapses. Importantly, this number was reverted to the WT condition in HTT-SD brains treated with sh-KIF1A. Together, this demonstrates that decreasing the phospho-HTT-induced SVP transport by reducing KIF1A levels in corticostriatal projecting neurons reverse the increase of vesicles at synapses induced by chronic HTT phosphorylation.

### **HTT-KIF1A-mediated axonal transport of SVPs in corticostriatal projecting neurons regulates procedural memory.**

We next investigated procedural memory in three-month old WT and HTT-SD mice injected with lentiviral sh-scr or sh-KIF1A. We used the same behavioral protocol described in Figure 1 except that the behavioral tests were performed three weeks after injection (Figure 7A). Analysis of the time to fall of the rotarod of the four groups of mice showed that in global, sh-KIF1A injection in WT mice reduced their performance as revealed by a significant reduction of the time spent on the rotarod. As previously observed (Fig 1), HTT-SD mice also performed less as compared to WT sh-Scr injected mice (Fig 7B-C). However, we observed that the lentiviral injection of sh-KIF1A significantly ameliorated the performance of the HTT-SD mice (Fig 7B-C). This increase was particularly evident in the first phase of habit formation that corresponds to the first 10 sessions of the first training day (Figure 7D-E). This indicates that the HTT-KIF1A-mediated transport of SVPs directly impact on SV at synapses and on procedural memory.

Interestingly, we found the rescue to be lost during the last day (Fig 6F, G) as HTT-SD mice injected with sh-KIF1A or sh-scr were indistinguishable. Conversely, we observed that the memory of WT mice injected with shKIF1A was impaired during the first three days but not at the end of the training (fig 6C). These observed defects in both WT mice injected with sh-KIF1A and HTT-SD mice suggest that procedural memory might be tightly linked to the efficacy of axonal transport and the subsequent number of SVs at synapses. We therefore scored the SVs number at synapses in individual animals and correlated this number to their performance on the first day of accelerating rotarod. Strikingly, we found that a tight balance of SVs at synapses is required for an efficient establishment of the procedural memory in mice ( $R^2=0,6$ ) (Figure 7H). Together, our findings indicate that HTT-KIF1A-mediated axonal transport of SVPs in the corticostriatal projecting neurons, a process regulated by phosphorylation, modulate the number of SVs at synapses, the probability of release and subsequently procedural memory.

## **Discussion**

### **HTT, a scaffold protein for KIF1A mediated transport.**

In this study, we show that HTT acts as a scaffold protein for SVP, regulating its transport, thus acting as an adaptor of SVP transport (Meng-meng Fu & Holzbaur, 2014). Other adaptors of SVP transport have been described in the literature like DENN/MADD binding to KIF1A by its death domain and to Rab3, located within the SVP membrane (Shigeo Takamori et al., 2006), by its MADD domain. DENN/MADD is known to regulate SVP binding to MTs according to the nucleotide state of Rab3 (Niwa et al., 2008; O. I. Wagner et al., 2009). Although DENN/MADD has not been found in HTT interactome, Rab3 isoforms are part of HTT interactome (Shirasaki et al., 2012). Rab3 is particularly noticeable because it has been shown to be transported by fast axonal transport of SVs or HTT positive vesicles through KIF1A and/or KIF1B $\beta$  transport (Kevenaer et al., 2016; J. A. White et al., 2015). Thus, Rab3 interaction with HTT on SVP would re-enforce the HTT role for scaffolding many proteins responsible for SVP transport regulation. Interestingly, HTT reduced levels have been shown to perturb Rab3 vesicle bidirectional transport (J. A. White et al., 2015). Moreover, the HTT mutation responsible for HD has been found not only to progressively decrease the levels of mRNA Rab3 in HD model mouse (Ruben Smith et al., 2005) but also to dysregulate Rab3 conversion from GTP to GDP state (Hong et al., 2016). Recently, it also has been demonstrated that HD mice show a decrease in glutamatergic transmission, amplifying HTT role for SVP transport (Fernandez-Garcia et al., 2020).

### **Too few SVs at the axon terminal is detrimental for the synapse ...**

Number of vesicles at the synapse seems not only to be crucial but also finely balanced since both too few vesicles and too many vesicles have already been shown to be detrimental for synaptic functions (L. B. Li et al., 2016; Phan et al., 2019) (figure 8). Too few vesicles at the synapse can be caused by decreased level of KIF1A or loss-of function mutation of KIF1A. Decreasing KIF1A levels in vivo by knocking down KIF1A or silencing KIF1A expression in mice is respectively postnatally lethal (Yonekawa et al., 1998) or responsible for procedural memory impairment. Loss-of-function mutation of KIF1A is detrimental for synaptic transmission, synaptic strength and learning and memory (Chiba et al., 2019; Esmaeeli Nieh et al., 2015; Guedes-dias et al., 2019; Yonekawa et al., 1998; Y. V. Zhang et al., 2017). Indeed, some KIF1A mutation lead to both a mEPSC frequency and quantal release decrease in the *Drosophila* NMJ (Y. V. Zhang et al., 2017). In humans, KIF1A T99M is known in human to be responsible for SPG30 causing cerebellar atrophy, intellectual disabilities, ataxia and stiffness of the legs (Esmaeeli Nieh et al., 2015).

In HD, although no quantification of the number of SV has been done yet, a recent study proved that glutamate neurotransmission is reduced in HD mice, and especially in the M2-DLS network. It would thus be interesting to quantify the number of SVs in HD. Furthermore, the same study showed that, local and optogenetic stimulation of this network improves motor learning and coordination of these

mice. This suggest first that glutamate transmission could be a key player in HD to cause the behavioral phenotypes and then that balancing the decreased glutamate transmission is sufficient to restore the phenotypes (Fernández-García et al., 2020).

### **... But too many SVs at the axon terminal is toxic for the synapse**

However, too many vesicles at the synapse are also detrimental since it participates to the procedural memory impairment in HT<sub>S421D</sub> mice by increasing the probability of release. Interestingly, another study proved, using ASIC KO mice, that an increase of the probability of release leads to a reduction of facilitation and an increase of mEPSC frequency, which could explain the deficits in learning and memory of these mice (Cho & Askwith, 2008).

Accumulation of SV can be caused by a disrupted axonal transport of SVP through HTT phosphorylation as we saw, but also through KIF1A gain of function mutation A255V (Chiba et al., 2019; Gabrych et al., 2019) or KBP non-sens mutation, known to cause Goldberg-Shprintzen syndrome characterized by intellectual disability, microcephaly and axonal neuropathy (Kevenaer et al., 2016; Lyons et al., 2008). Genetic regulation, affecting other target than KIF1A, can also lead to an accumulation of SV at the synapse in flies through stromalin expression, a cohesion complex member (Phan et al., 2019). This complex is mutated in cohesinopathies like cornelia de Lange syndrome where an accumulation of SVP at the synapse is a good candidate to explain some neurological deficits observed in this neurodegenerative disorder like seizures (Dowsett et al., 2019; Phan et al., 2019).

### **SV pools and probability of release**

Within the presynapse, SVs are organized into different pools according to their composition, age and distance from the active zone, namely the Readily releasable pool (RRP), the recycling pool and the reserve pool (Crawford & Kavalali, 2015; P. S. Kaeser & Regehr, 2017; Kavalali, 2006; Rizzoli, 2014; Truckenbrodt et al., 2018). RRP is considered as the pool containing the SV ready to be released very fast upon neuronal activity, docked and/or primed. Once the RRP is depleted, it is thought to be filled from SVs within the reserve pool by a slow process (hundreds of milliseconds) (Pulido & Marty, 2017). Facilitation is thought, by increasing SV docking, to compensate for the SV depletion of the RRP after a first stimulation which would then produce depression (Pulido & Marty, 2017). In our HT<sub>S421D</sub> mouse model, we could hypothesize that the higher number of SVs at the presynapse induces a higher number of docked SVs and SV released during the first stimuli, which could impair the increasing in docking normally observed during facilitation.

### **HTT phosphorylation in HD context**

Here, we point out the importance of HTT role through its phosphorylation on regulating the SV number reaching the synapse. Since HTT, when mutated in HD, is known to cause severe and deadly symptoms of motor incoordination, cognitive decline and psychiatric disorders, it is interesting to understand HTT phosphorylation on S421 role in HD. First, in HD, phosphorylation on S421 as well as

Akt levels are decreased and calcineurin levels, the phosphatase for S421, are increased (Colin et al., 2008; Humbert et al., 2002; Pineda et al., 2009; Warby et al., 2005). Consequences of this neuroprotective cellular pathway dysregulation and rescue strategies based on S421 phosphomimetism have been studied (Humbert et al., 2002; Kratter et al., 2016; Pardo, 2006; Pineda et al., 2009; Zala et al., 2008) and focused on BDNF transport or release as a read out of the rescue. However, it would be interesting to study the S421D impact on SVP transport in a rescue context for HD (Humbert et al., 2002; Kratter et al., 2016; Zala et al., 2008).

#### **Silencing KIF1A does not affect axonal BDNF transport**

As mentioned earlier, KIF1A has been shown to transport and regulate axonal entry of DCVs containing BDNF in neurites (Gumy et al., 2017; Hung & Coleman, 2016; Lim et al., 2017; Lo et al., 2011). So why don't we observe a reduction of BDNF vesicle transport in our shKIF1A transduced axons? To our knowledge, only few studies focused on BDNF transport upon KIF1A silencing and the main one reports different effects on flux, run length and speed according to the RNAi used (the mouse KIF1A RNAi showing little or no impairment on BDNF vesicle dynamics) (Lo et al., 2011). Moreover, other kinesins like KIF5B could compensate for the loss of KIF1A (Dompierre et al., 2007; Lo et al., 2011). All of these arguments lead us to think that it is possible that our shKIF1A is specific to SVP transport.

#### **DLS early effect on procedural memory**

Surprisingly, lowering KIF1A levels within M1 neurons projecting mainly to the DLS rescued the early phases of procedural memory establishment, usually attributed to the DMS area, rather than the late phase of the procedural memory establishment (Costa et al., 2004; Yin et al., 2009). The explanation might come from the engagement of both DMS and DLS during the first phase of the learning (Kupferschmidt et al., 2017; Perrin & Venance, 2019) thus, targeting DLS might be sufficient to induce a rescue of the procedural memory during the first days. However, how do we explain the loss of rescue during the late phases of learning? Studies focusing on the dynamics of DLS across training proved that the number of active cell clusters upon stimulation within the DLS is reduced with training, as a refinement strategy of the connections with training (Corbit et al., 2017) (Badreddine et al., *under revision*). Thus, it is possible that the small number of DLS connections responsible for the habit formation were not targeted by the shKIF1A virus, whose expression does not cover the entire DLS.

#### **Contact for reagent and resource sharing**

Further information and requests for resources and reagents should be directed to and will be fulfilled by the Lead Contact, Frédéric Saudou

## Material and methods

### Mice

*Hdh*<sup>S421A/S421A</sup> and *Hdh*<sup>S421D/S421D</sup> mice used in this study were described earlier (Thion et al., 2015) and generated by Mouse Clinical Institute (Strasbourg, France). Briefly, these C57Bl6/J mice were knocked in with a point mutation replacing the serine 421 by an alanine or an aspartic acid, respectively.

Animals were housed under standard conditions of temperature ( $21 \pm 2^\circ\text{C}$ ) and humidity ( $55 \pm 5\%$ ), with food and water *ad libitum* in a 12:12h day/night cycle. Animals were held in accordance with the French animal welfare act and the EU legislation (council directive 2010/63/EU). The French Ministry of Agriculture and the local ethics committee gave a specific authorization (authorization no. 18607) to conduct the experiments described in the present study.

### Behavior

Many behavioral tests aiming at characterizing the mice have already been performed (Bruyère et al., 2020; Y. Ehinger et al., 2020; Thion et al., 2015) and we focused here on the accelerating rotarod. The test was performed during the beginning of the light phase and mice had access to food and water *ad libitum*. All the precautions have been taken to limit the variability of the results while preserving animal well-being. For this purpose, we used only males and littermate mice were kept in the same cages (until their injection). Cages were transported to the experimental room at least 30 minutes prior the tests to allow the acclimatation.

#### ***Accelerating rotarod***

Procedural memory was tested with the accelerated rotarod paradigm. The rotarod LE8305 from BIOSEB was used. Before the accelerating rotarod phase, mice got used to the rod with a 4RPM speed for 1 minute the day preceding the 8-day test. Rotarod test was performed over 8 consecutive days with 10 sessions per day per mouse at increasing speed from 4 RPM to 40 RPM in 5 minutes. Each trial was separated by at least a 15-minute resting period. The latency and the speed to fall off from the rotarod were recorded.

### Plasmids and lentiviruses

shKIF1A plasmid was a kind gift from C. Hoogenraad's lab (JL-35, (Kevenaar et al., 2016) and its control, shscr is a mouse universal scramble (5' GACCCCTCGCTAAGTAGT 3'). Vglut-1 cDNA sequence was amplified from adult mouse and pHluorin plasmid was a kind gift from T.Ryan's lab (Fernandez-Alfonso & Ryan, 2008). Vglut-1-pHluorin was created by cloning vglut-1 sequence before the pHluorin sequence in a SmaI site. Vamp-2-mCherry plasmid was a kind gift from T.Ryan's lab (Calloway et al., 2015) and BDNF-mCherry construct was previously described in Hinckelmann et al., 2016 and used in Virlogeux et al., 2018.

shKIF1A plasmid has been cloned into pSIN lentiviral vector (Drouet et al., 2009) by Gateway system (Life Technology) using sense primer

5'-

GGGGACAAGTTTGTACAAAAAAGCAGGCTTCTGAATTCTGCAGTCGACGG-3' and anti-sens primer 5'-GGGGACCACTTTGTACAAGAAAGCTGGGTCGCGGCCGCCCTACTTGTACA-3' and recombination. Shscramble, Vamp-2-mCherry, BDNF-mCherry and vglut-1-pHluorin plasmids have been cloned into pSIN vector using the same strategy.

Vamp-2-mCherry, shKIF1A and shscramble lentiviruses were produced by ENS Lyon Vectorology Facility with titer higher than (vamp2:  $3.65 \times 10^9$  ui/l)  $10^8$  UI/ml. Vglut-1-pHluorin and BDNF-mCherry lentiviruses were homemade produced by the GIN virus production platform.

### **Stereotaxic injections**

Animals were anesthetized by inhalation of isoflurane associated with a mix of oxygen and air (3-5% of isoflurane for induction and 1-2% in the mask). Mouse head was then shaved and placed within the stereotaxic frame. Skin was incised and skull was bilaterally drilled. With a nanoinjector, diluted lentivirus (1/3 in saline solution) was bilaterally injected (500nl at 50nl/min speed) at position AP:1,54 ML: + or -1,6 DV: -0,8. Finally, skin was sutured and 1 ml of NaCl 0,9% was injected subcutaneously. After surgery, mice were put alone in a cage and monitored daily.

### **Electron microscopy**

Between 3 and 4 month-animals were anesthetized with 1ml/kg of Doléthal® and perfused transcardially with cold PBS followed by 2% paraformaldehyde 2% glutaraldehyde and 0,1M cacodylate cold solution. Brains were removed and dorsolateral striatum was punched either directly from the brain to obtain 1mm square piece of tissue, either from 100 µm-thick slices obtained from vibratome.

### **Electrophysiology**

#### **Microfluidics**

##### ***Neurons in microfluidic chambers***

As described in Virlogeux et al., 2018, primary cortical and striatal neurons were dissected from E15.5 wild type (C57Bl6/J) or *Hdh*<sup>S421A/S421A</sup> or *Hdh*<sup>S421D/S421D</sup> mouse embryos. They then underwent a chemical dissociation with papain cysteine solution, DNase (1/100) and FBS (1/10) and were finally mechanically dissociated. Dissociated cortical and striatal neurons were re-suspended in growing medium ( $5 \times 10^6$  cells in 120 µl) and plated in the chamber with a final density of  $\sim 7000$  cells/mm<sup>2</sup>. Growing medium was added in the synaptic chamber to equilibrate flux. Cortical neurons were plated in the presynaptic chamber and striatal neurons were plated in the postsynaptic chamber. Neurons were left in the incubator for 2 hours, then all compartments were gently filled with growing medium.

##### ***Vesicular transport***

Between DIV0 and DIV4, cortical neurons within the presynaptic compartment were transduced with lentivirus expressing VAMP2-mCherry or BDNF-mCherry. They were washed out the next day. At DIV 8, cortical neurons were transduced with shKIF1A or shScramble lentiviruses. Before recordings, DIV 12 neurons in microchamber were carefully inspected and selected based on the absence of cell



contamination. For double transduction, transport of mCherry-tagged cargo was analyzed within GFP-positive axons.

Images were acquired every 200 ms for 1min on inverted microscope (Axio Observer, Zeiss) with X63 oil-immersion objective (1.46NA) coupled to a spinning-disk confocal system (CSU-W1-T3; Yokogawa) connected to an electron-multiplying CCD (charge-coupled device) camera (ProEM+1024, Princeton Instrument) at 37 °C and 5% CO<sub>2</sub>.

### ***Immunolabelling***

Neurons from the reconstituted corticostriatal network within microfluidics device were fixed with a PFA/Sucrose solution (4%/4% in PBS) for 20 min at room temperature (RT). After three washes of PBS, neurons were incubated first with a blocking solution (BSA 1%, NGS 2%, Triton X-100 0.1%) and then with primary antibodies (KIF1A, HTT (4c8), mCherry) overnight at 4°C. The next day, neurons were washed with three washes of PBS followed by one-hour incubation at RT of appropriate secondary antibodies and finally washed again three times with PBS. Images were acquired with a X63 oil-immersion objective (1.4 NA) using an inverted confocal microscope (LSM 710, Zeiss) coupled to an Airyscan detector. Images were then smoothed and a similar percentage of threshold was applied. Mandel coefficient was calculated using coloc2 imageJ plugin and the numbers of colocalizing pixels were obtained by the multiplication between the number of pixels of one channel and the corresponding Mandel coefficient. Number of pixels was obtained by the following equation:  $(\text{area} * \text{mean fluorescence intensity}) / 255$ . Each condition was tested using at least 3 microfluidics device per culture from 2 independent cultures. In each microfluidics device, at least 3 fields were analyzed.

### ***Exocytosis event recording***

At DIV0, cortical neurons within the presynaptic compartment were transduced with lentivirus expressing vGlut-1-pHluorin. Lentivirus was washed out the next day. Before recordings, DIV 12 neurons in microchamber were carefully inspected and selected based on the absence of cell contamination.

Images were acquired every 200 ms for 1min on inverted microscope (Axio Observer, Zeiss) with X63 oil-immersion objective (1.46NA) coupled to a spinning-disk confocal system (CSU-W1-T3; Yokogawa) with TIRF microscopy at 37 °C and 5% CO<sub>2</sub>. The same three fields per microchambers were acquired before and after a 4AP-bicucullin (2.5mM and 50µM) stimulation of the presynaptic chamber, four times in total (1 before and three after stimulation). Analysis was automatized. Results from stimulated neurons are normalized with the activity of the same neuron without stimulation.

### **Biochemistry**

Cortical neurons were plated in free culture, transduced at DIV1 and lysed at DIV5 in NetN buffer (20 mM TrisHCl pH8, 120 mM NaCl, 1mM EDTA, 0.5% NP40) complemented with protease inhibitor cocktail (Roche).

Vesicular fraction from brains was prepared as described in (M.-V. Hinckelmann et al., 2016). Briefly, brains were homogenized in lysis buffer (10mM HEPES-KOH, 175 mM L-aspartic acid, 65 mM taurine, 85 mM betaine, 25 mM glycine, 6.5 mM MgCl<sub>2</sub>, 5mM EGTA, 0.5 mM D-glucose, 1.5 mM CaCl<sub>2</sub>, 20 mM DTT pH 7.2, protease inhibitor from Roche) on ice with a glass potter and then with a 25G needle. Lysates were then centrifuged (12000 RPM) and the supernatant, considered as the total fraction, is then centrifuged (3000RPM for 10 minutes). The resulting supernatant is centrifuged (12 000 RCF for 40 minutes). Supernatant is then ultracentrifuged (100 000g) to obtain the vesicular fraction (the pellet) and the cytosolic fraction (the supernatant).

Brains samples and punches of motor and visual cortex areas from injected mice were obtained by dissection under the binocular and homogenized in cold buffer containing 4 mM Hepes, pH 7.4, 320 mM sucrose and inhibitor cocktail (Roche).

All types of lysed samples were dosed by a Bradford reagent to quantify the protein concentration and then analyzed by SDS-PAGE transferred to PVDF membranes. Then, membranes were incubated for 45 minutes in a 5% BSA TBST (10mM Tris pH 8, 150 mM NaCl, 0.5% Tween 20) solution and incubated with primary antibodies against KIF1A (abcam ab180153, 1:1000), p150 (BD laboratories, #612708, 1:1000, Tubulin (Sigma, #F2168, 1:1000) at 4°C, overnight. The next day, membranes were washed at least three times with TBST and incubated in secondary antibodies (1:1000) for two hours at RT. Membranes were finally revealed with ECL (Amersham Biosciences) after three washes of TBST.

### **Mass spectrometry**

This analysis is extracted from Migazzi et al., 2020. Briefly, vesicular fraction from brains obtained as described earlier were first pre-cleared for an hour at 4°C with protein A Sepharose beads (Sigma Aldrich-P9424) and then immunoprecipitated for 3 hours at 4°C by agarose beads preincubated with anti-HTT D7F7 antibody (Cell Signaling-5656). To remove non-specific binding, the beads were washed three times with the lysis buffer and bound proteins are finally eluted with Laemmli buffer. The HTT corresponding band on the western blot was cut and analyzed. MS was performed with a LTQ Orbitrap XL mass spectrometer (Thermo Scientific), equipped with a nanoESI source (Proxeon). The top eight peaks in the mass spectra (Orbitrap; resolution, 60,000) were selected for fragmentation (CID; normalized collision energy, 35%; activation time, 30 ms, q-value, 0.25). Proteins were identified using the MaxQuant software package version 1.2.2.5 (MPI for Biochemistry, Germany) and UniProt database version 04/2013.

### **Immunolabelling**

For immunostaining, brains were incubated in PFA 4% overnight and washed with PBS three times the next day. Then, brains were cut into 100 µm-thick slices using vibratome. The slices were incubated with a blocking solution (0.3% triton, 10%NGD in PBS) for 2 hours at RT and then with antibody against GFP (Institut Curie, A-P-R#06) overnight at 4°C. The day after, primary antibody is removed by 3 washes of PBS before incubating the slices with the associated secondary antibody and finally with 3 washes of PBS. Finally, slices were mounted on Superfrost slides by using DAKO solution and coverslips and acquired with a x10 objective (0.45 NA) using a slide scanner (AxioScan Z1, Zeiss) and with a x10 objective (0.3 NA) using an inverted confocal microscope (LSM 710, Zeiss) coupled to an Airyscan detector to improve signal-to-noise ratio and to increase the resolution

### **Analysis**

Quantification of vesicle velocity, directional flow and vesicle number was done on 100 µm of neurite using KymoTool Box ImageJ plugin. Anterograde or retrograde speeds describe respectively the mean speed of anterograde or retrograde movement of a vesicle. The static vesicles are considered as the ones without any movement during the recording. Linear flow and directionality were calculated according to the following equations:

$$\text{linear flow} = |\text{anterograde speed} * \text{number of anterograde vesicles}| + |\text{retrograde speed} * \text{number of retrograde vesicles}|$$

$$\text{directionality} = \frac{\text{anterograde speed} * \text{number of anterograde vesicles} - \text{retrograde speed} * \text{number of retrograde vesicles}}{\text{anterograde speed} * \text{number of anterograde vesicles} + \text{retrograde speed} * \text{number of retrograde vesicles}}$$

### **Statistical analysis**

For each data set, outliers were identified and removed from the analysis using ROUT test (Q=1%). Then, Shapiro-Wilk normality test was performed to assess the normality of the data. According if the data set followed a normal repartition or not, parametric or non-parametric tests were performed, respectively. Then, if two conditions were analyzed, t-test (Mann-Whitney if nonparametric) was used. Then, if more than two conditions were compared, a two-way ANOVA or a one-way ANOVA (Kruskal-Wallis if nonparametric followed by a Dunn's post hoc analysis) were used according if the data set were dependent to another or not, respectively. \*p < 0.05; \*\*p < 0.01; \*\*\*p < 0.001; \*\*\*\*p < 0.0001; ns, not significant. Statistical calculations were performed using GraphPad Prism 6.0

### **Acknowledgements**

We thank Sebastien Carnicella, Alain Marty, members of the Saudou, Humbert and Venance labs for comments; Vicky Brandt for critical reading; Béatrice Blot, Aurélie Genoux, Chiara Scaramuzzino, Nagham Badreddine for technical help and/or initial experiments; T.Ryan for the gift of pHluorin plasmid C. Hoogenraad for the gift of shKIF1A plasmid, Y. Saoudi and the GIN imaging facility (PIC-GIN) for help with image acquisitions; G. Froment, D. Nègre, and C. Costa from SFR Biosciences (UMS3444/CNRS, US8/Inserm, ENS de Lyon, UCBL) for lentivirus production. This work was supported

by grants from ANR-15-IDEX-02 NeuroCoG (F.S.) in the framework of the “Investissements d’avenir” program, Fondation pour la Recherche Médicale (FRM, DEI20151234418, F.S.; DEQ20170336752, S.H.), Fondation pour la Recherche sur le Cerveau (FRC)(F.S.), Fondation Bettencourt Schueller (F.S.) and AGEMED program from INSERM (F.S. & S.H.). F.S. laboratory is member of the Grenoble Center of Excellence in Neurodegeneration (GREEN). H.V. was supported by a PhD fellowship from Association Huntington France and by a FRM fellowship (FDT201904008035)

### **Additional information**

**Supplementary files** include 3 Supplementary Figures

### **Competing financial interests:**

The authors declare that they have no competing interests

### **References**

- Alabi, A. A., & Tsien, R. W. (2012). Synaptic Vesicle Pools and Dynamics. 1–18.
- Barkus, R. V., Klyachko, O., Horiuchi, D., Dickson, B. J., & Saxton, W. M. (2008). Identification of an axonal kinesin-3 motor for fast anterograde vesicle transport that facilitates retrograde transport of neuropeptides. *Molecular Biology of the Cell*, 19(1), 274–283. <https://doi.org/10.1091/mbc.E07-03-0261>
- Bentley, M., & Banker, G. (2016). The cellular mechanisms that maintain neuronal polarity. *Nature Reviews Neuroscience*, 17(10), 611–622. <https://doi.org/10.1038/nrn.2016.100>
- Bruyère, J., Abada, Y.-S., Vitet, H., Fontaine, G., Deloulme, J.-C., Cès, A., Denarier, E., Pernet-Gallay, K., Andrieux, A., Humbert, S., Potier, M.-C., Delatour, B., & Saudou, F. (2020). Presynaptic APP levels and synaptic homeostasis are regulated by Akt phosphorylation of huntingtin. *ELife*, 9. <https://doi.org/10.7554/eLife.56371>
- Calloway, N., Gouzer, G., Xue, M., & Ryan, T. A. (2015). The active-zone protein Munc13 controls the use-dependence of presynaptic voltage-gated calcium channels. *ELife*, 4(JULY2015), 1–15. <https://doi.org/10.7554/eLife.07728>
- Chen, C. W., Peng, Y. F., Yen, Y. C., Bhan, P., Muthaiyan Shanmugam, M., Klopfenstein, D. R., & Wagner, O. I. (2019). Insights on UNC-104-dynein/dynactin interactions and their implications on axonal transport in *Caenorhabditis elegans*. *Journal of Neuroscience Research*, 97(2), 185–201. <https://doi.org/10.1002/jnr.24339>
- Chiba, K., Takahashi, H., Chen, M., Obinata, H., Arai, S., Hashimoto, K., & Oda, T. (2019). Disease-associated mutations hyperactivate KIF1A motility and anterograde axonal transport of synaptic vesicle precursors. *PNAS*, 116(37), 18429–18434. <https://doi.org/10.1073/pnas.1905690116>
- Cho, J. H., & Askwith, C. C. (2008). Presynaptic release probability is increased in hippocampal neurons from ASIC1 knockout mice. *Journal of Neurophysiology*, 99(2), 426–441. <https://doi.org/10.1152/jn.00940.2007>

- Colin, E., Zala, D., Liot, G., Rangone, H., Borrell-Pagès, M., Li, X.-J., Saudou, F., & Humbert, S. (2008). Huntingtin phosphorylation acts as a molecular switch for anterograde/retrograde transport in neurons. *The EMBO Journal*, *27*(15), 2124–2134. <https://doi.org/10.1038/emboj.2008.133>
- Corbit, V. L., Ahmari, S. E., & Gittis, A. H. (2017). A Corticostriatal Balancing Act Supports Skill Learning. *Neuron*, *96*(2), 253–255. <https://doi.org/10.1016/j.neuron.2017.09.046>
- Costa, R. M., Cohen, D., & Nicolells, M. A. (2004). Differential Corticostriatal Plasticity during Fast and Slow Motor Skill Learning in Mice. *Current Biology*, *14*, 1124–1134. <https://doi.org/10.1016/j.cub.2004.06.053>
- Crawford, D. C., & Kavalali, E. T. (2015). Molecular underpinnings of synaptic vesicle pool heterogeneity. *Traffic*, *16*(4), 338–364. <https://doi.org/10.1111/tra.12262>
- DiFiglia, M., Sapp, E., Chase, K., Schwarz, C., Meloni, A., Young, C., Martin, E., Vonsattel, J. P., Carraway, R., Reeves, S. A., Boyce, F. M., & Aronin, N. (1995). Huntingtin is a cytoplasmic protein associated with vesicles in human and rat brain neurons. *Neuron*, *14*(5), 1075–1081. [https://doi.org/10.1016/0896-6273\(95\)90346-1](https://doi.org/10.1016/0896-6273(95)90346-1)
- Dompierre, J. P., Godin, J. D., Charrin, B. C., Cordelières, F. P., King, S. J., Humbert, S., & Saudou, F. (2007). Histone deacetylase 6 inhibition compensates for the transport deficit in Huntington’s disease by increasing tubulin acetylation. *The Journal of Neuroscience: The Official Journal of the Society for Neuroscience*, *27*(13), 3571–3583. <https://doi.org/10.1523/JNEUROSCI.0037-07.2007>
- Dowsett, L., Porras, A. R., Kruszka, P., Davis, B., Hu, T., Honey, E., Badoe, E., Thong, M. K., Leon, E., Girisha, K. M., Shukla, A., Nayak, S. S., Shotelersuk, V., Megarbane, A., Phadke, S., Sirisena, N. D., Dissanayake, V. H. W., Ferreira, C. R., Kisling, M. S., ... Krantz, I. D. (2019). Cornelia de Lange syndrome in diverse populations. *American Journal of Medical Genetics, Part A*, *179*(2), 150–158. <https://doi.org/10.1002/ajmg.a.61033>
- Drouet, V., Perrin, V., Hassig, R., Dufour, N., Auregan, G., Alves, S., Bonvento, G., Brouillet, E., Luthi-Carter, R., Hantraye, P., & Déglon, N. (2009). Sustained effects of nonallele-specific huntingtin silencing. *Annals of Neurology*, *65*(3), 276–285. <https://doi.org/10.1002/ana.21569>
- Ehinger, Y., Bruyère, J., Panayotis, N., Abada, Y.-S., Borloz, E., Matagne, V., Scaramuzzino, C., Vitet, H., Delatour, B., Saidi, L., Villard, L., Saudou, F., & Roux, J.-C. (2020). Huntingtin phosphorylation governs BDNF homeostasis and improves the phenotype of *Mecp2* knockout mice. *EMBO Molecular Medicine*, *12*(2). <https://doi.org/10.15252/emmm.201910889>
- Esmaeeli Nieh, S., Madou, M. R. Z., Sirajuddin, M., Fregeau, B., Mcknight, D., Lexa, K., Strober, J., Spaeth, C., Hallinan, B. E., Smaoui, N., Pappas, J. G., Burrow, T. A., McDonald, M. T., Latibashvili, M., Leshinsky-Silver, E., Lev, D., Blumkin, L., Vale, R. D., Barkovich, A. J., & Sherr, E. H. (2015). De novo mutations in *KIF1A* cause progressive encephalopathy and brain atrophy. *Annals of Clinical and Translational Neurology*, *2*(6), 623–635. <https://doi.org/10.1002/acn3.198>
- Fernandez-Alfonso, T., & Ryan, T. A. (2008). A heterogeneous “resting” pool of synaptic vesicles that is dynamically interchanged across boutons in mammalian CNS synapses. *Brain Cell Biology*, *36*(1–4), 87–100. <https://doi.org/10.1007/s11068-008-9030-y>

Fernández-García, S., Conde-Berriozabal, S., García-García, E., Gort-Paniello, C., Bernal-Casas, D., Barriga, G. G.-D., López-Gil, J., Muñoz-Moreno, E., Sòria, G., Campa, L., Artigas, F., Rodriguez, M., Alberch, J., & Masana, M. (2020). M2 Cortex-Dorsolateral striatum stimulation reverses motor symptoms and synaptic deficits in Huntington's Disease. 1–24.  
<https://doi.org/10.1101/2020.04.08.032359>

Fogel, H., Frere, S., Segev, O., Bharill, S., Shapira, I., Gazit, N., O'Malley, T., Slomowitz, E., Berdichevsky, Y., Walsh, D. M., Isacoff, E. Y., Hirsch, J. A., & Slutsky, I. (2014). APP homodimers transduce an amyloid- $\beta$ -mediated increase in release probability at excitatory synapses. *Cell Reports*, 7(5), 1560–1576. <https://doi.org/10.1016/j.celrep.2014.04.024>

Fu, M., & Holzbaur, E. L. F. (2014). Integrated regulation of motor-driven organelle transport by scaffolding proteins. *Trends in Cell Biology*, 24(10), 564–574.  
<https://doi.org/10.1016/j.tcb.2014.05.002>

Furuta, K., Furuta, A., Toyoshima, Y. Y., Amino, M., Oiwa, K., & Kojima, H. (2013). Measuring collective transport by defined numbers of processive and nonprocessive kinesin motors. *Proceedings of the National Academy of Sciences of the United States of America*, 110(2), 501–506.  
<https://doi.org/10.1073/pnas.1201390110>

Gabrych, D. R., Lau, V. Z., Niwa, S., & Silverman, M. A. (2019). Going Too Far Is the Same as Falling Short†: Kinesin-3 Family Members in Hereditary Spastic Paraplegia. *Frontiers in Cellular Neuroscience*, 13(September), 1–24. <https://doi.org/10.3389/fncel.2019.00419>

Gauthier, L. R., Charrin, C., Dompierre, J. P., Borrell-page, M., Cordelie, F. P., Mey, J. De, Macdonald, M. E., Leßmann, V., Humbert, S., & Saudou, F. (2004). Huntingtin Controls Neurotrophic Support and Survival of Neurons by Enhancing BDNF Vesicular Transport along Microtubules. *Cell*, 118, 127–138.

Graybiel, A. M., & Grafton, S. T. (2015). The Striatum: Where Skills and Habits Meet. *Cold Spring Harb Perspect Biol*, 1–14.

Guedes-Dias, P., & Holzbaur, E. L. F. (2019). Axonal transport: Driving synaptic function. *Science*, 366(6462). <https://doi.org/10.1126/science.aaw9997>

Guedes-dias, P., Nirschl, J. J., Abreu, N., Tokito, M. K., Janke, C., Magiera, M. M., Holzbaur, E. L. F., (2019). Kinesin-3 Responds to Local Microtubule Dynamics to Target Synaptic Cargo Delivery to the Presynapse Article Kinesin-3 Responds to Local Microtubule Dynamics to Target Synaptic Cargo Delivery to the Presynapse. *Current Biology*, 29(2), 268-282.e8.  
<https://doi.org/10.1016/j.cub.2018.11.065>

Gumy, L. F., Katrukha, E. A., Grigoriev, I., Jaarsma, D., Kapitein, L. C., Akhmanova, A., & Hoogenraad, C. C. (2017). MAP2 Defines a Pre-axonal Filtering Zone to Regulate KIF1- versus KIF5-Dependent Cargo Transport in Sensory Neurons. *Neuron*, 94(2), 347-362.e7.  
<https://doi.org/10.1016/j.neuron.2017.03.046>

Hanse, E., & Gustafsson, B. (2001). Vesicle release probability and pre-primed pool at glutamatergic synapses in area CA1 of the rat neonatal hippocampus. *Journal of Physiology*, 531(2), 481–493.  
<https://doi.org/10.1111/j.1469-7793.2001.0481i.x>

- Hawes, S. L., Evans, R. C., Unruh, B. A., Benkert, E. E., Gillani, F., Dumas, T. C., & Blackwell, K. T. (2015). Multimodal plasticity in dorsal striatum while learning a lateralized navigation task. *Journal of Neuroscience*, 35(29), 10535–10549. <https://doi.org/10.1523/JNEUROSCI.4415-14.2015>
- Hayashi, K., Hasegawa, S., Sagawa, T., Tasaki, S., & Niwa, S. (2018). Non-invasive force measurement reveals the number of active kinesins on a synaptic vesicle precursor in axonal transport regulated by ARL-8. *Physical Chemistry Chemical Physics*, 20(5), 3403–3410. <https://doi.org/10.1039/c7cp05890j>
- Her, L., & Goldstein, L. S. B. (2008). Enhanced Sensitivity of Striatal Neurons to Axonal Transport Defects Induced by Mutant Huntingtin. 28(50), 13662–13672. <https://doi.org/10.1523/JNEUROSCI.4144-08.2008>
- Hinckelmann, M.-V., Virlogeux, A., Niehage, C., Poujol, C., Choquet, D., Hoflack, B., Zala, D., & Saudou, F. (2016). Self-propelling vesicles define glycolysis as the minimal energy machinery for neuronal transport. *Nature Communications*, 7, 13233. <https://doi.org/10.1038/ncomms13233>
- Hong, Y., Zhao, T., Li, X. J., & Li, S. (2016). Mutant huntingtin impairs BDNF release from astrocytes by disrupting conversion of Rab3a-GTP into Rab3a-GDP. *Journal of Neuroscience*, 36(34), 8790–8801. <https://doi.org/10.1523/JNEUROSCI.0168-16.2016>
- Humbert, S., Bryson, E. A., Cordelie, F. P., Connors, N. C., Datta, S. R., Finkbeiner, S., & Greenberg, M. E. (2001). The IGF-1 / Akt Pathway Is Neuroprotective in Huntington' s Disease and Involves Huntingtin Phosphorylation by Akt. 2, 831–837.
- Hung, C. O. Y., & Coleman, M. P. (2016). KIF1A mediates axonal transport of BACE1 and identification of independently moving cargoes in living SCG neurons. *Traffic*, 17(11), 1155–1167. <https://doi.org/10.1111/tra.12428>
- Kaesler, P. S., & Regehr, W. G. (2017). The readily releasable pool of synaptic vesicles. In *Current Opinion in Neurobiology* (Vol. 43, pp. 63–70). Elsevier Ltd. <https://doi.org/10.1016/j.conb.2016.12.012>
- Kaether, C., Skehel, P., & Dotti, C. G. (2000). Axonal Membrane Proteins Are Transported in Distinct Carriers: A Two-Color Video Microscopy Study in Cultured Hippocampal Neurons □. 11(April), 1213–1224.
- Katz B. (1969). *The Release of Neuronal Transmitter Substances*. Liverpool Univ. Press.
- Kavalali, E. T. (2006). Synaptic vesicle reuse and its implications. In *Neuroscientist* (Vol. 12, Issue 1, pp. 57–66). <https://doi.org/10.1177/1073858405281852>
- Kevenaar, J. T., Bianchi, S., Van Spronsen, M., Olieric, N., Lipka, J., Frias, C. P., Mikhaylova, M., Harterink, M., Keijzer, N., Wulf, P. S., Hilbert, M., Kapitein, L. C., De Graaff, E., Ahkmanova, A., Steinmetz, M. O., & Hoogenraad, C. C. (2016). Kinesin-Binding Protein Controls Microtubule Dynamics and Cargo Trafficking by Regulating Kinesin Motor Activity. *Current Biology*, 26(7), 849–861. <https://doi.org/10.1016/j.cub.2016.01.048>
- Koushika, S. P., Schaefer, A. M., Vincent, R., Willis, J. H., Bowerman, B., & Nonet, M. L. (2004). Mutations in *Caenorhabditis elegans* Cytoplasmic Dynein Components Reveal Specificity of Neuronal

Retrograde Cargo. *Journal of Neuroscience*, 24(16), 3907–3916.  
<https://doi.org/10.1523/JNEUROSCI.5039-03.2004>

Kratter, I. H., Zahed, H., Lau, A., Tsvetkov, A. S., Daub, A. C., Weiberth, K. F., Gu, X., Saudou, F., Humbert, S., Yang, X. W., Osmand, A., Steffan, J. S., Masliah, E., & Finkbeiner, S. (2016). Serine 421 regulates mutant huntingtin toxicity and clearance in mice. *Journal of Clinical Investigation*, 126(9), 3585–3597. <https://doi.org/10.1172/JCI80339>

Kupferschmidt, D. A., Juczewski, K., Cui, G., Johnson, K. A., & Lovinger, D. M. (2017). Parallel, but Dissociable, Processing in Discrete Corticostriatal Inputs Encodes Skill Learning. *Neuron*, 96(2), 476–489.e5. <https://doi.org/10.1016/j.neuron.2017.09.040>

Li, H., Wyman, T., Yu, Z. X., Li, S. H., & Li, X. J. (2003). Abnormal association of mutant huntingtin with synaptic vesicles inhibits glutamate release. *Human Molecular Genetics*, 12(16), 2021–2030.  
<https://doi.org/10.1093/hmg/ddg218>

Li, L. B., Lei, H., Arey, R. N., Li, P., Liu, J., Murphy, C. T., Xu, X. Z. S., & Shen, K. (2016). The Neuronal Kinesin UNC-104/KIF1A is a Key Regulator of Synaptic Aging and Insulin Signaling-Regulated Memory. *Current Biology*, 26(5), 605–615. <https://doi.org/10.1016/j.cub.2015.12.068>

Lim, A., Rechtsteiner, A., & Saxton, W. M. (2017). Two kinesins drive anterograde neuropeptide transport. *Molecular Biology of the Cell*, 28(24). <https://doi.org/10.1091/mbc.E16-12-0820>

Lipka, J., Kapitein, L. C., Jaworski, J., & Hoogenraad, C. C. (2016). Transport To Dendrites. *Embo J.*, 1(3), 1–17.

Liu, J. S., Schubert, C. R., Fu, X., Fourniol, F. J., Jaiswal, J. K., Houdusse, A., Stultz, C. M., Moores, C. A., & Walsh, C. A. (2012). Article Molecular Basis for Specific Regulation of Neuronal Kinesin-3 Motors by Doublecortin Family Proteins. *Molecular Cell*, 47(5), 707–721.  
<https://doi.org/10.1016/j.molcel.2012.06.025>

Lo, K. Y., Kuzmin, A., Unger, S. M., Petersen, J. D., & Silverman, M. A. (2011). KIF1A is the primary anterograde motor protein required for the axonal transport of dense-core vesicles in cultured hippocampal neurons. *Neuroscience Letters*, 491(3), 168–173.  
<https://doi.org/10.1016/j.neulet.2011.01.018>

Lyons, D. A., Naylor, S. G., Mercurio, S., Dominguez, C., & Talbot, W. S. (2008). KBP is essential for axonal structure, outgrowth and maintenance in zebrafish, providing insight into the cellular basis of Goldberg-Shprintzen syndrome. *Development*, 135(3), 599–608. <https://doi.org/10.1242/dev.012377>

Mahoney, T. R., Lin, Q., Itoh, T., Luo, S., Hadwiger, G., Vincent, R., Wang, Z. W., Fukuda, M., & Nonet, M. L. (2006). Regulation of synaptic transmission by RAB-3 and RAB-27 in *Caenorhabditis elegans*. *Molecular Biology of the Cell*, 17(6), 2617–2625. <https://doi.org/10.1091/mbc.E05-12-1170>

Mannella, F., Gurney, K., & Baldassarre, G. (2013). The nucleus accumbens as a nexus between values and goals in goal-directed behavior: A review and a new hypothesis. *Frontiers in Behavioral Neuroscience*, 7(OCT), 1–29. <https://doi.org/10.3389/fnbeh.2013.00135>



- Millicamps, S., & Julien, J. P. (2013). Axonal transport deficits and neurodegenerative diseases. *Nature Reviews Neuroscience*, 14(3), 161–176. <https://doi.org/10.1038/nrn3380>
- Monroy, B. Y., Tan, T. C., Oclaman, J. M., Han, J. S., Simó, S., Niwa, S., Nowakowski, D. W., McKenney, R. J., & Ori-McKenney, K. M. (2020). A Combinatorial MAP Code Dictates Polarized Microtubule Transport. *Developmental Cell*, 53(1), 60-72.e4. <https://doi.org/10.1016/j.devcel.2020.01.029>
- Niwa, S., Tanaka, Y., & Hirokawa, N. (2008). KIF1B  $\beta$  - and KIF1A-mediated axonal transport of presynaptic regulator Rab3 occurs in a GTP-dependent manner through DENN / MADD. 10(11). <https://doi.org/10.1038/ncb1785>
- Okada, Y., Yamazaki, H., Sekine-Aizawa, Y., & Hirokawa, N. (1995). The neuron-specific kinesin superfamily protein KIF1A is a unique monomeric motor for anterograde axonal transport of synaptic vesicle precursors. *Cell*, 81(5), 769–780. [https://doi.org/10.1016/0092-8674\(95\)90538-3](https://doi.org/10.1016/0092-8674(95)90538-3)
- Pace, R. De, Britt, D. J., Mercurio, J., Hoffmann, V., Abebe, D., Bonifacino, J. S., Pace, R. De, Britt, D. J., Mercurio, J., Foster, A. M., Djavaherian, L., Hoffmann, V., Abebe, D., & Bonifacino, J. S. (2020). Article Synaptic Vesicle Precursors and Lysosomes Are Transported by Different Mechanisms in the Axon of Mammalian Neurons II Synaptic Vesicle Precursors and Lysosomes Are Transported by Different Mechanisms in the Axon of Mammalian Neurons. *CellReports*, 31(11), 107775. <https://doi.org/10.1016/j.celrep.2020.107775>
- Pardo, R. (2006). Inhibition of Calcineurin by FK506 Protects against Polyglutamine-Huntingtin Toxicity through an Increase of Huntingtin Phosphorylation at S421. *Journal of Neuroscience*, 26(5), 1635–1645. <https://doi.org/10.1523/JNEUROSCI.3706-05.2006>
- Park, Hyekeun, Li, Y., & Tsien, R. W. (2012). Influence of synaptic vesicle position on release probability and exocytotic fusion mode. *Science*, 335(6074), 1362–1366. <https://doi.org/10.1126/science.1216937>
- Park, Hyungju, Popescu, A., & Poo, M. ming. (2014). Essential role of presynaptic NMDA receptors in activity-dependent BDNF secretion and corticostriatal LTP. *Neuron*, 84(5), 1009–1022. <https://doi.org/10.1016/j.neuron.2014.10.045>
- Perrin, E., & Venance, L. (2019). ScienceDirect Bridging the gap between striatal plasticity and learning. *Current Opinion in Neurobiology*, 54, 104–112. <https://doi.org/10.1016/j.conb.2018.09.007>
- Phan, A., Thomas, C. I., Chakraborty, M., Berry, J. A., Kamasawa, N., Davis, R. L., Phan, A., Thomas, C. I., Chakraborty, M., Berry, J. A., Kamasawa, N., & Davis, R. L. (2019). Stromalin Constrains Memory Acquisition by Developmentally Limiting Synaptic Vesicle Pool Size Article Stromalin Constrains Memory Acquisition by Developmentally Limiting Synaptic Vesicle Pool Size. *Neuron*, 101(1), 103-118.e5. <https://doi.org/10.1016/j.neuron.2018.11.003>
- Pineda, J. R., Pardo, R., Zala, D., Yu, H., Humbert, S., & Saudou, F. (2009). Genetic and pharmacological inhibition of calcineurin corrects the BDNF transport defect in Huntington’s disease. *Molecular Brain*, 2, 33. <https://doi.org/10.1186/1756-6606-2-33>

- Pulido, C., & Marty, A. (2017). Quantal Fluctuations in Central Mammalian Synapses: Functional Role of Vesicular Docking Sites. *Physiological Reviews*, 97(4), 1403–1430. <https://doi.org/10.1152/physrev.00032.2016>
- Rizzoli, S. O. (2014). Synaptic vesicle recycling: Steps and principles. *EMBO Journal*, 33(8), 788–822. <https://doi.org/10.1002/embj.201386357>
- Sampo, B., Kaech, S., Kunz, S., & Banker, G. (2003). Two distinct mechanisms target membrane proteins to the axonal surface. *Neuron*, 37(4), 611–624. [https://doi.org/10.1016/S0896-6273\(03\)00058-8](https://doi.org/10.1016/S0896-6273(03)00058-8)
- Saudou, F., & Humbert, S. (2016). The Biology of Huntingtin. *Neuron*, 89(5), 910–926. <https://doi.org/10.1016/j.neuron.2016.02.003>
- Sgro, A. E., Bajjalieh, S. M., & Chiu, D. T. (2013). Single-axonal organelle analysis method reveals new protein-motor associations. *ACS Chemical Neuroscience*, 4(2), 277–284. <https://doi.org/10.1021/cn300136y>
- Shirasaki, D. I., Greiner, E. R., Al-Ramahi, I., Gray, M., Boontheung, P., Geschwind, D. H., Botas, J., Coppola, G., Horvath, S., Loo, J. A., & Yang, X. W. (2012). Network organization of the huntingtin proteomic interactome in mammalian brain. *Neuron*, 75(1), 41–57. <https://doi.org/10.1016/j.neuron.2012.05.024>
- Smith, R., Petersén, Å., Bates, G. P., Brundin, P., & Li, J. Y. (2005). Depletion of rabphilin 3A in a transgenic mouse model (R6/1) of Huntington's disease, a possible culprit in synaptic dysfunction. *Neurobiology of Disease*, 20(3), 673–684. <https://doi.org/10.1016/j.nbd.2005.05.008>
- Staras, K., Branco, T., Burden, J. J., Pozo, K., Darcy, K., Marra, V., Ratnayaka, A., & Goda, Y. (2010). A Vesicle Superpool Spans Multiple Presynaptic Terminals in Hippocampal Neurons. *Neuron*, 66(1), 37–44. <https://doi.org/10.1016/j.neuron.2010.03.020>
- Stucchi, R., Plucińska, G., Hummel, J. J. A., Zahavi, E. E., Guerra San Juan, I., Klykov, O., Scheltema, R. A., Altelaar, A. F. M., & Hoogenraad, C. C. (2018). Regulation of KIF1A-Driven Dense Core Vesicle Transport: Ca<sup>2+</sup>/CaM Controls DCV Binding and Liprin- $\alpha$ /TANC2 Recruits DCVs to Postsynaptic Sites. *Cell Reports*, 24(3), 685–700. <https://doi.org/10.1016/j.celrep.2018.06.071>
- Takamori, S., Holt, M., Stenius, K., Lemke, E. A., Grønborg, M., Riedel, D., Urlaub, H., Schenck, S., Brügger, B., Ringler, P., Müller, S. A., Rammner, B., Gräter, F., Hub, J. S., De Groot, B. L., Mieskes, G., Moriyama, Y., Klingauf, J., Grubmüller, H., ... Jahn, R. (2006). Molecular Anatomy of a Trafficking Organelle. *Cell*, 127(4), 831–846. <https://doi.org/10.1016/j.cell.2006.10.030>
- Thion, M. S., McGuire, J. R., Sousa, C. M., Fuhrmann, L., Fitamant, J., Leboucher, S., Vacher, S., Du Montcel, S. T., Bièche, I., Bernet, A., Mehlen, P., Vincent-Salomon, A., & Humbert, S. (2015). Unraveling the Role of Huntingtin in Breast Cancer Metastasis. *Journal of the National Cancer Institute*, 107(10), 1–13. <https://doi.org/10.1093/jnci/djv208>
- Truckenbrodt, S., Viplav, A., Jähne, S., Vogts, A., Denker, A., Wildhagen, H., Fornasiero, E. F., & Rizzoli, S. O. (2018). Newly produced synaptic vesicle proteins are preferentially used in synaptic transmission. *The EMBO Journal*, 37(15), 1–24. <https://doi.org/10.15252/embj.201798044>

- Virlogeux, A., Moutaux, E., Christaller, W., Bruyere, J., Fino, E., Charlot, B., Cazorla, M., & Saudou, F. (2018). Reconstituting Corticostriatal Network on-a-Chip Reveals the Contribution of the Presynaptic Compartment to Huntington's Disease. *Cell Reports*, 22, 110–122. <https://doi.org/10.1016/j.celrep.2017.12.013>
- Vitet, H., Brandt, V., & Saudou, F. (2020). ScienceDirect Traffic signaling: new functions of huntingtin and axonal transport in neurological disease. <https://doi.org/10.1016/j.conb.2020.04.001>
- Wagner, O. I., Esposito, A., Köhler, B., Chen, C. W., Shen, C. P., Wu, G. H., Butkevich, E., Mandalapu, S., Wenzel, D., Wouters, F. S., & Klopfenstein, D. R. (2009). Synaptic scaffolding protein SYD-2 clusters and activates kinesin-3 UNC-104 in *C. elegans*. *Proceedings of the National Academy of Sciences of the United States of America*, 106(46), 19605–19610. <https://doi.org/10.1073/pnas.0902949106>
- Warby, S. C., Chan, E. Y., Metzler, M., Gan, L., Singaraja, R. R., Crocker, S. F., Robertson, H. A., & Hayden, M. R. (2005). Huntingtin phosphorylation on serine 421 is significantly reduced in the striatum and by polyglutamine expansion in vivo. *Human Molecular Genetics*, 14(11), 1569–1577. <https://doi.org/10.1093/hmg/ddi165>
- Weiss, K. R., & Littleton, J. T. (2016). Characterization of axonal transport defects in *Drosophila* Huntingtin mutants. *Journal of Neurogenetics*, 30(3–4), 212–221. <https://doi.org/10.1080/01677063.2016.1202950>
- White, J. A., Anderson, E., Zimmerman, K., Zheng, K. H., Rouhani, R., & Gunawardena, S. (2015). Huntingtin differentially regulates the axonal transport of a sub-set of Rab-containing vesicles in vivo. *Human Molecular Genetics*, 24(25), 7182–7195. <https://doi.org/10.1093/hmg/ddv415>
- White, J. Ag., Krzystek, T. J., Hoffmar-glennon, H., Thant, C., Zimmerman, K., Iacobucci, G., Vail, J., Thurston, L., Rahman, S., & Gunawardena, S. (2020). Excess Rab4 rescues synaptic and behavioral dysfunction caused by defective HTT-Rab4 axonal transport in Huntington's disease. 1–22.
- Wisco, D., Anderson, E. D., Chang, M. C., Norden, C., Boiko, T., Fölsch, H., & Winckler, B. (2003). Uncovering multiple axonal targeting pathways in hippocampal neurons. *Journal of Cell Biology*, 162(7), 1317–1328. <https://doi.org/10.1083/jcb.200307069>
- Wong, Y. C., & Holzbaur, E. L. F. (2014). The Regulation of Autophagosome Dynamics by Huntingtin and HAP1 Is Disrupted by Expression of Mutant Huntingtin, Leading to Defective Cargo Degradation. 34(4), 1293–1305. <https://doi.org/10.1523/JNEUROSCI.1870-13.2014>
- Yin, H. H., Prasad Mulcare, S., Hilario, M. R. F., Clouse, E., Holloway, T., Davis, M. I., Hansson, A. C., Lovinger, D. M., & Costa, R. M. (2009). Dynamic reorganization of striatal circuits during the acquisition and consolidation of a skill. *Nature Neuroscience*, 12(3), 333–341. <https://doi.org/10.1038/nn.2261>
- Yonekawa, V., Harada, A., Okada, Y., Funakoshi, T., Kanai, Y., Takei, Y., Terada, S., Noda, T., & Hirokawa, N. (1998). Defect in synaptic vesicle precursor transport and neuronal cell death in KIF1A motor protein-deficient mice. *Journal of Cell Biology*, 141(2), 431–441. <https://doi.org/10.1083/jcb.141.2.431>

Zala, D., Colin, E., Rangone, H., Liot, G., Humbert, S., & Saudou, F. (2008). Phosphorylation of mutant huntingtin at S421 restores anterograde and retrograde transport in neurons. *Human Molecular Genetics*, 17(24), 3837–3846. <https://doi.org/10.1093/hmg/ddn281>

Zhang, Y. V., Hannan, S. B., Kern, J. V., Stanchev, D. T., Koç, B., Jahn, T. R., & Rasse, T. M. (2017). The KIF1A homolog Unc-104 is important for spontaneous release, postsynaptic density maturation and perisynaptic scaffold organization. *Scientific Reports*, 7(November 2016), 1–9. <https://doi.org/10.1038/srep38172>

**Legends:**

**Figure 1. HTT phosphorylation at S421 impairs mouse procedural memory.** (A) Schematic representation of the accelerating rotarod protocol over 8 days (10 sessions per day) assessing the mouse procedural memory. Performance of 20 WT, 20 HTT<sub>SD</sub> (B)(C) or 13 WT and 18 HTT<sub>SA</sub> (D)(E) 3-month-old male mice over the 8 days (B to E) and over the first (F to I) or the last day (J to M) were assessed. Time to fall was represented as the mean of the sessions (B)(D)(F)(H)(J) and (L) during the associated period and per day (C)(E) or session (G)(I)(K) and (M). Histograms are represented with the means +/- SEM. Significance was determined using a two-way ANOVA for the analysis of the performance per day or sessions and by a Mann-Whitney test; \* p < 0.05, \*\*\*\* p < 0.0001, ns = not significant.

**Figure 2. HTT phosphorylation at S421 increases the probability of release in the corticostriatal network *ex vivo* and *in vitro*.**

(A) Representative traces of sEPSCs in WT and HTT<sub>SD</sub> MSNs within the S2-DLS network. (B) sEPSC frequency and amplitude were recorded on 10 WT and 10 HTT<sub>SD</sub> 2-3-month-old mice (C) Representative images and of SVs at the corticostriatal synapse obtained by electronic microscopy from punches of DLS from 3-month-old male WT and HTT<sub>SD</sub> mouse brains. Scale = 200 nm (D) Quantification of the number of SVs at the corticostriatal synapse in 5 WT and 3 HTT<sub>SD</sub> mouse brains on 253 WT and 171 HTT<sub>SD</sub> axon terminals. Histograms are represented with the means +/- SEM. Significance was determined using a Mann-Whitney test; \*\*\*\* p < 0.0001. Facilitation of the cortical neurons projecting to the DLS was assessed *ex vivo* by a paired pulse ratio after 2 repeated stimulations on 13 WT and 12 HTT<sub>SD</sub> 2-3-month-old mice (E, F). Exocytosis rate of vglut-1-pHluorin vesicles was recorded in microfluidics device. Scale bar=1 cm (G). Amplitude of the signal and number of events within WT and HTT<sub>SD</sub> corticostriatal network with 4 AP bicuculline stimulation were recorded. Ratio of the amplitude after and before the stimulation was calculated. Histograms represent means +/- SEM of 3 independent experiments (D1 to D3) and per microfluidics device. Significance was determined using a mixed model calculated with R software; \* p < 0.05, ns = not significant.

**Figure 3. HTT phosphorylation at S421 increases Vamp-2-mCherry vesicle directionality on corticostriatal network reproduced in microfluidics device.**

(A) Schematic representation of the 3-compartment microfluidics device allowing the reconstitution of a corticostriatal mature network compatible with live-cell imaging of axons. (B) Representative kymographs of Vamp-2-mCherry vesicle transport in axons for each genotype. Scale bar = 25 μm. From kymographs, segmental velocities (C), anterograde vesicle number (D), retrograde vesicle number (E), static vesicle number (F), linear flow (G) and directional net flux (H) of Vamp-2-mCherry axonal vesicles

were measured for 100µm of axon. Histograms represent means +/- SEM of 3 independent experiments studying the dynamics of 2107 WT and 3450 HTT-SD moving vesicles in 118 WT and 157 HTT-SD axons. Significance was determined using Mann-Whitney test; \*\*  $p < 0.01$ , \*\*\*\*  $p < 0.0001$ , ns = not significant.

**Figure 4. HTT phosphorylation at S421 increases KIF1A recruitment on Vamp-2-mCherry vesicles.**

(A) Western blot analysis from vesicular fraction of 6 WT and 6 HTT-SD brains. Significance was determined using Mann-Whitney test; \*  $p < 0.05$ . (B) LFQ intensity of proteins bound to vesicles immunoprecipitated with HTT. Gray: identified proteins, blue: motor complex, orange: synaptic proteins. (C) Scheme of overlapping HTT and KIF1A interactome. (D) Representative picture of a immunofluorescence labelling revealing HTT (magenta), KIF1A (green) and Vamp-2-mCherry (red) within cortical axons localized in long channels of the microfluidics device followed by gray value representation over distance. (E) Schematic representation of HTT scaffolding SVP molecular complex. KIF1A and HTT colocalization is quantified using Mandel's coefficient (F) and the number of colocalizing pixels (G). The random condition represents the number of randomly colocalizing pixels. Histograms represent means +/- SEM of 2 independent experiments reproducing a corticostriatal network of WT or HTT-SD neurons in at least 3 microfluidics device per experiment. Significance was determined using Mann and Whitney test.

**Figure 5. KIF1A silencing specifically restores axonal transport in HTT<sub>SD</sub> corticostriatal axons.**

(A) Schematic representation of the experimental set up using microfluidics device reproducing a corticostriatal network in which cortical neurons are transduced with Vamp-2-mCherry and sh-scr (sh-scr-GFP) or sh-KIF1A (sh-KIF1A-GFP) lentiviruses. (B) Representative kymographs of Vamp-2-mCherry vesicle transport within WT or HTT-SD axons in microfluidics device transduced with sh-scr or sh-KIF1A. Scale bar = 25 µm. From kymographs, segmental velocities (C), the repartition of Vamp-2-mCherry vesicles in terms of anterograde vesicles (significance determined as an interaction between the condition and the percentage of vesicles and the anterograde speed revealed by a two-way-ANOVA test) (D), anterograde vesicle number (E), retrograde vesicle number (F), linear flow (G) and directionality (H) of Vamp-2-mCherry axonal vesicles were measured for 100µm of axon. Histograms represent means +/- SEM of 2 independent experiments studying the dynamics of at least 1005 WT sh-scr, 1420 WT sh-KIF1A, 2411 HTT-SD sh-scr and 1248 HTT-SD sh-KIF1A vesicles in at least 57 WT sh-scr, 91 WT sh-KIF1A, 84 HTT-SD sh-scr and 87 HTT-SD sh-KIF1A axons. Significance was determined using Kruskal-Wallis test followed by a Dunn's post hoc analysis; \*  $p < 0.05$ , \*\*  $p < 0.01$ , \*\*\*  $p < 0.001$  \*\*\*\*  $p < 0.0001$ , ns = not significant. The same network on microfluidics was then used to study BDNF-mCherry axonal transport (H) and anterograde speed (I), linear flow (J) and

directionality (**K**) of BDNF-mCherry vesicle were also measured for 100 $\mu$ m of axon. Histograms represent means  $\pm$  SEM of at least 1 independent experiment studying the dynamics of at least 1144 WT sh-scr, 1606 WT sh-KIF1A, 4294 HTT-SD sh-scr and 2507 HTT-SD sh-KIF1A vesicles in at least 75 WT shscr, 103 WT shKIF1A, 125 HTT<sub>SD</sub> shscr and 156 HTT<sub>SD</sub> shKIF1A axons. Significance was determined using Kruskal-Wallis test followed by a Dunn's post hoc analysis; \*\*\*  $p < 0.001$ , \*\*\*\*  $p < 0.0001$ , ns = not significant.

**Figure 6. KIF1A silencing restores the number of SVs at the corticostriatal synapse in HTT<sub>SD</sub> brains.**

(**A**) schematic representation of bilateral stereotaxic injections sites. Scale = 1 cm (**B**) Immunolabeling of GFP localizing the injection site on a slice located at 1.5 mm before the bregma. Scale = 1 cm (insets, 100  $\mu$ m) (**C**) Western blot and the analysis for KIF1A level evaluation of punches of M1 injected area. At least 3 punches from 2 brains were analyzed. V1: visual cortex 1, M1: motor cortex 1, LH: left hemisphere, RH: right hemisphere Significance was determined using a two-way ANOVA test followed by a Sidak's multiple comparison test; \*\*  $p < 0.01$ . (**D**) Immunolabeling of GFP localizing the projection site on a slide located at -0.3 mm after the bregma. Scale = 1 cm (inset, 250  $\mu$ m). (**E**) Representative images from electron microscopy and quantification focusing on the number of SVs at the corticostriatal synapse of 3 WT male and littermate mice injected with either shscr (360 synapses) or shKIF1A (324 synapses) and 3 HTTSD mice injected with shscr (417 synapses) or shKIF1A (337 synapses). Scale = 200 nm. Histograms represent means  $\pm$  SEM. Significance was determined using Kruskal-Wallis test followed by a Dunn's post hoc analysis; \*\*  $p < 0.01$ , \*\*\*  $p < 0.001$ , \*\*\*\*  $p < 0.0001$ , ns = not significant.

**Figure 7. KIF1A silencing restores the impaired procedural memory of HTT<sub>SD</sub> mice.**

(**A**) Schematic representation of the accelerating rotarod protocol over 8 days (10 sessions per day) assessing the mouse procedural memory following stereotaxic injection of shscr or shKIF1A. Performance of 12 WT shscr, 11 WT shKIF1A, 10 HTT<sub>SD</sub> shscr and 10 HTT<sub>SD</sub> shKIF1A 3-month-old male mice over the 8 days (**B**)(**C**) and over the first (**D**)(**E**) or the last day (**F**)(**G**) were assessed. Time to fall was represented as the mean of the sessions (**B**)(**D**)(**F**) during the associated period and per day (**C**) or session (**E**)(**G**). Histograms are represented with the means  $\pm$  SEM. Significance was determined using a two-way ANOVA for the analysis of the performance per day or sessions followed by a Tukey's post hoc test and using a One-way ANOVA followed by a Tukey's post hoc test for (**B**, **D**, **F**); \*  $p < 0.05$ , \*\*  $p < 0.01$ , \*\*\*\*  $p < 0.0001$ , ns = not significant. (**H**) correlation between the number of SVs found at the synapse and the mean performance of the first day of the accelerating rotarod of 11 mice. The line represents the gaussian fit displaying a R square of 0.6.

**Figure Sup 1. HTT-SD and HTT-SA motor coordination is not impaired, unlike procedural memory.**

(A) time to fall of the accelerating rotarod during the first session of the first day of training. Data obtained from 20 WT mice and 20 HT-SD mice. (B) time to fall of the accelerating rotarod during the first session of the first day of training. Data obtained from 13 WT mice and 18 HTT-SA mice. (C) time to fall of the accelerating rotarod during the 10 sessions of the first day of 8 WT mice, 10 HTT-SD mice and 12 HTT-SA 18-month-old mice. Histograms are represented with the means  $\pm$  SEM. Significance was determined using a Mann-Whitney test; \*  $p < 0.05$ , \*\*  $p < 0.01$ , ns = not significant

**Figure Sup 2. Number of synapses in HTT-SD is not changed**

(A) number of synapses per  $100 \mu\text{m}^2$  in 3 WT and 3  $\text{HTT}_{\text{S421D}}$  brains from littermate mice. Histograms are represented with the means of at least 50 images per brains  $\pm$  SEM. Significance was determined using a Mann-Whitney test, ns = not significant.

**Figure Sup 3. KIF1A levels**

(A) Western blot and analysis of total fraction of 10 WT and 10 HTT-SD brains. (B) Western blot and analysis of KIF1A levels in cells transduced with shKIF1A or shscr lentiviruses. Corresponding quantification of KIF1A levels shows a 83% reduction of KIF1A expression. Histograms are represented with the means  $\pm$  SEM.



Figure 1

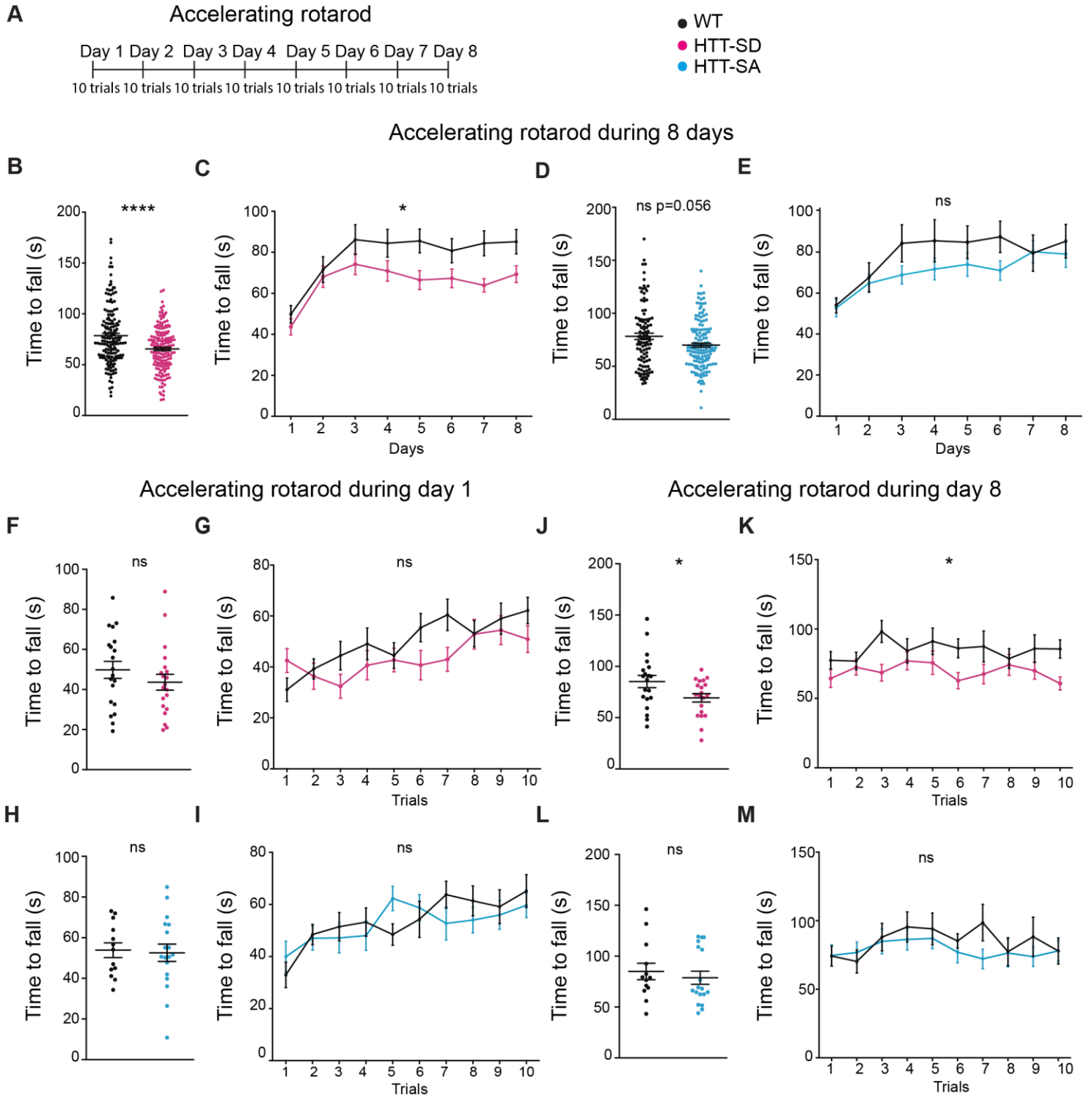


Figure 2

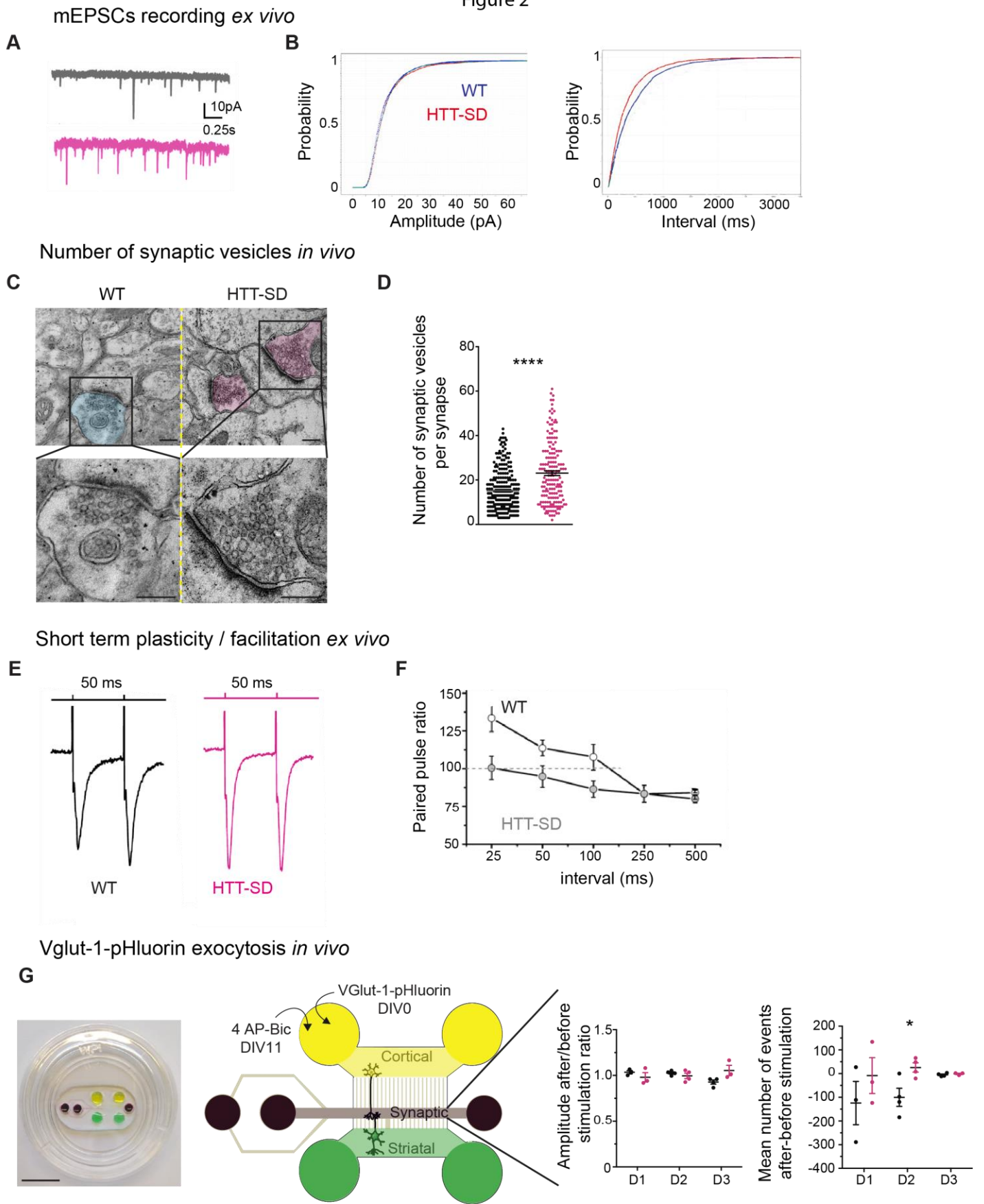


Figure 3

Vamp-2-mCherry axonal transport

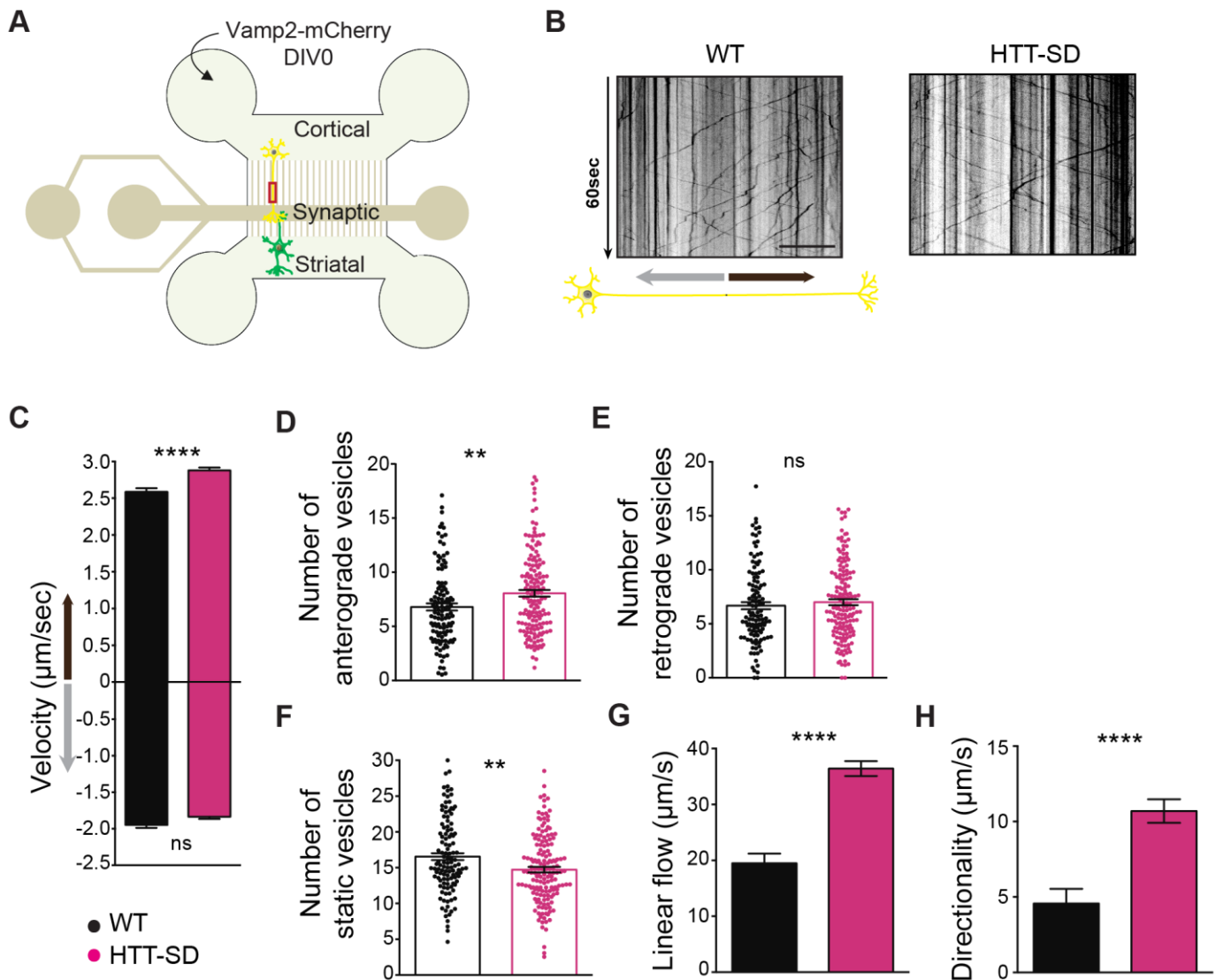
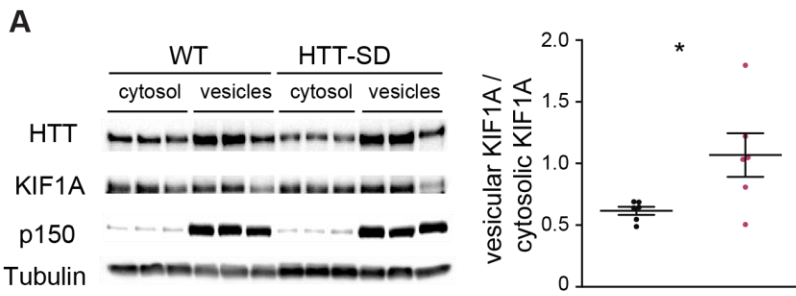
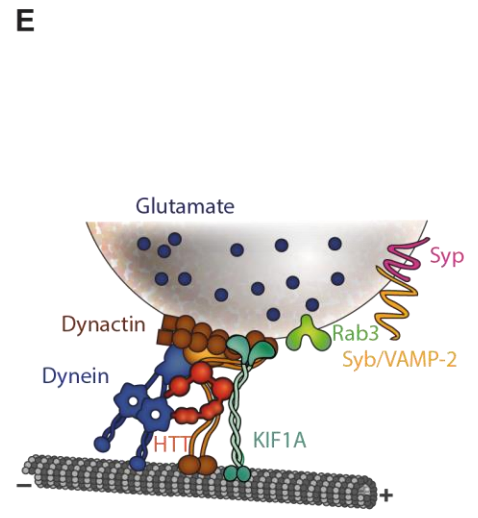
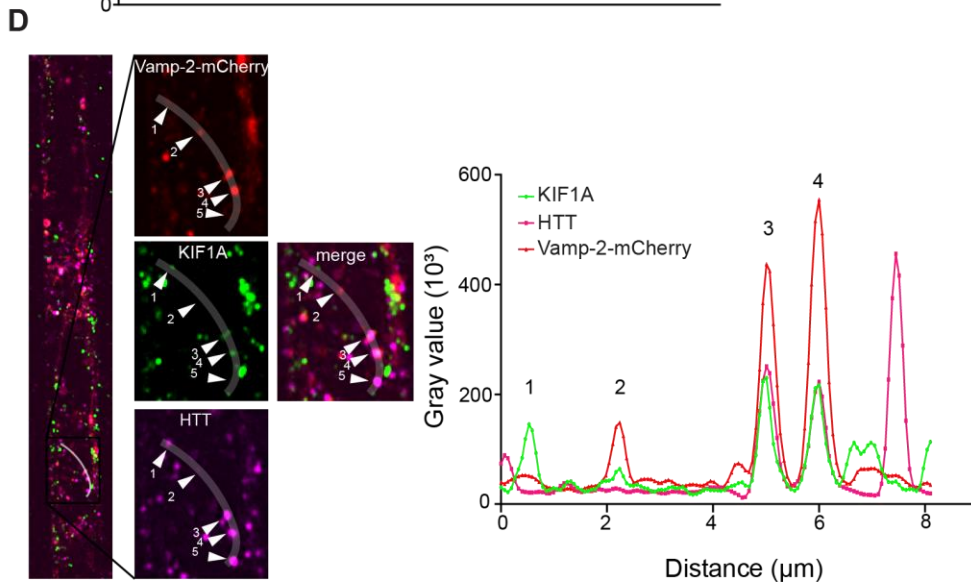
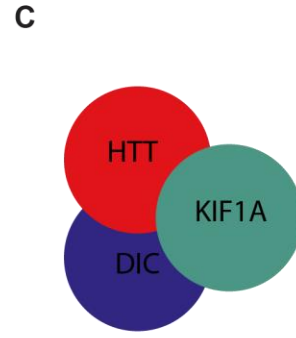
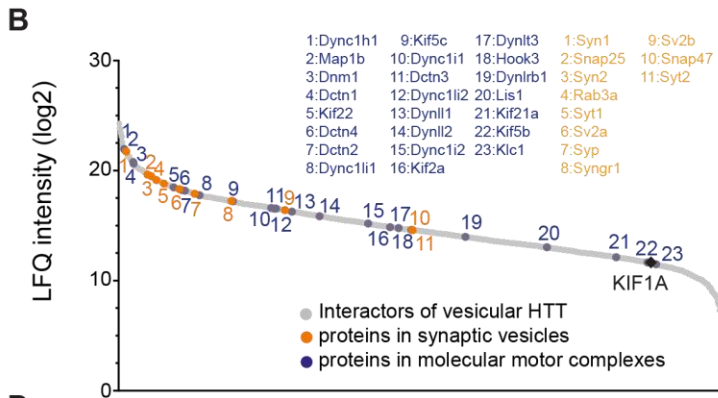


Figure 4

KIF1A levels on moving vesicles



KIF1A presence on HTT vesicles



HTT and KIF1A colocalization

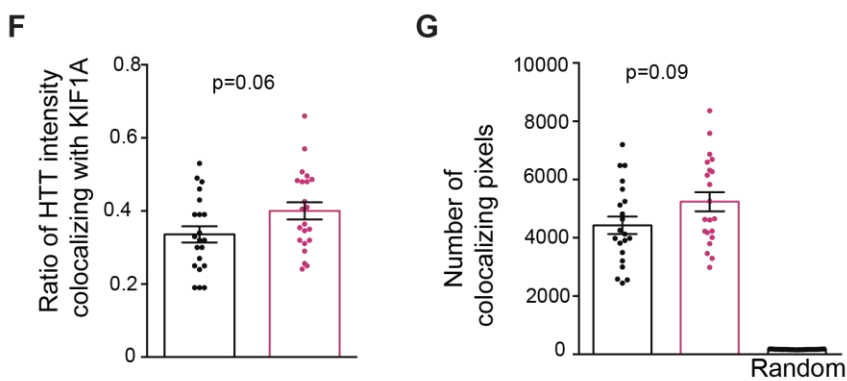
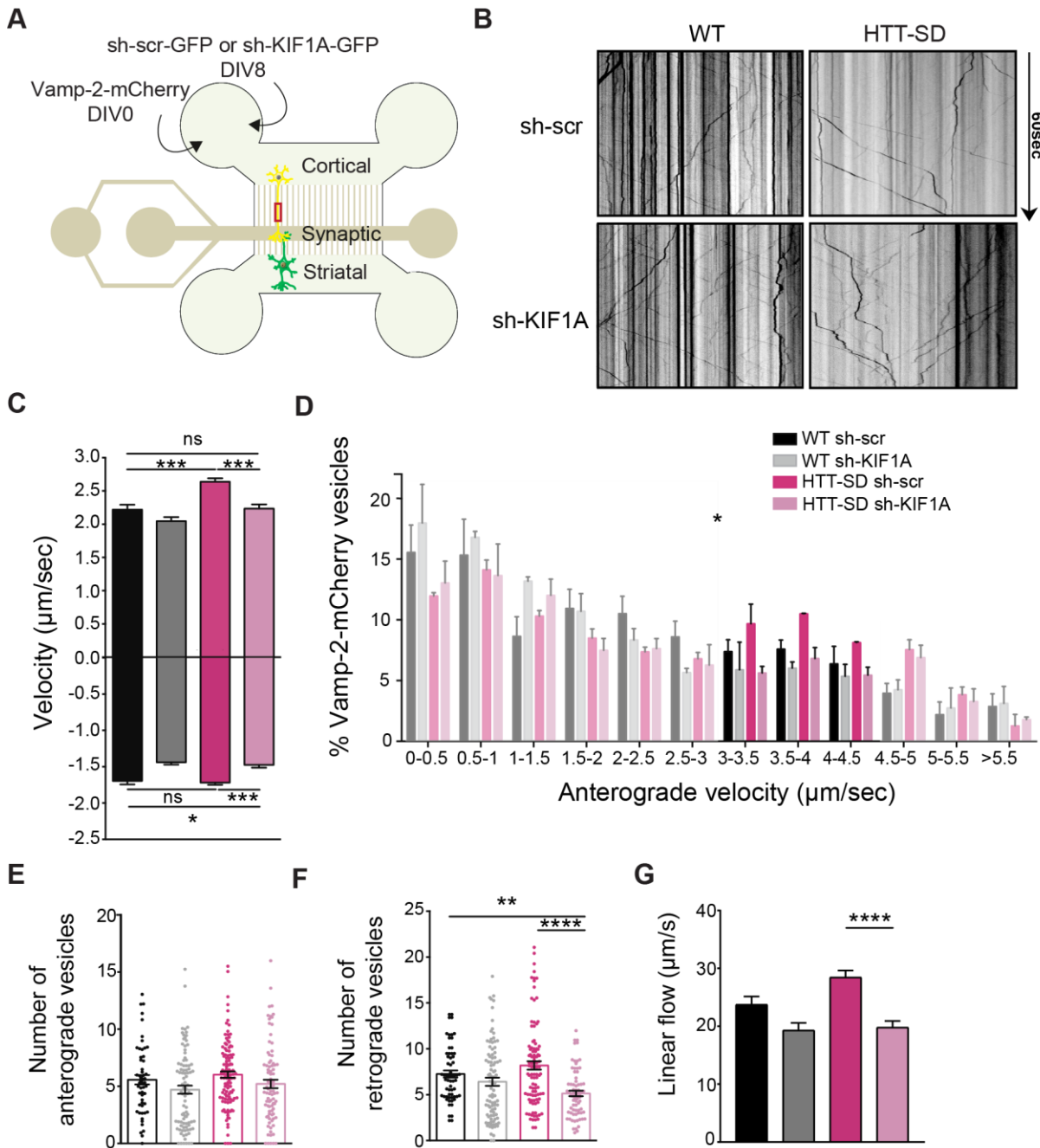


Figure 5

Vamp-2-mCherry transport with KIF1A silencing



BDNF-mCherry transport with KIF1A silencing

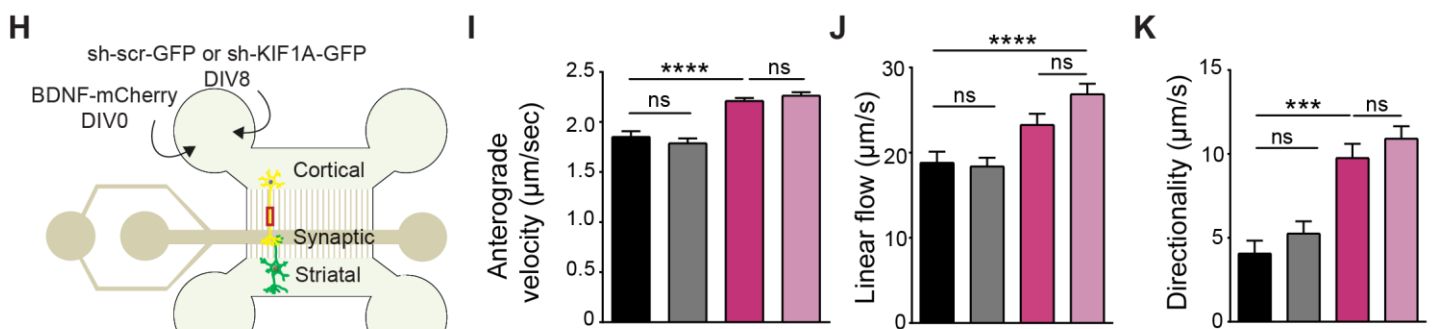


Figure 6

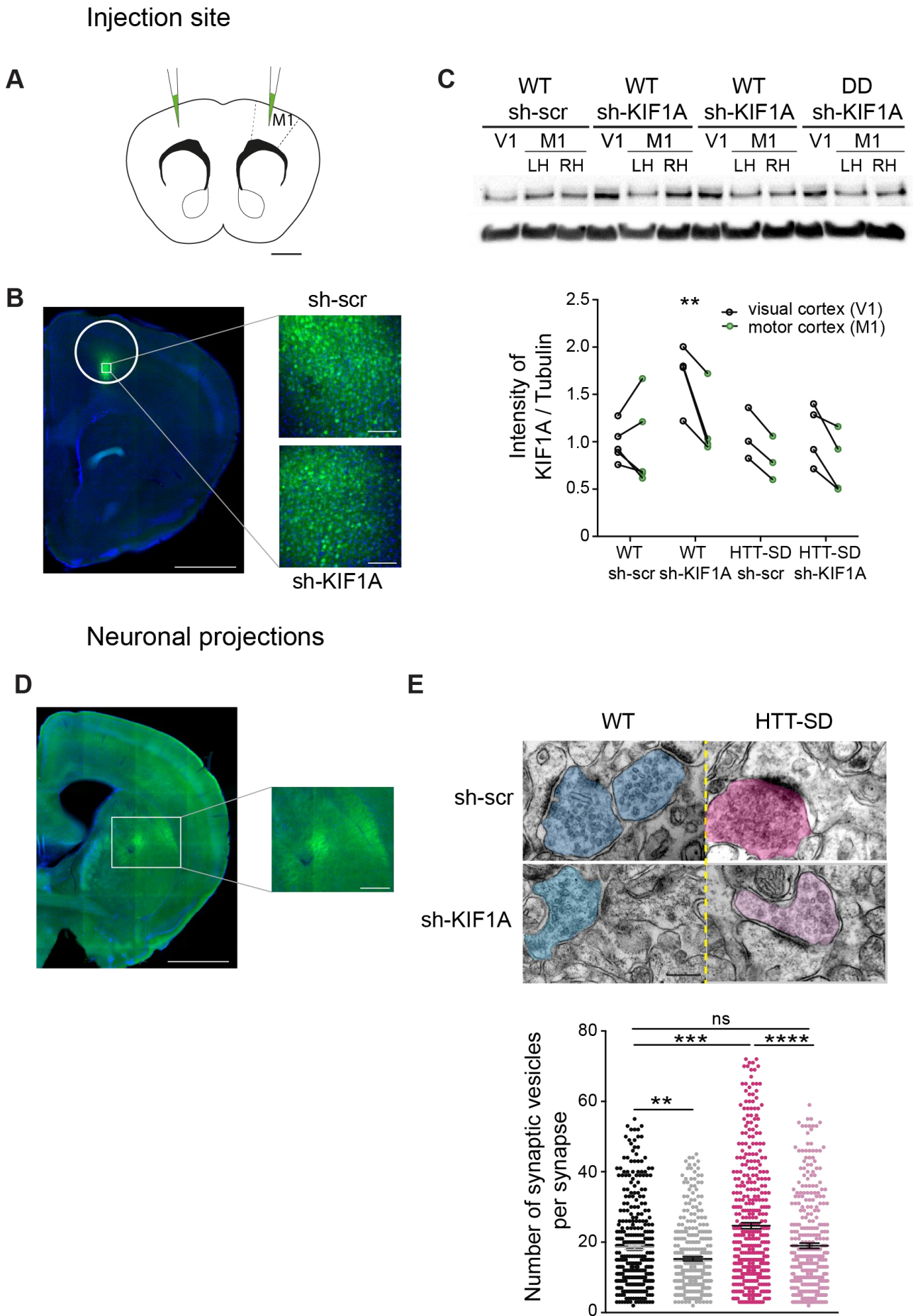


Figure 7

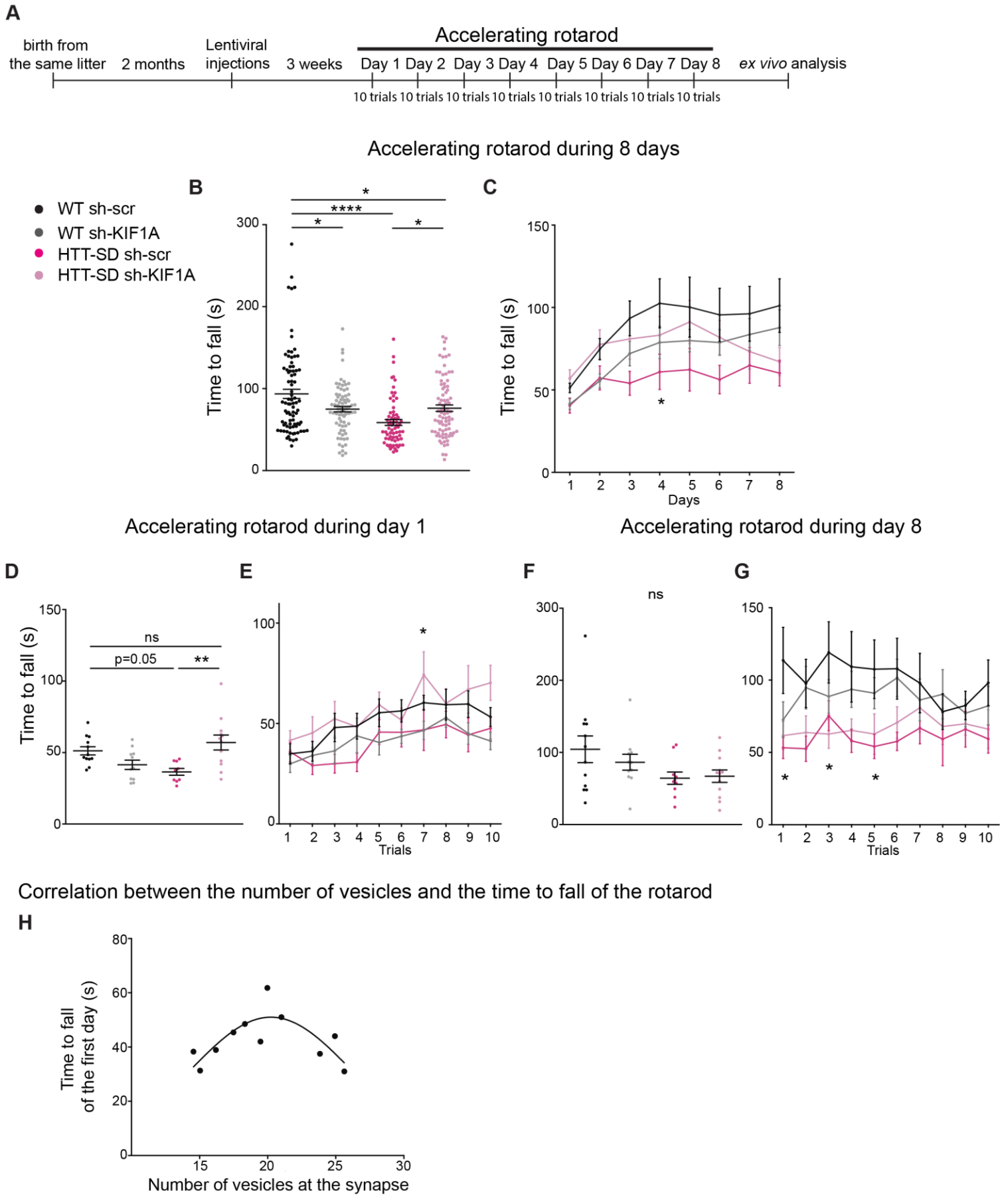


Figure 8

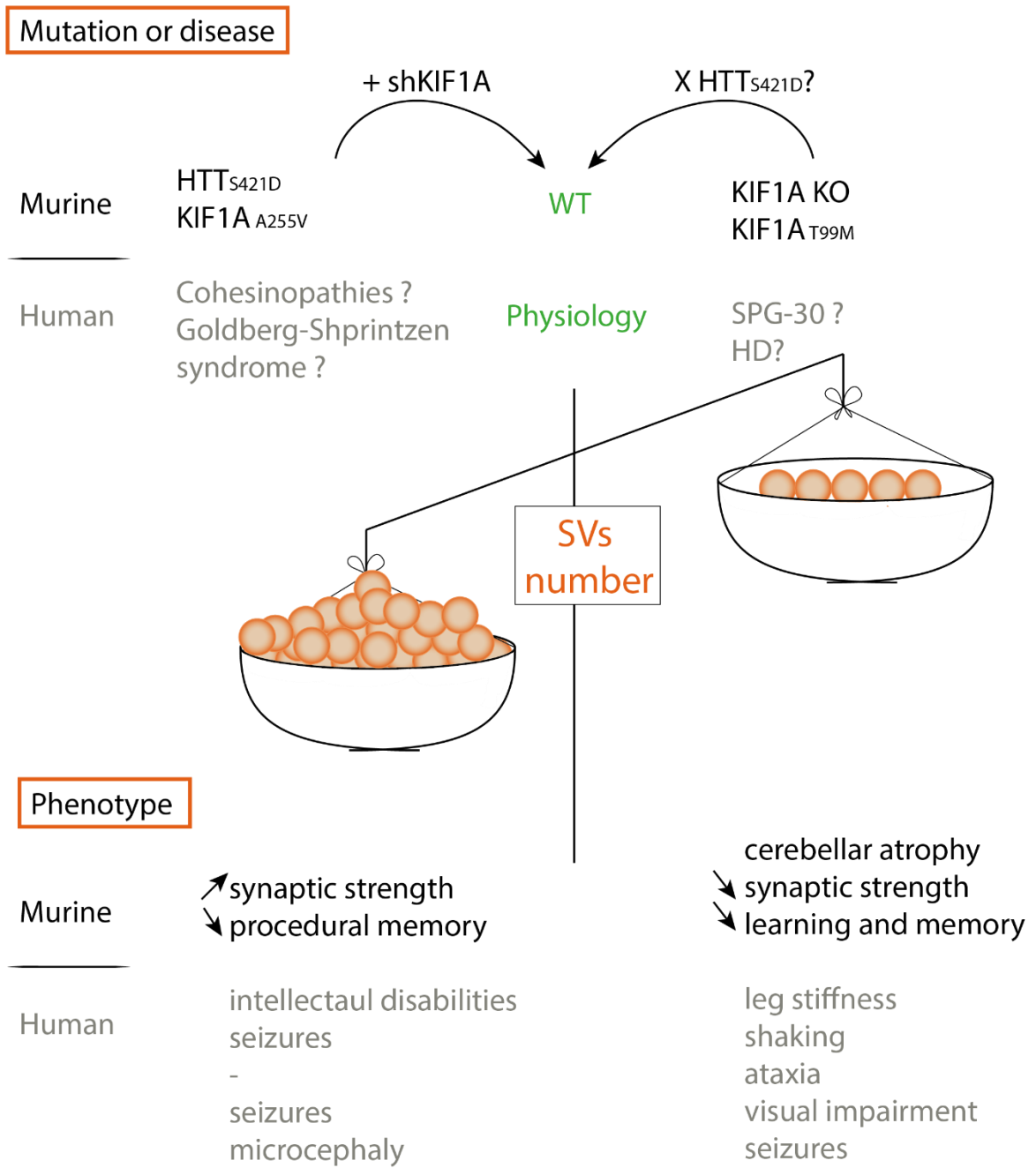
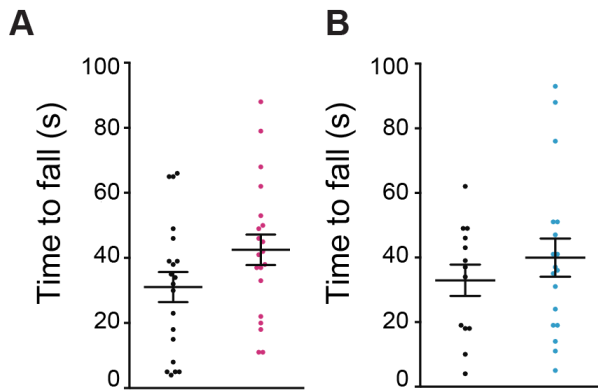




Figure S1

Accelerating rotarod - first trial of the first day



Accelerating rotarod - first day at 18 months

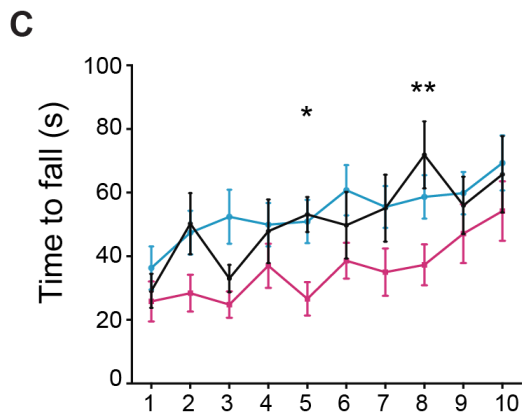


Figure S2

**A** Number of corticostriatal synapses in the DLS

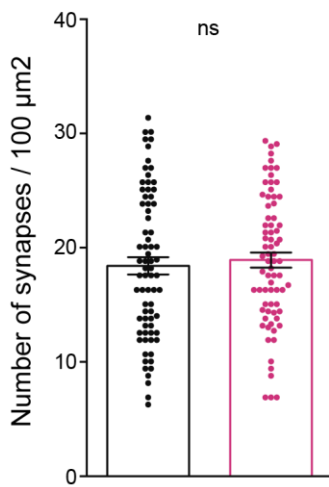
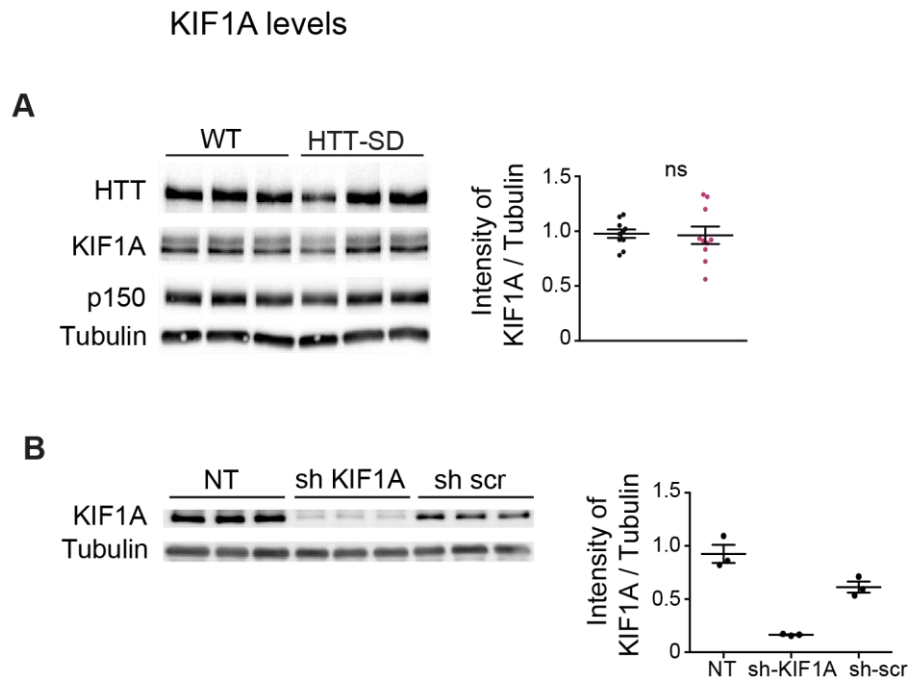
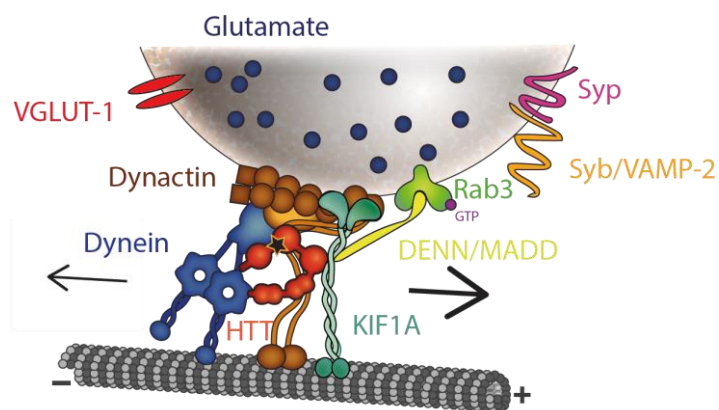


Figure S3



## Discussion

In our study, we linked HTT-mediated SVP transport in a corticostriatal network to the number of SVs at the synapse which we show, is correlated to the procedural memory in mice. Indeed, HTT could act as a scaffold protein stabilizing complexes containing molecular motor and adaptors (figure 104) but could also act as a regulator of SVP transport through its phosphorylation at S421. This transport regulation mechanism raises some questions related to physiological consequences of axonal transport.



**Figure 104: HTT acts as a scaffold for SVP transport.** Scheme of a possible HTT role on scaffolding SVP adaptor like DENN/MADD and molecular motors.

### **An abnormally high number of SVs at the axon terminal is detrimental for learning and memory**

This study showed that  $HTT_{S421D}$  mice exhibit impaired procedural memory consequently to an accumulation of SVs at the axon terminal that is caused by an increase in anterograde transport. Learning and memory is known to depend on SV density at the synapse consequently or not to KIF1A motility (L. B. Li et al., 2016; Phan et al., 2019). In humans, accumulation of SVPs at the axon terminal due to KIF1A gain of function mutation is thought to be pathogenic (Chiba et al., 2019; Gabrych et al., 2019).

In *C. elegans*, whereas reduced function of UNC-104 did not affect both learning and memory, similar to the  $HTT_{S421A}$  mice, UNC-104 overexpression causes a slight defect in learning but then improved short term memory and its maintenance (L. B. Li et al., 2016). These experiments suggest that level of KIF1A and thus, SV quantity at the synapse is crucial for learning and memory.

SV accumulation can also be observed in another ND where the cohesion complex is mutated. Although a better understanding of the role of this complex on axonal transport remains to be

established, a study in *Drosophila* revealed that, by mutating one of its members, stromalin, SVs accumulate at the axon terminal. This accumulation influences learning and synaptic strength and is thought to be detrimental for synaptic communication (Phan et al., 2019). In human, a mutation in the stromalin gene could lead to LDP, seizures and intellectual disabilities which are symptoms of cohesinopathies such as Cornelia de Lange syndrome (Dowsett et al., 2019; Phan et al., 2019).

Although this study focuses on the consequences within the presynaptic neuron of the SV accumulation, it is interesting to investigate the postsynaptic mechanisms also known to mediate learning and memory. For instance, the high release probability in the presynaptic neuron cause a higher frequency of NT release, which can lead to excitotoxicity mechanisms into the postsynaptic neuron. Although it is not known if excitotoxicity happens in HTTS421D mice, it is known that this glutamate-linked toxicity results in an overload of calcium (due to an excessive NT binding to NMDAR) within the postsynaptic neuron, which activates proteases and phospholipases producing free radicals known to be toxic for the cell (Dennis W. Choi, 1988; Zoghbi et al., 2000). Thus, impairing postsynaptic neuron homeostasis could also participate to the impaired procedural memory in HTTS421D mice. Interestingly, one solution found to decrease excitotoxicity was to reduce the glutamate release (D. W. Choi, 1990; Zoghbi et al., 2000).

### **HTT phosphorylation as a tool to regulate axonal transport and understand its mechanisms**

As said earlier, HTT phosphorylation represents an approach to investigate and potentially rescue a transportopathy. In this study, we demonstrated that by HTT phosphorylation increases anterograde transport of SVPs and causes procedural memory impairments. In the previous study, we demonstrated that APP transport is modulated by HTT phosphorylation and that its modulation can rescue memory of AD mouse model. Similarly, we can envision that KIF1A human mutations, known to generate either a loss of function or a gain of function of KIF1A in mice, could be attenuated respectively in HTTS421D or HTTS421A mice.

### **Anterograde SVP transport impairments affects retrograde SVP transport**

In this study, two modes of transport regulation can be seen. The first one through HTT phosphorylation at S421 impacts specifically the anterograde but not the retrograde transport of SVPs, as it is the case for BDNF and APP transport (Bruyère et al., 2020; Colin et al., 2008). This behavior fits with the fact that cellular regulation often leads to changes in only one direction (M. J. I. Müller et al., 2008). Indeed, cellular changes are often subtle and only modulate affinity or the number of recruited motors. However, when KIF1A is silenced, even if KIF1A is responsible for the anterograde transport,

both directions are affected. This trend has been seen in other studies for BACE-1 vesicles or DCVs where KIF1A has been knocked down, inhibited or mutated in superior cervical ganglion or *Drosophila* (Barkus et al., 2008; Hung & Coleman, 2016). The explanation may reside in the fact that with a lower anterograde transport, less vesicles are brought to the synapse and thus, less of them are available to be brought back towards the cell body by retrograde transport (Hung & Coleman, 2016). This behavior also fits with the steric disinhibition model in which one motor is essential to activate the other one. Indeed, it has been found that mutation impairing the binding rate or detachment force of one motor causes reduction of motion in the two directions by decreasing run lengths or velocities (Kaether et al., 2000; M. J. I. Müller et al., 2008).

In conclusion, this study unraveled a new role for HTT in the transport of SVs and also demonstrated a tight link between regulatory mechanisms of axonal transport (HTT phosphorylation), the stoichiometry of SVs at synapses and how this influences *in vivo* the probability of release, facilitation and subsequent procedural memory.

To conclude this study, we can claim that SV number at the synapse is crucial for neuronal homeostasis and subsequent behavior (figure 105). If it is increased like in HTTS421D mice or maybe in mice where KIF1A activity is increased by the A255V mutation, it could lead to learning deficits as a consequence of an increase of the probability of release. In human, accumulation of SVs might cause cohesinopathies or the Goldberg-Shprintzen syndrome leading to seizures and intellectual disabilities. Silencing KIF1A could be a way to overcome with SV accumulation in *Drosophila* (Phan et al., 2019), mice or humans. On the opposite, a lower number of SVs at the synapse could be found in KIF1A KO mice or KIF1AT99M mice and could be responsible for the decrease of the probability of release which is also thought to cause learning deficits. Future studies could focus on the phenotypes of mice coming from the crossing between HTTS421D mice and KIF1A T99M mice to investigate the S421 phosphorylation propensity to restore KIF1A T99M phenotypes.

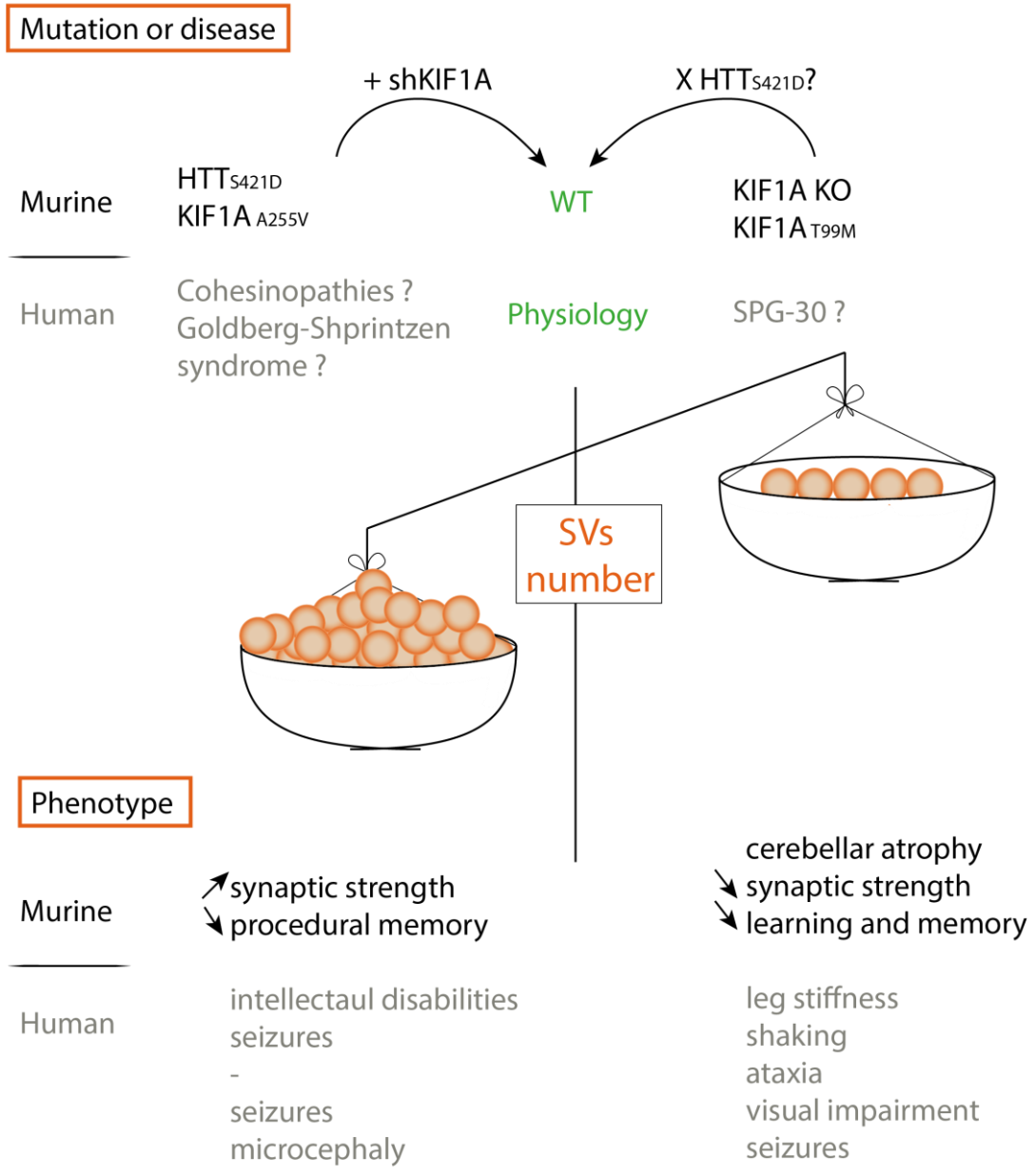


Figure 105: SV number at the synapse is crucial for neuronal homeostasis and subsequent behavior.



## Discussion

My thesis work allowed me to answer some questions regarding the contribution of vesicular transport in axons in both physio- and pathological contexts. However, science, by nature, leads us to put those answers into perspectives, raising new questions. These issues can be new because of the use of state-of-the-art technologies like the microfluidics or because of the new findings but can also validate or lend weight to previous theories.

### 1. Experimental set up: looking for more integrative and relevant studies

The main goal of this project was to study in a more integrated way, the consequences of HTT phosphorylation at S421. Indeed, the Saudou's lab previously showed that S421 phosphorylation acts as a molecular switch for vesicular directionality (Colin et al., 2008). However, this first study was carried out by techniques available then, namely N-terminal HTT fragment plasmid transfection of neurons grown in free cultures. Thanks to the development in the laboratory of new techniques (Moutaux, Christaller, et al., 2018; Virlogeux et al., 2018) and the use of KI mice designed by the Humbert's lab, we were able to investigate the consequences of HTT phosphorylation in a more physiologically way.

#### a. Microfluidics: an essential tool to study neuronal dynamics within networks

Although the use of microfluidics for neurosciences has been developed only recently, this tool now seems mandatory to investigate cellular and molecular dynamics, as illustrated by the growing number of various studies using this state-of-the-art technique (Bigler et al., 2017; J. T. S. Fernandes et al., 2016; Gummy et al., 2011; Katsikoudi et al., 2020; Schaedel et al., 2015; Sgro et al., 2013; Taylor et al., 2005, 2010; Wioland et al., 2017). However, it is important to understand its limitations and keep looking for improvements to compensate them.

##### i. Microfluidics: a tool to reproduce *in vitro* the *in vivo* networks

The first development of microfluidics allowed to separate axons from soma (Taylor et al., 2010). Here, we developed and used for several conditions new set ups allowing us to compartmentalize and connect two populations of neurons. The properties of the design (different channel lengths and compartments) and the use of chemical (laminin gradient) allow to control how these two populations of neurons communicate. By allowing specifically the axons to grow within long channels and the dendrites into the short channels, we reproduced the *in vivo* network of cortical neurons projecting to either the striatum or other cortical neurons. The functionalities of the reconstituted corticostriatal network have been assessed by different approaches. For instance,



postsynaptic signaling induced by the presynaptic influx like the phosphorylation of ERK, the binding of glutamate to its postsynaptic receptors (iGluSnFR) or MSNs calcium transient firing demonstrated that these inhibitory neurons, largely dependent on cortical afference for their survival, are communicating in a way similar to what happens in the brain to the cortical neurons (Virlogeux et al., 2018). Importantly, a careful analysis of the development and maturation of the network allowed us to set up the experimental conditions in which such network is fully mature and functional. The strength of this set-up is also to be able to specifically assess by biochemical or immunostaining methods neuronal homeostasis (synapse function, synapse number) or protein contents (APP or A $\beta$  peptides for example). Finally, the other important strength of such device is the possibility to assess at high spatial and temporal resolution to study, using spinning disk confocal microscope, neuronal dynamics such as vesicular transport in axons or in dendrites, exocytic events at the synapse or calcium transient dynamics.

## ii. Microfluidics limitations

However, as for all *in vitro* experiments, microfluidics device has limitations that have to be considered.

### 1. Neuronal cell diversity

Most cells within the devices are neurons. Although we have observed the presence of astrocytes, their presence is not properly controlled. As such, synapses formed in the synaptic compartment may lack the *in vivo* characteristic of the tripartite synapse (Perea et al., 2009). In addition, we did not observe the presence of oligodendrocytes or microglia. Oligodendrocytes are key components of neuronal networks as they form the myelin sheet around axons, known to modulate the speed of the neuronal communication. Microglia, that represents 10-15% of neuronal cells within the brain (Lawson et al., 1992), also play a crucial role because those immune cells are able to maintain homeostasis by secreting extracellular signaling proteins (cytokines) that are known to regulate synaptogenesis, synaptic maturation and axonal growth (Werneburg et al., 2017). For example, TNF- $\alpha$  is known to regulate postsynaptic homeostasis and its role in AD has been highlighted. TNF- $\alpha$  would indeed impair APP homeostasis by increasing A $\beta$  quantities through an increase of production (increase of BACE1 expression) and a decrease of its degradation by microglia (Styr & Slutsky, 2018). Thus, adding microglia into our microfluidics device could help to reproduce the complexity of some NDs like AD and get closer to the pathological processes.

## 2. *The brain as a communication between multiple structures*

As described in the first chapter, the brain is functioning as the result of neuronal networks formed between different brain structures. The loop regulating the movement coordination is a good example of the need of multiple brain structures to establish a movement or a behavior. The type of microfluidics we developed aimed at representing a two-structure network. However, in order to better understand the dynamics and the functionality of a network regulating behavior, and how neurons interact with each other, it would be of interest to create microfluidics containing several compartments hosting more than 2 types of neurons. For example, a way to study memory formation and long-term storage could be to use a three-chamber microfluidics device in which cortical axons would connect to hippocampal dendrites and whose axons would connect to other cortical dendrites.

### iii. From microfluidics to *in vivo* studies: a too big step?

One of the main reasons why *in vitro* experiments are carried out is because of the complexity to access to *in vivo* dynamics. However, thanks to the development of new technologies especially advances in microscopy and optic techniques, we are now able to study *in vivo* some neuronal dynamics like vesicular transport. Thus, we can compare the cellular processes obtained in microfluidics with those obtained by *in vivo* study. Despite the microfluidics limitations we discussed earlier, we have been able to obtain similar results *in vitro* and *in vivo* in term of BDNF axonal transport (Moutaux *et al.*, *in prep*), number of synapses (Bruyère *et al.*, 2020) or release of glutamate (Vitet *et al.*, *in prep*). Thus, it is tempting to conclude that microfluidics allows to reproduce the biological mechanisms observed *in vivo* and keeping some physiological relevance. In addition, such microfluidic can simplify the *in vivo* system by first studying the functioning of one circuit before the study of a more complex network. Moreover, for some applications (vesicular transport, drug testing), one can plate cell lines derived from patients into microfluidics thus reducing the number of animals used in research.

### b. Use of KI mice to endogenously control the phosphorylation status of a protein: a not so specific tool?

HTT<sub>S421D</sub> and HTT<sub>S421A</sub> mice used in this study were designed by a point mutation replacing an amino acid (serine) by another one (aspartic acid or alanine) to mimic respectively the constitutively phosphorylated or unphosphorylatable form of HTT.

It is known that HTT overexpression in cells and in mice changes cellular processes or homeostasis (Colin *et al.*, 2008; Gauthier *et al.*, 2004). For example, transgenic HD mice overexpressing the first exon of HTT with an expanded polyQ (R6/2) show strong and rapid phenotypes as compared

to Knock-In HD mice (KI) having the same polyQ length (around 140-150) (*Hdh*<sup>CAG140</sup> mice, (Menalled et al., 2003)). KI mice avoid overexpression artefacts on cellular processes and therefore they reproduce better the physiopathology. Here we also used KI mice carrying the point mutation on S421 allowing us to assess specifically the consequences of mutations either mimicking constitutive phosphorylation or the absence of phosphorylation on endogenous HTT.

However, although this mutation is made on endogenous HTT, the non-reversibility and ubiquitous nature of the mutation bring limitations to the approach.

Indeed, one of the characteristics of phosphorylation is its lability and high dynamicity (Gelens & Saurin, 2018; Tarrant & Cole, 2009), which allows protein to respond in a time-manner to cellular cues. The fact that the phosphorylation status is constitutively changed in our KI mice does not allow activation nor reversibility and thus can dysregulate cellular pathways or cell homeostasis by changing permanently the status of phosphorylation. Second, the presence of the mutation at the egg stage could interfere with embryonic development. Thus, we have to consider the possibility that the observed adulthood mechanisms could be, at least in part, due to compensatory feedback loops operating during the embryonic development.

The second point to consider is the ubiquitous nature of the mutation.

HTT is present in most tissues (Marques Sousa & Humbert, 2013) thus, HTT phosphorylation status is modified in all the tissues of the KI mouse model including peripheral tissues such as muscles or testis. Within the brain, HTT phosphorylation status is changed in neurons but also in astrocytes. One strategy to avoid the absence of control in time and space while preserving the physiological level of a protein would be to activate the phosphorylation at a specific time in specific compartments using optogenetics or the cre/lox system upon tamoxifen injection (Barnat et al., 2017). However, this strategy is possible only for short genes with a single exon. Another approach to be specific in time and space of expression could be the use of AAV or lentivirus injection of pHTT into the area of interest as the lab already did (Pardo, 2006). However, the induced overexpression abolishes the endogenous dimension desired in this project and the transgene is limited in its size.

Although we proceeded to many behavioral tests to characterize the behavior of the HTTS421 mice (anxiety, reproduction rate, muscle strength, motor coordination, memories, ...) and found no behavioral consequences except for procedural memory, we cannot exclude that additional cellular pathways are impaired and then compensated. This is why in the third study we put strong efforts to silence specifically KIF1A in the corticostriatal projecting neurons as a way to demonstrate the causative effect between axonal transport of SVPs in corticostriatal neurons and habit formation.

Therefore, one difficulty when linking a cellular mechanism to a specific behavior is to demonstrate its specificity not only regarding the neuronal circuit (the corticostriatal circuit in our case) but also at the molecular level. In support, HTT is not only involved in axonal transport but its phosphorylation could impact other functions controlled by HTT such as autophagy, ciliogenesis or neurogenesis. For example, besides its role on vesicular transport, HTT phosphorylation at S421 has been shown to be implicated in the regulation of HTT cleavage (Warby et al., 2009). Indeed, S421 phosphorylation would reduce HTT N-ter fragment accumulation in the nucleus by reducing HTT cleavage by caspase-6.

Another cellular function modified by HTT S421 phosphorylation could involve endo/exocytosis or scaffolding of glycolytic enzymes (figure 106).

For instance, it would be interesting to assess if S421 phosphorylation also regulates the traffic based on actin filaments. If it does, it could impact SV pool dynamics at the presynapse and maybe regulate the resulting number of docked vesicles, crucial for facilitation.

Another example, since molecular motors consume ATP to “walk” on the MTs, would be to assess if the number of active motors on a vesicle increases because of S421 phosphorylation. Indeed, the supply of ATP might need to be increased for the motor recruitment to be useful. Thus, we could imagine that S421 phosphorylation also regulates the recruitment of glycolytic enzymes on the vesicle.

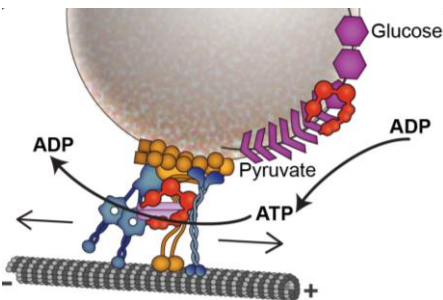


Figure 106: HTT acts as a scaffold for glycolytic enzymes on the vesicle

In order to discriminate between the different HTT roles during a cellular process, one solution

could be to modulate the expression of one of HTT’s partners in  $HTT_{S421D}$  or  $HTT_{S421A}$  neurons and see if it rescues the phenotype. For instance, in the third study, we demonstrated that the regulation of the probability of release is due to the HTT-mediated transport of SVP by silencing KIF1A, which interacts with HTT to regulate transport. However, this strategy does not imply that this is the only mechanism regulating the probability of release. In fact, endocytosis regulation by HTT could also be involved by regulating the size of the reserve pool or the number of docked vesicles. For example, an experiment modulating the expression or the function of dynamin-1 in  $HTT_{S421D}$  neurons, combined with a measure of glutamate release using the vglut-1-pHluorin probe, could give information about possible additional mechanisms.

Even if we consider that HTT phosphorylation acts mainly on axonal transport directionality, deciphering its consequences could be difficult. It is the case for vesicular transport since S421

phosphorylation acts as a molecular switch for the directionalities of at least TrkB vesicles, APP vesicles, BDNF vesicles and SVPs (Bruyère et al., 2020; Colin et al., 2008; Scaramuzzino et al., *in prep*).

The fact that HTT regulates the transport of several different vesicles (in terms of dynamics and functions) clearly adds complexity to the studies. How can we be sure that the cellular process we are observing is the result of the transport regulation of one type of vesicle? Theoretically, a vesicle possesses a specific function; SVPs regulate the NT release whereas BDNF regulates the survival. Thus, if we study NT release in HTT<sub>S421D</sub> neurons, its modification is probably mostly due to SVP transport regulation compared with BDNF transport regulation. However, in practice it is different, as the roles of cargoes can overlap with each other and induce similar phenotypes (e.g.: intensity of postsynaptic signaling, memory impairment or neuronal death). In addition, some transported factors could also impact the dynamics of other vesicles. Although this inter-vesicular regulation seems to have a lighter impact than direct vesicular transport regulation, it is still important not to neglect it. So, what are the tools or the methods used to counteract this issue?

We can use the overexpression or the silencing of a cargo in a physiological situation to understand the consequences on a given cellular process of the dysregulation of its homeostasis. This is the strategy we used to prove in the first study that APP homeostasis regulates the number of synapses. While in WT neurons, overexpressing APP decreases the number of synapses, it rescues the increased number of synapses observed in HTT<sub>S421A</sub> neurons, demonstrating that APP regulates the number of synapses *in vitro*. This is why we postulate that the change of synapse number *in vivo* could be due to APP homeostasis changes. However, we still cannot exclude that this mechanism does not imply a regulation of another vesicle dynamics, that could also be responsible for the synapse number regulation.

In the third study, the identification of KIF1A as a kinesin preferentially transporting SVPs allowed us to demonstrate that SVPs and not BDNF trafficking is responsible for the observed phenotype. However, it does not exclude the possibility that other cargoes are transported via KIF1A. Another strategy could have involved the regulation of DENN/MADD expression or function since it is also a regulator of SVP transport (Niwa et al., 2008). However, this signaling pathway regulates other cellular pathways such as TNF- $\alpha$ -induced apoptosis, Rab protein regulation or neurotransmission (K. Del Villar & Miller, 2004; Marat et al., 2011; Miyoshi & Takai, 2004) (figure 107).

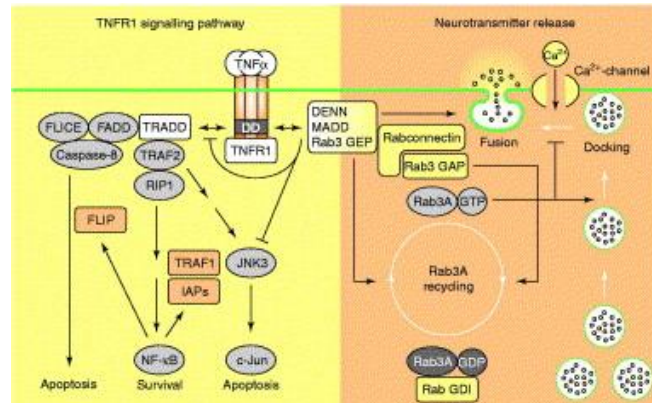


**Figure 107: DENN/MADD cellular functions.** Scheme from Miyoshi & Takai, 2004

In the second study, although the rescue of BDNF homeostasis is probably the main factor responsible for the amelioration of RTT mouse phenotypes because of its importance for striatal survival and down regulation in RTT, the restoration of other cargoes like APP or SVPs cannot be excluded (Roux et al., 2012). Indeed, in addition to BDNF, Roux and colleagues (Roux et al., 2012), found a decrease in HTT, HAP1 and dynactin suggesting that alteration of other cargo transport could be involved in RTT and that their restoration could also participate to the amelioration of the phenotype. For example, APP transport is also impaired, probably due to the down regulation of HTT (Roux et al., 2012). In addition, SVP transport could probably be also impaired because at least 18 different *de novo* missense variants of KIF1A motor domain gene have been described in RTT/RTT-like patients (Kaur et al., 2020). Thus, it is possible that the rescue of MECP2 KO mice through the increase of S421 phosphorylation by FK506 could also involve a restoration of the anterograde transport of APP vesicles and SVPs.

The possible involvement of several cargo transport in the rescue of phenotypes by S421 phosphorylation could also be involved in HD. Indeed, in Kratter et al., 2016, HTT<sub>S421D</sub> mice have been crossed with HD mouse model and a rescue of the HD phenotypes is observed. Although BDNF is the first cargo thought to be responsible for the rescue of the striatum-associated phenotypes, other cargoes like APP and SPs could also participate in the rescues of HD phenotypes. It is important to remember that HD patients do not only exhibit striatal-associated symptoms but also depression and cognitive impairments. Knowing the behavioral impact of the transport regulation of APP vesicle or SVPs, it is likely that these HD aspects are due to the disruption of the transport of those cargoes. As preliminary results, we indeed found that APP transport is impaired in HdhCAG140<sup>+/-</sup> corticostriatal network, which could be the cause of post signaling impairments like ERK phosphorylation, hypersynchrony of calcium transient or glutamate binding to its receptor (figure 108). However, the reduction of glutamate binding of to its receptor in HdhCAG140<sup>+/-</sup> neurons could also be due to the regulation of SVP transport, possibly impaired in HD. Indeed, in HD brains, SP representation within the PM is decreased (Morton et al., 2001; R. Smith et al., 2005) as well as the glutamate transmission

within M2-DLS network in HD mice correlated with impaired motor skill learning (Fernández-García et al., 2020).

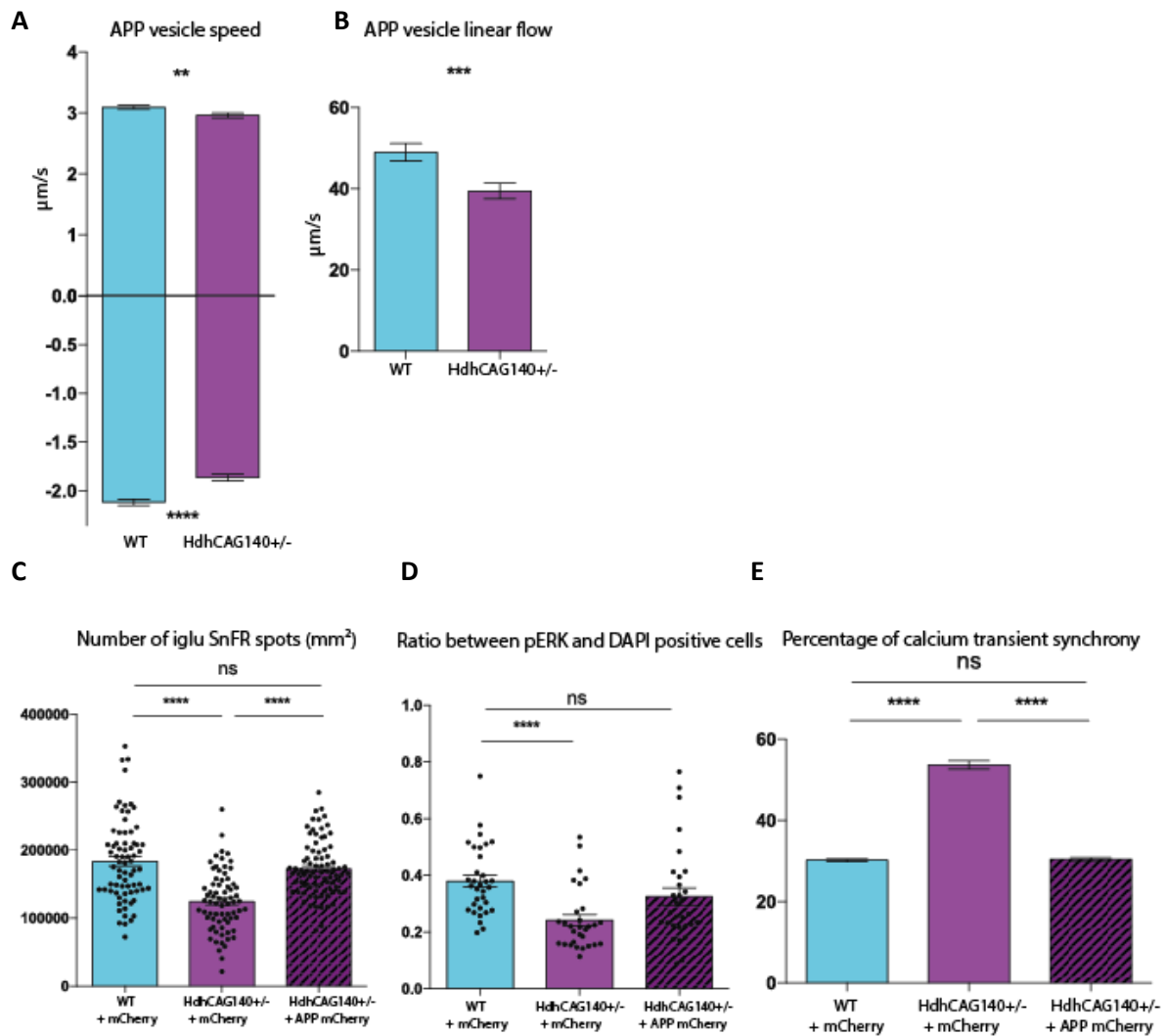


**Figure 108: APP transport and post signaling are impaired in HdhCAG140+/- corticostriatal network.** (A) anterograde and retrograde speed and (B) linear flow of APP-mCherry vesicles. (C) Number of iglu SnFR spots within the synaptic chamber after a 15-minute stimulation of glycine-strychnine. (D) ratio between pERK positive cells and DAPI within the postsynaptic chamber. (E) percentage of synchrony in GCamp6f signal in the postsynaptic chamber. Significance was estimated by Mann & Whitney test for (A) and (B) and with a One-way ANOVA followed by Dunn's test for (C) to (E). Data was obtained from at least 3 independent experiments in more than 3 microfluidics devices for each and at least 1200 vesicles within 150 axons were analyzed.

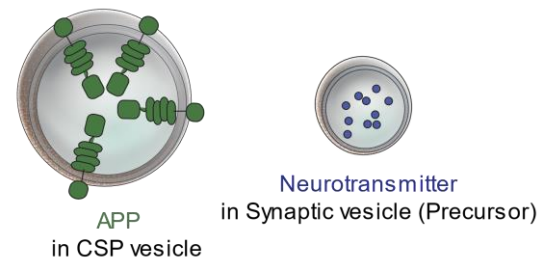
Taken together, our studies allowed to decipher the involvement of specific cargoes in specific circuits. However, a better understanding of the contribution of specific adaptors in the selective transport of cargoes will be necessary to decipher the contribution of individual cargoes to synapse homeostasis and function.

## Interaction between cargoes

As mentioned earlier, a phenotype is often due to the regulation of several players as components of a same homeostatic regulation mechanism. As an example, APP and its cleavage products, as well as BDNF, whose levels at the synapse are driven by their axonal transport, have been shown to regulate SV release which, consequently, might not be due only to SVP transport regulation.

### ***APP as a regulator of NT release***

APP has been recently described as a player able to regulate NT release at the active zone (Morton et al., 2001; R. Smith et al., 2005). For now, at least two mechanisms have been proposed to explain APP role on NT release.



The first one relies on APP ability to form homodimer. Activation of APP dimers are thought to be responsible for an increase of presynaptic calcium influx and SV release through a Gi/o protein signaling (Fogel et al., 2014).

The second mechanism involves APP and one of its homologs, APLP2 that can also interact with SPs like synaptophysin (syp), synaptotagmin (syt) or synaptobrevin (vamp2) to facilitate NT release (Fanutza et al., 2015; Laßek et al., 2013). Consequently, KO mice of these proteins exhibit a reduced SV density and active zone size (G. Yang et al., 2005).

Thus, by increasing APP anterograde transport in  $HTT_{S421D}$  mice, it is possible that APP levels at the synapse are increased, which could promote APP homodimerization and consequent NT release. On the contrary, in  $HTT_{S421A}$  mice, we observe a decrease in the levels of APP at the PM which could decrease its dimerization and thus the probability of release. This might be one mechanism to explain the rescue of AD mice in which the probability of release is increased.

Regulation of SVP transport might thus not be the only responsible for the change of probability of release.

### ***A $\beta$ as a regulator of the SV cycle***

A $\beta$  peptides have been described as a regulator of neurotransmission through their binding to NMDA receptors (Q. S. Chen et al., 2002) but they also act as NT release regulators within the presynaptic neuron. Indeed, A $\beta$  peptides are able to activate APP homodimerization at the PM thus increasing the probability of release. In this configuration, APP dimerization can be considered as a presynaptic receptor for A $\beta$  signaling regulating glutamate release (Fogel et al., 2014). In AD, excessive A $\beta$  peptides



production might then initiate a positive feedback loop through APP dimer activation leading to hyperactivity (Fogel, et al., 2014).

In addition, A $\beta$  peptides have also been described as a complex regulator of SV cycle; A $\beta$  peptides are able to exert a control according to their oligomerization, over exocytosis, endocytosis and the dynamics between SV pools. Indeed, A $\beta$  peptides can increase NT release by stimulating the formation of the fusion pore through binding to synaptophysin or decrease NT release by inhibiting exocytosis through binding to syntaxin. A $\beta$  peptides can also impair endocytosis by decreasing dynamin-1 levels or by preventing endocytosis synaptophysin-dependent triggering through its binding to vamp2. Finally, A $\beta$  peptides can increase synapsin 1 phosphorylation thus enhancing the number of SVs from the reserve pool migrating to the RRP and the consequent probability of release (Fagiani et al., 2019) (figure 109).

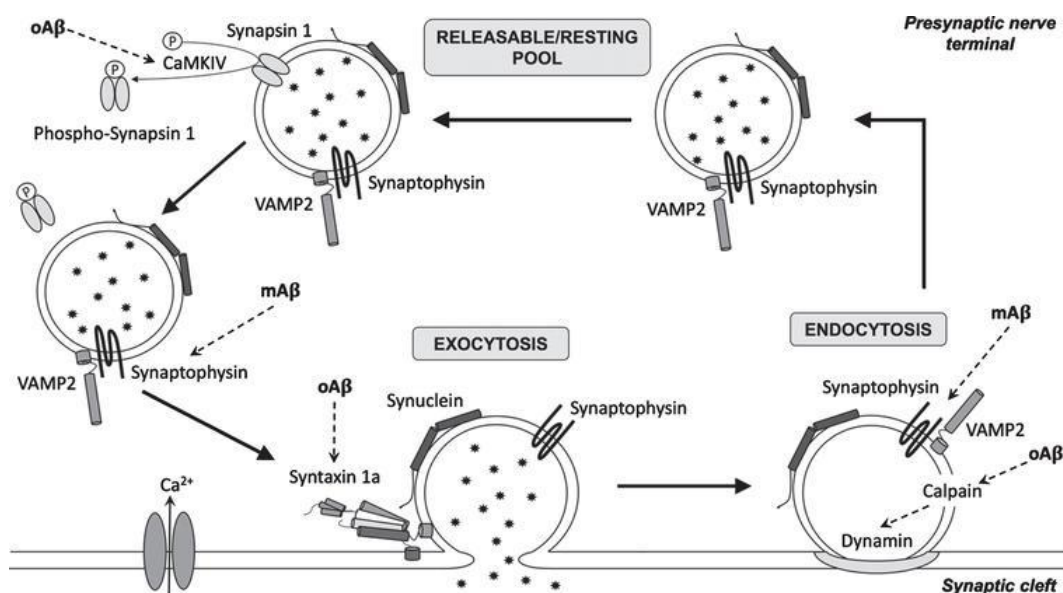


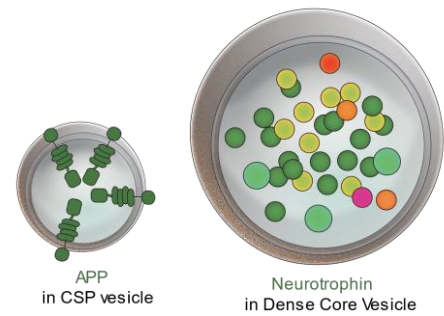
**Figure 109: A $\beta$  peptides regulates SV cycle.** Scheme from Fagiani *et al.*, 2019

Interestingly, increasing vamp2 production through epigenetic modulation restores A $\beta$ -induced synaptic transmission failure (S. Hu et al., 2015). Thus, increasing SVP transport and the consequent levels of SPs at the PM can be protective when A $\beta$  is overexpressed but toxic in physiological condition (HTT<sub>S421D</sub> mice).

Regarding A $\beta$  peptide role on NT release, we could also point out the consequences of KIF1A silencing, known to be responsible for BACE-1 transport at the synapse (Hung & Coleman, 2016). Indeed, we can speculate that reducing KIF1A-mediated transport of BACE1 to the synapse of WT neurons could also reduce A $\beta$  peptide production, which can reduce the NT release. This reduction in NT release is seen in the WT mice injected with shKIF1A (data not shown).

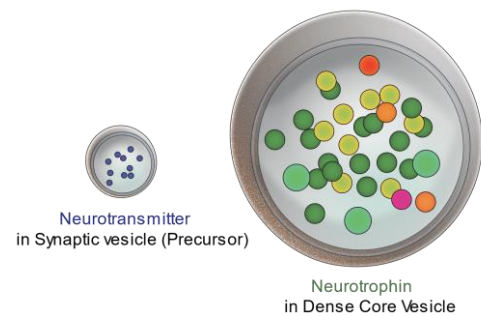
### ***Aβ as a regulator of BDNF homeostasis***

In addition to regulating NT release, 100 nM of Aβ peptides, through the activation of the IGF1R pathway, are also able to activate CREB (cyclic AMP response element-binding), a transcription factor known to sustain BDNF expression (Zimbone et al., 2018). Thus, regulating APP transport in MECP2 KO neurons in the second study may have restored the Aβ peptide homeostasis thus promoting BDNF production, amplifying the consequences of its increased released at the synapse.



### ***BDNF and the regulation of NT release***

BDNF is another regulator of NT release. BDNF, upon binding to its receptor, TrkB into the pre- or the postsynaptic neuron, is able to regulate neuronal activity, NT release and retrograde signaling (Y. Li et al., 2017). Long term BDNF treatment of neurons in a physiological condition induces an increase in EPSCs and in the number of endocytosed SVs, suggesting that BDNF is able to modulate the size of SV pools (Rauti et al., 2020; William J. Tyler et al., 2006). Mechanisms describing BDNF ability to regulate NT release have been reported. One of them relies on the ability of BDNF to activate a MAP kinase responsible for the phosphorylation of synapsin-1 leading to the mobilization of SVs from the recycling pool and a subsequent increased NT release (Jovanovic et al., 2000). Another study proposed that this results in an increased in the number of docked SV number impacting the size of the AZ in CA1 neurons (W. J. Tyler & Pozzo-Miller, 2001). Thus, reestablishing BDNF transport in MECP2 KO neurons or in HD mouse neurons (Maria Borrell-Pagès et al., 2006; Yann Ehinger et al., 2020; Zala et al., 2008) might also change the NT release thus amplifying the pro-survival consequences of the BDNF release at the synapse.



Although we have to consider the fact that cargoes can interact and regulate each other, this thesis work allowed to better define the physiological role of the S421 phosphorylation in axonal transport at the molecular, cellular and behavioral levels.

## 2. S421 phosphorylation of HTT as a physiological regulator of vesicle transport.

We previously described the cellular and behavioral consequences of HTT phosphorylation at S421 in contexts where it was constitutively active or inactive. However, it is important to realize that in physiological conditions, S421 oscillates between those two phosphorylation states. The following part focuses on understanding the physiological conditions and mechanisms in which HTT regulates vesicular transport.

### a. Why is transport regulation physiologically important?

Even though it is still difficult nowadays to access the phosphorylation rate of a protein, especially in human brains because of its dynamic properties, we can hypothesize that HTT phosphorylation in “healthy” human brains is tightly regulated. Indeed, upon several stimuli, during learning phases for instance, HTT might be more phosphorylated therefore stimulating transport of SVPs, thus allowing SVPs to rapidly overcome the emptying of SV pools and for APP to produce the STP-induced morphological and functional changes on synapse homeostasis. Then, the plastic property of neurons implies that they are able to change their morphology and function in the two ways. Right after the train of stimulations or when a neuronal network is not used anymore, the cell might favor retrograde transport to either (and respectively) sense the context at the synapse or to retrieve and recycle vesicles or proteins which became useless.

Thus, the fast regulation of neuronal transport is crucial for neuronal homeostasis. But what could be the triggering mechanism?

### b. Could S421 phosphorylation be a molecular signature of neuronal activity changes?

At the beginning of this century, the idea of the regulation of the vesicular transport as a consequence of neuronal activity came out (Carroll et al., 2001; Kamenetz et al., 2003; Malinow et al., 2000). In support, unpublished work from the lab suggest a mechanism involving the calcium-dependent recruitment of vesicles upon neuronal activity (Moutaux *et al.*, *in prep*). Interestingly, changes in neuronal activity has been observed in many NDs like AD (Frere & Slutsky, 2017; Styr & Slutsky, 2018) or HD (Blumenstock & Dudanova, 2020; Dougherty et al., 2014; Rebec et al., 2006; Virlogeux et al., 2018) which exhibit impaired transport of BDNF, TrkB and APP vesicles (Gauthier et al., 2004; Liot et al., 2013; Zala et al., 2008). In HD mouse models, pS421 has been found in lower levels in the cortex and the striatum (Metzler et al., 2010; Warby et al., 2005). Thus, we can speculate that HTT S421 phosphorylation could be a downstream process or a regulatory mechanism resulting from neuronal activity changes. In HD, Akt-mediated S421 phosphorylation is decreased due to the

abnormal activation of extrasynaptic NMDAR (Jablonski et al., 2011; Leavitt et al., 2006; Metzler et al., 2010; Zeron et al., 2002). In addition, Akt is cleaved and inactivated in HD postmortem brains (Humbert et al., 2002). The fact that NMDAR activation induces S421 phosphorylation adds a causative link between NMDA-Evoked current and S421 phosphorylation of HTT. Thus, S421 phosphorylation could appear as a regulatory mechanism counteracting the excessive NMDAR activation observed in HD to go back to homeostatic values. This strategy would follow many studies in which S421 phosphorylation has been found to counteract many toxic functions provoked by HTT mutation thus conferring a prosurvival role of S421 phosphorylation (Humbert et al., 2002). For instance, S421D mutation restores vesicular transport, HTT increased cleavage, mitochondrial function and neuronal survival in HD cells (Gauthier, et al., 2004; Humbert et al., 2002; Kratter et al., 2016; Metzler et al., 2010; Pardo, 2006; Rangone et al., 2004; Warby et al., 2009; X. Xu et al., 2020; Zala et al., 2008).

Thus, we saw how crucial the transport regulation is for the good functioning of a network, probably via a translation of neuronal activity. But is HTT the only regulator of neuronal transport directionality?

### c. Is HTT role of molecular switch for vesicular transport redundant?

We have demonstrated that HTT phosphorylation acts as a molecular switch for transport directionality of several cargoes (Bruyère et al., 2020; Colin et al., 2008; Ehinger et al., 2020; Vitet et al., *in prep*). It is interesting to note that JIP1 shares similar features with HTT in this function (Meng-meng Fu & Holzbaaur, 2013). JIP1 regulates vesicular directionality upon phosphorylation (also a phosphorylation at S421). However, the differences may reside in the signaling pathways that regulate these phosphorylations: Akt through IGF-1 pathway in the case of HTT and JNK in the case of JIP1 associated with cell survival regulation. Interestingly, according to the stimuli, the strength and the duration of JNK activation, the cellular outcomes can vary from induction of apoptosis to increased survival (E. F. Wagner & Nebreda, 2009). Thus, cells would be able to regulate the directionality of vesicles in response to different upstream signaling pathways. However, this dichotomy regarding these signaling pathways seems paradoxical since both HTT and JIP1 regulators were found to modulate the transport of the same vesicles, APP and autophagosomes, in a similar manner (Colin et al., 2008; Meng-meng Fu & Holzbaaur, 2013; Meng meng Fu et al., 2014; Wong & Holzbaaur, 2014). More studies are needed to decipher the specific properties of those two transport regulators. Do they localize on the same vesicles or are they specific to subtypes of vesicles?

#### **d. HTT: a transport regulator of all the types of vesicles encountered in neurons?**

We unraveled a role for HTT as a regulator of the transport of several types of vesicles namely, APP vesicles, BDNF vesicles and SVPs. Other studies demonstrated that HTT is also involved in transport of autophagosomes (Meng meng Fu et al., 2014; Wong & Holzbaur, 2014), signaling endosomes (Scaramuzzino et al., *in prep*) or late endosomes (Colin et al., 2008; J. A. White et al., 2015). Does HTT regulate the transport of most, if not all, vesicles within a neurite? This may depend on the vesicle subtypes. For example, HTT silencing has been found to affect one subpopulation of vesicles and not others according to the type of Rab protein that is present on these vesicles (J. A. White et al., 2015). For instance, some recycling endosomes (Rab 11 and 19 positive endosomes) are affected by HTT silencing but no others (Rab 14, 21, 26 and 32) (Power et al., 2012; J. A. White et al., 2015).

The presence of specific Rab proteins on vesicles might reflect different vesicle status and might dictate the need of a vesicle for a HTT-mediated regulation of its transport. It would thus be interesting to decipher Rab-HTT interaction; what is the dynamics of HTT-independent vesicles? Does Rab recruit HTT on a vesicle?

### **3. Restoring vesicular transport in NDs, an efficient therapeutic strategy?**

#### **a. Transport rescue through genetics**

For some NDs, it is theoretically quite easy to restore neuronal transport homeostasis without affecting other cellular process homeostasis. It is for example the case of transportopathies caused by mutation(s) in the genes coding for the transport machinery (molecular motor, MAPs or other neuronal transport regulators) like cohesinopathies, SPGs, HD or the Goldberg-Shprintzen syndrome. Indeed, the development of gene therapy or allele specific ASO treatment could bring future leads by reducing the weight of the mutated gene (De Vos & Hafezparast, 2017).

#### **b. Transport rescue through homeostasis regulation**

Such therapies might be more difficult to develop when neuronal dysregulations originate from homeostatic perturbances. This is why it is important to study these homeostatic perturbances by first deciphering the homeostatic mechanisms occurring in physiological conditions. Understanding the role of a protein of interest on homeostasis allows us to better characterize the feedback loop and the role of the protein of interest within the feedback loop. In other word, it is important to know if HTT is the effector, the sensor or the integrator acting on the studied variable (Macleod & Zinsmaier, 2006; Styr & Slutsky, 2018). By a better understanding of the actors involved in the loop, we could avoid acting on the effector, thus perturbing the negative feedbacks already set up by the homeostatic

loop to counteract the perturbation (Styr & Slutsky, 2018). A more trivial example would be to try to decrease the high body temperature caused by the flu even though increasing the body temperature is a feedback mechanism to sustain the immune response. In AD, absence of a clear idea of the homeostatic regulation, mainly caused by the complexity of the mechanisms involved, can explain why so many strategies failed to characterize and rescue the NDs (Styr & Slutsky, 2018). To go back to HTT regulation transport as a therapeutic strategy, if the transport is not considered as an effector in the studied homeostatic loop, as for our study as a sensor, this could be a good strategy (figure 110).

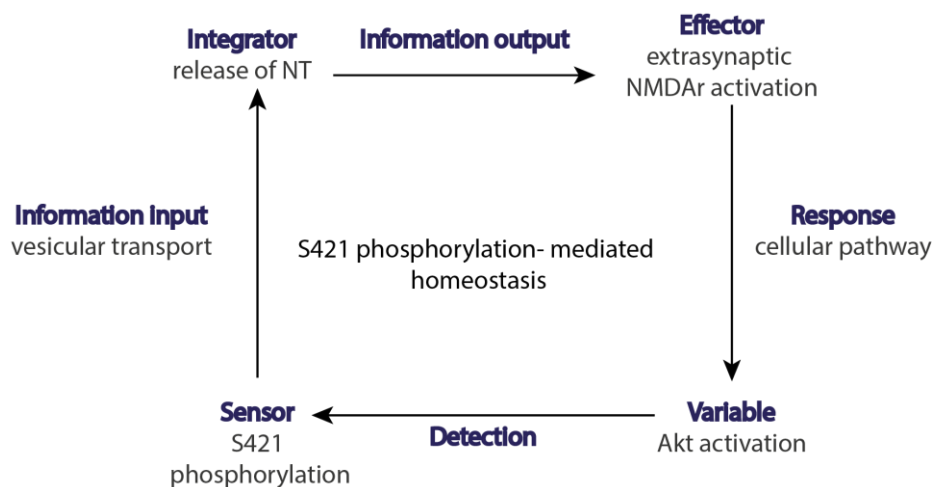


**Figure 110: S421 phosphorylation role in the homeostatic regulation of neurotransmission.** Scheme representing a possible mechanism.

*In vivo* studies that do not consider the vesicular transport as an essential player of the homeostatic loop, failed to fully restore some mouse phenotypes (Styr & Slutsky, 2018). This is for example the case of studies based on overexpression of a cargo in context where the transport of this cargo is impaired (Q. Chang et al., 2006; Hathorn et al., 2011; Simmons et al., 2009; Xie et al., 2010). In the latest studies, rescue of HD mouse behavioral phenotypes was not complete. On the opposite, when the transport is either restored or replaced by local and physiological supply of the cargo, the rescue is more complete (Bruyère et al., 2020; De Pins et al., 2019; Dey et al., 2010; Yann Ehinger et al., 2020). Indeed, using FK506 treatment for RTT mice, BDNF local delivery by astrocytes or crossings with HTT<sub>S421A</sub> mice for AD mice or BDNF delivery by mesenchymal stem cells implanted within the striatum of HD mice rescued motor phenotypes in RTT mice, memory in AD mice and motor coordination in HD mice.

# Conclusion

Throughout this manuscript, I aimed at emphasizing the role of HTT-mediated axonal transport as a regulator of neuronal homeostasis by its ability to target a cargo to its specific subcellular compartment where it is essential for network function and behavior. As illustrated in figure 111, the modulation of one actor of the transport machinery is enough to impact neuronal transport. The extreme sensibility of this finely tuned biosystem is depicted by the development of many NDs linked to a mutation or a homeostatic dysregulation of MAPs, molecular motor, regulator or scaffolding proteins. Consequently, theoretical and integrated studies is of importance to better characterize the homeostatic regulation of the vesicular transport to identify potential therapeutic candidates for these diseases.

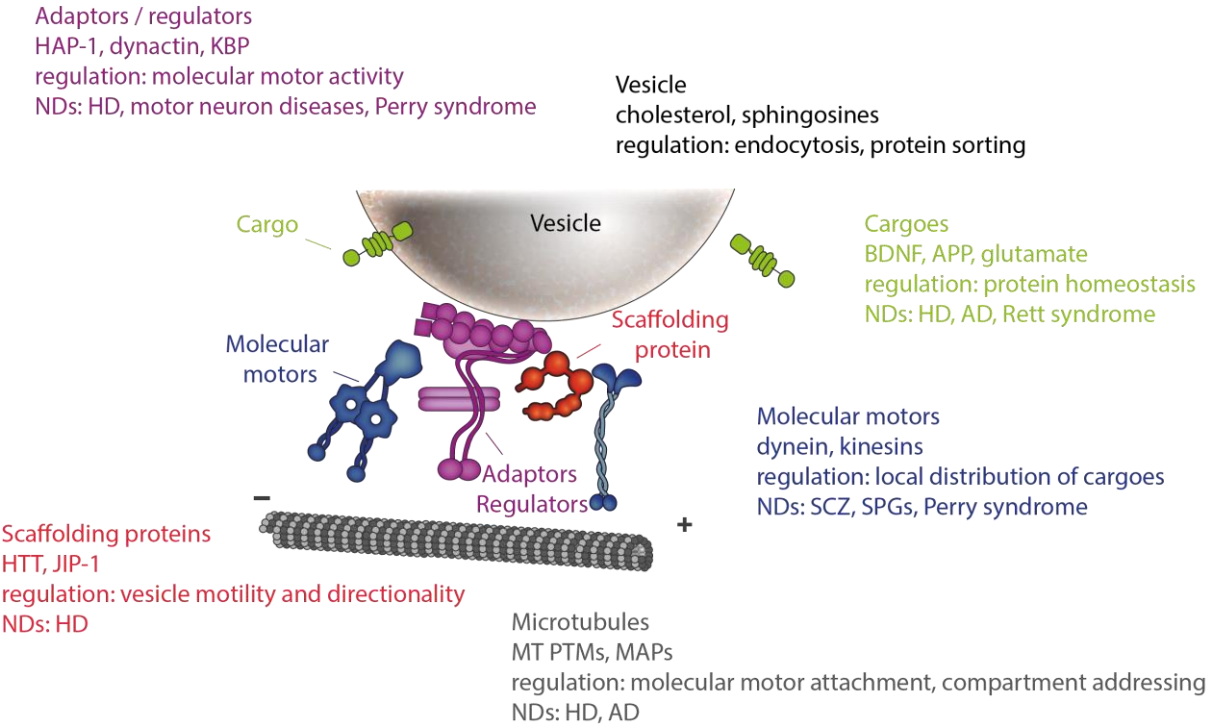


**Figure 111: axonal transport of a vesicle results from the coordinated action of molecular motors, adaptors, scaffolding protein and tracks.** If one of them is dysregulated, it leads to transportopathies and/or neurodegeneration.

## Perspectives

This study also opens new possibilities and challenges for both theoretical research and therapeutic perspectives.

### 1. Technical challenges and future plans for research

As mentioned earlier, although the use of this mouse line can be limited in some technical aspects due to the fact that the mutation affecting the phosphorylation status of HTT is permanent, we believe these mice could serve as a good tool to decipher some other aspects of axonal transport.

#### a. Investigate the role of energy

The lab has shown that HTT scaffolds glycolytic enzymes on the mobile vesicle allowing a local supply of ATP and thus promoting molecular motor function, (Hinckelmann et al., 2016; Zala et al., 2013; McCluskey *et al.*, *in prep*). HTT S421 phosphorylation, may also regulate and/or recruit glycolytic enzyme to maximize ATP production. This hypothesis could be challenged by assessing the level of glycolytic enzymes on vesicles isolated from HTT<sub>S421D</sub> brains by vesicular fractionation. We could then regulate the stoichiometry of glycolytic enzymes on WT vesicles (using a TM-GAPDH constructs for instance (M.-V. Hinckelmann et al., 2016)) and investigate if the increased ATP production is contributing for the increased anterograde transport caused by S421 phosphorylation. .

#### b. Investigate the role of neuronal activity

Neurons from HTTS421 mice could also be used to investigate the consequences of neuronal activity on S421 phosphorylation. This hypothesis could be tested by application of electric stimulation using MEA technique on microfluidics microchambers (Moutaux, Charlot, et al., 2018). In combination with the neuronal transduction of a tagged cargo and with a peptide biosensor, it would allow to understand the link between neuronal activity, S421 phosphorylation and vesicular transport. Indeed, the peptide biosensor could be a genetically encoded FRET-biosensor or a self-reporting biosensor able to fluoresce when HTT is phosphorylated (Tarrant & Cole, 2009). However, the large size of HTT might be another technical challenge to create a biosensor reporting its phosphorylation. Nevertheless, this could help us understand the physiological regulation of axonal transport through S421 phosphorylation and the consequences in term of S421 phosphorylation in NDs like AD or HD where neuronal activity is impaired.



## 2. Challenges in therapeutic strategies for pharmaceutical industry

### a. HD clinical trials & ASO strategy

My thesis work added new information regarding the physiological roles of HTT which could be useful for the design of drugs used in HD clinical trials. Unlike some studies (J. P. Liu & Zeitlin, 2017), this work emphasizes the need for HTT and its phosphorylation to maintain neuronal homeostasis. Our findings that levels of cargoes reaching the synapse are finely regulated, dysregulating WT HTT levels with ASO might have deleterious consequences. On the other hand, the specific reduction of mHTT expression would be more appropriate in removing the toxic functions as well as the potential dominant negative effect of mHTT on WT HTT.

### b. FK506: the answer to all the NDs with a deficit of transport?

Throughout this manuscript, we suggested that S421 phosphorylation, that can be increased by FK506, is protective and restores Rett syndrome in mice. Moreover, other studies performed in the lab demonstrated that FK506 treatment rescues cell death and BDNF transport impairments caused by the polyQ mutation of HTT (Pardo, 2006; Pineda et al., 2009). Therefore, we could wonder if FK506 treatment could be used as a therapeutic compound to rescue the deficit in transport observed in several NDs. Interestingly, FK506 is already employed in medicine nowadays as a FDA-approved immunosuppressant preventing allograft rejection (Y. Lee et al., 2018; Sigal & Dumont, 1992), making its use as a treatment for NDs likely to be authorized. Whether FK506 could be of therapeutic interest for other transportopathies like HD, Rett syndrome, HSP or cohesinopathies in humans remain of interest.

In case of RTT or HD, where the mutation impairs at least one regulator of the transport that is not specific to one type of cargo, FK506 could be beneficial because it could be able to rescue the transport of many (if not all) the cargoes. In the case of HD, the recovery of BDNF, APP and SVP transport might lead to a stronger therapeutic effect since these cargoes contribute to synaptic homeostasis and circuit function. However, rescuing axonal transport in humans by FK506 treatment might not be sufficient alone (De Vos & Hafezparast, 2017) and could have negative side effects. Indeed, FK506 could affect numerous off-targets because phosphorylation and dephosphorylation regulate many signaling pathways modulating many cellular processes (Gibbs et al., 2015). For instance, decreasing calcineurin activity could impair endocytosis in neurons and other several homeostatic regulation mechanisms in non-neural cells like T cells or kidney cells (Bremer et al., 2016).

For NDs based on mutation of one of the members of the transport machinery regulating the transport of a specific cargo like KIF1A in SPG-30 or the Goldberg-Shprintzen syndrome, FK506 may not

be appropriate. Although FK506 could have a beneficial effect for the KIF1A mediated transport by restoring it, other cargoes (like APP) whose transport is not impaired might then be dysregulated and lead to APP accumulation at synapses and consequently disrupt synapse homeostasis.

Together, my thesis work led to a better understanding on the cargoes that are transported by HTT, how their transport is regulated by HTT phosphorylation with consequences for Rett syndrome, AD and HD.

## Bibliography

- Abbott, L. F., & Regehr, W. G. (2004). *Synaptic computation*. [www.nature.com/nature](http://www.nature.com/nature)
- Abramov, E., Dolev, I., Fogel, H., Ciccotosto, G. D., Ruff, E., & Slutsky, I. (2009). Amyloid-beta as a positive endogenous regulator of release probability at hippocampal synapses. *Nature Neuroscience*, *12*(12), 1567–1576. <https://doi.org/10.1038/nn.2433>
- Adalbert, R., Milde, S., Durrant, C., Ando, K., Stygelbout, V., Yilmaz, Z., Gould, S., Brion, J. P., & Coleman, M. P. (2018). Interaction between a MAPT variant causing frontotemporal dementia and mutant APP affects axonal transport. *Neurobiology of Aging*, *68*, 68–75. <https://doi.org/10.1016/j.neurobiolaging.2018.03.033>
- Agasse, F., Mendez-David, I., Christaller, W., Carpentier, R., Braz, B. Y., David, D. J., Saudou, F., & Humbert, S. (2020). Chronic Corticosterone Elevation Suppresses Adult Hippocampal Neurogenesis by Hyperphosphorylating Huntingtin. *Cell Reports*, *32*(1). <https://doi.org/10.1016/j.celrep.2020.107865>
- Aillaud, C., Bosc, C., Peris, L., Bosson, A., Heemeryck, P., Dijk, J. Van, Friec, J. Le, Boulan, B., Vossier, F., Sanman, L. E., Syed, S., Amara, N., Couté, Y., Lafanechère, L., Denarier, E., Delphin, C., Pelletier, L., Humbert, S., Bogyo, M., & Andrieux, A. (2017). Regulate Neuron Differentiation. *Science*, *1453*(December), 1448–1453.
- Al-Bassam, J., & Nithianantham, S. (2018). Malleable folding of coiled-coils regulates kinesin-3 dimerization. *Proceedings of the National Academy of Sciences of the United States of America*, *115*(51), 12845–12847. <https://doi.org/10.1073/pnas.1818758115>
- Alabi, A. A., & Tsien, R. W. (2012). *Synaptic Vesicle Pools and Dynamics*. 1–18.
- Alder, J., Kanki, H., Valtorta, F., Greengard, P., & Poo, M. M. (1995). Overexpression of synaptophysin enhances neurotransmitter secretion at *Xenopus* neuromuscular synapses. *Journal of Neuroscience*, *15*(1 II), 511–519. <https://doi.org/10.1523/jneurosci.15-01-00511.1995>
- Alder, Janet, Xie, Z.-P., Valtorta, F., Creengard, P., & Poe, M.-M. (1992). Antibodies to Synaptophysin Interfere with Transmitter Secretion at Neuromuscular Synapses. In *Neuron* (Vol. 9).
- Allan, V. (2014). One, two, three, cytoplasmic dynein is go! *Science*, *345*(6194), 271–272. <https://doi.org/10.1126/science.1257245>
- Allen, C., & Stevens, C. F. (1994). An evaluation of causes for unreliability of synaptic transmission. *Proceedings of the National Academy of Sciences of the United States of America*, *91*(22), 10380–10383. <https://doi.org/10.1073/pnas.91.22.10380>
- Ally, S., Larson, A. G., Barlan, K., Rice, S. E., & Gelfand, V. I. (2009). Opposite-polarity motors activate one another to trigger cargo transport in live cells. *Journal of Cell Biology*, *187*(7), 1071–1082. <https://doi.org/10.1083/jcb.200908075>
- Altar, C. A., Cai, N., Bliven, T., Juhasz, M., Conner, J. M., Acheson, A. L., Lindsay, R. M., & Wiegand, S. J. (1997). *Anterograde transport of brain-derived neurotrophic factor and its role in the brain*. *389*(October), 856–860.
- Anderson, E. N., & li, J. A. W. (2014). *Axonal transport and neurodegenerative disease : vesicle-motor*

*complex formation and their regulation.* 29–47.

- Androuin, A., Potier, B., Nägerl, U. V., Cattaert, D., Danglot, L., Thierry, M., Youssef, I., Triller, A., Duyckaerts, C., El Hachimi, K. H., Dutar, P., Delatour, B., & Marty, S. (2018). Evidence for altered dendritic spine compartmentalization in Alzheimer's disease and functional effects in a mouse model. *Acta Neuropathologica*, *135*(6), 839–854. <https://doi.org/10.1007/s00401-018-1847-6>
- Araki, Y., Kawano, T., Saito, Y., Wada, S., Miyamoto, K., Kobayashi, H., Ishikawa, H. O., Ohsugi, Y., Yamamoto, T., Matsuno, K., Kinjo, M., & Suzuki, T. (2007). *The novel cargo Alcadin induces vesicle association of kinesin-1 motor components and activates axonal transport.* *26*(6), 1475–1486. <https://doi.org/10.1038/sj.emboj.7601609>
- Arpağ, G., Norris, S. R., Mousavi, S. I., Soppina, V., Verhey, K. J., Hancock, W. O., & Tüzel, E. (2019). Motor Dynamics Underlying Cargo Transport by Pairs of Kinesin-1 and Kinesin-3 Motors. *Biophysical Journal*, *116*(6), 1115–1126. <https://doi.org/10.1016/j.bpj.2019.01.036>
- Arthur, C. P., Dean, C., Pagratis, M., Chapman, E. R., & Stowell, M. H. B. (2010). Loss of synaptotagmin IV results in a reduction in synaptic vesicles and a distortion of the Golgi structure in cultured hippocampal neurons. *Neuroscience*, *167*(1), 135–142. <https://doi.org/10.1016/j.neuroscience.2010.01.056>
- Asselin, L., Rivera Alvarez, J., Heide, S., Bonnet, C. S., Tilly, P., Vitet, H., Weber, C., Bacino, C. A., Baranaño, K., Chassevent, A., Dameron, A., Faivre, L., Hanchard, N. A., Mahida, S., McWalter, K., Mignot, C., Nava, C., Rastetter, A., Streff, H., ... Godin, J. D. (2020). Mutations in the KIF21B kinesin gene cause neurodevelopmental disorders through imbalanced canonical motor activity. *Nature Communications*, *11*(1). <https://doi.org/10.1038/s41467-020-16294-6>
- Atherton, J., Farabella, I., Yu, I. M., Rosenfeld, S. S., Houdusse, A., Topf, M., & Moores, C. A. (2014). Conserved mechanisms of microtubule-stimulated ADP release, ATP binding, and force generation in transport kinesins. *ELife*, *3*, e03680. <https://doi.org/10.7554/eLife.03680>
- Ayloo, S., Guedes-Dias, P., Ghiretti, A. E., & Holzbaur, E. L. F. (2017). Dynein efficiently navigates the dendritic cytoskeleton to drive the retrograde trafficking of BDNF/TrkB signaling endosomes. *Molecular Biology of the Cell*, *28*(19), 2543–2554. <https://doi.org/10.1091/mbc.E17-01-0068>
- Baas, P. W., Deitch, J. S., Black, M. M., & Banker, G. A. (1988). Polarity orientation of microtubules in hippocampal neurons: Uniformity in the axon and nonuniformity in the dendrite. *Proceedings of the National Academy of Sciences of the United States of America*, *85*(21), 8335–8339. <https://doi.org/10.1073/pnas.85.21.8335>
- Bacaj, T., Wu, D., Burré, J., Malenka, R. C., Liu, X., & Südhof, T. C. (2015). Synaptotagmin-1 and -7 Are Redundantly Essential for Maintaining the Capacity of the Readily-Releasable Pool of Synaptic Vesicles. *PLoS Biology*, *13*(10), 1–26. <https://doi.org/10.1371/journal.pbio.1002267>
- Baker, R. R., Dowdall, M. J., & Whittaker, V. P. (1975). The effect of neurotransmitter release upon phospholipid composition and fatty acid turnover in synaptic vesicles of *Torpedo marmorata* electric organ and guinea pig cerebral cortex. *Biochemical Society Transactions*, *3*(2), 263–265. <https://doi.org/10.1042/bst0030263>
- Balcar, V. J., & Johnston, G. A. R. (1972). THE STRUCTURAL SPECIFICITY OF THE HIGH AFFINITY UPTAKE OF L-GLUTAMATE AND L-ASPARTATE BY RAT BRAIN SLICES. *Journal of Neurochemistry*, *19*(11), 2657–2666. <https://doi.org/10.1111/j.1471-4159.1972.tb01325.x>

- Baldelli, P., Fassio, A., Valtorta, F., & Benfenati, F. (2007). Lack of synapsin I reduces the readily releasable pool of synaptic vesicles at central inhibitory synapses. *Journal of Neuroscience*, *27*(49), 13520–13531. <https://doi.org/10.1523/JNEUROSCI.3151-07.2007>
- Baleriola, J., Walker, C. A., Jean, Y. Y., Crary, J. F., Troy, C. M., Nagy, P. L., & Hengst, U. (2014). Axonally synthesized ATF4 transmits a neurodegenerative signal across brain regions. *Cell*, *158*(5), 1159–1172. <https://doi.org/10.1016/j.cell.2014.07.001>
- Balsters, J. H., Zerbi, V., Sallet, J., Wenderoth, N., & Mars, R. B. (2020). Primate homologs of mouse cortico-striatal circuits. *eLife*, *9*, 1–24. <https://doi.org/10.7554/eLife.53680>
- Baquet, Z. C., Gorski, J. A., & Jones, K. R. (2004). Early Striatal Dendrite Deficits followed by Neuron Loss with Advanced Age in the Absence of Anterograde Cortical Brain-Derived Neurotrophic Factor. *Journal of Neuroscience*, *24*(17), 4250–4258. <https://doi.org/10.1523/JNEUROSCI.3920-03.2004>
- Barker, R. A., Fujimaki, M., Rogers, P., & Rubinsztein, D. C. (2020). Huntingtin-lowering strategies for Huntington's disease. *Expert Opinion on Investigational Drugs*, *0*(0). <https://doi.org/10.1080/13543784.2020.1804552>
- Barkus, R. V., Klyachko, O., Horiuchi, D., Dickson, B. J., & Saxton, W. M. (2008). Identification of an axonal kinesin-3 motor for fast anterograde vesicle transport that facilitates retrograde transport of neuropeptides. *Molecular Biology of the Cell*, *19*(1), 274–283. <https://doi.org/10.1091/mbc.E07-03-0261>
- Barnat, M., Capizzi, M., Aparicio, E., Boluda, S., Wennagel, D., Kacher, R., Kassem, R., Lenoir, S., Agasse, F., Braz, B. Y., Liu, J. P., Ighil, J., Tessier, A., Zeitlin, S. O., Duyckaerts, C., Dommergues, M., Durr, A., & Humbert, S. (2020). Huntington's disease alters human neurodevelopment. *Science (New York, N.Y.)*, *369*(6505), 787–793. <https://doi.org/10.1126/science.aax3338>
- Barnat, M., Le Fric, J., Benstaali, C., & Humbert, S. (2017). Huntingtin-Mediated Multipolar-Bipolar Transition of Newborn Cortical Neurons Is Critical for Their Postnatal Neuronal Morphology. *Neuron*, *93*(1), 99–114. <https://doi.org/10.1016/j.neuron.2016.11.035>
- Bayer, S. A. (Shirley A., & Altman, J. (1991). *Neocortical development*. Raven Press.
- Becanovic, K., Nørremølle, A., Neal, S. J., Kay, C., Collins, J. A., Arenillas, D., Lilja, T., Gaudenzi, G., Manoharan, S., Doty, C. N., Beck, J., Lahiri, N., Portales-Casamar, E., Warby, S. C., Connolly, C., De Souza, R. A. G., Tabrizi, S. J., Hermanson, O., Langbehn, D. R., ... Leavitt, B. R. (2015). A SNP in the HTT promoter alters NF-κB binding and is a bidirectional genetic modifier of Huntington disease. *Nature Neuroscience*, *18*(6), 807–816. <https://doi.org/10.1038/nn.4014>
- Bedse, G., Di Domenico, F., Serviddio, G., & Cassano, T. (2015). Aberrant insulin signaling in Alzheimer's disease: Current knowledge. *Frontiers in Neuroscience*, *9*(MAY), 1–13. <https://doi.org/10.3389/fnins.2015.00204>
- Belichenko, P. V., Masliah, E., Kleschevnikov, A. M., Villar, A. J., Epstein, C. J., Salehi, A., & Mobley, W. C. (2004). Synaptic structural abnormalities in the Ts65Dn mouse model of Down syndrome. *Journal of Comparative Neurology*, *480*(3), 281–298. <https://doi.org/10.1002/cne.20337>
- Bellocchio, E. E., Reimer, R. J., Fremeau, R. T., & Edwards, R. H. (2000). Uptake of Glutamate into Synaptic Vesicles by an Inorganic Phosphate Transporter. *Science*, *289*(5481), 957. <https://doi.org/10.1126/science.289.5481.957>

- Benfenati, F., Greengard, P., Brunner, J., & Bahler, M. (1989). Electrostatic and hydrophobic interactions of synapsin I and synapsin I fragments with phospholipid bilayers. *Journal of Cell Biology*, 108(5), 1851–1862. <https://doi.org/10.1083/jcb.108.5.1851>
- Bentley, M., & Banker, G. (2016). The cellular mechanisms that maintain neuronal polarity. *Nature Reviews Neuroscience*, 17(10), 611–622. <https://doi.org/10.1038/nrn.2016.100>
- Bharat, V., Siebrecht, M., Burk, K., Ahmed, S., Reissner, C., Kohansal-Nodehi, M., Steubler, V., Zweckstetter, M., Ting, J. T., & Dean, C. (2017). Capture of Dense Core Vesicles at Synapses by JNK-Dependent Phosphorylation of Synaptotagmin-4. *Cell Reports*, 21(8), 2118–2133. <https://doi.org/10.1016/j.celrep.2017.10.084>
- Bigler, R. L., Kamande, J. W., Dumitru, R., Niedringhaus, M., & Taylor, A. M. (2017). Messenger RNAs localized to distal projections of human stem cell derived neurons. *Scientific Reports*, 7(1), 1–11. <https://doi.org/10.1038/s41598-017-00676-w>
- Bircks, R., & MacIntosh, F. . (1961). Acetylcholine metabolism of a sympathetic ganglion. *Canadian Journal of Biochemistry and Physiology*, 39(4), 787–827.
- Biró, Á. A., Holderith, N. B., & Nusser, Z. (2005). Quantal size is independent of the release probability at hippocampal excitatory synapses. *Journal of Neuroscience*, 25(1), 223–232. <https://doi.org/10.1523/JNEUROSCI.3688-04.2005>
- Biol, M., & Melo, A. M. (2020). Untangling the Conformational Polymorphism of Disordered Proteins Associated With Neurodegeneration at the Single-Molecule Level. *Frontiers in Molecular Neuroscience*, 12(January), 1–10. <https://doi.org/10.3389/fnmol.2019.00309>
- Bitsikas, V., Riento, K., Howe, J. D., Barry, N. P., & Nichols, B. J. (2014). *The Role of Flotillins in Regulating A b Production , Investigated Using Flotillin 1- / - , Flotillin 2- / - Double Knockout Mice*. 9(1). <https://doi.org/10.1371/journal.pone.0085217>
- Bittner, T., Fuhrmann, M., Burgold, S., Jung, C. K. E., Volbracht, C., Steiner, H., Mitteregger, G., Kretzschmar, H. A., Haass, C., & Herms, J. (2009).  $\beta$ -Secretase Inhibition Reduces Spine Density In Vivo via an Amyloid Precursor Protein-Dependent Pathway. 29(33), 10405–10409. <https://doi.org/10.1523/JNEUROSCI.2288-09.2009>
- Blumenstock, S., & Dudanova, I. (2020). Cortical and Striatal Circuits in Huntington’s Disease. *Frontiers in Neuroscience*, 14(February). <https://doi.org/10.3389/fnins.2020.00082>
- Bohmbach, K., Schwarz, M. K., Schoch, S., & Henneberger, C. (2018). The structural and functional evidence for vesicular release from astrocytes in situ. *Brain Research Bulletin*, 136, 65–75. <https://doi.org/10.1016/j.brainresbull.2017.01.015>
- Bondy, C., Cheng, C., Zhong, J., & Lee, W. -H. (2006). *IGF-1 in Brain Growth and Repair Processes* (A. Laitha & R. Lim (eds.)). Springer US. [https://doi.org/10.1007/978-0-387-30381-9\\_7](https://doi.org/10.1007/978-0-387-30381-9_7)
- Borrell-Pagès, M., Zala, D., Humbert, S., & Saudou, F. (2006). Huntington’s disease: From huntingtin function and dysfunction to therapeutic strategies. *Cellular and Molecular Life Sciences*, 63(22), 2642–2660. <https://doi.org/10.1007/s00018-006-6242-0>
- Borrell-Pagès, Maria, Canals, J. M., Cordelières, F. P., Parker, J. A., Pineda, J. R., Grange, G., Bryson, E. A., Guillemier, M., Hirsch, E., Hantraye, P., Cheetham, M. E., Néri, C., Alberch, J., Brouillet, E., Saudou, F., & Humbert, S. (2006). Cystamine and cysteamine increase brain levels of BDNF in

- Huntington disease via HSJ1b and transglutaminase. *Journal of Clinical Investigation*, 116(5), 1410–1424. <https://doi.org/10.1172/JCI27607>
- Bosson, A., Paumier, A., Boisseau, S., Jacquier-Sarlin, M., Buisson, A., & Albrieux, M. (2017). TRPA1 channels promote astrocytic Ca<sup>2+</sup> hyperactivity and synaptic dysfunction mediated by oligomeric forms of amyloid- $\beta$  peptide. *Molecular Neurodegeneration*, 12(1), 1–19. <https://doi.org/10.1186/s13024-017-0194-8>
- Bourne, J. N., & Harris, K. M. (2011). Coordination of size and number of excitatory and inhibitory synapses results in a balanced structural plasticity along mature hippocampal CA1 dendrites during LTP. *Hippocampus*, 21(4), 354–373. <https://doi.org/10.1002/hipo.20768>
- Bowen, M. E., Engelman, D. M., & Brunger, A. T. (2002). Mutational analysis of synaptobrevin transmembrane domain oligomerization. *Biochemistry*, 41(52), 15861–15866. <https://doi.org/10.1021/bi0269411>
- Braak, H., & Braak, E. (1997). *Frequency of Stages of Alzheimer-Related Lesions in Different Age Categories*.
- Braak, Heiko, Alafuzoff, I., Arzberger, T., Kretschmar, H., & Tredici, K. (2006). Staging of Alzheimer disease-associated neurofibrillary pathology using paraffin sections and immunocytochemistry. *Acta Neuropathologica*, 112(4), 389–404. <https://doi.org/10.1007/s00401-006-0127-z>
- Brasted, P. J., & Wise, S. P. (2004). Comparison of learning-related neuronal activity in the dorsal premotor cortex and striatum. *European Journal of Neuroscience*, 19(3), 721–740. <https://doi.org/10.1111/j.0953-816X.2003.03181.x>
- Bremer, S., Vethe, N. T., & Bergan, S. (2016). Chapter 11. Monitoring calcineurin inhibitors response based on NFAT-regulated gene expression. In *Personalized Immunosuppression in Transplantation*. Elsevier Inc. <https://doi.org/10.1016/B978-0-12-800885-0.00011-4>
- Brimblecombe, K. R., & Cragg, S. J. (2015). Substance P weights striatal dopamine transmission differently within the striosome-matrix axis. *Journal of Neuroscience*, 35(24), 9017–9023. <https://doi.org/10.1523/JNEUROSCI.0870-15.2015>
- Bruce, A. W., Donaldson, I. J., Wood, I. C., Yerbury, S. A., Sadowski, M. I., Chapman, M., Göttgens, B., & Buckley, N. J. (2004). Genome-wide analysis of repressor element 1 silencing transcription factor/neuron-restrictive silencing factor (REST/NRSF) target genes. *Proceedings of the National Academy of Sciences of the United States of America*, 101(28), 10458–10463. <https://doi.org/10.1073/pnas.0401827101>
- Bruckner, R. J., Mansy, S. S., Ricardo, A., Mahadevan, L., & Szostak, J. W. (2009). Flip-flop-induced relaxation of bending energy: Implications for membrane remodeling. *Biophysical Journal*, 97(12), 3113–3122. <https://doi.org/10.1016/j.bpj.2009.09.025>
- Brunholz, S., Sisodia, S., Lorenzo, A., Deyts, C., Kins, S., & Morfini, G. (2012). Axonal transport of APP and the spatial regulation of APP cleavage and function in neuronal cells. *Experimental Brain Research*, 217(3–4), 353–364. <https://doi.org/10.1007/s00221-011-2870-1>
- Bruyère, J., Abada, Y.-S., Vitet, H., Fontaine, G., Deloulme, J.-C., Cès, A., Denarier, E., Pernet-Gallay, K., Andrieux, A., Humbert, S., Potier, M.-C., Delatour, B., & Saudou, F. (2020). Presynaptic APP levels and synaptic homeostasis are regulated by Akt phosphorylation of huntingtin. *ELife*, 9. <https://doi.org/10.7554/eLife.56371>

- Buée, L., Bussièrre, T., Buée-Scherrer, V., Delacourte, A., & Hof, P. R. (2000). Tau protein isoforms, phosphorylation and role in neurodegenerative disorders. *Brain Research Reviews*, 33(1), 95–130. [https://doi.org/10.1016/S0165-0173\(00\)00019-9](https://doi.org/10.1016/S0165-0173(00)00019-9)
- Bunge, M. . (1973). fine structure of nerve fibers and growth cones of isolated sympathetic neurons in culture. *The Journal of Cell Biology*, 56, 713–735.
- Burrus, C. J., Mckinstry, S. U., Kim, N., Zeitlin, S., Yin, H. H., Eroglu, C., Burrus, C. J., Mckinstry, S. U., Kim, N., Ozlu, M. I., Santoki, A. V, Fang, F. Y., & Ma, A. (2020). Striatal Projection Neurons Require Huntingtin for Synaptic Connectivity and Survival Article Striatal Projection Neurons Require Huntingtin for Synaptic Connectivity and Survival. *CellReports*, 30(3), 642-657.e6. <https://doi.org/10.1016/j.celrep.2019.12.069>
- Busche, M. A., Chen, X., Henning, H. A., Reichwald, J., Staufenbiel, M., Sakmann, B., & Konnerth, A. (2012). Critical role of soluble amyloid- $\beta$  for early hippocampal hyperactivity in a mouse model of Alzheimer's disease. *Proceedings of the National Academy of Sciences of the United States of America*, 109(22), 8740–8745. <https://doi.org/10.1073/pnas.1206171109>
- Butowt, R., & Von Bartheld, C. S. (2007). Conventional kinesin-I motors participate in the anterograde axonal transport of neurotrophins in the visual system. *Journal of Neuroscience Research*, 85(12), 2546–2556. <https://doi.org/10.1002/jnr.21165>
- Cai, H., Reinisch, K., & Ferro-Novick, S. (2007). Coats, Tethers, Rabs, and SNAREs Work Together to Mediate the Intracellular Destination of a Transport Vesicle. *Developmental Cell*, 12(5), 671–682. <https://doi.org/10.1016/j.devcel.2007.04.005>
- Cai, Q., Pan, P. Y., & Sheng, Z. H. (2007). Syntabulin-kinesin-1 family member 5B-mediated axonal transport contributes to activity-dependent presynaptic assembly. *Journal of Neuroscience*, 27(27), 7284–7296. <https://doi.org/10.1523/JNEUROSCI.0731-07.2007>
- Cai, Q., & Sheng, Z. H. (2009). Molecular motors and synaptic assembly. *Neuroscientist*, 15(1), 78–89. <https://doi.org/10.1177/1073858408329511>
- Calakos, N., & Scheller, R. H. (1994). Vesicle-associated membrane protein and synaptophysin are associated on the synaptic vesicle. *Journal of Biological Chemistry*, 269(40), 24534–24537.
- Calloway, N., Gouzer, G., Xue, M., & Ryan, T. A. (2015). The active-zone protein Munc13 controls the use-dependence of presynaptic voltage-gated calcium channels. *ELife*, 4(JULY2015), 1–15. <https://doi.org/10.7554/eLife.07728>
- Camina, E., & Güell, F. (2017). The neuroanatomical, neurophysiological and psychological basis of memory: Current models and their origins. *Frontiers in Pharmacology*, 8(JUN), 1–16. <https://doi.org/10.3389/fphar.2017.00438>
- Camoletto, P. G., Vara, H., Morando, L., Connell, E., Marletto, F. P., Giustetto, M., Sassoè-Pognetto, M., Van Veldhoven, P. P., & Ledesma, M. D. (2009). Synaptic vesicle docking: Sphingosine regulates syntaxin1 interaction with Munc18. *PLoS ONE*, 4(4). <https://doi.org/10.1371/journal.pone.0005310>
- CANNON, W. B., & ROSENBERG, C. E. (1932). The wisdom of the body. *London, UK: Kegan Paul, Trench Trbner*, 312.
- Carroll, R. C., Beattie, E. C., Von Zastrow, M., & Malenka, R. C. (2001). Role of AMPA receptor



- endocytosis in synaptic plasticity. *Nature Reviews Neuroscience*, 2(5), 315–324. <https://doi.org/10.1038/35072500>
- Cash, A. D., Aliev, G., Siedlak, S. L., Nunomura, A., Fujioka, H., Zhu, X., Raina, A. K., Vinters, H. V., Tabaton, M., Johnson, A. B., Paula-Barbosa, M., Avila, J., Jones, P. K., Castellani, R. J., Smith, M. A., & Perry, G. (2003). Microtubule reduction in Alzheimer's disease and aging is independent of  $\tau$  filament formation. *American Journal of Pathology*, 162(5), 1623–1627. [https://doi.org/10.1016/S0002-9440\(10\)64296-4](https://doi.org/10.1016/S0002-9440(10)64296-4)
- Cavallin, M., Hubert, L., Cantagrel, V., Munnich, A., Boddaert, N., Vincent-Delorme, C., Cuvellier, J. C., Masson, C., Besmond, C., & Bahi-Buisson, N. (2016). Recurrent KIF5C mutation leading to frontal pachygyria without microcephaly. *Neurogenetics*, 17(1), 79–82. <https://doi.org/10.1007/s10048-015-0459-8>
- Caviston, J. P., Ross, J. L., Antony, S. M., Tokito, M., & Holzbaur, E. L. F. (2007). Huntingtin facilitates dynein/dynactin-mediated vesicle transport. *Proceedings of the National Academy of Sciences*, 104(24), 10045–10050. <https://doi.org/10.1073/pnas.0610628104>
- Chanaday, N. L., Cousin, M. A., Milosevic, I., Watanabe, S., & Morgan, J. R. (2019). The synaptic vesicle cycle revisited: New insights into the modes and mechanisms. *Journal of Neuroscience*, 39(42), 8209–8216. <https://doi.org/10.1523/JNEUROSCI.1158-19.2019>
- Chang, Q., Khare, G., Dani, V., Nelson, S., & Jaenisch, R. (2006). The disease progression of Mecp2 mutant mice is affected by the level of BDNF expression. *Neuron*, 49(3), 341–348. <https://doi.org/10.1016/j.neuron.2005.12.027>
- Chang, S., Trimbuch, T., & Rosenmund, C. (2018). Synaptotagmin-1 drives synchronous Ca<sup>2+</sup>-triggered fusion by C2B-domain-mediated synaptic-vesicle-membrane attachment. *Nature Neuroscience*, 21(1), 33–42. <https://doi.org/10.1038/s41593-017-0037-5>
- Chaudhry, F. A., Edwards, R. H., & Fonnum, F. (2008). Vesicular Neurotransmitter Transporters as Targets for Endogenous and Exogenous Toxic Substances. *Annual Review of Pharmacology and Toxicology*, 48(1), 277–301. <https://doi.org/10.1146/annurev.pharmtox.46.120604.141146>
- Chen, C. W., Peng, Y. F., Yen, Y. C., Bhan, P., Muthaiyan Shanmugam, M., Klopfenstein, D. R., & Wagner, O. I. (2019). Insights on UNC-104-dynein/dynactin interactions and their implications on axonal transport in *Caenorhabditis elegans*. *Journal of Neuroscience Research*, 97(2), 185–201. <https://doi.org/10.1002/jnr.24339>
- Chen, Q. S., Wei, W. Z., Shimahara, T., & Xie, C. W. (2002). Alzheimer amyloid  $\beta$ -peptide inhibits the late phase of long-term potentiation through calcineurin-dependent mechanisms in the hippocampal dentate gyrus. *Neurobiology of Learning and Memory*, 77(3), 354–371. <https://doi.org/10.1006/nlme.2001.4034>
- Chen, W., Mahadomrongkul, V., Berger, U. V., Bassan, M., DeSilva, T., Tanaka, K., Irwin, N., Aoki, C., & Rosenberg, P. A. (2004). The Glutamate Transporter GLT1a Is Expressed in Excitatory Axon Terminals of Mature Hippocampal Neurons. *Journal of Neuroscience*, 24(5), 1136–1148. <https://doi.org/10.1523/JNEUROSCI.1586-03.2004>
- Cheon, C. K., Lim, S. H., Kim, Y. M., Kim, D., Lee, N. Y., Yoon, T. S., Kim, N. S., Kim, E., & Lee, J. R. (2017). Autosomal dominant transmission of complicated hereditary spastic paraplegia due to a dominant negative mutation of KIF1A, SPG30 gene. *Scientific Reports*, 7(1), 1–11. <https://doi.org/10.1038/s41598-017-12999-9>

- Chiba, K., Takahashi, H., Chen, M., Obinata, H., Arai, S., Hashimoto, K., & Oda, T. (2019). *Disease-associated mutations hyperactivate KIF1A motility and anterograde axonal transport of synaptic vesicle precursors*. *116*(37), 18429–18434. <https://doi.org/10.1073/pnas.1905690116>
- Chicka, M. C., Hui, E., Liu, H., & Chapman, E. R. (2008). Synaptotagmin arrests the SNARE complex before triggering fast, efficient membrane fusion in response to Ca<sup>2+</sup>. *Nature Structural and Molecular Biology*, *15*(8), 827–835. <https://doi.org/10.1038/nsmb.1463>
- Cho, J. H., & Askwith, C. C. (2008). Presynaptic release probability is increased in hippocampal neurons from ASIC1 knockout mice. *Journal of Neurophysiology*, *99*(2), 426–441. <https://doi.org/10.1152/jn.00940.2007>
- Choi, D. W. (1990). Methods for antagonizing glutamate neurotoxicity. *Cerebrovascular and Brain Metabolism Reviews*, *2*(2), 105–147. <https://pubmed.ncbi.nlm.nih.gov/2201346/>
- Choi, Dennis W. (1988). Glutamate neurotoxicity and diseases of the nervous system. *Neuron*, *1*(8), 623–634. [https://doi.org/10.1016/0896-6273\(88\)90162-6](https://doi.org/10.1016/0896-6273(88)90162-6)
- Cianfrocco, M. A., DeSantis, M. E., Leschziner, A. E., & Reck-Peterson, S. L. (2015). Mechanism and Regulation of Cytoplasmic Dynein. *Annual Review of Cell and Developmental Biology*, *31*(1), 83–108. <https://doi.org/10.1146/annurev-cellbio-100814-125438>
- Cohen, E., Paulsson, J. F., Blinder, P., Burstyn-Cohen, T., Du, D., Estepa, G., Adame, A., Pham, H. M., Holzenberger, M., Kelly, J. W., Masliah, E., & Dillin, A. (2009). Reduced IGF-1 Signaling Delays Age-Associated Proteotoxicity in Mice. *Cell*, *139*(6), 1157–1169. <https://doi.org/10.1016/j.cell.2009.11.014>
- Coimbra, J. R. M., Marques, D. F. F., Baptista, S. J., Pereira, C. M. F., Moreira, P. I., Dinis, T. C. P., Santos, A. E., & Salvador, J. A. R. (2018). Highlights in BACE1 inhibitors for Alzheimer's disease treatment. *Frontiers in Chemistry*, *6*(MAY), 1–10. <https://doi.org/10.3389/fchem.2018.00178>
- Colin, E., Zala, D., Liot, G., Rangone, H., Borrell-Pagès, M., Li, X.-J., Saudou, F., & Humbert, S. (2008a). Huntingtin phosphorylation acts as a molecular switch for anterograde/retrograde transport in neurons. *The EMBO Journal*, *27*(15), 2124–2134. <https://doi.org/10.1038/emboj.2008.133>
- Collins, S. C., Mikhaleva, A., Vrcelj, K., Vancollie, V. E., Wagner, C., Demeure, N., Whitley, H., Kannan, M., Balz, R., Anthony, L. F. E., Edwards, A., Moine, H., White, J. K., Adams, D. J., Reymond, A., Lelliott, C. J., Webber, C., & Yalcin, B. (2019). Large-scale neuroanatomical study uncovers 198 gene associations in mouse brain morphogenesis. *Nature Communications*, *10*(1), 1–12. <https://doi.org/10.1038/s41467-019-11431-2>
- Conde, C., & Cáceres, A. (2009). Microtubule assembly, organization and dynamics in axons and dendrites. *Nature Reviews Neuroscience*, *10*(5), 319–332. <https://doi.org/10.1038/nrn2631>
- Congdon, E. E., & Sigurdsson, E. M. (2018). Tau-targeting therapies for Alzheimer disease. *Nature Reviews Neurology*, *14*(7), 399–415. <https://doi.org/10.1038/s41582-018-0013-z>
- Cooper, L. N., & Bear, M. F. (2012). The BCM theory of synapse modification at 30: Interaction of theory with experiment. *Nature Reviews Neuroscience*, *13*(11), 798–810. <https://doi.org/10.1038/nrn3353>
- Corbit, V. L., Ahmari, S. E., & Gittis, A. H. (2017). A Corticostriatal Balancing Act Supports Skill Learning. *Neuron*, *96*(2), 253–255. <https://doi.org/10.1016/j.neuron.2017.09.046>

- Cornejo, A., Aguilar Sandoval, F., Caballero, L., Machuca, L., Muñoz, P., Caballero, J., Perry, G., Ardiles, A., Areche, C., & Melo, F. (2017). Rosmarinic acid prevents fibrillization and diminishes vibrational modes associated to  $\beta$  sheet in tau protein linked to Alzheimer's disease. *Journal of Enzyme Inhibition and Medicinal Chemistry*, 32(1), 945–953. <https://doi.org/10.1080/14756366.2017.1347783>
- Corradi, A., Zanardi, A., Giacomini, C., Onofri, F., Valtorta, F., Zoli, M., & Benfenati, F. (2008). Synapsin-I and synapsin-II-null mice display an increased age-dependent cognitive impairment. *Journal of Cell Science*, 121(18), 3042–3051. <https://doi.org/10.1242/jcs.035063>
- Cosker, K. E., Courchesne, S. L., & Segal, R. A. (2008). Action in the axon: generation and transport of signaling endosomes. *Current Opinion in Neurobiology*, 18(3), 270–275. <https://doi.org/10.1016/j.conb.2008.08.005>
- Costa, R. M., Cohen, D., & Nicolells, M. A. . (2004). Differential Corticostriatal Plasticity during Fast and Slow Motor Skill Learning in Mice. *Current Biology*, 14, 1124–1134. <https://doi.org/10.1016/j.cub.2004.06.053>
- Craft, S., Claxton, A., Baker, L. D., Hanson, A. J., Cholerton, B., Trittschuh, E. H., Dahl, D., Caulder, E., Neth, B., Montine, T. J., Jung, Y., Maldjian, J., Whitlow, C., Friedman, S., & De La Monte, S. (2017). Effects of Regular and Long-Acting Insulin on Cognition and Alzheimer's Disease Biomarkers: A Pilot Clinical Trial. *Journal of Alzheimer's Disease*, 57(4), 1325–1334. <https://doi.org/10.3233/JAD-161256>
- Crawford, D. C., & Kavalali, E. T. (2015). Molecular underpinnings of synaptic vesicle pool heterogeneity. *Traffic*, 16(4), 338–364. <https://doi.org/10.1111/tra.12262>
- Creus-Muncunill, J., & Ehrlich, M. E. (2019). Cell-Autonomous and Non-cell-Autonomous Pathogenic Mechanisms in Huntington's Disease: Insights from In Vitro and In Vivo Models. *Neurotherapeutics*, 16(4), 957–978. <https://doi.org/10.1007/s13311-019-00782-9>
- Crittenden, J. R., & Graybiel, A. M. (2011). Basal ganglia disorders associated with imbalances in the striatal striosome and matrix compartments. *Frontiers in Neuroanatomy*, 5(SEP), 1–25. <https://doi.org/10.3389/fnana.2011.00059>
- Cubo, E., Martinez-Horta, S. I., Santalo, F. S., Descalls, A. M., Calvo, S., Gil-Polo, C., Muñoz, I., Llano, K., Mariscal, N., Diaz, D., Gutierrez, A., Aguado, L., & Ramos-Arroyo, M. A. (2019). Clinical manifestations of homozygote allele carriers in Huntington disease. *Neurology*, 92(18), E2101–E2108. <https://doi.org/10.1212/WNL.00000000000007147>
- Culver, B. P., Savas, J. N., Park, S. K., Choi, J. H., Zheng, S., Zeitlin, S. O., Yates, J. R., & Tanese, N. (2012). Proteomic analysis of wild-type and mutant huntingtin-associated proteins in mouse brains identifies unique interactions and involvement in protein synthesis. *Journal of Biological Chemistry*, 287(26), 21599–21614. <https://doi.org/10.1074/jbc.M112.359307>
- Curtis, D. R., & Watkins, J. C. (1961). Analogues of Glutamic and  $\gamma$ -Amino-n-butyric acids having Potent Actions on Mammalian Neurones. *Nature*, 191(4792), 1010–1011. <https://doi.org/10.1038/1911010a0>
- Danbolt, N. C., Furness, D. N., & Zhou, Y. (2016). Neuronal vs glial glutamate uptake: Resolving the conundrum. In *Neurochemistry International* (Vol. 98, pp. 29–45). Elsevier Ltd. <https://doi.org/10.1016/j.neuint.2016.05.009>

- Davis, G. W., Raja, M. K., Preobraschenski, J., Olmo-Cabrera, S. Del, Martinez-Turrillas, R., Jahn, R., Perez-Otano, I., & Wesseling, J. F. (2019). Elevated synaptic vesicle release probability in synaptophysin/gyrin family quadruple knockouts. *Elife*. <https://doi.org/10.7554/eLife.40744.001>
- De Pins, B., Cifuentes-Díaz, C., Thamila Farah, A., López-Molina, L., Montalban, E., Sancho-Balsells, A., López, A., Ginés, S., Delgado-García, J. M., Alberch, J., Gruart, A., Girault, J. A., & Giralt, A. (2019). Conditional BDNF delivery from astrocytes rescues memory deficits, spine density, and synaptic properties in the 5xFAD mouse model of alzheimer disease. *Journal of Neuroscience*, *39*(13), 2441–2458. <https://doi.org/10.1523/JNEUROSCI.2121-18.2019>
- De Robertis, E. D., & Bennett, H. S. (1955). Some features of the submicroscopic morphology of synapses in frog and earthworm. *The Journal of Biophysical and Biochemical Cytology*, *1*(1), 47–58. <https://doi.org/10.1083/jcb.1.1.47>
- De Rossi, P., Nomura, T., Andrew, R. J., Masse, N. Y., Sampathkumar, V., Musial, T. F., Sudwarts, A., Recupero, A. J., Le Metayer, T., Hansen, M. T., Shim, H. N., Krause, S. V., Freedman, D. J., Bindokas, V. P., Kasthuri, N., Nicholson, D. A., Contractor, A., & Thinakaran, G. (2020). Neuronal BIN1 Regulates Presynaptic Neurotransmitter Release and Memory Consolidation. *Cell Reports*, *30*(10), 3520–3535.e7. <https://doi.org/10.1016/j.celrep.2020.02.026>
- De Vos, K. J., & Hafezparast, M. (2017). Neurobiology of axonal transport defects in motor neuron diseases: Opportunities for translational research? *Neurobiology of Disease*, *105*, 283–299. <https://doi.org/10.1016/j.nbd.2017.02.004>
- DeBoer, S. R., You, Y. M., Szodorai, A., Kaminska, A., Pigino, G., Nwabuisi, E., Wang, B., Estrada-Hernandez, T., Kins, S., Brady, S. T., & Morfini, G. (2008). Conventional kinesin holoenzymes are composed of heavy and light chain homodimers. *Biochemistry*, *47*(15), 4535–4543. <https://doi.org/10.1021/bi702445j>
- Dehmelt, L., & Halpain, S. (2004). Protein family review The MAP2 / Tau family of microtubule-associated proteins. *Genome Biology*, *6*(1), 1–10. <http://genomebiology.com/2004/6/1/204>
- Del Castillo, J., & Katz, B. (1954). *QUANTAL COMPONENTS OF THE END-PLATE POTENTIAL*.
- Del Prete, D., Lombino, F., Liu, X., & D'Adamio, L. (2014). APP is cleaved by bace1 in pre-synaptic vesicles and establishes a pre-synaptic interactome, vialts intracellular domain, with molecular complexes that regulate pre-synaptic vesicles functions. *PLoS ONE*, *9*(9). <https://doi.org/10.1371/journal.pone.0108576>
- Del Villar, K., & Miller, C. A. (2004). Down-regulation of DENN/MADD, a TNF receptor binding protein, correlates with neuronal cell death in Alzheimer's disease brain and hippocampal neurons. *Proceedings of the National Academy of Sciences of the United States of America*, *101*(12), 4210–4215. <https://doi.org/10.1073/pnas.0307349101>
- Delépine, C., Meziane, H., Nectoux, J., Opitz, M., Smith, A. B., Ballatore, C., Saillour, Y., Bennaceur-Griscelli, A., Chang, Q., Williams, E. C., Dahan, M., Duboin, A., Billuart, P., Herault, Y., & Bienvenu, T. (2016). Altered microtubule dynamics and vesicular transport in mouse and human MeCP2-deficient astrocytes. *Human Molecular Genetics*, *25*(1), 146–157. <https://doi.org/10.1093/hmg/ddv464>
- Denker, A., Krohnert, K., Bučkers, J., Neher, E., & Rizzoli, S. O. (2011). The reserve pool of synaptic vesicles acts as a buffer for proteins involved in synaptic vesicle recycling. *Proceedings of the National Academy of Sciences of the United States of America*, *108*(41), 17183–17188.

<https://doi.org/10.1073/pnas.1112690108>

- Denker, A., & Rizzoli, S. O. (2010). Synaptic vesicle pools: An update. *Frontiers in Synaptic Neuroscience*, 2(OCT), 1–12. <https://doi.org/10.3389/fnsyn.2010.00135>
- Deshpande, A., Win, K. M., & Busciglio, J. (2008). Tau isoform expression and regulation in human cortical neurons. *The FASEB Journal*, 22(7), 2357–2367. <https://doi.org/10.1096/fj.07-096909>
- Dey, N. D., Bombard, M. C., Roland, B. P., Davidson, S., Lu, M., Rossignol, J., Sandstrom, M. I., Skeel, R. L., Lescaudron, L., & Dunbar, G. L. (2010). Genetically engineered mesenchymal stem cells reduce behavioral deficits in the YAC 128 mouse model of Huntington's disease. *Behavioural Brain Research*, 214(2), 193–200. <https://doi.org/10.1016/j.bbr.2010.05.023>
- Deyts, C., Thinakaran, G., & Parent, A. T. (2016). APP Receptor? To Be or Not to Be. *Trends in Pharmacological Sciences*, 37(5), 390–411. <https://doi.org/10.1016/j.tips.2016.01.005>
- Di Paolo, G., Moskowitz, H. S., Gipson, K., Wenk, M. R., Voronov, S., Obayashi, M., Flavell, R., Fitzsimonds, R. M., Ryan, T. A., & De Camill, P. (2004). Impaired PtdIns(4,5)P<sub>2</sub> synthesis in nerve terminals produces defects in synaptic vesicle trafficking. *Nature*, 431(7007), 415–422. <https://doi.org/10.1038/nature02896>
- DiFiglia, M., Sapp, E., Chase, K., Schwarz, C., Meloni, A., Young, C., Martin, E., Vonsattel, J. P., Carraway, R., Reeves, S. A., Boyce, F. M., & Aronin, N. (1995). Huntingtin is a cytoplasmic protein associated with vesicles in human and rat brain neurons. *Neuron*, 14(5), 1075–1081. [https://doi.org/10.1016/0896-6273\(95\)90346-1](https://doi.org/10.1016/0896-6273(95)90346-1)
- Dittman, J., & Ryan, T. A. (2009). Molecular Circuitry of Endocytosis at Nerve Terminals. *Annual Review of Cell and Developmental Biology*, 25(1), 133–160. <https://doi.org/10.1146/annurev.cellbio.042308.113302>
- Dobrunz, L. E., & Stevens, C. F. (1997). Heterogeneity of release probability, facilitation, and depletion at central synapses. *Neuron*, 18(6), 995–1008. [https://doi.org/10.1016/S0896-6273\(00\)80338-4](https://doi.org/10.1016/S0896-6273(00)80338-4)
- Dominguez, N., van Weering, J. R. T., Borges, R., Toonen, R. F. G., & Verhage, M. (2018). Dense-core vesicle biogenesis and exocytosis in neurons lacking chromogranins A and B. *Journal of Neurochemistry*, 144(3), 241–254. <https://doi.org/10.1111/jnc.14263>
- Dompierre, J. P., Godin, J. D., Charrin, B. C., Cordelières, F. P., King, S. J., Humbert, S., & Saudou, F. (2007). Histone deacetylase 6 inhibition compensates for the transport deficit in Huntington's disease by increasing tubulin acetylation. *The Journal of Neuroscience : The Official Journal of the Society for Neuroscience*, 27(13), 3571–3583. <https://doi.org/10.1523/JNEUROSCI.0037-07.2007>
- Doran, E., Keator, D., Head, E., Phelan, M. J., Kim, R., Totoiu, M., Barrio, J. R., Small, G. W., Potkin, S. G., & Lott, I. T. (2017). Down Syndrome, Partial Trisomy 21, and Absence of Alzheimer's Disease: The Role of APP. *Journal of Alzheimer's Disease*, 56(2), 459–470. <https://doi.org/10.3233/JAD-160836>
- Dotti, C. G., Sullivan, C. A., & Banker, G. A. (1988). The Establishment of Polarity by Hippocampal Neurons in Culture. In *The Journal of Neuroscience: Vol. 1* (Issue 4).
- Dougherty, S. E., Hollimon, J. J., McMeekin, L. J., Bohannon, A. S., West, A. B., Lesort, M., Hablitz, J. J., & Cowell, R. M. (2014). Hyperactivity and cortical disinhibition in mice with restricted expression of mutant huntingtin to parvalbumin-positive cells. *Neurobiology of Disease*, 62, 160–171. <https://doi.org/10.1016/j.nbd.2013.10.002>

- Dowsett, L., Porras, A. R., Kruszka, P., Davis, B., Hu, T., Honey, E., Badoe, E., Thong, M. K., Leon, E., Girisha, K. M., Shukla, A., Nayak, S. S., Shotelersuk, V., Megarbane, A., Phadke, S., Sirisena, N. D., Dissanayake, V. H. W., Ferreira, C. R., Kisling, M. S., ... Krantz, I. D. (2019). Cornelia de Lange syndrome in diverse populations. *American Journal of Medical Genetics, Part A*, *179*(2), 150–158. <https://doi.org/10.1002/ajmg.a.61033>
- Dragatsis, I., Levine, M. S., & Zeitlin, S. (2000). Inactivation of Hdh in the brain and testis results in progressive neurodegeneration and sterility in mice. *Nature Genetics*, *26*(3), 300–306. <https://doi.org/10.1038/81593>
- Drewe, E. A. (1974). The Effect of Type and Area of Brain Lesion on Wisconsin Card Sorting Test Performance. *Cortex*, *10*(2), 159–170. [https://doi.org/10.1016/S0010-9452\(74\)80006-7](https://doi.org/10.1016/S0010-9452(74)80006-7)
- Drouet, V., Perrin, V., Hassig, R., Dufour, N., Auregan, G., Alves, S., Bonvento, G., Brouillet, E., Luthi-Carter, R., Hantraye, P., & Déglon, N. (2009). Sustained effects of nonallele-specific huntingtin silencing. *Annals of Neurology*, *65*(3), 276–285. <https://doi.org/10.1002/ana.21569>
- Drouet, V., Ruiz, M., Zala, D., Feyeux, M., Auregan, G., Cambon, K., Troquier, L., Carpentier, J., Aubert, S., Merienne, N., Bourgois-Rocha, F., Hassig, R., Rey, M., Dufour, N., Saudou, F., Perrier, A. L., Hantraye, P., & Déglon, N. (2014). Allele-specific silencing of mutant huntingtin in rodent brain and human stem cells. *PLoS ONE*, *9*(6). <https://doi.org/10.1371/journal.pone.0099341>
- Durán, E., Montes, M. Á., Jemal, I., Satterfield, R., Young, S., & Álvarez de Toledo, G. (2018). Synaptotagmin-7 controls the size of the reserve and resting pools of synaptic vesicles in hippocampal neurons. *Cell Calcium*, *74*, 53–60. <https://doi.org/10.1016/j.ceca.2018.06.004>
- Eccles, J. . (1957). Physiology of nerve cells. *John Hopkins Press*.
- Echeverri, C. J., Paschal, B. M., Vaughan, K. T., & Vallee, R. B. (1996). Molecular characterization of the 50-kD subunit of dynactin reveals function for the complex in chromosome alignment and spindle organization during mitosis. *Journal of Cell Biology*, *132*(4), 617–633. <https://doi.org/10.1083/jcb.132.4.617>
- Eckley, D. M., Gill, S. R., Melkonian, K. A., Bingham, J. B., Goodson, H. V., Heuser, J. E., & Schroer, T. A. (1999). Analysis of dynactin subcomplexes reveals a novel actin-related protein associated with the Arp1 minifilament pointed end. *Journal of Cell Biology*, *147*(2), 307–319. <https://doi.org/10.1083/jcb.147.2.307>
- Eddings, C. R., Arbez, N., Akimov, S., Geva, M., Hayden, M. R., & Ross, C. A. (2019). Pridopidine protects neurons from mutant-huntingtin toxicity via the sigma-1 receptor. *Neurobiology of Disease*, *129*(May), 118–129. <https://doi.org/10.1016/j.nbd.2019.05.009>
- Edelman, G. M., & Gally, J. A. (2001). Degeneracy and complexity in biological systems. *Proceedings of the National Academy of Sciences of the United States of America*, *98*(24), 13763–13768. <https://doi.org/10.1073/pnas.231499798>
- Edelmann, L., Hanson, P. I., Chapman, E. R., & Jahn, R. (1995). Synaptobrevin binding to synaptophysin: a potential mechanism for controlling the exocytotic fusion machine. *The EMBO Journal*, *14*(2), 224–231. <https://doi.org/10.1002/j.1460-2075.1995.tb06995.x>
- Edgar, J. R. (2016). Q & A: What are exosomes, exactly? *BMC Biology*, *14*(1). <https://doi.org/10.1186/s12915-016-0268-z>

- Edwards, R. H. (2007). *Review The Neurotransmitter Cycle and Quantal Size*. 835–858. <https://doi.org/10.1016/j.neuron.2007.09.001>
- Edwards, S. R., Hamlin, A. S., Marks, N., Coulson, E. J., & Smith, M. T. (2014). Comparative studies using the Morris water maze to assess spatial memory deficits in two transgenic mouse models of Alzheimer's disease. *Clinical and Experimental Pharmacology and Physiology*, *41*(10), 798–806. <https://doi.org/10.1111/1440-1681.12277>
- Egan, M. F., Kost, J., Voss, T., Mukai, Y., Aisen, P. S., Cummings, J. L., Tariot, P. N., Vellas, B., Van Dyck, C. H., Boada, M., Zhang, Y., Li, W., Furtek, C., Mahoney, E., Mozley, L. H., Mo, Y., Sur, C., & Michelson, D. (2019). Randomized trial of verubecestat for prodromal Alzheimer's disease. *New England Journal of Medicine*, *380*(15), 1408–1420. <https://doi.org/10.1056/NEJMoa1812840>
- Egan, M. J., Tan, K., & Reck-Peterson, S. L. (2012). Lis1 is an initiation factor for dynein-driven organelle transport. *Journal of Cell Biology*, *197*(7), 971–982. <https://doi.org/10.1083/jcb.201112101>
- Ehinger, Y., Bruyère, J., Panayotis, N., Abada, Y.-S., Borloz, E., Matagne, V., Scaramuzzino, C., Vitet, H., Delatour, B., Saidi, L., Villard, L., Saudou, F., & Roux, J.-C. (2020). Huntingtin phosphorylation governs BDNF homeostasis and improves the phenotype of Mecp2 knockout mice. *EMBO Molecular Medicine*, *12*(2). <https://doi.org/10.15252/emmm.201910889>
- Ehrnhoefer, D. E., Sutton, L., & Hayden, M. R. (2011). Small changes, big impact: Posttranslational modifications and function of huntingtin in huntington disease. *Neuroscientist*, *17*(5), 475–492. <https://doi.org/10.1177/1073858410390378>
- El-Daher, M.-T., Hangen, E., Bruyère, J., Poizat, G., Al-Ramahi, I., Pardo, R., Bourg, N., Souquere, S., Mayet, C., Pierron, G., Lévêque-Fort, S., Botas, J., Humbert, S., & Saudou, F. (2015). Huntingtin proteolysis releases non-polyQ fragments that cause toxicity through dynamin 1 dysregulation. *The EMBO Journal*, *34*(17), 2255–2271. <https://doi.org/10.15252/embj.201490808>
- Elias, S., McGuire, J. R., Yu, H., & Humbert, S. (2015). Huntingtin Is Required for Epithelial Polarity through RAB11A-Mediated Apical Trafficking of PAR3-aPKC. *PLoS Biology*, *13*(5), 1–26. <https://doi.org/10.1371/journal.pbio.1002142>
- Elias, S., Thion, M. S., Yu, H., Sousa, C. M., Lasgi, C., Morin, X., & Humbert, S. (2014). Huntingtin regulates mammary stem cell division and differentiation. *Stem Cell Reports*, *2*(4), 491–506. <https://doi.org/10.1016/j.stemcr.2014.02.011>
- Elmqvist, D., & Quastel, D. M. J. (1965). A quantitative study of end-plate potentials in isolated human muscle. *J. Physiol*, *178*, 505–529.
- Elshenawy, M. M., Kusakci, E., Volz, S., Baumbach, J., Bullock, S. L., & Yildiz, A. (2020). Lis1 activates dynein motility by modulating its pairing with dynactin. *Nature Cell Biology*, *22*(May). <https://doi.org/10.1038/s41556-020-0501-4>
- Encalada, S. E., Szpankowski, L., Xia, C. H., & Goldstein, L. S. B. (2011). Stable kinesin and dynein assemblies drive the axonal transport of mammalian prion protein vesicles. *Cell*, *144*(4), 551–565. <https://doi.org/10.1016/j.cell.2011.01.021>
- Ernfors, P., Lee, K., & Jaenisch, R. (1994). Mice lacking brain-derived neurotrophic factor develop with sensory deficits. *Nature*, *368*(March), 147–150.
- Esmaeeli Nieh, S., Madou, M. R. Z., Sirajuddin, M., Fregeau, B., Mcknight, D., Lexa, K., Strober, J.,

- Spaeth, C., Hallinan, B. E., Smaoui, N., Pappas, J. G., Burrow, T. A., McDonald, M. T., Latibashvili, M., Leshinsky-Silver, E., Lev, D., Blumkin, L., Vale, R. D., Barkovich, A. J., & Sherr, E. H. (2015). De novo mutations in KIF1A cause progressive encephalopathy and brain atrophy. *Annals of Clinical and Translational Neurology*, 2(6), 623–635. <https://doi.org/10.1002/acn3.198>
- Even, A., Morelli, G., Broix, L., Scaramuzzino, C., Turchetto, S., Gladwyn-Ng, I., Le Bail, R., Shilian, M., Freeman, S., Magiera, M. M., Jijumon, A. S., Krusy, N., Malgrange, B., Brone, B., Dietrich, P., Dragatsis, I., Janke, C., Saudou, F., Weil, M., & Nguyen, L. (2019). ATAT1-enriched vesicles promote microtubule acetylation via axonal transport. *Science Advances*, 5(12). <https://doi.org/10.1126/sciadv.aax2705>
- Fagiani, F., Lanni, C., Racchi, M., Pascale, A., & Govoni, S. (2019). Amyloid- $\beta$  and Synaptic Vesicle Dynamics: A Cacophonous Orchestra. *Journal of Alzheimer's Disease*, 72(1), 1–14. <https://doi.org/10.3233/JAD-190771>
- Fang, Q., & Lindau, M. (2014). How could SNARE proteins open a fusion pore? *Physiology*, 29(4), 278–285. <https://doi.org/10.1152/physiol.00026.2013>
- Fanutza, T., del Prete, D., Ford, M. J., Castillo, P. E., & D'Adamio, L. (2015). APP and APLP2 interact with the synaptic release machinery and facilitate transmitter release at hippocampal synapses. *eLife*, 4(NOVEMBER2015). <https://doi.org/10.7554/eLife.09743>
- Fassier, C., Tarrade, A., Peris, L., Courageot, S., Mailly, P., Dalard, C., Delga, S., Roblot, N., Lefeuvre, J., Job, D., Hazan, J., Curmi, P. A., & Melki, J. (2013). Microtubule-targeting drugs rescue axonal swellings in cortical neurons from spastin knockout mice. *DMM Disease Models and Mechanisms*, 6(1), 72–83. <https://doi.org/10.1242/dmm.008946>
- Fassio, A., Patry, L., Congia, S., Onofri, F., Piton, A., Gauthier, J., Pozzi, D., Messa, M., Defranchi, E., Fadda, M., Corradi, A., Baldelli, P., Lapointe, L., St-Onge, J., Meloche, C., Mottron, L., Valtorta, F., Nguyen, D. K., Rouleau, G. A., ... Cossette, P. (2011). SYN1 loss-of-function mutations in autism and partial epilepsy cause impaired synaptic function. *Human Molecular Genetics*, 20(12), 2297–2307. <https://doi.org/10.1093/hmg/ddr122>
- Fatt, P., & Katz, B. (1952). SPONTANEOUS SUBTHRESHOLD ACTIVITY AT MOTOR NERVE ENDINGS. In *J. Physiol* (Vol. 7).
- Feinstein, S. C., & Wilson, L. (2005). Inability of tau to properly regulate neuronal microtubule dynamics: A loss-of-function mechanism by which tau might mediate neuronal cell death. *Biochimica et Biophysica Acta - Molecular Basis of Disease*, 1739(2), 268–279. <https://doi.org/10.1016/j.bbdis.2004.07.002>
- Fernandes, D., & Carvalho, A. L. (2016). Mechanisms of homeostatic plasticity in the excitatory synapse. *Journal of Neurochemistry*, 139(6), 973–996. <https://doi.org/10.1111/jnc.13687>
- Fernandes, J. T. S., Chutna, O., Chu, V., Conde, J. P., & Outeiro, T. F. (2016). A novel microfluidic cell co-culture platform for the study of the molecular mechanisms of Parkinson's disease and other synucleinopathies. *Frontiers in Neuroscience*, 10(NOV), 1–11. <https://doi.org/10.3389/fnins.2016.00511>
- Fernandez-Alfonso, T., & Ryan, T. A. (2008). A heterogeneous “resting” pool of synaptic vesicles that is dynamically interchanged across boutons in mammalian CNS synapses. *Brain Cell Biology*, 36(1–4), 87–100. <https://doi.org/10.1007/s11068-008-9030-y>



- Fernández-García, S., Conde-Berriozabal, S., García-García, E., Gort-Paniello, C., Bernal-Casas, D., Barriga, G. G.-D., López-Gil, J., Muñoz-Moreno, E., Sòria, G., Campa, L., Artigas, F., Rodríguez, M., Alberch, J., & Masana, M. (2020). *M2 Cortex-Dorsolateral striatum stimulation reverses motor symptoms and synaptic deficits in Huntington's Disease*. 1–24. <https://doi.org/10.1101/2020.04.08.032359>
- Fields, R. D., & Ellisman, M. H. (1985). Synaptic morphology and differences in sensitivity. *Science*, 228(4696), 197–199. <https://doi.org/10.1126/science.3975637>
- Fogel, H., Frere, S., Segev, O., Bharill, S., Shapira, I., Gazit, N., Malley, T. O., Slomowitz, E., Berdichevsky, Y., Walsh, D. M., Isacoff, E. Y., Hirsch, J. A., & Slutsky, I. (2014). APP Homodimers Transduce an Amyloid- $\beta$ -Mediated Increase in Release Probability at Excitatory Synapses. *CellReports*, 7(5), 1560–1576. <https://doi.org/10.1016/j.celrep.2014.04.024>
- Fonnum, F. (1984). Glutamate: A Neurotransmitter in Mammalian Brain. *Journal of Neurochemistry*, 42(1), 1–11. <https://doi.org/10.1111/j.1471-4159.1984.tb09689.x>
- Fowler, M. W., & Staras, K. (2015). Synaptic vesicle pools: Principles, properties and limitations. *Experimental Cell Research*, 335(2), 150–156. <https://doi.org/10.1016/j.yexcr.2015.03.007>
- Francelle, L., Lotz, C., Outeiro, T., Brouillet, E., & Merienne, K. (2017). Contribution of neuroepigenetics to Huntington's disease. *Frontiers in Human Neuroscience*, 11(January), 1–15. <https://doi.org/10.3389/fnhum.2017.00017>
- Fredj, N. Ben, & Burrone, J. (2009). A resting pool of vesicles is responsible for spontaneous vesicle fusion at the synapse. *Nature Neuroscience*, 12(6), 751–758. <https://doi.org/10.1038/nn.2317>
- Frere, S., & Slutsky, I. (2017). Review Alzheimer ' s Disease : From Firing Instability to Homeostasis Network Collapse. *Neuron*, 97(1), 32–58. <https://doi.org/10.1016/j.neuron.2017.11.028>
- Fu, Meng-meng, & Holzbaur, E. L. F. (2013). *JIP1 regulates the directionality of APP axonal transport by coordinating kinesin and dynein motors*. 202(3), 495–508. <https://doi.org/10.1083/jcb.201302078>
- Fu, Meng-meng, & Holzbaur, E. L. F. (2014). Integrated regulation of motor-driven organelle transport by scaffolding proteins. *Trends in Cell Biology*, 24(10), 564–574. <https://doi.org/10.1016/j.tcb.2014.05.002>
- Fu, Meng meng, Nirschl, J. J., & Holzbaur, E. L. F. (2014). LC3 Binding to the scaffolding protein jip1 regulates processive dynein-driven transport of autophagosomes. *Developmental Cell*, 29(5), 577–590. <https://doi.org/10.1016/j.devcel.2014.04.015>
- Fu, Min, & Zuo, Y. (2011). Experience-dependent structural plasticity in the cortex. *Trends in Neurosciences*, 34(4), 177–187. <https://doi.org/10.1016/j.tins.2011.02.001>
- Fukushima, N., Furuta, D., Hidaka, Y., Moriyama, R., & Tsujiuchi, T. (2009). Post-translational modifications of tubulin in the nervous system. *Journal of Neurochemistry*, 109(3), 683–693. <https://doi.org/10.1111/j.1471-4159.2009.06013.x>
- Furness, D. N., Dehnes, Y., Akhtar, A. Q., Rossi, D. J., Hamann, M., Grutle, N. J., Gundersen, V., Holmseth, S., Lehre, K. P., Ullensvang, K., Wojewodzc, M., Zhou, Y., Attwell, D., & Danbolt, N. C. (2008). A quantitative assessment of glutamate uptake into hippocampal synaptic terminals and astrocytes: New insights into a neuronal role for excitatory amino acid transporter 2 (EAAT2).

*Neuroscience*, 157(1), 80–94. <https://doi.org/10.1016/j.neuroscience.2008.08.043>

- Furuta, K., Furuta, A., Toyoshima, Y. Y., Amino, M., Oiwa, K., & Kojima, H. (2013). Measuring collective transport by defined numbers of processive and nonprocessive kinesin motors. *Proceedings of the National Academy of Sciences of the United States of America*, 110(2), 501–506. <https://doi.org/10.1073/pnas.1201390110>
- Fuxe, K., & Agnati, L. . (1991). *Volume Transmission in the Brain: Novel Mechanisms for Neural Transmission* (Vol. 1). Raven press.
- Gabrych, D. R., Lau, V. Z., Niwa, S., & Silverman, M. A. (2019). Going Too Far Is the Same as Falling Short†: Kinesin-3 Family Members in Hereditary Spastic Paraplegia. *Frontiers in Cellular Neuroscience*, 13(September), 1–24. <https://doi.org/10.3389/fncel.2019.00419>
- Gan, Q., & Watanabe, S. (2018). Synaptic vesicle endocytosis in different model systems. In *Frontiers in Cellular Neuroscience* (Vol. 12). Frontiers Media S.A. <https://doi.org/10.3389/fncel.2018.00171>
- Gangarossa, G., Perez, S., Dembitskaya, Y., Prokin, I., Berry, H., & Venance, L. (2020). BDNF Controls Bidirectional Endocannabinoid Plasticity at Corticostriatal Synapses. *Cerebral Cortex*, 30(1), 197–214. <https://doi.org/10.1093/cercor/bhz081>
- Garcia, C. C., Blair, H. J., Seager, M., Coulthard, A., Tennant, S., Buddles, M., Curtis, A., & Goodship, J. A. (2004). Identification of a mutation in synapsin I, a synaptic vesicle protein, in a family with epilepsy. *Journal of Medical Genetics*, 41(3), 183–186. <https://doi.org/10.1136/jmg.2003.013680>
- Gauthier, L. R., Charrin, B. C., Borrell-Pagès, M., Dompierre, J. P., Rangone, H., Cordelières, F. P., De Mey, J., MacDonald, M. E., Leßmann, V., Humbert, S., & Saudou, F. (2004). Huntingtin controls neurotrophic support and survival of neurons by enhancing BDNF vesicular transport along microtubules. *Cell*, 118(1), 127–138. <https://doi.org/10.1016/j.cell.2004.06.018>
- Gelens, L., & Saurin, A. T. (2018). Exploring the Function of Dynamic Phosphorylation-Dephosphorylation Cycles. *Developmental Cell*, 44(6), 659–663. <https://doi.org/10.1016/j.devcel.2018.03.002>
- Genc, B., Gozutok, O., & Hande Ozdinler, P. (2019). Complexity of generating mouse models to study the upper motor neurons: Let us shift focus from mice to neurons. *International Journal of Molecular Sciences*, 20(16), 1–26. <https://doi.org/10.3390/ijms20163848>
- George, C., Gontier, G., Lacube, P., François, J. C., Holzenberger, M., & Aïd, S. (2017). The Alzheimer's disease transcriptome mimics the neuroprotective signature of IGF-1 receptor-deficient neurons. *Brain*, 140(7), 2012–2027. <https://doi.org/10.1093/brain/awx132>
- Georgiev, D. D., & Glazebrook, J. F. (2018). The quantum physics of synaptic communication via the SNARE protein complex. *Progress in Biophysics and Molecular Biology*, 135, 16–29. <https://doi.org/10.1016/j.pbiomolbio.2018.01.006>
- Geppert, M., Goda, Y., Hammer, R. E., Li, C., Rosahl, T. W., Stevens, C. F., & Südhof, T. C. (1994). Synaptotagmin I: A major Ca<sup>2+</sup> sensor for transmitter release at a central synapse. *Cell*, 79(4), 717–727. [https://doi.org/10.1016/0092-8674\(94\)90556-8](https://doi.org/10.1016/0092-8674(94)90556-8)
- Ghiretti, A. E., Thies, E., Tokito, M. K., Lin, T., Ostap, E. M., Kneussel, M., & Holzbaur, E. L. F. (2016). Activity-Dependent Regulation of Distinct Transport and Cytoskeletal Remodeling Functions of the Dendritic Kinesin KIF21B. *Neuron*, 92(4), 857–872.

<https://doi.org/10.1016/j.neuron.2016.10.003>

- Gibbs, K. L., Greensmith, L., & Schiavo, G. (2015). Regulation of Axonal Transport by Protein Kinases. *Trends in Biochemical Sciences*, 40(10), 597–610. <https://doi.org/10.1016/j.tibs.2015.08.003>
- Ginty, D. D., & Segal, R. A. (2002). Retrograde neurotrophin signaling: Trk-ing along the axon. *Current Opinion in Neurobiology*, 12(3), 268–274. [https://doi.org/10.1016/S0959-4388\(02\)00326-4](https://doi.org/10.1016/S0959-4388(02)00326-4)
- Gitler, D., Cheng, Q., Greengard, P., & Augustine, G. J. (2008). Synapsin IIa controls the reserve pool of glutamatergic synaptic vesicles. *Journal of Neuroscience*, 28(43), 10835–10843. <https://doi.org/10.1523/JNEUROSCI.0924-08.2008>
- Glaze, D. G., Neul, J. L., Kaufmann, W. E., & Berry-kraavis, E. (2019). *study of tro fi netide in pediatric Rett syndrome. 0*. <https://doi.org/10.1212/WNL.0000000000007316>
- Gleeson, J. G., Minnerath, S. R., Fox, J. W., Allen, K. M., Luo, R. F., Hong, S. E., Berg, M. J., Kuzniecky, R., Reitnauer, P. J., Borgatti, R., Mira, A. P., Guerrini, R., Holmes, G. L., Rooney, C. M., Berkovic, S., Scheffer, I., Cooper, E. C., Ricci, S., Cusmai, R., ... Walsh, C. A. (1999). Characterization of mutations in the gene doublecortin in patients with double cortex syndrome. *Annals of Neurology*, 45(2), 146–153. [https://doi.org/10.1002/1531-8249\(199902\)45:2<146::AID-ANA3>3.0.CO;2-N](https://doi.org/10.1002/1531-8249(199902)45:2<146::AID-ANA3>3.0.CO;2-N)
- Goda, Y., & Stevens, C. F. (1998). Readily releasable pool size changes associated with long term depression. In *Neurobiology* (Vol. 95). [www.pnas.org](http://www.pnas.org).
- Godin, J. D., Colombo, K., Molina-Calavita, M., Keryer, G., Zala, D., Charrin, B. E. C., Dietrich, P., Volvert, M. L., Guillemot, F., Dragatsis, I., Bellaïche, Y., Saudou, F., Nguyen, L., & Humbert, S. (2010). Huntingtin Is Required for Mitotic Spindle Orientation and Mammalian Neurogenesis. *Neuron*, 67(3), 392–406. <https://doi.org/10.1016/j.neuron.2010.06.027>
- Gondré-Lewis, M. C., Park, J. J., & Loh, Y. P. (2012). Cellular Mechanisms for the Biogenesis and Transport of Synaptic and Dense-Core Vesicles. In *International Review of Cell and Molecular Biology* (Vol. 299). Elsevier. <https://doi.org/10.1016/B978-0-12-394310-1.00002-3>
- Gordon, S. L., Harper, C. B., Smillie, K. J., & Cousin, M. A. (2016). A fine balance of synaptophysin levels underlies efficient retrieval of synaptobrevin II to synaptic vesicles. *PLoS ONE*, 11(2), 1–12. <https://doi.org/10.1371/journal.pone.0149457>
- Götz, J., Ittner, L. M., & Kins, S. (2006). Do axonal defects in tau and amyloid precursor protein transgenic animals model axonopathy in Alzheimer's disease? *Journal of Neurochemistry*, 98(4), 993–1006. <https://doi.org/10.1111/j.1471-4159.2006.03955.x>
- Grafmüller, A., Shillcock, J., & Lipowsky, R. (2009). The fusion of membranes and vesicles: Pathway and energy barriers from dissipative particle dynamics. *Biophysical Journal*, 96(7), 2658–2675. <https://doi.org/10.1016/j.bpj.2008.11.073>
- Gray, E. G. (1969). Electron Microscopy of Excitatory and Inhibitory Synapses: A Brief Review. *Progress in Brain Research*, 31(C), 141–155. [https://doi.org/10.1016/S0079-6123\(08\)63235-5](https://doi.org/10.1016/S0079-6123(08)63235-5)
- Gray, E. G., & Guillery, R. W. (1966). Synaptic Morphology in the Normal and Degenerating Nervous System. *International Review of Cytology*, 19(C), 111–182. [https://doi.org/10.1016/S0074-7696\(08\)60566-5](https://doi.org/10.1016/S0074-7696(08)60566-5)
- Graybiel, A. M., & Grafton, S. T. (2015). The Striatum : Where Skills and Habits Meet. *Cold Spring Harb*

- Gritton, H. J., Howe, W. M., Romano, M. F., DiFeliceantonio, A. G., Kramer, M. A., Saligrama, V., Bucklin, M. E., Zemel, D., & Han, X. (2019). Unique contributions of parvalbumin and cholinergic interneurons in organizing striatal networks during movement. *Nature Neuroscience*, *22*(4), 586–597. <https://doi.org/10.1038/s41593-019-0341-3>
- Groemer, T. W., Thiel, C. S., Holt, M., Riedel, D., Hua, Y., Hüve, J., Wilhelm, B. G., & Klingauf, J. (2011). Amyloid precursor protein is trafficked and secreted via synaptic vesicles. *PLoS ONE*, *6*(4). <https://doi.org/10.1371/journal.pone.0018754>
- Gromova, K. V., Muhia, M., Rothhammer, N., Gee, C. E., Thies, E., Schaefer, I., Kress, S., Kilimann, M. W., Shevchuk, O., Oertner, T. G., & Kneussel, M. (2018). Neurobeachin and the Kinesin KIF21B Are Critical for Endocytic Recycling of NMDA Receptors and Regulate Social Behavior. *Cell Reports*, *23*(9), 2705–2717. <https://doi.org/10.1016/j.celrep.2018.04.112>
- Gruenberg, J., & Stenmark, H. (2004). The biogenesis of multivesicular endosomes. *Nature Reviews Molecular Cell Biology*, *5*(4), 317–323. <https://doi.org/10.1038/nrm1360>
- Guardia-Laguarta, C., Coma, M., Pera, M., Clarimón, J., Sereno, L., Agulló, J. M., Molina-Porcel, L., Gallardo, E., Deng, A., Berezovska, O., Hyman, B. T., Blesa, R., Gómez-Isla, T., & Lleó, A. (2009). Mild cholesterol depletion reduces amyloid- $\beta$  production by impairing APP trafficking to the cell surface. *Journal of Neurochemistry*, *110*(1), 220–230. <https://doi.org/10.1111/j.1471-4159.2009.06126.x>
- Guedes-Dias, P., & Holzbaaur, E. L. F. (2019). Axonal transport: Driving synaptic function. *Science*, *366*(6462). <https://doi.org/10.1126/science.aaw9997>
- Guedes-dias, P., Nirschl, J. J., Abreu, N., Tokito, M. K., Janke, C., Magiera, M. M., Holzbaaur, E. L. F., Guedes-dias, P., Nirschl, J. J., Abreu, N., Tokito, M. K., Janke, C., & Magiera, M. M. (2019). Kinesin-3 Responds to Local Microtubule Dynamics to Target Synaptic Cargo Delivery to the Presynapse Article Kinesin-3 Responds to Local Microtubule Dynamics to Target Synaptic Cargo Delivery to the Presynapse. *Current Biology*, *29*(2), 268-282.e8. <https://doi.org/10.1016/j.cub.2018.11.065>
- Gumy, L. F., Katrukha, E. A., Grigoriev, I., Jaarsma, D., Kapitein, L. C., Akhmanova, A., & Hoogenraad, C. C. (2017). MAP2 Defines a Pre-axonal Filtering Zone to Regulate KIF1- versus KIF5-Dependent Cargo Transport in Sensory Neurons. *Neuron*, *94*(2), 347-362.e7. <https://doi.org/10.1016/j.neuron.2017.03.046>
- Gumy, L. F., Yeo, G. S. H., Tung, Y. C. L., Zivraj, K. H., Willis, D., Coppola, G., Lam, B. Y. H., Twiss, J. L., Holt, C. E., & Fawcett, J. W. (2011). Transcriptome analysis of embryonic and adult sensory axons reveals changes in mRNA repertoire localization. *Rna*, *17*(1), 85–98. <https://doi.org/10.1261/rna.2386111>
- Gunawardena, S., & Goldstein, L. S. B. (2001). Disruption of axonal transport and neuronal viability by amyloid precursor protein mutations in *Drosophila*. *Neuron*, *32*(3), 389–401. [https://doi.org/10.1016/S0896-6273\(01\)00496-2](https://doi.org/10.1016/S0896-6273(01)00496-2)
- Gunawardena, S., Her, L., Bruschi, R. G., Laymon, R. A., Niesman, I. R., Gordesky-gold, B., Sintasath, L., Bonini, N. M., & Goldstein, L. S. B. (2003). *Disruption of Axonal Transport by Loss of Huntingtin or Expression of Pathogenic PolyQ Proteins in Drosophila*. *40*, 25–40.
- Gunawardena, S., Yang, G., & Goldstein, L. S. B. (2013). *Presenilin controls kinesin-1 and dynein function*

- during APP-vesicle transport in vivo. 22(19), 3828–3843. <https://doi.org/10.1093/hmg/ddt237>
- Guo, Q., Huang, B., Cheng, J., Seefelder, M., Engler, T., Pfeifer, G., Oeckl, P., Otto, M., Moser, F., Maurer, M., Pautsch, A., Baumeister, W., Fernández-busnadiego, R., & Kochanek, S. (2018). The cryo-electron microscopy structure of huntingtin. *Nature Publishing Group*. <https://doi.org/10.1038/nature25502>
- Gutiérrez-Medina, B., Buendía Padilla, M., Gutiérrez-Esparza, A. J., & Oaxaca Camacho, A. R. (2018). Differential effect of multiple kinesin motors on run length, force and microtubule binding rate. *Biophysical Chemistry*, 242(August), 28–33. <https://doi.org/10.1016/j.bpc.2018.08.007>
- Habets, R. L. P., & Borst, J. G. G. (2007). Dynamics of the readily releasable pool during post-tetanic potentiation in the rat calyx of Held synapse. *Journal of Physiology*, 581(2), 467–478. <https://doi.org/10.1113/jphysiol.2006.127365>
- Hammond, J. W., Cai, D., Blasius, T. L., Li, Z., Jiang, Y., Jih, G. T., Meyhofer, E., & Verhey, K. J. (2009). Mammalian Kinesin-3 motors are dimeric in vivo and move by processive motility upon release of autoinhibition. *PLoS Biology*, 7(3), 0650–0663. <https://doi.org/10.1371/journal.pbio.1000072>
- Hancock, W. O. (2014). Bidirectional cargo transport: Moving beyond tug of war. *Nature Reviews Molecular Cell Biology*, 15(9), 615–628. <https://doi.org/10.1038/nrm3853>
- Hanse, E., & Gustafsson, B. (2001). Vesicle release probability and pre-primed pool at glutamatergic synapses in area CA1 of the rat neonatal hippocampus. *Journal of Physiology*, 531(2), 481–493. <https://doi.org/10.1111/j.1469-7793.2001.0481i.x>
- Harada, A., Takei, Y., Kanai, Y., Tanaka, Y., Nonaka, S., & Hirokawa, N. (1998). Golgi vesiculation and lysosome dispersion in cells lacking cytoplasmic dynein. *Journal of Cell Biology*, 141(1), 51–59. <https://doi.org/10.1083/jcb.141.1.51>
- Harper, C. B., Mancini, G. M. S., van Slegtenhorst, M., & Cousin, M. A. (2017). Altered synaptobrevin-II trafficking in neurons expressing a synaptophysin mutation associated with a severe neurodevelopmental disorder. *Neurobiology of Disease*, 108(April), 298–306. <https://doi.org/10.1016/j.nbd.2017.08.021>
- Harris, K. D., & Shepherd, G. M. G. (2015). The neocortical circuit: Themes and variations. *Nature Neuroscience*, 18(2), 170–181. <https://doi.org/10.1038/nn.3917>
- Harris, K. M., & Sultan, P. (1995). Variation in the Number, Location and Size of Synaptic Vesicles Provides an Anatomical Basis for the Nonuniform Probability of Release at Hippocampal CA1 Synapses. In *S Neuropharmacology* (Vol. 34, Issue 95).
- Harvey, L. F., Berk, A., Kaiser, C., Krieger, M., Scott, M. P., Bretscher, A., Ploegh, H. L., & Matsudaira, P. T. (2008). *Molecular Cell Biology 6th edition*. W.H. Freeman.
- Hathorn, T., Snyder-Keller, A., & Messer, A. (2011). Nicotinamide improves motor deficits and upregulates PGC-1 $\alpha$  and BDNF gene expression in a mouse model of Huntington's disease. *Neurobiology of Disease*, 41(1), 43–50. <https://doi.org/10.1016/j.nbd.2010.08.017>
- Hattula, K., & Peränen, J. (2000). FIP-2, a coiled-coil protein, links Huntingtin to Rab8 and modulates cellular morphogenesis. *Current Biology*, 10(24), 1603–1606. [https://doi.org/10.1016/S0960-9822\(00\)00864-2](https://doi.org/10.1016/S0960-9822(00)00864-2)

- Hawes, S. L., Evans, R. C., Unruh, B. A., Benkert, E. E., Gillani, F., Dumas, T. C., & Blackwell, K. T. (2015). Multimodal plasticity in dorsal striatum while learning a lateralized navigation task. *Journal of Neuroscience*, 35(29), 10535–10549. <https://doi.org/10.1523/JNEUROSCI.4415-14.2015>
- Hayashi, K., Hasegawa, S., Sagawa, T., Tasaki, S., & Niwa, S. (2018). Non-invasive force measurement reveals the number of active kinesins on a synaptic vesicle precursor in axonal transport regulated by ARL-8. *Physical Chemistry Chemical Physics*, 20(5), 3403–3410. <https://doi.org/10.1039/c7cp05890j>
- Hebb, D. (1949). *The organization of behavior*. John Wiley & Sons.
- Hedera, P. (2000). Hereditary Spastic Paraplegia Overview. In *GeneReviews*. University of Washington, Seattle; 1993-2020. <https://www.ncbi.nlm.nih.gov/books/>
- Heindel, W. C., Salmon, D. P., Shults, C. W., Walicke, P. A., & Butters, N. (1989). Neuropsychological evidence for multiple implicit memory systems: A comparison of Alzheimer's, Huntington's, and Parkinson's disease patients. *Journal of Neuroscience*, 9(2), 582–587. <https://doi.org/10.1523/jneurosci.09-02-00582.1989>
- Hendricks, A. G., Holzbaur, E. L. F., & Goldman, Y. E. (2012). Force measurements on cargoes in living cells reveal collective dynamics of microtubule motors. *Proceedings of the National Academy of Sciences of the United States of America*, 109(45), 18447–18452. <https://doi.org/10.1073/pnas.1215462109>
- Her, L.-S., & Goldstein, L. S. B. (2008). Enhanced Sensitivity of Striatal Neurons to Axonal Transport Defects Induced by Mutant Huntingtin. *The Journal of Neuroscience*, 28(50), 13662 LP – 13672. <http://www.jneurosci.org/content/28/50/13662.abstract>
- Her, L., & Goldstein, L. S. B. (2008). *Enhanced Sensitivity of Striatal Neurons to Axonal Transport Defects Induced by Mutant Huntingtin*. 28(50), 13662–13672. <https://doi.org/10.1523/JNEUROSCI.4144-08.2008>
- Hinckelmann, M.-V., Virlogeux, A., Niehage, C., Poujol, C., Choquet, D., Hoflack, B., Zala, D., & Saudou, F. (2016). Self-propelling vesicles define glycolysis as the minimal energy machinery for neuronal transport. *Nature Communications*, 7, 13233. <https://doi.org/10.1038/ncomms13233>
- Hinckelmann, M. V., Zala, D., & Saudou, F. (2013). Releasing the brake: Restoring fast axonal transport in neurodegenerative disorders. *Trends in Cell Biology*, 23(12), 634–643. <https://doi.org/10.1016/j.tcb.2013.08.007>
- Hirokawa, N., Nitta, R., & Okada, Y. (2009). The mechanisms of kinesin motor motility: Lessons from the monomeric motor KIF1A. *Nature Reviews Molecular Cell Biology*, 10(12), 877–884. <https://doi.org/10.1038/nrm2807>
- Hirokawa, N., Niwa, S., & Tanaka, Y. (2010). Review Molecular Motors in Neurons : Transport Mechanisms and Roles in Brain Function , Development , and Disease. *Neuron*, 68(4), 610–638. <https://doi.org/10.1016/j.neuron.2010.09.039>
- Hirokawa, N., & Tanaka, Y. (2015). Kinesin superfamily proteins (KIFs): Various functions and their relevance for important phenomena in life and diseases. *Experimental Cell Research*, 334(1), 16–25. <https://doi.org/10.1016/j.yexcr.2015.02.016>
- Hnasko, T. S., Chuhma, N., Zhang, H., Goh, G. Y., Sulzer, D., Palmiter, R. D., Rayport, S., & Edwards, R.

- H. (2010). Vesicular Glutamate Transport Promotes Dopamine Storage and Glutamate Corelease In Vivo. *Neuron*, 65(5), 643–656. <https://doi.org/10.1016/j.neuron.2010.02.012>
- Hoe, H. S., Lee, H. K., & Pak, D. T. S. (2012). The upside of APP at synapses. *CNS Neuroscience and Therapeutics*, 18(1), 47–56. <https://doi.org/10.1111/j.1755-5949.2010.00221.x>
- Holler-Rickauer, S., Köstinger, G., Martin, K., Schuhknecht, G., & Stratford, K. (2019). *Structure and function of a neocortical synapse*. <https://doi.org/10.1101/2019.12.13.875971>
- Holzbaur, E. L. F., & Scherer, S. S. (2011). Microtubules, axonal transport, and neuropathy. *New England Journal of Medicine*, 365(24), 2330–2332. <https://doi.org/10.1056/NEJMcibr1112481>
- Hong, Y., Zhao, T., Li, X. J., & Li, S. (2016). Mutant huntingtin impairs BDNF release from astrocytes by disrupting conversion of Rab3a-GTP into Rab3a-GDP. *Journal of Neuroscience*, 36(34), 8790–8801. <https://doi.org/10.1523/JNEUROSCI.0168-16.2016>
- Höning, S., Ricotta, D., Krauss, M., Späte, K., Spolaore, B., Motley, A., Robinson, M., Robinson, C., Haucke, V., & Owen, D. J. (2005). Phosphatidylinositol-(4,5)-bisphosphate regulates sorting signal recognition by the clathrin-associated adaptor complex AP2. *Molecular Cell*, 18(5), 519–531. <https://doi.org/10.1016/j.molcel.2005.04.019>
- Hornbeck, P. V., Kornhauser, J. M., Tkachev, S., Zhang, B., Skrzypek, E., Murray, B., Latham, V., & Sullivan, M. (2012). PhosphoSitePlus: A comprehensive resource for investigating the structure and function of experimentally determined post-translational modifications in man and mouse. *Nucleic Acids Research*, 40(D1), 261–270. <https://doi.org/10.1093/nar/gkr1122>
- Hsu, C. C., Moncaleano, J. D., & Wagner, O. I. (2011). Sub-cellular distribution of UNC-104(KIF1A) upon binding to adaptors as UNC-16(JIP3), DNC-1(DCTN1/Glued) and SYD-2(Liprin- $\alpha$ ) in *C. elegans* neurons. *Neuroscience*, 176, 39–52. <https://doi.org/10.1016/j.neuroscience.2010.12.044>
- Htet, Z. M., Gillies, J. P., Baker, R. W., Leschziner, A. E., DeSantis, M. E., & Reck-Peterson, S. L. (2020). LIS1 promotes the formation of activated cytoplasmic dynein-1 complexes. *Nature Cell Biology*, 22(May). <https://doi.org/10.1038/s41556-020-0506-z>
- Hu, S., Wang, H., Chen, K., Cheng, P., Gao, S., Liu, J., Li, X., & Sun, X. (2015). MicroRNA-34c Downregulation Ameliorates Amyloid- $\beta$ -Induced Synaptic Failure and Memory Deficits by Targeting VAMP2. *Journal of Alzheimer's Disease*, 48(3), 673–686. <https://doi.org/10.3233/JAD-150432>
- Hu, Y., Qu, L., & Schikorski, T. (2008). Mean synaptic vesicle size varies among individual excitatory hippocampal synapses. *Synapse*, 62(12), 953–957. <https://doi.org/10.1002/syn.20567>
- Hu, Y. S., Long, N., Pigino, G., Brady, S. T., & Lazarov, O. (2013). Molecular Mechanisms of Environmental Enrichment: Impairments in Akt/GSK3 $\beta$ , Neurotrophin-3 and CREB Signaling. *PLoS ONE*, 8(5). <https://doi.org/10.1371/journal.pone.0064460>
- Huber, K. M. (2018). Synaptic homeostasis: Quality vs. quantity. *Nature Neuroscience*, 21(6), 774–776. <https://doi.org/10.1038/s41593-018-0159-4>
- Humbert, S., Bryson, E. A., Cordelières, F. P., Connors, N. C., Datta, S. R., Finkbeiner, S., Greenberg, M. E., & Saudou, F. (2002). The IGF-1/Akt pathway is neuroprotective in Huntington's disease and involves huntingtin phosphorylation by Akt. *Developmental Cell*, 2(6), 831–837. [https://doi.org/10.1016/S1534-5807\(02\)00188-0](https://doi.org/10.1016/S1534-5807(02)00188-0)

- Hung, C. O. Y., & Coleman, M. P. (2016). KIF1A mediates axonal transport of BACE1 and identification of independently moving cargoes in living SCG neurons. *Traffic*, *17*(11), 1155–1167. <https://doi.org/10.1111/tra.12428>
- Huo, L., Yue, Y., Ren, J., Yu, J., Liu, J., Yu, Y., Ye, F., Xu, T., Zhang, M., & Feng, W. (2012). The CC1-FHA tandem as a central hub for controlling the dimerization and activation of kinesin-3 KIF1A. *Structure*, *20*(9), 1550–1561. <https://doi.org/10.1016/j.str.2012.07.002>
- li, J. A. W., Anderson, E., Zimmerman, K., Zheng, K. H., Rouhani, R., & Gunawardena, S. (2015). *Huntingtin differentially regulates the axonal transport of a sub-set of Rab-containing vesicles in vivo*. *24*(25). <https://doi.org/10.1093/hmg/ddv415>
- Iijima, K. I., Ando, K., Takeda, S., Satoh, Y., Seki, T., Itoharu, S., Greengard, P., Kirino, Y., Nairn, A. C., & Suzuki, T. (2000). Neuron-specific phosphorylation of Alzheimer's  $\beta$ -amyloid precursor protein by cyclin-dependent kinase 5. *Journal of Neurochemistry*, *75*(3), 1085–1091. <https://doi.org/10.1046/j.1471-4159.2000.0751085.x>
- Ikin, A. F., Annaert, W. G., Takei, K., De Camilli, P., Jahn, R., Greengard, P., & Buxbaum, J. D. (1996). Alzheimer amyloid protein precursor is localized in nerve terminal preparations to rab5-containing vesicular organelles distinct from those implicated in the synaptic vesicle pathway. *Journal of Biological Chemistry*, *271*(50), 31783–31786. <https://doi.org/10.1074/jbc.271.50.31783>
- Imig, C., Min, S. W., Krinner, S., Arancillo, M., Rosenmund, C., Südhof, T. C., Rhee, J. S., Brose, N., & Cooper, B. H. (2014). The Morphological and Molecular Nature of Synaptic Vesicle Priming at Presynaptic Active Zones. *Neuron*, *84*(2), 416–431. <https://doi.org/10.1016/j.neuron.2014.10.009>
- Itakura, E., Kishi-Itakura, C., & Mizushima, N. (2012). The hairpin-type tail-anchored SNARE syntaxin 17 targets to autophagosomes for fusion with endosomes/lysosomes. *Cell*. <https://doi.org/10.1016/j.cell.2012.11.001>
- Ivanova, D., Imig, C., Camacho, M., Reinhold, A., Guhathakurta, D., Montenegro-Venegas, C., Cousin, M. A., Gundelfinger, E. D., Rosenmund, C., Cooper, B., & Fejtova, A. (2020). CtBP1-Mediated Membrane Fission Contributes to Effective Recycling of Synaptic Vesicles. *Cell Reports*, *30*(7), 2444–2459.e7. <https://doi.org/10.1016/j.celrep.2020.01.079>
- Jablonski, M. R., Cooper, L., & Jacob, D. A. (2011). NMDA receptor excitotoxicity: Impact on phosphatase activity and phosphorylation of huntingtin. *Journal of Neuroscience*, *31*(12), 4357–4359. <https://doi.org/10.1523/JNEUROSCI.6747-10.2011>
- Jackman, S. L., & Regehr, W. G. (2017). The Mechanisms and Functions of Synaptic Facilitation. *Neuron*, *94*(3), 447–464. <https://doi.org/10.1016/j.neuron.2017.02.047>
- Jahn, R., & Südhof, T. C. (1993). Synaptic Vesicle Traffic: Rush Hour in the Nerve Terminal. *Journal of Neurochemistry*, *61*(1), 12–21. <https://doi.org/10.1111/j.1471-4159.1993.tb03533.x>
- Jahn, R., Thomas, ", & Südhof, C. (1994). *Synaptic Vesicle Traffic: Rush Hour in the Nerve Terminal*.
- Janke, C., & Magiera, M. M. (2020). The tubulin code and its role in controlling microtubule properties and functions. *Nature Reviews Molecular Cell Biology*, *21*(6), 307–326. <https://doi.org/10.1038/s41580-020-0214-3>



- Janz, R., Sü Dhof, T. C., Hammer, R. E., Unni, V., Siegelbaum, S. A., & Bolshakov, V. Y. (1999). Essential Roles in Synaptic Plasticity for Synaptogyrin I and Synaptophysin I they are phosphorylated by an endogenous src-like tyro-sine kinase on synaptic vesicles (Barnekow et al indicates that synaptophysin I and synaptogyrin I are physiological substrates for togyrin I and bred double knockout mice deficient in. In *Neuron* (Vol. 24).
- Jeong, H., Then, F., Melia, T. J., Mazzulli, J. R., Cui, L., Savas, J. N., Voisine, C., Paganetti, P., Tanese, N., Hart, A. C., Yamamoto, A., & Krainc, D. (2009). Acetylation Targets Mutant Huntingtin to Autophagosomes for Degradation. *Cell*, 137(1), 60–72. <https://doi.org/10.1016/j.cell.2009.03.018>
- Jia, J. Y., Lamer, S., Schümann, M., Schmidt, M. R., Krause, E., & Haucke, V. (2006). Quantitative proteomics analysis of detergent-resistant membranes from chemical synapses: Evidence for cholesterol as spatial organizer of synaptic vesicle cycling. *Molecular and Cellular Proteomics*, 5(11), 2060–2071. <https://doi.org/10.1074/mcp.M600161-MCP200>
- Jiang, Z. G., & North, R. A. (1991). Membrane properties and synaptic responses of rat striatal neurones in vitro. *The Journal of Physiology*, 443(1), 533–553. <https://doi.org/10.1113/jphysiol.1991.sp018850>
- Jovanovic, J. N., Czernik, A. J., Fienberg, A. A., Greengard, P., & Sihra, T. S. (2000). Synapsins as mediators of BDNF-enhanced neurotransmitter release. *Nature Neuroscience*, 3(4), 323–329. <https://doi.org/10.1038/73888>
- Jung, J., Grant, T., Thomas, D. R., Diehnelt, C. W., Grigorieff, N., & Joshua-Tor, L. (2019). High-resolution cryo-EM structures of outbreak strain human norovirus shells reveal size variations. *Proceedings of the National Academy of Sciences of the United States of America*, 116(26), 12828–12832. <https://doi.org/10.1073/pnas.1903562116>
- Kaan, H. Y. K., Hackney, D. D., & Kozielski, F. (2011). The structure of the kinesin-1 motor-tail complex reveals the mechanism of autoinhibition. *Science*, 333(6044), 883–885. <https://doi.org/10.1126/science.1204824>
- Kádková, A., Radecke, J., & Sørensen, J. B. (2019). The SNAP-25 Protein Family. In *Neuroscience* (Vol. 420, pp. 50–71). Elsevier Ltd. <https://doi.org/10.1016/j.neuroscience.2018.09.020>
- Kaesler, P. (2011). Pushing synaptic vesicles over the RIM. *Cellular Logistics*, 1(3), 106–110. <https://doi.org/10.4161/cl.1.3.16429>
- Kaesler, P. S., & Regehr, W. G. (2017). The readily releasable pool of synaptic vesicles. In *Current Opinion in Neurobiology* (Vol. 43, pp. 63–70). Elsevier Ltd. <https://doi.org/10.1016/j.conb.2016.12.012>
- Kaether, C., Skehel, P., & Dotti, C. G. (2000). Axonal Membrane Proteins Are Transported in Distinct Carriers : A Two-Color Video Microscopy Study in Cultured Hippocampal Neurons □. 11(April), 1213–1224.
- Kamenetz, F., Tomita, T., Hsieh, H., Seabrook, G., Borchelt, D., Iwatsubo, T., Sisodia, S., & Malinow, R. (2003). APP processing and synaptic function. *Neuron*, 37(6), 925–937. [https://doi.org/10.1016/S0896-6273\(03\)00124-7](https://doi.org/10.1016/S0896-6273(03)00124-7)
- Kametani, F., & Hasegawa, M. (2018). Reconsideration of amyloid hypothesis and tau hypothesis in Alzheimer's disease. *Frontiers in Neuroscience*, 12(JAN). <https://doi.org/10.3389/fnins.2018.00025>

- Kapitein, L. C., & Hoogenraad, C. C. (2015). Building the Neuronal Microtubule Cytoskeleton. *Neuron*, 87(3), 492–506. <https://doi.org/10.1016/j.neuron.2015.05.046>
- Karasmanis, E. P., Phan, C. T., Angelis, D., Kesisova, I. A., Hoogenraad, C. C., McKenney, R. J., & Spiliotis, E. T. (2018). Polarity of Neuronal Membrane Traffic Requires Sorting of Kinesin Motor Cargo during Entry into Dendrites by a Microtubule-Associated Septin. *Developmental Cell*, 46(2), 204–218.e7. <https://doi.org/10.1016/j.devcel.2018.06.013>
- Karmakar, S., Sharma, L. G., Roy, A., Patel, A., & Pandey, L. M. (2019). Neuronal SNARE complex: A protein folding system with intricate protein-protein interactions, and its common neuropathological hallmark, SNAP25. *Neurochemistry International*, 122(December 2018), 196–207. <https://doi.org/10.1016/j.neuint.2018.12.001>
- Karran, E., & De Strooper, B. (2016). The amyloid cascade hypothesis: are we poised for success or failure? *Journal of Neurochemistry*, 139, 237–252. <https://doi.org/10.1111/jnc.13632>
- Katsikoudi, A., Ficulle, E., Cavallini, A., Sharman, G., Guyot, A., Zagnoni, M., Eastwood, B. J., Hutton, M., & Bose, S. (2020). Quantitative propagation of assembled human Tau from Alzheimer's disease brain in microfluidic neuronal cultures. *Journal of Biological Chemistry*, 295, jbc.RA120.013325. <https://doi.org/10.1074/jbc.ra120.013325>
- Katz B. (1969). *The Release of Neuronal Transmitter Substances*. Liverpool Univ. Press.
- Kaur, S., Van Bergen, N. J., Verhey, K. J., Nowell, C. J., Budaitis, B., Yue, Y., Ellaway, C., Brunetti-Pierri, N., Cappuccio, G., Bruno, I., Boyle, L., Nigro, V., Torella, A., Roscioli, T., Cowley, M. J., Massey, S., Sonawane, R., Burton, M. D., Schonewolf-Greulich, B., ... Christodoulou, J. (2020). Expansion of the phenotypic spectrum of de novo missense variants in kinesin family member 1A (KIF1A). *Human Mutation*. <https://doi.org/10.1002/humu.24079>
- Kavalali, E. T. (2006). Synaptic vesicle reuse and its implications. In *Neuroscientist* (Vol. 12, Issue 1, pp. 57–66). <https://doi.org/10.1177/1073858405281852>
- Kelliher, M. T., Saunders, H. A., & Wildonger, J. (2019). Microtubule control of functional architecture in neurons. *Current Opinion in Neurobiology*, 57, 39–45. <https://doi.org/10.1016/j.conb.2019.01.003>
- Kelliher, M. T., Yue, Y., Ng, A., Kamiyama, D., Huang, B., Verhey, K. J., & Wildonger, J. (2018). Autoinhibition of kinesin-1 is essential to the dendrite-specific localization of Golgi outposts. *Journal of Cell Biology*, 217(7), 2531–2547. <https://doi.org/10.1083/jcb.201708096>
- Kendrick, A. A., Dickey, A. M., Redwine, W. B., Tran, P. T., Vaites, L. P., Dzieciatkowska, M., Harper, J. W., & Reck-Peterson, S. L. (2019). Hook3 is a scaffold for the opposite-polarity microtubule-based motors cytoplasmic dynein-1 and KIF1C. *The Journal of Cell Biology*, 218(9), 2982–3001. <https://doi.org/10.1083/jcb.201812170>
- Kern, J. V., Zhang, Y. V., Kramer, S., Brenman, J. E., & Rasse, T. M. (2013). *The Kinesin-3, Unc-104 Regulates Dendrite Morphogenesis and Synaptic Development in Drosophila*. 195(September), 59–72. <https://doi.org/10.1534/genetics.113.151639>
- Keryer, G., Pineda, J. R., Liot, G., Kim, J., Dietrich, P., Benstaali, C., Smith, K., Cordelières, F. P., Spassky, N., Ferrante, R. J., Dragatsis, I., & Saudou, F. (2011). Ciliogenesis is regulated by a huntingtin-HAP1-PCM1 pathway and is altered in Huntington disease. *Journal of Clinical Investigation*, 121(11), 4372–4382. <https://doi.org/10.1172/JCI57552>

- Kevenaar, J. T., Bianchi, S., Van Spronsen, M., Olieric, N., Lipka, J., Frias, C. P., Mikhaylova, M., Harterink, M., Keijzer, N., Wulf, P. S., Hilbert, M., Kapitein, L. C., De Graaff, E., Ahkmanova, A., Steinmetz, M. O., & Hoogenraad, C. C. (2016). Kinesin-Binding Protein Controls Microtubule Dynamics and Cargo Trafficking by Regulating Kinesin Motor Activity. *Current Biology*, *26*(7), 849–861. <https://doi.org/10.1016/j.cub.2016.01.048>
- Kim, A. Y., Oh, C., Im, H. J., & Baek, H. M. (2020). Enhanced bidirectional connectivity of the subthalamo-pallidal pathway in 6-OHDA-mouse model of Parkinson's disease revealed by probabilistic tractography of diffusion-weighted MRI at 9.4T. *Experimental Neurobiology*, *29*(1), 80–92. <https://doi.org/10.5607/en.2020.29.1.80>
- Kim, B., Elzinga, S. E., Henn, R. E., McGinley, L. M., & Feldman, E. L. (2019). The effects of insulin and insulin-like growth factor I on amyloid precursor protein phosphorylation in in vitro and in vivo models of Alzheimer's disease. *Neurobiology of Disease*, *132*(July), 104541. <https://doi.org/10.1016/j.nbd.2019.104541>
- Kim, B., & Feldman, E. L. (2012). Insulin resistance in the nervous system. *Trends in Endocrinology and Metabolism*, *23*(3), 133–141. <https://doi.org/10.1016/j.tem.2011.12.004>
- Kim, B., & Feldman, E. L. (2015). Insulin resistance as a key link for the increased risk of cognitive impairment in the metabolic syndrome. *Experimental & Molecular Medicine*, *47*(November 2014), e149. <https://doi.org/10.1038/emm.2015.3>
- Kim, E. K., & Choi, E. J. (2010). Pathological roles of MAPK signaling pathways in human diseases. *Biochimica et Biophysica Acta - Molecular Basis of Disease*, *1802*(4), 396–405. <https://doi.org/10.1016/j.bbadis.2009.12.009>
- Kim, T., Gondré-Lewis, M. C., Arnaoutova, I., & Loh, Y. P. (2006). Dense-core secretory granule biogenesis. *Physiology*, *21*(2), 124–133. <https://doi.org/10.1152/physiol.00043.2005>
- Kirch, R. D., Pinnell, R. C., Hofmann, U. G., & Cassel, J. (2015). *The Double-H Maze : A Robust Behavioral Test for Learning and Memory in Rodents*. July, 1–19. <https://doi.org/10.3791/52667>
- Kitagishi, Y., Nakanishi, A., Ogura, Y., & Matsuda, S. (2014). Dietary regulation of PI3K/AKT/GSK-3 $\beta$  pathway in Alzheimer's disease. *Alzheimer's Research and Therapy*, *6*(3), 1–7. <https://doi.org/10.1186/alzrt265>
- Kitamura, T., Ogawa, S. K., Roy, D. S., Okuyama, T., Morrissey, M. D., Smith, L. M., Redondo, R. L., & Tonegawa, S. (2017). Engrams and circuits crucial for systems consolidation of a memory. *Science*, *356*(6333), 73–78. <https://doi.org/10.1126/science.aam6808>
- Klapstein, G. J., Fisher, R. S., Zanjani, H., Cepeda, C., Jokel, E. S., Chesselet, M. F., & Levine, M. S. (2001). Electrophysiological and morphological changes in striatal spiny neurons in R6/2 Huntington's disease transgenic mice. *Journal of Neurophysiology*, *86*(6), 2667–2677. <https://doi.org/10.1152/jn.2001.86.6.2667>
- Klassen, M. P., Wu, Y. E., Maeder, C. I., Nakae, I., Cueva, J. G., Lehrman, E. K., Tada, M., Gengyo-Ando, K., Wang, G. J., Goodman, M., Mitani, S., Kontani, K., Katada, T., & Shen, K. (2010). An Arf-like Small G Protein, ARL-8, Promotes the Axonal Transport of Presynaptic Cargoes by Suppressing Vesicle Aggregation. *Neuron*, *66*(5), 710–723. <https://doi.org/10.1016/j.neuron.2010.04.033>
- Kleim, J. A., Barbay, S., & Nudo, R. J. (1998). Functional reorganization of the rat motor cortex following motor skill learning. *Journal of Neurophysiology*, *80*(6), 3321–3325.

<https://doi.org/10.1152/jn.1998.80.6.3321>

- Klopfenstein, D. R., & Vale, R. D. (2004). The Lipid Binding Pleckstrin Homology Domain in UNC-104 Kinesin is Necessary for Synaptic Vesicle Transport in *Caenorhabditis elegans*. *Molecular Biology of the Cell*, *15*, 3729–3739. <https://doi.org/10.1091/mbc.E04>
- Koenig, E. (1965). Synthetic Mechanisms in the Axon—I. Local Axonal Synthesis of Acetylcholinesterase. *Journal of Neurochemistry*, *12*(5), 343–355. <https://doi.org/10.1111/j.1471-4159.1965.tb04235.x>
- Kohli, B. M., Pflieger, D., Mueller, L. N., Carbonetti, G., Aebersold, R., Nitsch, R. M., & Konietzko, U. (2012). Interactome of the amyloid precursor protein APP in brain reveals a protein network involved in synaptic vesicle turnover and a close association with synaptotagmin-1. *Journal of Proteome Research*, *11*(8), 4075–4090. <https://doi.org/10.1021/pr300123g>
- Kokotos, A. C., Harper, C. B., Marland, J. R. K., Smillie, K. J., Cousin, M. A., & Gordon, S. L. (2019). Synaptophysin sustains presynaptic performance by preserving vesicular synaptobrevin-II levels. *Journal of Neurochemistry*, *151*(1), 28–37. <https://doi.org/10.1111/jnc.14797>
- Kolter, T., & Sandhoff, K. (2006). Sphingolipid metabolism diseases. In *Biochimica et Biophysica Acta - Biomembranes* (Vol. 1758, Issue 12, pp. 2057–2079). <https://doi.org/10.1016/j.bbamem.2006.05.027>
- Kondo, M., Takei, Y., & Hirokawa, N. (2012). Motor Protein KIF1A Is Essential for Hippocampal Synaptogenesis and Learning Enhancement in an Enriched Environment. *Neuron*, *73*(4), 743–757. <https://doi.org/10.1016/j.neuron.2011.12.020>
- Konishi, Y., & Setou, M. (2009). Tubulin tyrosination navigates the kinesin-1 motor domain to axons. *Nature Neuroscience*, *12*(5), 559–567. <https://doi.org/10.1038/nn.2314>
- Kononenko, N. L., Diril, M. K., Puchkov, D., Kintscher, M., Koo, S. J., Pfuhl, G., Winter, Y., Wienisch, M., Klingauf, J., Breustedt, J., Schmitz, D., Maritzen, T., & Haucke, V. (2013). Compromised fidelity of endocytic synaptic vesicle protein sorting in the absence of stonin 2. *Proceedings of the National Academy of Sciences of the United States of America*, *110*(6). <https://doi.org/10.1073/pnas.1218432110>
- Kononenko, N. L., & Haucke, V. (2015). Molecular mechanisms of presynaptic membrane retrieval and synaptic vesicle reformation. *Neuron*, *85*(3), 484–496. <https://doi.org/10.1016/j.neuron.2014.12.016>
- Kopke, E., Tung, Y. C., Shaikh, S., Del Alonso, C. A., Iqbal, K., & Grundke-Iqbal, I. (1993). Microtubule-associated protein tau. Abnormal phosphorylation of a non-paired helical filament pool in Alzheimer disease. *Journal of Biological Chemistry*, *268*(32), 24374–24384.
- Koralek, A. C., Jin, X., Long, J. D., Costa, R. M., & Carmena, J. M. (2012). Corticostriatal plasticity is necessary for learning intentional neuroprosthetic skills. *Nature*, *483*(7389), 331–335. <https://doi.org/10.1038/nature10845>
- Koushika, S. P., Schaefer, A. M., Vincent, R., Willis, J. H., Bowerman, B., & Nonet, M. L. (2004). Mutations in *Caenorhabditis elegans* Cytoplasmic Dynein Components Reveal Specificity of Neuronal Retrograde Cargo. *Journal of Neuroscience*, *24*(16), 3907–3916. <https://doi.org/10.1523/JNEUROSCI.5039-03.2004>

- Kratter, I. H., Zahed, H., Lau, A., Tsvetkov, A. S., Daub, A. C., Weiberth, K. F., Gu, X., Saudou, F., Humbert, S., Yang, X. W., Osmann, A., Steffan, J. S., Masliah, E., & Finkbeiner, S. (2016). Serine 421 regulates mutant huntingtin toxicity and clearance in mice. *Journal of Clinical Investigation*, *126*(9), 3585–3597. <https://doi.org/10.1172/JCI80339>
- Krebs, C. E., Karkheiran, S., Powell, J. C., Cao, M., Makarov, V., Darvish, H., Di Paolo, G., Walker, R. H., Shahidi, G. A., Buxbaum, J. D., De Camilli, P., Yue, Z., & Paisán-Ruiz, C. (2013). The sac1 domain of SYNJ1 identified mutated in a family with early-onset progressive parkinsonism with generalized seizures. *Human Mutation*, *34*(9), 1200–1207. <https://doi.org/10.1002/humu.22372>
- Kunwar, A., Vershinin, M., Xu, J., & Gross, S. P. (2008). Stepping, Strain Gating, and an Unexpected Force-Velocity Curve for Multiple-Motor-Based Transport. *Current Biology*, *18*(16), 1173–1183. <https://doi.org/10.1016/j.cub.2008.07.027>
- Kupferschmidt, D. A., Juczewski, K., Cui, G., Johnson, K. A., & Lovinger, D. M. (2017). Parallel, but Dissociable, Processing in Discrete Corticostriatal Inputs Encodes Skill Learning. *Neuron*, *96*(2), 476–489.e5. <https://doi.org/10.1016/j.neuron.2017.09.040>
- Kuster, A., Nola, S., Dingli, F., Vacca, B., Gauchy, C., Beaujouan, J. C., Nunez, M., Moncion, T., Loew, D., Formstecher, E., Galli, T., & Proux-Gillardeaux, V. (2015). The Q-soluble N-ethylmaleimide-sensitive factor attachment protein receptor (Q-SNARE) SNAP-47 regulates trafficking of selected vesicle-associated membrane proteins (VAMPs). *Journal of Biological Chemistry*, *290*(47), 28056–28069. <https://doi.org/10.1074/jbc.M115.666362>
- Lacey, S. E., He, S., Scheres, S. H. W., & Carter, A. P. (2019). Cryo-EM of dynein microtubule-binding domains shows how an axonemal dynein distorts the microtubule. *ELife*, *8*, 1–21. <https://doi.org/10.7554/eLife.47145>
- LaMonte, B. H., Wallace, K. E., Holloway, B. A., Shelly, S. S., Ascaño, J., Tokito, M., Van Winkle, T., Howland, D. S., & Holzbaur, E. L. F. (2002). Disruption of dynein/dynactin inhibits axonal transport in motor neurons causing late-onset progressive degeneration. *Neuron*, *34*(5), 715–727. [https://doi.org/10.1016/S0896-6273\(02\)00696-7](https://doi.org/10.1016/S0896-6273(02)00696-7)
- Laßek, M., Weingarten, J., Einsfelder, U., Brendel, P., Müller, U., & Volkandt, W. (2013). Amyloid precursor proteins are constituents of the presynaptic active zone. *Journal of Neurochemistry*, *127*(1), 48–56. <https://doi.org/10.1111/jnc.12358>
- Lauwers, E., Goodchild, R., & Verstreken, P. (2016). Membrane Lipids in Presynaptic Function and Disease. In *Neuron* (Vol. 90, Issue 1, pp. 11–25). Cell Press. <https://doi.org/10.1016/j.neuron.2016.02.033>
- Lawson, L. J., Perry, V. H., & Gordon, S. (1992). Turnover of resident microglia in the normal adult mouse brain. *Neuroscience*, *48*(2), 405–415. [https://doi.org/10.1016/0306-4522\(92\)90500-2](https://doi.org/10.1016/0306-4522(92)90500-2)
- Lazarov, O., Morfini, G. A., Pigino, G., Gadadhar, A., Chen, X., Robinson, J., Ho, H., Brady, S. T., & Sisodia, S. S. (2007). Impairments in Fast Axonal Transport and Motor Neuron Deficits in Transgenic Mice Expressing Familial Alzheimer ' s Disease-Linked Mutant Presenilin 1. *Journal of Neurochemistry*, *101*(26), 7011–7020. <https://doi.org/10.1523/JNEUROSCI.4272-06.2007>
- Leavitt, B. R., Van Raamsdonk, J. M., Shehadeh, J., Fernandes, H., Murphy, Z., Graham, R. K., Wellington, C. L., Raymond, L. A., & Hayden, M. R. (2006). Wild-type huntingtin protects neurons from excitotoxicity. *Journal of Neurochemistry*, *96*(4), 1121–1129. <https://doi.org/10.1111/j.1471-4159.2005.03605.x>

- Lee, K. J., Moussa, C. E. H., Lee, Y., Sung, Y., Howell, B. W., Turner, R. S., Pak, D. T. S., & Hoe, H. S. (2010). Beta amyloid-independent role of amyloid precursor protein in generation and maintenance of dendritic spines. *Neuroscience*, *169*(1), 344–356. <https://doi.org/10.1016/j.neuroscience.2010.04.078>
- Lee, M. S., Kao, S. C., Lemere, C. A., Xia, W., Tseng, H. C., Zhou, Y., Neve, R., Ahljianian, M. K., & Tsai, L. H. (2003). APP processing is regulated by cytoplasmic phosphorylation. *Journal of Cell Biology*, *163*(1), 83–95. <https://doi.org/10.1083/jcb.200301115>
- Lee, Y., Lee, K., Lee, J., Beom, Y., Hwangbo, A., Jung, J. A., & Song, C. (2018). *crossm In Vitro and In Vivo Assessment of FK506 Analogs as Novel*. *62*(11), 1–17.
- Leidel, C., Longoria, R. A., Gutierrez, F. M., & Shubeita, G. T. (2012). Measuring molecular motor forces in VIVO: Implications for tug-of-war models of bidirectional transport. *Biophysical Journal*, *103*(3), 492–500. <https://doi.org/10.1016/j.bpj.2012.06.038>
- Lessard, D. V., Zinder, O. J., Hotta, T., Verhey, K. J., Ohi, R., & Berger, C. L. (2019). Polyglutamylation of tubulin's C-terminal tail controls pausing and motility of kinesin-3 family member KIF1A. *Journal of Biological Chemistry*, *294*(16), 6353–6363. <https://doi.org/10.1074/jbc.RA118.005765>
- Leterrier, C. (2018). The axon initial segment: An updated viewpoint. *Journal of Neuroscience*, *38*(9), 2135–2145. <https://doi.org/10.1523/JNEUROSCI.1922-17.2018>
- Leterrier, C., Dubey, P., & Roy, S. (2017). The nano-architecture of the axonal cytoskeleton. *Nature Reviews Neuroscience*, *18*(12), 713–726. <https://doi.org/10.1038/nrn.2017.129>
- Lewis, K. T., Maddipati, K. R., Naik, A. R., & Jena, B. P. (2017). Unique Lipid Chemistry of Synaptic Vesicle and Synaptosome Membrane Revealed Using Mass Spectrometry. *ACS Chemical Neuroscience*, *8*(6), 1163–1169. <https://doi.org/10.1021/acschemneuro.7b00030>
- Li, H., Wyman, T., Yu, Z. X., Li, S. H., & Li, X. J. (2003). Abnormal association of mutant huntingtin with synaptic vesicles inhibits glutamate release. *Human Molecular Genetics*, *12*(16), 2021–2030. <https://doi.org/10.1093/hmg/ddg218>
- Li, L. B., Lei, H., Arey, R. N., Li, P., Liu, J., Murphy, C. T., Xu, X. Z. S., & Shen, K. (2016). The Neuronal Kinesin UNC-104/KIF1A is a Key Regulator of Synaptic Aging and Insulin Signaling-Regulated Memory. *Current Biology*, *26*(5), 605–615. <https://doi.org/10.1016/j.cub.2015.12.068>
- Li, Y., Wang, D., Li, Y., Chu, H., Zhang, L., Hou, M., Jiang, X., Chen, Z., Su, B., & Sun, T. (2017). Pre-synaptic TrkB in basolateral amygdala neurons mediates BDNF signaling transmission in memory extinction. *Cell Death & Disease*, *8*(7), e2959. <https://doi.org/10.1038/cddis.2017.302>
- Liévens, J. C., Woodman, B., Mahal, A., & Bates, G. P. (2002). Abnormal phosphorylation of synapsin I predicts a neuronal transmission impairment in the R6/2 Huntington's disease transgenic mice. *Molecular and Cellular Neuroscience*, *20*(4), 638–648. <https://doi.org/10.1006/mcne.2002.1152>
- Liley, A. W., & North, K. A. K. (1953). *An electrical investigation of effects of repetitive stimulation on mam-malian neuromuscular junction*. [www.physiology.org/journal/jn](http://www.physiology.org/journal/jn)
- Lim, A., Rechtsteiner, A., & Saxton, W. M. (2017). Two kinesins drive anterograde neuropeptide transport. *Molecular Biology of the Cell*, *28*(24). <https://doi.org/10.1091/mbc.E16-12-0820>
- Lingwood, D., & Simons, K. (2010). Lipid Rafts As a Membrane-Organizing Principle. *Science*, *327*(5961),

46. <https://doi.org/10.1126/science.1174621>

- Liot, G., Zala, D., Pla, P., Mottet, G., Piel, M., & Saudou, F. (2013). Mutant Huntingtin alters retrograde transport of TrkB receptors in striatal dendrites. *The Journal of Neuroscience : The Official Journal of the Society for Neuroscience*, 33(15), 6298–6309. <https://doi.org/10.1523/JNEUROSCI.2033-12.2013>
- Lipka, J., Kapitein, L. C., Jaworski, J., & Hoogenraad, C. C. (2016). Transport To Dendrites. *Embo J.*, 1(3), 1–17.
- Lipka, J., Kuijpers, M., Jaworski, J., & Hoogenraad, C. C. (2013). Mutations in cytoplasmic dynein and its regulators cause malformations of cortical development and neurodegenerative diseases. *Biochemical Society Transactions*, 41(6), 1605–1612. <https://doi.org/10.1042/BST20130188>
- Littleton, J. T., Stern, M., Schuize, K., Perin, M., & Bellen's, H. J. (1993). Mutational Analysis of Drosophila synaptotagmin Demonstrates Its Essential Role in Ca<sup>2+</sup>-Activated Neurotransmitter Release. In *Cell* (Vol. 74).
- Liu, J. P., & Zeitlin, S. O. (2017). Is huntingtin dispensable in the adult brain? In *Journal of Huntington's Disease* (Vol. 6, Issue 1). <https://doi.org/10.3233/JHD-170235>
- Liu, J. S., Schubert, C. R., Fu, X., Fourniol, F. J., Jaiswal, J. K., Houdusse, A., Stultz, C. M., Moores, C. A., & Walsh, C. A. (2012). Article Molecular Basis for Specific Regulation of Neuronal Kinesin-3 Motors by Doublecortin Family Proteins. *Molecular Cell*, 47(5), 707–721. <https://doi.org/10.1016/j.molcel.2012.06.025>
- Liu, X. H., Geng, Z., Yan, J., Li, T., Chen, Q., Zhang, Q. Y., & Chen, Z. Y. (2015). Blocking GSK3 $\beta$ -mediated dynamin1 phosphorylation enhances BDNF-dependent TrkB endocytosis and the protective effects of BDNF in neuronal and mouse models of Alzheimer's disease. *Neurobiology of Disease*, 74(1), 377–391. <https://doi.org/10.1016/j.nbd.2014.11.020>
- Liu, Y. S., Dai, X., Wu, W., Yuan, F. fen, Gu, X., Chen, J. G., Zhu, L. Q., & Wu, J. (2017). The Association of SNAP25 Gene Polymorphisms in Attention Deficit/Hyperactivity Disorder: a Systematic Review and Meta-Analysis. *Molecular Neurobiology*, 54(3), 2189–2200. <https://doi.org/10.1007/s12035-016-9810-9>
- Liu, Y., Sugiura, Y., & Lin, W. (2011). The role of Synaptobrevin1/VAMP1 in Ca<sup>2+</sup>-triggered neurotransmitter release at the mouse neuromuscular junction. *Journal of Physiology*, 589(7), 1603–1618. <https://doi.org/10.1113/jphysiol.2010.201939>
- Llinás, R. R. (2003). The contribution of Santiago Ramon y Cajal to functional neuroscience. *Nature Reviews Neuroscience*, 4(1), 77–80. <https://doi.org/10.1038/nrn1011>
- Lo, K. Y., Kuzmin, A., Unger, S. M., Petersen, J. D., & Silverman, M. A. (2011). KIF1A is the primary anterograde motor protein required for the axonal transport of dense-core vesicles in cultured hippocampal neurons. *Neuroscience Letters*, 491(3), 168–173. <https://doi.org/10.1016/j.neulet.2011.01.018>
- Lou, H., Kim, S. K., Zaitsev, E., Snell, C. R., Lu, B., & Loh, Y. P. (2005). Sorting and activity-dependent secretion of BDNF require interaction of a specific motif with the sorting receptor carboxypeptidase E. *Neuron*, 45(2), 245–255. <https://doi.org/10.1016/j.neuron.2004.12.037>
- Lundgren, J. L., Ahmed, S., Schedin-Weiss, S., Gouras, G. K., Winblad, B., Tjernberg, L. O., & Frykman,

- S. (2015). ADAM10 and BACE1 are localized to synaptic vesicles. *Journal of Neurochemistry*, *135*(3), 606–615. <https://doi.org/10.1111/jnc.13287>
- Lyons, D. A., Naylor, S. G., Mercurio, S., Dominguez, C., & Talbot, W. S. (2008). KBP is essential for axonal structure, outgrowth and maintenance in zebrafish, providing insight into the cellular basis of Goldberg-Shprintzen syndrome. *Development*, *135*(3), 599–608. <https://doi.org/10.1242/dev.012377>
- Ma, T., Cheng, Y., Hellard, E. R., Wang, X., Lu, J., Gao, X., Huang, C. C. Y., Wei, X., Ji, J., & Wang, J. (2018). Bidirectional and long-lasting control of alcohol-seeking behavior by corticostriatal LTP and LTD. *Nature Neuroscience*. <https://doi.org/10.1038/s41593-018-0081-9>
- MacDonald, M. E., Ambrose, C. M., Duyao, M. P., Myers, R. H., Lin, C., Srinidhi, L., Barnes, G., Taylor, S. A., James, M., Groot, N., MacFarlane, H., Jenkins, B., Anderson, M. A., Wexler, N. S., Gusella, J. F., Bates, G. P., Baxendale, S., Hummerich, H., Kirby, S., ... Harper, P. S. (1993). A novel gene containing a trinucleotide repeat that is expanded and unstable on Huntington's disease chromosomes. *Cell*, *72*(6), 971–983. [https://doi.org/10.1016/0092-8674\(93\)90585-E](https://doi.org/10.1016/0092-8674(93)90585-E)
- Macleod, G. T., & Zinsmaier, K. E. (2006). Synaptic Homeostasis on the Fast Track. *Neuron*, *52*(4), 570–571. <https://doi.org/10.1016/j.neuron.2006.11.006>
- Maday, S., Twelvetrees, A. E., Moughamian, A. J., & Holzbaur, E. L. F. (2014). Axonal Transport: Cargo-Specific Mechanisms of Motility and Regulation. *Neuron*, *84*(2), 292–309. <https://doi.org/10.1016/j.neuron.2014.10.019>
- Maday, S., Wallace, K. E., & Holzbaur, E. L. F. (2012). Autophagosomes initiate distally and mature during transport toward the cell soma in primary neurons. *Journal of Cell Biology*, *196*(4), 407–417. <https://doi.org/10.1083/jcb.201106120>
- Maeder, C. I., San-Miguel, A., Wu, E. Y., Lu, H., & Shen, K. (2014). In vivo neuron-wide analysis of synaptic vesicle precursor trafficking. *Traffic*, *15*(3), 273–291. <https://doi.org/10.1111/tra.12142>
- Magiera, M. M., Singh, P., Gadadhar, S., & Janke, C. (2018). Tubulin Posttranslational Modifications and Emerging Links to Human Disease. *Cell*, *173*(6), 1323–1327. <https://doi.org/10.1016/j.cell.2018.05.018>
- Mahapatra, S., Fan, F., & Lou, X. (2016). Tissue-specific dynamin-1 deletion at the calyx of Held decreases short-term depression through a mechanism distinct from vesicle resupply. *Proceedings of the National Academy of Sciences of the United States of America*, *113*(22), E3150–E3158. <https://doi.org/10.1073/pnas.1520937113>
- Mahoney, T. R., Lin, Q., Itoh, T., Luo, S., Hadwiger, G., Vincent, R., Wang, Z. W., Fukuda, M., & Nonet, M. L. (2006). Regulation of synaptic transmission by RAB-3 and RAB-27 in *Caenorhabditis elegans*. *Molecular Biology of the Cell*, *17*(6), 2617–2625. <https://doi.org/10.1091/mbc.E05-12-1170>
- Malagon, G., Miki, T., Tran, V., Gomez, L., & Marty, A. (2020). Incomplete vesicular docking limits synaptic strength under high release probability conditions. *eLife*, *9*, 1–18. <https://doi.org/10.7554/eLife.52137>
- Malinow, R., Mainen, Z. F., & Hayashi, Y. (2000). LTP mechanisms: From silence to four-lane traffic. *Current Opinion in Neurobiology*, *10*(3), 352–357. [https://doi.org/10.1016/S0959-4388\(00\)00099-4](https://doi.org/10.1016/S0959-4388(00)00099-4)



- Mannella, F., Gurney, K., & Baldassarre, G. (2013). The nucleus accumbens as a nexus between values and goals in goal-directed behavior: A review and a new hypothesis. *Frontiers in Behavioral Neuroscience*, 7(OCT), 1–29. <https://doi.org/10.3389/fnbeh.2013.00135>
- Marat, A. L., Dokainish, H., & McPherson, P. S. (2011). DENN domain proteins: Regulators of Rab GTPases. *Journal of Biological Chemistry*, 286(16), 13791–13800. <https://doi.org/10.1074/jbc.R110.217067>
- Marder, E. (1999). Neural signalling: Does colocalization imply cotransmission? *Current Biology*, 9(21), 809–811. [https://doi.org/10.1016/s0960-9822\(99\)80496-5](https://doi.org/10.1016/s0960-9822(99)80496-5)
- Marques Sousa, C., & Humbert, S. (2013). Huntingtin: here, there, everywhere! *Journal of Huntington's Disease*, 2(4), 395–403. <https://doi.org/10.3233/JHD-130082>
- Marrone, D. F., & Petit, T. L. (2002). The role of synaptic morphology in neural plasticity: Structural interactions underlying synaptic power. *Brain Research Reviews*, 38(3), 291–308. [https://doi.org/10.1016/S0165-0173\(01\)00147-3](https://doi.org/10.1016/S0165-0173(01)00147-3)
- Martens, S., Kozlov, M. M., & McMahon, H. T. (2007). How Synaptotagmin Promotes Membrane Fusion. *Science*, 316(5828), 1205. <https://doi.org/10.1126/science.1142614>
- Martineau, M., Guzman, R. E., Fahlke, C., & Klingauf, J. (2017). VGLUT1 functions as a glutamate/proton exchanger with chloride channel activity in hippocampal glutamatergic synapses. *Nature Communications*, 8(1). <https://doi.org/10.1038/s41467-017-02367-6>
- Martínez-Mármol, R., Mohannak, N., Qian, L., Wang, T., Gormal, R. S., Ruitenber, M. J., Vanhaesebroeck, B., Coulson, E. J., & Meunier, F. A. (2019). p110 $\delta$  PI3-Kinase Inhibition Perturbs APP and TNF $\alpha$  Trafficking, Reduces Plaque Burden, Dampens Neuroinflammation, and Prevents Cognitive Decline in an Alzheimer's Disease Mouse Model. *The Journal of Neuroscience: The Official Journal of the Society for Neuroscience*, 39(40), 7976–7991. <https://doi.org/10.1523/JNEUROSCI.0674-19.2019>
- Marzo, M. G., Griswold, J. M., & Markus, S. M. (2020). Pac1/LIS1 stabilizes an uninhibited conformation of dynein to coordinate its localization and activity. *Nature Cell Biology*, 22(May). <https://doi.org/10.1038/s41556-020-0492-1>
- Matrone, C. (2013). A new molecular explanation for age-related neurodegeneration: The Tyr682 residue of amyloid precursor protein. *BioEssays*, 35(10), 847–852. <https://doi.org/10.1002/bies.201300041>
- Matrone, C., Iannuzzi, F., & Annunziato, L. (2019). The Y682ENPTY687 motif of APP: Progress and insights toward a targeted therapy for Alzheimer's disease patients. *Ageing Research Reviews*, 52(November 2018), 120–128. <https://doi.org/10.1016/j.arr.2019.04.003>
- Matsumoto, T., Rauskolb, S., Polack, M., Klose, J., Kolbeck, R., Korte, M., & Barde, Y. A. (2008). Biosynthesis and processing of endogenous BDNF: CNS neurons store and secrete BDNF, not pro-BDNF. *Nature Neuroscience*, 11(2), 131–133. <https://doi.org/10.1038/nn2038>
- Matteoli, M., Coco, S., Schenk, U., & Verderio, C. (2004). Vesicle turnover in developing neurons: How to build a presynaptic terminal. *Trends in Cell Biology*, 14(3), 133–140. <https://doi.org/10.1016/j.tcb.2004.01.007>
- Matz, J., Gilyan, A., Kolar, A., McCarvill, T., & Krueger, S. R. (2010). Rapid structural alterations of the

- active zone lead to sustained changes in neurotransmitter release. *Proceedings of the National Academy of Sciences of the United States of America*, 107(19), 8836–8841. <https://doi.org/10.1073/pnas.0906087107>
- McAdam, R. L., Morton, A., Gordon, S. L., Alterman, J. F., Khvorova, A., Cousin, M. A., & Smillie, K. J. (2020). Loss of huntingtin function slows synaptic vesicle endocytosis in striatal neurons from the httQ140/Q140 mouse model of Huntington's disease. *Neurobiology of Disease*, 134(October 2019), 104637. <https://doi.org/10.1016/j.nbd.2019.104637>
- McGeorge, A. J., & Faull, R. L. M. (1989). The organization of the projection from the cerebral cortex to the striatum in the rat. *Neuroscience*, 29(3), 503–537. [https://doi.org/10.1016/0306-4522\(89\)90128-0](https://doi.org/10.1016/0306-4522(89)90128-0)
- McGuire, J. R., Rong, J., Li, S., & Li, X. (2006). *Interaction of Huntingtin-associated Protein-1 with Kinesin Light Chain*. 281(6), 3552–3559. <https://doi.org/10.1074/jbc.M509806200>
- McKenna, M. C. (2007). The glutamate-glutamine cycle is not stoichiometric: Fates of glutamate in brain. *Journal of Neuroscience Research*, 85(15), 3347–3358. <https://doi.org/10.1002/jnr.21444>
- McKenney, R. J. (2020). LIS1 cracks open dynein. *Nature Cell Biology*, 22(5), 515–517. <https://doi.org/10.1038/s41556-020-0500-5>
- Mcmahon, H. T., BOLSHAKOVt, V. Y., Janz, R., Hammer, R. E., SIEGELBAUMt, S. A., & SIIDHOF, T. C. (1996). Synaptophysin, a major synaptic vesicle protein, is not essential for neurotransmitter release. In *Neurobiology* (Vol. 93).
- Menalled, L. B., Sison, J. D., Dragatsis, I., Zeitlin, S., & Chesselet, M. F. (2003). Time course of early motor and neuropathological anomalies in a knock-in mouse model of Huntington's disease with 140 CAG repeats. *Journal of Comparative Neurology*, 465(1), 11–26. <https://doi.org/10.1002/cne.10776>
- Merchán-Pérez, A., Rodríguez, J. R., Alonso-Nanclares, L., Schertel, A., & DeFelipe, J. (2009). Counting synapses using FIB/SEM microscopy: A true revolution for ultrastructural volume reconstruction. *Frontiers in Neuroanatomy*, 3(OCT). <https://doi.org/10.3389/neuro.05.018.2009>
- Merchán-Pérez, A., Rodríguez, J. R., Ribak, C. E., & DeFelipe, J. (2009). Proximity of excitatory and inhibitory axon terminals adjacent to pyramidal cell bodies provides a putative basis for nonsynaptic interactions. *Proceedings of the National Academy of Sciences of the United States of America*, 106(24), 9878–9883. <https://doi.org/10.1073/pnas.0900330106>
- Metzler, M., Gan, L., Mazarei, G., Graham, R. K., Liu, L., Bissada, N., Lu, G., Leavitt, B. R., & Hayden, M. R. (2010). Phosphorylation of huntingtin at Ser421 in YAC128 neurons is associated with protection of YAC128 neurons from NMDA-mediated excitotoxicity and is modulated by PP1 and PP2A. *Journal of Neuroscience*, 30(43), 14318–14329. <https://doi.org/10.1523/JNEUROSCI.1589-10.2010>
- Michaelson, D. M., Barkai, G., & Barenholz, Y. (1983). Asymmetry of lipid organization in cholinergic synaptic vesicle membranes. *The Biochemical Journal*, 211(1), 155–162. <https://doi.org/10.1042/bj2110155>
- Miki, T., Malagon, G., Pulido, C., Llano, I., Neher, E., & Marty, A. (2016). Actin- and Myosin-Dependent Vesicle Loading of Presynaptic Docking Sites Prior to Exocytosis. *Neuron*, 91(4), 808–823. <https://doi.org/10.1016/j.neuron.2016.07.033>

- Miki, T., Nakamura, Y., Malagon, G., Neher, E., & Marty, A. (2018). Two-component latency distributions indicate two-step vesicular release at simple glutamatergic synapses. *Nature Communications*, *9*(1), 1–3. <https://doi.org/10.1038/s41467-018-06336-5>
- Millecamps, S., & Julien, J. P. (2013). Axonal transport deficits and neurodegenerative diseases. *Nature Reviews Neuroscience*, *14*(3), 161–176. <https://doi.org/10.1038/nrn3380>
- Miller, K. E., Deproto, J., Kaufmann, N., Patel, B. N., Duckworth, A., & Vactor, D. Van. (2005). *Direct Observation Demonstrates that Liprin- $\gamma$  Is Required for Trafficking of Synaptic Vesicles*. *15*, 684–689. <https://doi.org/10.1016/j.cub.2005.02.061>
- Mitter, D., Reisinger, C., Hinz, B., Hollmann, S., Yelamanchili, S. V., Treiber-Held, S., Ohm, T. G., Herrmann, A., & Ahnert-Hilger, G. (2003). The synaptophysin/synaptobrevin interaction critically depends on the cholesterol content. *Journal of Neurochemistry*, *84*(1), 35–42. <https://doi.org/10.1046/j.1471-4159.2003.01258.x>
- Miyachi, S., Hikosaka, O., & Lu, X. (2002). Differential activation of monkey striatal neurons in the early and late stages of procedural learning. *Experimental Brain Research*, *146*(1), 122–126. <https://doi.org/10.1007/s00221-002-1213-7>
- Miyachi, S., Hikosaka, O., Miyashita, K., Kárádi, Z., & Rand, M. K. (1997). Differential roles of monkey striatum in learning of sequential hand movement. *Experimental Brain Research*, *115*(1), 1–5. <https://doi.org/10.1007/PL00005669>
- Miyoshi, J., & Takai, Y. (2004). Dual role of DENN/MADD (Rab3GEP) in neurotransmission and neuroprotection. *Trends in Molecular Medicine*, *10*(10), 476–480. <https://doi.org/10.1016/j.molmed.2004.08.002>
- Mizuno, N., Toba, S., Edamatsu, M., Watai-Nishii, J., Hirokawa, N., Toyoshima, Y. Y., & Kikkawa, M. (2004). Dynein and kinesin share an overlapping microtubule-binding site. *EMBO Journal*, *23*(13), 2459–2467. <https://doi.org/10.1038/sj.emboj.7600240>
- Mochel, F., Lipids, F. M., Metabolic, I., Verlag, S., & Mochel, F. (2018). *Lipids and synaptic functions To cite this version : HAL Id : hal-01957839 Lipids and synaptic functions*.
- Mochida, S., Hida, Y., Tanifuji, S., Hagiwara, A., Hamada, S., Abe, M., Ma, H., Yasumura, M., Kitajima, I., Sakimura, K., & Ohtsuka, T. (2016). SAD-B Phosphorylation of CAST Controls Active Zone Vesicle Recycling for Synaptic Depression. *Cell Reports*, *16*(11), 2901–2913. <https://doi.org/10.1016/j.celrep.2016.08.020>
- Mohrmann, R., De Wit, H., Verhage, M., Neher, E., & Sørensen, J. B. (2010). Fast vesicle fusion in living cells requires at least three SNARE complexes. *Science*, *330*(6003), 502–505. <https://doi.org/10.1126/science.1193134>
- Monroy, B. Y., Tan, T. C., Oclaman, J. M., Han, J. S., Simó, S., Niwa, S., Nowakowski, D. W., McKenney, R. J., & Ori-McKenney, K. M. (2020). A Combinatorial MAP Code Dictates Polarized Microtubule Transport. *Developmental Cell*, *53*(1), 60–72.e4. <https://doi.org/10.1016/j.devcel.2020.01.029>
- Montagna, E., Dorostkar, M. M., & Herms, J. (2017). The role of APP in structural spine plasticity. *Frontiers in Molecular Neuroscience*, *10*(May), 1–7. <https://doi.org/10.3389/fnmol.2017.00136>
- Morfini, G. A., Burns, M., Binder, L. I., Kanaan, N. M., Lapointe, N., Bosco, D. A., Brown, R. H., Brown, H., Tiwari, A., Hayward, L., Edgar, J., Nave, K. A., Garberrn, J., Atagi, Y., Song, Y., Pigino, G., &

- Brady, S. T. (2009). Axonal transport defects in neurodegenerative diseases. *Journal of Neuroscience*, *29*(41), 12776–12786. <https://doi.org/10.1523/JNEUROSCI.3463-09.2009>
- Morton, A. J., Faull, R. L. M., & Edwardson, J. M. (2001). Abnormalities in the synaptic vesicle fusion machinery in Huntington's disease. *Brain Research Bulletin*, *56*(2), 111–117. [https://doi.org/10.1016/S0361-9230\(01\)00611-6](https://doi.org/10.1016/S0361-9230(01)00611-6)
- Moutaux, E., Charlot, B., Genoux, A., Saudou, F., & Cazorla, M. (2018). *Lab on a Chip for the study of activity-dependent intracellular dynamics in neuronal networks †*. 3425–3435. <https://doi.org/10.1039/c8lc00694f>
- Moutaux, E., Christaller, W., Scaramuzzino, C., Genoux, A., Charlot, B., Cazorla, M., & Saudou, F. (2018). Neuronal network maturation differently affects secretory vesicles and mitochondria transport in axons. *Scientific Reports*, *8*(1), 1–14. <https://doi.org/10.1038/s41598-018-31759-x>
- Mowla, S. J., Pareek, S., Farhadi, H. F., Petrecca, K., Fawcett, J. P., Seidah, N. G., Morris, S. J., Sossin, W. S., & Murphy, R. A. (1999). Differential sorting of nerve growth factor and brain-derived neurotrophic factor in hippocampal neurons. *Journal of Neuroscience*, *19*(6), 2069–2080. <https://doi.org/10.1523/jneurosci.19-06-02069.1999>
- Muhia, M., Thies, E., Labonté, D., Ghiretti, A. E., Gromova, K. V., Xompero, F., Lappe-Siefke, C., Hermans-Borgmeyer, I., Kuhl, D., Schweizer, M., Ohana, O., Schwarz, J. R., Holzbaur, E. L. F., & Kneussel, M. (2016). The Kinesin KIF21B Regulates Microtubule Dynamics and Is Essential for Neuronal Morphology, Synapse Function, and Learning and Memory. *Cell Reports*, *15*(5), 968–977. <https://doi.org/10.1016/j.celrep.2016.03.086>
- Müller, M. J. I., Klumpp, S., & Lipowsky, R. (2008). Tug-of-war as a cooperative mechanism for bidirectional cargo transport by molecular motors. *Proceedings of the National Academy of Sciences of the United States of America*, *105*(12), 4609–4614. <https://doi.org/10.1073/pnas.0706825105>
- Müller, M., Liu, K. S. Y., Sigrist, S. J., & Davis, G. W. (2012). RIM controls homeostatic plasticity through modulation of the readily-releasable vesicle pool. *Journal of Neuroscience*, *32*(47), 16574–16585. <https://doi.org/10.1523/JNEUROSCI.0981-12.2012>
- Müller, N. G., & Knight, R. T. (2006). The functional neuroanatomy of working memory: Contributions of human brain lesion studies. *Neuroscience*, *139*(1), 51–58. <https://doi.org/10.1016/j.neuroscience.2005.09.018>
- Muresan, Z., & Muresan, V. (2005). c-Jun NH2-terminal kinase-interacting protein-3 facilitates phosphorylation and controls localization of amyloid- $\beta$  precursor protein. *Journal of Neuroscience*, *25*(15), 3741–3751. <https://doi.org/10.1523/JNEUROSCI.0152-05.2005>
- Murthy, V. N. (1998). *Synaptic plasticity : Step-wise strengthening*. 650–653.
- Murthy, V. N., Schikorski, T., Stevens, C. F., & Zhu, Y. (2001). Inactivity produces increases in neurotransmitter release and synapse size. *Neuron*, *32*(4), 673–682. [https://doi.org/10.1016/S0896-6273\(01\)00500-1](https://doi.org/10.1016/S0896-6273(01)00500-1)
- Murthy, V. N., Sejnowski, T. J., & Stevens, C. F. (1997). Heterogeneous release properties of visualized individual hippocampal synapses. *Neuron*, *18*(4), 599–612. [https://doi.org/10.1016/S0896-6273\(00\)80301-3](https://doi.org/10.1016/S0896-6273(00)80301-3)

- N. Siddiqui, & A. Straube. (2017). Intracellular Cargo Transport by Kinesin. *Biochemistry (Moscow)*, *82*(7), 803–815.
- Nakatsu, F., Okada, M., Mori, F., Kumazawa, N., Iwasa, H., Zhu, G., Kasagi, Y., Kamiya, H., Harada, A., Nishimura, K., Takeuchi, A., Miyazaki, T., Watanabe, M., Yuasa, S., Manabe, T., Wakabayashi, K., Kaneko, S., Saito, T., & Ohno, H. (2004). Defective function of GABA-containing synaptic vesicles in mice lacking the AP-3B clathrin adaptor. *Journal of Cell Biology*, *167*(2), 293–302. <https://doi.org/10.1083/jcb.200405032>
- Neuman, K. M., Molina-Campos, E., Musial, T. F., Price, A. L., Oh, K. J., Wolke, M. L., Buss, E. W., Scheff, S. W., Mufson, E. J., & Nicholson, D. A. (2015). Evidence for Alzheimer’s disease-linked synapse loss and compensation in mouse and human hippocampal CA1 pyramidal neurons. *Brain Structure and Function*, *220*(6), 3143–3165. <https://doi.org/10.1007/s00429-014-0848-z>
- Neves, G., & Lagnado, L. (1999). The kinetics of exocytosis and endocytosis in the synaptic terminal of goldfish retinal bipolar cells. In *Journal of Physiology*.
- Nigam, S. M., Xu, S., Ackermann, F., Gregory, J. A., Lundkvist, J., Lendahl, U., & Brodin, L. (2016). Endogenous APP accumulates in synapses after BACE1 inhibition. *Neuroscience Research*, *109*, 9–15. <https://doi.org/10.1016/j.neures.2016.02.002>
- Nissenkorn, A., Kidon, M., & Ben-Zeev, B. (2017). A Potential Life-Threatening Reaction to Glatiramer Acetate in Rett Syndrome. *Pediatric Neurology*, *68*, 40–43. <https://doi.org/10.1016/j.pediatrneurol.2016.11.006>
- Niwa, S., Lipton, D. M., Morikawa, M., Zhao, C., Hirokawa, N., Lu, H., & Shen, K. (2016). Autoinhibition of a Neuronal Kinesin UNC-104/KIF1A Regulates the Size and Density of Synapses. *Cell Reports*, *16*(8), 2129–2141. <https://doi.org/10.1016/j.celrep.2016.07.043>
- Niwa, S., Tanaka, Y., & Hirokawa, N. (2008). *KIF1B*  $\beta$  - and *KIF1A*-mediated axonal transport of presynaptic regulator *Rab3* occurs in a GTP-dependent manner through *DENN / MADD*. *10*(11). <https://doi.org/10.1038/ncb1785>
- Niwa, S., Tao, L., Lu, S. Y., Liew, G. M., Feng, W., Nachury, M. V., & Shen, K. (2017). BORC Regulates the Axonal Transport of Synaptic Vesicle Precursors by Activating ARL-8. *Current Biology*, *27*(17), 2569–2578.e4. <https://doi.org/10.1016/j.cub.2017.07.013>
- Nonet, M. L., Holgado, A. M., Brewer, F., Serpe, C. J., Norbeck, B. A., Holleran, J., Wei, L., Hartweg, E., Jorgensen, M., & Alfonso, A. (1999). Regulates the Size and Protein Composition of Synaptic Vesicles. *Molecular Biology of the Cell*, *10*(July), 2343–2360.
- Nordborg, C., & Johansson, B. B. (1995). Secondary thalamic lesions after ligation of the middle cerebral artery: an ultrastructural study. *Acta Neuropathologica*, *91*(1), 61–66. <https://doi.org/10.1007/s004010050392>
- Nyenhuis, S. B., Thapa, A., & Cafiso, D. S. (2019). Phosphatidylinositol 4,5 Bisphosphate Controls the cis and trans Interactions of Synaptotagmin 1. *Biophysical Journal*, *117*(2), 247–257. <https://doi.org/10.1016/j.bpj.2019.06.016>
- O’Hare, J. K., Ade, K. K., Sukharnikova, T., Van Hooser, S. D., Palmeri, M. L., Yin, H. H., & Calakos, N. (2016). Pathway-Specific Striatal Substrates for Habitual Behavior. *Neuron*, *89*(3), 472–479. <https://doi.org/10.1016/j.neuron.2015.12.032>

- Ochaba, J., Lukacsovich, T., Csikos, G., Zheng, S., Margulis, J., Salazar, L., Mao, K., Lau, A. L., Yeung, S. Y., Humbert, S., Saudou, F., Klionsky, D. J., Finkbeiner, S., Zeitlin, S. O., Marsh, J. L., Housman, D. E., Thompson, L. M., & Steffan, J. S. (2014). Potential function for the Huntingtin protein as a scaffold for selective autophagy. *Proceedings of the National Academy of Sciences of the United States of America*, *111*(47), 16889–16894. <https://doi.org/10.1073/pnas.1420103111>
- Octave, J. N., Pierrot, N., Ferao Santos, S., Nalivaeva, N. N., & Turner, A. J. (2013). From synaptic spines to nuclear signaling: Nuclear and synaptic actions of the amyloid precursor protein. *Journal of Neurochemistry*, *126*(2), 183–190. <https://doi.org/10.1111/jnc.12239>
- Ohba, C., Haginoya, K., Osaka, H., Kubota, K., Ishiyama, A., Hiraide, T., Komaki, H., Sasaki, M., Miyatake, S., Nakashima, M., Tsurusaki, Y., Miyake, N., Tanaka, F., Saitsu, H., & Matsumoto, N. (2015). *De novo KIF1A mutations cause intellectual de fi cit , cerebellar atrophy , lower limb spasticity and visual disturbance*. *60*(12), 739–742. <https://doi.org/10.1038/jhg.2015.108>
- Okada, Y., & Hirokawa, N. (1999). A processive single-headed motor: Kinesin superfamily protein KIF1A. *Science*, *283*(5405), 1152–1157. <https://doi.org/10.1126/science.283.5405.1152>
- Okada, Y., Yamazaki, H., Sekine-Aizawa, Y., & Hirokawa, N. (1995). The neuron-specific kinesin superfamily protein KIF1A is a unique monomeric motor for anterograde axonal transport of synaptic vesicle precursors. *Cell*, *81*(5), 769–780. [https://doi.org/10.1016/0092-8674\(95\)90538-3](https://doi.org/10.1016/0092-8674(95)90538-3)
- Olenick, M. A., & Holzbaur, E. L. F. (2019). Cell science at a glance dynein activators and adaptors at a glance. *Journal of Cell Science*, *132*(6), 1–7. <https://doi.org/10.1242/jcs.227132>
- Oliveira, A. M. M., Hawk, J. D., Abel, T., & Havekes, R. (2010). Post-training reversible inactivation of the hippocampus enhances novel object recognition memory. *Learning and Memory*, *17*(3), 155–160. <https://doi.org/10.1101/lm.1625310>
- Osunbayo, O., Butterfield, J., Bergman, J., Mershon, L., Rodionov, V., & Vershinin, M. (2015). Cargo transport at microtubule crossings: Evidence for prolonged tug-of-war between kinesin motors. *Biophysical Journal*, *108*(6), 1480–1483. <https://doi.org/10.1016/j.bpj.2015.02.016>
- Otsuka, A. J., Jeyaprakash, A., García-Añoveros, J., Tang, L. Z., Fisk, G., Hartshorne, T., Franco, R., & Bornt, T. (1991). The *C. elegans unc-104* 4 gene encodes a putative kinesin heavy chain-like protein. *Neuron*, *6*(1), 113–122. [https://doi.org/10.1016/0896-6273\(91\)90126-K](https://doi.org/10.1016/0896-6273(91)90126-K)
- Owe, S. G., Jensen, V., Evergren, E., Ruiz, A., Shupliakov, O., Kullmann, D. M., Storm-Mathisen, J., Walaas, S. I., Hvalby, Ø., & Bergersen, L. H. (2009). Synapsin- and actin-dependent frequency enhancement in mouse hippocampal mossy fiber synapses. *Cerebral Cortex*, *19*(3), 511–523. <https://doi.org/10.1093/cercor/bhn101>
- Pace, R. De, Britt, D. J., Mercurio, J., Hoffmann, V., Abebe, D., Bonifacino, J. S., Pace, R. De, Britt, D. J., Mercurio, J., Foster, A. M., Djavaherian, L., Hoffmann, V., Abebe, D., & Bonifacino, J. S. (2020). Article Synaptic Vesicle Precursors and Lysosomes Are Transported by Different Mechanisms in the Axon of Mammalian Neurons II II Synaptic Vesicle Precursors and Lysosomes Are Transported by Different Mechanisms in the Axon of Mammalian Neurons. *CellReports*, *31*(11), 107775. <https://doi.org/10.1016/j.celrep.2020.107775>
- Pack-chung, E., Kurshan, P. T., Dickman, D. K., & Schwarz, T. L. (2007). *A Drosophila kinesin required for synaptic bouton formation and synaptic vesicle transport*. *10*(8), 980–989. <https://doi.org/10.1038/nn1936>

- Paddock, B. E., Wang, Z., Biela, L. M., Chen, K., Getzy, M. D., Striegel, A., Richmond, J. E., Chapman, E. R., Featherstone, D. E., & Reist, N. E. (2011). Membrane penetration by synaptotagmin is required for coupling calcium binding to vesicle fusion in vivo. *Journal of Neuroscience*, *31*(6), 2248–2257. <https://doi.org/10.1523/JNEUROSCI.3153-09.2011>
- Padzik, A., Deshpande, P., Hollos, P., Franker, M., Rannikko, E. H., Cai, D., Prus, P., Mågård, M., & Westerlund, N. (2016). *KIF5C S176 Phosphorylation Regulates Microtubule Binding and Transport Efficiency in Mammalian Neurons*. *10*(March), 1–15. <https://doi.org/10.3389/fncel.2016.00057>
- Pal, A., Severin, F., Lommer, B., Shevchenko, A., & Zerial, M. (2006). Huntingtin-HAP40 complex is a novel Rab5 effector that regulates early endosome motility and is up-regulated in Huntington's disease. *Journal of Cell Biology*, *172*(4), 605–618. <https://doi.org/10.1083/jcb.200509091>
- Palidwor, G. A., Shcherbinin, S., Huska, M. R., Rasko, T., Stelzl, U., Arumughan, A., Foulle, R., Porras, P., Sanchez-Pulido, L., Wanker, E. E., & Andrade-Navarro, M. A. (2009). Detection of alpha-rod protein repeats using a neural network and application to huntingtin. *PLoS Computational Biology*, *5*(3). <https://doi.org/10.1371/journal.pcbi.1000304>
- Palop, J. J., Chin, J., Roberson, E. D., Wang, J., Thwin, M. T., Bien-ly, N., Yoo, J., Ho, K. O., Yu, G., Kreitzer, A., Finkbeiner, S., & Noebels, J. L. (2007). *Article Aberrant Excitatory Neuronal Activity and Compensatory Remodeling of Inhibitory Hippocampal Circuits in Mouse Models of Alzheimer ' s Disease*. 697–711. <https://doi.org/10.1016/j.neuron.2007.07.025>
- Pang, Z. P., & Südhof, T. C. (2010). Cell biology of Ca<sup>2+</sup>-triggered exocytosis. In *Current Opinion in Cell Biology* (Vol. 22, Issue 4, pp. 496–505). <https://doi.org/10.1016/j.ceb.2010.05.001>
- Papandréou, M. J., & Leterrier, C. (2018). The functional architecture of axonal actin. *Molecular and Cellular Neuroscience*, *91*(February), 151–159. <https://doi.org/10.1016/j.mcn.2018.05.003>
- Pardo, R. (2006). Inhibition of Calcineurin by FK506 Protects against Polyglutamine-Huntingtin Toxicity through an Increase of Huntingtin Phosphorylation at S421. *Journal of Neuroscience*, *26*(5), 1635–1645. <https://doi.org/10.1523/JNEUROSCI.3706-05.2006>
- Park, Hyekeun, Li, Y., & Tsien, R. W. (2012). Influence of synaptic vesicle position on release probability and exocytotic fusion mode. *Science*, *335*(6074), 1362–1366. <https://doi.org/10.1126/science.1216937>
- Park, Hyungju, & Poo, M. M. (2013). Neurotrophin regulation of neural circuit development and function. *Nature Reviews Neuroscience*, *14*(1), 7–23. <https://doi.org/10.1038/nrn3379>
- Park, Hyungju, Popescu, A., & Poo, M. ming. (2014). Essential role of presynaptic NMDA receptors in activity-dependent BDNF secretion and corticostriatal LTP. *Neuron*, *84*(5), 1009–1022. <https://doi.org/10.1016/j.neuron.2014.10.045>
- Pennuto, M., Bonanomi, D., Benfenati, F., & Valtorta, F. (2003). Synaptophysin I Controls the Targeting of VAMP2/ Synaptobrevin II to Synaptic Vesicles. *Molecular Biology of the Cell*, *14*, 4909–4919. <https://doi.org/10.1091/mbc.E03-06>
- Perea, G., Navarrete, M., & Araque, A. (2009). Tripartite synapses: astrocytes process and control synaptic information. *Trends in Neurosciences*, *32*(8), 421–431. <https://doi.org/10.1016/j.tins.2009.05.001>
- Peris, L., Wagenbach, M., Lafanechère, L., Brocard, J., Moore, A. T., Kozielski, F., Job, D., Wordeman,

- L., & Andrieux, A. (2009). Motor-dependent microtubule disassembly driven by tubulin tyrosination. *Journal of Cell Biology*, *185*(7), 1159–1166. <https://doi.org/10.1083/jcb.200902142>
- Perrin, E., & Venance, L. (2019). ScienceDirect Bridging the gap between striatal plasticity and learning. *Current Opinion in Neurobiology*, *54*, 104–112. <https://doi.org/10.1016/j.conb.2018.09.007>
- Perry, R. B., & Fainzilber Mike. (2013). Local Translation in Neuronal Processes - In Vivo Tests of a 'HereticalHypothesis.' *Developmental Neurobiology*, n/a-n/a. <https://doi.org/10.1002/dneu.22115>
- Persoon, C. M., Moro, A., Nassal, J. P., Farina, M., Broeke, J. H., Arora, S., Dominguez, N., Weering, J. R., Toonen, R. F., & Verhage, M. (2018). Pool size estimations for dense-core vesicles in mammalian CNS neurons. *The EMBO Journal*, *37*(20), 1–18. <https://doi.org/10.15252/embj.201899672>
- Phan, A., Thomas, C. I., Chakraborty, M., Berry, J. A., Kamasawa, N., Davis, R. L., Phan, A., Thomas, C. I., Chakraborty, M., Berry, J. A., Kamasawa, N., & Davis, R. L. (2019). Stromalin Constrains Memory Acquisition by Developmentally Limiting Synaptic Vesicle Pool Size Article Stromalin Constrains Memory Acquisition by Developmentally Limiting Synaptic Vesicle Pool Size. *Neuron*, *101*(1), 103–118.e5. <https://doi.org/10.1016/j.neuron.2018.11.003>
- Pineda, J. R., Pardo, R., Zala, D., Yu, H., Humbert, S., & Saudou, F. (2009). Genetic and pharmacological inhibition of calcineurin corrects the BDNF transport defect in Huntington's disease. *Molecular Brain*, *2*, 33. <https://doi.org/10.1186/1756-6606-2-33>
- Poll, S., Mittag, M., Musacchio, F., Justus, L. C., Giovannetti, E. A., Steffen, J., Wagner, J., Zohren, L., Schoch, S., Schmidt, B., Jackson, W. S., Ehninger, D., & Fuhrmann, M. (2020). Memory trace interference impairs recall in a mouse model of Alzheimer's disease. *Nature Neuroscience*, *23*(8), 952–958. <https://doi.org/10.1038/s41593-020-0652-4>
- Postila, P. A., & Róg, T. (2019). A Perspective: Active Role of Lipids in Neurotransmitter Dynamics. In *Molecular Neurobiology*. Humana Press Inc. <https://doi.org/10.1007/s12035-019-01775-7>
- Poudel, K. R., & Bai, J. (2014). ScienceDirect Synaptic vesicle morphology : a case of protein sorting ? *Current Opinion in Cell Biology*, *26*, 28–33. <https://doi.org/10.1016/j.ceb.2013.09.001>
- Poulsen, E. T., Iannuzzi, F., Rasmussen, H. F., Maier, T. J., Enghild, J. J., Jørgensen, A. L., & Matrone, C. (2017). An aberrant phosphorylation of amyloid precursor protein tyrosine regulates its trafficking and the binding to the clathrin endocytic complex in neural stem cells of alzheimer's disease patients. *Frontiers in Molecular Neuroscience*, *10*(March). <https://doi.org/10.3389/fnmol.2017.00059>
- Power, D., Srinivasan, S., & Gunawardena, S. (2012). In-vivo evidence for the disruption of Rab11 vesicle transport by loss of huntingtin. *NeuroReport*, *23*(16), 970–977. <https://doi.org/10.1097/WNR.0b013e328359d990>
- Preobraschenski, J., Cheret, C., Ganzella, M., Schenck, S., Jahn, R., Ahnert-hilger, G., Preobraschenski, J., Cheret, C., Ganzella, M., Zander, J. F., Richter, K., & Schenck, S. (2018). Dual and Direction-Selective Mechanisms of Phosphate Transport by the Vesicular Glutamate Article Dual and Direction-Selective Mechanisms of Phosphate Transport by the Vesicular Glutamate Transporter. *CellReports*, *23*(2), 535–545. <https://doi.org/10.1016/j.celrep.2018.03.055>
- Priller, C., Bauer, T., Mitteregger, G., Krebs, B., Kretschmar, H. A., & Herms, J. (2006). Synapse



- formation and function is modulated by the amyloid precursor protein. *The Journal of Neuroscience: The Official Journal of the Society for Neuroscience*, 26(27), 7212–7221. <https://doi.org/10.1523/JNEUROSCI.1450-06.2006>
- Puchkov, D., & Haucke, V. (2013). Greasing the synaptic vesicle cycle by membrane lipids. *Trends in Cell Biology*, 23(10), 493–503. <https://doi.org/10.1016/j.tcb.2013.05.002>
- Pulido, C., & Marty, A. (2017). Quantal Fluctuations in Central Mammalian Synapses: Functional Role of Vesicular Docking Sites. *Physiological Reviews*, 97(4), 1403–1430. <https://doi.org/10.1152/physrev.00032.2016>
- Pulido, C., Trigo, F. F., Llano, I., & Marty, A. (2015). Vesicular Release Statistics and Unitary Postsynaptic Current at Single GABAergic Synapses. *Neuron*, 85(1), 159–172. <https://doi.org/10.1016/j.neuron.2014.12.006>
- Puzzo, D., Lee, L., Palmeri, A., Calabrese, G., & Arancio, O. (2014). Behavioral assays with mouse models of Alzheimer's disease: Practical considerations and guidelines. *Biochemical Pharmacology*, 88(4), 450–467. <https://doi.org/10.1016/j.bcp.2014.01.011>
- Puzzo, D., Privitera, L., Leznik, E., Fà, M., Staniszewski, A., Palmeri, A., & Arancio, O. (2008). Picomolar amyloid-beta positively modulates synaptic plasticity and memory in hippocampus. *The Journal of Neuroscience: The Official Journal of the Society for Neuroscience*, 28(53), 14537–14545. <https://doi.org/10.1523/JNEUROSCI.2692-08.2008>
- Qu, L., Akbergenova, Y., Hu, Y., & Schikorski, T. (2009). Synapse-to-synapse variation in mean synaptic vesicle size and its relationship with synaptic morphology and function. *Journal of Comparative Neurology*, 514(4), 343–352.
- Quentin, E., Belmer, A., & Maroteaux, L. (2018). Somato-Dendritic Regulation of Raphe Serotonin Neurons; A Key to Antidepressant Action. *Frontiers in Neuroscience*, 12(December), 1–11. <https://doi.org/10.3389/fnins.2018.00982>
- Quetglas, S., Iborra, C., Sasakawa, N., De Haro, L., Kumakura, K., Sato, K., Leveque, C., & Seagar, M. (2002). Calmodulin and lipid binding to synaptobrevin regulates calcium-dependent exocytosis. *EMBO Journal*, 21(15), 3970–3979. <https://doi.org/10.1093/emboj/cdf404>
- Quillfeldt, J. a. (2010). Behavioral Methods to Study Learning in Rats. *Animal Models as Tools in Ethical Biomedical Research*, 341–383.
- Radde, R., Bolmont, T., Kaeser, S. A., Coomaraswamy, J., Lindau, D., Stoltze, L., Calhoun, M. E., Jäggi, F., Wolburg, H., Gengler, S., Haass, C., Ghetti, B., Czech, C., Hölscher, C., Mathews, P. M., & Jucker, M. (2006). A $\beta$ 42-driven cerebral amyloidosis in transgenic mice reveals early and robust pathology. *EMBO Reports*, 7(9), 940–946. <https://doi.org/10.1038/sj.embor.7400784>
- Rajappa, R., Gauthier-Kemper, A., Böning, D., Hüve, J., & Klingauf, J. (2016). Synaptophysin 1 Clears Synaptobrevin 2 from the Presynaptic Active Zone to Prevent Short-Term Depression. *Cell Reports*, 14(6), 1369–1381. <https://doi.org/10.1016/j.celrep.2016.01.031>
- Rajendran, L., Hoshino, M., Zahn, T. R., Keller, P., Geiger, K. D., Verkade, P., & Simons, K. (2006). Alzheimer's disease  $\beta$ -amyloid peptides are released in association with exosomes. *Proceedings of the National Academy of Sciences of the United States of America*, 103(30), 11172–11177. <https://doi.org/10.1073/pnas.0603838103>

- Ramos-Miguel, A., Gicas, K., Alamri, J., Beasley, C. L., Dwork, A. J., Mann, J. J., Rosoklija, G., Cai, F., Song, W., Barr, A. M., & Honer, W. G. (2019). Reduced SNAP25 Protein Fragmentation Contributes to SNARE Complex Dysregulation in Schizophrenia Postmortem Brain. *Neuroscience*, *420*, 112–128. <https://doi.org/10.1016/j.neuroscience.2018.12.015>
- Rangone, H., Pardo, R., Colin, E., Girault, J. A., Saudou, F., & Humbert, S. (2005). Phosphorylation of arfaptin 2 at Ser260 by Akt inhibits PolyQ-huntingtin-induced toxicity by rescuing proteasome impairment. *Journal of Biological Chemistry*, *280*(23), 22021–22028. <https://doi.org/10.1074/jbc.M407528200>
- Rangone, H., Poizat, G., Troncoso, J., Ross, C. A., MacDonald, M. E., Saudou, F., & Humbert, S. (2004). The serum- and glucocorticoid-induced kinase SGK inhibits mutant huntingtin-induced toxicity by phosphorylating serine 421 of huntingtin. *European Journal of Neuroscience*, *19*(2), 273–279. <https://doi.org/10.1111/j.0953-816X.2003.03131.x>
- Raposo, G., & Stoorvogel, W. (2013). Extracellular vesicles: Exosomes, microvesicles, and friends. *Journal of Cell Biology*, *200*(4), 373–383. <https://doi.org/10.1083/jcb.201211138>
- Ratovitski, T., Chighladze, E., Arbez, N., Boronina, T., Herbrich, S., Cole, R. N., & Ross, C. A. (2012). Huntingtin protein interactions altered by polyglutamine expansion as determined by quantitative proteomic analysis. *Cell Cycle*, *11*(10), 2006–2021. <https://doi.org/10.4161/cc.20423>
- Rauti, R., Cellot, G., D'Andrea, P., Colliva, A., Scaini, D., Tongiorgi, E., & Ballerini, L. (2020). BDNF impact on synaptic dynamics: Extra or intracellular long-term release differently regulates cultured hippocampal synapses. *Molecular Brain*, *13*(1), 1–16. <https://doi.org/10.1186/s13041-020-00582-9>
- Rebec, G. V., Conroy, S. K., & Barton, S. J. (2006). Hyperactive striatal neurons in symptomatic Huntington R6/2 mice: Variations with behavioral state and repeated ascorbate treatment. *Neuroscience*, *137*(1), 327–336. <https://doi.org/10.1016/j.neuroscience.2005.08.062>
- Reck-Peterson, S. L., Redwine, W. B., Vale, R. D., & Carter, A. P. (2018). The cytoplasmic dynein transport machinery and its many cargoes. *Nature Reviews Molecular Cell Biology*, *19*(6), 382–398. <https://doi.org/10.1038/s41580-018-0004-3>
- Régnier-Vigouroux, A., Tooze, S. A., & Huttner, W. B. (1991). Newly synthesized synaptophysin is transported to synaptic-like microvesicles via constitutive secretory vesicles and the plasma membrane. *The EMBO Journal*, *10*(12), 3589–3601. <https://doi.org/10.1002/j.1460-2075.1991.tb04925.x>
- Reid, E., Kloos, M., Ashley-Koch, A., Hughes, L., Bevan, S., Svenson, I. K., Graham, F. L., Gaskell, P. C., Dearlove, A., Pericak-Vance, M. A., Rubinsztein, D. C., & Marchuk, D. A. (2002). A kinesin heavy chain (KIF5A) mutation in hereditary spastic paraplegia (SPG10). *American Journal of Human Genetics*, *71*(5), 1189–1194. <https://doi.org/10.1086/344210>
- Rey, S., Marra, V., Smith, C., & Staras, K. (2020). Nanoscale Remodeling of Functional Synaptic Vesicle Pools in Hebbian Plasticity. *Cell Reports*, *30*(6), 2006–2017.e3. <https://doi.org/10.1016/j.celrep.2020.01.051>
- Ricard, J. (2006). CHAPTER 1 Molecular stereospecific recognition and reduction in cell biology. *New Comprehensive Biochemistry*, *40*(PART C), 1–26. [https://doi.org/10.1016/S0167-7306\(05\)40001-0](https://doi.org/10.1016/S0167-7306(05)40001-0)

- Riganti, L., Antonucci, F., Gabrielli, M., Prada, I., Giussani, P., Viani, P., Valtorta, F., Menna, E., Matteoli, M., & Verderio, C. (2016). Sphingosine-1-phosphate (S1P) impacts presynaptic functions by regulating synapsin I localization in the presynaptic compartment. *Journal of Neuroscience*, *36*(16), 4624–4634. <https://doi.org/10.1523/JNEUROSCI.3588-15.2016>
- Rivire, J. B., Ramalingam, S., Lavastre, V., Shekarabi, M., Holbert, S., Lafontaine, J., Srour, M., Merner, N., Rochefort, D., Hince, P., Gaudet, R., Mes-Masson, A. M., Baets, J., Houlden, H., Brais, B., Nicholson, G. A., Van Esch, H., Nafissi, S., De Jonghe, P., ... Rouleau, G. A. (2011). KIF1A, an axonal transporter of synaptic vesicles, is mutated in hereditary sensory and autonomic neuropathy type 2. *American Journal of Human Genetics*, *89*(2), 219–230. <https://doi.org/10.1016/j.ajhg.2011.06.013>
- Rizo, J., & Rosenmund, C. (2008). Synaptic vesicle fusion. *Nature Structural and Molecular Biology*, *15*(7), 665–674. <https://doi.org/10.1038/nsmb.1450>
- Rizzoli, S. O. (2014). Synaptic vesicle recycling: Steps and principles. *EMBO Journal*, *33*(8), 788–822. <https://doi.org/10.1002/embj.201386357>
- Rizzoli, S. O., & Betz, W. J. (2005). Synaptic vesicle pools. *Nature Reviews Neuroscience*, *6*(1), 57–69. <https://doi.org/10.1038/nrn1583>
- Rodan, L. H., Cohen, J., Fatemi, A., Gillis, T., Lucente, D., Gusella, J., & Picker, J. D. (2016). A novel neurodevelopmental disorder associated with compound heterozygous variants in the huntingtin gene. *European Journal of Human Genetics*, *24*(12), 1826–1827. <https://doi.org/10.1038/ejhg.2016.74>
- Rohrbough, J., & Broadie, K. (2005). Lipid regulation of the synaptic vesicle cycle. In *Nature Reviews Neuroscience* (Vol. 6, Issue 2, pp. 139–150). <https://doi.org/10.1038/nrn1608>
- Rosas, H. D., Salat, D. H., Lee, S. Y., Zaleta, A. K., Hevelone, N., & Hersch, S. M. (2008). Complexity and heterogeneity: What drives the ever-changing brain in Huntington's disease? *Annals of the New York Academy of Sciences*, *1147*, 196–205. <https://doi.org/10.1196/annals.1427.034>
- Roux, J.-C., Zala, D., Panayotis, N., Borges-Correia, A., Saudou, F., & Villard, L. (2012). [Unexpected link between Huntington disease and Rett syndrome]. *Medicine Sciences: M/S*, *28*(1), 44–46. <https://doi.org/10.1051/medsci/2012281016>
- Russo, A. F. (2017). Overview of Neuropeptides: Awakening the Senses? *Headache*, *57*, 37–46. <https://doi.org/10.1111/head.13084>
- Rust, M. B., & Maritzen, T. (2015). Relevance of presynaptic actin dynamics for synapse function and mouse behavior. *Experimental Cell Research*, *335*(2), 165–171. <https://doi.org/10.1016/j.yexcr.2014.12.020>
- Rusu, P., Jansen, A., Soba, P., Kirsch, J., Löwer, A., Merdes, G., Kuan, Y. H., Jung, A., Beyreuther, K., Kjaerulf, O., & Kins, S. (2007). Axonal accumulation of synaptic markers in APP transgenic *Drosophila* depends on the NPTY motif and is paralleled by defects in synaptic plasticity. *European Journal of Neuroscience*, *25*(4), 1079–1086. <https://doi.org/10.1111/j.1460-9568.2007.05341.x>
- Ryu, J. K., Jahn, R., & Yoon, T. Y. (2016). Review: Progresses in understanding N-ethylmaleimide sensitive factor (NSF) mediated disassembly of SNARE complexes. *Biopolymers*, *105*(8), 518–531. <https://doi.org/10.1002/bip.22854>

- Sadoul, K., Joubert, C., Michallet, S., Nolte, E., Peronne, L., Ramirez-Rios, S., Ribba, A.-S., & Lafanechère, L. (2018). Déchiffrement du code tubuline. *Médecine/Sciences*, *34*(12), 1047–1055. <https://doi.org/10.1051/medsci/2018295>
- Sahlender, D. A., Roberts, R. C., Arden, S. D., Spudich, G., Taylor, M. J., Luzio, J. P., Kendrick-Jones, J., & Buss, F. (2005). Optineurin links myosin VI to the Golgi complex and is involved in Golgi organization and exocytosis. *Journal of Cell Biology*, *169*(2), 285–295. <https://doi.org/10.1083/jcb.200501162>
- Sahoo, P. K., Smith, D. S., Perrone-Bizzozero, N., & Twiss, J. L. (2018). Axonal mRNA transport and translation at a glance. *Journal of Cell Science*, *131*(8). <https://doi.org/10.1242/jcs.196808>
- Sahu, B. S., Manna, P. T., Edgar, J. R., Antrobus, R., Mahata, S. K., Bartolomucci, A., Borner, G. H. H., & Robinson, M. S. (2017). Role of clathrin in dense core vesicle biogenesis. *Molecular Biology of the Cell*, *28*(20), 2676–2685. <https://doi.org/10.1091/mbc.E16-10-0742>
- Salinas, S., Bilsland, L. G., & Schiavo, G. (2008). Molecular landmarks along the axonal route: axonal transport in health and disease. *Current Opinion in Cell Biology*, *20*(4), 445–453. <https://doi.org/10.1016/j.ceb.2008.04.002>
- Salpietro, V., Malintan, N. T., Llano-Rivas, I., Spaeth, C. G., Efthymiou, S., Striano, P., Vandrovcova, J., Cutrupi, M. C., Chimenz, R., David, E., Di Rosa, G., Marce-Grau, A., Raspall-Chaure, M., Martin-Hernandez, E., Zara, F., Minetti, C., Kriouile, Y., El Khorassani, M., Aguenouz, M., ... Krishnakumar, S. S. (2019). Mutations in the Neuronal Vesicular SNARE VAMP2 Affect Synaptic Membrane Fusion and Impair Human Neurodevelopment. *American Journal of Human Genetics*, *104*(4), 721–730. <https://doi.org/10.1016/j.ajhg.2019.02.016>
- Sámano, C., Cifuentes, F., & Morales, M. A. (2012). Neurotransmitter segregation: Functional and plastic implications. *Progress in Neurobiology*, *97*(3), 277–287. <https://doi.org/10.1016/j.pneurobio.2012.04.004>
- Sampo, B., Kaech, S., Kunz, S., & Banker, G. (2003). Two distinct mechanisms target membrane proteins to the axonal surface. *Neuron*, *37*(4), 611–624. [https://doi.org/10.1016/S0896-6273\(03\)00058-8](https://doi.org/10.1016/S0896-6273(03)00058-8)
- Sandweiss, A. J., Brandt, V. L., & Zoghbi, H. Y. (2020). Advances in understanding of Rett syndrome and MECP2 duplication syndrome: prospects for future therapies. *The Lancet Neurology*, *19*(8), 689–698. [https://doi.org/10.1016/S1474-4422\(20\)30217-9](https://doi.org/10.1016/S1474-4422(20)30217-9)
- Santos, M. S., Li, H., & Voglmaier, S. M. (2009). Synaptic vesicle protein trafficking at the glutamate synapse. *Neuroscience*, *158*(1), 189–203. <https://doi.org/10.1016/j.neuroscience.2008.03.029>
- Saudou, F., & Humbert, S. (2016). The Biology of Huntingtin. *Neuron*, *89*(5), 910–926. <https://doi.org/10.1016/j.neuron.2016.02.003>
- Schaedel, L., John, K., Gaillard, J., Nachury, M. V., Blanchoin, L., & Théry, M. (2015). Microtubules self-repair in response to mechanical stress. *Nature Materials*, *14*(11), 1156–1163. <https://doi.org/10.1038/nmat4396>
- Scheinfeld, M. H., Ghersi, E., Davies, P., & D'Adamio, L. (2003). Amyloid  $\beta$  Protein Precursor Is Phosphorylated by JNK-1 Independent of, yet Facilitated by, JNK-Interacting Protein (JIP)-1. *Journal of Biological Chemistry*, *278*(43), 42058–42063. <https://doi.org/10.1074/jbc.M304853200>

- Schiavo, G., Matteoli, M., & Montecucco, C. (2000). Neurotoxins affecting neuroexocytosis. *Physiological Reviews*, *80*(2), 717–766. <https://doi.org/10.1152/physrev.2000.80.2.717>
- Schikorski, T. (2014). Readily releasable vesicles recycle at the active zone of hippocampal synapses. *Proceedings of the National Academy of Sciences of the United States of America*, *111*(14), 5415–5420. <https://doi.org/10.1073/pnas.1321541111>
- Schikorski, T., & Stevens, C. F. (1997). Quantitative Ultrastructural Analysis of Hippocampal. *J. Neurosci.*, *17*(15), 5858–5867. <https://pdfs.semanticscholar.org/6317/17f04ca52a47f6c909b5e614a4a2afa6c141.pdf>
- Schlager, M. A., & Hoogenraad, C. C. (2009). Basic mechanisms for recognition and transport of synaptic cargos. *Molecular Brain*, *2*(1), 1–12. <https://doi.org/10.1186/1756-6606-2-25>
- Schlüter, O. M., Basu, J., Südhof, T. C., & Rosenmund, C. (2006). Rab3 superprimes synaptic vesicles for release: Implications for short-term synaptic plasticity. *Journal of Neuroscience*, *26*(4), 1239–1246. <https://doi.org/10.1523/JNEUROSCI.3553-05.2006>
- Schmitz, T. W., & Nathan Spreng, R. (2016). Basal forebrain degeneration precedes and predicts the cortical spread of Alzheimer’s pathology. *Nature Communications*, *7*, 1–13. <https://doi.org/10.1038/ncomms13249>
- Schoch, S., Deák, F., Königstorfer, A., Mozhayeva, M., Sara, Y., Südhof, T. C., & Kavalali, E. T. (1999). SNARE Function Analyzed in Synaptobrevin/VAMP Knockout Mice Downloaded from. In *J. Comp. Physiol. A* (Vol. 126, Issue 9). [www.sciencemag.org/SCIENCEVOL294](http://www.sciencemag.org/SCIENCEVOL294)
- Schousboe, A., Scafidi, S., Bak, L. K., Waagepetersen, H. S., & McKenna, M. C. (2014). *Glutamate Metabolism in the Brain Focusing on Astrocytes* (pp. 13–30). [https://doi.org/10.1007/978-3-319-08894-5\\_2](https://doi.org/10.1007/978-3-319-08894-5_2)
- Seal, R. P., & Edwards, R. H. (2006). Functional implications of neurotransmitter co-release: Glutamate and GABA share the load. *Current Opinion in Pharmacology*, *6*(1 SPEC. ISS.), 114–119. <https://doi.org/10.1016/j.coph.2005.12.001>
- Seong, I. S., Woda, J. M., Song, J. J., Lloret, A., Abeyrathne, P. D., Woo, C. J., Gregory, G., Lee, J. M., Wheeler, V. C., Walz, T., Kingston, R. E., Gusella, J. F., Conlon, R. A., & MacDonald, M. E. (2009). Huntingtin facilitates polycomb repressive complex 2. *Human Molecular Genetics*, *19*(4), 573–583. <https://doi.org/10.1093/hmg/ddp524>
- Sgro, A. E., Bajjalieh, S. M., & Chiu, D. T. (2013). Single-axonal organelle analysis method reveals new protein-motor associations. *ACS Chemical Neuroscience*, *4*(2), 277–284. <https://doi.org/10.1021/cn300136y>
- Shan, Q., Ge, M., Christie, M. J., & Balleine, B. W. (2014). The acquisition of goal-directed actions generates opposing plasticity in direct and indirect pathways in dorsomedial striatum. *Journal of Neuroscience*, *34*(28), 9196–9201. <https://doi.org/10.1523/JNEUROSCI.0313-14.2014>
- Shankar, G. M., & Walsh, D. M. (2009). Alzheimer’s disease: Synaptic dysfunction and A $\beta$ . *Molecular Neurodegeneration*, *4*(1), 1–13. <https://doi.org/10.1186/1750-1326-4-48>
- Shashi, V., Magiera, M. M., Klein, D., Zaki, M., Schoch, K., Rudnik-Schöneborn, S., Norman, A., Lopes Abath Neto, O., Dusl, M., Yuan, X., Bartesaghi, L., De Marco, P., Alfares, A. A., Marom, R., Arold, S. T., Guzmán-Vega, F. J., Pena, L. D., Smith, E. C., Steinlin, M., ... Senderek, J. (2018). Loss of

- tubulin deglutamylase CCP 1 causes infantile-onset neurodegeneration. *The EMBO Journal*, 37(23), 1–12. <https://doi.org/10.15252/embj.2018100540>
- Shastry, S., & Hancock, W. O. (2010). Neck Linker Length Determines the Degree of Processivity in Kinesin-1 and Kinesin-2 Motors. *Current Biology*, 20(10), 939–943. <https://doi.org/10.1016/j.cub.2010.03.065>
- Shimizu, H., Kawamura, S., & Ozaki, K. (2003). An essential role of Rab5 in uniformity of synaptic vesicle size. *Journal of Cell Science*, 116(17), 3583–3590. <https://doi.org/10.1242/jcs.00676>
- Shimizu, Y., Morii, H., Arisaka, F., & Tanokura, M. (2005). Stalk region of kinesin-related protein Unc104 has moderate ability to form coiled-coil dimer. *Biochemical and Biophysical Research Communications*, 337(3), 868–874. <https://doi.org/10.1016/j.bbrc.2005.09.126>
- Shimojo, M., Courchet, J., Pieraut, S., Torabi-Rander, N., Sando, R., Polleux, F., & Maximov, A. (2015). SNAREs Controlling Vesicular Release of BDNF and Development of Callosal Axons. *Cell Reports*, 11(7), 1054–1066. <https://doi.org/10.1016/j.celrep.2015.04.032>
- Shin, H., Wyszynski, M., Huh, K. H., Valtschanoff, J. G., Lee, J. R., Ko, J., Streuli, M., Weinberg, R. J., Sheng, M., & Kim, E. (2003). Association of the kinesin motor KIF1A with the multimodular protein liprin- $\alpha$ . *Journal of Biological Chemistry*, 278(13), 11393–11401. <https://doi.org/10.1074/jbc.M211874200>
- Shineman, D. W., Dain, A. S., Kim, M. L., & Lee, V. M. Y. (2009). Constitutively active Akt inhibits trafficking of amyloid precursor protein and amyloid precursor protein metabolites through feedback inhibition of phosphoinositide 3-kinase. *Biochemistry*, 48(17), 3787–3794. <https://doi.org/10.1021/bi802070j>
- Shirasaki, D. I., Greiner, E. R., Al-Ramahi, I., Gray, M., Boontheung, P., Geschwind, D. H., Botas, J., Coppola, G., Horvath, S., Loo, J. A., & Yang, X. W. (2012). Network organization of the huntingtin proteomic interactome in mammalian brain. *Neuron*, 75(1), 41–57. <https://doi.org/10.1016/j.neuron.2012.05.024>
- Sieburth, D., Ch'ng, Q., Dybbs, M., Tavazoie, M., Kennedy, S., Wang, D., Dupuy, D., Rual, J. F., Hill, D. E., Vidal, M., Ruvkun, G., & Kaplan, J. M. (2005). Systematic analysis of genes required for synapse structure and function. *Nature*, 436(7050), 510–516. <https://doi.org/10.1038/nature03809>
- Sigal, N. ., & Dumont, F. . (1992). CYCLOSPORIN A, FK-506, and rapamycin: Pharmacologic Probes of Lymphocyte Signal Transduction. *Annual Reviews Immunology*, 10, 519–560.
- Simmons, D. A., Rex, C. S., Palmer, L., Pandeyarajan, V., Fedulov, V., Gall, C. M., & Lynch, G. (2009). Up-regulating BDNF with an ampakine rescues synaptic plasticity and memory in Huntington ' s disease knockin mice. 106(12).
- Sinha, R., Ahmed, S., Jahn, R., & Klingauf, J. (2011). Two synaptobrevin molecules are sufficient for vesicle fusion in central nervous system synapses. *Proceedings of the National Academy of Sciences of the United States of America*, 108(34), 14318–14323. <https://doi.org/10.1073/pnas.1101818108>
- Skorobogatko, Y., Landicho, A., Chalkley, R. J., Kossenkov, A. V., Gallo, G., & Vosseller, K. (2014). O-Linked  $\beta$ -N-Acetylglucosamine (O-GlcNAc) site Thr-87 Regulates Synapsin I localization to Synapses and size of the reserve pool of synaptic vesicles. *Journal of Biological Chemistry*, 289(6), 3602–3612. <https://doi.org/10.1074/jbc.M113.512814>

- Smith, R., Brundin, P., & Li, J. Y. (2005). Synaptic dysfunction in Huntington's disease: A new perspective. *Cellular and Molecular Life Sciences*, 62(17), 1901–1912. <https://doi.org/10.1007/s00018-005-5084-5>
- Smith, Ruben, Petersén, Å., Bates, G. P., Brundin, P., & Li, J. Y. (2005). Depletion of rabphilin 3A in a transgenic mouse model (R6/1) of Huntington's disease, a possible culprit in synaptic dysfunction. *Neurobiology of Disease*, 20(3), 673–684. <https://doi.org/10.1016/j.nbd.2005.05.008>
- Snyder, J. M., Hagan, C. E., Bolon, B., & Keene, C. D. (2018). 20. Nervous System. In *Comparative Anatomy and Histology*. Elsevier Inc. <https://doi.org/10.1016/B978-0-12-802900-8.00020-8>
- Song, Y. H., & Mandelkow, E. (1993). Recombinant kinesin motor domain binds to  $\beta$ -tubulin and decorates microtubules with a B surface lattice. *Proceedings of the National Academy of Sciences of the United States of America*, 90(5), 1671–1675. <https://doi.org/10.1073/pnas.90.5.1671>
- Soppina, V., Norris, S. R., Dizaji, A. S., Kortus, M., Veatch, S., Peckham, M., & Verhey, K. J. (2014). Dimerization of mammalian kinesin-3 motors results in superprocessive motion. *Proceedings of the National Academy of Sciences of the United States of America*, 111(15), 5562–5567. <https://doi.org/10.1073/pnas.1400759111>
- Soppina, V., Rai, A. K., Ramaiya, A. J., Barak, P., & Mallik, R. (2009). Tug-of-war between dissimilar teams of microtubule motors regulates transport and fission of endosomes. *Proceedings of the National Academy of Sciences of the United States of America*, 106(46), 19381–19386. <https://doi.org/10.1073/pnas.0906524106>
- Soppina, V., & Verhey, K. J. (2014). The family-specific K-loop influences the microtubule on-rate but not the superprocessivity of kinesin-3 motors. *Molecular Biology of the Cell*, 25(14), 2161–2170. <https://doi.org/10.1091/mbc.E14-01-0696>
- Soukup, S., Vanhauwaert, R., & Verstreken, P. (2018). Parkinson's disease: convergence on synaptic homeostasis. *The EMBO Journal*, 37(18), 1–16. <https://doi.org/10.15252/embj.201898960>
- Southwell, A. L., Kordasiewicz, H. B., Langbehn, D., Skotte, N. H., Parsons, M. P., Villanueva, E. B., Caron, N. S., Ostergaard, M. E., Anderson, L. M., Xie, Y., Cengio, L. D., Findlay-Black, H., Doty, C. N., Fitsimmons, B., Swayze, E. E., Seth, P. P., Raymond, L. A., Bennett, C. F., & Hayden, M. R. (2018). Huntingtin suppression restores cognitive function in a mouse model of Huntington's disease. *Science Translational Medicine*, 10(461), 1–13. <https://doi.org/10.1126/scitranslmed.aar3959>
- Spiwoks-Becker, I., Vollrath, L., Seeliger, M. W., Jaissle, G., Eshkind, L. G., & Leube, R. E. (2001). *SYNAPTIC VESICLE ALTERATIONS IN ROD PHOTORECEPTORS OF SYNAPTOPHYSIN-DEFICIENT MICE*. [www.neuroscience-ibro.com](http://www.neuroscience-ibro.com)
- Staras, K., Branco, T., Burden, J. J., Pozo, K., Darcy, K., Marra, V., Ratnayaka, A., & Goda, Y. (2010). A Vesicle Superpool Spans Multiple Presynaptic Terminals in Hippocampal Neurons. *Neuron*, 66(1), 37–44. <https://doi.org/10.1016/j.neuron.2010.03.020>
- Stavoe, A. K. H., Hill, S. E., Hall, D. H., & Colón-Ramos, D. A. (2016). KIF1A/UNC-104 Transports ATG-9 to Regulate Neurodevelopment and Autophagy at Synapses. *Developmental Cell*, 38(2), 171–185. <https://doi.org/10.1016/j.devcel.2016.06.012>
- Stenmark, H. (2009). Rab GTPases as coordinators of vesicle traffic. *Nature Reviews Molecular Cell Biology*, 10(8), 513–525. <https://doi.org/10.1038/nrm2728>

- Stevens, C. ., & Sullivan, J. . (1998). Regulation of the Readily Releasable Vesicle Pool by Protein Kinase C. *Neuron*, *21*, 885–893.
- Steward, O. (1997). mRNA localization in neurons: A multipurpose mechanism? *Neuron*, *18*(1), 9–12. [https://doi.org/10.1016/S0896-6273\(01\)80041-6](https://doi.org/10.1016/S0896-6273(01)80041-6)
- Stokin, G. B., Lillo, C., Falzone, T. L., Bruschi, R. G., Rockenstein, E., Mount, S. L., Raman, R., Davies, P., Masliah, E., Williams, D. S., & Goldstein, L. S. B. (2005). Axonopathy and transport deficits early in the pathogenesis of Alzheimer's diseases. *Science*, *307*(5713), 1282–1288. <https://doi.org/10.1126/science.1105681>
- Stuber, G. D., Hnasko, T. S., Britt, J. P., Edwards, R. H., & Bonci, A. (2010). Dopaminergic terminals in the nucleus accumbens but not the dorsal striatum corelease glutamate. *Journal of Neuroscience*, *30*(24), 8229–8233. <https://doi.org/10.1523/JNEUROSCI.1754-10.2010>
- Stucchi, R., Plucińska, G., Hummel, J. J. A., Zahavi, E. E., Guerra San Juan, I., Klykov, O., Scheltema, R. A., Altelaar, A. F. M., & Hoogenraad, C. C. (2018). Regulation of KIF1A-Driven Dense Core Vesicle Transport: Ca<sup>2+</sup>/CaM Controls DCV Binding and Liprin- $\alpha$ /TANC2 Recruits DCVs to Postsynaptic Sites. *Cell Reports*, *24*(3), 685–700. <https://doi.org/10.1016/j.celrep.2018.06.071>
- Styr, B., & Slutsky, I. (2018). Imbalance between firing homeostasis and synaptic plasticity drives early-phase Alzheimer's disease. *Nature Neuroscience*, *21*(4), 463–473. <https://doi.org/10.1038/s41593-018-0080-x>
- Südhof, T. C. (2013). A molecular machine for neurotransmitter release: Synaptotagmin and beyond. *Nature Medicine*, *19*(10), 1227–1231. <https://doi.org/10.1038/nm.3338>
- Szodorai, A., Kuan, Y. H., Hunzelmann, S., Engel, U., Sakane, A., Sasaki, T., Takai, Y., Kirsch, J., Müller, U., Beyreuther, K., Brady, S., Morfini, G., & Kins, S. (2009). APP anterograde transport requires Rab3A GTPase activity for assembly of the transport vesicle. *Journal of Neuroscience*, *29*(46), 14534–14544. <https://doi.org/10.1523/JNEUROSCI.1546-09.2009>
- Szpankowski, L., Encalada, S. E., & Goldstein, L. S. B. (2012). Subpixel colocalization reveals amyloid precursor protein-dependent kinesin-1 and dynein association with axonal vesicles. *Proceedings of the National Academy of Sciences of the United States of America*, *109*(22), 8582–8587. <https://doi.org/10.1073/pnas.1120510109>
- Tabrizi, S. J., Ghosh, R., & Leavitt, B. R. (2019). Huntingtin Lowering Strategies for Disease Modification in Huntington's Disease. *Neuron*, *101*(5), 801–819. <https://doi.org/10.1016/j.neuron.2019.01.039>
- Tabrizi, S. J., Leavitt, B. R., Landwehrmeyer, G. B., Wild, E. J., Saft, C., Barker, R. A., Blair, N. F., Craufurd, D., Priller, J., Rickards, H., Rosser, A., Kordasiewicz, H. B., Czech, C., Swayze, E. E., Norris, D. A., Baumann, T., Gerlach, I., Schobel, S. A., Paz, E., ... Lane, R. M. (2019). Targeting huntingtin expression in patients with Huntington's disease. *New England Journal of Medicine*, *380*(24), 2307–2316. <https://doi.org/10.1056/NEJMoa1900907>
- Takamori, S., Rhee, J. S., Rosenmund, C., & Jahn, R. (2001). Identification of differentiation-associated brain-specific phosphate transporter as a second vesicular glutamate transporter (VGLUT2). *The Journal of Neuroscience: The Official Journal of the Society for Neuroscience*, *21*(22), 1–6. <https://doi.org/10.1523/jneurosci.21-22-j0002.2001>
- Takamori, Shigeo, Holt, M., Stenius, K., Lemke, E. A., Grønborg, M., Riedel, D., Urlaub, H., Schenck, S.,



- Brügger, B., Ringler, P., Müller, S. A., Rammner, B., Gräter, F., Hub, J. S., De Groot, B. L., Mieskes, G., Moriyama, Y., Klingauf, J., Grubmüller, H., ... Jahn, R. (2006). Molecular Anatomy of a Trafficking Organelle. *Cell*, *127*(4), 831–846. <https://doi.org/10.1016/j.cell.2006.10.030>
- Tan, J. Z. A., & Gleeson, P. A. (2019). The role of membrane trafficking in the processing of amyloid precursor protein and production of amyloid peptides in Alzheimer's disease. *Biochimica et Biophysica Acta - Biomembranes*, *1861*(4), 697–712. <https://doi.org/10.1016/j.bbamem.2018.11.013>
- Tanaka, Y., Niwa, S., Dong, M., Farkhondeh, A., Wang, L., Zhou, R., & Hirokawa, N. (2016). The Molecular Motor KIF1A Transports the TrkA Neurotrophin Receptor and Is Essential for Sensory Neuron Survival and Function. *Neuron*, *90*(6), 1215–1229. <https://doi.org/10.1016/j.neuron.2016.05.002>
- Tani, H., Dulla, C. G., Farzampour, Z., Taylor-Weiner, A., Huguenard, J. R., & Reimer, R. J. (2014). A local glutamate-glutamine cycle sustains synaptic excitatory transmitter release. *Neuron*, *81*(4), 888–900. <https://doi.org/10.1016/j.neuron.2013.12.026>
- Tarrade, A., Fassier, C., Courageot, S., Charvin, D., Vitte, J., Peris, L., Thorel, A., Mouisel, E., Fonknechten, N., Roblot, N., Seilhean, D., Diérich, A., Hauw, J. J., & Melki, J. (2006). A mutation of spastin is responsible for swellings and impairment of transport in a region of axon characterized by changes in microtubule composition. *Human Molecular Genetics*, *15*(24), 3544–3558. <https://doi.org/10.1093/hmg/ddl431>
- Tarrant, M. K., & Cole, P. A. (2009). *The Chemical Biology of Protein Phosphorylation*. <https://doi.org/10.1146/annurev.biochem.78.070907.103047>
- Taruno, A., Ohmori, H., & Kuba, H. (2012). Inhibition of presynaptic Na<sup>+</sup>/K<sup>+</sup>-ATPase reduces readily releasable pool size at the avian end-bulb of Held synapse. *Neuroscience Research*, *72*(2), 117–128. <https://doi.org/10.1016/j.neures.2011.11.003>
- Tas, R. P., Chazeau, A., Cloin, B. M. C., Lambers, M. L. A., Hoogenraad, C. C., & Kapitein, L. C. (2017). Differentiation between Oppositely Oriented Microtubules Controls Polarized Neuronal Transport. *Neuron*, *96*(6), 1264-1271.e5. <https://doi.org/10.1016/j.neuron.2017.11.018>
- Taylor, A. M., Blurton-Jones, M., Rhee, S. W., Cribbs, D. H., Cotman, C. W., & Jeon, N. L. (2005). A microfluidic culture platform for CNS axonal injury, regeneration and transport. *Nature Methods*, *2*(8), 599–605. <https://doi.org/10.1038/nmeth777>
- Taylor, A. M., Dieterich, D. C., Ito, H. T., Kim, S. A., & Schuman, E. M. (2010). Microfluidic Local Perfusion Chambers for the Visualization and Manipulation of Synapses. *Neuron*, *66*(1), 57–68. <https://doi.org/10.1016/j.neuron.2010.03.022>
- Thanawala, M. S., & Regehr, W. G. (2013). Presynaptic calcium influx controls neurotransmitter release in part by regulating the effective size of the readily releasable pool. *Journal of Neuroscience*, *33*(11), 4625–4633. <https://doi.org/10.1523/JNEUROSCI.4031-12.2013>
- Thanawala, M. S., & Regehr, W. G. (2016). Determining synaptic parameters using high-frequency activation. *Journal of Neuroscience Methods*, *264*, 136–152. <https://doi.org/10.1016/j.jneumeth.2016.02.021>
- Thiele, C., Hannah, M. J., Fahrenholz, F., & Huttner, W. B. (2000). Cholesterol binds to synaptophysin and is required for biogenesis of synaptic vesicles. In *NATURE CELL BIOLOGY* (Vol. 2).

- Thinakaran, G., & Koo, E. H. (2008). Amyloid precursor protein trafficking, processing, and function. *Journal of Biological Chemistry*, *283*(44), 29615–29619. <https://doi.org/10.1074/jbc.R800019200>
- Thion, M. S., McGuire, J. R., Sousa, C. M., Fuhrmann, L., Fitamant, J., Leboucher, S., Vacher, S., Du Montcel, S. T., Bièche, I., Bernet, A., Mehlen, P., Vincent-Salomon, A., & Humbert, S. (2015). Unraveling the Role of Huntingtin in Breast Cancer Metastasis. *Journal of the National Cancer Institute*, *107*(10), 1–13. <https://doi.org/10.1093/jnci/djv208>
- Thomas, L., Hartung, K., Langosch, D., Rehm, H., Bamberg, E., Franke, W. W., & Betz, H. (1988). Identification of Synaptophysin as a Hexameric. *Science*, *242*, 1050–1053.
- Thomson, A. M. (2000). Facilitation, augmentation and potentiation at central synapses. *Trends in Neurosciences*, *23*, 305–312.
- Ting, L., Lu, H., Yen, S., Ngo, T. H., Tu, F., Tsai, I., & Tsai, Y. (2019). Expression of *AH11* Rescues Amyloidogenic Pathology in Alzheimer's Disease Model Cells. 7572–7582.
- Tomishige, M., Klopfenstein, D. R., & Vale, R. D. (2002). Conversion of Unc104/KIF1A kinesin into a processive motor after dimerization. *Science*, *297*(5590), 2263–2267. <https://doi.org/10.1126/science.1073386>
- Tonegawa, S., Morrissey, M. D., & Kitamura, T. (2018). The role of engram cells in the systems consolidation of memory. *Nature Reviews Neuroscience*, *19*(8), 485–498. <https://doi.org/10.1038/s41583-018-0031-2>
- Toshiyuki, N., Hong, Z., Nobuhiro, M., En, L., Jin, X., Bruce, A. Y., & Junying, Y. (2000). Caspase-12 mediates endoplasmic reticulum specific apoptosis and cytotoxicity by amyloid- $\beta$ . *Nature*, *403*(January), 98–103.
- Triaca, V., Sposato, V., Bolasco, G., Ciotti, M. T., Pelicci, P., Bruni, A. C., Cupidi, C., Maletta, R., Feligioni, M., Nisticò, R., Canu, N., & Calissano, P. (2016). NGF controls APP cleavage by downregulating APP phosphorylation at Thr668: relevance for Alzheimer's disease. *Aging Cell*, *15*(4), 661–672. <https://doi.org/10.1111/acel.12473>
- Tropea, D., Giacometti, E., Wilson, N. R., Beard, C., McCurry, C., Dong, D. F., Flannery, R., Jaenisch, R., & Sur, M. (2009). Partial reversal of Rett Syndrome-like symptoms in MeCP2 mutant mice. *Proceedings of the National Academy of Sciences of the United States of America*, *106*(6), 2029–2034. <https://doi.org/10.1073/pnas.0812394106>
- Truckenbrodt, S., Viplav, A., Jähne, S., Vogts, A., Denker, A., Wildhagen, H., Fornasiero, E. F., & Rizzoli, S. O. (2018). Newly produced synaptic vesicle proteins are preferentially used in synaptic transmission. *The EMBO Journal*, *37*(15), 1–24. <https://doi.org/10.15252/embj.201798044>
- Trudeau, L. , & Gutiérrez, R. (2007). On cotransmission & neurotransmitter phenotype plasticity. *Molecular Interventions*, *7*(3), 138–146.
- Tucker, W. C., Weber, T., & Chapman, E. R. (2004). Reconstitution of Ca<sup>2+</sup>-Regulated Membrane Fusion by Synaptotagmin and SNAREs. *Science*, *304*(5669), 435–438. <https://doi.org/10.1126/science.1097196>
- Turrigiano, G. (2012). Homeostatic synaptic plasticity: Local and global mechanisms for stabilizing neuronal function. *Cold Spring Harbor Perspectives in Biology*, *4*(1), 1–18. <https://doi.org/10.1101/cshperspect.a005736>

- Turrigiano, G. G. (1999). Homeostatic plasticity in neuronal networks: The more things change, the more they stay the same. *Trends in Neurosciences*, 22(5), 221–227. [https://doi.org/10.1016/S0166-2236\(98\)01341-1](https://doi.org/10.1016/S0166-2236(98)01341-1)
- Turrigiano, G. G. (2017). The dialectic of hebb and homeostasis. *Philosophical Transactions of the Royal Society B: Biological Sciences*, 372(1715), 4–6. <https://doi.org/10.1098/rstb.2016.0258>
- Twelvetrees, A. E., Yuen, E. Y., Arancibia-Carcamo, I. L., MacAskill, A. F., Rostaing, P., Lumb, M. J., Humbert, S., Triller, A., Saudou, F., Yan, Z., & Kittler, J. T. (2010). Delivery of GABAARs to Synapses Is Mediated by HAP1-KIF5 and Disrupted by Mutant Huntingtin. *Neuron*, 65(1), 53–65. <https://doi.org/10.1016/j.neuron.2009.12.007>
- Tyler, W. J., & Pozzo-Miller, L. D. (2001). BDNF enhances quantal neurotransmitter release and increases the number of docked vesicles at the active zones of hippocampal excitatory synapses. *Journal of Neuroscience*, 21(12), 4249–4258. <https://doi.org/10.1523/jneurosci.21-12-04249.2001>
- Tyler, William J., Zhang, X. L., Hartman, K., Winterer, J., Muller, W., Stanton, P. K., & Pozzo-Miller, L. (2006). BDNF increases release probability and the size of a rapidly recycling vesicle pool within rat hippocampal excitatory synapses. *Journal of Physiology*, 574(3), 787–803. <https://doi.org/10.1113/jphysiol.2006.111310>
- Umeda, T., Ramser, E. M., Yamashita, M., Nakajima, K., Mori, H., Silverman, M. A., & Tomiyama, T. (2015). Intracellular amyloid  $\beta$  oligomers impair organelle transport and induce dendritic spine loss in primary neurons. *Acta Neuropathologica Communications*, 3, 51. <https://doi.org/10.1186/s40478-015-0230-2>
- Vagnoni, A., Perkinson, M. S., Gray, E. H., Francis, P. T., Noble, W., & Miller, C. C. J. (2012). Calsyntenin-1 mediates axonal transport of the amyloid precursor protein and regulates  $\alpha\beta$  production. *Human Molecular Genetics*, 21(13), 2845–2854. <https://doi.org/10.1093/hmg/dds109>
- Vale, R. D. (2003). The molecular motor toolbox for intracellular transport. *Cell*, 112(4), 467–480. [https://doi.org/10.1016/S0092-8674\(03\)00111-9](https://doi.org/10.1016/S0092-8674(03)00111-9)
- Vale, R. D., & Milligan, R. A. (2000). The way things move: Looking under the hood of molecular motor proteins. *Science*, 288(5463), 88. <https://doi.org/10.1126/science.288.5463.88>
- Valenzuela, J. I., Jaureguierry-Bravo, M., Salas, D. A., Ramírez, O. A., Cornejo, V. H., Lu, H. E., Blanpied, T. A., & Couve, A. (2014). Transport along the dendritic endoplasmic reticulum mediates the trafficking of GABAB receptors. *Journal of Cell Science*, 127(15), 3382–3395. <https://doi.org/10.1242/jcs.151092>
- Valtorta, F., Pennuto, M., Bonanomi, D., & Benfenati, F. (2004). Synaptophysin: Leading actor or walk-on role in synaptic vesicle exocytosis? *BioEssays*, 26(4), 445–453. <https://doi.org/10.1002/bies.20012>
- Van Asselen, M., Almeida, I., Júlio, F., Januário, C., Campos, E. B., Simões, M., & Castelo-Branco, M. (2012). Implicit contextual learning in prodromal and early stage Huntington's disease patients. *Journal of the International Neuropsychological Society*, 18(4), 689–696. <https://doi.org/10.1017/S1355617712000288>
- Van Dam, P. S., & Aleman, A. (2004). Insulin-like growth factor-I, cognition and brain aging. *European Journal of Pharmacology*, 490(1–3), 87–95. <https://doi.org/10.1016/j.ejphar.2004.02.047>

- Van Den Bogaart, G., Holt, M. G., Bunt, G., Riedel, D., Wouters, F. S., & Jahn, R. (2010). One SNARE complex is sufficient for membrane fusion. *Nature Structural and Molecular Biology*, *17*(3), 358–364. <https://doi.org/10.1038/nsmb.1748>
- Van Esch, H. (2012). MECP2 duplication syndrome. *Molecular Syndromology*, *2*(3–5), 128–136. <https://doi.org/10.1159/000329580>
- Varoqueaux, F., Sigler, A., Rhee, J. S., Brose, N., Enk, C., Reim, K., & Rosenmund, C. (2002). Total arrest of spontaneous and evoked synaptic transmission but normal synaptogenesis in the absence of Munc13-mediated vesicle priming. *Proceedings of the National Academy of Sciences of the United States of America*, *99*(13), 9037–9042. <https://doi.org/10.1073/pnas.122623799>
- Vassilopoulos, S., Gibaud, S., Jimenez, A., Caillol, G., & Leterrier, C. (2019). Ultrastructure of the axonal periodic scaffold reveals a braid-like organization of actin rings. *Nature Communications*, *10*(1), 1–13. <https://doi.org/10.1038/s41467-019-13835-6>
- Venkatramani, A., & Panda, D. (2019). Regulation of neuronal microtubule dynamics by tau: Implications for tauopathies. *International Journal of Biological Macromolecules*, *133*, 473–483. <https://doi.org/10.1016/j.ijbiomac.2019.04.120>
- Verhey, K. J., & Gaertig, J. (2007). The tubulin code. *Cell Cycle*, *6*(17), 2152–2160. <https://doi.org/10.4161/cc.6.17.4633>
- Verhey, K. J., & Hammond, J. W. (2009). Traffic control: Regulation of kinesin motors. *Nature Reviews Molecular Cell Biology*, *10*(11), 765–777. <https://doi.org/10.1038/nrm2782>
- Verkhatsky, A., Matteoli, M., Parpura, V., Mothet, J., & Zorec, R. (2016). Astrocytes as secretory cells of the central nervous system: idiosyncrasies of vesicular secretion. *The EMBO Journal*, *35*(3), 239–257. <https://doi.org/10.15252/embj.201592705>
- Verret, L., Mann, E. O., Hang, G. B., Barth, A. M. I., Cobos, I., Ho, K., Devidze, N., Masliah, E., Kreitzer, A. C., Mody, I., Mucke, L., & Palop, J. J. (2012). Inhibitory interneuron deficit links altered network activity and cognitive dysfunction in alzheimer model. *Cell*, *149*(3), 708–721. <https://doi.org/10.1016/j.cell.2012.02.046>
- Vijayvargia, R., Epand, R., Leitner, A., Jung, T., Shin, B., Jung, R., Lloret, A., Atwal, R. S., Lee, H., Lee, J., Aebersold, R., & Hebert, H. (2016). *Huntingtin 's spherical solenoid structure enables polyglutamine tract-dependent modulation of its structure and function.* 1–16. <https://doi.org/10.7554/eLife.11184>
- Villar, A. J., Belichenko, P. V., Gillespie, A. M., Kozy, H. M., Mobley, W. C., & Epstein, C. J. (2005). Identification and characterization of a new Down syndrome model, Ts[Rb(12.1716)]2Cje, resulting from a spontaneous Robertsonian fusion between T(1716)65Dn and mouse Chromosome 12. *Mammalian Genome*, *16*(2), 79–90. <https://doi.org/10.1007/s00335-004-2428-7>
- Virlogeux, A., Moutaux, E., Christaller, W., Charlot, B., & Bruye, J. (2018). *Reconstituting Corticostriatal Network on-a-Chip Reveals the Contribution of the Presynaptic Compartment to Huntington 's Disease Article Reconstituting Corticostriatal Network on-a-Chip Reveals the Contribution of the Presynaptic Compartment to Huntingt.* 110–122. <https://doi.org/10.1016/j.celrep.2017.12.013>
- Vitet, H., Brandt, V., & Saudou, F. (2020). Traffic signaling: new functions of huntingtin and axonal transport in neurological disease. *Current Opinion in Neurobiology*, *63*.

<https://doi.org/10.1016/j.conb.2020.04.001>

- Vonsattel, J. P., Myers, R. H., Stevens, T. J., Ferrante, R. J., Bird, E. D., & Richardson, E. P. (1985). Neuropathological classification of huntington's disease. *Journal of Neuropathology and Experimental Neurology*, *44*(6), 559–577. <https://doi.org/10.1097/00005072-198511000-00003>
- Vossel, K. A., Beagle, A. J., Rabinovici, G. D., Shu, H., Lee, S. E., Naasan, G., Hegde, M., Cornes, S. B., Henry, M. L., Nelson, A. B., Seeley, W. W., Geschwind, M. D., Gorno-Tempini, M. L., Shih, T., Kirsch, H. E., Garcia, P. A., Miller, B. L., & Mucke, L. (2013). Seizures and epileptiform activity in the early stages of Alzheimer disease. *JAMA Neurology*, *70*(9), 1158–1166. <https://doi.org/10.1001/jamaneurol.2013.136>
- Wagner, E. F., & Nebreda, Á. R. (2009). Signal integration by JNK and development. *Nature Publishing Group*. <https://doi.org/10.1038/nrc2694>
- Wagner, O. I., Esposito, A., Köhler, B., Chen, C. W., Shen, C. P., Wu, G. H., Butkevich, E., Mandalapu, S., Wenzel, D., Wouters, F. S., & Klopfenstein, D. R. (2009). Synaptic scaffolding protein SYD-2 clusters and activates kinesin-3 UNC-104 in *C. elegans*. *Proceedings of the National Academy of Sciences of the United States of America*, *106*(46), 19605–19610. <https://doi.org/10.1073/pnas.0902949106>
- Walter, W. J., Beránek, V., Fischermeier, E., & Diez, S. (2012). Tubulin Acetylation alone does not affect kinesin-1 velocity and run length in vitro. *PLoS ONE*, *7*(8), 1–5. <https://doi.org/10.1371/journal.pone.0042218>
- Wang, H., Megill, A., He, K., Kirkwood, A., & Lee, H. K. (2012). Consequences of inhibiting amyloid precursor protein processing enzymes on synaptic function and plasticity. *Neural Plasticity*, *2012*. <https://doi.org/10.1155/2012/272374>
- Wang, Y., & Tang, B. L. (2006). SNAREs in neurons - Beyond synaptic vesicle exocytosis (review). *Molecular Membrane Biology*, *23*(5), 377–384. <https://doi.org/10.1080/09687860600776734>
- Warby, S. C., Chan, E. Y., Metzler, M., Gan, L., Singaraja, R. R., Crocker, S. F., Robertson, H. A., & Hayden, M. R. (2005). Huntingtin phosphorylation on serine 421 is significantly reduced in the striatum and by polyglutamine expansion in vivo. *Human Molecular Genetics*, *14*(11), 1569–1577. <https://doi.org/10.1093/hmg/ddi165>
- Warby, S. C., Doty, C. N., Graham, R. K., Shively, J., Singaraja, R. R., & Hayden, M. R. (2009). Phosphorylation of huntingtin reduces the accumulation of its nuclear fragments. *Molecular and Cellular Neuroscience*, *40*(2), 121–127. <https://doi.org/10.1016/j.mcn.2008.09.007>
- Washbourne, P., Schiavo, G., & Montecucco, C. (1995). Vesicle-associated membrane protein-2 (synaptobrevin-2) forms a complex with synaptophysin. *Biochemical Journal*, *305*(3), 721–724. <https://doi.org/10.1042/bj3050721>
- Washbourne, Philip, Thompson, P. M., Carta, M., Costa, E. T., Mathews, J. R., Lopez-Bendito, G., Molnár, Z., Becher, M. W., Valenzuela, C. F., Partridge, L. D., & Wilson, M. C. (2002). Genetic ablation of the t-SNARE SNAP-25 distinguishes mechanisms of neuroexocytosis. *Nature Neuroscience*, *5*(1), 19–26. <https://doi.org/10.1038/nn783>
- Washburn, C. L., Bean, J. E., Silverman, M. A., Pellegrino, M. J., Yates, P. A., & Allen, R. G. (2002). Regulation of peptidergic vesicle mobility by secretagogues. *Traffic*, *3*(11), 801–809. <https://doi.org/10.1034/j.1600-0854.2002.31105.x>

- Weingarten, J., Weingarten, M., Wegner, M., & Volkandt, W. (2017). APP—A novel player within the presynaptic active zone proteome. *Frontiers in Molecular Neuroscience*, *10*(February), 1–6. <https://doi.org/10.3389/fnmol.2017.00043>
- Weiss, K. R., & Littleton, J. T. (2016). Characterization of axonal transport defects in *Drosophila* Huntingtin mutants. *Journal of Neurogenetics*, *30*(3–4), 212–221. <https://doi.org/10.1080/01677063.2016.1202950>
- Weissman, L., de Souza-Pinto, N. C., Stevnsner, T., & Bohr, V. A. (2007). DNA repair, mitochondria, and neurodegeneration. *Neuroscience*, *145*(4), 1318–1329. <https://doi.org/10.1016/j.neuroscience.2006.08.061>
- Wen, H., Linhoff, M. W., McGinley, M. J., Li, G. L., Corson, G. M., Mandel, G., & Brehm, P. (2010). Distinct roles for two synaptotagmin isoforms in synchronous and asynchronous transmitter release at zebrafish neuromuscular junction. *Proceedings of the National Academy of Sciences of the United States of America*, *107*(31), 13906–13911. <https://doi.org/10.1073/pnas.1008598107>
- Werneburg, S., Feinberg, P. A., Johnson, K. M., & Schafer, D. P. (2017). A microglia-cytokine axis to modulate synaptic connectivity and function. *Current Opinion in Neurobiology*, *47*, 138–145. <https://doi.org/10.1016/j.conb.2017.10.002>
- Westhead, E. W. (1987). Lipid Composition and Orientation in Secretory Vesicles. *Annals of the New York Academy of Sciences*, *493*(1), 92–100. <https://doi.org/10.1111/j.1749-6632.1987.tb27186.x>
- Weyer, S. W., Zagrebelsky, M., Herrmann, U., Hick, M., Ganss, L., Gobbert, J., Gruber, M., Altmann, C., Korte, M., Deller, T., & Müller, U. C. (2014). *Comparative analysis of single and combined APP / APLP knockouts reveals reduced spine density in APP-KO mice that is prevented by APPs  $\alpha$  expression*. 1–15.
- White, J. A., Anderson, E., Zimmerman, K., Zheng, K. H., Rouhani, R., & Gunawardena, S. (2015). Huntingtin differentially regulates the axonal transport of a sub-set of Rab-containing vesicles in vivo. *Human Molecular Genetics*, *24*(25), 7182–7195. <https://doi.org/10.1093/hmg/ddv415>
- White, J. Ag. then diffuses back into neurons where it is hydrolyzed by the phosphate-activated-glutaminase (PAG) into glutamate within mitochondria localized close to a synapse, Krzystek, T. J., Hoffmar-glennon, H., Thant, C., Zimmerman, K., Iacobucci, G., Vail, J., Thurston, L., Rahman, S., & Gunawardena, S. (2020). *Excess Rab4 rescues synaptic and behavioral dysfunction caused by defective HTT-Rab4 axonal transport in Huntington ' s disease*. 1–22.
- Wilson, C. . (1995). The contribution of cortical neurons to the firing pattern of striatal spiny neurons. *Models of Information Processing in the Basal Ganglia*, Davies and Beiser, 29–50.
- Wioland, H., Guichard, B., Senju, Y., Myram, S., Lappalainen, P., Jégou, A., & Romet-Lemonne, G. (2017). ADF/Cofilin Accelerates Actin Dynamics by Severing Filaments and Promoting Their Depolymerization at Both Ends. *Current Biology*, *27*(13), 1956-1967.e7. <https://doi.org/10.1016/j.cub.2017.05.048>
- Wisco, D., Anderson, E. D., Chang, M. C., Norden, C., Boiko, T., Fölsch, H., & Winckler, B. (2003). Uncovering multiple axonal targeting pathways in hippocampal neurons. *Journal of Cell Biology*, *162*(7), 1317–1328. <https://doi.org/10.1083/jcb.200307069>
- Wong, Y. C., & Holzbaur, E. L. F. (2014). *The Regulation of Autophagosome Dynamics by Huntingtin and HAP1 Is Disrupted by Expression of Mutant Huntingtin , Leading to Defective Cargo Degradation*.

34(4), 1293–1305. <https://doi.org/10.1523/JNEUROSCI.1870-13.2014>

- Woodruff, G., Reyna, S. M., Dunlap, M., Van Der Kant, R., Callender, J. A., Young, J. E., Roberts, E. A., & Goldstein, L. S. B. (2016). Defective Transcytosis of APP and Lipoproteins in Human iPSC-Derived Neurons with Familial Alzheimer's Disease Mutations. *Cell Reports*, *17*(3), 759–773. <https://doi.org/10.1016/j.celrep.2016.09.034>
- Wu, G. H., Muthaiyan Shanmugam, M., Bhan, P., Huang, Y. H., & Wagner, O. I. (2016). Identification and Characterization of LIN-2(CASK) as a Regulator of Kinesin-3 UNC-104(KIF1A) Motility and Clustering in Neurons. *Traffic*, *17*(8), 891–907. <https://doi.org/10.1111/tra.12413>
- Wu, Y. E., Huo, L., Maeder, C. I., Feng, W., & Shen, K. (2013). The Balance between Capture and Dissociation of Presynaptic Proteins Controls the Spatial Distribution of Synapses. *Neuron*, *78*(6), 994–1011. <https://doi.org/10.1016/j.neuron.2013.04.035>
- Wu, Y., O'Toole, E. T., Girard, M., Ritter, B., Messa, M., Liu, X., McPherson, P. S., Ferguson, S. M., & De Camilli, P. (2014). A dynamin 1-, dynamin 3- and clathrin-independent pathway of synaptic vesicle recycling mediated by bulk endocytosis. *ELife*, *3*, 1–26. <https://doi.org/10.7554/elife.01621>
- Wu, Y., Whiteus, C., Xu, C. S., Hayworth, K. J., Weinberg, R. J., Hess, H. F., & De Camilli, P. (2017). Contacts between the endoplasmic reticulum and other membranes in neurons. *Proceedings of the National Academy of Sciences of the United States of America*, *114*(24), E4859–E4867. <https://doi.org/10.1073/pnas.1701078114>
- Xie, Y., Hayden, M. R., & Xu, B. (2010). BDNF overexpression in the forebrain rescues Huntington's disease phenotypes in YAC128 mice. *Journal of Neuroscience*, *30*(44), 14708–14718. <https://doi.org/10.1523/JNEUROSCI.1637-10.2010>
- Xu, K., Zhong, G., & Zhuang, X. (2013). Actin, spectrin, and associated proteins form a periodic cytoskeletal structure in axons. *Science*, *339*(6118), 452–456. <https://doi.org/10.1126/science.1232251>
- Xu, X., Ng, B., Sim, B., Radulescu, C. I., Yusof, N. A. B. M., Goh, W. I., Lin, S., Lim, J. S. Y., Cha, Y., Kusko, R., Kay, C., Ratovitski, T., Ross, C., Hayden, M. R., Wright, G., & Pouladi, M. A. (2020). pS421 huntingtin modulates mitochondrial phenotypes and confers neuroprotection in an HD hiPSC model. *Cell Death and Disease*, *11*(9). <https://doi.org/10.1038/s41419-020-02983-z>
- Yamashita, N., & Kuruvilla, R. (2016). Neurotrophin signaling endosomes: Biogenesis, regulation, and functions. *Current Opinion in Neurobiology*, *39*, 139–145. <https://doi.org/10.1016/j.conb.2016.06.004>
- Yang, G., Gong, Y. D., Gong, K., Jiang, W. L., Kwon, E., Wang, P., Zheng, H., Zhang, X. F., Gan, W. B., & Zhao, N. M. (2005). Reduced synaptic vesicle density and active zone size in mice lacking amyloid precursor protein (APP) and APP-like protein 2. *Neuroscience Letters*, *384*(1–2), 66–71. <https://doi.org/10.1016/j.neulet.2005.04.040>
- Yang, G. Z., Yang, M., Lim, Y., Lu, J. J., Wang, T. H., Qi, J. G., Zhong, J. H., & Zhou, X. F. (2012). Huntingtin associated protein 1 regulates trafficking of the amyloid precursor protein and modulates amyloid beta levels in neurons. *Journal of Neurochemistry*, *122*(5), 1010–1022. <https://doi.org/10.1111/j.1471-4159.2012.07845.x>
- Yang, R., Bostick, Z., Garbouchian, A., Luisi, J., Banker, G., & Bentley, M. (2019). A novel strategy to visualize vesicle-bound kinesins reveals the diversity of kinesin-mediated transport. *Traffic*,

20(11), 851–866. <https://doi.org/10.1111/tra.12692>

- Yano, H., & Chao, M. V. (2004). Mechanisms of Neurotrophin Receptor Vesicular Transport. *Journal of Neurobiology*, 58(2), 244–257. <https://doi.org/10.1002/neu.10321>
- Yap, C. C., Digilio, L., McMahon, L. P., Garcia, A. D. R., & Winckler, B. (2018). Degradation of dendritic cargos requires Rab7-dependent transport to somatic lysosomes. *Journal of Cell Biology*, 217(9), 3141–3159. <https://doi.org/10.1083/jcb.201711039>
- Yee, A. X., Hsu, Y. T., & Chen, L. (2017). A metaplasticity view of the interaction between homeostatic and hebbian plasticity. *Philosophical Transactions of the Royal Society B: Biological Sciences*, 372(1715). <https://doi.org/10.1098/rstb.2016.0155>
- Yin, H. H., Prasad Mulcare, S., Hilario, M. R. F., Clouse, E., Holloway, T., Davis, M. I., Hansson, A. C., Lovinger, D. M., & Costa, R. M. (2009). Dynamic reorganization of striatal circuits during the acquisition and consolidation of a skill. *Nature Neuroscience*, 12(3), 333–341. <https://doi.org/10.1038/nn.2261>
- Yogev, S., Cooper, R., Fetter, R., Horowitz, M., & Shen, K. (2016). Microtubule Organization Determines Axonal Transport Dynamics. *Neuron*, 92(2), 449–460. <https://doi.org/10.1016/j.neuron.2016.09.036>
- Yonekawa, V., Harada, A., Okada, Y., Funakoshi, T., Kanai, Y., Takei, Y., Terada, S., Noda, T., & Hirokawa, N. (1998). Defect in synaptic vesicle precursor transport and neuronal cell death in KIF1A motor protein-deficient mice. *Journal of Cell Biology*, 141(2), 431–441. <https://doi.org/10.1083/jcb.141.2.431>
- Yuan, A., Rao, M. V., Veeranna, & Nixon, R. A. (2017). Neurofilaments and neurofilament proteins in health and disease. *Cold Spring Harbor Perspectives in Biology*, 9(4). <https://doi.org/10.1101/cshperspect.a018309>
- Yue, Y., Sheng, Y., Zhang, H. N., Yu, Y., Huo, L., Feng, W., & Xu, T. (2013). The CC1-FHA dimer is essential for KIF1A-mediated axonal transport of synaptic vesicles in *C. elegans*. *Biochemical and Biophysical Research Communications*, 435(3), 441–446. <https://doi.org/10.1016/j.bbrc.2013.05.005>
- Zala, D., Colin, E., Rangone, H., Liot, G., Humbert, S., & Saudou, F. (2008). Phosphorylation of mutant huntingtin at S421 restores anterograde and retrograde transport in neurons. *Human Molecular Genetics*, 17(24), 3837–3846. <https://doi.org/10.1093/hmg/ddn281>
- Zala, D., Hinckelmann, M. V., & Saudou, F. (2013). Huntingtin's Function in Axonal Transport Is Conserved in *Drosophila melanogaster*. *PLoS ONE*, 8(3), 1–10. <https://doi.org/10.1371/journal.pone.0060162>
- Zala, D., Hinckelmann, M. V., Yu, H., Lyra Da Cunha, M. M., Liot, G., Cordelières, F. P., Marco, S., & Saudou, F. (2013). Vesicular glycolysis provides on-board energy for fast axonal transport. *Cell*, 152(3), 479–491. <https://doi.org/10.1016/j.cell.2012.12.029>
- Zeitler, B., Froelich, S., Marlen, K., Shivak, D. A., Yu, Q., Li, D., Pearl, J. R., Miller, J. C., Zhang, L., Paschon, D. E., Hinkley, S. J., Ankoudinova, I., Lam, S., Guschin, D., Kopan, L., Cherone, J. M., Nguyen, H. O. B., Qiao, G., Ataei, Y., ... Zhang, H. S. (2019). Allele-selective transcriptional repression of mutant HTT for the treatment of Huntington's disease. *Nature Medicine*, 25(7), 1131–1142. <https://doi.org/10.1038/s41591-019-0478-3>



- Zeitlin, S., Liu, J. P., Chapman, D. L., Papaioannou, V. E., & Efstratiadis, A. (1995). Increased apoptosis and early embryonic lethality in mice nullizygous for the Huntington's disease gene homologue. *Nature Genetics*, *11*(2), 155–163. <https://doi.org/10.1038/ng1095-155>
- Zekert, N., & Fischer, R. (2009). The *Aspergillus nidulans* Kinesin-3 UncA Motor Moves Vesicles along a Subpopulation of Microtubules. *Molecular Biology of the Cell*, *20*, 673–684. <https://doi.org/10.1091/mbc.E08>
- Zeron, M. M., Hansson, O., Chen, N., Wellington, C. L., Leavitt, B. R., Brundin, P., Hayden, M. R., & Raymond, L. A. (2002). Increased Sensitivity to N-Methyl-D-Aspartate in a Mouse Model of Huntington's Disease. *Neuron*, *33*, 849–860.
- Zhang, B., Koh, Y. H., Beckstead, R. B., Budnik, V., Ganetzky, B., & Bellen, H. J. (1998). Synaptic vesicle size and number are regulated by a clathrin adaptor protein required for endocytosis. *Neuron*, *21*(6), 1465–1475. [https://doi.org/10.1016/S0896-6273\(00\)80664-9](https://doi.org/10.1016/S0896-6273(00)80664-9)
- Zhang, F. X., Ge, S. N., Dong, Y. L., Shi, J., Feng, Y. P., Li, Y., Li, Y. Q., & Li, J. L. (2018). Vesicular glutamate transporter isoforms: The essential players in the somatosensory systems. In *Progress in Neurobiology* (Vol. 171, pp. 72–89). Elsevier Ltd. <https://doi.org/10.1016/j.pneurobio.2018.09.006>
- Zhang, K., Foster, H. E., Rondelet, A., Lacey, S. E., Bahi-Buisson, N., Bird, A. W., & Carter, A. P. (2017). Cryo-EM Reveals How Human Cytoplasmic Dynein Is Auto-inhibited and Activated. *Cell*, *169*(7), 1303-1314.e18. <https://doi.org/10.1016/j.cell.2017.05.025>
- Zhang, Y. V., Hannan, S. B., Kern, J. V., Stanchev, D. T., Koç, B., Jahn, T. R., & Rasse, T. M. (2017). The KIF1A homolog Unc-104 is important for spontaneous release, postsynaptic density maturation and perisynaptic scaffold organization. *Scientific Reports*, *7*(November 2016), 1–9. <https://doi.org/10.1038/srep38172>
- Zhang, X., & Song, W. (2013). *The role of APP and BACE1 trafficking in APP processing and amyloid-β generation. Figure 1, 1.*
- Zhang, Y. W., Thompson, R., Zhang, H., & Xu, H. (2011). APP processing in Alzheimer's disease. *Molecular Brain*, *4*(1), 1–13. <https://doi.org/10.1186/1756-6606-4-3>
- Zhao, C., Takita, J., Tanaka, Y., Setou, M., Nakagawa, T., Takeda, S., Yang, H. W., Terada, S., Nakata, T., Takei, Y., Saito, M., Tsuji, S., Hayashi, Y., & Hirokawa, N. (2001). Charcot-Marie-Tooth Disease Type 2A Caused by Mutation in a Microtubule Motor KIF1B gaku et al., 1994; termed KIF1B hereafter) that we call KIF1B. The two isoforms, splice variants of the same gene mapped on mouse chromosome 4E, share the N-terminal motor. *Cell*, *105*, 587–597. <http://www>.
- Zhao, X. L., Wang, W. A., Tan, J. X., Huang, J. K., Zhang, X., Zhang, B. Z., Wang, Y. H., YangCheng, H. Y., Zhu, H. L., Sun, X. J., & Huang, F. De. (2010). Expression of β-amyloid induced age-dependent presynaptic and axonal changes in *Drosophila*. *Journal of Neuroscience*, *30*(4), 1512–1522. <https://doi.org/10.1523/JNEUROSCI.3699-09.2010>
- Zheng, Q., Ahlawat, S., Schaefer, A., Mahoney, T., Koushika, S. P., & Nonet, M. L. (2014). The Vesicle Protein SAM-4 Regulates the Processivity of Synaptic Vesicle Transport. *PLoS Genetics*, *10*(10). <https://doi.org/10.1371/journal.pgen.1004644>
- Zheng, W. H., & Quirion, R. (2006). Insulin-like growth factor-1 (IGF-1) induces the activation/phosphorylation of Akt kinase and cAMP response element-binding protein (CREB) by

- activating different signaling pathways in PC12 cells. *BMC Neuroscience*, 7, 1–10. <https://doi.org/10.1186/1471-2202-7-51>
- Zimbone, S., Monaco, I., Gianì, F., Pandini, G., Copani, A. G., Giuffrida, M. L., & Rizzarelli, E. (2018). Amyloid Beta monomers regulate cyclic adenosine monophosphate response element binding protein functions by activating type-1 insulin-like growth factor receptors in neuronal cells. *Aging Cell*, 17(1), 1–10. <https://doi.org/10.1111/acel.12684>
- Zoghbi, H. ., Gage, F. ., & Choi D.W. (2000). Neurobiology of disease. *Current Opinion in Neurobiology*, 10, 655–660.
- Zuccato, C., Ciammola, A., Rigamonti, D., Leavitt, B. R., Goffredo, D., Conti, L., MacDonald, M. E., Friedlander, R. M., Silani, V., Hayden, M. R., Timmusk, T., Sipione, S., & Cattaneo, E. (2001). Loss of huntingtin-mediated BDNF gene transcription in Huntington's disease. *Science*, 293(5529), 493–498. <https://doi.org/10.1126/science.1059581>
- Zuccato, Chiara, Tartari, M., Crotti, A., Goffredo, D., Valenza, M., Conti, L., Cataudella, T., Leavitt, B. R., Hayden, M. R., Timmusk, T., Rigamonti, D., & Cattaneo, E. (2003). Huntingtin interacts with REST/NRSF to modulate the transcription of NRSE-controlled neuronal genes. *Nature Genetics*, 35(1), 76–83. <https://doi.org/10.1038/ng1219>
- Zucker, R. S., & Regehr, W. G. (2002). Short-term synaptic plasticity. *Annual Review of Physiology*, 64, 355–405. <https://doi.org/10.1146/annurev.physiol.64.092501.114547>
- Zurawski, Z., Page, B., Chicka, M. C., Brindley, R. L., Wells, C. A., Preininger, A. M., Hyde, K., Gilbert, J. A., Cruz-Rodriguez, O., Currie, K. P. M., Chapman, E. R., Alford, S., & Hamm, H. E. (2017). Gβγ directly modulates vesicle fusion by competing with synaptotagmin for binding to neuronal SNARE proteins embedded in membranes. *Journal of Biological Chemistry*, 292(29), 12165–12177. <https://doi.org/10.1074/jbc.M116.773523>

## Annex

# Mutations in the *KIF21B* kinesin gene cause neurodevelopmental disorders through imbalanced canonical motor activity

Laure Asselin<sup>1,2,3,4</sup>, José Rivera Alvarez<sup>1,2,3,4,20</sup>, Solveig Heide<sup>5,6,7,20</sup>, Camille S. Bonnet<sup>1,2,3,4,20</sup>, Peggy Tilly<sup>1,2,3,4</sup>, Hélène Vitet<sup>8</sup>, Chantal Weber<sup>1,2,3,4</sup>, Carlos A. Bacino<sup>9,10</sup>, Kristin Baranaño<sup>11</sup>, Anna Chassevent<sup>11</sup>, Amy Dameron<sup>12</sup>, Laurence Faivre<sup>13,14</sup>, Neil A. Hanchard<sup>9</sup>, Sonal Mahida<sup>15</sup>, Kirsty McWalter<sup>16</sup>, Cyril Mignot<sup>5,6,7,16</sup>, Caroline Nava<sup>5,16</sup>, Agnès Rastetter<sup>16</sup>, Haley Streff<sup>9,10</sup>, Christel Thauvin-Robinet<sup>13,17</sup>, Marjan M. Weiss<sup>18</sup>, Gladys Zapata<sup>10</sup>, Petra J. G. Zwijnenburg<sup>18</sup>, Frédéric Saudou<sup>8</sup>, Christel Depienne<sup>1,2,3,4,16,19</sup>, Christelle Golzio<sup>1,2,3,4</sup>, Delphine Héron<sup>5,6,7</sup> & Juliette D. Godin<sup>1,2,3,4</sup>✉

*KIF21B* is a kinesin protein that promotes intracellular transport and controls microtubule dynamics. We report three missense variants and one duplication in *KIF21B* in individuals with neurodevelopmental disorders associated with brain malformations, including corpus callosum agenesis (ACC) and microcephaly. We demonstrate, in vivo, that the expression of *KIF21B* missense variants specifically recapitulates patients' neurodevelopmental abnormalities, including microcephaly and reduced intra- and inter-hemispheric connectivity. We establish that missense *KIF21B* variants impede neuronal migration through attenuation of kinesin autoinhibition leading to aberrant *KIF21B* motility activity. We also show that the ACC-related *KIF21B* variant independently perturbs axonal growth and ipsilateral axon branching through two distinct mechanisms, both leading to deregulation of canonical kinesin motor activity. The duplication introduces a premature termination codon leading to nonsense-mediated mRNA decay. Although we demonstrate that *Kif21b* haploinsufficiency leads to an impaired neuronal positioning, the duplication variant might not be pathogenic. Altogether, our data indicate that impaired *KIF21B* autoregulation and function play a critical role in the pathogenicity of human neurodevelopmental disorder.

A list of author affiliations appears at the end of the paper.

The development of the mammalian cerebral cortex depends on microtubule (MT)-related processes that coordinate birth, migration and differentiation of excitatory and inhibitory neurons. MT cytoskeleton acts in concert with microtubule associated proteins (MAP) and motor proteins to promote the structural changes that underlie key developmental events such as neurogenesis, migration, neuritegenesis, axon pathfinding and synapse formation. Kinesin superfamily proteins (KIFs) are important molecular motors that control MT organization and dynamics in both axons and dendrites and mediate intracellular transport of various cargo, including vesicles, organelles, cellular proteins and mRNAs, along MTs<sup>1,2</sup>. The importance of both the force-generating and MT-regulating functions of KIFs for brain development has become evident with loss of function studies demonstrating defects in mitosis<sup>3–9</sup>, cytokinesis<sup>10,11</sup>, polarity<sup>3</sup>, migration<sup>12–14</sup>, axonal growth and branching<sup>14–18</sup>, survival<sup>19</sup> and synaptogenesis<sup>20–24</sup>. Further reflecting the key role of KIFs in neuronal development, variants in human KIF-encoding genes (*KIF4A*<sup>24</sup>, *KIF7*<sup>25–28</sup>, *KIF11*<sup>29</sup>, *KIF2A*<sup>30–32</sup>, *KIF5C*<sup>24,28,30,33</sup>, *KIF1A*<sup>28,34</sup>, *KIF6*<sup>35</sup>, *KIF14*<sup>11,36,37</sup>, *KIF26A*<sup>28</sup>) have been associated with various neurodevelopmental disorders, including malformation of cortical development (MCD), acrocallosal syndrome, ciliopathies, epilepsy and intellectual disability. Most KIF variants have been predicted to be highly pathogenic in silico but their direct implication in disease and the underlying pathophysiological mechanisms have only been elicited for only a few of them<sup>11,26,35,38</sup>.

The MT-plus-end directed kinesin-4 motor KIF21B is mainly expressed in spleen, testes and central nervous tissues and is particularly enriched in neurons<sup>39,40</sup>. Within neurons, KIF21B is present in both axons and dendrites and especially abundant in growth cones<sup>40,41</sup>. KIF21B has dual functions in neurons. First, it promotes intracellular transport through its N-terminal processive motor activity<sup>21,42–44</sup>. However, except for BDNF-TrkB signaling endosomes<sup>44</sup>, 2-subunit-containing GABAA receptor<sup>45</sup> and neurobeachin recycling endosomes<sup>43</sup>, our knowledge of KIF21B-transported cargoes is very limited. Second, KIF21B influences MT dynamics through distinct MT binding domains<sup>21,42,44</sup>. KIF21B positively regulates MTs dynamicity in dendrites by favoring MT growth and catastrophes<sup>21,44</sup>. In addition, in vitro studies demonstrate that KIF21B can also act as a MT pausing factor by accumulating at the MT-plus ends<sup>42</sup>. Notably, KIF21B functions can be modulated by neuronal activity, which favors KIF21B trafficking activity at the expense of MT dynamics regulatory function<sup>44</sup> as well as through an auto-inhibitory interaction between the N-terminal motor domain and an internal regulatory coiled-coil region (rCC)<sup>42,46</sup>.

KIF21B homozygous knockout (KO) mice display severe morphological abnormalities including microcephaly and partial loss of commissural fibers<sup>47</sup>, cognitive deficits<sup>21,43,48</sup> and altered synaptic transmission<sup>21,23</sup>. Together with the reduced dendritic complexity and spines density observed in KIF21B<sup>-/-</sup> neurons in culture<sup>21</sup>, these results highlight a critical role for KIF21B in brain development and function. Though, there are no clear KIF21B-related neurodevelopmental disorders, a duplication of the locus bearing *KIF21B* has been found in individuals with neurodevelopmental delay and intellectual disability (ID)<sup>49</sup>.

Here we provide the evidence of a causal relationship between variants in *KIF21B* and neurodevelopmental disorders. We report the identification of three missense variants and one truncating variant in patients with neurodevelopmental delay and brain malformations including corpus callosum (CC) agenesis (ACC) and microcephaly. By combining in vivo modeling tools, we show that *KIF21B* pathogenic variants impede neuronal migration and connectivity through at least two distinct mechanisms both leading to dysregulation of canonical kinesin motor activity.

Taken together our data suggest that *KIF21B* is a novel gene for ID associated with heterogeneous brain morphological anomalies.

## Results

**Identification of human *KIF21B* variants.** Using trio whole-exome sequencing, we identified a de novo variant (NM\_001252100.1, c.2032A>C, p.Ile678Leu) in the *KIF21B* gene in a first patient (P1) presenting with developmental delay, learning and motor disabilities, associated with isolated complete agenesis of the corpus callosum (ACC) (Fig. 1a, e, Table 1, Supplementary Note 1). Through the GeneMatcher platform<sup>50</sup>, variants in *KIF21B* were found in three additional patients. Patient 2 (P2) (NM\_001252100.1, c.937C>A, p.Gln313Lys) presented with severe ID associated with microcephaly (Fig. 1b, f); patient 3 (P3) (NM\_001252100.1, c.3001G>A, p. Ala1001Thr) presented with global developmental delay and mild to moderate ID (Fig. 1c) but normal brain structure at the MRI. This variant was inherited from the father, who presented with developmental delay and learning difficulties; and patient 4 (P4) (NM\_001252100.1, c.2959\_2962dup, p.Asn988Serfs\*4) presented with mild developmental delays and hypotonia, but no brain structural anomalies on brain MRI (Fig. 1d, g). The three identified *KIF21B* missense variants occur within highly conserved residues positioned in the motor domain (NM\_001252100.1, c.937C>A, p.Gln313Lys-P2), the regulatory coiled-coil (rCC) region (NM\_001252100.1, c.3001G>A, p. Ala1001Thr-P3), and the coiled-coil domain (NM\_001252100.1, c.2032A>C, p.Ile678Leu-P1) (Fig. 1h, Supplementary Fig. 1a–c). The fourth variant is a duplication (NM\_001252100.1, c.2959\_2962dup, p.Asn988Serfs\*4-P4) that leads to the introduction of a premature termination codon in exon 20. RT-qPCR analysis and sequencing of *KIF21B* transcripts isolated from P4's blood revealed haploinsufficiency, likely due to the degradation of the mutant mRNA by nonsense-mediated decay (Supplementary Fig. 1d, e). All variants were predicted pathogenic by commonly used in silico software (Polyphen-2, Mutation Taster, SIFT and CADD; Supplementary Fig. 1f) and co-segregated with the phenotype in each pedigree (Fig. 1a–d). Of note, we found two other de novo variants of unknown significance in patients: one hemizygous variant in *ARHGAP4* (chromosome X) in P1 that also segregated in his healthy brother and one de novo in *UBR3* (NM\_172070.3, c.5023G>C; p.Glu1675Gln) in P4, that showed a weak pathogenic score based on in silico predictions. None of the four *KIF21B* variants is reported in public databases, including dbSNP, 1000 Genomes and gnomAD. Overall, we identified variants in *KIF21B* gene in four patients presenting with mild to severe neurodevelopmental delay associated with heterogeneous brain malformations (Table 1, Supplementary Note 1).

**Kif21b expression is restricted to neurons.** We first examined the expression pattern of Kif21b in the mouse developing cortex. Although levels of *Kif21b* mRNA transcripts are rather stable during development (Fig. 2a), protein expression tends to increase from embryonic day (E) 12.5 to postnatal day (P) 2 (Fig. 2b). *mKif21b* transcripts were mostly observed in the cortical plate (CP) and almost entirely excluded from the ventricular (VZ) and sub-ventricular (SVZ) zones, where progenitors and newborn neurons reside (Supplementary Fig. 2a). As corticogenesis proceeds, *mKif21b* mRNAs accumulated in the intermediate zone, which is enriched in growing axons (Supplementary Fig. 2a). Immunolabeling of E12.5 to E18.5 embryo brain sections showed a restricted expression of mKif21b proteins to postmitotic compartments of the neuronal epithelium with a particularly intense signal in the axon-rich zone

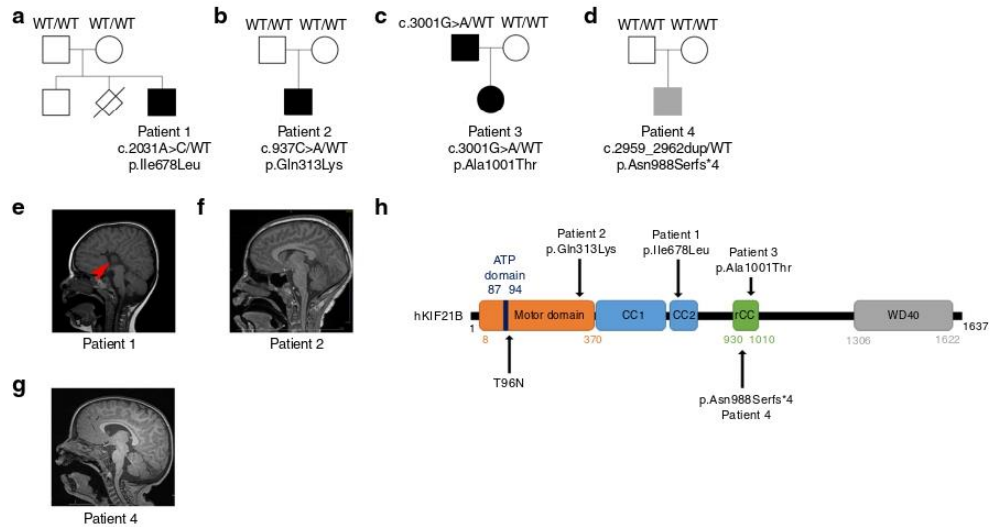


**Fig. 1** Patients with *KIF21B* variants. **a-d** Pedigrees of patients with identified *KIF21B* variants. **e-g** Sagittal brain section of patient's MRI showing a complete agenesis of the corpus callosum in patient 1 (**e**, red arrow) and microcephaly in patient 2 (**f**). **h** Schematic representation of the human *KIF21B* (h*KIF21B*) protein indicating the different domains (motor domain, ATP binding site, coiled-coil domain (CC) 1 and 2, regulatory coiled-coil domain (rCC) and WD40 domain) and the position of the mutated amino acids for patient 1 (p.Ile678Leu), 2 (p.Gln313Lys), 3 (p.Ala1001Thr) and 4 (p.Asn988Serfs\*4). T96N substitution that abolishes *KIF21B* mobility is also depicted.

(Fig. 2c and Supplementary Fig. 2b, c). m*Kif21b* staining specificity was validated by the absence of labeling in *Kif21b* knockout brain sections at birth (Supplementary Fig. 2e, f). Further immunostainings with antibodies against m*Kif21b* and  $\beta$ III-Tubulin or *Tbr2* that label neurons and intermediate progenitors respectively, confirmed that *Kif21b* is exclusively expressed in post mitotic neurons at all stages of development (Fig. 2c, d and Supplementary Fig. 2b, c). To undoubtedly exclude any expression of *Kif21b* in progenitors, we analyzed m*Kif21b* protein in progenitor (YFP<sup>+</sup>; CD24<sup>-</sup>) and neuron populations (YFP<sup>+</sup>; CD24<sup>+</sup>) isolated from Rosa26-lox-STOP-YFP; NEX<sup>CRE/+</sup> E16.5 cortices by fluorescent-activated cell sorting. No *Kif21b* protein was detected in cortical progenitors by immunoblotting (Supplementary Fig. 2d). Although *Kif21b* was previously thought to be mainly localized to dendrites<sup>40</sup>, our data suggest an axonal localization in the developing cortex (Supplementary Fig. 2b). To ascertain the axonal distribution of m*Kif21b*, we used a 2-chambers microfluidic device to analyze separately the axons from cell bodies and dendrites<sup>51</sup> (Fig. 2e, f). Channels separating both chambers are 450- $\mu$ m-long so only axons from neurons located in the proximal compartment can reach the distal chamber<sup>51</sup>. Immunolabelings of mouse primary cortical neurons with *Kif21b* and Tau antibodies in these devices confirmed the expression of *Kif21b* in Tau-positive axons and its accumulation at the axonal tips (Fig. 2e, f). *Kif21b* is thus moderately but stably expressed in both dendrites and axons of postmitotic neurons from early to late corticogenesis.

***KIF21B* variants impair migration of projection neurons.** To evaluate the pathogenic nature of *KIF21B* variants, we assessed the consequences of overexpressing h*KIF21B* variants on neuronal migration using in utero electroporation (IUE) in mice. Given that *KIF21B* is a post mitotic kinesin, we used plasmids allowing expression of human *KIF21B* under the control of the NeuroD promoter (NeuroD-h*KIF21B*). Transfection in N2A neuroblastoma cell line showed even expression of wild-type (WT) and all three missense h*KIF21B* variants by western blot, suggesting that

p.Gln313Lys, p.Ile678Leu and p.Ala1001Thr missense variants are unlikely to affect the production, stability or turnover of the h*KIF21B* proteins (Supplementary Fig. 3a). Consistently, cycloheximide chase experiments in N2A cells revealed a similar half-life of WT and mutant h*KIF21B* proteins (Supplementary Fig. 3b).

To investigate the effects of the variants on neuronal positioning, we individually induced neuron-specific expression of the h*KIF21B* mutants using IUE of NeuroD-h*KIF21B* constructs together with a NeuroD-IRES-GFP reporter plasmid in mouse embryonic cortices at E14.5. Four days after IUE, whereas most of the GFP<sup>+</sup> postmitotic neurons expressing full-length WT-h*KIF21B* reached the CP as in the control (Fig. 3a), neurons expressing missense variants accumulated in the intermediate zone, with a decrease of 27.7%, 60.3% and 23% of the cells reaching the upper CP in the p.Gln313Lys, p.Ile678Leu and p.Ala1001Thr conditions, respectively (Bonferroni adjusted  $P = 0.0001$ ) (Fig. 3b). Noteworthy, h*KIF21B* missense variants likely disturbed neuronal migration in a cell-autonomous manner as their expression did not affect cell survival and glia scaffold integrity (Supplementary Fig. 3c). To assess the functional consequences of the p.Asn988Serfs\*4 protein truncated variant (Supplementary Fig. 1d), we silenced m*Kif21b* specifically in post mitotic neurons using IUE of CRE-dependent inducible shRNA vector<sup>52</sup> together with a NeuroD-CRE-IRES-GFP construct at E14.5. Efficacy of the two shRNAs was confirmed by RT-qPCR (-61.4% for sh-*Kif21b* #1, -45.1% for sh-*Kif21b* #2) (Supplementary Fig. 3d). Four days after IUE, *Kif21b*-silenced neurons displayed migration defects compared to control shRNA-electroporated cells with a reduction of 23.5% and 32.2% of cells distributed in the upper CP for sh-*Kif21b* #1 and sh-*Kif21b* #2, respectively (Supplementary Fig. 3e, f). To note, the migratory phenotype induced by sh-*Kif21b* #2 was fully recovered by co-electroporation of wild-type NeuroD-m*Kif21b* construct (Supplementary Fig. 3e, f). Most of the cells overexpressing the p.Gln313Lys and p.Ala1001Thr mutants or silenced for *Kif21b* showed a correct positioning with nearly all cells found in

**Table 1 Clinical summary of patients with hKIF21B variants.**

	Patient 1	Patient 2	Patient 3	Patient 4
Age at last evaluation	10 y	12 y 1 m	9 y	3 y 8 m
Sex	Male	Male	Female	Male
Genetics	KIF21B c.2032A>C p.Ile678Leu	KIF21B c.937C>A p.Gln313Lys	KIF21B c.3001G>A p.Ala1001Thr	KIF21B c.2959_2962dupGCCA p.Asn988Serfs*4
Inheritance	De novo	De novo	Inherited from the affected father	De novo
Pregnancy and delivery	Normal	Oligohydramnios and IUGR	Normal	Small for gestational age
Height (perc)/weight (perc)/head circumference (perc) at birth	51 cm (97th p), 3.750 kg (97th p), 33 cm (15th p)	49 cm (49th p), 2.584 kg (7th p), 32 cm (5th p)	3.480 kg (50th p)	46.4 cm (7th p), 2.633 kg (5.87th p), *34 cm (25th p), *Measurements done at age 6 days
Neonatal findings	None	Nuchal cord at birth and was blue, mild respiratory distress, but discharged with mother	None	Feeding issues, NG tube
Developmental stages				
Age of sitting (months)	10	Does not	14	9
Age of walking (months)	18	Does not	24	15–16
Language delay	Yes	Yes	Yes	No
Age of first words (m: months, y: years)	36 m	36 m	36 m	12 m
Age of first sentences (m: months, y: years)	NA	NA	N/A	24 m
Current language ability	Short sentences, dysarthria	Non-verbal	Sentences	Short sentences
Intellectual disability (ID) (mild, moderate, severe)	Borderline	Severe	Mild to moderate	Mild
Estimated level of ID				
Age at evaluation (y)	10 y	12 y 1 m	9 y	3 y 8 m
Total IQ	66–79 (WISC V)	139 cm (–1.3), 20 kg (–3.4), 48.5 cm (–3.9)	54–59 (WISC V)	90.7 cm (–1.1), 17.8 kg (+1.8), 49.6 cm (–0.2)
Clinical examination				
Age at examination (years)	5 y	12 y 1 m	3 y 9 m	3 y 8 m
Height (SD)/weight (SD)/head circumference (SD)	118 cm (+1.5), 21.3 kg (+2), 52 cm (+0.5)	Poor visual fixation, constant tongue thrusting, poor gag, poor head control, bilateral ankle tightness, right wrist contracture	Mildly hypertonic legs	90.7 cm (–1.1), 16.3 kg (+0.09), 50.7 cm (+0.72)
Neurologic examination	Slow	Large eyes, fleshy ears, hypertelorism		Hypotonia
Dysmorphic features	Plagiocephaly		Epicanthic folds, mild ptosis, tented upperlip	Upslanting palpebral fissures, prominent eyebrows, broad nose with bulbous tip, anteverted nares, Micrognathia, Right-sided Duane syndrome
Brain imaging (MRI)				
Age at examination (m: months, y: years)	3 y	6 m and 12 y	2 y	1 y 9 m
Brain anomalies (MRI)	Complete agenesis of the corpus callosum	Normal	No structural abnormalities, myelinisation not completed yet, Normal differentiation white and gray matter. No focal lesions. Normal spectroscopy	A few scattered punctate foci of T2 prolongation in subcortical white matter and periventricular white matter of bilateral cerebral hemispheres with no associated restricted diffusion or hemorrhage
Other				History of falling spells with normal EEG. Severe constipation, Central sleep apnea, History of feeding issues requiring G tube

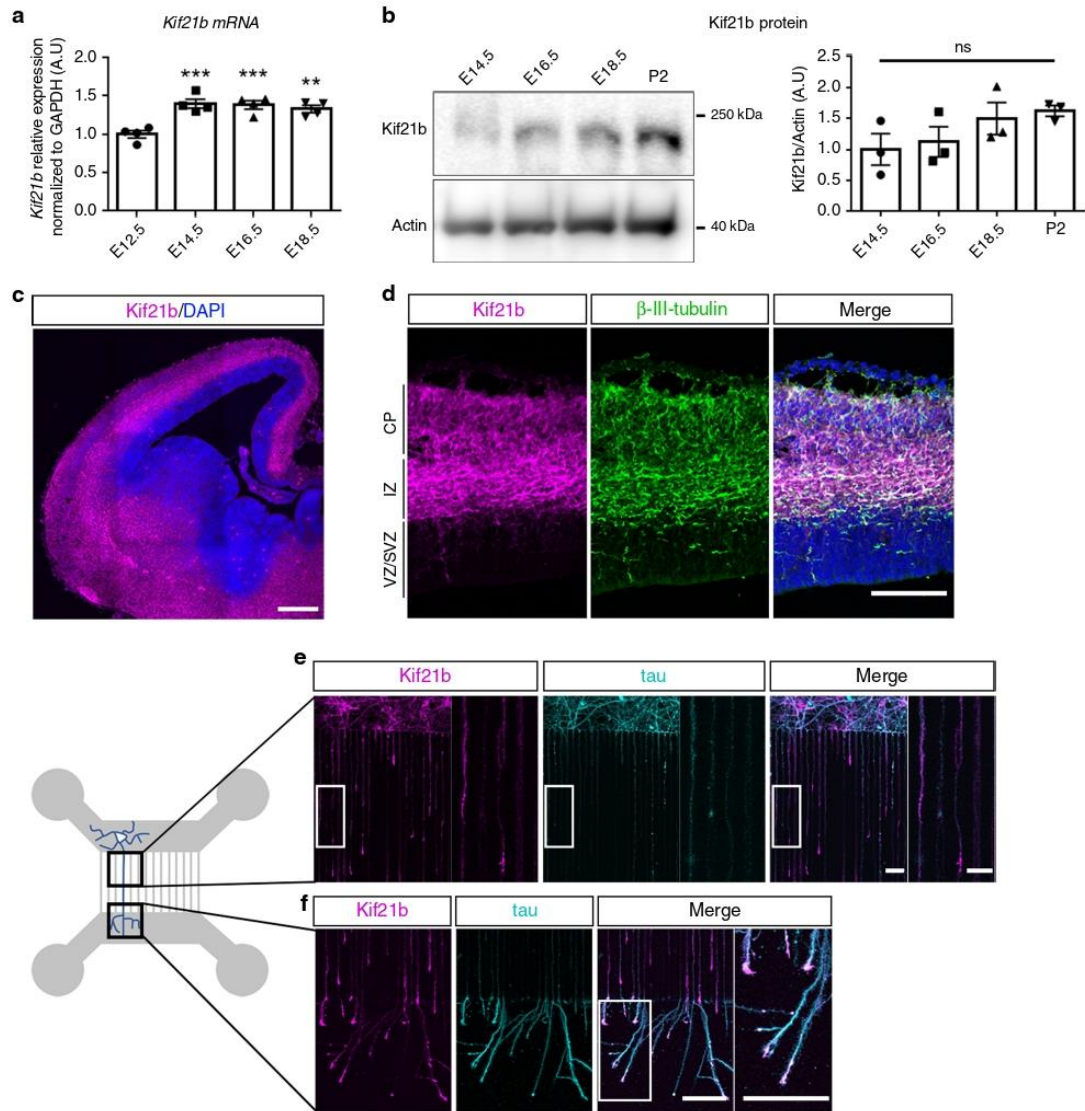


**Fig. 2** **Kif21b** expression in mouse developing cortex. **a** RT-qPCR analyses showing expression of *Kif21b* transcripts in mouse cortices at different embryonic stages (from E12.5 to E18.5) ( $n = 4$  brains per stage). **b** Western blot analyses of mouse cortical extracts showing similar expression of Kif21b protein from E14.5 to P2 ( $n = 3$  brains per stage). **a, b** Data are represented as means  $\pm$  S.E.M. Significance was calculated by one-way ANOVA (Bonferroni's multiple comparisons test), ns non-significant;  $**P < 0.005$ ;  $***P < 0.001$ . **c, d** E14.5 mouse forebrain coronal sections immunolabelled for Kif21b (magenta) and  $\beta$ -III-tubulin (neuronal marker, green) and counterstained with DAPI (blue) showing that Kif21b expression is restricted to post mitotic neurons. **e, f** Left panel: schematic representation of a 2-compartment microfluidic chamber. Cortical neurons (in cyan) plated in the upper chamber (gray) grow their axons through 450- $\mu$ m-long microchannels. The length of the microchannels allows axons but not dendrites to reach the lower chamber. Right panel: immunolabeling of Kif21b (magenta) and tau (axonal marker, cyan) on mouse primary cortical neurons at DIV5 in microdevices showing expression of Kif21b in axons (**e**) with an enrichment in growth cones (**f**). CP cortical plate, IZ intermediate zone, SVZ subventricular zone, VZ ventricular zone. Scale bars, (**c**) 250  $\mu$ m and (**d-f**) 100  $\mu$ m, magnifications (**e, f**) 20  $\mu$ m. Source data are provided in the Source Data file.

the upper layer of the cortex after birth, indicating a delay in migration rather than a permanent arrest (Fig. 3c, d, Supplementary Fig. 3g, h). By contrast, the p.Ile678Leu variant induced a permanent migration defect as a large number of p.Ile678Leu-expressing neurons remained in the white matter and deep-layers at P2 (Fig. 3c, d). Remarkably, p.Ile678Leu-expressing

projection neurons permanently arrested in the white matter were expressing the upper-layer marker *Cux1*, which supports a faulty migration rather than specification defects (Fig. 3e). Altogether, these results demonstrate that missense *hKIF21B* variants and *Kif21b* haploinsufficiency impede, to various extents, the radial migration of projection neurons.



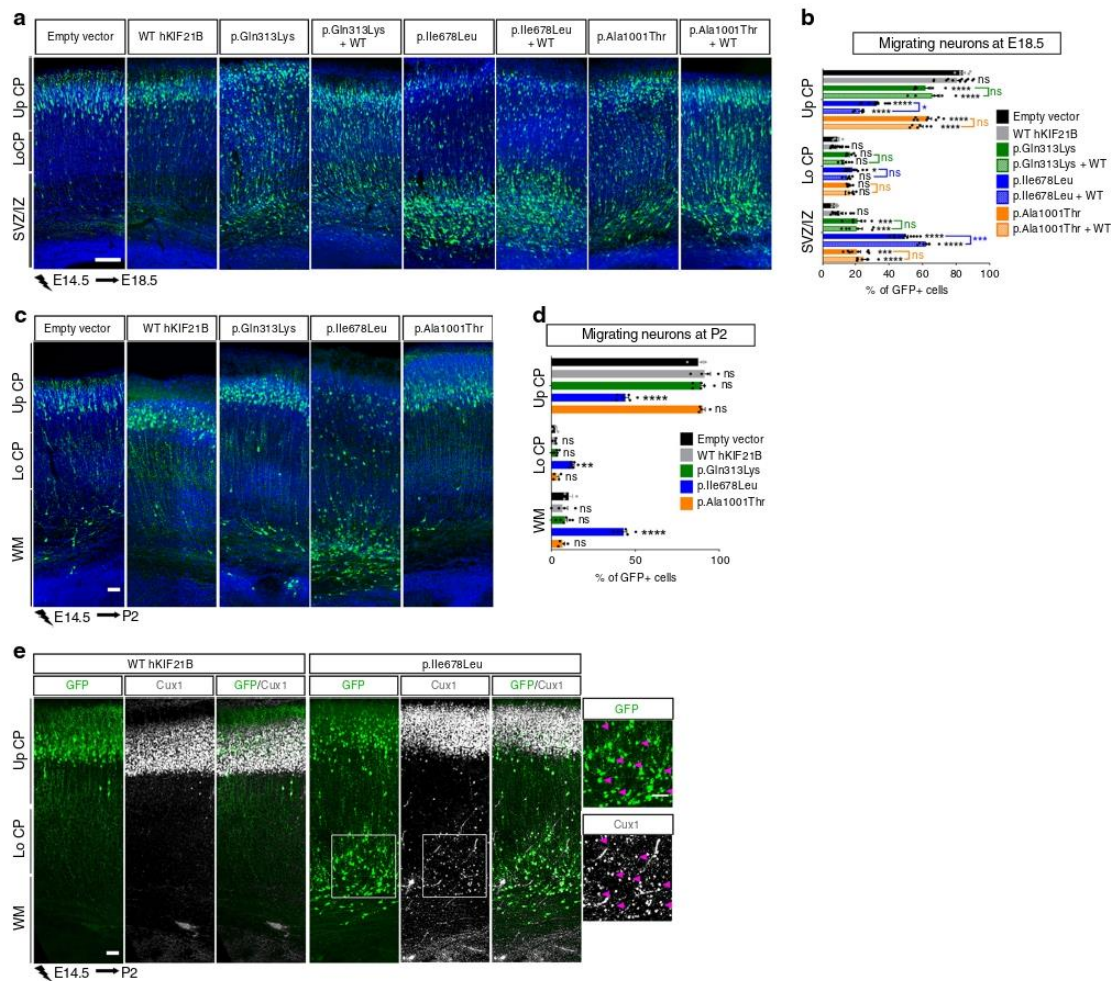
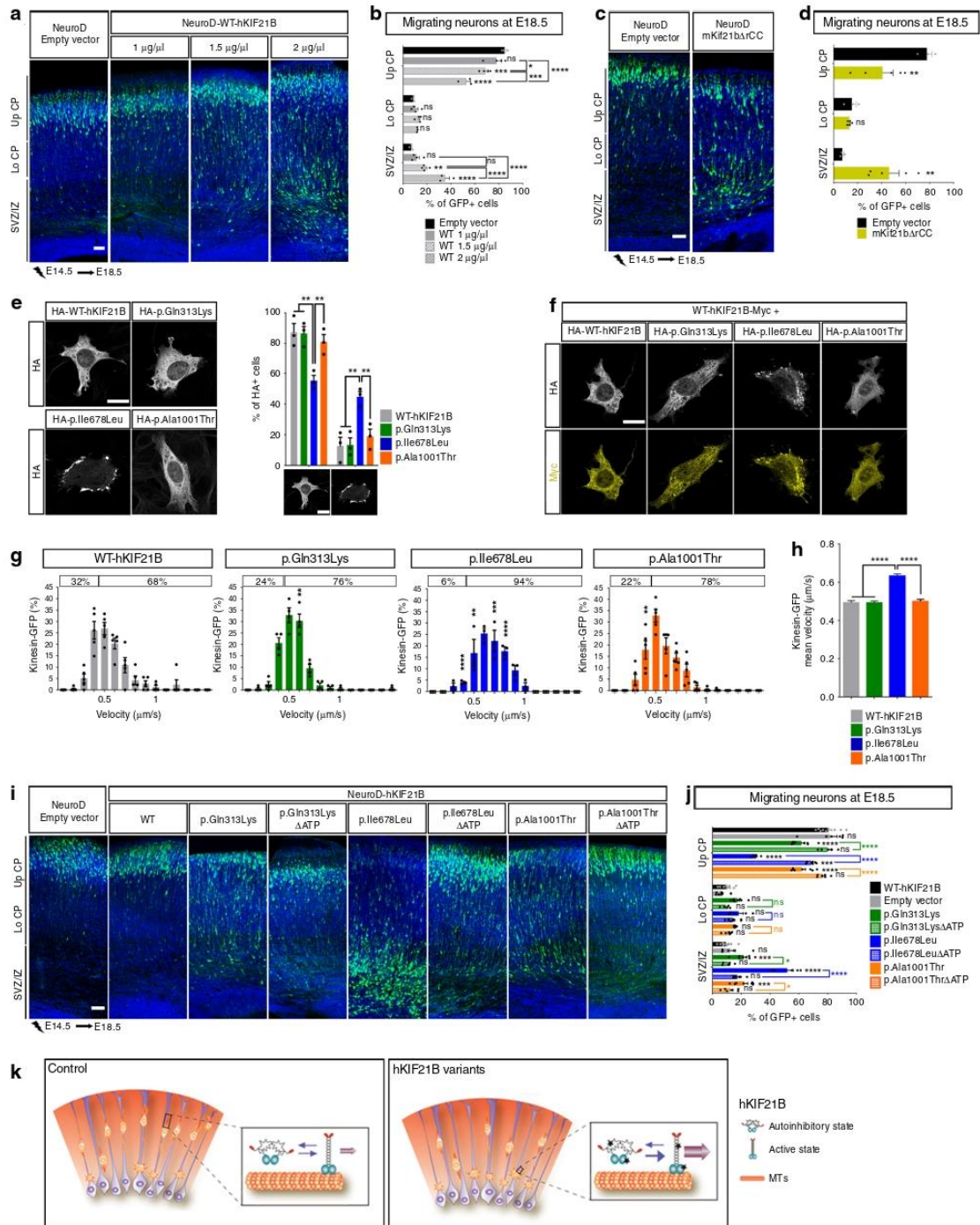


**Fig. 3 Expression of hKIF21B missense variants induces abnormal neuronal migration. a, c** Coronal sections of E18.5 (**a**) or P2 (**c**) mouse cortices electroporated at E14.5 with NeuroD-IRES-GFP empty vector (1 μg/μL) or WT, p.Gln313Lys, p.Ile678Leu or p.Ala1001Thr NeuroD-hKIF21B or co-expressing WT-hKIF21B together with mutated hKIF21B constructs (ratio 1:1). GFP-positive electroporated cells are depicted in green. Nuclei are stained with DAPI. **b, d** Analysis (means ± S.E.M.) of the percentage of electroporated GFP-cells in different regions (Up CP: upper cortical plate, Lo CP: lower cortical plate, IZ: intermediate zone, SVZ: subventricular zone) showing effect of expressing hKIF21B variants. Data were analyzed by two-way ANOVA (Bonferroni's multiple comparisons test). Number of embryos analyzed: **b** Empty vector,  $n = 6$ ; WT,  $n = 13$ ; p.Gln313Lys,  $n = 6$ ; p.Ile678Leu,  $n = 11$ ; p.Ala1001Thr,  $n = 8$ . Rescue experiments:  $n = 6$  for each condition. **d** Empty vector,  $n = 3$ ; WT,  $n = 4$ ; p.Gln313Lys,  $n = 6$ ; p.Ile678Leu,  $n = 6$ ; p.Ala1001Thr,  $n = 4$ . ns non-significant; \* $P < 0.05$ ; \*\* $P < 0.005$ ; \*\*\* $P < 0.001$ ; \*\*\*\* $P < 0.0001$ . **e** Cux1-immunolabeling (gray) of P2 coronal sections of mouse brains electroporated at E14.5 with the WT or p.Ile678Leu NeuroD-hKIF21B constructs showing no specification defects of arrested neurons (green). Scale bars (**a, c, e**) 50 μm. Source data are provided in the Source Data file.

**KIF21B variants lead to aberrant KIF21B motility activity.** To understand the molecular mechanisms by which variants in hKIF21B gene lead to defective radial migration, we tested for restoration of the hKIF21B variant-induced phenotype by increasing amount of wild-type protein. IUE of wild-type hKIF21B together with hKIF21B mutants at a 1:1 ratio failed to rescue the migration phenotype (Fig. 3a, b). Strikingly, neurons overexpressing large amount of WT-hKIF21B (2 units of NeuroD-hKIF21B) failed to reach the upper CP 4 days after IUE (Fig. 4a, b). Collectively, these results raise the possibility that hKIF21B variants impair migration by enhancing KIF21B activity in a dominant manner. One possible mechanism by which hKIF21B mutants might exert this effect is by relieving

autoinhibition imposed by the rCC to the motor domain as shown for CFEOM-causing variants in KIF21A<sup>46,53,54</sup>, a kinesin-4 family member that shares 61% identity with KIF21B<sup>40</sup>. Consistent with the hypothesis that KIF21B hyperactivation cause migration phenotypes, expression of a truncated mouse mKif21b protein that lacks the rCC domain (1 unit of NeuroD-mKif21bΔrCC) led to faulty migration (Fig. 4c, d).

To test whether identified variants alter KIF21B autoinhibition, we next sought to explore the functions of KIF21B that were enhanced by KIF21B autoinhibition release in mutant conditions. Given the processive activity of KIF21B, we assessed the effect of the variants on KIF21B motility activity. Using immunofluorescence, we first compared the localization of the wild-type (WT)



and the three missense mutant proteins in ST cells transfected with pcDNA-HA-hKIF21B cDNA constructs (Fig. 4e, Supplementary Fig. 4a). Although WT, p.Gln313Lys and p.Ala1001Thr proteins showed similar diffuse cytoplasmic localization, the p.Ile678Leu KIF21B protein tended to form aggregates localized

mainly at the periphery of the cells, suggesting an enhanced motility toward the plus end of the microtubules (Fig. 4e). To note, WT and all mutant proteins showed similar distribution in soma and neurites when overexpressed in primary cortical neurons (Supplementary Fig. 4c). Interestingly, in 100% of the

**Fig. 4** *hKIF21B* variants induce abnormal migration through enhanced *KIF21B* motor activity. **a, c, i** Coronal sections of E18.5 cortices, 4 days after IUE with the indicated NeuroD-IRES-GFP constructs. GFP-positive electroporated cells are depicted in green. Nuclei are stained with DAPI. **b, d, j** Percentage (means  $\pm$  S.E.M.) of electroporated cells in upper (Up CP) and lower (Lo CP) cortical plate, intermediate (IZ) and subventricular zone (SVZ), showing the effect of increasing (**b**) amount or (**d**) activity of *hKIF21B* and (**j**) contribution of the processive activity to the phenotype. Data were analyzed by two-way ANOVA (Bonferroni's multiple comparisons test). Number of embryos analyzed: **b** Empty vector and WT 2  $\mu\text{g}/\mu\text{L}$ ,  $n = 3$ ; WT 1 and 1.5  $\mu\text{g}/\mu\text{L}$ ,  $n = 4$ ; **d**  $n = 3$  for each condition; **j** Empty vector,  $n = 9$ ; WT,  $n = 6$ ; p.Gln313Lys,  $n = 8$ ; p.Ile678Leu,  $n = 5$ ; p.Ala1001Thr,  $n = 8$ ; p.Gln313Lys $\Delta$ ATP,  $n = 5$ ; p.Ile678Leu $\Delta$ ATP,  $n = 8$ ; p.Ala1001Thr $\Delta$ ATP,  $n = 6$ . **e** Immunolabeling of ST cells transfected with indicated HA-tagged *hKIF21B* constructs showing impaired localization of p.Ile678Leu variant. Histogram (means  $\pm$  S.E.M.) represents the percentage of cells with a diffuse versus an impaired localization of the HA-tagged proteins. Data were analyzed by two-way ANOVA (Bonferroni's multiple comparisons test). Number of cells analyzed: WT,  $n = 467$ ; p.Gln313Lys,  $n = 429$ ; p.Ile678Leu,  $n = 540$ ; p.Ala1001Thr,  $n = 387$ ; from three independent experiments. **f** Immunolabeling of ST cells transfected with the indicated Myc- and HA-tagged *hKIF21B* constructs showing that the p.Ile678Leu variant alters the localization of the WT protein. **g, h** Live imaging of Cos7 cells transfected with the indicated GFP-tagged *hKIF21B* constructs. Histograms (means  $\pm$  S.E.M.) represent (**g**) velocities distribution and (**h**) mean velocities. 20–32 cells from 3–5 independent experiments were analyzed by (**g**) two-way ANOVA or (**h**) one-way ANOVA (Bonferroni's multiple comparisons test). Total number of particles analyzed: WT,  $n = 203$ ; p.Gln313Lys,  $n = 182$ ; p.Ile678Leu,  $n = 195$ ; p.Ala1001Thr,  $n = 237$ . ns non-significant; \* $P < 0.05$ ; \*\* $P < 0.005$ ; \*\*\* $P < 0.001$ ; \*\*\*\* $P < 0.0001$ . Scale bars: (**a, c, i**) 50  $\mu\text{m}$ ; (**e, f**) 20  $\mu\text{m}$ . **k** Model: WT *KIF21B* switches between an autoinhibition and an active (purple arrows) state. *hKIF21B* variants (marked by a star) conformation favors the active state. *KIF21B* hyper-motility (pink arrow) leads to migration defects. Source data are provided in the Source Data file.

ST cells where the p.Ile678Leu variant is mislocalized, the cellular localization of the WT protein is altered, suggesting that the p.Ile678Leu protein might act as a dominant negative protein (Fig. 4f). In accordance, the p.Ile678Leu variant is competing with the WT protein to form *KIF21B* homodimer. Indeed, anti-Myc immunoprecipitation on extracts from HEK293T cells expressing myc-tagged WT, HA-tagged WT and WT or p.Ile678Leu GFP-tagged *hKIF21B* proteins revealed that the binding of the Myc and HA-tagged WT proteins was affected by the expression of the p.Ile678Leu missense variant (Supplementary Fig. 4d). We further analyzed the processivity of mutant *hKIF21B* in Cos7 cells transfected with GFP-tagged *hKIF21B* constructs (Supplementary Fig. 4b). Live-cell imaging revealed a shift of GFP-*hKIF21B* velocity toward high speed for all variant proteins compared to the WT protein (Fig. 4g). Notably the p.Ile678Leu variant showed a more drastic effect with an increased average velocity of 28% compared to the WT protein (Fig. 4h). We next assessed the effect of *hKIF21B* variants on the trafficking of BDNF vesicles and mitochondria, two potential cargoes of *KIF21B*<sup>21,44</sup>. Fast videomicroscopy experiments performed in Cos7 cells transfected with WT and mutant pDNA-HA-*hKIF21B* cDNA (Supplementary Fig. 4b) and BDNF-mCherry or Mito-RFP constructs did not reveal any change in the dynamics of neither BDNF-mCherry-containing vesicles (Supplementary Fig. 4e–g) or mitochondria (Supplementary Fig. 4h, i), suggesting that *hKIF21B* variants might lead to excessive motility of other unidentified cargoes. Collectively, these data indicate that the variants enhanced *KIF21B* processive activity through lessening of the kinesin autoinhibition.

We finally tested the effect of expressing immotile *hKIF21B* mutant proteins on neuronal migration. We performed IUE of truncated WT and mutant *hKIF21B* that lacks the ATP binding domain (Fig. 1h) in wild-type E14.5 mouse cortices. Although a significant number of neurons expressing the p.Gln313Lys, p.Ile678Leu and p.Ala1001Thr *hKIF21B* variants were trapped in the IZ at E18.5, most of the cells expressing the immotile variants (NeuroD-p.Gln313Lys- $\Delta$ ATP*hKIF21B*, NeuroD-p.Ile678Leu- $\Delta$ ATP-*hKIF21B*, NeuroD-p.Ala1001Thr- $\Delta$ ATP*hKIF21B*) showed a correct distribution (Fig. 4i, j, Supplementary Fig. 3a), demonstrating that preventing the motility of the mutant proteins decreases the severity of the migration phenotype. These results confirmed that the mutant protein impairs radial migration at least by enhancing *KIF21B* motility activity through the release of the kinesin autoinhibition (Fig. 4k). Collectively, our data indicate that modulation of kinesin autoregulation is critical in *KIF21B*-associated cortical migration phenotypes.

***KIF21B* p.Gln313Lys variant reduced head size in zebrafish.** Considering the presence of microcephaly in the subject with p.Gln313Lys variant, we asked whether this mutant could induce head size defects in an appropriate animal model. We therefore turned toward the developing zebrafish embryo, a model that has been extensively used for microcephaly modeling, the measure of head size being a relevant proxy for brain size<sup>55</sup>. *drKIF21B* protein is broadly distributed in zebrafish larval brain at 5 days post-fertilization (dpf), a stage characterized by strong upregulation of *drKIF21B* transcripts (Supplementary Fig. 5a, b). Larvae injected with p.Gln313Lys human mRNA showed a significant and physiologically relevant reduction of head size compared to control at 5 dpf (–6%, Welch two sample *t*-test  $P = 1.185 \times 10^{-9}$ ), therefore exhibiting a phenotype analogous to the microcephaly observed in the human clinical condition (Fig. 5). By contrast, introduction of WT mRNAs or the two other missense variants (p.Ala1001Thr and p.Ile678Leu), that do not lead to head circumference defects in patients, barely affected zebrafish head size (Fig. 5, Supplementary Fig. 5c, d). These data suggest that this particular p.Gln313Lys variant in the motor domain of *KIF21B* likely drives the microcephaly phenotype observed in the individual carrier.

**p.Gln313Lys *KIF21B* variant does not impair proliferation.** We next sought to understand the mechanisms by which the p.Gln313Lys variant impairs brain size. Expression of *hKIF21B* missense variants in mouse cortical neurons did not induce cell death (Supplementary Fig. 3c), excluding the possibility that the microcephaly phenotype arises from a poor survival of neurons. Although *KIF21B* expression is restricted to neurons, we further tested whether expression of the p.Gln313Lys variant could non-cell autonomously affect the progenitors' biology. We performed IUE of NeuroD-p.Gln313Lys *hKIF21B* at E14.5 in wild-type cortices and analyzed the progenitors located in the electroporated area at E16.5. The total number and the proliferative fraction (Ki67<sup>+</sup>) of both apical (Pax6<sup>+</sup>) and intermediate progenitors (Tbr2<sup>+</sup>) were indistinguishable from control condition (Supplementary Fig. 5e–j), suggesting that the brain size phenotype induced by the p.Gln313Lys *hKIF21B* variant was unlikely to have arisen from impaired neurogenesis. Altogether these results suggested that neither impaired birth nor poor survival of neurons or their progenitors contributed to the microcephaly phenotype observed in the subject with the p.Gln313Lys variant.

**p.Ile678Leu *hKIF21B* variant expression impedes axogenesis.** The corpus callosum (CC), the major commissure connecting

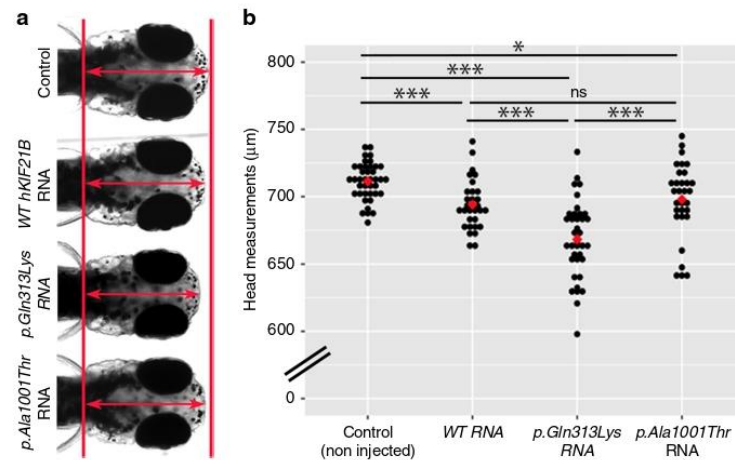


**Fig. 5** Expression of p.Gln313Lys hKIF21B decreases head size in zebrafish larvae. **a** Dorsal view of representative control zebrafish larvae (non-injected) or injected with 100 pg of wild-type (WT) or mutated *hKIF21B* mRNAs (p.Gln313Lys and p.Ala1001Thr) at 5 days post-fertilization (5 dpf). Double arrow indicates the distance between the forebrain and hindbrain, a measure used as a proxy for head size. **b** Dot plot of the head measurements (red double arrow) of control and injected larvae at 5 dpf. Red diamond corresponds to the mean of the batch measured. Number of embryos analyzed for this specific batch: control,  $n = 40$ ; WT,  $n = 31$ ; p.Gln313Lys,  $n = 38$ ; p.Ala1001Thr,  $n = 31$ . Experiments were repeated six times for non-injected control embryos ( $n = 231$ ), four times for WT-injected embryos ( $n = 127$ ), three times for p.Gln313Lys-injected embryos ( $n = 108$ ) and four times for p.Ala1001Thr-injected embryos ( $n = 158$ ). ns, non-significant,  $*P < 0.05$ ,  $**P < 0.005$ ,  $***P < 0.001$ . Significance was calculated by unpaired two-tailed Student's *t*-test or a Welch's two sample *t*-test between control and RNA-injected larvae. ns non-significant,  $*P < 0.05$ ,  $**P < 0.005$ ,  $***P < 0.001$ . Source data are provided in the Source Data file.

the two cerebral hemispheres, is formed of hundreds of millions of axons projecting contralaterally from the callosal projection neurons. Callosal axons cross the midline around birth to reach, in the first postnatal week, the contralateral cortex where they branch extensively at layer II/III and V. Given the ACC in the patient carrying the p.Ile678Leu variant, we investigated how the missense variants in *hKIF21B* lead to aberrant inter-hemispheric connectivity by introducing WT or mutant cDNA (NeuroD-hKIF21B) together with a mScarlet-expressing vector (pCAG2-mScarlet) in wild-type callosal projection neuron via IUE of E15.5 mouse cortical progenitors. The p.Gln313Lys substitution variant was used as a negative control as we did not expect any commissural defects according to the patient clinical features (Table 1). At P4, soon after the axons cross the midline and at P8, when axons start invading the contralateral CP, neither the expression of WT-hKIF21B nor of any of the variants perturbed midline crossing, as indicated by an equivalent scarlet intensity on each side of the CC (Fig. 6a–c, Supplementary Fig. 6a–c). In addition, at P22, when callosal axons achieve their adult-like arborization pattern, axons correctly invaded the homotopic contralateral cortex and successfully branched in layer II–III and V in all conditions (Supplementary Fig. 6g, h). Nonetheless, expression of the p.Ile678Leu, but not WT nor p.Gln313Lys mutant reduced by half the density of scarlet-positive axons in the white matter compared to the control both at P4 and P8 ( $-49.7\%$  at P8,  $P = 0.0043$ ) (Fig. 6a, b, d, e, Supplementary Fig. 6a, b, d). These defects were unlikely due to delayed innervation, as the poor inter-hemispheric connections persisted at P22 (Supplementary Fig. 6e, f). Rerouting through alternate commissures was also excluded as no aberrant axonal projections were observed after electroporation of callosal neurons and as no other commissures were shown enlarged in the patient (P1). Altogether, these results indicate that the faulty CC innervation is due to an impaired axonal growth rather than to defective contralateral targeting. Accordingly, we

measured the length of the longest neurites in primary cortical neurons transfected with pcDNA-HA-hKIF21B cDNA constructs. Although primary cortical neurons expressing WT-hKIF21B or p.Ala1001Thr and p.Gln313Lys hKIF21B variants showed normal axonal growth, expression of p.Ile678Leu mutant severely impaired axonogenesis at DIV2 and DIV5 (Fig. 6f, g, Supplementary Fig. 7a, b). To dig deeper into the pathogenic mechanism of the p.Ile678Leu hKIF21B variant, we performed a complementation experiment by co-electroporating p.Ile678Leu hKIF21B with increasing amounts of WT-hKIF21B at E15.5 and analyzed the percentage of projecting neurons at P8. Equivalent amounts of WT-hKIF21B failed to rescue the CC innervation phenotype (Fig. 6b, e). Further in vitro analysis of neurite length in primary cortical neurons expressing WT-hKIF21B together with p.Ile678Leu hKIF21B mutant at a 1:1 ratio confirmed the lack of rescue of axonal growth (Fig. 6f, g). We next reasoned that the p.Ile678Leu variant might exert its effect through attenuation of KIF21B autoinhibition. Accordingly, primary neurons transfected with two units of NeuroD-hKIF21B displayed shorter longest neurites in vitro (Fig. 6f, g), suggesting that enhanced KIF21B activity induces axonogenesis defects. To corroborate these findings in vivo, we assessed the ability of neurons electroporated with  $\Delta$ ATP p.Ile678Leu variant (NeuroD-p.Ile678Leu- $\Delta$ ATPhKIF21B) to project axons contralaterally at P8 (Fig. 6b, c, e). There was no significant difference between the control and the immotile p.Ile678Leu- $\Delta$ ATPhKIF21B, suggesting that the p.Ile678Leu variant impedes CC innervation through aberrant motor activity. Consistent with a hyperactivation of KIF21B, neurons expressing NeuroD-mKif21b $\Delta$ rCC failed to project axons at P8 (Fig. 6b, e). Altogether these results indicate that the loss of inter-hemispheric connectivity induced by the p.Ile678Leu hKIF21B variant, and the subsequent release of KIF21B autoinhibition, arises from impaired axonal growth rather than defective innervation and arborization in the contralateral cortex.

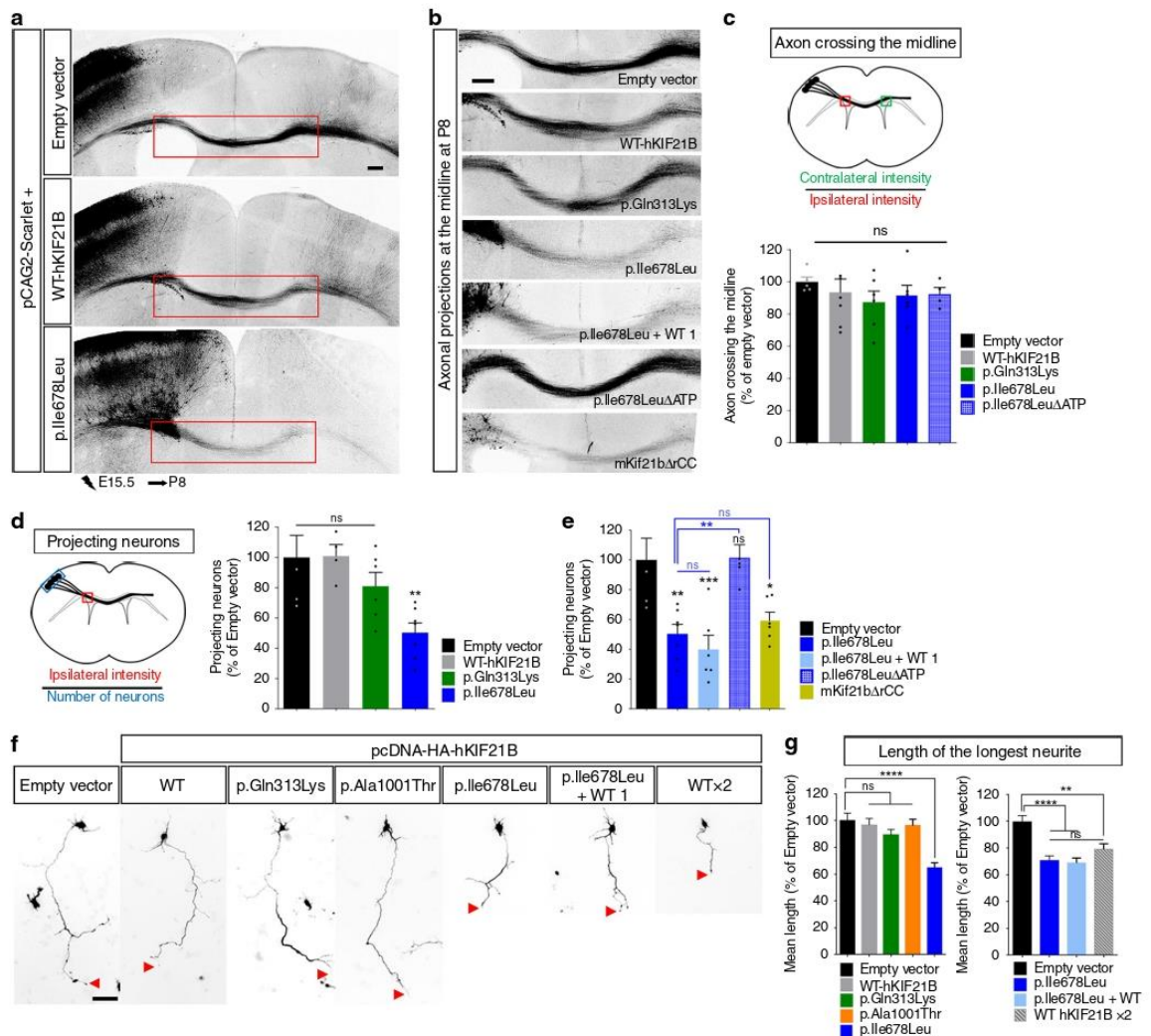
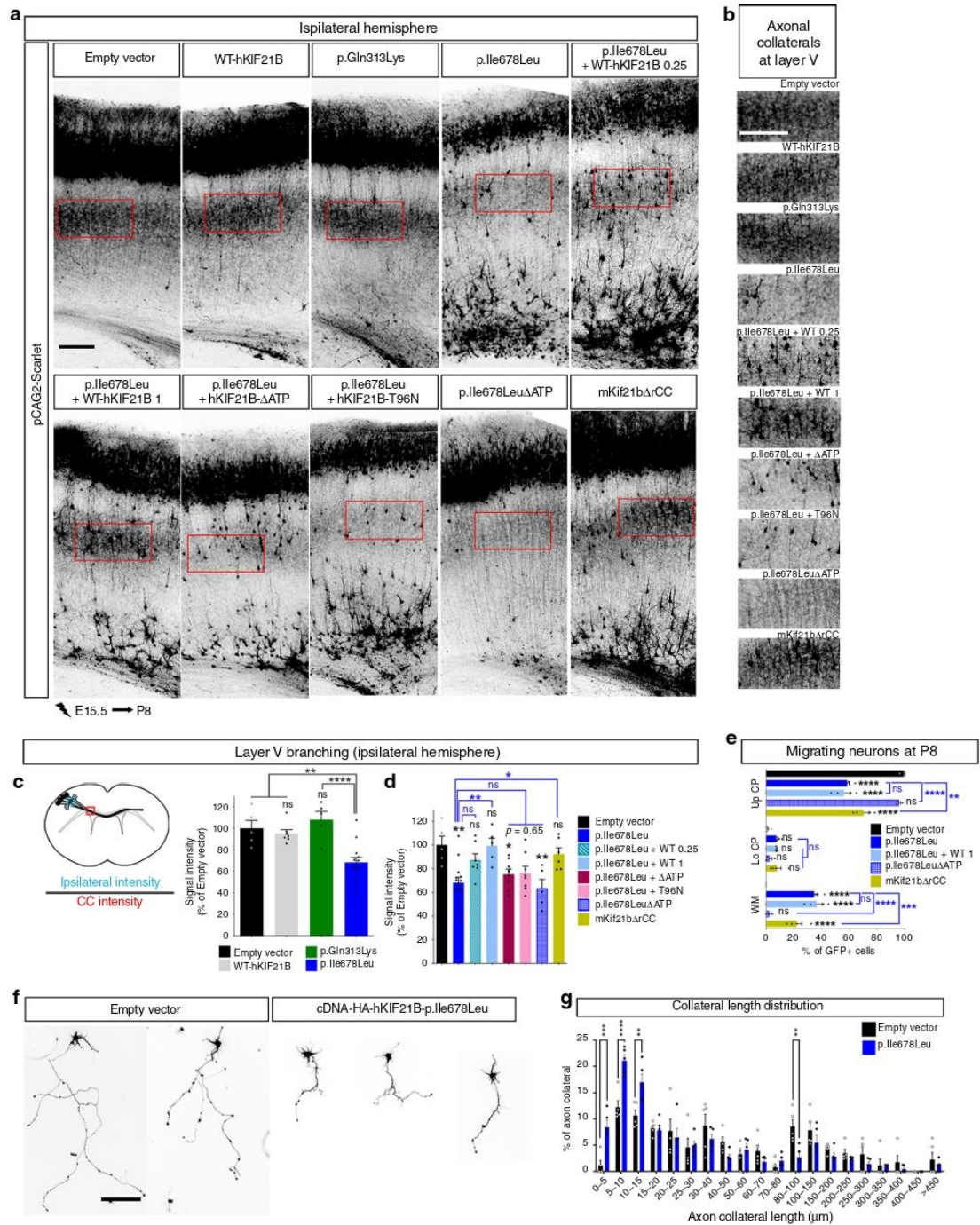


**Fig. 6** p.Ile678Leu hKIF21B variant impedes inter-hemispheric connectivity. **a** Coronal sections of P8 brains after IUE with pCAG2-Scarlet and indicated NeuroD-IRES-GFP constructs. **b** Close-up views of the red boxed area in **a** showing impaired inter-hemispheric connectivity upon expression of the p.Ile678Leu variant or the hyperactive mKif21bΔrCC but not upon expression of WT, p.Gln313Lys or immotile p.Ile678LeuΔATP. Rescue experiments were done by co-expressing p.Ile678Leu-hKIF21B (1 μg/μL) together with WT-hKIF21B constructs at 1 μg/μL (p.Ile678Leu + WT 1). Scale bars, 250 μm. **c, d** Upper (**c**) or left (**d**) panels, schematic describing methods used to quantify the percentage (**c**) of axon crossing the midline and (**d**) of projecting neurons. Lower (**c**) or right (**d**) panels, histograms presenting the percentage (**c**) of axon crossing the midline and (**d, e**) of projecting neurons. Data (means ± S.E.M.) were analyzed by one-way ANOVA (Bonferroni's multiple comparisons test). Number of pups analyzed: **c** Empty vector, *n* = 5; WT, *n* = 7; p.Gln313Lys, *n* = 6; p.Ile678Leu, *n* = 6; p.Ile678LeuΔATP, *n* = 4; **d, e** empty vector, *n* = 5; WT, *n* = 4; p.Gln313Lys, *n* = 6; p.Ile678Leu, *n* = 7; p.Ile678LeuΔATP, *n* = 5; p.Ile678Leu + WT, *n* = 6; mKif21bΔrCC, *n* = 6. **f** Representative DIV2 cortical neurons transfected at DIV0 with pCAG2-Scarlet together with empty pcDNA-HA or WT (at 1 (WT) or 2 μg/μL (WT x2)) or mutant pcDNA-HA-hKIF21B constructs. Rescue experiments were done by co-expressing mutated p.Ile678Leu hKIF21B variant together with NeuroD-WT-hKIF21B (ratio 1:1; p.Ile678Leu + WT 1). Red arrowheads point to the axon tip. **g** Quantification of the longest neurite length (axon) at DIV2. Bars represent the means of the longest neurite length ± S.E.M. Significance was calculated by one-way ANOVA (Bonferroni's multiple comparisons test). Number of neurons analyzed: (left graph) Empty vector, *n* = 94; WT, *n* = 96; p.Gln313Lys, *n* = 104; p.Ile678Leu, *n* = 144; p.Ala1001Thr, *n* = 133, from four (Empty vector, WT, p.Ile678Leu) or three (p.Gln313Lys, p.Ala1001Thr) independent experiments; (right graph) empty vector, *n* = 132; WT 2 μg/μL, *n* = 125; p.Ile678Leu + WT, *n* = 146; p.Ile678Leu, *n* = 134; from four independent experiments. ns non-significant; \**P* < 0.05; \*\**P* < 0.005; \*\*\**P* < 0.001; \*\*\*\**P* < 0.0001. Scale bars, (**a**) 200 μm, (**b**) 250 μm (**f**) 50 μm. Source data are provided in the Source Data file.

**hKIF21B p.Ile678Leu variant impairs ipsilateral connectivity.** Callosal neurons not only branch contralaterally, but also send multiple ipsilateral axon collaterals within layer II-III and even more strongly to layer V. We further examined whether this

hKIF21B missense variant also impacts the establishment of intracortical connections. We performed IUE of WT and mutant hKIF21B in wild-type embryos at E15.5 and analyzed ipsilateral cortical collaterals at P8. Although callosal neurons expressing



WT or p.Gln313Lys hKIF21B displayed prominent ipsilateral branching, overexpression of the p.Ile678Leu variant greatly reduced the intracortical branching (−32%, Bonferroni adjusted  $P = 0.0016$ ) (Fig. 7a–c). Co-electroporation of p.Ile678Leu hKIF21B variant with either half or equivalent dose of WT-hKIF21B gradually restored the intrahemispheric connectivity

phenotype, suggesting that p.Ile678Leu hKIF21B possibly impairs formation of ipsilateral collaterals through a dominant negative mechanism (Fig. 7a, b, d). Notably, migration defects were not rescued in these experiments (Fig. 7e) demonstrating that the branching phenotype is not an indirect consequence of neuron mispositioning. Conversely, p.Ile678Leu-ΔATPhKIF21B

**Fig. 7 p.Ile678Leu hKIF21B variant impairs ipsilateral axon collaterals formation.** **a** Representative images of ipsilateral P8 cortices after IUE, with pCAG2-Scarlet and indicated NeuroD-IRES-GFP constructs. Rescue experiments were done by co-expressing mutated p.Ile678Leu hKIF21B together with increasing amount of WT-hKIF21B (at 0.25  $\mu\text{g}/\mu\text{L}$  (WT 0.25) or 1  $\mu\text{g}/\mu\text{L}$  (WT 1)) or equivalent amount of hKIF21B- $\Delta\text{ATP}$  or hKIF21B-T96N, that both lost their processivity. **b** Close-up views of red boxed area in **(a)** showing axon ipsilateral branching within layer V for all the indicated conditions. **c–e** Histograms (means  $\pm$  S.E.M.) showing **(c, d)** the quantification of the ipsilateral branching in layer V (intensity of scarlet signal in layer V (blue box) normalized on the intensity of the scarlet signal in the corpus callosum (red box) — as shown on the schematic in the upper panel) and **(e)** the distribution of electroporated neurons in three different regions (Up CP (upper cortical plate), Lo CP (lower cortical plate), and WM (White matter)). Data from were analyzed by **(c, d)** one-way ANOVA or **(e)** two-ways ANOVA (Bonferroni's multiple comparisons test). Number of pups analyzed: **c, d** Empty vector,  $n = 5$ ; WT,  $n = 7$ ; p.Gln313Lys,  $n = 5$ ; p.Ile678Leu,  $n = 14$ ; p.Ile678Leu + WT 0.25  $\mu\text{g}/\mu\text{L}$ ,  $n = 7$ ; p.Ile678Leu + WT 1  $\mu\text{g}/\mu\text{L}$ ,  $n = 5$ ; p.Ile678Leu +  $\Delta\text{ATP}$ ,  $n = 8$ ; p.Ile678Leu + T96N,  $n = 8$ ; p.Ile678Leu $\Delta\text{ATP}$ ,  $n = 5$ ; mKif21b $\Delta\text{rCC}$ ,  $n = 6$ ; **e** Empty vector,  $n = 5$ ; p.Ile678Leu,  $n = 6$ ; p.Ile678Leu + WT 1  $\mu\text{g}/\mu\text{L}$ ,  $n = 4$ ; p.Ile678Leu $\Delta\text{ATP}$ ,  $n = 3$ ; mKif21b $\Delta\text{rCC}$ ,  $n = 4$ . **f** Representative DIV5 cortical neurons transfected at DIV2 with pCAG2-Scarlet together with the indicated pcDNA-HA-hKIF21B constructs. **g** Distribution (means  $\pm$  S.E.M.) of axonal collateral branches length at DIV5. Significance was calculated by two-way ANOVA (Bonferroni's multiple comparisons test). Number of collaterals analyzed: Empty vector,  $n = 265$ ; p.Ile678Leu,  $n = 385$ ; from 51 (Empty vector) and 66 (p.Ile678Leu) neurons from five independent experiments. ns non-significant, \* $P < 0.05$ ; \*\* $P < 0.005$ ; \*\*\* $P < 0.001$ ; \*\*\*\* $P < 0.0001$ . Scale bars, **(a, b)** 250  $\mu\text{m}$ , **(f)** 150  $\mu\text{m}$ . Source data are provided in the Source Data file.

overexpressing neurons that migrated normally (Fig. 7e), failed to send axonal collaterals ipsilaterally in layer V (Fig. 7a, b, d). Also, those neurons (p.Ile678Leu- $\Delta\text{ATP}$ hKIF21B) showed normal axonal growth (Fig. 6b, c, e), ruling out the possibility that defective intracortical branching arises from impaired axonogenesis (Fig. 7a, b, d). Accordingly, branching defects likely arose from impaired collateral growth as revealed by in vitro analysis of axon branching in primary neurons at DIV5. Expression of p.Ile678Leu hKIF21B variant but not WT nor p.Gln313Lys or p.Ala1001Thr mutants led to a shift of branch length toward short branch classes that resulted in a large decrease of the mean length of axon collaterals (Fig. 7f, g, Supplementary Fig. 7a, c, d). Consistent with a dominant negative effect, intrahemispheric connectivity is not affected upon KIF21B hyperactivation with neurons expressing NeuroD-mKif21b $\Delta\text{rCC}$  displaying normal ipsilateral collaterals (Fig. 7a, b, d). We finally investigated which function of WT-hKIF21B was negatively modulated by the mutant protein. We induced expression of p.Ile678Leu variant together with hKIF21B that either cannot bind (NeuroD- $\Delta\text{ATP}$ hKIF21B; Fig. 1h) or hydrolyze ATP (T96N-hKIF21B; Fig. 1h)<sup>21</sup> at a 1:1 ratio using IUE at E15.5. Both constructs failed to rescue the branching phenotype induced by p.Ile678Leu hKIF21B at P8, suggesting that p.Ile678Leu hKIF21B exerts its dominant negative effect on the processive activity of KIF21B (Fig. 7a, b, d, Supplementary Fig. 3a). Collectively, our results showed that the p.Ile678Leu variant alters the intrahemispheric connectivity beyond its effect on migration and axonal growth through a dominant negative effect on motility.

## Discussion

Our findings highlight the critical role of KIF21B in the regulation of processes involved in cortical development and implicate variants in *KIF21B* in ID and brain malformation. We identified three missense variants and one duplication of four nucleotides. The duplication leads to a frameshift introducing a premature termination codon in exon 20. The resulting mutant mRNA is likely degraded by nonsense-mediated mRNA decay. Although we demonstrated in mice that *Kif21b* haploinsufficiency leads to an impaired neuronal positioning (Supplementary Fig. 3d–f), the p.Asn988Serfs\*4 protein truncated variant is possibly not pathogenic. Indeed, hKIF21B gene might partially tolerate loss-of-function variants: in the gnomAD (Genome Aggregation Database, v2.1.1 “non-neuro”) populations that is supposed to be depleted in severe pediatric conditions, 28 loss-of-function variants have been reported. Nonetheless, the ratio of the observed/expected loss-of-function variants in the gnomAD populations is

low (0.32, confidence interval 0.23–0.43), still questioning the penetrance of loss-of-function variants in *KIF21B*.

Our study provides the molecular mechanisms by which the identified variants lead to an abnormal brain phenotype. We showed that all missense variants, to various extents, impaired neuronal migration by enhancing KIF21B motor activity. Several lines of evidence suggest that hKIF21B missense variants exert a gain-of-function effect by enhancing KIF21B motility activity through lessening of the kinesin autoinhibition (Fig. 4). First, WT-hKIF21B is unable to rescue the variant-induced migratory defects at equivalent dose (Fig. 3a, b). Second, the phenotype induced by overexpression of the variants is phenocopied by the expression of a constitutively active form of KIF21B (that is truncated for the rCC domain) (Fig. 4c, d). Third, loss of ATP binding is sufficient to abrogate the phenotype induced by the missense variants ( $\Delta\text{ATP}$ -hKIF21B; Figs. 4i, j and 7e). Fourth, mutant hKIF21B proteins showed enhanced microtubule-based motility compared to the WT protein (Fig. 4g, h). How do hKIF21B variants lead to autoinhibition release? KIF21B autoinhibition is mediated by a regulatory segment (rCC) within the second coiled-coil domain (CC2, Fig. 1h) that fastens the CC2 domain to the motor head<sup>42,46</sup>. We hypothesize that the position of the missense variants within the motor (p.Gln313Lys), coiled-coil (p.Ile678Leu) and rCC (p.Ala1001Thr) domains (Fig. 1h) alters the protein conformation so that it varies the impact on the intramolecular interaction between the motor and the internal coiled-coil domains. This model raises the possibility that the level of disruption of these interactions correlates with the degree of autoinhibition release imposed by the different missense variants and therefore dictates the severity of the phenotype. In accordance, the increase in KIF21B processivity correlated with the extent of migration defects, the velocity of the p.Ile678Leu variant being the most drastically enhanced (Fig. 4g, h). We therefore propose a model in which a minimal level of autoinhibition is required to ensure proper function of KIF21B in the developing cortex. Below this threshold, the more KIF21B gets overactivated, the more severe and broad the phenotypes will present. In this model, the p.Gln313Lys and p.Ala1001Thr variants would partially relieve autoinhibition, whereas the p.Ile678Leu variant would completely loose autoinhibition. Consistently, p.Gln313Lys and p.Ala1001Thr KIF21B induce a delay of migration, whereas the p.Ile678Leu variant leads to a permanent arrest of migration and an additional connectivity phenotype (Figs. 3 and 6).

Beyond autoinhibition, maintaining a proper level of KIF21B activity seems to be crucial for its function during development. Indeed, *KIF21B* haploinsufficiency also leads to migratory defects. Whether those defects are caused by a loss of trafficking or MT

regulator functions is not clear and should be further assessed. Overall, the model could be expanded to a threshold of activity, below (haploinsufficiency) or above (identified missense variants) which KIF21B would not be properly functional leading to neurodevelopmental defects.

Convergent evidence suggests that the p.Ile678Leu variant alters axon branching through a dominant negative effect on KIF21B processivity (Fig. 7). First, co-expression of increasing amount of WT-hKIF21B together with the mutant protein gradually restored the intrahemispheric connectivity phenotype. Second, an immotile form of KIF21B failed to rescue the variant-induced branching defect. Third, expression of a constitutive active form ( $\Delta$ rCC) of KIF21B does not affect the formation of axon branches. Fourth, p.Ile678Leu- $\Delta$ ATPhKIF21B over-expressing neurons display abnormal ipsilateral collaterals. Fifth, consistent with a dominant negative effect, the WT KIF21B protein fails to form homodimer and is mislocalized when co-expressed with the p.Ile678Leu variant. Intriguingly, the p.Ile678Leu variant also perturbs axonal growth (Fig. 6) and migration (Figs. 3 and 4) through attenuation of autoinhibition, suggesting, as discussed above, a possible gain-of-function effect. To reconcile these seemingly conflicting findings, we propose that it could imply that KIF21B regulates the trafficking of different cargoes in axon and branches. p.Ile678Leu-induced over-activation of KIF21B might therefore lead to excessive motility of specific cargoes within axons. Conversely, the same variant could impede the transport of branch-specific cargoes by interfering with the function of the wild-type protein. At this time, none of the few KIF21B cargoes identified is specific to axon or branches<sup>44,45</sup>, so further work is needed to identify cargoes in the different cellular compartments and validate this hypothesis.

Expression of the KIF21B p.Gln313Lys variant recapitulates the microcephaly phenotype observed in the reported subject. Given that introduction of the p.Ala1001Thr variant that is expected to attenuate KIF21B autoinhibition at the same extent as the p.Gln313Lys substitution variant, but does not reduce brain size in zebrafish (Fig. 5), the hyperactivation of KIF21B is unlikely to be driving the phenotype of microcephaly. In a search for possible microcephaly-underlying mechanism, we exclude any non-cell autonomous effect on progenitors' proliferation, or any impact on cell survival. Abnormal postnatal neuronal maturation may also contribute to the global microcephaly phenotype. Accordingly microcephaly may worsen with time: the patient carrying the KIF21B p.Gly313Lys variant was born with a head circumference (HC) of 32 cm (5<sup>th</sup> percentile), but microcephaly progressed and at the age of 12 was 48.5 cm (<1st percentile, -3.9 SD). These maturation defects may result from regulation of neuronal soma size<sup>56,57</sup> or from connectivity defects. Although the axonal branching is not impaired in callosal neurons overexpressing the microcephaly-related variant, we cannot rule out the possibility that reduced dendritic arborization of projection neurons influences the microcephaly phenotype.

In conclusion, the mechanism proposed here for the role of KIF21B in attenuating (p.Gln313Lys and p.Ala1001Thr) or abrogating autoinhibition (p.Ile678Leu) of one or several kinesin functions, might be expanded to other kinesins (KIF1A<sup>28</sup>, KIF5C<sup>30</sup>, KIF7<sup>26</sup>, KIF4A<sup>24</sup>) known to be regulated by autoinhibition and for which the pathophysiological mechanisms underlying the migration and inter-hemispheric connectivity phenotypes have not yet been elucidated. In addition, autoinhibition of kinesins has been implicated in several physiological processes including the regulation of innervation, synaptogenesis and compartment-specific localization of cargo<sup>53,54,58,59</sup>. Our results indicate that fine-tuning of KIF21B activities is critical for proper neuronal migration and axonal growth, adding novel physiological roles of kinesin autoinhibition.

## Methods

**Whole-exome sequencing (WES).** A parent-offspring trio approach was used for whole-exome sequencing (WES) in each family. Exomes were sequenced using DNA isolated from blood according to standard procedures. Informed consent was obtained from all participants in accordance with site-specific institutional review board. Patient 1: The SeqCap EZ MedExome Enrichment Kit (Roche) was used for library preparation with 12 samples multiplexing, according to manufacturer's protocol. This library was then sequenced on a NextSeq 500 (Illumina) with a 2 × 150 bp high output flowcell. The bioinformatic analyses was conducted by Polyweb using BWA 0.7.12, picard-tools-1.121, GenomeAnalysisTK-2014.3-17-g0583013, SNPEff-4.2. Patient 2: The SeqCap EZ VCRome 2.0 (Roche) was used for library preparation. Exome libraries were sequenced on an Illumina HiSeq 2500 instrument and the following sites are used to search for previously described gene pathogenic variants and polymorphisms: the Human Gene Mutation Database (HGMD), the single Nucleotide Polymorphism database (dbSNP), 1000 genomes, HapMap data. Patient 3: Exome capture was done using the Nimblegen SeqCap-*p\_EZ\_Exome\_v3* (Nimblegen). Exome libraries were sequenced on an Illumina HiSeq instrument (Illumina, San Diego, USA) with 150 bp paired-end reads at a median coverage of 100×. Sequence reads were aligned to the hg19 reference genome using BWA. Variants were subsequently called by the GATK unified genotyper, and annotated using a custom diagnostic annotation pipeline. Patient 4: Exome was captured using the Clinical Research Exome kit (Agilent Technologies, Santa Clara, CA). Massively parallel (NextGen) sequencing was done on an Illumina system with 100 bp or greater paired-end reads. Reads were aligned to human genome build GRCh37/UCSC hg19, and analyzed for sequence variants using GeneDx's XomeAnalyzer (a custom-developed variant annotation, filtering and viewing interface for WES data)<sup>60</sup>. The general assertion criteria for variant classification are publicly available on the GeneDx ClinVar submission page (<http://www.ncbi.nlm.nih.gov/clinvar/submitters/26957/>).

Inclusion and genetic studies were approved by local ethics committee in France (CCP Ile de France, CPP No. 71-10/ ID RCB: 2010-A00802-37) and USA (Institutional Review Board at Baylor College of Medicine, protocol H-29697 and at the John Hopkins School of Medicine).

**Cloning and plasmid constructs.** Wild-type (WT) human *KIF21B* cDNA (NCBI Reference Sequence: NM\_001252100.1) was obtained from Vector Builder by gene synthesis and subcloned by restriction-ligation into the NeuroD-iresGFP<sup>61</sup>, the pCDNA3.1+/N-HA and in the pEGFP-N1 vectors. Myc-tagged hKIF21B constructs were obtained by replacing the GFP sequence of the pEGFP-N1 containing the hKIF21B gene by a Myc-tag sequence. Human *KIF21B* variants c.937C>A (p.Gln313Lys), c.2032A>C (p.Ile678Leu), c.3001G>A (p.Ala1001Thr) and the c.288C>T (T96N) substitution that abolishes KIF21B mobility<sup>21</sup> were created from WT CDS by Sequence and Ligation Independent Cloning (SLIC). *hKIF21B* ATP binding site (amino acids 87-94; UniProtKB O75037) was deleted by SLIC from NeuroD-WT-hKIF21B-iresGFP, NeuroD-hKIF21B-p.Gln313Lys-iresGFP, NeuroD-hKIF21B-p.Ile678Leu-iresGFP and NeuroD-hKIF21B-p.Ala1001Thr-iresGFP to generate p.Ile678Leu- $\Delta$ ATPhKIF21B WT- $\Delta$ ATPhKIF21B, p.Gln313Lys- $\Delta$ ATPhKIF21B, p.Ile678Leu- $\Delta$ ATPhKIF21B and p.Ala1001Thr- $\Delta$ ATPhKIF21B constructs, respectively.

Wild-type mouse *Kif21b* CDS was isolated from E18.5 cDNA mouse cortices by PCR and a new isoform has been amplified. This isoform is 4920 bp-long and has an insertion (c.4905\_4906 ins C; NM\_001039472.2) that leads to a frameshift and to the introduction of a premature stop codon in exon 35. This isoform has been subcloned by restriction-ligation into the NeuroD-IRES-GFP plasmid. This new isoform has also been fused to eGFP in the N-terminal part (pEGFP-C1-WT-mKif21b) via subcloning in pEGFP-C1 plasmid (NovoPro V12024). The amino acids 930-1010 corresponding to autoinhibitory domain (rCC)<sup>42</sup> were deleted by site-directed mutagenesis to generate NeuroD-mKif21b- $\Delta$ rCC construct. Mouse *Kif21b* 3'UTR sequence (NCBI Reference Sequence: NM\_001039472.2) were amplified by PCR and cloned by restriction-ligation into the pEGFP-C1 plasmid and fused to eGFP in the N-terminal part. pCR-BluntII-TOPO-mKif21b 3'UTR used to synthesize RNA probes was generated by cloning part of the mKif21b 3' UTR (255 bp, Genepaint template T36548) in pCR-BluntII-TOPO vector.

shRNAs against coding sequence 3390-3410 (NM\_001252100.1) (sh-*Kif21b* #1) or the 3' UTR (sh-*Kif21b* #2) of mouse *Kif21b* were generated by annealing of sense and antisense oligos, the resulting duplex were subcloned in pCALSL-mir30<sup>52</sup> backbone vector digested with *XhoI* and *EcoRI*. The following oligos were used: sh-*Kif21b* #1:

sense: 5'TCGAGaaggtatattgctgttgacagttagcgcCCACGATGACTTCAAGITCA AtagtgaagccacagatgtaTTGAACTTGAAGTCATCGTGGTgctactgctcctgG 3'; antisense: 5'AATTCcaggcagtaggcaCCACGATGACTTCAAGITCAAtacatctgtggcttcaactTTGAACTTGAAGTCATCGTGGcctcactgtcaacagcaatatacttC 3'; sh-*Kif21b* #2: sense: 5'TCGAGaaggtatattgctgttgacagttagcgcGCCTTTAAACACCCAGAGATAtagtagaagccacagatgtaTATACTCTGGITGTTAAAGGCTgctactgctcctgG 3'; antisense: 5'AATTCcaggcagtaggcaGCCTTTAAACACCCAGAGATAtacatctgtggcttcaactTATACTCTGGITGTTAAAGGCGcctcactgtcaacagcaatatacttC 3'; Scrambled shRNA: Sense: 5'TCGAGaaggtatattgctgttgacagttagcgcGCCGATAGCGCTAATAATTtagtgaagccacagatgtaAAATATTATGCGCTATCGCGCtggcctgctcctgG 3'; Antisense: 5'AATTCcaggcagtaggcaGCCGATAGCGCT



AATAATTTTtacatctgtgcttcaactAAATTATTAGCGCTATCGCGCGcgtcactgtcaacagcaataatctc 3'

pCAG2-mScarlet and pSCV2-CAG-mVENUS<sup>61</sup> expressing vectors were provided by J. Courchet (INMG, Lyon, France). Plasmid DNAs used in this study were prepared using the EndoFree plasmid purification kit (Macherey Nagel).

**Mouse.** All animal studies were conducted in accordance with French regulations (EU Directive 86/609 – French Act Rural Code R 214-87 to 126) and all procedures were approved by the local ethics committee and the Research Ministry (APA-FIS#15691-20180627/1458609). Mice were bred at the IGBMC animal facility under controlled light/dark cycles, stable temperature (19 °C) and humidity (50% condition) and were provided with food and water ad libitum.

Timed-pregnant wild-type (WT) NMRI (Janvier-labs) and CD1 (Charles River Laboratories) females were used for in utero electroporation (IUE) of sh-*Kif21b* and NeuroD-hKIF21B constructs, respectively, at embryonic day 14.5 (E14.5). Hybrid F1 females were obtained by mating inbred 129/SvJ females (Janvier-labs) with C57Bl/6J males (Charles River Laboratories). F1 females were crossed with C57Bl/6J males (Charles River Laboratories) to obtain timed-pregnant females for IUE at E15.5.

Kif21b KO mice were generated using the International Mouse Phenotyping Consortium targeting mutation strategy<sup>62</sup> and obtained from UC Davis/ KOMP repository (Kif21b<sup>tm1a(KOMP)Wtsi</sup>). Genotyping was done as follows: Genomic DNA was extracted from tail biopsies using PCR reagent (Viagen) supplemented with Proteinase K (1 mg/mL), heated at 55 °C for 5 h. Proteinase K was inactivated for 45 min at 85 °C, and cell debris was removed by centrifugation. Samples were processed for PCR using the following primers: KIF21B forward: 5'-GGGGTACTTTCACATTTGACCCAG-3', KIF21B reverse: 5'-GAAGGGACCAAACTGGGGC-3' for KIF21B targeted exon amplification and Mq forward 5'-GCTATGACTGGG CACAACAGACAATC-3' and Mq reverse 5'-CAAGGTGAGATGACAGGAG ATCTCG-3' for Neomycin gene amplification. The presence of the wild-type and knockout alleles was indicated by 346 and 261 bp products, respectively, which were detected on a 2% agarose gel.

**In utero electroporation (IUE).** Timed-pregnant mice were anesthetized with isoflurane (2 L per min of oxygen, 4% isoflurane in the induction phase and 2% isoflurane during surgery operation; Tem Segá). The uterine horns were exposed, and a lateral ventricle of each embryo was injected using pulled glass capillaries (Harvard apparatus, 1.0 OD\*0.58 ID\*100 mmL) with Fast Green (1 µg/µL; Sigma) combined with different amounts of DNA constructs using a micro injector (Eppendorf Femto Jet). We injected 1 µg/µL of WT or mutant NeuroD-hKIF21B-IRES-GFP constructs together with 0.5 µg/µL of empty NeuroD-IRES-GFP vector at E14.5. 1.5 µg/µL of NeuroD-IRES-GFP vector were used as control. We injected 1 µg/µL of NeuroD-Cre-GFP vector together with 3 µg/µL of either Cre inducible pCALS-miR30-shRNA-*Kif21b* #1 or #2 or pCALS-miR30-sh-scramble sequence and 1 µg/µL of NeuroD-IRES-GFP or NeuroD-mKif21b-IRES-GFP (rescue experiment). For axonal pathfinding experiments, we injected 1 µg/µL of NeuroD-IRES-GFP (empty or containing WT or mutated human KIF21B cDNA) together with 0.8 µg/µL of pCAG2-mScarlet at E15.5. For rescue experiments, we co-injected 1 µg/µL of NeuroD-IRES-GFP (WT or mutated human KIF21B cDNA) together with 0.25, 0.5 or 1 µg/µL of the indicated NeuroD-IRES-GFP constructs. Plasmids were further electroporated into the neuronal progenitors adjacent to the ventricle by discharging five electric pulses (40 V) for 50 ms at 950 ns intervals using electrodes (diameter 3 mm; Sonidel CUY650P3) and ECM-830 BTX square wave electroporator (VWR International). After electroporation, embryos were placed back in the abdominal cavity and the abdomen was sutured using surgical needle and thread. For E16.5 and E18.5 analysis, pregnant mice were killed by cervical dislocation 2 and 4 days after surgery. For postnatal analysis, electroporated pups were killed 2, 4, or 8 days after birth (P2, P4, P8) by head sectioning or 22 days after birth (P22) by terminal perfusion.

**Mouse brain fixation, cutting and immunolabeling.** E12.5 to P8 animals were killed by head sectioning and brains were fixed in 4% paraformaldehyde (PFA, Electron Microscopy Sciences) in Phosphate buffered saline (PBS, HyClone) 2 h at room temperature (RT) or overnight (O/N) at 4 °C. P22 animals were killed by terminal perfusion of PBS then 4% PFA followed by overnight post-fixation at 4 °C in 4% PFA. For Kif21b expression pattern (Fig. 2 and Supplementary Fig. 2), immunolabeling was performed on cryosections as follows: after fixation, brains were rinsed and equilibrated in 20% sucrose in PBS overnight at 4 °C, embedded in Tissue-Tek O.C.T. (Sakura), frozen on dry ice and coronal sections were cut at the cryostat (12 to 18 µm thickness, Leica CM3050S) and processed for In situ hybridization or immunolabeling. Sections were maintained at -80 °C. For IUE analyses (Figs. 3–7, Supplementary Figs. 3–7), immunolabeling was performed on vibratome sections as follows: after fixation, brains were rinsed and embedded in a solution of 4% low-melting agarose (Bio-Rad) and cut into coronal sections (60-µm-thick for E18.5 and P2 mice, 100-µm-thick for P4 to P22 mice) using a vibrating-blade microtome (Leica VT1000S, Leica Microsystems) and processed for immunolabeling. Sections were maintained in PBS-azide 0.05% for short-term storage and in an Antifreeze solution (30% Ethyleneglycol, 20% Glycerol, 30% DH<sub>2</sub>O, 20% PO<sub>4</sub> Buffer) for long-term storage.

For cryosections only, an antigen retrieval was performed by boiling sections in sodium citrate buffer (0.01 M, pH 6) during 15 min. Cryo- and vibratome sections were permeabilized and blocked with 5% Normal Donkey Serum (NDS, Dominic Dutsher), 0.1% Triton X-100 in PBS. Slides were incubated with primary antibodies diluted in blocking solution overnight at 4 °C and secondary antibodies diluted in PBS-0.1% Triton one hour at room temperature, whereas cell nuclei were identified using DAPI (1 mg/mL Sigma). Slices were mounted in Aquapolymount mounting medium (Polysciences Inc). All primary and secondary antibodies used for immunolabeling are described in Supplementary Table 1.

**RNA in situ hybridization.** Mouse *Kif21b* sense and antisense probes were synthesized from pCR-BluntII-TOPO-mKif21b 3'UTR by either *Bam*HI digestion followed by synthesis with T7 RNA polymerase (Roche) (sense probe) or *Eco*RV digestion followed by synthesis with SP6 RNA polymerase (Roche) (antisense probe). Kif21b digoxigenin-labeled probes using the DIG RNA labeling Kit SP6/T7 (Roche) according to the manufacturer's protocol. In situ hybridization was performed on E12.5 to E18.5 WT NMRI coronal embryonic brain cryosections as follows: sections were first rinsed in Phosphate buffered saline (PBS, HyClone) and dehydrated for 5 min in successive ethanol baths (70%, 95% and 100%) diluted in sterile milliQ water. The same amount of each antisense or sense Kif21b digoxigenin-labeled probes were diluted at 0.1 µg/µL in pre-warm Hybridization Buffer (4 M NaCl 0.2 M, 5 mM EDTA pH 8, 10 mM Tris-HCl pH 7.5, 10 mM NaH<sub>2</sub>PO<sub>4</sub>·2H<sub>2</sub>O, 10 mM Na<sub>2</sub>HPO<sub>4</sub>, 2 mg/mL Ficoll, 2 mg/mL polyvinylpyrrolidone, 2 mg/mL bovine serum albumin, 10% Dextran Sulfate, 1 mg/mL Yeast tRNA (ThermoFisher Scientific), 50% deionized formamide) and denatured for 10 min at 70 °C. Sections were then incubated with the probe mix in a water-bath O/N at 70 °C in a sealed humidified chamber. Slides were then washed twice with the pre-warmed 1× Saline Sodium Citrate solution (SSC, 0.15 M NaCl, 15 mM Na Citrate) at 70 °C for 30 min and in the 0.2× SSC solution for one hour at 70 °C and for 5 min at RT. Slides were then washed twice in the MABT solution (0.1 M Maleic Acid, 0.15 M NaCl, 0.1% Tween-20, pH 6) for 30 min at RT under slow agitation and blocked in MABT solution supplemented with 2% blocking reagent (Roche) and 20% heat-inactivated Normal Donkey Serum (NDS, Dominic Dutsher) for 1 hour at RT. Slides were then incubated with the anti-DIG antibody (Abcam ab76907, 1:2500 diluted in blocking solution) O/N in humidified chamber at 4 °C. Slides were then washed four times in MABT for 15 min at RT then twice in Alkaline Phosphatase Buffer (NTMT, 100 mM NaCl, 100 mM Tris pH 9.5, 50 mM MgCl<sub>2</sub>·H<sub>2</sub>O, 0.1% Tween-20) for 10 min at RT and stained in NTMT supplemented with NBT (Sigma-Aldrich, 0.3 mg/mL) and BCIP (Sigma-Aldrich, 0.175 mg/mL) for 4 hours at RT in a box protected from the light. Reaction was stopped by transferring slides into PBS for 15 min, then slides were post-fixed in PFA4% diluted in PBS for 10 min at 4 °C. Slides were then washed 3 times in PBS for 10 min, air-dried and mount in Pertex mounting medium (Leica Microsystems). Images were taken using a microscope (Leica M420) connected to a Photometrics camera with the CoolSNAP software (v. 1.2).

**Primary neuronal culture, magnetofection and immunolabeling.** Cortices from E15.5 CD1 mouse embryos were dissected in cold PBS supplemented with BSA (3 mg/mL), MgSO<sub>4</sub> (1 mM, Sigma), and D-glucose (30 mM, Sigma). Cortices were dissociated in Neurobasal media containing papain (20 U/mL, Worthington) and DNase I (100 µg/mL, Sigma) for 20 min at 37 °C, washed 5 min with Neurobasal media containing Ovomucoide (15 mg/mL, Worthington), and manually triturated in OptiMeM supplemented with D-Glucose (20 mM). Cells were then plated at 2 × 10<sup>5</sup> cells per 24-well plate coated with poly-D-lysine (1 mg/mL, Sigma) overnight at 4 °C and cultured for 2–5 days in Neurobasal medium supplemented with B27 (1×), L-glutamine (2 mM) and penicillin (5 units/mL)-streptomycin (50 mg/mL). To transfected cultured neurons, we performed magnetofection at DIV0 (for analysis at DIV2) or DIV2 (for analysis at DIV5) using NeuroMag (OZ Bioscience) according to the manufacturer's protocol. Cells were fixed at DIV2 or DIV5 for 15 min at room temperature in 4% PFA, 4% sucrose in PBS, and incubated for 1 h in 0.1% Triton X-100, 5% NDS in PBS. Primary antibodies were incubated overnight at 4 °C and secondary antibodies were incubated for 1 h at room temperature (see Supplementary Table 1 for antibodies). DNA was stained using DAPI (1/1000). Slides were air-dried and mounted in Aquapolymount mounting medium (Polysciences Inc).

**Fluorescent-activated cell sorting (FACS).** Cortices from 3 to 4 E16.5 mouse Rosa26-loxSTOP-YFP; NEXCRE/+ embryos were dissected and dissociated as described above. After dissociation, cells were resuspended in 500 µL of staining solution (10% Fetal Bovine Serum (FBS) + 0.02% Sodium Azide in PBS) and stained for 20 min on ice in dark with CD24-APC Antibody (0.06 µg/100 µL final; clone MI/69, ThermoFisher Scientific (#17-0242-82)). Cells were then washed twice with HBSS (Gibco) and passed through a 40 µm filter (Falcon FACS). YFP-/CD24- population was sorted to enrich for progenitors and YFP+/CD24+ population was used to enrich for neurons using the BD Aria II flow cytometer with 488 and 633 lasers to excite YFP and APC respectively. Littermate YFP- embryos (Rosa26-loxSTOP-YFP; NEXCRE-) were processed the same way, stained with the Rat IgG2b-APC isotype control antibody (clone eB149/10H5, ThermoFisher Scientific (#17-4031-82)) and used as controls to set the YFP and CD24 gates.

**Microfluidic fabrication and neurons plating.** Design of polydimethylsiloxane microfluidic device is based on the one described by Taylor et al.<sup>51</sup> with modifications of the size of the microchannels (3- $\mu$ m width, 3- $\mu$ m height and 450- $\mu$ m length to reduce the number of axons per microchannels)<sup>63</sup>. Briefly, microfluidics chambers were positioned and sealed on Iwaki boxes using plasma cleaner and then coated with poly-D-lysine (0.1 mg/mL) in the upper chamber, and with poly-D-lysine (0.1 mg/mL) and laminin (10  $\mu$ g/mL) in the lower chamber. After overnight incubation at 4 °C microfluidic devices were washed two times with Neurobasal medium and once with growing medium (Neurobasal medium supplemented with 2% B27, 2 mM Glutamax, and 1% penicillin/streptomycin). Microchambers were then placed in the incubator until neurons were plated. Primary cortical neurons were prepared as follows: E15.5 C57Bl/6j mouse embryos were collected and cortices were dissected, followed by papain and cysteine digestion and trypsin inhibitor incubation. After mechanical dissociation, cortical neurons were resuspended in growing medium ( $5 \times 10^6$  cells in 120  $\mu$ L) and plated in the upper chamber with a final density of  $\sim 7000$  cells/mm<sup>2</sup>. Neurons were kept in the incubator for 1 h. Then, the two compartments were gently filled with growing medium.

Immunostaining in microchambers was performed from DIV5 culture<sup>64</sup>; after 30 min fixation in 4% PFA/Sucrose dissolved in PBS, all the compartments were blocked with a solution containing BSA 1%, normal goat serum 2%, Triton X-100 0.1%. For these two solutions, a bigger volume in the upper chamber was applied to create a pressure gradient. After 1 h incubation with blocking solution, neurites in both compartments were incubated overnight at 4 °C with primary antibody recognizing KIF21B and Tau. Secondary antibodies were added the following day for 4 h and microchambers were maintained in PBS for a few days in the dark at 4 °C (see Supplementary Table 1 for antibodies).

**RNA extraction, cDNA synthesis and RT-qPCR.** To assess Kif21b mRNA expression in mouse and zebrafish, total RNA was extracted from the cortices of WT NMRI mouse embryos or from whole zebrafish (*Danio rerio*) embryos (AB strain) at different time points of development, with TRIzol reagent (ThermoFisher Scientific). We used mKif21b ex2-3 and drKif21b ex2-3 primers to target *mKif21b* or *zkif21b* cDNA and mGAPDH or drElfA (Elongation factor 1- $\alpha$ ) as housekeeping genes normalizer (Table 2). shRNA-*Kif21b* knock-down efficacy was assessed by RT-qPCR. Total RNA was prepared from HEK293T cells overexpressing sh-scrambled or shRNA-*Kif21b* #2 together with pEGFP-C1-3'UTR mKif21B or from HEK 293K cells overexpressing sh-scrambled or shRNA-*Kif21b* #1 together with pEGFP-C1-WT-mKif21b. We used GFP primers to target the 3' UTR sequence of *mKif21b* cDNA fused to GFP and mKif21B ex2-3 primers to target *mKif21b* cDNA. We used mGAPDH or Hprt1 primers as housekeeping genes normalizer (Table 2). cDNA samples were synthesized with SuperScript IV Reverse Transcriptase (Invitrogen) and submitted to DNase I treatment (TurboDNase, ThermoFisher). RT-qPCR was performed in a LightCycler PCR instrument (Roche) using SYBR Green Master Mix (Roche). RT-qPCR was also performed to assess the degradation of the mutant mRNA by nonsense-mediated decay (NMD). A blood sample was obtained from patient 4 in PAXgene Blood RNA Tube (Qiagen, Germantown, CA, USA) and total RNA extracted using Qiagen PAXgene Blood miRNA kit (Qiagen, Germantown, CA, USA). As controls, total RNA was prepared with TRIzol reagent (ThermoFisher Scientific) from blood sample obtained three male individuals aged between 3 and 8 years who do not carry any *KIF21B* variants in PAXgene Blood RNA Tube. We used hKIF21B ex2-3 and hKIF21B ex33-34 coupled primers to target *hKIF21B* cDNA and hTBP as housekeeping gene normalizer.

**Cell culture, transfections and immunolabeling.** All cells used in this study are provided by the cell culture platform of the IGBMC (Strasbourg), are guaranteed mycoplasma free (PCR test Venorgem) and have not been authenticated. Mouse neuroblastoma N2A (ATCC) cells and Cos7 (ATCC) cells were cultured in DMEM (1 g/L glucose, GIBCO) supplemented with 5% Fetal Calf Serum (FCS) and Gentamycin 40  $\mu$ g/mL in a humidified atmosphere containing 5% CO<sub>2</sub> at 37 °C. Human embryonic kidney (HEK) 293T cells were cultured in DMEM (1 g/L glucose) (GIBCO) supplemented with 10% FCS, penicillin 100 UI/mL, streptomycin

100  $\mu$ g/mL in a humidified atmosphere containing 5% CO<sub>2</sub> at 37 °C. Mouse ST cells are neuronal progenitor cell lines from E14 striatal primordia of WT embryos immortalized using tsA58 SV40 large T antigen<sup>65</sup>. ST cells were cultured DMEM (1 g/L glucose) supplemented with 10% FCS heat-inactivated, non-essential amino acids, penicillin 100 UI/mL, streptomycin 100  $\mu$ g/mL and G418 400  $\mu$ g/mL in a humidified atmosphere containing 5% CO<sub>2</sub> at 33 °C. Cells were transfected using Lipofectamine 2000 (Invitrogen) according to the manufacturer's protocol. Expression of transfected genes was analyzed 48 h after transfection by immunoblotting. For localization experiments, ST cells were fixed 48 h after transfection for 5 min in -20 °C MeOH/AcOH solution (1:1), and incubated for 1 h in 0.5% Triton X-100, 5% NDS in PBS. Primary antibodies were incubated overnight at 4 °C and secondary antibodies were incubated for 1 h at room temperature (see Supplementary Table 1 for antibodies). DNA was stained using DAPI (1/1000). Slides were air-dried and mounted in Aquapolymount mounting medium (Polysciences Inc).

**Immunoprecipitation.** Immunoprecipitation (IP) experiments were done using the Pierce Anti-Myc Magnetic Beads kit (ThermoScientific) according to the manufacturer's protocol. HEK293T cells were transfected with the indicated HA-tagged, GFP-tagged and Myc-tagged constructs (ratio 1:1:2) using X-treme GENE 9 DNA transfection reagent (Roche). Cells were lysed 24 h after transfection in ice-cold IP buffer from the kit, supplemented with EDTA-free protease inhibitors (cOmplete<sup>™</sup>, Roche) and 0.01 M phosphatase inhibitor PMSF, for 30 min on ice. Cells debris were removed by high speed centrifugation at 4 °C for 15 min. After protein concentration measurement, samples were diluted to 1  $\mu$ g/ $\mu$ L. Half of the protein were kept (Input) and diluted in 2x Laemmli Elution Buffer (Bio-Rad) containing 2%  $\beta$ -mercaptoethanol. 400  $\mu$ g of proteins were then incubated with 15  $\mu$ L of pre-washed magnetic Myc-coupled beads for 2 h at 4 °C under gentle shaking. Beads were collected using a magnetic stand and supernatants were discarded. Beads were then washed twice with IP buffer and proteins were eluted at 95 °C by adding 2x Laemmli Elution Buffer containing 2%  $\beta$ -mercaptoethanol. The same volume of sample for all condition were loaded and analyzed by western blot as described below.

**Protein extraction and western blot.** Proteins from mouse cortices (E14.5 to P2) or from transfected cells (N2A, HEK293T, Cos7 and ST cells) were extracted as follows: cells were lysed in RIPA buffer (50 mM Tris pH 8.0, 150 mM NaCl, 5 mM EDTA pH 8.0, 1% Triton X-100, 0.5% sodium deoxycholate, 0.1% SDS) supplemented with EDTA-free protease inhibitors (cOmplete<sup>™</sup>, Roche) for 30 min, then cells debris were removed by high speed centrifugation at 4 °C for 25 min. Protein concentration was measured by spectrophotometry using Bio-Rad Bradford protein assay reagent. Samples were denatured at 95 °C for 10 min in Laemmli buffer (Bio-Rad) supplemented with 2%  $\beta$ -mercaptoethanol and then resolved by SDS-PAGE and transferred onto nitrocellulose membranes. Membranes were blocked in 5% milk in PBS buffer with 0.1% Tween (PBS-T) and incubated overnight at 4 °C with the appropriate primary antibody in blocking solution. Membranes were washed three times in PBS-T, incubated at room temperature for 1 h with HRP-coupled secondary antibodies (Invitrogen) at 1:10,000 dilution in PBS-T, followed by three times PBS-T washes. Visualization was performed by quantitative chemiluminescence using SuperSignal West Pico PLUS Chemiluminescent Substrate (Sigma). Signal intensity was quantified using ImageQuant LAS 600 (GE Healthcare). Primary and secondary coupled HRP antibodies used for western blot are described in Supplementary Table 1. Relative protein expression was quantified using ImageJ software (Java 1.8.0\_112).

**Cycloheximide (CHX) treatment.** To assess the protein half-life of WT- and mutated hKIF21B proteins, treatments using the translational inhibitor cycloheximide (CHX) were performed. N2A cells were cultured on 6-well plates and transfected with the adequate NeuroD- hKIF21B constructs using Lipofectamine 2000 (Invitrogen) according to the manufacturer's protocol. The day after, cells were treated with CHX (Sigma) diluted in media at 10  $\mu$ g/mL for either 2, 4, 6, 8 or

**Table 2** List of primers used for RT-qPCR.

Gene	Specie	Forward sequence	Reverse sequence
mKIF21B ex2-3	Mouse	AAGGCTGCTTTGAGGGCTAT	AAAGCCGGTGCCCATAGTA
hKIF21B ex3-4	Human	GTCACTTCTCGCTCATCCA	CTCTGCACGTTATCTGGGT
hKIF21B ex33-34	Human	TCAGTGGCTCCCGAGATAAC	CTTGTGCGCATTTGGGGATT
drKIF21B ex2-3	Zebrafish	TCACTGAGGGCTGCTTTGAG	GACACGCTCAGCTCAAAACC
GFP		TACGGCAAGCTGACCTGAAGT	GAAGTCGTGCTGCTTATGTGG
mGAPDH	Mouse	TGATGACATCAAGAAGGTGGTGAAG	TCCTTGGAGGCCATGTAGGCCAT
drElfA	Zebrafish	CTTCTCAGGCTGACTGTGC	CCGCTAGCATTACCCTCC
hTBP	Human	CGGCTGTTAACTTCGCTTC	CACACGCCAAGAAACAGTGA
Hprt1	Human	AGGCGAACCTCTCGGCTTTC	TCATCATCACTAATCACGAGCC

10 h. Cells were lysed as described above. For analysis, 10 µg of protein of each sample were loaded on a SDS-gel followed by western blotting analysis as described above. Experiments consisted of at least three independent replicates. Relative protein expression was quantified using ImageJ software (Java 1.8.0\_112).

**Zebrafish manipulation.** Zebrafish (*D. rerio*) embryos (AB strain) maintenance and experiments were performed as described here [https://zfinfo.org/zf\\_info/zfbook/cont.html#cont1](https://zfinfo.org/zf_info/zfbook/cont.html#cont1). Human WT and mutant full-length cDNA were cloned into pCS2 vector and transcribed using the SP6 Message Machine kit (Ambion). We injected 1 nL of diluted RNAs (WT or mutants) at 100 ng/µL into wild-type zebrafish eggs at 1- to 2-cell stage. Length of the head was measured at 5 dpf as shown by the double arrow headed red lines (Fig. 5a). All the experiments were repeated at least three times and an unpaired two-tailed Student's *t*-test or a Welch's two samples *t*-test (when the variances are unequal) was performed to determine significance. All images were taken using a microscope (Leica M420) dedicated to brightfield acquisitions equipped with a Coolsnap CF camera controlled by Coolsnap software. To perform zebrafish whole-mount immunolabeling, larvae were fixed at 5 dpf in Dent's fixative (80% methanol, 20% dimethylsulfoxide [DMSO]) overnight at 4 °C. The larvae were rehydrated slowly by decreasing concentrations of methanol. Larvae were then washed in PBS buffer with 0.1% Tween (PBS-T). After bleaching for 30 min in (10% H<sub>2</sub>O<sub>2</sub> in PBS-T with KOH (0.5 g/mL)), the larvae were rinsed in PBS-T, twice for 10 min each. Then larvae were permeabilized with proteinase K, then post-fixed with 4% PFA and washed in PBS-T. PFA-fixed larvae were washed in IF buffer (0.1% Tween-20, 1% BSA in PBS) for 10 min, then incubated in the blocking buffer (10% FBS, 1% BSA in PBS) for 1 h at room temperature. Larvae were incubated with primary antibody diluted in blocking solution, overnight at 4 °C (see Supplementary Table 1 for antibodies). After two washes in IF Buffer for 10 min each, larvae were incubated in secondary antibody diluted in blocking solution 2 h at room temperature. Larvae were washed in IF buffer for 10 min, twice. All images were taken using an epifluorescence microscope at ×5 magnification equipped with a Coolsnap CF camera controlled by Coolsnap software v1.2.

**Image acquisition and analysis.** Cell counting and in vivo branching analyses were done in at least three different brain slices of at least three different embryos or pups for each condition. After histological examination, only brains with comparative electroporated regions and efficiencies were conserved for quantification.

For neuronal migration analyses, proliferation analyses and brain immunofluorescence experiments, a *z* stack of 1.55 µm was acquired in 1024 × 1024 mode using a confocal microscope (Leica TCS SP5 equipped with an hybrid camera and a HC PL APO ×20/0.70 objective) controlled by Leica Las X software v3.7 and analyzed using ImageJ software (Java 1.8.0\_112). Cortical wall areas (upper cortical plate (Up CP), lower cortical plate (Lo CP), intermediate zone (IZ), subventricular zone (SVZ)/ventricular zone (VZ)) were identified according to cell density (nuclei staining with DAPI). The total number of GFP-positive cells in the embryonic brain sections was quantified by counting positive cells within a box of fixed size and the percentage of positive cells in each cortical area was calculated. For proliferation analyses, the total number of markers-positive cells in embryonic brain sections was quantified by counting positive cells in the intermediate zone (IZ) and in the subventricular zone (SVZ) below the electroporated region using square of 100-µm width or 50-µm width, respectively, with anatomically matched positions in experimental groups.

For in vivo branching analyses, a *z* stack of 3 µm was acquired in 1024 × 1024 mode using confocal microscope (Leica TCS SP5 equipped with an hybrid camera and a PL FL ×10/0.30 objective) and analyzed using ImageJ software (Java 1.8.0\_112). For axonal midline crossing analyses, the fluorescence within a box of fixed size placed at the contralateral side of the midline of the brain section was measured and divided by the fluorescence at the ipsilateral side of the midline area (Fig. 6c). This value was normalized to empty vector (control) value. For projecting neurons analyses, the fluorescence intensity within a box of fixed size placed at the ipsilateral side of the midline of the brain section was measured using ImageJ (Java 1.8.0\_112) and this value was divided by the number of Scarlet-positive neurons within a box of fixed size placed at the upper cortical plate (Fig. 6d). For quantification of layer V (ipsilateral) collateral branching, a box of fixed size was drawn encompassing layer V and the fluorescence area within this box was measured. This value was then divided by the fluorescence at the ipsilateral side of the midline area (Fig. 7c). We quantified contralateral branching<sup>66</sup> as follows: fluorescence within a box of fixed size placed contralaterally is measured on a vertical axis (from ventricular boundaries to pial surface) and converted from pixel size to percentile (0%: ventricular zone, 100%: pial surface) using the ProfilePlot plugin from Fiji software. Signal intensity of 100% is set as the maximum signal intensity in migration percentile 0 to 20 (considered as the white matter).

For in vitro branching analyses, primary neuronal cultures were done independently at least two (DIV5) or three (DIV2) times. DIV2 and DIV5 axonal length measures were performed in 125–146 and 30–66 independent cells respectively. For DIV5 axon collateral length distribution analyses, measures were performed in 187–385 collaterals from 30 to 66 independent cells. Images were acquired using upright fluorescence (DM 4000B; Leica) equipped with a HC PL APO20/×0.70 objective and a Coolsnap FX monochrome camera (Photometrics)

controlled by Leica Las X software v3.7. To measure the axonal length (longest neurite) at DIV2 and DIV5, the longest Scarlet-positive-labeled neurite was traced and the length was measured using Simple Neurite Tracer plugin ([https://imagej.net/Simple\\_Neurite\\_Tracer](https://imagej.net/Simple_Neurite_Tracer)) from Fiji software. Branch number and length was measured at DIV5 using Simple Neurite Tracer plugin.

For variant subcellular localization analysis (Fig. 4e, f), a *z* stack of 0.13 µm was acquired in 1024 × 1024 mode using a confocal microscope (Leica TCS SP5 equipped with an hybrid camera, using a HCX PL APO ×63/1.40–0.60 oil objective) controlled by Leica Las X software v3.7. For each condition, 67 to 229 independent cells from three independent transfections were segregated according to the subcellular localization of HA-tagged constructs (diffuse localization versus impaired localization).

**Live-cell imaging procedure and analysis.** Cos7 cells were grown on 35-mm glass bottom microwell dishes No. 0 (MatTek, U.S.A.). Cells were transfected with the different pcEGFP-N1-hKIF21B constructs or co-transfected with BDNF-mCherry (gift from Gary Banker, Oregon Health and Science University, Portland, USA) or Mito-RFP (gift from Hélène Puccio, IGBMC, Illkirch, France) and the different pcDNA3.1+/N-HA-hKIF21B constructs or empty vector with a DNA ratio of 1:2 as described above. Live-cell imaging was done 24 h after transfection. Live videomicroscopy was performed on an inverted microscope Leica CSU W1 DM18 (Leica) with an Adaptive Focus Control (AFC) controlled by Metamorph software v 7.6, using an HCX PL APO Lambda blue ×63/1.40 oil objective or an HC PL APO 100 × 1.47 oil objective. The microscope and the chamber were kept at 37 °C and 5% CO<sub>2</sub>. Images were collected using an Orca Flash 4.0 camera with an exposure time of 80–150 ms. Images were acquired every 250 ms for 30 s to 1 min. Single GFP-positive kinesin were tracked using Manual Tracking plugin (<https://imagej.nih.gov/ij/plugins/track/track.html>) from Fiji software. For each condition, 182–203 kinesin particles in 25–32 independent cells were analyzed from at least three independent transfections. BDNF vesicles velocities and RFP-positive mitochondria were obtained from kymograph analysis, using Fiji plugin Kymo Tool-Box v.1.01 ([https://github.com/fabricecordelieres/IJ-Plugin\\_KymoToolBox/releases](https://github.com/fabricecordelieres/IJ-Plugin_KymoToolBox/releases)). For each condition, 250–322 BDNF particles in 10–19 independent cells were analyzed from at least three independent transfections. For each condition, 173–256 Mito-RFP particles in 19–31 independent cells were analyzed from four independent transfections.

**Statistics and reproducibility.** Immunofluorescence, in situ hybridization, FACS-sorting and western blot experiments (Figs. 2c–e and 3e; Supplementary Figs. 2a–d, 3c, 4c, 5b) were repeated three times independently and gave similar results. Experiments on Kif21b WT and knockout mouse brain (Supplementary Fig. 2e, f) were performed on *n* = 3 and *n* = 5 different brains per genotype, respectively, and gave similar results. Western blot expression profile of NeuroD-IRES-GFP constructs (Supplementary Fig. 3a), HA-tagged, Myc-tagged (Supplementary Fig. 4a) and GFP-tagged constructs (Supplementary Fig. 4b) were performed once. For in utero electroporation experiments, only brains with comparative electroporated regions and efficiencies were conserved for quantification and statistical analyses. Analysis of IUE experiments were performed blinded. For one embryo or pup brain, cell counting and in vivo branching analyses were performed in three different slices. The exact numbers (*n*) of samples, animals, cells, particles, axons or branches used to derive statistics are mentioned in figure legends along with the respective data and are also reported in Supplementary Data 1. The number of times each experiment was repeated independently (i.e. the number of independent transfection or magnetofection) and statistical tests are mentioned in figure legends along with the respective data whenever possible, and are also reported in Supplementary Data 1. Statistical details (adjustments made for multiple comparisons, confidence intervals and exact *P*-values) for Figs. 2a; 3b, d; 4b, d, e—right panel, g, h, j; 5b; 6d, e, g; 7c–e, g; Supplementary Figs. 3d, f; 4d—right panel, f, g; 6d; 7b–d, are reported in Supplementary Data 1. All statistics were calculated using Prism (GraphPad, version 6) and are represented as mean ± S.E.M. Graphs were generated using Prism and images were assembled with Adobe Photoshop 13.0.1 (Adobe Systems).

**Reporting summary.** Further information on research design is available in the Nature Research Reporting Summary linked to this article.

#### Data availability

The source data underlying Figs. 2a, b; 3b, d; 4b, d, e, g, h, j; 5b; 6c, d, e, g; 7c, d, e, g; and Supplementary Figs. 1d; 2d, f; 3a, b, d, f, h; 4a, b, d, f, g, h, i; 5a, d, g, j; 6c, d, h; 7b, c, d are provided as a Source Data file. All other relevant data included in the article are available from the authors upon request. The following databases and in silico software were used in the study: Human Gene Mutation Databases (<http://www.hgmd.cf.ac.uk/ac/introduction.php?lang=english>), the single Nucleotide Polymorphism database (<http://ftp.ncbi.nih.gov/snp/>), genome aggregation database (gnomAD, <https://gnomad.broadinstitute.org/>), 1000 genomes (<https://www.internationalgenome.org/>), Polyphen-2 (<http://genetics.bwh.harvard.edu/pph2/>), Mutation Taster (<http://www.mutationtaster.org/>), Sorting Intolerant from Tolerant (SIFT, <https://sift.bii.a-star.edu.sg/>) and Combined Annotation Dependent Depletion (CADD, <https://cadd.gs.washington.edu/>).

The three *hKIF21B* missense variants have been deposited in LOVD (Leiden Open Variation Database) v3.0 (<https://databases.lovd.nl/shared/genes/KIF21B>) under the accession numbers 0000663938 (p.Ile678Leu), 0000663939 (p.Gln313Lys) and 0000663940 (p.Ala1001Thr).

Received: 17 June 2019; Accepted: 26 April 2020;

Published online: 15 May 2020

## References

- Hirokawa, N. Kinesin and dynein superfamily proteins and the mechanism of organelle transport. *Science* **279**, 519–526 (1998).
- Hirokawa, N. & Tanaka, Y. Kinesin superfamily proteins (KIFs): various functions and their relevance for important phenomena in life and diseases. *Exp. Cell Res.* **334**, 16–25 (2015).
- Caraballona, A., Hu, D. J. & Vallee, R. B. KIF1A inhibition immortalizes brain stem cells but blocks BDNF-mediated neuronal migration. *Nat. Neurosci.* **19**, 253–262 (2016).
- Chen, J. L., Chang, C. H. & Tsai, J. W. Gli2 rescues delays in brain development induced by Kif3a dysfunction. *Cereb. Cortex* **29**, 751–764 (2018).
- Foerster, P. et al. mTORC1 signaling and primary cilia are required for brain ventricle morphogenesis. *Development* **144**, 201–210 (2017).
- Sun, D. et al. Regulation of neural stem cell proliferation and differentiation by Kinesin family member 2a. *PLoS ONE* **12**, e0179047 (2017).
- Tsai, J. W., Lian, W. N., Kemal, S., Kriegstein, A. R. & Vallee, R. B. Kinesin 3 and cytoplasmic dynein mediate interkinetic nuclear migration in neural stem cells. *Nat. Neurosci.* **13**, 1463–1471 (2010).
- Wilson, S. L., Wilson, J. P., Wang, C., Wang, B. & McConnell, S. K. Primary cilia and Gli3 activity regulate cerebral cortical size. *Dev. Neurobiol.* **72**, 1196–1212 (2012).
- Geng, A. et al. KIF20A/MKLP2 regulates the division modes of neural progenitor cells during cortical development. *Nat. Commun.* **9**, 2707 (2018).
- Janisch, K. M. et al. The vertebrate-specific Kinesin-6, Kif20b, is required for normal cytokinesis of polarized cortical stem cells and cerebral cortex size. *Development* **140**, 4672–4682 (2013).
- Reilly, M. L. et al. Loss of function mutations in KIF14 cause severe microcephaly and kidney development defects in humans and zebrafish. *Hum. Mol. Genet.* **28**, 778–795 (2018).
- Falnikar, A., Tole, S. & Baas, P. W. Kinesin-5, a mitotic microtubule-associated motor protein, modulates neuronal migration. *Mol. Biol. Cell* **22**, 1561–1574 (2011).
- Falnikar, A., Tole, S., Liu, M., Liu, J. S. & Baas, P. W. Polarity in migrating neurons is related to a mechanism analogous to cytokinesis. *Curr. Biol.* **23**, 1215–1220 (2013).
- Homma, N. et al. Kinesin superfamily protein 2A (KIF2A) functions in suppression of collateral branch extension. *Cell* **114**, 229–239 (2003).
- Liu, M. et al. Kinesin-12, a mitotic microtubule-associated motor protein, impacts axonal growth, navigation, and branching. *J. Neurosci.* **30**, 14896–14906 (2010).
- Myers, K. A. & Baas, P. W. Kinesin-5 regulates the growth of the axon by acting as a brake on its microtubule array. *J. Cell Biol.* **178**, 1081–1091 (2007).
- Peretti, D., Peris, L., Rosso, S., Quiroga, S. & Caceres, A. Evidence for the involvement of KIF4 in the anterograde transport of L1-containing vesicles. *J. Cell Biol.* **149**, 141–152 (2000).
- Xu, M. et al. Kinesin-12 influences axonal growth during zebrafish neural development. *Cytoskeleton* **71**, 555–563 (2014).
- Midorikawa, R., Takei, Y. & Hirokawa, N. KIF4 motor regulates activity-dependent neuronal survival by suppressing PARP-1 enzymatic activity. *Cell* **125**, 371–383 (2006).
- Kondo, M., Takei, Y. & Hirokawa, N. Motor protein KIF1A is essential for hippocampal synaptogenesis and learning enhancement in an enriched environment. *Neuron* **73**, 743–757 (2012).
- Muhia, M. et al. The kinesin KIF21B regulates microtubule dynamics and is essential for neuronal morphology, synapse function, and learning and memory. *Cell Rep.* **15**, 968–977 (2016).
- Nakajima, K. et al. Molecular motor KIF5A is essential for GABA(A) receptor transport, and KIF5A deletion causes epilepsy. *Neuron* **76**, 945–961 (2012).
- Swarnkar, S., Avchalumov, Y., Raveendra, B. L., Grinman, E. & Puthanveetil, S. V. Kinesin family of proteins Kif1 and Kif21B act as inhibitory constraints of excitatory synaptic transmission through distinct mechanisms. *Sci. Rep.* **8**, 17419 (2018).
- Willemssen, M. H. et al. Involvement of the kinesin family members KIF4A and KIF5C in intellectual disability and synaptic function. *J. Med. Genet.* **51**, 487–494 (2014).
- Najmabadi, H. et al. Deep sequencing reveals 50 novel genes for recessive cognitive disorders. *Nature* **478**, 57–63 (2011).
- Putoux, A. et al. KIF7 mutations cause fetal hydroletharus and acrocallosal syndromes. *Nat. Genet.* **43**, 601–606 (2011).
- Dafinger, C. et al. Mutations in KIF7 link Joubert syndrome with Sonic Hedgehog signaling and microtubule dynamics. *J. Clin. Invest.* **121**, 2662–2667 (2011).
- Jamuar, S. S. et al. Somatic mutations in cerebral cortical malformations. *N. Engl. J. Med.* **371**, 733–743 (2014).
- Ostergaard, P. et al. Mutations in KIF11 cause autosomal-dominant microcephaly variably associated with congenital lymphedema and chorioretinopathy. *Am. J. Hum. Genet.* **90**, 356–362 (2012).
- Poirier, K. et al. Mutations in TUBG1, DYNC1H1, KIF5C and KIF2A cause malformations of cortical development and microcephaly. *Nat. Genet.* **45**, 639–647 (2013).
- Tian, G. et al. A patient with lissencephaly, developmental delay, and infantile spasms, due to de novo heterozygous mutation of KIF2A. *Mol. Genet. Genomic Med.* **4**, 599–603 (2016).
- Cavallin, M. et al. Recurrent KIF2A mutations are responsible for classic lissencephaly. *Neurogenetics* **18**, 73–79 (2017).
- Michels, S. et al. Mutations of KIF5C cause a neurodevelopmental disorder of infantile-onset epilepsy, absent language, and distinctive malformations of cortical development. *Am. J. Med. Genet. A* **173**, 3127–3131 (2017).
- Ohba, C. et al. De novo KIF1A mutations cause intellectual deficit, cerebellar atrophy, lower limb spasticity and visual disturbance. *J. Hum. Genet.* **60**, 739–742 (2015).
- Konjikusic, M. J. et al. Mutations in Kinesin family member 6 reveal specific role in ependymal cell gliogenesis and human neurological development. *PLoS Genet.* **14**, e1007817 (2018).
- Filges, I. et al. Exome sequencing identifies mutations in KIF14 as a novel cause of an autosomal recessive lethal fetal ciliopathy phenotype. *Clin. Genet.* **86**, 220–228 (2014).
- Makrythanasis, P. et al. Biallelic variants in KIF14 cause intellectual disability with microcephaly. *Eur. J. Hum. Genet.* **26**, 330–339 (2018).
- Broix, L. et al. Gliogenesis and cell cycle alterations contribute to KIF2A-related malformations of cortical development. *Hum. Mol. Genet.* **27**, 224–238 (2018).
- Labonte, D., Thies, E. & Kneussel, M. The kinesin KIF21B participates in the cell surface delivery of gamma2 subunit-containing GABAA receptors. *Eur. J. Cell Biol.* **93**, 338–346 (2014).
- Marszalek, J. R., Weiner, J. A., Farlow, S. J., Chun, J. & Goldstein, L. S. Novel dendritic kinesin sorting identified by different process targeting of two related kinesins: KIF21A and KIF21B. *J. Cell Biol.* **145**, 469–479 (1999).
- Huang, C. F. & Banker, G. The translocation selectivity of the kinesins that mediate neuronal organelle transport. *Traffic* **13**, 549–564 (2012).
- van Riel, W. E. et al. Kinesin-4 KIF21B is a potent microtubule pausing factor. *Elife* **6**, e24746 (2017).
- Gromova, K. V. et al. Neurobeachin and the kinesin KIF21B are critical for endocytic recycling of NMDA receptors and regulate social behavior. *Cell Rep.* **23**, 2705–2717 (2018).
- Ghirelli, A. E. et al. Activity-dependent regulation of distinct transport and cytoskeletal remodeling functions of the dendritic kinesin KIF21B. *Neuron* **92**, 857–872 (2016).
- Labonte, D. et al. TRIM3 regulates the motility of the kinesin motor protein KIF21B. *PLoS ONE* **8**, e75603 (2013).
- Bianchi, S. et al. Structural basis for misregulation of kinesin KIF21A autoinhibition by CFEOM1 disease mutations. *Sci. Rep.* **6**, 30668 (2016).
- Kannan, M. et al. WD40-repeat 47, a microtubule-associated protein, is essential for brain development and autophagy. *Proc. Natl Acad. Sci. USA* **114**, E9308–E9317 (2017).
- Morikawa, M., Tanaka, Y., Cho, H. S., Yoshihara, M. & Hirokawa, N. The molecular motor KIF21B mediates synaptic plasticity and fear extinction by terminating Rac1 activation. *Cell Rep.* **23**, 3864–3877 (2018).
- Olson, H. E. et al. Micro-duplications of 1q32.1 associated with neurodevelopmental delay. *Eur. J. Med. Genet.* **55**, 145–150 (2012).
- Sobreira, N., Schiettecatte, F., Valle, D. & Hamosh, A. GeneMatcher: a matching tool for connecting investigators with an interest in the same gene. *Hum. Mutat.* **36**, 928–930 (2015).
- Taylor, A. M. et al. A microfluidic culture platform for CNS axonal injury, regeneration and transport. *Nat. Methods* **2**, 599–605 (2005).
- Matsuda, T. & Cepko, C. L. Controlled expression of transgenes introduced by in vivo electroporation. *Proc. Natl Acad. Sci. USA* **104**, 1027–1032 (2007).
- Cheng, L. et al. Human CFEOM1 mutations attenuate KIF21A autoinhibition and cause oculomotor axon stalling. *Neuron* **82**, 334–349 (2014).
- van der Vaart, B. et al. CFEOM1-associated kinesin KIF21A is a cortical microtubule growth inhibitor. *Dev. Cell* **27**, 145–160 (2013).
- Golzio, C. et al. KCTD13 is a major driver of mirrored neuroanatomical phenotypes of the 16p11.2 copy number variant. *Nature* **485**, 363–367 (2012).

56. Igarashi, A. et al. Nuclear PTEN deficiency causes microcephaly with decreased neuronal soma size and increased seizure susceptibility. *J. Biol. Chem.* **293**, 9292–9300 (2018).
57. Thomanetz, V. et al. Ablation of the mTORC2 component rictor in brain or Purkinje cells affects size and neuron morphology. *J. Cell Biol.* **201**, 293–308 (2013).
58. Kelliher, M. T. et al. Autoinhibition of kinesin-1 is essential to the dendrite-specific localization of Golgi outposts. *J. Cell Biol.* **217**, 2531–2547 (2018).
59. Niwa, S. et al. Autoinhibition of a neuronal kinesin UNC-104/KIF1A regulates the size and density of synapses. *Cell Rep.* **16**, 2129–2141 (2016).
60. Retterer, K. et al. Clinical application of whole-exome sequencing across clinical indications. *Genet Med* **18**, 696–704 (2016).
61. Hand, R. & Polleux, F. Neurogenin2 regulates the initial axon guidance of cortical pyramidal neurons projecting medially to the corpus callosum. *Neural Dev.* **6**, 30 (2011).
62. Skarnes, W. C. et al. A conditional knockout resource for the genome-wide study of mouse gene function. *Nature* **474**, 337–342 (2011).
63. Zala, D. et al. Vesicular glycolysis provides on-board energy for fast axonal transport. *Cell* **152**, 479–491 (2013).
64. Virlogeux, A. et al. Reconstituting corticostriatal network on-a-chip reveals the contribution of the presynaptic compartment to Huntington's disease. *Cell Rep.* **22**, 110–122 (2018).
65. Trettel, F. et al. Dominant phenotypes produced by the HD mutation in *STHdh(Q111)* striatal cells. *Hum. Mol. Genet* **9**, 2799–2809 (2000).
66. Courchet, J. et al. Terminal axon branching is regulated by the LKB1-NUAK1 kinase pathway via presynaptic mitochondrial capture. *Cell* **153**, 1510–1525 (2013).

### Acknowledgements

This work was funded by grants from INSERM (ATIP-Avenir program, J.D.G.), the Fyssen foundation (J.D.G.), the French state funds through the Agence Nationale de la Recherche under the project JJC CREDO ANR-14-CE13-0008-01 (J.D.G.), CILAXCAL (C.D.) and AXION ANR-18-CE16-0009-01 (F.S.), and the program Investissements d'Avenir labeled (ANR-10-IDEX-0002-02, ANR-10-LABX-0030-INRT, to J.D.G. and C.G.), the Fondation pour la recherche sur le cerveau (F.S.), INSERM/CNRS and University of Strasbourg. N.A.H. and G.Z. are supported by USDA Grant Number 3092-51000-057-04S. L.A. and J.R.A. are funded through the IGBMC PhD program (ANR-10-IDEX-0002-02, ANR-10-LABX-0030-INRT). L.A. is currently supported by Fondation pour la recherche médicale (FDT201805005184). P.T. and C.W. are, respectively, research assistant and research engineer at the University of Strasbourg. J.D.G. and C.G. are INSERM investigators. F.S. is a professor at Univ. Grenoble Alpes. H.V. is supported by a PhD fellowship from Association Huntington France. We thank the Imaging Center of IGBMC ([ici.igbmc.fr](http://ici.igbmc.fr)), in particular, Elvire Guiot and Erwan Grandgirard for their assistance in the imaging experiments. We are grateful to the staff of the mouse facilities of the Institut Clinique de la souris (ICS) and Institut de Génétique et de Biologie Moléculaire et Cellulaire (IGBMC), the staff of the zebrafish facility of the IGBMC and, the molecular biology service (in particular Thierry Lerouge and Paola Rossillo) for their involvement in the project. We thank Sandra Bour and IGBMC communication service. We also thank Dr Courchet, Dr Banker, Dr Puccio and member of Chelly lab for sharing reagents and for discussion. We are really grateful to Pr Jamel Chelly and Dr Laurent Nguyen for their continuous support, discussion and time reading this manuscript. We warmly thank Dr Sandrine Humbert and Dr Binnaz Yalcin for helpful comments and advices. We are also grateful to members of J.D.G. and Chelly

laboratories for discussion and technical assistance. In particular, we thank Dr Efil Bayam for cell sorting and advices in writing the manuscript. We thank Dr Gabrielle Rudolf for reading the manuscript and for her suggestions. We finally thank Paula Hernandez for her help collecting patient samples.

### Author contributions

L.A. and J.R.A. conceived and designed the experiments, performed the experiments, performed statistical analysis and analyzed the data related to cellular, and functional studies in mice. P.T. provided technical assistance and performed in utero electroporation. C.G. and C.S.B. conceived, designed and performed experiments in zebrafish. C.W. provided technical assistance for zebrafish studies. S.H., K.B., C.A.B., A.C., A.D., S.M., L.F., N.A.H., K.M., C.M., H.S., C.T.R., M.M.W., P.J.G.Z., G.Z. and D.H. contributed clinical and imaging data and follow-up of patients and families. S.H., A.R., C.N. and C.D. contributed to the generation of whole-exome sequencing, bioinformatics tools and analysis of sequencing data. H.V. and F.S. conceived and performed the expression analysis in microdevices. J.D.G. conceived, coordinated and supervised the study, designed experiments, analyzed data and wrote the manuscript.

### Competing interests

A.D. and K.M. are employees of GeneDx, Inc. The other authors declare no competing interest.

### Additional information

**Supplementary information** is available for this paper at <https://doi.org/10.1038/s41467-020-16294-6>.

**Correspondence** and requests for materials should be addressed to J.D.G.

**Peer review information** *Nature Communications* thanks the anonymous reviewer(s) for their contribution to the peer review of this work. Peer reviewer reports are available.

**Reprints and permission information** is available at <http://www.nature.com/reprints>

**Publisher's note** Springer Nature remains neutral with regard to jurisdictional claims in published maps and institutional affiliations.



**Open Access** This article is licensed under a Creative Commons Attribution 4.0 International License, which permits use, sharing, adaptation, distribution and reproduction in any medium or format, as long as you give appropriate credit to the original author(s) and the source, provide a link to the Creative Commons license, and indicate if changes were made. The images or other third party material in this article are included in the article's Creative Commons license, unless indicated otherwise in a credit line to the material. If material is not included in the article's Creative Commons license and your intended use is not permitted by statutory regulation or exceeds the permitted use, you will need to obtain permission directly from the copyright holder. To view a copy of this license, visit <http://creativecommons.org/licenses/by/4.0/>.

© The Author(s) 2020

<sup>1</sup>Institut de Génétique et de Biologie Moléculaire et Cellulaire, Illkirch, France. <sup>2</sup>Centre National de la Recherche Scientifique, UMR7104, Illkirch, France. <sup>3</sup>Institut National de la Santé et de la Recherche Médicale, INSERM, U1258 Illkirch, France. <sup>4</sup>Université de Strasbourg, Strasbourg, France. <sup>5</sup>Département de Génétique, AP-HP, Hôpital de la Pitié-Salpêtrière, Paris, France. <sup>6</sup>Groupe de Recherche Clinique (GRC) "Déficience Intellectuelle et Autisme", UPMC, Paris, France. <sup>7</sup>Centre de Référence Déficiences Intellectuelles de Causes Rares, Hôpital de la Pitié-Salpêtrière, Paris, France. <sup>8</sup>Univ. Grenoble Alpes, INSERM, U1216, CHU Grenoble Alpes, Grenoble Institut Neurosciences, Grenoble, France. <sup>9</sup>Department of Molecular and Human Genetics, Baylor College of Medicine, Houston, TX, USA. <sup>10</sup>Texas Children's Hospital, Houston, TX, USA. <sup>11</sup>Department of Neurogenetics, Kennedy Krieger Institute, Baltimore, MD 21205, USA. <sup>12</sup>GeneDx, Gaithersburg, MD 20877, USA. <sup>13</sup>Centre de Référence Anomalies du Développement et Syndromes Malformatifs, Fédération Hospitalo-Universitaire Médecine Translationnelle et Anomalies du Développement (TRANSLAD), Centre Hospitalier Universitaire Dijon et Université de Bourgogne, Dijon, France. <sup>14</sup>Equipe GAD, INSERM LNC UMR 1231, Faculté de Médecine, Université de Bourgogne Franche-Comté, Dijon, France. <sup>15</sup>Department of Neurology, Boston Children's Hospital, Boston, MA 02115, USA. <sup>16</sup>INSERM, U 1127, CNRS UMR 7225, Faculté de Médecine de Sorbonne Université, UMR S 1127, Institut du Cerveau et de la Moelle épinière, ICM, Paris, France. <sup>17</sup>Centre de Référence Déficiences Intellectuelles de Causes Rares, Centre Hospitalier Universitaire Dijon, Dijon, France. <sup>18</sup>Department of Clinical Genetics, Amsterdam UMC, Vrije Universiteit Amsterdam, Amsterdam, The Netherlands. <sup>19</sup>Institute of Human Genetics, University Hospital Essen, University of Duisburg-Essen, Essen, Germany. <sup>20</sup>These authors contributed equally: José Rivera Alvarez, Solveig Heide, Camille S. Bonnet <sup>✉</sup>email: [godin@igbmc.fr](mailto:godin@igbmc.fr)

